



*forests*

# Historical Wood Structure, Properties and Conservation

---

Edited by

Magdalena Broda and Callum A. S. Hill

Printed Edition of the Special Issue Published in *Forests*

# **Historical Wood: Structure, Properties and Conservation**



# Historical Wood: Structure, Properties and Conservation

Editors

**Magdalena Broda**

**Callum A. S. Hill**

MDPI • Basel • Beijing • Wuhan • Barcelona • Belgrade • Manchester • Tokyo • Cluj • Tianjin



*Editors*

Magdalena Broda  
Faculty of Forestry and  
Wood Technology  
Poznan University  
of Life Sciences  
Poznan  
Poland

Callum A. S. Hill  
Norwegian Institute of  
Bioeconomy Research  
NIBIO  
Ås  
Norway

*Editorial Office*

MDPI  
St. Alban-Anlage 66  
4052 Basel, Switzerland

This is a reprint of articles from the Special Issue published online in the open access journal *Forests* (ISSN 1999-4907) (available at: [www.mdpi.com/journal/forests/special\\_issues/historical\\_wood](http://www.mdpi.com/journal/forests/special_issues/historical_wood)).

For citation purposes, cite each article independently as indicated on the article page online and as indicated below:

LastName, A.A.; LastName, B.B.; LastName, C.C. Article Title. <i>Journal Name</i> <b>Year</b> , <i>Volume Number</i> , Page Range.
--

**ISBN 978-3-0365-3153-3 (Hbk)**

**ISBN 978-3-0365-3152-6 (PDF)**

© 2022 by the authors. Articles in this book are Open Access and distributed under the Creative Commons Attribution (CC BY) license, which allows users to download, copy and build upon published articles, as long as the author and publisher are properly credited, which ensures maximum dissemination and a wider impact of our publications.

The book as a whole is distributed by MDPI under the terms and conditions of the Creative Commons license CC BY-NC-ND.

# Contents

<b>About the Editors</b> . . . . .	<b>vii</b>
<b>Preface to "Historical Wood: Structure, Properties and Conservation"</b> . . . . .	<b>ix</b>
<b>Angeliki Zisi</b> Forest Wood through the Eyes of a Cultural Conservator Reprinted from: <i>Forests</i> <b>2021</b> , <i>12</i> , 1001, doi:10.3390/f12081001 . . . . .	<b>1</b>
<b>Magdalena Broda and Callum A. S. Hill</b> Conservation of Waterlogged Wood—Past, Present and Future Perspectives Reprinted from: <i>Forests</i> <b>2021</b> , <i>12</i> , 1193, doi:10.3390/f12091193 . . . . .	<b>25</b>
<b>Zarah Walsh-Korb</b> Sustainability in Heritage Wood Conservation: Challenges and Directions for Future Research Reprinted from: <i>Forests</i> <b>2021</b> , <i>13</i> , 18, doi:10.3390/f13010018 . . . . .	<b>81</b>
<b>Hugh Collett, Florian Bouville, Finn Giuliani and Eleanor Schofield</b> Structural Monitoring of a Large Archaeological Wooden Structure in Real Time, Post PEG Treatment Reprinted from: <i>Forests</i> <b>2021</b> , <i>12</i> , 1788, doi:10.3390/f12121788 . . . . .	<b>117</b>
<b>Sarah Hunt, Josep Grau-Bove, Eleanor Schofield and Simon Gaisford</b> Effect of Polyethylene Glycol Treatment on Acetic Acid Emissions from Wood Reprinted from: <i>Forests</i> <b>2021</b> , <i>12</i> , 1629, doi:10.3390/f12121629 . . . . .	<b>131</b>
<b>Gabriel Lipkowitz, Karoline Sofie Hennem, Eleonora Piva and Eleanor Schofield</b> Numerical Modelling of Moisture Loss during Controlled Drying of Marine Archaeological Wood Reprinted from: <i>Forests</i> <b>2021</b> , <i>12</i> , 1662, doi:10.3390/f12121662 . . . . .	<b>139</b>
<b>Yeqing Han, Jing Du, Xinduo Huang, Kaixuan Ma, Yu Wang and Peifeng Guo et al.</b> Chemical Properties and Microbial Analysis of Waterlogged Archaeological Wood from the Nanhai No. 1 Shipwreck Reprinted from: <i>Forests</i> <b>2021</b> , <i>12</i> , 587, doi:10.3390/f12050587 . . . . .	<b>151</b>
<b>Carmen-Mihaela Popescu and Magdalena Broda</b> Interactions between Different Organosilicons and Archaeological Waterlogged Wood Evaluated by Infrared Spectroscopy Reprinted from: <i>Forests</i> <b>2021</b> , <i>12</i> , 268, doi:10.3390/f12030268 . . . . .	<b>161</b>
<b>Jeannette J. Łucejko, Anne de Lamotte, Fabrizio Andriulo, Hartmut Kutzke, Stephen Harding and Mary Phillips-Jones et al.</b> Evaluation of Soda Lignin from Wheat Straw/Sarkanda Grass as a Potential Future Consolidant for Archaeological Wood Reprinted from: <i>Forests</i> <b>2021</b> , <i>12</i> , 911, doi:10.3390/f12070911 . . . . .	<b>177</b>
<b>Eirini Mitsi, Stamatis Boyatzis and Anastasia Pournou</b> Chemical Characterization of Waterlogged Charred Wood: The Case of a Medieval Shipwreck Reprinted from: <i>Forests</i> <b>2021</b> , <i>12</i> , 1594, doi:10.3390/f12111594 . . . . .	<b>205</b>

<b>Petros Choidis, Dimitrios Kraniotis, Ilari Lehtonen and Bente Hellum</b> A Modelling Approach for the Assessment of Climate Change Impact on the Fungal Colonization of Historic Timber Structures Reprinted from: <i>Forests</i> <b>2021</b> , <i>12</i> , 819, doi:10.3390/f12070819 . . . . .	<b>217</b>
<b>Giuseppina Fiore Bettina, Belinda Giambra, Giuseppe Cavallaro, Giuseppe Lazzara, Bartolomeo Megna and Ramil Fakhrullin et al.</b> Restoration of a XVII Century's <i>predella reliquary</i> : From Physico-Chemical Characterization to the Conservation Process Reprinted from: <i>Forests</i> <b>2021</b> , <i>12</i> , 345, doi:10.3390/f12030345 . . . . .	<b>245</b>
<b>Miha Humar, Angela Balzano, Davor Kržišnik and Boštjan Lesar</b> Assessment of Wooden Foundation Piles after 125 Years of Service Reprinted from: <i>Forests</i> <b>2021</b> , <i>12</i> , 143, doi:10.3390/f12020143 . . . . .	<b>257</b>
<b>Amir Ghavidel, Reza Hosseinpourpia, Holger Militz, Viorica Vasilache and Ion Sandu</b> Characterization of Archaeological European White Elm ( <i>Ulmus laevis</i> P.) and Black Poplar ( <i>Populus nigra</i> L.) Reprinted from: <i>Forests</i> <b>2020</b> , <i>11</i> , 1329, doi:10.3390/f11121329 . . . . .	<b>271</b>
<b>Magdalena Broda, Paulina Kryg and Graham Alan Ormondroyd</b> Gap-Fillers for Wooden Artefacts Exposed Outdoors—A Review Reprinted from: <i>Forests</i> <b>2021</b> , <i>12</i> , 606, doi:10.3390/f12050606 . . . . .	<b>285</b>

# About the Editors

## **Magdalena Broda**

A researcher at the Faculty of Forestry and Wood Technology, Poznań University of Life Sciences, Poland. A biotechnologist by education but involved in wood science for several years. Her work focuses on the new conservation methods for waterlogged archaeological wood, relations between wood structure and properties, and biodegradation in general.

## **Callum A. S. Hill**

An independent consultant and a visiting researcher at NIBIO. He previously held the Edinburgh Research Partnership Chair of Renewable Materials at Edinburgh Napier University between 2007 and 2013. Prior to that, he was a Senior Lecturer in Wood Science at Bangor University (1994-2007). He is a widely published researcher, having authored two textbooks, eight book chapters, and over 200 research papers.





# **Preface to “Historical Wood: Structure, Properties and Conservation”**

Nowadays, the majority of research concentrates on applied science that regards issues crucial from the socio-economical perspective, such as new functional materials and super-efficient technologies, clean energy, improvement of human health, or tackling climate change. However, we cannot forget about our culture and history, which define our humanity. Wooden cultural heritage is an integral part of it. Therefore, we are obliged to protect it, save it from oblivion, and preserve it for future generations.

This Special Issue presents the methods for the historical wooden artefacts conservation, reliable modern techniques for characterisation of the wood structure, properties and degree of degradation. It also discusses problems and doubts related to all aspects of conservation and re-conservation of wooden cultural heritage.

We hope that this book will meet the expectations of readers interested in historical wood.

**Magdalena Broda, Callum A. S. Hill**  
*Editors*



Article

# Forest Wood through the Eyes of a Cultural Conservator

Angeliki Zisi

Department of Collection Management, Museum of Cultural History, University of Oslo, Kabelgata 34, 0580 Oslo, Norway; angeliki.zisi@khm.uio.no

**Abstract:** If prehistoric and historical time were placed into the time span of the existence of our universe, then the act of archaeology could be defined as the act of digging up what was only buried yesterday. So, conservation is about preserving a moment that has just become past time, yet significant. It is a moment of human creativity and ingenuity. It is not strange that forest wood has become the material to convey such moments. Forest wood is a living, everlasting source growing without human intervention, within reach, easy to use and shape thinking both great and small. It does not have to be a wooden ship; it can be a mere piece of charcoal. For it is what surrounded humans in the past which archaeologists seek and use to weave human history, and what conservators bring back to context by reviving it. This work presents forest wood as an artefact and its preservation challenges as such. It touches on its natural degradation processes through burial, compromised properties and eventual conservation. Both dry and waterlogged wood are included. The overarching aim of this paper is to pay tribute, preserve and inspire the long-standing, open dialog and fruitful collaboration between cultural conservators and forest and wood scientists.

**Keywords:** historical wood; archaeological wood; wood degradation; artefact; heritage; conservation; cultural conservator



**Citation:** Zisi, A. Forest Wood through the Eyes of a Cultural Conservator. *Forests* **2021**, *12*, 1001. <https://doi.org/10.3390/f12081001>

Academic Editors: Magdalena Broda and Callum A. S. Hill

Received: 15 June 2021  
Accepted: 26 July 2021  
Published: 28 July 2021

**Publisher's Note:** MDPI stays neutral with regard to jurisdictional claims in published maps and institutional affiliations.



**Copyright:** © 2021 by the author. Licensee MDPI, Basel, Switzerland. This article is an open access article distributed under the terms and conditions of the Creative Commons Attribution (CC BY) license (<https://creativecommons.org/licenses/by/4.0/>).

## 1. Introduction

The purpose of this paper is to present basic concepts of wood structure and its physicochemical and mechanical properties from the point of view of a cultural conservator assigned with the task of preserving wooden artefacts and the practical as well as ethical problems involved when doing so. The intention is to avoid providing specific solutions to specific problems, and rather offer to the reader a way of critical thinking when challenged with the study and preservation of a piece of historical wood regardless of the burial environment it was found in. As it is not feasible to include all aspects of wood, let alone degraded wood, it is also a wish to communicate to wood scientists those wood terms and issues with an immediate interest to conservators brought together with the societal role of the latter. Last, it is hoped that the paper will be a useful introduction to those conservators new to the field of wood conservation.

Here, both archaeological and historical wood are referred to as 'historical wood', meaning generally wood of historical as well as cultural value. Besides, historical time becomes irrelevant with regard to wood degradation. Wood degradation and severity of degradation is partially about the wood species and deterioration already present at the moment of 'discard' and, more importantly, the burial process and type and duration of subsequent prevailing environmental conditions to which wood is exposed. Even so, it would be advisable for the reader to keep in mind throughout the text that the word 'historical' wood will also imply some meaning of degradation apart from its value.

## 2. Why Wood?

The answer to this question emerges plainly in Perlin's introductory line of his book *A Forest Journey: The role of wood in the development of civilization*—'Ancient writers observed that forests always recede as civilizations develop and grow' [1] (p. 25). The connection

between human evolution and forests is inextricably tied. For when wood was critically limited, humans engineered ways of acquiring iron from copper slag, carelessly marking the beginning of a new historical era [1] (p. 17).

In an ancient world already covered with trees for hundreds of millions of years, humans picked up wood and started building it around them. It warmed them, housed them, carried them, protected them, and its beauty even filled them with awe. Wood still lies out there to speak to us of life during the Mesolithic time in the Western Solent, UK [2]. It has helped us reconstruct a Mycenaean shipwright's toolkit from the Late Bronze Age, Greece [3]. It has also taught us about pioneering maritime engineering and stuns us with the scale of wooden constructions humans were capable of building, a case in point being the emergence of the harbour of King Herod of Judea Caesarea Palaestinae (ca. 23–15 BCE) out in the open sea (Figure 1) [4]. For a resourceful collection of references to Greek and Roman wood technology, including entries on energy conversion, fire and fuels, the research by Humphrey et al. is certainly worth a glance [5].

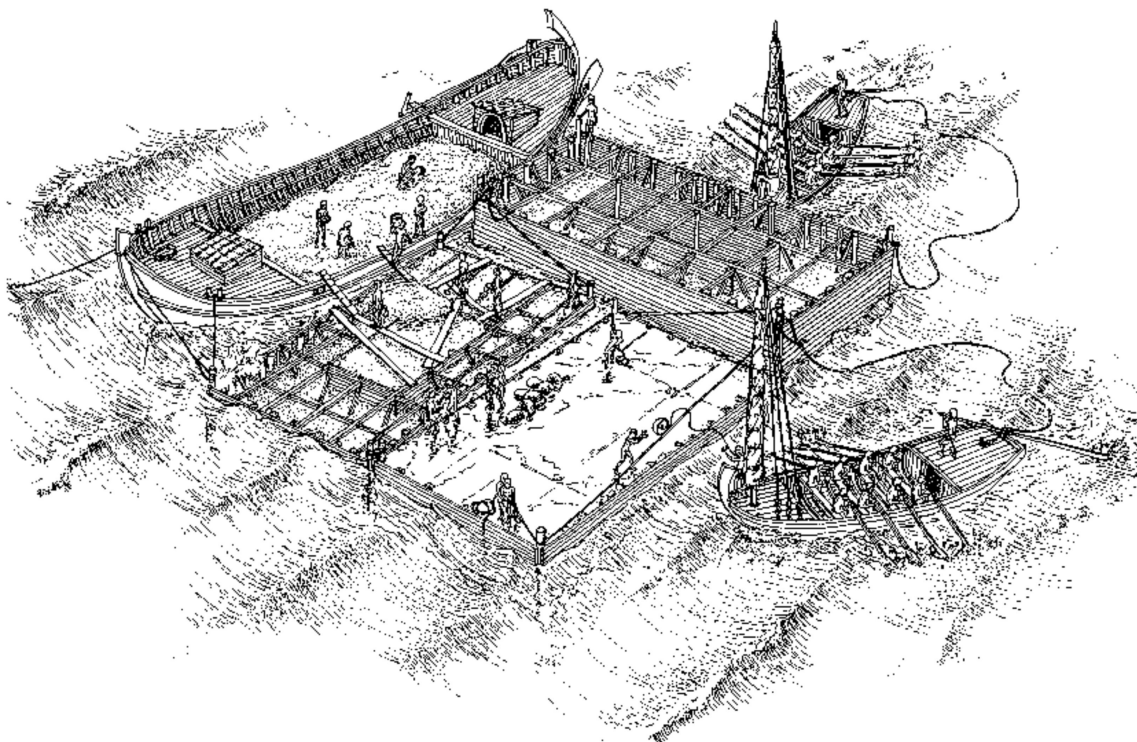


**Figure 1.** Reconstruction of prefabricated caissons being positioned and loaded with concrete at Area K at the northern end of the main enclosing mole at Caesarea [4] (p. 213). Drawing: C.J. Brandon; used with kind permission.

An artificial harbour on a far smaller scale is now being unravelled at Lechaion in Corinth, Greece, with much of the wooden infrastructure still preserved in situ [6]. Along with its value in understanding the role of the city and port of Ancient Corinth during the Roman and Byzantine (Late Antiquity) period, its excavation gives us a unique opportunity to access yet another source of information—tree-rings. It is hoped that it will be possible to expand tree-ring chronological sequences in the Aegean [7], and so, add fixed points for archaeologists for dating finds based on dendrochronology [8]. It will also enhance our knowledge of forestry practices in ancient times. Reconstruction of the paleoclimate and evaluation of climate model simulations constitutes yet another dynamic aspect offered by tree-rings [9,10].

Faced closely with something made in the past, the role of a conservator is to preserve the find and therefore, preserve history for today's humans to reflect on before handing it down to a later time. Humbly drawn from our short cosmic lives, the perception of

our personal role as individuals is that of rather small significance for the continuation of history, yet history fully resonates within us. It only takes a visit to a museum to make even an unwitting soul aware of their part in this abiding history, intertwined, no matter the distance, with the events that generated what we today admire as artefacts in displays. The museum that truthfully brings about this self-consciousness to its visitor has fulfilled its purpose. History becomes essential reference points for perpetual evolution of life. It imparts confidence and provides comfort: '[ . . . ] but even unfinished wood, as it darkens and the grain grows more subtle with the years, acquires an inexplicable power to calm and soothe.' [11] (p. 12).

Conservation of wood of historical and cultural value goes hand-in-hand with wood science. They are both built around the theory of wood as raw material, its structure and properties. Conservation consults wood science and adopts ways of studying wood within the ethics that now define it as an artefact. For in the majority of cases, particularly in the Western world, historical wood can no longer serve its original purpose especially if that was functional. An artefact is unique and now destined for study and appreciation and interventions, therefore, have to be minimal and well justified to serve its longevity. The reader is greatly encouraged to refer to the work by Muñoz Viñas 'Contemporary Theory of Conservation' which discusses intervention with great deliberation, reflecting on the way to adhere to the authenticity of an object [12]. A fine use of both 'science conservation', which seeks the truth of the object, as well as 'contemporary conservation theory' which values the object for the immaterial matters it represents such as art, meaning and feeling, is to this author, central. So, in a way, both worlds are reflected in the word 'artefact'.

Meanwhile, historical wood deteriorates as any piece of wood. Expertise knowledge of the structure and properties of wood helps the conservator assess its current state of preservation by knowing what to look for and how, in order to understand what care it needs and how best to give it. Many decades of collaboration with forest and wood experts have advanced the conservation of wood by establishing solutions both simple and sophisticated to be utilized reasonably. It is true that even after so much progress it is still difficult to predict how a conserved piece of historic wood will fair in time, regardless of the time and most conscientious efforts spent on this. Having said that, we can assume that if it is in existence today, it will be so in the future, for responsible care is underway.

### 3. Basic Wood Structure and Properties concerning Conservation

Hort in his translation of Theophrastus (ca. 370-285 BCE) *Enquiry into Plants* (Greek: Περὶ φυτῶν ἱστορία, Latin: *Historia Plantarum*), remarks Theophrastus's continuous wonder as to which essential characteristics distinguish one plant from another [13] (p. xxii). It is notable that the first systematic botanist based his ratiocination on direct comparisons with the other division of Aristotle's kingdoms of life, that of the animals: 'Fibre and veins (Hort note: 'muscles and veins') have no special names in relation to plants, but, because of the resemblance, borrow the names of the corresponding parts of animals.' [13] (p. 19). Theophrastus's work builds on that of his contemporary mentor Aristotle in *History of Animals* (Τῶν περὶ τὰ ζῶα ἱστοριῶν or *Historia Animalium*): 'However, since it is by the help of the better known that we must pursue the unknown [ . . . ] it is clear that it is right to speak of these things in the way indicated' [13] (p. 19); a core science lesson still holding true today.

A long history past these cornerstones, Linnaeus carries this inner need to understand and rationalise an apparent chaotic plant diversity and submits it in his *Systema Naturae* (1735). Linnaeus's early work in the classification of flowers seemed to work well for the then known plants, but there was a problem (solved by Swedish botanist, Florin in the 1950s) when trying to fit the first, in evolutionary terms, order of trees—the Coniferales [14]. It is well known that gymnosperms—of which conifers are a group—are the primitive state and that the angiosperms are the derivative, an evolution taking place sometime in the mid-Mesozoic and certainly by the end of it, at the Lower Cretaceous [14]. Setting aside for a moment the thriving diversity of angiosperms, Farjon shows his respect for conifers,

these ancient living and intelligent organisms, with a life that covers more than 300 million years of existence and evolution, and whimsically notes: in contrast to the much-admired dinosaurs, conifers did not become extinct at the end of the Cretaceous. That the internal structure of conifer wood remained virtually unchanged for millions of years, efficient in its simplicity and homogeneity and capable of adapting to a wide range of climates from the very cold to the very dry, has allowed conifers to continue to prosper on Earth.

A rich fossil plant record informs us that during the Late Cretaceous angiosperms became an important component of the vegetation in the warm subtropical climates of Antarctica [15]. Although heading into the Pleistocene deep-freeze this vegetation disappeared from the continent, angiosperms managed to succeed and even force out conifers from the lowland tropical rainforests, which instead resided in mountains, on coasts, in high deserts, and in cold climates [14]. Today angiosperms account for about 300,000 species, whereas conifers a mere 630 species.

Angiosperms produce what is called hardwood whereas conifers produce softwood. The terms are based on the hardness of wood and its weight, or density, although names do not necessarily correspond to the actual wood properties even today [16]. Theophrastus already excludes hardwood lime wood for it is especially soft and easy to work [13] (p. 445).

### 3.1. Macroscopic Structural Characteristics

Softwood and hardwood artefacts are equally stored in museum collections or found still standing in the open air or submerged in the seas and lakes. A quick guide to distinguishing between the two is the presence or absence of wood rays in its cross-section, easily noticed with the naked eye. While wide and conspicuous in hardwoods like oak, beech and sycamore, rays are difficult to distinguish in softwoods like pine and spruce, even with a hand lens. A second feature of hardwoods only, more often than not visible to the naked eye, but certainly with the use of a hand lens, is the presence of pores, the small openings within growth rings. These openings correspond to the cell lumina of the vessel members, a cell type unique to hardwoods only. Depending on their arrangement in relation to the rings, hardwood is classified as ring-porous, semi-ring-porous or diffuse porous. Equally, some softwoods like those of the Pineaceae family also have small openings in their cross-section. However, these openings are not cells, but intercellular spaces corresponding to axial resin canals (traumatic canals included). They are found scattered on the cross-section mainly as solitary openings or in pairs, or in small groups aligned with the rings.

Furthermore, looking at the cross-section of both types of woods, one can easily identify an inner dark wood portion expanding outwards from the central part of the tree trunk (pith), called heartwood which is surrounded by a lighter and narrower in width wood portion called sapwood (Figure 2). Heartwood is the result of the progressive transformation of the living sapwood into dead tissue. As such, heartwood does not participate in the translocation and storage of food, solely run by sapwood, but provides mechanical support to the tree. The formation of heartwood is a natural aging process and associated with bordered pits aspiration, formation of tyloses and deposition of extractives, all of which protect the wood from decay by occluding pathways.

With this initial distinction between hardwood and softwood, the conservator can assume from the outset that penetration depth of a conservation material will be difficult in hardwood like oak because its heartwood is rich with tyloses; similarly, it will be difficult in the prominent by pit-aspiration heartwood of softwoods. That conservators are more likely holding in their hands such wood, is a valid probability as, unless restricted by supply, local availability and the time allowed to grow, heartwood was chiefly used for its superior mechanical properties and resistance to attack by microorganisms, attributes ancient people were very well aware of [17] (p. 28).

Woodworking is also of importance when it comes to the impregnation of wood with conservation agents (Figure 2). Standing trees or dead wood generally absorb fluids along the main growth axis, the longitudinal. Flow follows naturally along the open pathways

formed by stacked cell lumina of myriad wood cells aligned with their long axis almost in parallel to the tree trunk [18]. Impregnation drops for the transverse directions by a factor of  $10^4$ . Therefore, permeability, or else, penetration depth, of a conservation agent depends additionally on this wood structural characteristic. It is not surprising that techniques as deep incising, radial drilling and through-boring are utilised to substantially improve penetration depth of preservatives in service wood poles today [19]. Certainly, one cannot so light-heartedly perforate wood of historical value, but can surely mimic the idea behind the procedure starting by using existing lateral entry points, usually pre-existing cracks or openings. Instances might still rise when such drastic interventions are a one-way street, but for reasons other than rushing through conservation treatments.

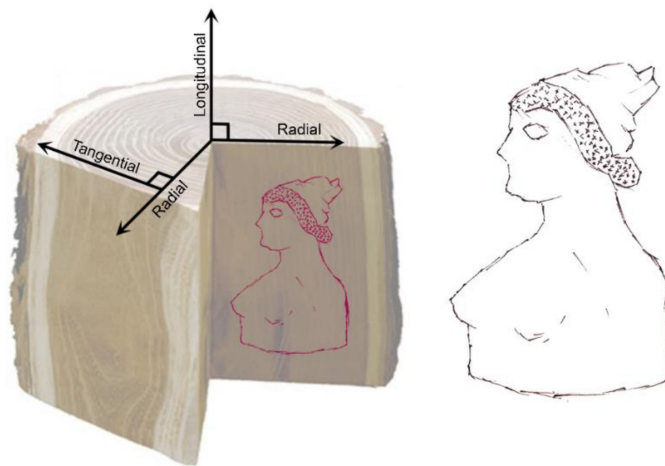


**Figure 2.** Artefact orientation inside a tree-trunk. Artistic interpretation of a female wooden figurine found in waterlogged condition at the excavations of the Temple of Artemis in Brauron, Greece (2500 years old) [20]. Image from a sector of coniferous wood stem adopted from <http://www.woodanatomy.ch/macro.html> (accessed on 8 May 2015). In ref. [21]. Image of figurine from <https://www.tovima.gr/2011/10/03/culture/ksylino-eidwlio-kai-soles-papoytsiwn-ilikias-2500-etwn/> (accessed on 11 June 2021). Drawing: A. Zisi.

The larger the available cross-section surface area for accessing is, the lesser time it can take a conservation agent to impregnate wood, and the less time the drying process will take afterwards. The drying rate of smaller objects is expected to be faster than for larger objects explained by the ratio of the surface area to the volume [22]. As an object becomes bigger the surface/volume ratio becomes smaller, so the drying rate depends on the available surface area. This is of significant importance for orthotropic wood where evaporation happens more readily in the cross-section than the lateral surface (radial, tangential). Therefore, large and especially long wooden objects request longer drying times than small objects. However, longer drying times favour good results regarding avoiding adverse shrinkage or shape distortions, as well as consolidant migration to the wood surface if impregnated wood is left to dry too fast [23]. Devising ways to slower and control solvent evaporation rate is advisable for any size wooden object.

Growth abnormalities in wood like, spiral grain and reaction wood, as well as natural growth characteristics as is the pith and knots, are further structural characteristics that should concern conservators and those involved in historical wood research. Their sometimes unavoidable inclusion in objects or structures can also affect data measurements or conservation results. The latter concerns, namely the reduced permeability to conservation agents in such wood and the release of tensions upon drying after immersion in either water or non-water-based consolidants. These could result in significant alterations of, for example, important carved surfaces or make it impossible to rejoin fragmented artefacts or complex structures as planks on frames of wooden hulls. Even small misalignments can



propagate the fault further away and end up distorting considerably the original shape of an object or a structure.

Meticulous study of the wood structure per case, and mapping and flagging of potential shortcomings before treatment is essential not only for conservators to design and execute conservation schemes but also for researchers to design methodological approaches tailored to the specifics of research questions with useful answers. For example, the use of *clear*, straight-grained, quarter-sawn wood from unseasoned, that is, with moisture content (MC) already over the fibre saturation point (FSP) 30% and free from drying-induced defects, oak and pine wood, allowed the acquisition of reliable and reproducible results for studying ultrasound wave propagation in historical wood whilst in a waterlogged state (in this case  $MC_{max}$ ) [24]. Moreover, taking into account the directional dependency of fluid permeability in wood, the longitudinal dimension of testing specimens was set shorter than the radial and tangential dimensions. This benefitted water absorption along the grain and tried to gain time from the waterlogging procedure, as long durations could be expected given the rather large size of the specimens [25]. Additional attention was paid to introducing a gradual vacuum power into the water bath so as to avoid possible rupturing of the pit membranes and tripping the waterlogging procedure [26]. If anything, the experiments proved that with the right knowledge of the material it is possible to control for the naturally high variability in wood, by taking a few crucial decisions right at the beginning of planning.

If not for a specific need for using hardwood species, the use of softwoods for experimental material is encouraged, for its greater structural uniformity allows easier interpretations of the effect of various applications on wood, especially at the outset of a study (e.g., [27]).

### 3.2. Microscopic Structural Characteristics

A closer look at thin, transparent wood sections or macerated wood substance under the light microscope, reveals a variety of wood cells bundled in different ways to form the wood tissue of conifers and angiosperms [28]. Images of sections representative of the transverse, radial and tangential planes, reveal diagnostic features for wood identification. Stitching together the three wood planes enables the conservator to see beyond the wooden surface and visualise its three-dimensional structure in greater detail than the initial dichotomous question—softwood or hardwood—allows him or her to do [29,30].

Wood under the microscope reveals that tracheid cells, which form up to 90% of the wood cell type in conifers, and fibre cells, which may contribute 50% or more of the total wood cell type in angiosperms, have tapered ends that are closed. With the ends of the tracheids closed, the transport and distribution of fluids in conifers is primarily dependent on the pitting of longitudinal tracheids. These pits conduct fluids in the tangential direction due to their positioning mainly along the radial wood surfaces (Figure 3). Although it seems that this depends on the species, as fluids in *Pinus sylvestris* L. end up filling the longitudinal tracheids having first travelled through the ray cells especially in thin and long wooden structures [31]. In the more cell type variable angiosperms, the vessel members, having large diameter cell lumen, are the actual fluid conducting cells, leaving the fibres functioning mainly as the wood strengthening cells in the living tree [32]. Vessel members form stacks of indeterminate length where fluid gets transferred through perforation plates of various typology, located at the ends of each cell—as long as there are no tyloses blocking the flow (Figures 4 and 5). From inside the vessel chamber, fluid can be transferred also in a radial manner via the intervessel pits formed on the vessel walls where a vessel member touches another one (Figure 6). Pits also exist where a vessel member meets ray cells, forming diversified vessel-ray pitting (Figure 7).

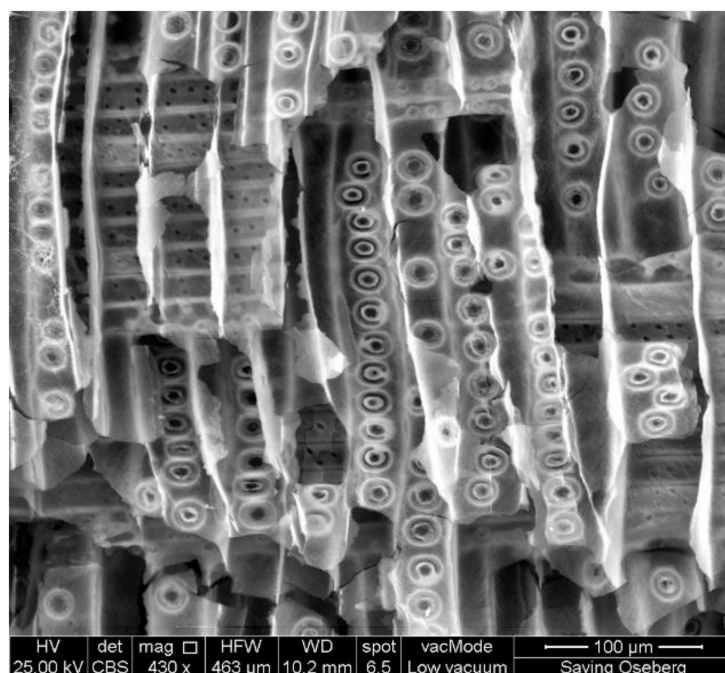


**Figure 3.** Scanning electron micrograph of a radial-longitudinal section from historical waterlogged *Picea abies* (L.) H.Karst. wood. Border pits in the longitudinal tracheids appear degraded whilst signs of attack by fungi are also visible along the tracheid lumen (left-hand side of image). The wood sample belongs to an assemblage of wooden stocks used for the construction of a road excavated from the medieval part of Oslo (ca. 1200–1300 CE). Image: A. Zisi, © Museum of Cultural History.

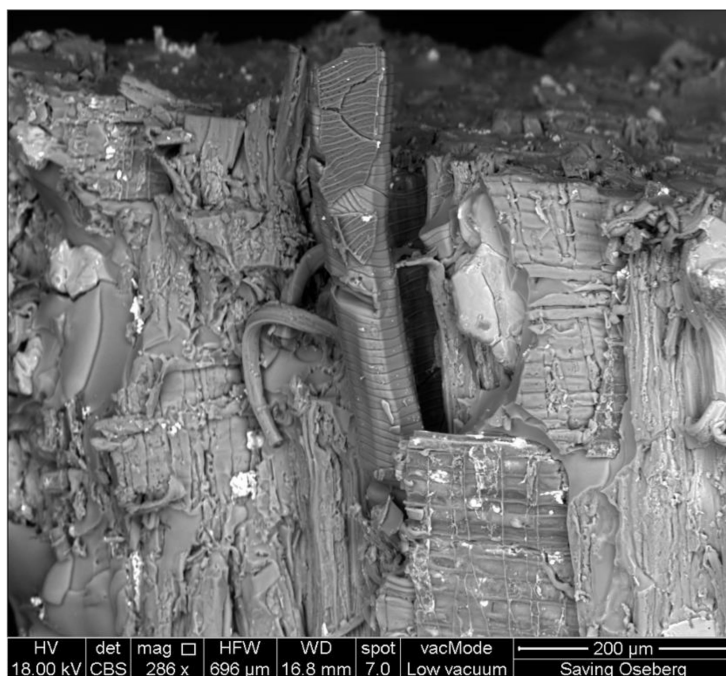


**Figure 4.** Scanning electron micrograph of a radial-longitudinal section from heavily degraded alum-treated wood (*Betula* spp.) from the Oseberg wooden collection. Protruding in the middle of the image is a perfect casting of the lumen of a vessel member with the bars of the scalariform perforation plate indented on its surface. Attached to the casting are pieces of the actual cell wall. The wood sample was treated with a silanol-based consolidant during re-conservation trials [33]. Image: A. Zisi, © Museum of Cultural History.

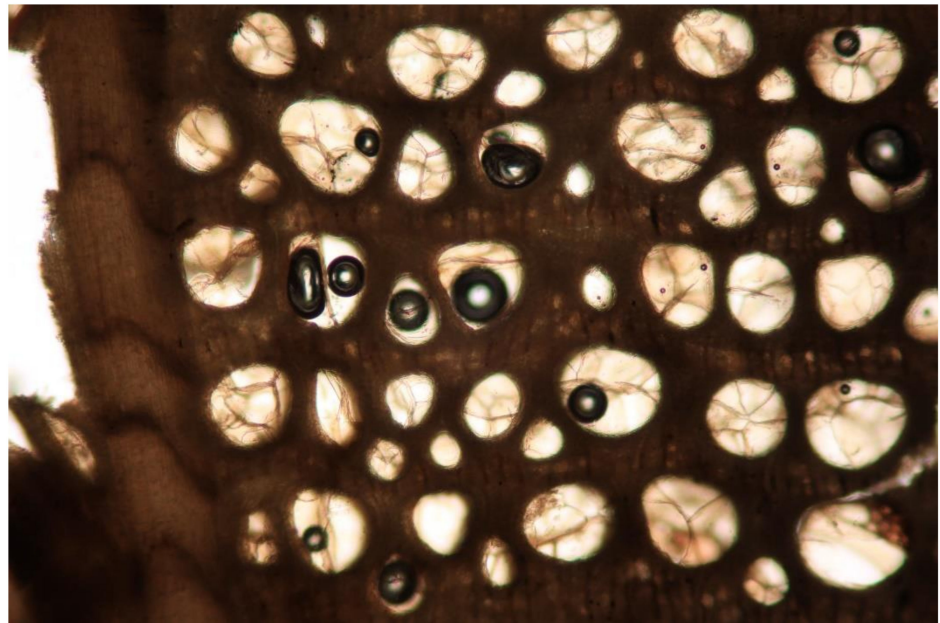


**Figure 5.** Light microscope image of a transverse section of a slow-grown *Quercus* spp. wood belonging to the White oak group (50×). Formation of tyloses in vessel members is prominent. The waterlogged wood sample derives from an underwater excavation site at the mouth of Ropotamo River located along the Bulgarian coast [34]. Image: A. Zisi, © Black Sea MAP.



**Figure 6.** Light microscope image of a tangential-longitudinal section of a *Pistacia* spp. wood (100×). Intervessel pits alternate. The waterlogged wood sample derives from an underwater excavation site at the mouth of Ropotamo River located along the Bulgarian coast [34]. Image: A. Zisi, © Black Sea MAP.

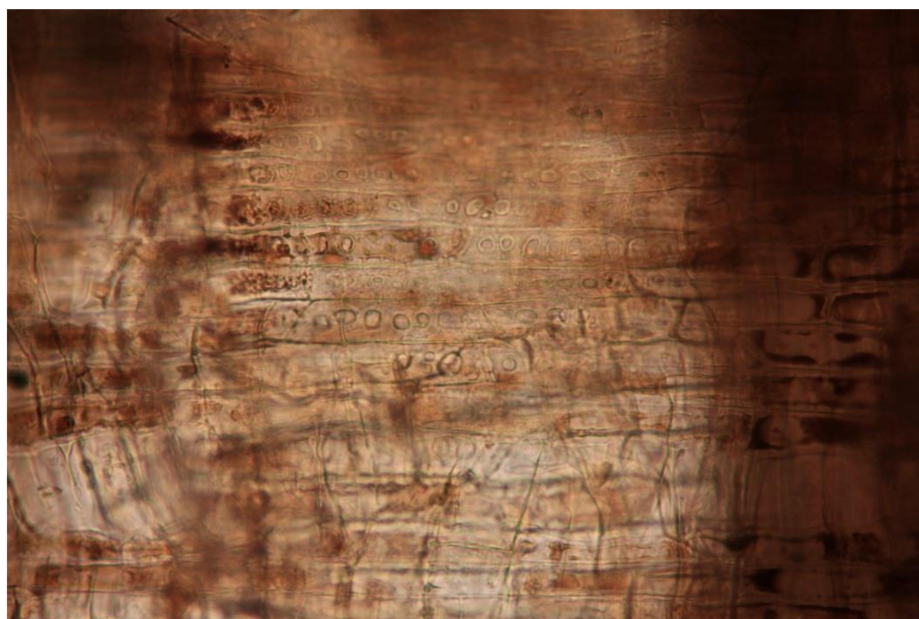


**Figure 7.** Light microscope image of a radial-longitudinal section of a *Quercus* spp. wood belonging to the White oak group (400×). Vessel-ray pitting with much reduced borders to apparently simple. The pits are rounded or angular. The wood sample belongs to one out of a number of piles forming a retaining wall found to the east of Lechaion’s ancient harbour entrance canal during underwater excavations in Greece. Image: A. Zisi, © Lechaion Harbour Project.

Wood identification requires good knowledge of wood anatomy, training, access to reference collections, experience and continuous practice. That historical wood can be degraded, and in many cases heavily degraded, can add complexity to the process of identification and can mislead an untrained eye. Deriving a species can also prove impossible. If left unsure, the best solution is to seek advice from a wood anatomist. Besides, the first interest for the conservator is not to identify the wood type but to recognise and assess the preservation state of these wood anatomical features.

It is broadly through these pathways and the fact that in the dead wood cells the lumen is predominantly empty, on which the conservator can rely, together with any other voids and their interconnection for transferring conservation agents inside wood (Figure 8). Identifying these microstructural characteristics and their preservation state [35,36], gives valuable insight into the type of conservation agent, means of application and success of conservation treatment.

### 3.3. Physical Properties

#### 3.3.1. Basic Density

Identifying the wood type has yet another importance for conservators. Whether dry or waterlogged, wood loses mass or else its density decreases due to deterioration. It is noted here that in contrast to the fields of timber industry and wood science, where ‘dry wood’ can denote oven-dried wood with 0% moisture content, in the fields of historical wood conservation and archaeology, the term ‘dry wood’ has been established to separate wood with moisture content in an air-dried condition from wood found in waterlogged contexts and therefore in a waterlogged condition, termed ‘waterlogged wood’. As the degree of wood deterioration is a function of the amount of mass lost, knowledge of approximately the amount of wood that would be expected as in the healthy wood species counterpart, allows calculations to be made and classifications of a degradation level to be defined [37].

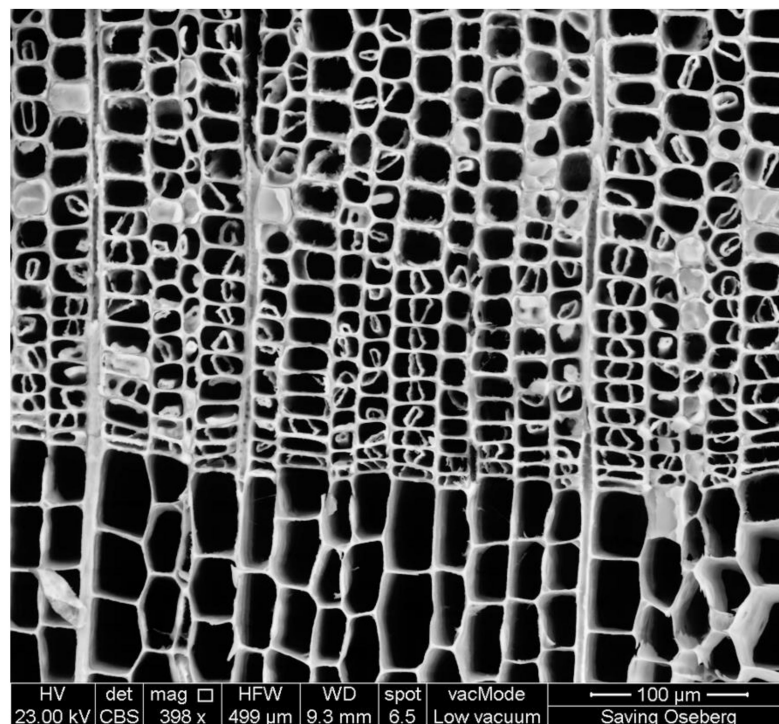


**Figure 8.** Scanning electron micrograph of a transverse section from historical waterlogged *Picea abies* wood. Latewood cells show severe degradation. There is pronounced secondary wall separation and collapse, with mainly parts of the primary wall and the middle lamella still in place. Seen also is the lumen of only a few latewood cells filled (or plugged) with 20% Paraloid B72 in acetone; the lumen of the earlywood cells remained empty after impregnation. The wood sample belongs to an assemblage of wooden stocks used for the construction of a road excavated from the medieval part of Oslo (ca. 1200–1300 CE). Image: A. Zisi, © Museum of Cultural History.

Basic density (based on oven-dried weight/wet or waterlogged volume) is a wood degradation benchmark for conservators. With a special note always in mind that density comparisons between that of historical wood and the average of a recent counterpart cannot be considered accurate, especially if assessed without a morphological evaluation of the wood's microstructural condition—Macchioni classifies wood samples with residual basic density (RBD%) lower than 65–70% as degraded, and with lower than 40% as heavily degraded [38]. Similarly, Jensen and Gregory suggest a density as low as  $100 \text{ kg}\cdot\text{m}^{-3}$  to be representative of a severely degraded piece of wood, while densities around  $400\text{--}500 \text{ kg}\cdot\text{m}^{-3}$  correspond to well-preserved wood irrespective of species [39].

Basic density is one of the first physical wood properties to be defined and can be easily performed and understood by every conservation laboratory. For wood in a waterlogged condition, density is calculated based on its oven-dried weight (at  $103 \pm 2 \text{ }^\circ\text{C}$  till constant weight is reached) and waterlogged volume. The same applies to dry wood, although, the challenge for the conservator to precisely measure the volume of dry fragile and irregularly shaped wooden artefacts would be greatly benefited by using a low-cost device developed by Kavvouras and Fotopoulou [40].

### 3.3.2. Hygroscopicity

It is well known that wood absorbs and releases water vapours due to its cellular make-up. Responsible for this are the hydroxyl groups of cellulose and hemicellulose due to their good affiliation to water molecules. Lignin, the third component of the cell wall which holds things together, is comparatively less hydrophilic. Wood cell walls will thus respond to changes in the relative humidity and temperature in the air or soil it is preserved in, until it reaches an equilibrium. That is when it neither gains nor loses

moisture, a condition called equilibrium moisture content (EMC). It can be deduced that historical wood will not necessarily reach the same moisture equilibrium levels compared to sound wood under the same environmental conditions. It depends not only on the residual amount of chemicals in its cell wall and cell wall integrity, but also on the presence of any extraneous inclusions or previous treatments.

Degraded waterlogged heartwood *Pinus sylvestris* retrieved from excavations in historical Oslo with a measured density of  $314 \text{ kg}\cdot\text{m}^{-3}$  (*o.d.* weight), that is RBD 63% compared to recent sound heartwood of the same species from Norway, reached EMC 11% after freeze-drying and conditioning at 50% ( $\pm 2\%$ ) RH and 20 °C. After immersion in water for 24h, the same wood raised the MC to 63% and after another 24h under vacuum application to  $\text{MC}_{\text{max}}$  249%. Although in its dried state the moisture content of the historical wood did agree perfectly with that of its recent counterpart, the latter reached  $\text{MC}_{\text{max}}$  just 101% [41]. The amount of water intake by historical wood echoes the process of wood mass loss. Empirical data reveal a very strong linear relationship between moisture content and basic density advancing wood degradation, with water now substituting the voids in historical waterlogged wood (Figure 9). For conservators woods with moisture content of more than 400% coupled with RBD less than 40% are classed as highly deteriorated. Water contents of more than 1000% for historical wood have been reported in the past [42].

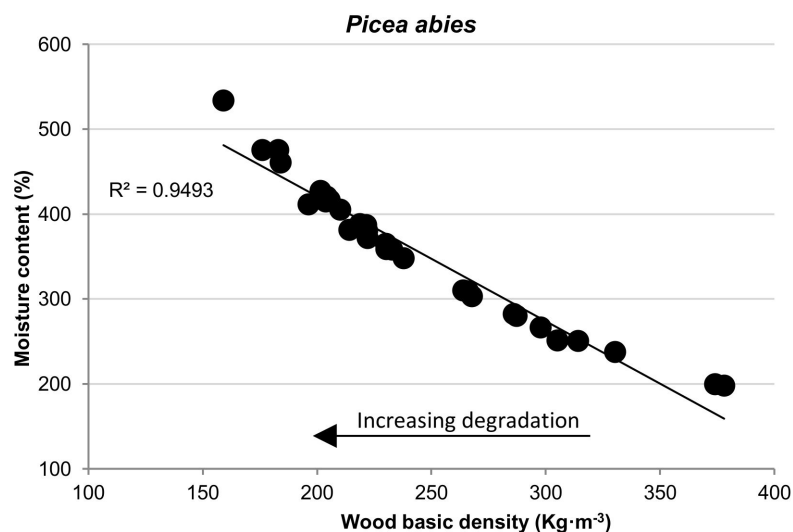


**Figure 9.** A strong linear relationship ( $r^2 = 0.949$ ) exists between wood basic density and moisture content increasing wood degradation ( $n = 30$ ) (author's unpublished work). A quadratic polynomial seems to better explain the relationship between the two variables ( $r^2 = 0.993$ ), however, a linear is given here just for reasons of simplicity.

### 3.3.3. Dimensional Stability

Wood cell walls will react to changes in surrounding humidity by either swelling or shrinking. The challenge for the conservator is to minimise and control for likely dimensional changes. For dry wood, when strengthening of the cell wall is not required due to a fairly good condition of the wood, this could be accomplished passively by storing or displaying it in a controlled environment—usually 50–55% RH and 20 °C. For dry wood in need of mechanical reinforcement or for wood in a waterlogged condition, invasive methods have to be used [43].

Ideally, treatment will not amplify some possible shrinking or swelling that could be expected when invasively dealing with an object. This is most certainly true for objects with interlocking parts where possible tensions towards different directions could build up during treatment, particularly when not all parts are degraded to the same level (e.g., either repairs made whilst the object was in use [44], or later repairs). Concern rises for objects that are not in a strong enough state to be dismantled and treated separately, or when it is rather

doubtful if the separated pieces will match well after treatment. This is a fairly common phenomenon in historical wood conservation or re-conservation, with an immediate impact on the readability of the object. A good conservation agent would therefore be inert to, or even able to counteract such tensions, possibly by improving elastic properties.

Rowell and Youngs [45] calculate the antishrink efficiency (ASE) on the basis of the treated volumetric swelling coefficient which includes dimensional changes along all three wood directions, radial, tangential and longitudinal. Yet, the contribution of the longitudinal shrinkage could be omitted, as very low to negligible changes are expected along this axis and because it is chiefly influenced by the fibre organisation. A focus on the transverse shrinkage is more useful as changes across this area are mostly influenced by the density of the wood [46], upon which conservators base basic condition assessments, as already mentioned. Nonetheless, consideration should be shown to objects including juvenile wood as this part of the tree can exhibit significant longitudinal shrinkage in undegraded wood.

Grattan et al. note that the higher the transverse ASE, the better the treatment for waterlogged wood [22]. A hundred percent ASE signifies no dimensional change; equal to zero a total ineffectual treatment; and more than 75%, a reasonable result unless the wood is highly degraded, whereupon the ASE aimed at has to be very high for a treatment to be of a significant value for waterlogged wood conservation. Johns rightfully emphasises that antishrink efficiency values need to be evaluated cautiously since the comparison is made between two different populations, the untreated controls and the treated one [47]. This is important when designing experiments for testing various different conservation agents on wood, to aim for consistency among the groups being tested. For example, when experiments are run using directly historical material rather than one specially selected or engineered for the purpose, where the advantage of dealing with the authentic material outweighs the disadvantage of a loss of control over experimental variables [48]. Thus, interpretation of results would benefit from a careful distribution of the material so that any 'irregularities', that is, wood grain orientation, conversion type, especially flat-sawn, growth ring curvature, presence of reaction wood, inclusions like knots, amount and distribution of latewood bands, etc. that could affect ASE anyway, are represented in all groups and as equally as possible. Lastly, Johns raises a concern regarding ASE measurement precision when it comes to lightly degraded wood where dimensional changes might be small [47].

The amount of acceptable dimensional change is something that has to be defined by collection curators. For example, after the first conservation attempt of a wet wooden table from Gordion tumulus in Turkey in 1957, results were deemed unsatisfactory due to intense wood shrinkage, 9% tangentially and 6% radially after solvent-drying wood with ethanol and consolidating it with a solution of paraffin wax in benzene (in ref. [49]).

Similarly, this author noted tangential and radial shrinkage of 7.5% and 2.7%, respectively for degraded *Picea abies* treated via immersion in 15% Butvar B98 in 60:40 toluene/ethanol, and 6.1% and 3.5% after immersion in 20% Paraloid B72 in acetone [41]. The wood had first gone through a dehydration process from a waterlogged state ( $MC_{max} = 216\%$ ) via solvent exchange in successive baths, starting with 70% ethanol in water and finishing in pure acetone. Values might look reasonable for the timber industry, yet a 2.7% dimensional change could make tool marks disappear. It is suggested here that, responsible for the rather large dimensional change is a combination of extractives removal by the solvents and the subsequent use of a low resin concentration. As mentioned, extractives are deposited in cell lumina and cell walls and can be extracted by organic solvents as are alcohol and acetone. If extractives are removed from the cell wall, a definite impact on the shrinkage of wood is expected [46,50,51]. Moreover, fragments of the structural cell wall polymers could also have been removed by the solvents in this case. Therefore, the dehydration of the waterlogged wood undermined further its already compromised preservation by increasing the void volume in wood, which the low resin concentration was incompetent to support adequately. Further reduction of the initial resin concentration can be assumed due to the already solvent-wet state of the wood. Also, the solubility of wood in ethanol/benzene

(replaced by toluene as it is less carcinogenic) is an ASTM standard to measure extractive contents [52].

Recent work has shown a strong linear relationship between the weight percentage gain of water-based polyethylene glycol (PEG) by degraded wood and its transverse swelling. In a direct comparison, when non-water-based consolidants were used to treat the same experimental material, the relationship between weight gain and dimensional change (in the transverse direction) was either very weak or nonexistent, therefore, highlighting different chemical interactions taking place between the wood cell wall and aqueous- and non-aqueous-based treatments [41].

### 3.4. Chemical Properties

Carbon, hydrogen and oxygen combine to form the principal organic components of wood substance, namely cellulose, hemicellulose and lignin. Lignin is the cell wall component that differentiates wood from other cellulosic materials produced by nature due to its higher contribution to wood [53,54]. Moreover, extractives and ash content in wood are also relevant to conservation.

The mainly crystalline structure of cellulose makes it harder for fluid penetration. However, the fewer amorphous cellulose regions could be characterised as the polymer's weak points. The reason is that these areas account for moisture-absorbing structures in the cellulose microfibrils [55,56], which attract more water molecules by direct hydrogen bonding with them and so forth, setting-off a process of cellulose hydrolysis, although its rate seems to be significantly slowed down by the way cellulose structures water molecules above its surface [57]. In an alkaline environment, for example, submerged in the sea, cellulose swells. When the pH is too high the polymer's end units detach without further extensive depolymerisation. However, depolymerisation occurs in an acidic environment and affects the wood's mechanical strength. Hemicellulose is more readily degraded than cellulose due to side groups branching out of the main polymer axis, which prevents a tighter arrangement among chains as in cellulose [49]. Semi-crystalline hemicelluloses are attacked by strong alkalis, whereas they are easily hydrolysable in acidic environments, where extensive chain breakdown also occurs. The amorphous lignin is chemically far more stable than the other two components of the cell wall and is commonly found to be the last one to go. It imparts rigidity and dimensional stability to the cell wall. It is, however, sensitive to ultraviolet light which is a major factor for its degradation when wood is exposed to it. An example of the effect of ultraviolet light on lignin is shown in a dry Chinese fir sample from a 170-year-old wooden building in China, where 4% lesser lignin content (determined according to GB/T 744-1989) was found in the outermost wood layer exposed to the sun than the immediate middle and innermost areas [58].

Fungi and bacteria are capable of depolymerising wood for food in all types of environments—dry, wet or waterlogged. In general, deterioration by microorganisms starts from the least resistant component and moves on: hemicellulose <  $\alpha$ -cellulose < lignin [59]. Non-biological chemical deterioration also takes place. For example, degradation of the cell wall and modification of the residual lignin that could not be ascribed to the act of microorganisms was found on wood from the high Arctic buried or frozen for 20–60 million years [60]. The proximity of wood to metal objects and metal corrosion in burial environments or in composite artefacts is another reason for chemical decomposition, as well as past conservation treatments. Thorough analyses of wood from the Oseberg collection, treated with alum more than 100 years ago, showed that the source of acidity was the alum treatment itself. With pH values even close to zero, wood is now mainly composed of lignin with up to 97% relative abundance (measured by pyrolysis-gas chromatography-mass spectrometry (Py GC-MS)) whereas, in this case, holocellulose has a 3% relative abundance [61]. For comparison, sound wood had relative abundances ranging between 21–42% for lignin and 58–78% for holocellulose [62]—the term ascribed to the total fraction of cellulose and hemicellulose.



An 8000-year-old waterlogged piece of oak wood from a Neolithic lakeside settlement in northern Greece [63], was found to contain an average of 76% lignin and 37% holocellulose (measured in accordance with ASTM D 1106-96 and ASTM D 1109-84) with values for sound wood from the literature, approximately 24% lignin and 20% holocellulose [48]. The careful reader will notice that numbers in the historical wood exceed 100%. That is because values were derived separately, using two different methods. As Florian notes, using methods for characterising and quantifying degraded wood chemicals would seem more appropriate than those designed for normal wood [64].

Lastly, regarding ash content—the inorganic content in wood. High values even up to 28% as those found in a waterlogged wood sample from the Gjelstad ship (author's unpublished work), are values that should not surprise conservators and researchers. In this case, the wood has been filtering the minerals from the soil around it like a sponge due to its severe degradation and loss in mass. Ash quantities as high as this are considerable and need to be accounted for when determining the degree of degradation—can lead, for example, to density overestimation—and when designing conservation actions and research for suitable conservation agents as wood might have lost its woody nature.

### 3.5. Mechanical Properties

Moisture content in wood has a very strong effect on its mechanical properties up to its fibre saturation point. Severely deteriorated wood loses its strength because of reductions of the crystal structure in the remaining cellulose. Cell walls can turn thin and weak and become prone to shrinkage and collapse. In weathered wood deterioration of earlywood cells is faster than that of the latewood cells, which show a two- to six-fold endurance to weathering; although as a whole, deterioration due to weathering is a very slow process [49]. Mass loss might occur, but not detected if replaced by minerals, typical of deteriorated waterlogged wood (or intentionally as in the conservation of the Oseberg wood). Careful study of the mechanical properties of buried historical waterlogged wood indicated a broad reduction of its compression strength parallel to the grain, static bending and stiffness [65]. Strength losses are not directly proportional to mass losses but are affected by integrity disturbances of the remaining substance. An increase in the plasticity of deteriorated cell walls [66] has been suggested as a possible explanation for the high values of impact bending strength matched with low stiffness values [65]. The comparison of Oseberg alum-treated wood to crisp-bread, retaining approximately 2–5% of the bending strength and 6–8% of the modulus of elasticity of fresh wood is representative of the challenges conservators are faced with [67]. Life becomes a bit more challenging for those involved when the artefact is furthermore a structural member of a construction such as temples, bridges, roofs [68,69] or the mothership of conserved shipwrecks, the Vasa [70].

## 4. Burial Environment and Wood Deterioration

Extreme environments [71], favour wood preservation: the dry dessert [72], sea water [73], rivers [74] and lakes, peat bogs [75], the cool and dry conditions of permafrost [76,77], any anoxic environment [78].

Shrouded in an old romantic narrative, organic wood, as indeed all types of cultural material, does not really reach an equilibrium with the surrounding environment only to be disturbed upon discovery. Wood never stops interacting with the dynamic natural environment surrounding it either passively as a source of food for organisms or energetically by the exchange of material (sediment, water, organics and inorganics), or by energy itself (sun, wind, wave, tide, currents, storm), until it reaches final disintegration [79,80]. Conservation of cultural wood has benefited from work demystifying historical wood degradation by microorganisms from dry, wet and waterlogged environments, from researchers as Blanchette [81–85] and Björdal [86–89]. Eaton and Hale [90], as well as Zabel and Morell [91], give collective background knowledge on wood microbiology and decay also for the interest of wood conservators, as is the latest extensive contribution in bio-deterioration of wooden cultural heritage from both aquatic and terrestrial sites by the

conservator Pournou [92]. Below, emphasis is given to presenting wood from marine burial environments as these are usually out of sight and reach for most (probably also because of the author's bias). Although, there are no serious reasons forbidding extrapolating, to some extent, the approach in understanding the burial processes and their effects on cultural material, from the marine to the terrestrial environment.

Wooden shipwrecks on the ocean floor will first interact with it physically as would any newly introduced object to the underwater environment [93]. Over time, shipwrecks transform into fragments of the natural geological configuration and their physical effect is less significant [94]. Biochemical deterioration, however, does carry on. Even in the deep sea [78], wood will be used to its highest potential [95,96], as a whale carcass reaching the deep-sea bed [97]. Even so, the suggestion by Muckelroy that it is the composition of the seabed, rather than the depth at which a wreck lies, determines its preservation, does have basis [98]. Especially if preservation means 'existence' and not the degree of degradation, as archaeologists tend to believe. For wood that will quickly cave in on itself in a featureless bed of mud and hard clay, assisted by scouring and tides is better protected from biological and erosive actions than exposed parts. The Mary Rose ship in Portsmouth is a clear example of this. Like a clam missing one of its shells, her once-buried and so preserved half, stages today a unique glimpse into life on board a warship in the early-mid 16th century northern Europe.

By classifying marine environments based on characteristics of the biozone, as are types of seabed, seabed movement by waves and currents, levels of sunlight, water temperature and salinity fluctuations, it is easier to identify the physical, chemical, geological and biological characteristics of the environment surrounding and interacting with a site. A shipwreck lying in abyssal zones will be subjected to a different deteriorating environment compared to a wreck in the intertidal and neritic zones. Depth seems to inversely influence the variability of the deterioration of a wreck within the same zone across the geographical map, with that of the abyssal being the most constant (Figure 10) [99,100]. Although this can be challenged as new research from these remote waters is coming into light [101]. Jordan gives a thorough insight into the site characteristics affecting the survival of historical waterlogged wood [102]. Parameters such as water level, pH and evaluations of dissolved oxygen content, redox potential and concentrations of chemical elements of a site, are very useful when possible [103].

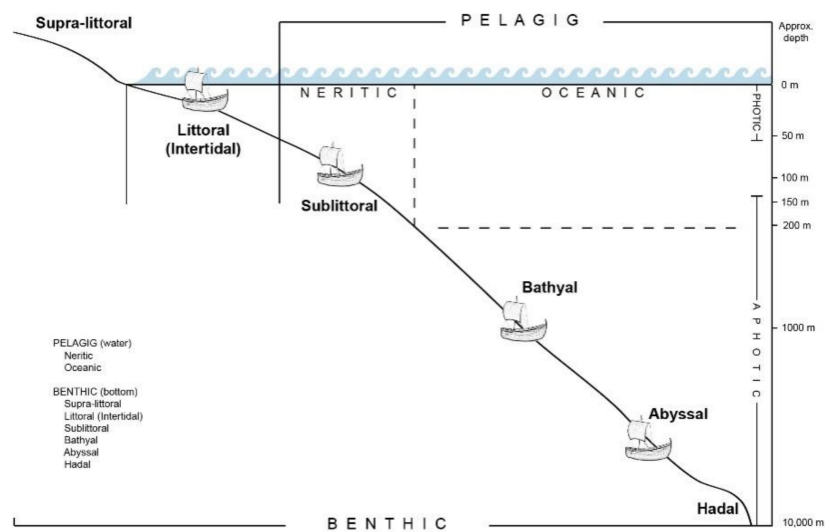


**Figure 10.** Classification of marine environments based on characteristics of the biozone [21] (after [99,100]). Artistic representation by A. Zisi of the Kyrenia, a 4th century BCE ancient Greek merchant ship.

The possibility of a ship's timbers being preserved and to what extent depends on the microenvironment or else the wood/marine environment interface, as this defines the speed of deterioration [89]. Two conditions play a chief role, the interface affiliation and the chemical environment [100]. Theoretically, the part of the wooden ship in contact with the sediment is preserved in good condition. It is favoured by fairly anoxic conditions promoted in close relation to sediment type and inclusions (e.g., organic matter poor), and environmental conditions. Analysis of the silt/clay sediment from around the Kolding cog shipwreck, Kolding Fjord, Denmark, for instance, showed that anoxic conditions were prevalent at a depth of only 6 mm below the sediment/water interface [104]. Jordan suggests that wood degradation from microbial activity is more likely related to the exposition of wood's end-grain surface rather than the depth of anoxia in the sediment [104].

In the clear blue waters of Lechaion, Greece, substantial amounts of wood remains from the infrastructure of the ancient harbour are still buried or exposed to the warm, saline and, in some cases, very shallow (50 cm deep) sea. Even with physical, chemical and micro-morphological analyses to define their preservation state under way, the main challenging factor for wood preservation, and indeed existence, is their 'natural' excavation, exposure and eventual perish. Lying in a dynamic underwater environment, their documentation is a brave against nature and time.

### 5. Assessing Degradation State

In 1970, Christensen, conservator at the National Museum of Denmark, wrote in his book [105] (p. 9): 'We cannot standardize the artifacts and other productions of our ancestors. [...] objects passing through the hands of conservators and restorers will go on being hopelessly heterogeneous, not only typologically but also as regards materials and condition'. Fifty-one years of wood conservation progress later, this learning is a fact describing the best part of wooden artefacts across conservation laboratories worldwide. Christensen's approach to making sense of the degradation state of cultural wood by training himself so as to anticipate results remains one of the greatly motivating written resources for those new to the field, both conservators and wood scientists. For the best way to manage expectations, whether conservation attempts or research on historical wood, dry or waterlogged, one has to put this truth wholeheartedly and design actions stemming from it.

In 1981, Hoffmann [106], a wood scientist, introduced for the first time in wood conservation, a number of chemical tests by the Technical Association of the Pulp and Paper Industry (TAPPI) in an effort to standardise, insofar as possible, the characterisation of cultural wood. His aim was to give confidence to wood conservation laboratories in choosing conservation treatments for their collections based on educated decisions beyond personal experience. Jagels et al. [66] and Schniewind and Kronkright [107], most wood scientists themselves, but also one conservator, extended the assessment by adding the evaluation of the residual mechanical strength for both waterlogged and dry wood, practices borrowed from forestry and wood science sectors.

Starting from what was known to approach the unknown, today a vast selection of methods exist or have been adopted for assessing the degradation state of historical wood [108–110]. This is a result of cultural conservators receiving exponentially more scientific education and training than four decades ago and because of 'rapid developments in new instrumentation technology, computer technology, physics and chemistry, and by easier access to large scale instrumental facilities' [111]. However, it is also a response to more material coming to light that needs special care, or new problems arising from past conservation treatments as there has been time for them to age; and it is well known that with age come problems. It is the nature of conservation of cultural heritage to rely on cross-disciplinary research in finding suitable solutions to today's challenges [112]. This 'increasingly evidence-based approach' [108], '[...] is easy to foresee that [...] will continue and accelerate even more' [111].

Away from the bright lights, the bench conservator may well still find herself or himself depending on poking a piece of art wood with a humble needle to assess the degradation state. Not only because there has to be training as well as a rationalization behind using novel methods, but also, because the advantages of development are not equally shared in all parts of the world. This is unfortunate considering that the need for preserving every culture is of equal significance. This imbalance needs our attention together with our appreciation (even among conservation colleagues), combined with the fact that, more often than not, preservation of tangible and intangible culture—the *raison d'être*—still relies on the intuition, experience, skills and responsibility of the conservator.

## 6. Conservation

‘A storyteller arrives, one hundred millions of years from now, to tell the tale of human species. It is an interval that will add a couple of per cent to the age of Earth and a little under one per cent to the age of the Universe.’ [113] (p. 7). ‘Contemporary society throws away infinitely more [...] if fossilized, might overwhelm the interpretive capacities of our far-future observers’ [113] (p. 170).

In a world full of inanimate objects, the antique meaning of the word ‘conservation’ has rather faded away, certainly in the Western world. Resources and labour producing things in the past were too valuable to cast away compared to the present day. As this author experienced at terrestrial excavations in Corinthia in Greece, when a *pithos*—a ceramic storing vessel with a diameter of more than a meter—was broken in the past, the breakage would have been repaired by drilling holes and mounting lead staples, thus, prolonging its service life. Yet, as Dooijes and Nieuwenhuys suggest, ‘extending the social life of the object’ seems additionally imprinted in ancient repairs [114]. The authors justly bring out the value of ancient repairs as fragments of the cultural biography of objects, since repairs reflect the perception and ideals of the time, even the ever-changing ones. Naturally, one cannot think through the minds of those people of the past, so as to claim they were thinking beyond their life span, millennia far into the future, to us, when doing so.

However, preserving the evidence of existence is a conscious act by the conservator of today. Conservators are here to assist, in hand with archaeologists and art historians, to not lose contact with past time; and they do it first and foremost for the people of the present. Our aim is not necessarily to force future generations to accept the values or use of heritage in the same way as past generations defined them and used them [115], but rather to allow the present generation to contemplate, question, feel, become inspired and participate in discussions, if not more. Nagmeldeen Morshed Hamza from the Conservation Center Giza in Egypt stated in his presentation during the last ICOM-CC Triennial Conference in Beijing (19 May 2021): ‘Conservation is not only treatment of objects, conservation is a successful communication of interdisciplinary collaboration to conduct a meaningful and successful conservation methodology’. Today, as never before, has conservation of cultural material brought together conservators, scientists and experts from various backgrounds from all over the world, to communicate and understand each other. Perhaps that is a value past generations unknowingly handed down to us through their creations. It is the tangible as well as the intangible fruits of this communication, together with conserved heritage, which we are passing on to generations yet to come for use as they seem fit.

More than 30 years ago, Peterson perceptually remarked that ‘artistic and social science definitions have a strong influence on conservation definitions’ [116]. He continues: ‘If we are to successfully encourage wood scientists to research areas that have application to conservation problems, scientists must be able to understand, if not appreciate, what constitutes both conservation problems and conservation solutions’. Success can be reached if conservators also make their way towards the middle ground by receiving more education on what wood and the science of wood are. Together with better dialog, ‘problems of communication between disciplines will be solved’ [116].

Indeed, through these past decades, far more conservators have added academic skills to their manual skills. An existing and continuously growing scientific literature of

cross-disciplinary research answering thousands of questions proves this. The disciplines of wood conservation and wood science (if not many other), and cultural heritage itself, have benefitted from significant findings and new knowledge, triggered by the challenge of dealing with wood as an artefact. This generates brilliance for future generations.

For those who have worked closely with historical finds, solutions do not always rely on numbers. Intriguingly, they rely on the experience and intuition acquired by practising conservation. Conservators are practical people ‘resourceful and good technologists’ [116]. They are capable of seeing the bigger picture and bridging the expectations with the reality called historical wood. Their inclusion in research projects from the very start will ensure work goes in the right direction. It is not that the efforts that do not involve conservators lack real science, but rather that the solutions offered may not become popular. At the same time, if conservators lose their manual skills and confidence, and are only focused on their academic side or other administrative work, they may not be able to offer instrumental insight to such endeavours [117].

## 7. Instead of Conclusions

This contribution has for the most part a Western-centred approach. Yet, conservation philosophy in the Far East, as in China and Japan, differentiates. There, it is a custom to replace deteriorated elements of, for example, wooden temples and lacquers, with new materials using the original recipes and techniques [118]. Methods and materials might be irreversible to the eye of the sometimes strongly ethical-oriented Western conservator, and difficult to use. However, the answer is that materials have been tested for so long and there is no concern as to the level of difficulty in applying them because with this philosophy it has been possible to preserve the skillset, tradition and culture uninterrupted for so long. As Jaeschke notes [118], ‘the historical significance lies in the construction of the monument and the restoration process itself’ and allows reuse.

In the aftermath of his translation of Tanizaki’s ‘*In Praise of Shadows*’ written in 1933, Harper notes that: ‘[ . . . ] for Tanizaki a museum piece is no cause for rejoicing. [ . . . ] art must live as a part of our daily lives or we had better give it up. We can admire it for what it once was, and try to understand what made it so [ . . . ] but to pretend that we can still participate in it is mere posturing’ [11] (p. 72).

**Funding:** This contribution was made possible with support from the Museum of Cultural History, University of Oslo, Norway.

**Data Availability Statement:** Contact author for data on Figure 9 or other mentioned in the manuscript which refer to her personal work.

**Acknowledgments:** The author wishes to first and foremost acknowledge the Museum of Cultural History, University of Oslo, Norway, for counting reflection as part of our daily working tasks, in addition to its generous financial support. Furthermore, identification by the author of woods from Ropotamo, Bulgaria was possible thanks to funding from Julia and Hans Rausing Foundation through the Expedition and Education Foundation (EEF), as part of the Black Sea Maritime Archaeology Project (Black Sea MAP). The anonymous reviewers are equally thanked for their useful comments on the manuscript. Lastly, the author wishes to express her warm gratitude to Sophia Palos for her instrumental editing of the manuscript. This work is dedicated to Maria Zisi.

**Conflicts of Interest:** The author declares no conflict of interest.

## References

1. Perlin, J. *A Forest Journey: The Role of Wood in the Development of Civilization*, 1st ed.; W. W. Norton & Company Inc.: New York, NY, USA, 1989; p. 445.
2. Momber, G.; Tomalin, D.; Scaife, R.; Satchell, J.; Gillespie, J. *Mesolithic Occupation at Bouldnor Cliff and the Submerged Prehistoric Landscapes of the Solent*; Council for British Archaeology: York, UK, 2011; p. 197.
3. Maragoudaki, E.; Kavvouras, P.K. Mycenaean shipwright took kit: Its reconstruction and evaluation. *Archaeol. Anthropol. Sci.* **2012**, *4*, 199–208. [CrossRef]
4. Brandon, C.J. Roman formwork used for underwater concrete construction. In *Building for Eternity: The History and Technology of Roman Concrete Engineering in the Sea*; Oleson, J.P., Ed.; Oxbow Books: Oxford, UK, 2014; pp. 189–222.

5. Humphrey, J.W.; Oleson, J.P.; Sherwood, A.N. *Greek and Roman Technology: A Sourcebook*; Routledge: Abingdon, UK, 1998; p. 623.
6. Zisi, A.; Athanasopoulos, P. *The Ancient Harbour of Lechaion: The Use of Wood in Harbour Construction During Late Antiquity*; Monographs of the Danish Institute at Athens: Athens, Greece; Volume I.1, in preparation.
7. Hughes, M.K.; Kuniholm, P.I.; Eischeid, J.K.; Garfin, G.; Griggs, C.B.; Latini, C. Aegean tree-ring signature years explained. *Tree Ring Res.* **2001**, *57*, 67–73.
8. Bonde, N.; Christensen, A.E. Dendrochronological dating of the Viking Age ship burials at Oseberg, Gokstad and Tune. *Antiquity* **1993**, *67*, 575–583. [CrossRef]
9. Sheppard, P.R. Dendroclimatology: Extracting climate from trees. *Wiley Interdiscip. Rev. Clim. Chang.* **2010**, *1*, 343–352. [CrossRef]
10. Büntgen, U.; Wacker, L.; Galván, J.D.; Arnold, S.; Arseneault, D.; Baillie, M.; Beer, J.; Bernabei, M.; Bleicher, N.; Boswijk, G.; et al. Tree rings reveal globally coherent signature of cosmogenic radiocarbon events in 774 and 993 CE. *Nat. Commun.* **2018**, *1*–7. [CrossRef]
11. Tanizaki, J. *In Praise of Shadows*; Vintage 2001: London, UK, 1977; p. 73.
12. Muñoz Viñas, S. Contemporary theory of conservation. *Stud. Conserv.* **2002**, *47*, 25–34. [CrossRef]
13. Hort, A. *Theophrastus: Enquiry into Plants, Book I–V*; Harvard University Press: Cambridge, MA, USA, 1916; p. 475.
14. Farjon, A. *A Natural History of Conifers*; Timber Press, Inc.: London, UK, 2008; p. 304.
15. Francis, J.E.; Ashworth, A.; Cantrill, D.J.; Crame, J.A.; Howe, J.; Stephens, R.; Tosolini, A.-M.; Thorn, V. 100 million years of Antarctic climate evolution: Evidence from fossil plants. In *Antarctica: A Keystone in a Changing World, Proceedings of the 10th International Symposium on Antarctic Earth Sciences, Santa Barbara, CA, USA, 26 August–1 September 2007*; Cooper, A.K., Barrett, P.J., Stagg, H., Storey, B., Stump, E., Wise, W., The 10th ISAES Editorial Team, Eds.; The National Academies Press: Washington, DC, USA, 2008; pp. 19–27. [CrossRef]
16. Bergman, R.; Cai, Z.; Carll, C.G.; Clausen, C.A.; Dietsberger, M.A.; Falk, R.H.; Frihart, C.R.; Glass, S.V.; Hunt, C.G.; Ibach, R.E.; et al. *Wood Handbook, Wood as an Engineering Material (All Chapters)*; General Technical Report FPL–GTR–190; Forest Products Laboratory United States Department of Agriculture Forest Service: Madison, WI, USA, 2010; p. 508.
17. McGrail, S. *Ancient Boats in North-West Europe: The Archaeology of Water Transport to AD 1500*; Routledge: Abingdon-on-Thames, UK, 1998; p. 354.
18. Peck, E.C. How wood shrinks and swells. *For. Prod. J.* **1957**, *7*, 235–244.
19. Morrell, J.J. *Wood Pole Maintenance Manual: 2012 Edition*; Forest Research Laboratory, Oregon State University: Corvallis, OR, USA, 2012; p. 56.
20. Papathoma, E.; Kavvouras, P.K.; Moraitou, G. Diagnostic study methodology applied on the wooden finds from Brauron—Towards the development of an informed conservation protocol. In Proceedings of the 12th ICOM-CC Working Group on Wet Organic Archaeological Materials, Istanbul, Turkey, 13–17 May 2013; Grant, T., Cook, C., Eds.; International Council of Museums, Committee for Conservation (ICOM-CC): Paris, France, 2016; pp. 77–84.
21. Zisi, A. Relationship between Wood Density and Ultrasound Propagation Velocity: A Non-Destructive Evaluation of Waterlogged Archaeological Wood State of Preservation Based on Its Underwater Acoustic Properties. Ph.D. Thesis, University of Southampton, Southampton, UK, October 2015.
22. Grattan, D.W.; McCawley, J.C.; Cook, C. The potential of the Canadian winter for the freeze-drying of degraded waterlogged wood: Part II. *Stud. Conserv.* **1980**, *25*, 118–136.
23. Horie, V. *Materials for Conservation: Organic Consolidants, Adhesives and Coatings*, 2nd ed.; Elsevier Ltd.: Oxford, UK, 2010; p. 504.
24. Zisi, A.; Dix, J.K. Simulating mass loss of decaying waterlogged wood: A technique for studying ultrasound propagation velocity in waterlogged archaeological wood. *J. Cult. Herit.* **2018**, *33*, 39–47. [CrossRef]
25. Smith, D.M. *Maximum Moisture Content Method for Determining Specific Gravity of Small Wood Samples*; Forest Products Laboratory, United States Department of Agriculture Forest Service: Madison, WI, USA; University of Wisconsin: Madison, WI, USA, 1954; p. 9.
26. Matsumura, J.; Booker, R.E.; Ridoutt, B.G.; Donaldson, L.A.; Mikajiri, N.; Matsunaga, H.; Oda, K. Impregnation of radiata pine wood by vacuum treatment II: Effect of pre-steaming on wood structure and resin content. *J. Wood Sci.* **1999**, *45*, 456–462. [CrossRef]
27. Feeney, F.E.; Chivers, R.C.; Evertsen, J.A.; Keating, J. The influence of inhomogeneity on the propagation of ultrasound in wood. *Ultrasonics* **1998**, *36*, 449–453. [CrossRef]
28. Tsoumis, G. *Wood as Raw Material: Source, Structure, Chemical Composition, Growth, Degradation and Identification*, 1st ed.; Pergamon Press Inc.: Oxford, UK, 1968; p. 276.
29. Wheeler, E.A.; Baas, P.; Gasson, P.E.; IAWA Committee (Eds.) IAWA list of microscopic features for hardwood identification. *IAWA J.* **1989**, *10*, 219–332.
30. Richter, H.G.; Grosser, D.; Heinz, I.; Gasson, P.E.; IAWA Committee (Eds.) IAWA list of microscopic features for softwood identification. *IAWA J.* **2004**, *25*, 1–70. [CrossRef]
31. Siau, J.F. *Transport Processes in Wood*; Springer: Berlin/Heidelberg, Germany; New York, NY, USA, 1984; p. 254. [CrossRef]
32. Côte, W.A. Structural factors affecting the permeability of wood. *J. Polym. Sci. Part. C Polym. Symp.* **1963**, *2*, 231–242. [CrossRef]
33. Zisi, A. *Silanol-Based Consolidant for Retreating Oseberg Wood: Adjusting a Method Initially Developed for Conserving Waterlogged Archaeological Wood. Saving Oseberg Phase II. Internal Report*; University of Oslo, Museum of Cultural History: Oslo, Norway, 2020; p. 137.

34. Peev, P.; Farr, R.H.; Slavchev, V.; Grant, M.J.; Adams, J.; Bailey, G. Bulgaria: Sea-level change and submerged settlements on the Black Sea. In *The Archaeology of Europe's Drowned Landscapes*; Coastal Research Library; Bailey, G., Galanidou, N., Peeters, H., Jöns, H., Mennenga, M., Eds.; Springer: Cham, Switzerland, 2020; Volume 35, pp. 393–412. [CrossRef]
35. Macchioni, N.; Capretti, C.; Sozzi, L.; Pizzo, B. Grading the decay of waterlogged archaeological wood according to anatomical characterisation. The case of the Fiauvé site (N-E Italy). *Int. Biodeterior. Biodegrad.* **2013**, *84*, 54–64. [CrossRef]
36. Klaassen, R.K.W.M. Bacterial decay in wooden foundation piles—Patterns and causes: A study of historical pile foundations in the Netherlands. *Int. Biodeterior. Biodegrad.* **2008**, *61*, 45–60. [CrossRef]
37. Barbour, R.J. The condition and dimensional stabilization of highly deteriorated waterlogged hardwoods. In *Waterlogged Wood: Study and Conservation, Proceedings of the 2nd ICOM-CC Working Group on Wet Organic Archaeological Materials Conference, Grenoble, France, 28–31 August 1984*; Ramier, R., Colardelle, M., Eds.; CETBGE: Grenoble, France, 1984; pp. 23–37.
38. Macchioni, N. Physical characteristics of the wood from the excavations of the ancient port of Pisa. *J. Cult. Herit.* **2003**, *4*, 85–89. [CrossRef]
39. Jensen, P.; Gregory, D.J. Selected physical parameters to characterize the state of preservation of waterlogged archaeological wood: A practical guide for their determination. *J. Archaeol. Sci.* **2006**, *33*, 551–559. [CrossRef]
40. Kavvouras, P.K.; Fotopoulou, M. A note on a simple device for measuring wooden artefact volume. *Stud. Conserv.* **2006**, *51*, 291–296. [CrossRef]
41. Zisi, A.; Steindal, C.; Andriulo, F.; Vespignani, L.; Braovac, S. *A Comparative Study of Non-Aqueous Consolidants Using Modern and Archaeological Wood Test Specimens. Saving Oseberg Phase II. Internal Report*; University of Oslo, Museum of Cultural History: Oslo, Norway, 2021; p. 124.
42. Fengel, D. Aging and fossilization of wood and its components. *Wood Sci. Technol.* **1991**, *25*, 153–177. [CrossRef]
43. Rowell, R.M. Chemical modification of cell wall polymers as potential treatments of archaeological wood. In *Archaeological Wood: Properties, Chemistry, and Preservation*; Rowell, R.M., Barbour, R.J., Eds.; American Chemical Society: Washington, DC, USA, 1990; pp. 421–431.
44. Goodburn, D.M.; Thomas, C. Reused medieval ship planks from Westminster, England, possibly derived from a vessel built in the cog style. *Int. J. Naut. Archaeol.* **1997**, *26*, 26–38. [CrossRef]
45. Rowell, R.; Youngs, R. *Dimensional Stabilization of Wood in Use*; Forest Products Laboratory, United States Department of Agriculture Forest Service: Madison, WI, USA; University of Wisconsin: Madison, WI, USA, 1981; p. 10.
46. Bossu, J.; Beauchêne, J.; Estevez, Y.; Duplais, C.; Clair, B. New insights on wood dimensional stability influenced by secondary metabolites: The case of a fast-growing tropical species *Bagassa guianensis* Aubl. *PLoS ONE* **2016**, *11*, 1–17. [CrossRef] [PubMed]
47. Johns, D.A. Observations resulting from the treatment of waterlogged wood bowls in Aotearoa (New Zealand). In *Hidden Dimensions: The Cultural Significance of Wetland Archaeology*; Bernick, K., Ed.; UBC Press: Vancouver, BC, Canada, 1998; pp. 319–328.
48. Kavvouras, P.K.; Kostarelou, C.; Zisi, A.; Petrou, M.; Moraitou, G. Use of silanol-terminated polydimethylsiloxane in the conservation of waterlogged archaeological wood. *Stud. Conserv.* **2009**, *54*, 65–76. [CrossRef]
49. Kavvouras, P.K. *Οργάνικά Υλικά II, Συντήρηση Αρχαιολογικού Ξύλου: Εργαστηριακές σημειώσεις*; University of West Attica: Athens, Greece, 2002; p. 145.
50. Stamm, A.J.; Loughborough, W.K. Variation in shrinking and swelling of wood. *Trans. Amer. Soc. Mech. Eng.* **1942**, *64*, 379–386.
51. Mantanis, G.I.; Young, R.A.; Rowell, R.M. Swelling of wood: Part 1. Swelling in water. *Wood Sci. Technol.* **1994**, *28*, 119–134. [CrossRef]
52. Pettersen, R.C. The chemical composition of wood. In *The Chemistry of Solid Wood*; Advances in Chemistry Series 207; Rowell, R.M., Ed.; American Chemical Society: Washington, DC, USA, 1984; pp. 57–126.
53. Madsen, B.; Gamstedt, E.K. Wood versus plant fibers: Similarities and differences in composite applications. *Adv. Mater. Sci. Eng.* **2013**, 1–14. [CrossRef]
54. Han, J.S. Properties of nonwood fibers. In Proceedings of the Korean Society of Wood Science and Technology Annual Meeting, Seoul, Korea, 24–25 April 1998; pp. 3–12.
55. Salmén, L.; Bergström, E. Cellulose structural arrangement in relation to spectral changes in tensile loading FTIR. *Cellulose* **2009**, *16*, 975–982. [CrossRef]
56. Salmén, L. Wood cell wall structure and organisation in relation to mechanics. In *Plant Biomechanics: From Structure to Function at Multiple Scales*, 1st ed.; Geitmann, A., Gril, J., Eds.; Springer: Cham, Switzerland, 2018; pp. 3–19. [CrossRef]
57. Matthews, J.F.; Skopec, C.E.; Mason, P.E.; Zuccato, P.; Torget, R.W.; Sugiyama, J.; Himmel, M.E.; Brady, J.W. Computer simulation studies of microcrystalline cellulose I $\beta$ . *Carbohydr. Res.* **2006**, *341*, 138–152. [CrossRef]
58. Zhao, C.; Zhang, X.; Liu, L.; Yu, Y.; Zheng, W.; Song, P. Probing chemical changes in holocellulose and lignin of timbers in ancient buildings. *Polymers* **2019**, *11*, 809. [CrossRef] [PubMed]
59. Hedges, J.L.; Cowie, G.L.; Ertel, J.R.; Barbour, R.J.; Hatcher, P.G. Degradation of carbohydrates and lignins in buried woods. *Geochim. Cosmochim. Acta* **1985**, *49*, 701–711. [CrossRef]
60. Obst, J.R.; McMillan, N.J.; Blanchette, R.A.; Christensen, D.J.; Faix, O.; Han, J.S.; Kuster, T.A.; Landucci, L.L.; Newman, R.H.; Pettersen, R.C.; et al. Characterization of Canadian Arctic fossil woods. In *Tertiary Fossil Forests of the Geodetic Hills, Axel Heiberg Island, Arctic Archipelago*; Christie, R.L., McMillan, N.J., Eds.; Geological Survey of Canada: Ottawa, ON, USA, 1991; pp. 123–146.
61. Braovac, S.; McQueen, C.M.A.; Sahlstedt, M.; Kutzke, H.; Łucejko, J.J.; Klokkernes, T. Navigating conservation strategies: Linking material research on alum-treated wood from the Oseberg collection to conservation decisions. *Herit. Sci.* **2018**, *6*, 1–16. [CrossRef]

62. Braovac, S.; Tamburini, D.; Łucejko, J.J.; McQueen, C.M.A.; Kutzke, H.; Colombini, M.P. Chemical analyses of extremely degraded wood using analytical pyrolysis and inductively coupled plasma atomic emission spectroscopy. *Microchem. J.* **2016**, *124*, 368–379. [CrossRef]
63. Chrysostomou, P.; Jagoulis, P.; Mäder, A. The “Culture of Four Lakes”: Prehistoric lakeside settlements (6th–2nd mill. BC) in the Amindeon Basin, Western Macedonia, Greece. *Archäol. Schweiz* **2015**, *24*–32. [CrossRef]
64. Florian, M.L.E. Scope and history of archaeological wood. In *Archaeological Wood: Properties, Chemistry, and Preservation*; Rowell, R.M., Barbour, R.J., Eds.; American Chemical Society: Washington, DC, USA, 1990; pp. 3–32.
65. Schniewind, A.P. Physical and mechanical properties of archaeological wood. In *Archaeological Wood: Properties, Chemistry, and Preservation*; Rowell, R.M., Barbour, R.J., Eds.; American Chemical Society: Washington, DC, USA, 1990; pp. 87–109.
66. Jagels, R.; Seifert, B.; Shottafter, J.E.; Wolfhagen, J.L.; Carlise, J.D. Analysis of wet-site archaeological wood samples. *For. Prod. J.* **1988**, *38*, 33–38.
67. Hoffmann, P.; Schwab, E.; Bonde, H. *Report on Strength Tests Performed on Wood Samples from the Gokstad Ship and Boats, and from the Oseberg Finds Complex, and Some Observations on Strakes from the Gokstad, Oseberg, and Tune Ships*; Bøe, A., Ed.; Vikingskips Seminaret, University of Oslo: Oslo, Norway, 2002; pp. 60–74.
68. Lüke, M.; Unger, W.; Nellessen, D. An historical roof timber system in the Old Town of Berlin-Spandau. In Proceedings of the International Research Group on Wood Protection, IRG50 Scientific Conference on Wood Protection, Quebec, QC, Canada, 12–16 May 2018; pp. 2–5.
69. Hudson-McAulay, K.J. The Structural and Mechanical Integrity of Historic Wood. Ph.D. Thesis, University of Glasgow, Glasgow, UK, August 2016.
70. Afshar, R.; Alavyoon, N.; Ahlgren, A.; Gamstedt, E. Full scale finite element modelling and analysis of the 17th-century warship Vasa: A methodological approach and preliminary results. *Eng. Struct.* **2021**, *231*, 1–16. [CrossRef]
71. Rothschild, L.J.; Mancinelli, R.L. Life in extreme environments. *Nature* **2001**, *409*, 1092–1101. [CrossRef]
72. Ward, C.; Zazzaro, C. Evidence for pharaonic seagoing ships at Mersa/Wadi Gawasis, Egypt. *Int. J. Naut. Archaeol.* **2010**, *39*, 1–17. [CrossRef]
73. Demesticha, S.; Skarlatos, D.; Neophytou, A. The 4th-century B.C. shipwreck at Mazotos, Cyprus: New techniques and methodologies in the 3D mapping of shipwreck excavations. *J. Field Archaeol.* **2014**, *39*, 134–150. [CrossRef]
74. Plets, R.; Dix, J.K.; Adams, J.R.; Bull, J.R.; Henstock, T.J.; Gutowski, M.; Best, A.I. The use of high-resolution 3D Chirp sub-bottom profiler for the reconstruction of the shallow water archaeological site of the Grace Dieu (1439), River Hamble, UK. *J. Archaeol. Sci.* **2009**, *36*, 408–418. [CrossRef]
75. Koksharov, S.F. A new subject in the study of the Great Idol. *Q. Int.* **2021**, *573*, 30–37. [CrossRef]
76. Peakcock, E.E.; Callanan, M. The challenge of developing sustainable heritage management and preservation strategies for perennial snow patch artefacts. Contributions of the SPARC Project. In Proceedings of the 13th ICOM-CC Working Group on Wet Organic Archaeological Materials, Florence, Italy, 16–21 May 2016; Williams, E., Hocker, E., Eds.; ICOM Committee for Conservation: Paris, France, 2018; pp. 22–26.
77. Matthiesen, H.; Jensen, J.B.; Gregory, D.; Hollesen, J.; Elberling, B. Degradation of archaeological wood under freezing and thawing conditions—Effects of permafrost and climate change. *Archaeometry* **2014**, *56*, 479–495. [CrossRef]
78. Pacheco-Ruiz, R.; Adams, J.; Pedrotti, F.; Grant, M.; Holmlund, J.; Bailey, C. Deep sea archaeological survey in the Black Sea—Robotic documentation of 2500 years of human seafaring. *Deep Sea Res. Part I Oceanogr. Res. Pap.* **2019**, *152*, 1–16.
79. Gregory, D. Experiments into the deterioration characteristics of materials on the Duart Point wreck-site: An interim report. *Int. J. Naut. Archaeol.* **1995**, *24*, 61–65. [CrossRef]
80. Quinn, R. The role of scour in shipwreck site formation processes and the preservation of wreck-associated scour signatures in the sedimentary—Evidence from seabed and sub-surface data. *J. Archaeol. Sci.* **2006**, *33*, 1419–1432. [CrossRef]
81. Blanchette, R.A.; Held, B.W.; Jurgens, J.; Stear, A.; Dupont, C. Fungi attacking historic wood of Fort Conger and the Peary Huts in the High Arctic. *PLoS ONE* **2021**, *16*, 1–16. [CrossRef]
82. Blanchette, R.A. A review of microbial deterioration found in archaeological wood from different environments. *Int. Biodeterior. Biodegrad.* **2000**, *46*, 189–204. [CrossRef]
83. Blanchette, R.A.; Haight, J.E.; Koestler, R.J.; Hatchfield, P.B.; Arnold, D. Assessment of deterioration in archaeological wood from Ancient Egypt. *J. Am. Inst. Conserv.* **1994**, *33*, 55–70. [CrossRef]
84. Blanchette, R.A.; Cease, K.R.; Abad, A.R.; Koestler, R.J.; Simpson, E.; Sams, G.K. An evaluation of different forms of deterioration found in archaeological wood. *Int. Biodeterior. Biodegrad.* **1991**, *28*, 3–22. [CrossRef]
85. Blanchette, R.A.; Nilsson, T.; Daniel, G.; Abad, A. Biological degradation of wood. In *Archaeological Wood: Properties, Chemistry, and Preservation*; Rowell, R.M., Barbour, R.J., Eds.; American Chemical Society: Washington, DC, USA, 1990; pp. 141–174.
86. Björdal, C.G. Submerged archaeological wooden structures. In *Biodeterioration and Preservation in Art, Archaeology and Architecture*; Mitchell, R., Clifford, J., Eds.; Archetype Publications Ltd.: London, UK, 2018; pp. 153–166.
87. Björdal, C.G. Microbial degradation of waterlogged archaeological wood. *J. Cult. Herit.* **2012**, *13S*, S118–S122. [CrossRef]
88. Björdal, C.G. Evaluation of microbial degradation of shipwrecks in the Baltic Sea. *Int. Biodeterior. Biodegrad.* **2012**, *70*, 126–140. [CrossRef]
89. Björdal, C.G.; Nilsson, T. Observation on microbial growth during conservation treatment of waterlogged archaeological wood. *Stud. Conserv.* **2001**, *46*, 211–220.



90. Eaton, R.A.; Hale, M.D.C. *Wood: Decay, Pests, and Protection*, 1st ed.; Chapman & Hall: London, UK, 1993; p. 546.
91. Zabel, R.A.; Morrell, J.J. *Wood Microbiology: Decay and Its Preservation*, 2nd ed.; Academic Press: London UK, 2020; p. 576.
92. Pournou, A. *Biodeterioration of Wooden Cultural Heritage: Organisms and Decay Mechanisms in Aquatic and Terrestrial Ecosystems*; Springer Nature: Cham, Switzerland, 2020; p. 538.
93. Keith, M. (Ed.) *Site Formation Processes of Submerged Shipwrecks*; University Press of Florida: Gainesville, FL, USA, 2016; p. 304. [CrossRef]
94. Ferrari, B.; Adams, J. Biogenic modifications of marine sediments and their influence on archaeological material. *Int. J. Naut. Archaeol.* **1990**, *19*, 139–151. [CrossRef]
95. Bienhold, C.; Ristova, P.P.; Wenzhöfer, F.; Dittmar, T.; Boetius, A. How deep-sea wood falls sustain chemosynthetic life. *PLoS ONE* **2013**, *8*, 1–17. [CrossRef]
96. Frizzell, T.J. In-Situ Preservation of Deep-Sea Shipwrecks: Understanding Biological Interactions and Environmental Impacts. Master's Thesis, Texas A&M University, College Station, TX, USA, May 2020.
97. Amon, D.J.; Glover, A.G.; Wiklund, H.; Marsh, L.; Linse, K.; Rogers, A.D.; Copley, J.T. The discovery of a natural whale fall in the Antarctic deep sea. *Deep Sea Res. Part. II Top. Stud. Oceanogr.* **2013**, *92*, 87–96. [CrossRef]
98. Van Doorninck, F.H. Maritime archaeology by Keith Muckelroy, Review by: Frederick, H. van Doorninck, Jr. *Am. Antiq.* **1981**, *46*, 226–228.
99. Hedgpeth, J.W. Classification of marine environments. In *Treatise on Marine Ecology and Paleontology*; Geological Society of America: Boulder, CO, USA, 1957; pp. 17–28.
100. Florian, M.-L.E. The underwater environment. In *Conservation of Marine Archaeological Objects*, 1st ed.; Pearson, C., Ed.; Butterworth & Co. Ltd.: London, UK, 1987; pp. 1–20.
101. Zeppilli, D.; Leduc, D.; Fontanier, C.; Fontanero, D.; Fuchs, S.; Gooday, A.J.; Goineau, A.; Ingels, J.; Ivanenko, V.N.; Kristensen, R.M.; et al. Characteristics of meiofauna in extreme marine ecosystems: A review. *Mar. Biodiv.* **2018**, *48*, 35–71. [CrossRef]
102. Jordan, B.A. Site characteristics impacting historic waterlogged wood: A review. *Int. Biodeterior. Biodegrad.* **2001**, *47*, 47–54. [CrossRef]
103. Gregory, D.J.; Jensen, P. The importance of analysing waterlogged wooden artefacts and the environmental conditions when considering their in situ preservation. *J. Wetl. Archaeol.* **2006**, *6*, 65–81. [CrossRef]
104. Jordan, B.A. Analysis of Environmental Conditions and Types of Biodeterioration Affecting the Preservation of Archaeological Wood and the Kolding Shipwreck Site. Ph.D. Thesis, University of Minnesota, Minneapolis, MN, USA, April 2003.
105. Christensen, B.B. *The Conservation of Waterlogged Wood in the National Museum of Denmark*; National Museum of Denmark: Copenhagen, Denmark, 1970; p. 118.
106. Hoffmann, P. Chemical wood analysis as a means of characterising archaeological wood. In Proceedings of the ICOM Waterlogged Wood Working Group Conference, Ottawa, ON, Canada, 15–18 September 1981; Grattan, E.D.W., Ed.; ICOM Waterlogged Wood Working Group: Ottawa, ON, Canada, 1981; pp. 78–83.
107. Schniewind, A.P.; Kronkright, D.P. Strength evaluation of deteriorated wood treated with consolidants. In *Adhesives and Consolidants, Proceedings of the Preprints of the Contributions to the IIC Paris Congress, Paris, France, 2–8 September 1984*; Brommelle, N.S., Ed.; International Institute for Conservation: London, UK, 1984; pp. 146–150.
108. High, K.E.; Penkman, K.E.H. A review of analytical methods for assessing preservation in waterlogged archaeological wood and their application in practice. *Herit. Sci.* **2020**, *8*, 1–33. [CrossRef]
109. Niemz, P.; Mannes, D. Non-destructive testing of wood and wood-based materials. *J. Cult. Herit.* **2012**, *13*, S26–S34. [CrossRef]
110. Antonelli, F.; Esposito, A.; Galotta, G.; Petriaggi, B.D.; Piazza, S.; Romagnoli, M.; Guerrieri, F. Microbiota in waterlogged archaeological wood: Use of next-generation sequencing to evaluate the risk of biodegradation. *Appl. Sci.* **2020**, *10*, 4636. [CrossRef]
111. Elding, L.I. Science for conservation of the cultural heritage. In *The Safeguard of Cultural Heritage—A Challenge from the Past for the Europe of Tomorrow, Proceedings of the COST Strategic Workshop—Safeguard of the Cultural Heritage, Florence, Italy, 11–13 July 2011*; Fioravanti, M., Mecca, S., Eds.; Firenze University Press: Florence, Italy, 2011; pp. 129–134.
112. Braovac, S. Practical experiences with cross-disciplinary research—The case of Saving Oseberg. *Primit. Tider* **2019**, *21*, 143–148. [CrossRef]
113. Zalasiewicz, J. *The Earth After Us. What Legacy Will Humans Leave in the Rocks?* Oxford University Press: New York, NY, USA, 2008; p. 251.
114. Dooijes, R.; Nieuwenhuys, O.P. Ancient repairs: Techniques and social meaning. In *Konservieren Oder Restaurieren, Die Restaurierung Griechischer Vasen von der Antike bis Heute*; Bentz, M., Kästner, U., Eds.; Verlag, C.H. Beck: Munich, Germany, 2007; pp. 17–22.
115. Lelyveld, M.; Taylor, J. What do we talk about when we talk about 'future generations'? In *Transcending Boundaries: Integrated Approaches to Conservation, Proceedings of the ICOM-CC 19th Triennial Conference Preprints, Beijing, China, 17–21 May 2021*; Bridgland, J., Ed.; International Council of Museums: Paris, France, 2021; pp. 1–10.
116. Peterson, C.E. New directions in the conservation of archaeological wood. In *Archaeological Wood: Properties, Chemistry, and Preservation*; Rowell, R.M., Barbour, R.J., Eds.; American Chemical Society: Washington, DC, USA, 1990; pp. 433–449.

117. Ashley-Smith, J. The ethics of doing nothing. *J. Inst. Conserv.* **2018**, *41*, 6–15. [CrossRef]
118. Jaeschke, R.L. When does history end? In *Archaeological Conservation and Its Consequences, Proceedings of the Preprints of the Contributions to the Copenhagen Congress, Copenhagen, Denmark, 26–30 August 1996*; Roy, A., Smith, P., Eds.; The International Institute for Conservation of Historic and Artistic Works: London, UK, 1996; pp. 86–88.



Review

# Conservation of Waterlogged Wood—Past, Present and Future Perspectives

Magdalena Broda <sup>1,2,\*</sup>  and Callum A. S. Hill <sup>3,4</sup> 

<sup>1</sup> Department of Wood Science and Thermal Techniques, Faculty of Forestry and Wood Technology, Poznań University of Life Sciences, Wojska Polskiego 38/42, 60-637 Poznań, Poland

<sup>2</sup> The BioComposites Centre, Bangor University, Deiniol Road, Bangor LL57 2UW, UK

<sup>3</sup> JCH Industrial Ecology Ltd., Bangor LL57 1LJ, UK; enquiries@jchindustrial.co.uk

<sup>4</sup> Norwegian Institute of Bioeconomy Research (NIBIO), P.O. Box 115, Postboks 115, NO-1431 Ås, Norway

\* Correspondence: magdalena.broda@up.poznan.pl

**Abstract:** This paper reviews the degradation, preservation and conservation of waterlogged archaeological wood. Degradation due to bacteria in anoxic and soft-rot fungi and bacteria in oxic waterlogged conditions is discussed with consideration of the effect on the chemical composition of wood, as well as the deposition of sulphur and iron within the structure. The effects on physical properties are also considered. The paper then discusses the role of consolidants in preserving waterlogged archaeological wood after it is excavated as well as issues to be considered when reburial is used as a means of preservation. The use of alum and polyethylene glycol (PEG) as consolidants is presented along with various case studies with particular emphasis on marine artefacts. The properties of consolidated wood are examined, especially with respect to the degradation of the wood post-conservation. Different consolidants are reviewed along with their use and properties. The merits and risks of reburial and in situ preservation are considered as an alternative to conservation.

**Keywords:** waterlogged wood; consolidation; archaeological wood; sorption; degradation; drying; wood conservation; PEG; alum; reburial; in situ preservation



**Citation:** Broda, M.; Hill, C.A.S. Conservation of Waterlogged Wood—Past, Present and Future Perspectives. *Forests* **2021**, *12*, 1193. <https://doi.org/10.3390/f12091193>

Academic Editor: Miha Humar

Received: 5 July 2021

Accepted: 27 August 2021

Published: 2 September 2021

**Publisher's Note:** MDPI stays neutral with regard to jurisdictional claims in published maps and institutional affiliations.



**Copyright:** © 2021 by the authors. Licensee MDPI, Basel, Switzerland. This article is an open access article distributed under the terms and conditions of the Creative Commons Attribution (CC BY) license (<https://creativecommons.org/licenses/by/4.0/>).

## 1. Introduction

Archaeological wood is defined as old wood that shows evidence of having been worked by humans, while “waterlogged” means that all the pore spaces, including capillaries and microcapillaries, are entirely filled with water [1,2].

Wood is an important material that has been used for shelter, tools and weapons since the time of the earliest hominids. It is a composite material with a hierarchical structure that is primarily composed of three polymers: cellulose, hemicellulose and lignin. When a tree dies, the wood decays under conditions where there is sufficient water and oxygen to allow decay organisms to metabolise the chemical constituents, but in the absence of either component in the environment, fungal decay does not occur. In arid conditions, wooden objects from ancient Egypt have been preserved for 5000 years, and under waterlogged conditions, where there is limited oxygen access, it is possible that wood can survive for a considerable period of time. The Shigir Idol, which was discovered in a peat bog in the Sverdlovsk region of the Urals, has been dated to the late Younger Dryas, about 12,000 years ago [3], although this age is insignificant compared with the Schöningen spears, which are over 300,000 years old [4]. Whereas no wood was recovered from the Sutton Hoo ship burial, which was located in sandy soil with good air permeability, wooden objects from the Oseberg and Gokstad ship burials, located in waterlogged environments, were extremely well preserved [5,6].

Although the appearance and structure of waterlogged wooden artefacts may be preserved, the wood is still degraded. Water-logging and anoxic conditions prevent fungal metabolism, but bacterial attack and chemical degradation can still occur, leading to a

loss of strength and structural integrity of the object. As a consequence, it is necessary to undertake some sort of conservation measures to preserve the wood, to prevent collapse during drying and maintain some mechanical strength, but many of these consolidation methods have subsequently resulted in problems that were not foreseen. In the past, alum was used as a consolidant, but there are now problems of extreme degradation of the wood. Polyethylene glycol (PEG) has often been used as the consolidant of choice because it is relatively inexpensive, stable and reversible. However, it produces objects that are heavy, with a dark and waxy appearance and is corrosive to metal [7].

The 1992 Valletta Treaty obliges signatory countries to protect their buried archaeological heritage, in situ, if possible. Where this is not possible, rescue excavation has to be undertaken with the remains protected from degradation. When archaeologically important sites are discovered, it is important to know whether the sites have favourable or unfavourable conditions for the preservation of remains. Based on this knowledge, it is then possible to determine the best strategy for the preservation of the artefacts. Although site reburial is one strategy for the preservation of archaeological remains, this can involve risks because the waterlogged conditions that resulted in the original preservation of the wood may not continue into the future [8–10]. Defining the characteristics of burial sites and their suitability for the ongoing preservation of their remains is a problem [11]. The most common parameters used to characterise sites are pH, redox potential (Eh), dissolved oxygen content, and the presence of ions, such as ammonium and nitrate. Depending on the dissolved oxygen content, the sites can be classified as anoxic, suboxic, dysoxic, or oxic. It is reported that oxygen levels of less than  $0.3 \text{ mL L}^{-1}$  prevent fungal growth, and environments are often characterised as being oxic or anoxic based upon the presence or absence of soft-rot fungi [8].

Consolidants for protecting waterlogged archaeological wood are available, but they all have disadvantages; is there one available that has optimal properties, or is more research needed to find the perfect material? Conservation agents for waterlogged wood should primarily provide integrity and dimensional stabilisation upon drying. They should also prevent further dimensional changes of the object, maintain, or improve its mechanical strength, and protect it against biotic and abiotic degradation. Conservation agents should be chemically stable, resistant to ageing/weathering, compatible with wood structure, and preferably bio-friendly and cost-efficient. Conservation ethics also impose the desirability to allow for the reversibility of the applied treatment or the possibility of further re-conservation using different agents. Due to the nature of conservation work: preserving the dimensions and appearance of ancient artefacts and making their history accessible to the public, treatments must be “gentle” in order to inflict as little damage as possible to the objects themselves. This often means long timescales and processes governed, for example, by diffusion of chemical treatments into artefacts lasting for periods of up to a year for immersion of smaller objects in tanks or, as for the Mary Rose, a spraying programme lasting over twenty years [12].

## 2. Degradation of Waterlogged Wood

Several different abiotic and biotic factors, including UV radiation, temperature and humidity changes, wind, precipitation, fungi, bacteria and insects, affect wood in the natural surroundings causing its degradation. Despite the multiple causes of wood degradation, the main decay mechanisms are similar at a molecular level. They involve hydrolysis of acetal linkages in polysaccharides (cellulose and hemicelluloses) and various redox and radical reactions of carbon, ester and ether linkages in the aromatic structure of lignin. However, in waterlogged environments, the range of the degrading factors is highly restricted, which significantly slows the decay rate, thus allowing the wood to survive even hundreds and thousands of years.

### 2.1. Microbiological Attack

Waterlogged wooden artefacts are generally discovered buried in bottom sediments of water reservoirs, wet soil or peatlands. All these environments offer highly reduced oxygen conditions, insufficient for typical terrestrial wood degraders such as brown rot and white-rot fungi. Therefore, they enable the growth of a restricted range of microorganisms. In anoxic or nearly anoxic waterlogged conditions, biodeterioration of the wood is mainly bacterial, while more oxygenated environments additionally facilitate decay caused by soft-rot fungi [2,13–15].

Wood-degrading bacteria are categorised into erosion, tunnelling and cavitation bacteria, based on the micromorphological degradation pattern they produce (the bacterial types do not represent any form of taxonomic classification) [16–18]. The most common form of microbiological attack in anaerobic or nearly anaerobic waterlogged environments is by erosion bacteria (EB). Erosion bacteria are spherical or rod-shaped Gram-negative cells that lack flagella. They are associated with a thick, polysaccharide-derived, slime layer and are motile via gliding [18–21]. The colonisation of wood by EB takes place from the surface, with invasion occurring via rays and pits and through the cell lumina. There is also degradation of the margo of the pits of the cell walls, leading to an increase in permeability of the wood [22]. The EB start attacking from the cell lumen, align themselves with the microfibrils and begin digesting cellulose and hemicelluloses from the cell wall starting at the S3 layer, leaving characteristic grooves. Attack proceeds through the cellulose-rich S2 and then the S1 layer towards the middle lamella. It is accompanied by the production of amorphous mucilage, which can be further colonised by different types of scavenging bacteria [20,21,23]. Even at advanced stages of decay, when the secondary wall layers are entirely decomposed, the lignin-rich middle lamella appears to be unaffected (only some minor modifications in lignin occur [24]). The remaining porous waterlogged lignin-rich material can still support itself and exhibit traces of its original manufacture. However, it may be very soft and easily deformed and will collapse upon drying. Because the bacterial attack is associated with the polysaccharide content only, changes in mechanical properties can be correlated with the relative lignin content of the wood [20,21,23,25].

Erosion bacteria can tolerate both low-oxygen and near-anoxic conditions; therefore, they can even decompose wooden artefacts that are buried deep in sediments; however, the decay is more intense when more oxygen is available [21,26]. They are slow degraders, and even after years of burial, they can still be actively degrading the wood [27]. A characteristic feature of bacterial attack is the lack of homogeneity, with heavily degraded regions of wood surrounded by regions that are unaffected [28], as well as variation in the extent of degradation of the different cell wall layers (Figures 1 and 2) [29]. The outer regions of the wood are usually characteristically more heavily degraded compared with the interior, which may remain relatively intact [30,31]. The extent of degradation is dependent upon timber species, dimensions, and whether the site is in marine or freshwater conditions [25], but is not necessarily related to the time of burial [2,13,32], and the role of nutrient enrichment on bacterial activity is poorly understood [19,33]. It seems that water flow stimulates EB degradation activity, which results from the low availability of nutrients in the surrounding area [26]. Interestingly, compression wood of pine apparently shows different degradation characteristics depending on the amount and severity of compression wood present, when compared to normal wood of the same species. In particular, severe compression wood showed a high degree of resistance of the outer S2 layer to bacterial erosion [34].



**Figure 1.** Slice of medieval waterlogged oak excavated from the Lednica Lake, in the Wielkopolska region, Poland, with a severely degraded, soft and light outer ring of sapwood (the loss of wood substance of about 70–80%) and a better-preserved, hard and much darker central part of heartwood (the loss of wood substance of about 10–20%) [35].

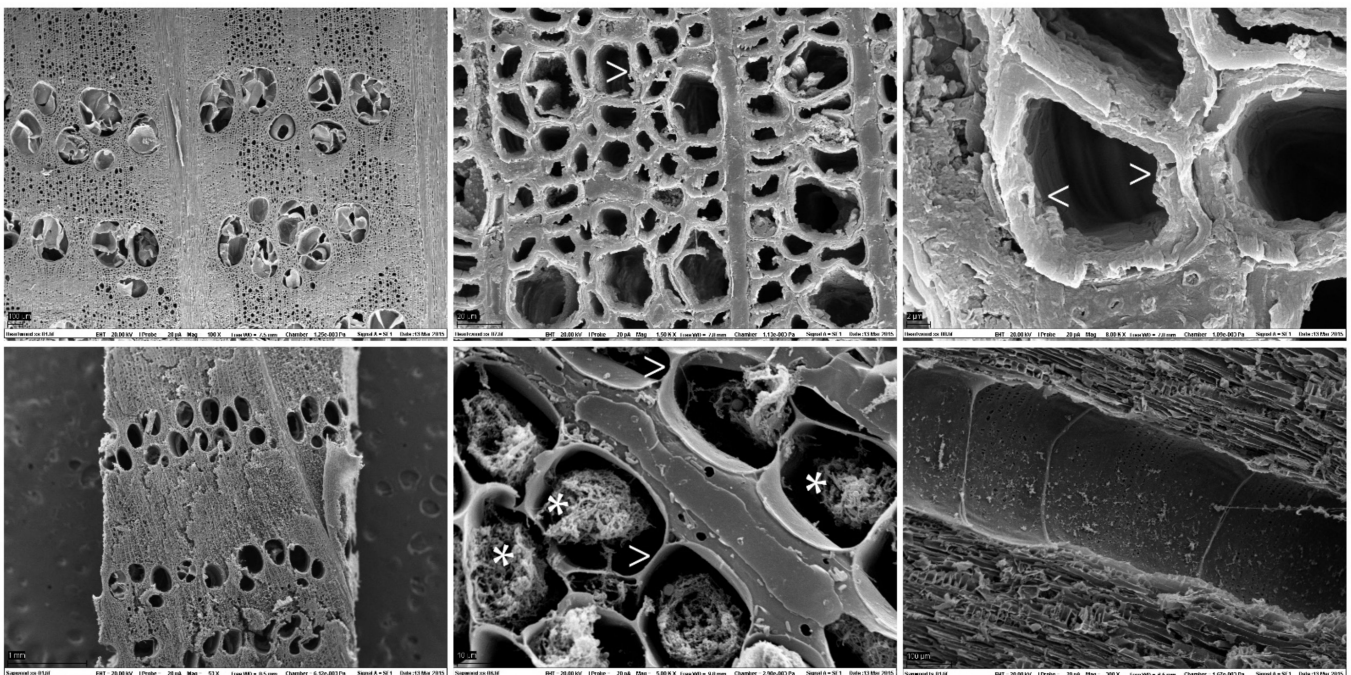


**Figure 2.** SEM images (Carl Zeiss AG-EVO<sup>®</sup> 50 scanning electron microscope using a cryo-SEM technique) of waterlogged oak excavated from the Lednica Lake; upper row—better-preserved heartwood (loss of wood substance about 10–20%) with thick cell walls (arrows) still consisting of all their layers (however sometimes partially degraded or detached); lower row—highly degraded sapwood (loss of wood substance about 70–80%) with a residue of the degraded secondary cell walls visible inside cell lumina (asterisks) and much thinner cell walls consisting mainly of the middle lamella (arrows).

Although degradation by erosion bacteria has been known since the 1980s, the bacteria responsible have not been isolated. Consequently, little is known about the conditions under which such organisms are most active. Culturing bacteria experiments and molecular DNA techniques have shown that bacteria in waterlogged wood belong to the *Cytophaga-*

*Flavobacterium-Bacteroides* complex, *Pseudomonas*, *Cellovibrio*, and *Brevundimonas* groups [36]. It was impossible to reproduce the decay patterns by monocultures in the laboratory, only by mixed cultures, which suggests that EB are active only when they form a synergistic, site-specific consortium with other degradative bacteria. However, they seem to be responsible for the initial attack of water-logged wood in anoxic or near-anoxic conditions [16,37,38]. Other opportunistic organisms, such as scavenging bacteria then begin to colonise and metabolise degraded polysaccharide material in the environment surrounding the erosion bacteria.

In conditions where there is some oxygen present, tunnelling and cavitation bacteria may also be responsible for wood degradation, and they often share this habitat with soft-rot fungi [13,20,21]. Tunnelling bacteria (TB) are unicellular, non-flagellated, motile, Gram-negative, spherical or rod-shaped bacteria. They can endure in a wide range of temperature and humidity conditions and are ubiquitous throughout terrestrial and aquatic environments. In nature, they often coexist with soft-rot fungi, degrading wooden substrates (of both coniferous and deciduous species) together [18,39,40]. Tunnelling bacteria colonise wood from the surface via nutrient-rich rays, and proceed through other lignified wood elements (tracheids, vessels and fibres) via pits or by direct cell wall penetration. TB adhere to the lumen side of the S3 layer using specific polysaccharides produced by themselves and then penetrate through the S2 and S1 layers towards the middle lamella, producing minute tunnels in different directions. They can degrade not only the polysaccharide fraction of the wood, but also the lignin-rich primary cell wall and middle lamella; however, much of the lignin still remains in the decomposed residual material. The ramified tunnels never cross each other, but when the wood is severely degraded, they may collapse, destroying the whole cell wall [17,24,39,40].

The third type of wood degrading bacteria are cavitation bacteria (CB). However, they are rarely reported and sometimes even considered a form of erosion bacteria under restricted conditions. Similarly to EB and TB, cavitation bacteria attach to the cell wall surface using polysaccharide slime. They pass through the small holes in the S3 layer towards the S2 and S1 cell walls, where they digest the polysaccharide fraction creating diamond-shaped or angular cavities. The middle lamella remains untouched. In contrast to EB and TB, degradation is localised mainly within the S2 layer and extends beyond the area where the bacteria are present. This suggests that cavitation bacteria produce diffusible enzymes which can penetrate the cell wall causing its degradation even at some distance from bacterial cells. The S3 layer usually remains undegraded or only slightly modified [16,17,20,24].

Wood from waterlogged sites, where some oxygen is available, shows evidence of soft-rot decay [14,18,25]. Soft-rot fungi belong to *Ascomycota* and *Fungi imperfecti* and are easily distinguishable from other wood-decaying fungi by the ability to degrade wood not only in terrestrial, but also in aquatic environments, and by the decay patterns they produce in wood. There are two decay patterns of soft-rot: type 1 and type 2. In type 1, common in gymnosperm woods, soft-rot produces specific spiral cavities within the S2 layer that follow the orientation of cellulose microfibrils. Depending on the wood anatomical orientation, the pattern can be seen as holes of different sizes (transverse sections) or long cavities with pointed ends (radial or tangential sections) in the secondary cell walls. At advanced decay stages, the entire secondary cell walls can be fully eroded, pointing at the ability of soft-rot to decompose all the cell wall components. However, lignin-rich cell structures or cell types (initial pit borders, middle lamella, ray tracheids of radiata pine) seem to be highly resistant to this type of decay. In type 2, typical for angiosperm woods, a diffuse form of cell wall degradation occurs. Fungal hyphae can colonise cell lumina and degrade the polysaccharide fraction of cell walls, leaving only lignin residues. However, in severely degraded wood, the whole secondary walls can be decomposed, leaving only relatively intact middle lamellae, which suggests that although soft-rot can easily metabolise cellulose and hemicelluloses, it is also able to modify lignin to some extent [14,39]. Sometimes also



type 3 of soft-rot decay is described, when fungal hyphae actively penetrate cells and colonise wood tissue through a traverse perforation of adjacent cells [16].

Several freshwater (*Allescheria terrestris*, *Chaetomium thermophilum*, *Sporotrichum thermophilum*, *Thermoascus aurantiacus*) and marine species (*Ceriporiopsis halima*, *Humicola alopalonella*, *Lulworthia* spp., *Monodictys pelagica*) of soft-rot fungi have been described [18]. They can actively decay waterlogged wood in a broad pH range (3.7–8.6), but as sediments accumulate and cover wooden artefacts (or the decay reaches deep inside large wooden pieces) and the oxygen availability reduces, the soft-rot stops and wood degradation proceeds only by anaerobic or nearly anaerobic bacterial attack [18,21]. Different decay patterns observed in waterlogged wood tell the history of the object and its burial environment, e.g., evidence of the presence of tunnelling bacteria in the Uluburun ship suggests that the water was oxygenated enough to promote the growth of these types of microorganisms [17]. Usually, the outer parts are heavily decayed by soft-rot and tunnelling bacteria, while the inner regions mainly present the pattern of degradation by erosion bacteria that can survive in almost anoxic conditions [13,17,18,20]. Although it is commonly assumed that erosion bacteria are the only form of bacterial attack in anoxic conditions, this may not be entirely reliable since little is known about the influence of different environmental factors on bacterial activity [8], and the bacterial community may be composed of both aerobic and anaerobic bacteria [41].

The main problem resulting from microbial degradation of waterlogged wood is associated with the loss of wood strength. The excavated wood usually looks good (Figures 1 and 3A,B), although its outer layers may feel soft and spongy to the touch. The residual cell wall substances (in highly degraded wood mainly in the form of a lignin-rich skeleton of middle lamellae (Figure 2 lower row, Figure 4B1–B3) keeps the wood integrity as long as it remains waterlogged (Figure 3B). However, upon drying, the capillary forces of evaporating water may cause a collapse of the weakened and fragile cell walls, which leads to irreversible wood shrinkage and cracking (Figures 3C and 4B1–B3).

A wooden artefact destroyed this way loses its historical and aesthetic value. To prevent this, immediate conservation treatment is essential directly after excavation if the wood is intended to be saved in a dry state [13,15,21]. The choice of a proper conservation agent requires knowledge of both the alterations in the degraded wood and the phenomena that have resulted in these changes [21].

During excavation, storage and restoration, the wood may be exposed to oxygen, and fungal or bacterial decay may then occur (white-rot fungi can further degrade even heavily decayed artefacts deprived of most of the cell wall polysaccharides) [2,17,43–45]. The same may happen during excavation and reburial of the objects, when greater oxygen concentrations can reactivate the extant bacteria or support wood colonisation by a new population of microorganisms [17]. Microbial colonisation can also occur on the surface layers of archaeological wood during the treatment with PEG, sugars or other nutrient-rich compounds, which may affect the penetration of the conservation agent into the wood matrix but usually does not endanger the integrity of the treated artefact [43].

## 2.2. Waterlogged Wood, Sulphur and Iron

In anoxic environments with low redox potentials, sulphate reducing bacteria (SRB) compete with other anaerobes, and in conditions of high sulphate concentration, SRB can outcompete such organisms, resulting in the enrichment of H<sub>2</sub>S in the local environment [46], which inhibits the activity of aerobic microorganisms. Where iron is present, the H<sub>2</sub>S reacts with Fe<sup>2+</sup> to produce iron sulphides, such as pyrite (FeS<sub>2</sub>), mackinawite (FeS), or greigite (Fe<sub>3</sub>S<sub>4</sub>) [47]. Iron is a common contaminant in waterlogged wood, especially associated with shipwrecks, although iron concentrations in wood can vary considerably between and within sites [48].



**Figure 3.** Highly degraded waterlogged elm wood excavated from the Lednica Lake, the Wielkopolska region, Poland (the loss of wood substance was about 70–80% with highly reduced cellulose and hemicelluloses content [42]); (A) part of a log shortly after excavation (upper photo) and cutting (lower photo); (B) untreated waterlogged elm samples (completely filled with water); (C) untreated samples shrunken upon air-drying.

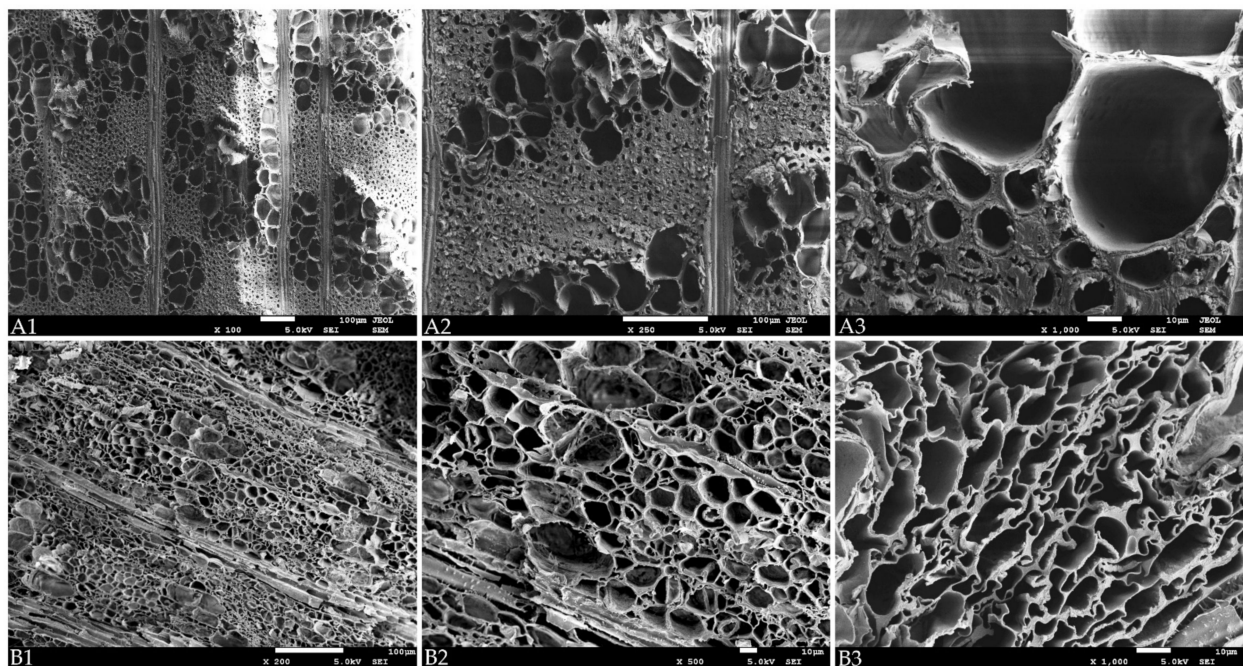


**Figure 4.** SEM (JEOL 7001F Scanning Electron Microscope (JEOL Ltd., Tokyo, Japan)) images of contemporary elm with undegraded thick cell walls (A1–A3) and heavily degraded waterlogged elm shrunken upon drying, with very thin and collapsed cell walls consisting mainly of the skeleton of lignin-made middle lamellae (B1–B3).

SRB are a group of prokaryotes that include members of the *Bacteria* and *Archaea* domains. SRB reduce sulphate to sulphur when metabolising simple organic molecules,

although any sulphur compound with an oxidation state above  $-2$  can act as an electron acceptor [49] as well as nitrate or nitrite; and even oxygen respiration is possible [46]. The sulphate ion acts as an electron-acceptor in a reaction chain, where the carbohydrate moiety acts as an electron-donor; other potential electron acceptors include Fe(III). A wide variety of organic compounds can act as electron-donors, including phenolic compounds, such as lignin and tannins, although the metabolic process does not involve the destruction of the aromatic ring. However, SRB do not metabolise polysaccharide and phenolic substrates directly, but rather use the by-products of other bacteria as their food source [46]. Thus, the activity of erosion bacteria and soft-rot fungi can stimulate the accumulation of both sulphur and iron. Although the activity of SRBs is dominant in anoxic conditions, some strains are facultative and able to operate in anoxic environments and in low oxygen concentrations [50]. SRB have been found in marine sediments, mud volcanoes, hydrothermal vents, hydrocarbon seeps and hypersaline microbial mats, in extreme pH environments (pH 2–10) [46].

Although thought to be associated exclusively with anaerobic conditions, it has been suggested that aerobic or fluctuating oxygen levels promote the deposition of sulphur in marine artefacts, indicating the importance of the local environmental conditions and their temporal and spatial variation affecting sulphur profiles in the wood even at the same site [51,52]. This includes the potential for localised anaerobic conditions to be produced in the vicinity of oxygen-consuming microorganisms. Modelling of sulphur deposition in wood was studied by immersing fresh pine sapwood samples in a solution of Fe(II) sulphate which was inoculated with a bacterial consortium obtained from seawater. The deposition of thiols in the wood was demonstrated through the use of scanning X-ray spectro-microscopy and sulphur K-edge X-ray near edge structure (XANES) spectroscopy. It was found that the thiols accumulated in the lignin-rich middle lamella of areas of wood that exhibited erosion bacteria attack. The presence of iron sulphides was also demonstrated. It was found that penetration by sulphate-reducing bacteria was restricted to regions of the wood where tunnelling bacteria were active. The generation of hydrogen sulphide by SRB produces a strongly reducing environment capable of changing the oxidation state of metals (e.g.,  $\text{Fe}^{3+} \rightarrow \text{Fe}^{2+}$ ,  $\text{Mn}^{4+} \rightarrow \text{Mn}^{2+}$ ) [8]. In this way, soluble iron can migrate through the wood to regions of SRB activity and react to form insoluble iron sulphide deposits. The timbers of the Batavia contained a range of iron sulphate compounds and the Mary Rose contained a mixture of reduced sulphur compounds of iron as well as iron sulphate [53]. It has been observed that shipwrecks from the Baltic sea, such as the Vasa, the Crown and the Riksnickeln tend to show high accumulations of iron and sulphur in the surface regions of the wood, whereas the Mary Rose and the Göta shipwreck from the Swedish west coast show a more uniform distribution of these elements [48]. The Sword shipwreck dating from the 17th Century contains iron-tannin precipitates, which makes extraction using chelates difficult [54]. In the case of the Batavia, a Dutch East Indiaman that sank off the coast of Australia in 1629, the timbers were sealed within a marine concretion that provided an anaerobic environment. Trapped within this concretion were also iron objects, such as cannon and cannon balls, which corroded and reacted with hydrogen sulfide to form pyrite ( $\text{FeS}_2$ ) and pyrrhotite ( $\text{FeS}$ ) [55].

In anaerobic freshwater environments, there are usually low concentrations of sulphate ions and the potential for sulphur enrichment of archaeological wood is much reduced, although SRB are still active in oxidising organic compounds, often in combination with methanogens [46]. It is thought that under conditions of low sulphate concentration, that SRB can utilise hydrogen, lactate and ethanol as substrates. The terminal electron acceptor used in the metabolic process depends upon the pH and the redox potential in the local environment [20].

### 2.3. Waterlogged Wood in Saltwater

Waterlogged wood in marine conditions is usually exposed to two very different environments. In open seawater, the wooden artefacts are susceptible to sediment erosion

and degradation by the wood-boring organisms: gribble and shipworm *Teredo navalis*, although the risk of attack of the latter is reduced considerably if the cellulose content of the wood is low. If the wood is buried in the sediments, the limited oxygen availability prevents respiration of wood borers, and only microbial degradation is possible, which often results in a relatively good state of wood preservation [56,57].

Sea salt present in wood excavated from salt waters can crystallise during drying and damage the wood structure. It can also increase water absorption by wood and promote corrosion [58]. However, archaeological wood that has been exposed to hyper-saline environments (e.g., the Dead Sea) shows little sign of physical or chemical degradation, where the presence of salts in the wood act to physically bulk the material, as well as inhibit microbial colonisation [59].

#### 2.4. Chemical Degradation

Waterlogged wood exhibits losses of the polysaccharide component primarily. Degradation of the cellulose in waterlogged wood involves a reduction in relative crystallinity, although crystal width appears to be unaffected [15]. Xylan in the oak wood of the Vasa ship was found to be depolymerised with the formation of water-soluble fragments [60,61]. Loss of carboxyl groups associated with glucuronic acid residues in hemicelluloses, as well as some loss of ester linkages in the lignin-carbohydrate complex (LCC) has been reported [15]. Degradation of lignin is much less severe compared to the carbohydrate components, but does involve some loss of  $\beta$ -O-4 linkages and degradation of syringyl moieties [15], as well as minor oxidation, which probably occurs after excavation or before oxygen is consumed following burial or immersion [62–64], but might indicate an oxic phase in the history of the sample [65]. A large increase in fluorescence background in the Raman spectrum was attributed to greater mobility of the lignin structure, due to the breakdown of LCC bonds, as well as a higher relative proportion of lignin in the wood [15]. Lignin extracted from waterlogged wood was characterised by direct exposure mass spectrometry (DE-MS) and compared with lignin extracted from fresh spruce wood [66]. It was concluded that combining this analytical technique with principal component analysis was a promising method for studying lignin degradation in archaeological wood.

Information about the degradation state of the molecular components of waterlogged wood can be obtained using a variety of instrumental techniques, including nuclear magnetic resonance (NMR), pyrolysis mass spectrometry (py-MS), pyrolysis-gas chromatography-mass spectrometry (py-GC-MS), direct exposure mass spectrometry (DE-MS), evolved gas analysis mass spectrometry (EGA-MS) and gel permeation chromatography (GPC) [67–71]. Silylation and py-GC-MS can be used to examine the lignin in waterlogged wood, revealing evidence of natural or anthropogenic heating of the wood [72]. Solid-state NMR of waterlogged wood showed that the hemicelluloses were completely removed, but that the lignin was intact [73]. Signals in the NMR spectrum can be significantly broadened due to the presence of iron ions in the waterlogged wood [74], and solid-state NMR is not sensitive enough to detect some important chemical features. For this reason, there has been an interest in employing ionic liquid dissolution techniques for NMR, sometimes combined with derivatization in order to improve solubility [67]. It is generally observed that the lignin structure is not significantly altered by the ageing process in waterlogged conditions [75]. Fourier transform infrared (FTIR) spectroscopy has been used to characterise waterlogged wood samples in order to determine the extent of bacterial attack, but this method requires prior calibration in order to determine the correlation between the FTIR spectrum and lignin content [76,77]. FT-Raman spectroscopy has also been used for the same purpose [78]. The chemical composition (holocellulose and lignin) of degraded waterlogged wood has been determined by using near-infrared spectroscopy (NIR) in combination with partial least squares regression [79]. The region between 1600 and 1800  $\text{cm}^{-1}$  can be used to identify the chemical state of the wood, and the pH can be determined by measuring the band ratios of the peaks at 1710  $\text{cm}^{-1}$  (-COOH) and 1608  $\text{cm}^{-1}$  (-COO-) [80]. A band at 1400  $\text{cm}^{-1}$  in the IR has been assigned to a com-

plex of iron and cellulose oxidation products [81]. Raman spectroscopy has been used to study iron sulphides in waterlogged wood [82]. Electron spin resonance has been used to determine the original charring temperature of charred waterlogged wood [83].

There have been reports of the presence of volatile monoterpenes present in waterlogged archaeological wood, which can be used as an aid to identification [84]. Sesquiterpenes may also be present (abietic, dehydroabietic, neoabietic, pimaric, sandaracopimaric acids), which are derived from the use of pine resins for caulking/waterproofing [75,85]. Oak wood, obtained from the Riksapplet shipwreck dating to 1676 was analysed and found to still contain tannins, particularly ellagic acid, indicating a partial loss of the more water-soluble extractive fraction [75]. Where tannins and iron are present, they can form complexes that are not amenable to extraction [54]. The presence of tannins in oak is an important factor in promoting iron accumulation.

### 2.5. Physical Degradation

The increase in porosity of the degraded wood due to microbiological degradation results in a higher maximum water content (MWC) and a reduction in residual basic density (RBD) compared to fresh wood from the same species. The MWC (also referred to as moisture content, or maximum moisture content) is the ratio of the dry wood weight to the total weight of wood plus water expressed as a percentage; the RBD is the ratio of the density of the archaeological wood sample compared to a typical value for a fresh wood sample of the same species, also expressed as a percentage. Waterlogged wood is considered to be degraded when the MWC is greater than 150% (depending on species) and severely degraded when the MWC exceeds 400% and RBD is less than 40% [86]. There has been some debate regarding the best method to determine the MWC, with some workers advocating vacuum-pressure treatments of the wood to ensure that all air bubbles are removed, but this carries with it the risk of damage to the wood. A study of pre-treatments concluded that they were unnecessary, but that waterlogged wood must be stored fully in water and immersed in watertight containers prior to any conservation activity and that MWC measurements must be carried out within a few days of sampling [87]. The density of the wood can be used to determine the degree of collapse of the wood when dried from the waterlogged state and hence the most appropriate method of conservation. The weight of the waterlogged wood can usually be readily determined, but measurement of the volume of the wood is not usually straightforward, unless the objects are regular geometric shapes and it is necessary to resort to pycnometric or buoyancy force techniques [88]. Although used as a measure of the extent of wood degradation, there has been found to be no correlation between MWC and holocellulose content, although a clearer relationship between holocellulose/lignin ratio was found, albeit with considerable scatter [89]. Water in waterlogged wood is in different environments depending upon whether it is in the macropores of the wood, or located in the cell wall and density corrections may be necessary to take this into account. It is common to find that wooden artefacts exhibit degradation gradients between surface and interior, upper and lower regions, or between heartwood and sapwood. Average values for samples may not therefore necessarily be that informative when determining the extent of degradation of the whole sample and the appropriate conservation technique to employ.

Porosity determination of waterlogged wood can be challenging to measure. Techniques, such as nitrogen sorption require dry samples and this risks collapse occurring, even when using methods such as solvent exchange or supercritical drying [90]. Porosity measurements on water-saturated samples, such as solute exclusion, thermoporometry, or NMR relaxation may be compromised by the presence of degradation products in the wood. Nitrogen sorption studies of waterlogged wood have shown that there is an increase in mesoporosity [15,91]. Helium pycnometry has been used to determine the cell wall density of degraded waterlogged wood after drying [92].

There has been interest in the use of ultrasound as a means of determining the degradation state of waterlogged archaeological wood in situ [86]. This technique determines

the density of the wood by analysing the compression (p-wave) velocity of ultrasound waves propagating through the wood.

The use of dynamic mechanical analysis (DMA) can be used to find the direct relationship between the viscoelasticity of the degraded wood and its chemical composition (precisely, the cellulose content) that translates to the degree of wood degradation. An exponential decrease in the storage modulus ( $E'$ ) and the loss modulus ( $E''$ ) was observed for both waterlogged softwoods and hardwoods. The decrease in  $E'$  in heavily degraded wood results from the progressive reduction in the amount of crystalline cellulose fraction in the cell wall, while the decrease in  $E''$  is due to the degradation of its amorphous part. The ratio  $E''/E'$  ( $\tan\delta$ ) varies with the frequency, depending on the degree of wood degradation; it is higher for slightly decayed wood, while for severely degraded wood, the  $\tan\delta$  values at low frequencies are lower (or similar) than for sound wood of the same species. The DMA technique can then serve as a useful tool for identification of the state of waterlogged wood preservation (in both a wet and a dry state), based on the magnitude of the storage and loss modulus and the changes in secondary relaxation peaks in the loss factor (their location and intensity) [42,93].

### 3. Properties of Commonly Encountered Consolidants and Some Case-Studies from the Conservation Practice

Waterlogged wood differs considerably depending on the species, growth anomalies, degree of degradation, permeability or history of use. Therefore, it is impossible to apply one versatile treatment to all wooden objects. To date, different methods and chemicals have been used for wood consolidation and stabilisation, including many treatment types (e.g., bulking, impregnation, in situ polymerisation) and various drying methods (slow air-drying, freeze-drying, polar solvent drying) [94].

The purpose of a consolidant is to prevent the collapse of the treated wood during conservation and drying and to ensure that the wood has sufficient structural integrity that it can withstand handling and display. Early attempts to conserve waterlogged wood used solvents, oils or waxes, but these failed to provide sufficient support to the degraded wooden objects [95]. Historical chemical methods include an alum treatment [96] and more recent treatments with PEG and sugars [97]. From the mid-1800s until the 1950s many waterlogged finds (especially in Scandinavia) were treated with alum ( $KAl(SO_4)_2 \cdot 12H_2O$ ), which was used to treat many artefacts of the Oseberg find, dating from 834 AD, which was excavated in 1904 [67]. Over time, this has resulted in significant conservation problems due to the presence of sulphuric acid which has severely degraded the wood. With great good fortune, the wood of the ship was not SO-treated. The alum treatment involved the soaking of wooden artefacts in concentrated alum solutions at 90 °C for up to 36 h [5]. This resulted in two distinct regions within the larger wooden objects, with a hard alum-rich outer zone and a softer alum-poor inner zone. The treated wood is now highly acidic (pH 1–2.5) and it has been found that the carbohydrate component of the wood is absent and the lignin is highly oxidised. Apart from alum, there are other inorganic components present and it is thought that the presence of iron, in particular, might have a catalytic effect on the degradation process [98], but this is not certain. For example, during reconstruction, an iron rod was used to strengthen the sled and other objects contain remnants of the original iron nails. Although decorative iron nails were removed from most objects prior to treatment, they were later replaced. Other inorganic components include zinc and mercury from the treatment of the wooden objects in zinc containers containing a solution of mercuric chloride, used as a biocide. Many of the alum treated objects were subsequently impregnated with linseed oil either by immersion or by brushing until fully saturated. The reconstructed objects were then coated with a matt varnish to remove the shine caused by the linseed oil treatment. An epoxy-based coating was also applied during the 1950s. The linseed oil-impregnated region provides the only remaining structural integrity for many of the finds and appears to limit the diffusion of sulphate into the treated areas [99]. Although not used on the Oseberg finds, glycerol was often added to the alum-treatment solution after 1910, which means that objects SO-treated are now extremely sensitive to ambient

relative humidity. The alum-treated zones of the Oseberg objects show pH values ranging from 1 to 4.5, with the source of acidity being the alum. During the impregnation process, the heating of the alum solution to 90 °C results in a drop in solution pH from 3.5 to 2, due to the precipitation of alunite ( $KAl_3(SO_4)_2(OH)_6$ ), which is only formed in heated solutions. This reaction results in the production of excess sulphate ions, which enter the wood structure [96]. The use of alum was the standard method for the treatment of archaeological wood at the Danish National Museum in Copenhagen, where it was in use for a century [100]. The Hjortspring boat was treated with a mixture of alum and glycerol in the 1920s, but the hygroscopic properties of this mixture caused stability problems and the boat was re-treated between 1966 and 1979 with PEG solution. Alum was also used to treat the County Hall Roman ship that was found in London in 1910, but very little of this artefact now remains.

Currently, polyethylene glycol (PEG) is the most common conservation agent. PEGs are linear polyethers with terminal hydroxyl groups, commercially available in a wide range of molecular weights from 300–600 (liquids at room temperature), through 1000–1500 (semi-liquids), to 3250–6000 (wax-like substances), freely soluble in water or alcohols and easy to use [101–105]. PEGs are hygroscopic, and exhibit deliquescence associated with a large increase in sorbed water at a critical air relative humidity (RH) [106], which depends upon temperature, molecular weight (MW) of polymer and the presence of any additives. This can cause problems for artefacts that are not located in controlled humidity conditions. The oxygen atoms of the PEG backbone and the terminal OH groups of the polymer chain can both form hydrogen bonds with the sorbed water molecules. As the polymer chain length increases there is a reduction in the proportion of terminal OH groups and in the entropy of mixing of the polymer with water molecules. This results in a decreased solubility of higher MW PEGs in water, which plateaus at an MW of approximately 6000, with little change in solubility thereafter. Increasing the temperature will increase the solubility of the PEG in water, requiring heating when treating with longer chain PEGs which can cause technical problems when treating large objects. The penetration of PEGs into wooden objects depends upon the MW and the degradation state of the artefact. There is no single PEG that can stabilise both lightly and heavily degraded waterlogged wood. High MW PEGs are suitable for stabilising heavily degraded waterlogged wood, but are unable to penetrate the microporous structure of the wood, whereas low MW PEGs can penetrate wood easily but are not solid at room temperature as well as being hygroscopic. By using a two-step treatment, the low MW PEG is able to stabilise the heavily degraded wood and this is then protected by an envelope of high MW PEG so that hygroscopicity is not a problem.

PEG was first used in the preservation of wooden artefacts after research at the Forest Products Laboratory in Madison WI in the 1950s [107–110]. The diffusion of PEG into waterlogged wood is a slow process, which is influenced by the MW and composition of the consolidant, the orientation of the wood sample with respect to the diffusant, anatomical characteristics of the wood and extent of deterioration of the wood, as well as physical conditions, such as the temperature of treatment [111]. Heavily degraded wood with a low density will exhibit severe collapse on drying and is usually treated with high MW PEG, followed by freeze-drying. Waterlogged wood that is less degraded can be treated with low MW PEG prior to freeze-drying [88]. Conservation usually involves a two-step treatment using a low and then a high MW PEG. Two-step treatments have been employed for many conservation projects including the Mary Rose in the UK, the Kinneret boat in Israel, the Bremen Cog in Germany, the Vasa in Sweden, the Shinan Treasure Ship in Korea, the Copper ship in Poland and the Hasholme logboat in Hull, UK.

The Mary Rose sank off Portsmouth (UK) in 1545 and the site remained largely undisturbed until 1965. It was decided to raise and conserve the ship in 1978. She was raised in 1982 and the mainly oak timbers were initially sprayed with fresh, chilled water for 12 years to remove the marine salts. From 1994 until 2013 she was conserved using a two-step PEG treatment which involved continuous spraying with an aqueous solution

of PEG 200 (40% *w/w*) for 12 years followed by spraying with a heated aqueous solution of PEG 2000 (60% *w/w*) for a further 7 years. During the spraying operation, a broad spectrum biocide was added in order to prevent microbiological degradation during the conservation process. This was followed by a controlled air-drying process at 55% RH and 20 °C. During this time, additional PEG 4000 was brush-applied to selected parts of the timbers [112–114].

The Kinneret boat (called by the press “Boat of Jesus”), dated back between the 1st century BC and 2nd century AD, was excavated from the muds of the Sea of Galilee in 1986. A two-step PEG treatment was chosen to conserve at least seven various types of wood in different states of degradation. The conservation process started with using PEG 600 with an increasing concentration up to 50%, then PEG 3500 was applied, and the concentration was slowly increasing up to 90%. The immersion method was proposed to shorten the conservation time to seven or eight years. Thirty-five tons of PEG were used during the process [115].

The conservation of the Bremen Cog of 1380 took 38 years from excavation to displaying the artefacts to the public. The ship was reconstructed in the display hall by suspending the wooden pieces from the ceiling and building a conservation tank around the hull [30,116]. The consolidation process involved treatment using two consecutive baths of aqueous solutions of PEG 200 and PEG 3000. The Bremen Cog was treated in the low MW PEG bath for ten years. It was found that the low MW PEG solution very quickly became contaminated with bacteria, resulting in the solution becoming very cloudy, which was dealt with by adding a flocculant and passing the solution through gravel filters. At the end of the impregnation procedure, it was necessary to dispose of 1600 tonnes of used PEG solution. It was established that PEG 200 was completely biodegradable in municipal wastewater treatment facilities, which allowed for the disposal of the drains at a slow rate. The treatment with PEG solution was simplified because PEG 200 is a liquid at room temperature and could be pumped directly into the conservation tank. However, PEG 3000 is solid at room temperature, requiring the PEG to be delivered using lorries with heated tanks so that the hot PEG could be pumped together with water into the treatment tank. Treatment with PEG 3000 was initially at a concentration of 60% in water, which was later increased to 70%, requiring a temperature of 40 °C to keep the PEG in solution. Treatment with PEG 3000 took three years. Once the conservation tank had been removed it was necessary to remove the surface encrustation of PEG 3000 to expose the treated wood surface. Residual shrinkage of the treated wood ranged from 0–2.7%, compared to 14.5% for untreated timbers.

The Vasa sank in Stockholm harbour in 1628 and was re-discovered in 1956. She was recovered from Stockholm harbour in 1961 and the timbers were treated with aqueous solutions of PEG 600, 1500 and 4000, with some additional manual applications of PEG 4000 and 1500 to selected parts between 1962 and 1965. The wood was sprayed using an aqueous PEG 1500 solution from 1965 to 1971, followed by PEG 600 from 1971 to 1979. PEG 600 and 4000 were applied manually between 1979 and 1991 with the excess PEG 4000 melted off the surface [117]. The presence of PEG 600 makes the Vasa sensitive to changes in RH, since PEG 600 is hygroscopic [117]. The timbers of the Danish Skuldelev ships which were found in Roskilde Fjord in the 1960s were treated in a single-stage process by submersion in a tank containing an aqueous solution of PEG 4000 followed by freeze-drying.

The excavation of the Shinan treasure ship, a medieval Chinese vessel found in the waters of the south-western coast of the Korean peninsula, took nine years, from 1976 to 1984. Her priceless cargo was excavated along with the ship that included 28 tons of copper coins, sandalwood, sherds, and plenty of metal, stone, and other objects. A two-step PEG treatment was applied to the ship’s Chinese red pine and Chinese fir timbers. It started with the removal of iron corrosion products. Then wooden elements were immersed in a 5% solution of PEG 400 at room temperature. The concentration was raised by 5% up to 20% in 3–4 month intervals. Then the impregnation continued in 25% PEG 4000 solution at



40°C, and the concentration was raised every 2–3 months by 5% up to 75%. Small heavily degraded parts were treated only with PEG 4000 [118].

The Copper ship, found in the Gulf of Gdańsk, Poland, was built in 1400 and served only eight years. She sank due to a fire during her route from Gdańsk to Western Europe transporting metal and woodland products. Surprisingly, the excavated wooden parts (mainly oak) remained in a well-preserved state despite 567 years of submersion in the sea sediments and salt water. The first conservation employed slow drying and surface impregnation with linseed oil and turpentine. Then, in the 1980s, when PEG was introduced as a new consolidant, it was employed for Copper ship conservation as well. The treatment involved the application of increasing concentrations (from 10% to 70% or 90%) of a mixture of lower MW PEGs (400 and 1500) or PEG 4000 using different methods, including soaking in warm PEG solutions (higher temperature increases the rate of PEG diffusion into the wood), spraying or paint brushing, adding biocides to prevent microbial activity in the conservation solution. Impregnation lasted from one up to three years, followed by slow air-drying of the artefacts until they reached moisture equilibrium with the surrounding air. Two-step impregnation was applied on an 8 metres long starboard, starting with spraying with an increasing concentration of PEG 300 (from 10% to 40%), followed by applying 40–50% solution of PEG 3000. No cracks were observed in the treated wood, the ASE was 73%, but wood hygroscopicity increased significantly due to a mixture of PEG 300 and 3000 present on the wood surface [119].

The Iron Age oak dug-out Hasholme logboat was discovered in 1984 at the Hasholme site in the parish of Holme-on-Spalding Moor in East Yorkshire, UK. After excavation, it was stored at the National Maritime Museum for two years and then transported to Hull, where it was conserved by spraying with PEG for 19 years (a two-step treatment). At the end of 2009, the conservation was completed, and the boat was left for natural air-drying after being washed down to remove the remains of PEG and the mould from its surface. A biocide was applied to prevent further mould growth. Some parts (e.g., the large decorated transom) were freeze-dried. Today, the boat is displayed in the Hull and East Riding Museum galleries under controlled humidity conditions to prevent further wood shrinkage or cracking and is regularly monitored for any signs of deterioration [120,121].

The Yenikapı Byzantine-Era Shipwrecks, Istanbul, Turkey were placed in desalination tanks after excavation where salt was removed in a running water bath, iron traces were then removed using disodium EDTA and oxalic acid followed by treatment in flowing water, with a repetition of the process until the iron was removed entirely. For conservation, both PEG and Kauramin (melamine formaldehyde) were employed, with the Kauramin treatment reserved for highly degraded non-durable materials. The other objects were soaked in a solution of 45% PEG 2000, followed by freeze-drying [122].

In order to determine if the consolidation process is complete, it is important to know the concentration of PEG inside the wood. Methods to determine PEG in solution include gravimetric and refractometry, but determination in wood requires extraction combined with an analysis technique, such as thin-layer chromatography (TLC) or high-performance liquid chromatography (HPLC). Semi-quantitative information can be obtained using TLC, but much more accurate information is obtained using HPLC, or size exclusion chromatography (SEC). However, such procedures can be time-consuming. It is known that PEG forms coloured complexes with bismuth, cobalt, molybdenum or iodine compounds and the reaction of aqueous solutions of PEG of different molecular weights (MW) with Dragendorff reagent (a mixture of bismuth subnitrate, hydrochloric acid and potassium iodide) has been examined. No reaction was observed with PEGs of MW 200–600, but a concentration-dependent change in the spectrum was observed with PEGs with an MW of 2000 and above. The colourimetric method was found to be MW-specific and the spectrum of admixtures of PEG 4000 was unaffected by additions of PEG 300. The method was applicable to PEG extracts from treated wood samples. Low MW PEGs for 200–400 did not interfere with the analysis [123]. In-situ Raman spectroscopy has been used to quantify the level of PEG in waterlogged archaeological wood, in order to avoid the need for removal

of samples and using extraction techniques [124]. Magnetic resonance imaging has also been used to visualise the distribution of PEG in waterlogged wood [125].

Impregnation with PEG in hot baths over extended periods can result in the relaxation of growth stresses, resulting in the distortion of treated timbers. It is also known that PEGs are susceptible to thermal-oxidative degradation under accelerated conditions, resulting in the formation of lower MW fragments which may be a concern for the long-term stability of conserved objects [53,117]. Examination of the distribution of PEG in treated wood from the Vasa and the Danish Skuldelev Viking ships showed that although large amounts of PEG could be extracted from degraded wood, there was very little found in the sound parts [117]. PEG 4000 was found only in the surface layers of the wood, whereas PEGs 1500 and 600 were found at all depths. Low MW PEG was detected in one of the Skuldelev ships which was thought to be due to degradation of the PEG 4000, but there was no evidence of degradation otherwise. However, if the starting material composition is not known, it is difficult to eliminate degradation with certainty. An alternative approach is to measure formic acid, which is a degradation by-product of PEG; although there may be other sources [53].

Alternatively to polyethylene glycols, sugars (mainly lactitol, less frequently trehalose or a mixture thereof) have been commonly applied for waterlogged wood conservation since the late 1980s. Conservation treatment includes impregnation with heated or unheated sugar solutions; it is appropriate for both large and small objects and can be applied as a pre-treatment followed by freeze-drying. The method provides several benefits to the treated wood, including increased strength, good dimensional stabilisation, and natural colour, being entirely reversible, safe, and more cost-effective than PEG treatment. However, sugars are highly susceptible to microbial attack, and biocides must be added to the impregnation solution [97,126].

Nowadays, more than thirty museums and private conservation laboratories worldwide use lactitol for waterlogged wood conservation. Among the largest artefacts treated with this method are the Poole logboat and the Friesland Smalschip. The pure “cold” lactitol method was applied, *inter alia*, for the conservation of 4 m-long elements of a pipeline from the Nango oohigashi site in Nara Prefecture, Japan (dated back to the 5th century AD), and included pre-treatment, decolouring and washing (1 month), impregnation with lactitol (3 years), drying at 50 °C (1.5 months), surface cleaning and further drying (0.5 months). A six metres long waterlogged pine coffin, dated back to the end of the 3rd century AD, excavated in 1995 from Simoikeyama tomb in Tenri City, Japan, was conserved using the “warm” lactitol method. The treatment included pre-treatment, decolouring (water plus 1% EDTA-2Na) and washing (1 month), lactitol impregnation at 50 °C started from a concentration of 40% up to 60% (13 months), dusting with pulverised monohydrate lactitol crystals to initiate crystallisation, drying at 50 °C (2 months), surface cleaning and further heat-drying. The total time of the treatment was 16 months. The “warm” lactitol plus 10% trehalose mixture method was applied to conserve the 1st-century BC heavily degraded waterlogged wooden figures excavated at the tomb of one of the kings of the ancient Shisui Kingdom (Han dynasty, 1st c. BC) in Shanzhuang village, China. The treatment included the removal of iron ions (water plus 1% EDTA-2Na, 1–2 weeks), washing in water (3 weeks), impregnation with a mixture of lactitol, 10% trehalose in water and 0.01% Kathon CG biocide at 50 °C started from 15% solution up to 50%, then the temperature was raised to 60 °C, and the impregnation was continued using 65%, 70% and 80%, subsequently (3 months for few centimetres thick artefacts, 6 months for thicker objects up to 10 cm, 18 months for the thickest ones), dusting with pulverised lactitol monohydrate crystals to initiate crystallisation, air-drying, and surface cleaning. The results of the applied treatments were assessed as satisfactory [97].

Consolidants historically used in waterlogged wood conservation are listed and briefly described in Table 1.

**Table 1.** A historical overview of waterlogged wood consolidants [127].

Consolidant	Exemplary Conservation Methods	Comments
Inorganic compounds		
Aluminum sulfate	Parts of the Oseberg find were boiled in aluminium sulfate in 1913 by Gustafson, dried and then impregnated with linseed oil.	Good dimensional stabilisation, wood sensitive to moisture changes, deposits on wood surface; no longer in use.
Aluminum potassium sulfate (alum)	The method first described by C.F. Herbst (and Speerschneider) in 1861—boiling an object in supersaturated alum solution, then drying and dipping it in linseed oil. The method used in the Danish National Museum (1858–1958) for more than 80% of all waterlogged wooden artefacts collected; applied to some parts of Oseberg Ship in Norway.	Prevents shrinkage, crystals can destroy fragile cells, wood is brittle, prone to cracking and deformations, deposits on the surface, iron elements must be removed, no longer in use.
Boron compounds	The Thessaloniki process for medium-degraded waterlogged wood described by Borgin (1978)—soaking wood in a concentrated solution of sodium tetraborate with sodium silicate and an organic polymer. After drying, wood is treated with a concentrated barium hydroxide solution to force precipitation of barium borate and barium silicate inside wood tissue.	Wood stabilisation and appearance are not always satisfactory; no longer in use.
Chromium compounds	Conservation by exchanging water in wood for a 2–10% solution of chromium(VI)oxide with the addition of 10–20% sodium dichromate (1965, French patent by Garrouste). Bouis proposed a similar method in 1975 but with the addition of linseed oil after drying (chromium compounds harden linseed oil).	Good dimensional stability, low weight and high porosity, resistance against fungi and fire, brittle, unnatural colour, the high toxicity of the chemicals; hardly used.
Silicon compounds (sodium and potassium silicate)	Scout (1921–1926) applied silicon glass for restoration objects in the museum; Cebertowicz and Jasienski (1951) used a mixture containing water glass by electrokinetic method on wooden elements in Biskupin, Poland; a dugout canoe consolidated by slow drying and brushing with a sodium silicate solution (Plenderleith).	Improved strength and hardness, cracks can close, unaesthetic appearance, irreversible; alkali silicates or water glass are no longer in use.
Organic compounds		
Animal glues	Glue solutions used for conservation of dugout canoes in Switzerland (1850–1900); Rathgen (1924) proposed using an aqueous glue solution in combination with drying and impregnation with resins; waterlogged wood conservation in Hungary (1959).	Glues are sensitive to moisture and microbial attack, shrink and become brittle, have poor penetrability, darkened wood colour; no longer in use.
Linseed oil	Oseberg Ship treated with creosote and linseed oil (since 1904) or linseed oil and white spirit (1957), parts of Oseberg Ship and funeral artefacts treated with linseed oil (1913); a boat treated with a mixture of turpentine, linseed oil, colophony and Carbolineum (1958).	Insufficient stabilisation, no longer in use.
Tung oil	Used for surface treatment of parts of the Hjortespring Find (Denmark) impregnated with alum (1921).	Poor strengthening effect, spotting on the surface, unnatural brown colour; no longer in use.
Lanolin	Lanolin method proposed by Vynckier (1982/83).	Method not important in wood conservation.

Table 1. Cont.

Consolidant	Exemplary Conservation Methods	Comments
Beeswax	Small wooden artefacts heated in a mixture of rapeseed oil, wax, spruce resin and benzene by Speerschneider (1861); pouring melted wax on a wooden object (1924); protective coating of melted beeswax for wood treated with alcohol and resin (1979).	Sometimes used for small and fragile artefacts, or as a compound of some conservation mixtures.
Carnauba wax	Dehydrated waterlogged wood submerged in melted paraffin, then in a mixture of dammar, carnauba wax, paraffin and beeswax by Brorson Christensen (1949–1956).	High durability, good stabilisation effect; no longer in use.
Paraffin	Dripping or pouring melted paraffin on wood, or storage in liquid paraffin (1924); wood dehydration with methanol and toluene, then impregnation with melted paraffin (Leechman 1929); dehydration with ethanol prior to paraffin treatment (Kisser and Pittioni, 1935); the paraffin method used in Hungary (1950–1960).	Good dimensional stabilisation for soft objects with low density; occasionally used for small highly degraded artefacts and wood/metal composites.
Microcrystalline wax	Mentioned as waterlogged wood consolidant by Werner (1959) and Sujanova (1972).	Not used for wood stabilisation.
Dammar	As a component of a conservation mixture (1949–1956); the alcohol–ether–dammar method described by Plenderleith (1956); wooden writing tablets treated with dammar after water–methanol–ether exchange (Blackshaw, 1974).	Good consolidation effects for heavily degraded wood, appropriate for smaller objects; chemicals applied pose a risk of explosion and fire; not commonly used.
Colophony	The acetone–rosin method published by McKerrell (1972); used for conservation of hardwood objects such as dead eyes, pulley blocks, and other ship’s fittings by Fox and for inlays of wood and ivory of a sword handle by Payton (1987).	Good dimensional stabilisation, suitable for low-permeability hardwoods; occasionally applied for better-reserved small objects.
Shellac	Alum-treated wood coated with shellac after drying and brushed with linseed oil (Herbst 1858–1860); heavy waterlogged object dewatered with glycerol and dried can be coated with a shellac solution (Plenderleith, 1956).	Low weight of treated object, good dimensional stabilisation; not in use anymore.
Ethylene glycol	Soaking wood with ethylene glycol until the final treatment (Miihlethaler, 1969); used to swell dried and shrunken waterlogged wood (De Jong, 1977); as an anti-shrink agent in the Thessaloniki process (Borgin, 1978).	Insufficient wood swelling by low-molecular glycols; rarely used.
Glycerol	For storing and soaking of wooden artefacts (1900); mixed alum–glycerol treatment (Brorson Christensen, 1910); Celtic monumental sculpture treated with rosin/glycerol (after 1911); parts of the Hjortespring Boat treated with glycerol (method developed by Rosenberg, 1921); as pre-treatment followed by freeze-drying (1986).	Crack formation or warping can occur, very hygroscopic; not in use.

Table 1. Cont.

Consolidant	Exemplary Conservation Methods	Comments
Polyethylene glycols (PEGs)	Recognised as suitable consolidant for waterlogged wood by Moren and Centerwall (1961) and Stamm (1956); parts of Oseberg Ship treated with melted PEG 4000 by Rosenqvist; the beginning of the conservation of the Vasa ship in Sweden (1961); conservation of the Bremen Cog (recommendations by Noack, 1965); treatment of parts of the Sjøvollen Ship in Norway (1968); PEG pre-treatment followed by freeze-drying developed by Iwasaki and Higuchi and Ambrose (1969–1970); the beginning of the Mary Rose conservation, Great Britain (1982).	Direct exchange of water by PEG, good stabilisation effect, darkened wood colour, high weight of the treated object, susceptible to microbial degradation, corrosive to metals, not stable in the long-term; the most common conservation method for waterlogged wood.
Sucrose	Noack proposed sucrose for the Bremen Cog treatment (1965); Franguelli and Loda (1970–1972) investigate wood conservation with sucrose; sucrose as a pre-treatment to freeze-drying (Parrent, 1983);	Good stabilisation and consolidation effect, best for better-preserved wood, natural wood appearance; used for objects of not particular historical value, when PEG-treatment is too expensive and time-consuming.
Sugar alcohols	Suitability of mannitol and sorbitol studied by Barbour and Murray (1982); mannitol as a pre-treatment followed by freeze-drying (Murray, 1985); two-stage treatment with mannitol and PEG prior to freeze-drying (Imazu, 1988); treatment of a 6-m-long wooden coffin (1998) and dugout pipeline (1999).	Insufficient stabilisation and white deposits—mannitol, better results for lactitol; not commonly used.
Cellulose ethers	A wooden coffin treated with Methyl cellulose solution (Schlabow, 1961); reports about not satisfactory results of methyl cellulose impregnation (Van der Heide, 1963; Ankner, 1969).	Reversible, but not suitable as consolidants because of poor penetration; not in use.
Cellulose esters	Nitrocellulose varnish used for sealing of the alum-treated parts of the Hjortespring Find, Denmark (1921); treatment of wooden scabbard with a solution of celluloid in amyl acetate and acetone (Plenderleith, 1954).	Low penetration, insufficient strengthening, brittleness of treated objects, nitrocellulose is highly flammable; not in use.
Phenol-formaldehyde resins (PF resins)	Considered as waterlogged wood consolidant since 1965–69 by Noack and Mühlethaler; USSR patent by Vichrov (the method of Minsk) for conservation of archaeological artefacts (1972); combined treatment with sucrose solution and phenol alcohol by Kolčín (1973), and sucrose with PF resin by Kazanska and Nikitina (1984).	Not suitable for large objects due to the short hardening time, imparts dark colour; not in use.
Urea-formaldehyde resins (UF resins)	First experiments with water-soluble UF resins (Celodal, 1938) and with hardening using a catalyst (von Stockar 1938); conservation of wooden bucket (1968); a combination of UF resins with alum (Szalay, 1980).	Not suitable for large objects; rarely used.
Melamine-formaldehyde resins (MF resins)	Used for waterlogged wood conservation since 1957 by Mueller-Beck and Haas; successful conservation of a paddle with Piazep ME/2 by Cott (1968); application of Kauramin CE 5549 for conservation of coat and ship elements by Witköpper and Hoffmann (1998).	Sufficient penetration and stabilisation, wood can bleach; occasionally used for smaller objects.

Table 1. Cont.

Consolidant	Exemplary Conservation Methods	Comments
Polyvinyl compounds	Poly(vinyl acetate) used for preliminary conservation of waterlogged wood (Losos, 1958); further experiments on the method by Brorson Christensen (1970). Poly(vinyl alcohol) used by Losos (1958); a mixture of Poly(vinyl alcohol) and glycerol for wood conservation used by Rumâncev (1958); medieval artefacts consolidated by Müller and Thieme (1966). Gilroy used Poly(vinyl butyral) to conserve a pulley shave from the Dutch ship Zeevijk in 1978. Poly(vinyl chloride) was tried for spoon conservation by Ypey in 1964.	Poly(vinyl acetate) is not hard enough for wood stabilisation, low dimensional stabilisation; Poly(vinyl alcohol) is reversible, poor dimensional stabilisation; Poly(vinyl butyral) has poor penetrability, gives good strengthening effects; not in use.
Poly(methyl methacrylate) (PMMA/MMA)	Used for in situ polymerisation in waterlogged wood by Brendel in 1966 and Munnikendam in 1967. PMMA used for the conservation of some artefacts from the Oseberg find stored in formalin by Rosenkvist.	MMA requires wood dehydration which can lead to its shrinkage, heat released during polymerisation can cause warping or shrinkage in wood; PMMA has a plasticising effect, wood can swell; occasionally used for small artefacts.
Poly(ethyl methacrylate)	Sawada used a solution of Paraloid B72 in xylene for consolidation of a vermilion Japanese lacquer vessel (1981).	Used only in exceptional cases.
Poly(butyl methacrylate) (PBMA/BMA)	Bowls, spoons, arrows, spheres, and wedges of wood treated with BMA by Nogid and Podzdnák (1964/65); modification of the method by De Jong (1977).	Strength improvement, colour and grain pattern not changed; rarely used.
Poly(2-hydroxyethyl methacrylate) (HEMA)	In situ polymerisation of HEMA in oak samples by Munnikendam (1967) resulted in crack formation; modification of the method by De Jong (1975–77) using different catalysts; the method considered by Grattan as less effective than others (1982).	Good strength improvement; can lead to crack formation; not used in practice.
Styrene	Neolithic ash samples treated with styrene by De Guichen et al. (1966) without satisfactory results; impregnation of wood after an exchange of water with a mixture of styrene and acrylonitrile using irradiation polymerisation (1970).	Improvement in wood strength, suitable for artefacts destroyed by insects or fungi, wood becomes brittle and hard; sometimes used for small wooden objects.
Unsaturated polyester resins	Application of resin to wood filled with acetone after water exchange by Ketelsen (1959) resulted in 7% wood shrinkage; using irradiation curing for styrene/polyester treated wood (De Tassigny and Ginier-Gillet, 1979); consolidation of a freeze-dried wood with Ludopal U 150 and irradiation curing (Schaudy et al., 1985); poly(caprolactone) oligomers tested for the conservation of waterlogged wood by Gerasimova et al. (1981)	Permanent and homogenous strengthening, cracks close upon curing, resistant to UV radiation and moisture changes; used occasionally for small artefacts.
Epoxy resins	Used only for dewatered (dried) wood; alum-treated parts of Oseberg Ship were sealed with Epolack (1954–56); conservation by brushing the surface of dugout canoe (Werner, 1961); treatment of a woven helmet by Bill (1979).	Resistant to biodegradation, does not improve wood dimensional stability, can deepen wood colour and produce a gloss on the surface; rarely used for already dried wood.
Polyurethanes	Used for glueing PEG-treated wood by Noack (1965).	Not used for consolidation, it can serve as a protective foam.

Table 1. Cont.

Consolidant	Exemplary Conservation Methods	Comments
Organosilicon compounds	The hull of Vasa ship sprayed with a mixture of PEG, borax, boric acid and methyl polysiloxane (1965); tetraethoxysilane (TEOS) tested for waterlogged wood by Semczak (1975); acrylate dimethylsiloxane oligomers tested by Yashvili (1975); a canoe treated with TEOS by Bright (1979); in situ polymerisation of organosilicon compounds mentioned by Xu (1983).	Good dimensional stability, hydrophobizing effect, TEOS reverses wood grain pattern, white deposits on the surface, wood becomes brittle; acrylate-siloxane oligomers preserve natural wood appearance; rarely used.

#### 4. Properties of Consolidated Wood

##### 4.1. Drying of Consolidated Wood

Once a wooden artefact has been treated with a consolidant and is stabilised, it is then necessary to dry the object so that it can be displayed. Depending on the size of the artefact and the budget available, the main choices are air drying, freeze-drying or supercritical drying. With most large objects, air drying is the only viable option. During the drying process, the wood may be subject to shrinkage or collapse, due to water being removed from the pore structure of the wood and surface tension forces operating at the meniscus surface of the water in the pores. Even sound wood exhibits shrinkage and even collapse when dried, but archaeological wood is especially prone to collapse because it is seriously weakened due to degradation. Consolidants mitigate this collapse occurring because they fill the pore spaces of the degraded wood, but damage can still occur if the drying is not performed properly. It is also essential that the consolidant enters the pore spaces of the degraded cell wall as well as the larger voids in the wood. If air drying is the chosen method, then it is important to carefully control the temperature and humidity of the environment to ensure that the drying does not take place too rapidly, requiring long drying times for large objects [128]. The surface tension collapsing forces at the water/wood interface can be reduced by incorporating other solvents, or by using solvent exchange to ensure that the final solvent is of low polarity, but this can add to the costs and introduce safety concerns. Where the wood has already collapsed prior to consolidation treatment, the options for recovering the original dimensions are limited, but there has been use of treatment with a low concentration of aqueous NaOH solution, or with a urea/ethylene diamine/PEG 200 mixture to swell the wood [129].

Consolidation with PEG prior to drying gives the best results when a low MW PEG is used to prevent cell wall collapse and a higher MW PEG is used to give the wood some structural strength [101]. Drying conditions can affect the distribution of the lower MW PEG in the cell wall, since a concentration gradient is set up between the PEG solution in the lumens and the cell wall, which encourages further diffusion of the PEG under slow-drying conditions, which can be advantageous [130].

Freeze drying is a relatively expensive process that requires long process times, expensive equipment and is not normally used for large conserved objects. The process involves the formation of ice in the object, which is then removed by sublimation under a vacuum. Since ice is of lower density than water, the freezing process involves an expansion that could damage artefacts and for this reason, a cryoprotectant is required. Most commonly, a low MW PEG is used as the cryoprotectant, but mannitol, trehalose, lactose, sucrose and many others are suitable. A successful freeze-drying process is one that occurs without collapse, shrinkage or cracking of the artefact under treatment. When performed correctly, freeze-drying of wooden artefacts after consolidation has been shown to result in reduced shrinkage after drying [131,132]. In order to prevent the collapse of the treated wooden artefact, it is necessary to keep the temperature inside the object lower than the eutectic PEG-water solution, so that there are no liquid phases present and only sublimation of the ice occurs [104,133]. The presence of liquid phases during the sublimation of the ice would give rise to the capillary forces which cause the collapse of the wood structure [12]. Problems arise because these necessary conditions can result in very long drying times

for large objects, with low temperatures required in order to maintain a solid PEG/water phase, but higher temperatures being favourable to more rapid drying and careful optimisation is required to minimise costs. Large objects also require custom-made dedicated equipment, which adds considerably to the expense of conservation. Supercritical drying has been examined as an alternative to freeze-drying, but is also expensive, only suitable for relatively small objects and requires an intermediate solvent-exchange step [134]. In other cases, larger objects have been sawn into sizes suitable for the available equipment, as was carried out for the Carpow logboat [135].

#### 4.2. Sorption Behaviour

Sorption isotherms of PEG-treated wood show much higher moisture uptakes at relative humidities in excess of 50% [136]. Wood treated with a variety of different PEG solutions showed lower EMC below 80% RH, but much higher levels of sorption thereafter [137]. Archaeological oak wood treated with PEG exhibits a reduced moisture uptake at RH below 80%, but greater moisture uptake above this value [138]. Similar behaviour is observed with pure PEG or PEG combined with pharmaceutical formulations [106,139]. It is often assumed that PEG in the cell wall exhibits lower hygroscopicity due to immobilisation caused by the surrounding cell wall polymers and that changes in hygroscopic behaviour are solely attributable to PEG in the lumens and large void structures [140]. If PEG is essentially immobilised in the cell wall and not responsible for sorption changes, then it should be possible to determine the location of the PEG by examining the sorption behaviour at different PEG loadings. There is also a large reduction in sorption hysteresis observed with PEG-treated wood, whereas untreated ancient oak shows increased sorption hysteresis [141]. Wood treated with a mixture of lactitol and trehalose also showed a reduction in sorption compared to untreated wood, except at RH levels in excess of 90%, as well as a marked reduction in hysteresis [142]. Two explanations can be given for the reduced moisture uptake at lower RH:

If the EMC is determined on the basis of the mass of the sample (e.g., wood plus consolidant) then even at the same level of moisture uptake as untreated wood a lower EMC will be recorded. In order to determine whether the reduction in EMC is genuine, it is necessary to determine the EMC on the basis of wood mass only (sometimes referred to as the reduced EMC).

If the PEG has entered the cell wall, there is a bulking effect and some of the cell wall volume is no longer available to accommodate sorbed water molecules. This property will depend on the extent of the penetration of the cell wall.

The reduction in hysteresis can be attributed to a plasticisation effect on the substrate caused by the consolidants in combination with the sorbed water. This will have the property of reducing the glass transition temperature of the wood cell wall matrix, resulting in a decrease in sorption hysteresis [143,144]; assuming that water molecules are able to penetrate the PEG-cell wall polymer void system. Higher MW PEGs do not enter the sound cell wall [145], but the extent of penetration of the pore structure of degraded wood by PEGs of different sizes is not known. Nanopores exhibit a partitioning effect on solutions of PEGs of different MW (and radius of gyration) and that changing the concentration of PEG in solution influences the radius of gyration [146]. Even if the cell wall pore structure of the cell wall of degraded wood was completely filled by PEG (which seems unlikely) the molecular dynamics of PEG in the wood would still allow for the transport of water molecules through the PEG network, including PEG in the cell wall voids. Furthermore, the changes in creep behaviour of wood afforded by impregnation with PEG (next section) suggest an intimate association between the PEG molecules and those of the degraded cell wall, a property that is also affected by the presence of sorbed water. The molecular dynamics of the interaction of PEG with cell wall polymers has been analysed using high resolution solid-state  $^{13}\text{C}$  NMR, showing that there is, indeed, an interaction between PEG and the cell wall polymers [147,148].



Wood samples treated with alum are not as sensitive to relative humidity as freeze-dried archaeological wood, since potassium alum and ammonium alum salts are not hygroscopic in the range 30–75% RH at 20 °C [95]. However, changes in RH levels can lead to stresses occurring between alum-rich and alum-poor zones in the treated wood, resulting in the degradation of wooden artefacts.

#### 4.3. Physical Properties

PEG impregnation results in a softening of wood, because the PEG acts as a plasticiser [149,150]. Creep deformation and support of large wooden structures treated with PEG is an issue that requires careful consideration [151]. PEG-impregnated wood exhibits much higher levels of creep compared to sound wood [152]. The easiest way of determining the elastic properties of wood is through the use of quasi-static loading, where the load is applied at a slow rate to avoid dynamic effects. For rare archaeological wood samples, it is better to use cubic wood samples loaded in compression within the elastic limit, allowing the material to be saved [140,153]. However, one problem with such an approach is that the evaluation of data from such experiments can be complicated due to sample inhomogeneity. Creep behaviour of large samples, such as planks, can be more representative, but requires large amounts of material, which may not be available. Ultrasonic testing methods are proving to be a rapid technique for determining elastic properties, but care is needed with the interpretation of results. Resonant ultrasonic spectroscopy (RUS) has been used to determine the dynamic stiffness of wood samples. A comparison of quasi-static compression and RUS performed on recent oak and oak obtained from the Vasa showed that the two techniques were complementary and allowed for the experimental determination of shear moduli and Poisson's ratios. Creep behaviour is affected by the ambient RH and temperature conditions and is especially sensitive to fluctuations in these conditions. Low MW PEG also has a melting point (17–22 °C) which is close to the ambient temperature of many museums and this can also affect behaviour. The effect of PEG impregnation on cell wall properties was investigated by using nano-indentation [154]. Wood cell walls of sound oak containing PEG were found to exhibit lower stiffness, indentation hardness and higher creep deformations compared to untreated wood. Furthermore, these properties were affected by the presence of moisture, with higher sensitivity found with the PEG-treated samples. These findings were based upon the EMC of the wood samples in total (dry wood mass plus PEG), rather than solely on the dry wood mass. The untreated samples of Vasa wood had slightly higher indentation hardness, stiffness and lower creep deformation compared with the sound wood reference samples. The reason for this was not explained, but is likely to be due to the increased relative lignin content and loss of the plasticising effect of the hemicelluloses, similar to thermal degradation [155]. The observed cell wall softening effect indicates that the PEG is able to plasticise the cell wall both through direct interaction and in the presence of sorbed water, showing that there is no discernable restraining effect of the PEG when located in the cell wall nano-pore space. In waterlogged wood which has been treated with PEG, it is often difficult to determine whether mechanical properties have been changed because of the presence of PEG, or due to post-conservation degradation of the wood. Sound wood which has been impregnated with PEG exhibits a decrease in modulus of elasticity (MOE), work to maximum load, work to proportional limit and compressive strength, properties that are also influenced by the moisture content of the treated wood [156].

#### 4.4. Degradation of Consolidated Wood

Although waterlogged wood exhibits degradation of the holocellulose content especially, further degradation post-conservation remains a possibility and the challenge then is to determine whether this is occurring, why it is occurring and what measures can be adopted to arrest this. The rate of oxygen consumption of a treated wooden artefact is an important determinant of its chemical stability after conservation [157]. Early investigations of this property used sawdust prepared from archaeological wood, but results from

such studies can be misleading, since the mechanical process used for the production of sawdust creates free radicals which affect the rate of oxygen consumption. It is important to use solid wood samples to determine the actual rates of oxygen consumption of wooden artefacts that would occur in the museum. A study of different conserved wood samples was unable to identify any single factor that was responsible for the varying rates of oxygen consumption between samples [157]. It was thought that the reaction most likely to be dominant was autooxidation of the wood polymers. Treatment of wood with hot alum solution to mimic the preservation of the Oseberg artefacts significantly increased the oxygen consumption of the treated wood [158], with the presence of iron salts enhancing the oxygen consumption further. The oxygen consumption of the Oseberg samples was found to be consistently higher than that of untreated wood. Treatment of wood with  $\text{FeCl}_2$  was also found to enhance oxygen consumption markedly, although co-addition of calcium chloride had a slight inhibitory effect. A model study of the effect of deposited sulphur and iron on the degradation of archaeological wood was undertaken by treating balsa wood with reduced iron and sulphur species which concluded that this approach was viable to study the degradation of archaeological samples [47].

The Swedish warship *Vasa* is a 1200 tonne displacement vessel, which is largely a self-supporting structure, requiring considerable structural integrity of the oak elements. In 2000, salt deposits were discovered on the wood surfaces, which were associated in part with the oxidation of sulphur compounds present in the wood [159]. Sulphur K-edge X-ray absorption near edge structure spectroscopy (XANES) showed that the sulphur in the preserved *Vasa* wood had oxidation states between 0 and +VI [160], with further oxidation leading to the generation of sulphuric acid/sulphates. Although most of the deposited salts are sulphates, some borates are also present which are derived from the original use of the antimicrobial boric acid/borax combination which was added to the spraying liquid used during the conservation treatment. The large amounts of iron compounds present originate from the different iron objects associated with the ship in service. In-situ, the sulphur and iron compounds in the wood were in a reduced form, due to the anoxic conditions in which the wreck was located. When the hull was reconstructed during the restoration process, a large number of epoxy or zinc-coated iron bolts were used to hold the structure together; many of which are now severely corroded. The iron compounds present in the wood were thought to be capable of catalysing various degradation reactions, including the oxidation of reduced sulphur to sulphuric acid, depolymerisation of cellulose and decomposition of PEG, via Fenton-type reaction pathways [60,81,161,162]. Iron and sulphur particles of various sizes and compositions are present in the surface regions of the wood and present within the cell walls, but there are fewer particles in the wood interior [163]. There is an increase in acidity deeper into the wood, apparently associated with a higher iron to sulphur ratio. Moreover, there is a decrease in the strength of the wood which is thought to be linked to oxygen exposure post-recovery [164]. Remedial action has been attempted by applying wet carbonate/bicarbonate poultices to some areas, or ammonia treatment which is of dubious efficacy [165,166]. However, the application of magnesium and calcium nanoparticles and calcium hydroxide nanoparticles from solvothermal reactions on the *Vasa* wood samples turned out more effective. The particles penetrated the cell walls and effectively neutralised the existing acids. The excess of their amount was converted into carbonate form, providing an alkaline reservoir that guarantees long-term wood de-acidification [167,168].

Henry VIII's flagship, the *Mary Rose*, faces similar problems since, for over 400 years, she was resting on a seabed under environmental conditions that promoted the formation of reduced sulphur compounds. Fe K-edge XANES spectra combined with micro-images obtained from S K-edge  $\mu$ -XANES analysis confirmed the presence of various iron and sulphur compounds at different oxidation levels in the *Mary Rose* timber, as in the *Vasa* case, and allowed to study their spatial correlations. To prevent wood degradation by the resulting formation of salts and acids, apart from neutralising the acidic environment by mixtures of soda and bicarbonate and removing iron ions using chelating agents, the

application of strontium carbonate nanoparticles is also considered. It could reduce the production of acid formation by reacting directly with sulphur compounds. The tests on small wood samples treated with PEG 200 confirmed the usefulness of this method, which offers hope for appropriate preservation of the endangered valuable shipwrecks [169,170].

Examination of the holocellulose content of wood from the Vasa using size exclusion chromatography showed that the outer 15 mm or so of the wood has a higher MW compared with the interior [160]. It was also found that the outer regions of the wood exhibited a higher tensile strength, which gradually decreased when progressing to the centre of the wood. This result was not expected given that the outer regions of the wood were subject to much higher levels of microbial degradation and also have the highest concentrations of PEG. Iron content was found to increase slightly when going from the exterior to the interior of the wood samples, whereas sulphur content was relatively stable. Significantly higher levels of acetic, formic, glycolic and oxalic acids were found in the interior of the wood, compared to the surface regions. It was noted that depolymerisation of the holocellulose content has not been found in never-dried Vasa wood and other wet-reference waterlogged archaeological wood samples. The oxalic acid is capable of depolymerising holocellulose and can be formed in Fenton-type reactions. Rather than simply considering the iron content it may be that the iron-sulphur ratio is important and it has been suggested that reduced organic sulphur species could function as antioxidants, but this was not observed in the reported study. It was hypothesised that the PEG was exerting some sort of protective effect in the surface regions. Although PEG in the surface layers (0–3 cm) of Vasa wood appeared to be undegraded, further into the wood the PEG exhibited signs of random depolymerisation, which was associated with high iron content. However, samples with higher sulphur to iron ratio did not exhibit degradation to the same extent. This was taken as evidence that the main degradation mechanism was not due to sulphuric acid, but rather an oxidative degradation process catalysed by iron, possibly a Fenton's reaction [61,171]. This hypothesis was tested by reacting holocellulose from undegraded oak and PEG-1500 with hydroxyl radicals generated in a Fenton's system (Fe(II)/H<sub>2</sub>O<sub>2</sub>) [161]. The results obtained with the PEG showed evidence of random chain scission, with alcohol, aldehydic and formate ester end groups, similar to what is observed with degraded PEG from the Vasa. Degradation of the holocellulose was also observed in the model studies and it was noted that exposure of cellulose to Fenton's reagent resulted in the generation of oxalic acid (among other species). This evidence was taken as supporting the hypothesis that Fenton's reactions were occurring within the conserved Vasa wood. Chemical characterisation of degraded waterlogged wood from ancient shipwrecks in the Roman harbour of Pisa showed the presence of high levels of calcium and iron, mostly associated with sulphates [172]. Higher concentrations of iron were associated with a lower degree of crystallinity of cellulose, which was thought to point to iron being a catalyst of random cellulose degradation, again suggesting Fenton's reactions. Studies of the excavated Mary Rose timbers show that the proportion of oxidised sulphur species declines from the surface to the interior of the wood and that the oxidation process was accelerated by the presence of iron [173]. Furthermore, oxidation of sulphur was occurring during the conservation process, in part promoted by the use of PEG solutions which were mediating redox cycling of the iron [113].

Iron sulphides will undergo oxidation reactions in the presence of high levels of humidity to produce hydrated iron sulphates and sulphuric acid, as well as natrojarosite (NaFe<sub>3</sub>(SO<sub>4</sub>)<sub>2</sub>(OH)<sub>6</sub>), or goethite ( $\alpha$ -FeOOH) [166,174] and the oxidation of iron pyrites to produce sulphuric acid is a very well-known phenomenon associated with mines [55]. The hygroscopic nature of the reaction products encourages further moisture sorption, which promotes the oxidative process. There appears to be a critical RH limit above which iron pyrite oxidation occurs, although there is some uncertainty where this limit lies [55]. The generation of sulphuric acid in conserved marine exhibits results in polysaccharide degradation and depolymerisation, although the lignin and remaining tannins remain relatively intact [175]. By contrast, an oxidative mechanism based upon a putative Fenton's

reaction, as proposed in several studies [161,164,176], would be non-discriminatory and would oxidise phenolic as well as polysaccharide content [177–179].

Aerobic oxidation of sulphur can be performed by bacteria, generating sulphuric acid [41,180,181] and acidophilic bacteria, which are capable of oxidising both iron and sulphur, have been identified in the unpreserved timbers of the Mary Rose and this bacterial community undergoes a change in the presence of PEG [113]. In acidic environments, the iron oxidising bacteria *Thiobacillus ferrooxidans* will accelerate the oxidation of  $\text{Fe}^{2+}$  ions [55]. It is also known that bacteria can degrade PEG [182]. Although bacterial oxidation may be a problem during the often extended period during which conservation takes place, the generally dry environments of museums in which the display of the objects occurs is probably unfavourable to bacterial activity.

There are now many studies underway to identify the best strategy for the removal of iron from the wood [183]. Iron can be removed by the use of chelating agents, such as ethylenediiminobis(2-hydroxy-4-methyl-phenyl)acetic acid (EDMA) [159]. Other suggested methods for iron removal prior to consolidation include electrophoresis [183] and microbial-mediated extraction [181,184]. Although soluble iron salts can be removed from waterlogged wood prior to conservation, iron sulphides are much more intractable [185]. An alternative approach is to accept the continued presence of iron and sulphur compounds, but prevent the ingress of oxygen by the application of a suitable gas-impermeable coating or envelope [55].

However, it has been suggested that removal of iron may not only be unnecessary, but may actually be damaging to the wood. The surface of the Vasa timbers has a higher concentration of iron, a higher pH and the cellulose has a higher molecular weight, compared with the interior of the timbers [176]. The interior of the wood has a lower pH, associated with a decrease in iron content, but an increase in oxalic acid concentration. These results are thought to indicate a reaction between oxalic acid and iron(III)oxides and iron(III)hydroxides to form iron(III)oxalato complexes. The observation that the iron content of the surface of the wood is greater than that of the interior contrasts with some studies [160,186], but is in agreement with others, e.g., [163]. The deposition of iron and sulphur in archaeological marine deposits is a complex process, involving microbiological and chemical mechanisms, depending on local site conditions and may also be different in different wood species [187]. A study of the lignin in the timber of the Vasa used thioacidolysis in combination with gas chromatography-mass spectroscopy in order to determine  $\beta$ -O-4 bonds and syringyl/guaiacyl ratios [188]. No major differences were observed between the lignin of fresh oak samples and that of PEG-treated oak from the Vasa. The lack of any significant degradation of the lignin was taken as evidence that the degradation of the cellulose could not be via an oxidative mechanism involving iron, but rather through the action of sulphuric acid. The lack of tannin in the Vasa oak also indicated that polysaccharide degradation was not mediated by any iron-tannin oxidative process, which is a known mechanism in oak-gall inks.

The rate of corrosion of iron in PEG-400 solutions is dependent upon the concentration of the polymer in the water. The corrosion of iron fasteners in wood can be described in terms of crevice corrosion theory, where one end of the fastener acts as a cathode and the end which is embedded in the wood as an anode. In the presence of oxygen,  $\text{Fe}^{2+}$  ions are liberated at the anodic end of the fastener, where they react to form iron peroxide ( $\text{FeOOH}$ ). The corrosion of metal fasteners is also affected by the presence of ions such as chloride. The issue of corrosion of iron fixings in archaeological wood that has been treated with PEG has been addressed by the use of corrosion inhibitors [189]. It is known that iron catalyses the oxidation of sulfur in the presence of PEG at 100 °C, but whether this would be an issue at room temperature is uncertain [190]. Oxidation of PEG is accelerated by the presence of hydrogen peroxide and trace metals with the concomitant formation of formic acid, whereas acidic pH promotes the generation of acetaldehyde and acetic acid [191]. PEG is known to strongly bind to iron oxide nanoparticles [192].

A high level of degradation of wood, evidenced by low levels of polysaccharide and extensive lignin oxidation was found in alum-treated wood samples from the Oseberg find, whereas the untreated wood from the timbers of the ship was found to be in good condition [67,95]. A combination of dissolution and derivatization was employed to study the chemical composition of wood in the Oseberg collection, using NMR, gel permeation chromatography (GPC) and pyrolysis coupled with gas chromatography and mass spectrometry (Py-GC-MS) [67]. The study showed that there was an increase in the carboxylic group content of the lignin, an almost total loss of hemicelluloses and significant cellulose depolymerisation, as well as the presence of monomeric sugars in the alum-treated samples. Lignin oxidation products include vanillin, syringaldehyde and syringic and vanillic carboxylic acids, found at much higher levels than encountered in sound wood. The main polysaccharide degradation products are composed of anhydrosugars. The alum-treated woods have been slowly degrading since the time of treatment and are now extremely fragile. The various iron items associated with the finds have also been corroded.

Other techniques for examining the extent of degradation of post-treated wood include evolved gas analysis mass spectrometry (EGA-MS) and a pyrolysis method coupled with gas chromatography and mass spectrometry with in situ silylation (Py(HMDS)-GC/MS), which appear promising providing more detailed information about both the degraded wood and the consolidant [193].

## 5. What Research Has Been Performed and Future Perspectives

Since polyethylene glycol has turned out to be detrimental to wooden artefacts in the long term, a need to find a new, more reliable alternative to preserve newly excavated waterlogged wooden objects has emerged. There is also an urgent necessity to search for solutions that would enable re-conserving the fragile artefacts degraded by the previous treatment (such as Viking artefacts from the Oseberg find or the Vasa ship), effectively strengthening their structure and maintaining them for posterity.

There are three different approaches to these problems. One of them is biomimetics, based on the idea of learning from nature and employing the solutions used and proven effective in nature. In the case of wood conservation, it involves the application of natural materials with hierarchical structure and structural functionalities such as natural polymers (polysaccharides, proteins and their derivatives) to reinforce the degraded wood tissue and simultaneously provide it with stability and flexibility. They are non-toxic, renewable and reduce environmental impact, and are stated to be a “green” alternative to polyethylene glycol. Another approach is to use synthetic polymers with structural properties that mimic natural materials but are much more durable. Finally, the third way is to develop multi-component conservation systems tailored to multiple needs of wooden objects, e.g., providing simultaneous consolidation of the wooden tissue, protection against biodegradation and deacidification.

### 5.1. Sugars and Sugar Alcohols

Sugars have been tried for wood preservation since the early 1900s. They can effectively protect wood against decay and reduce wood shrinkage and swelling. However, the treated wood becomes damp and sticky under humid conditions [194]. Since they are cheap, non-corrosive, non-toxic, non-volatile, easily soluble in water (which enables reversibility of the treatment by soaking/rinsing with water) and compatible with the size of the pores in the wood, they also found application in the conservation of waterlogged wooden artefacts in the early 1970s. Since that time, their use has been developed and thoroughly studied [97,195].

#### 5.1.1. Sucrose

Sucrose (a disaccharide composed of glucose and fructose) was the first sugar applied for the consolidation of waterlogged wood, including small laboratory samples and large artefacts such as boats and ships [97,195,196]. The impregnation procedure starts with

soaking wood pieces in a 5% or 10% aqueous sucrose solution. The concentration is incrementally increased by 5% or 10% until the object reaches equilibrium with the previous solution (or in one- or two-week intervals) [97,126,195]. To increase the stabilisation effectiveness, freeze-drying is suggested following the impregnation. There are two sucrose methods: “cold” at room temperature and “warm” when the solution is heated up to 60 °C. The “cold” method is considered the cheapest conservation treatment for large artefacts and is still in use. In contrast, the “warm” method is not recommended since it often results in the decomposition of sucrose into a non-crystallisable monosaccharide mixture that decreases its consolidation effectiveness [97]. Stabilisation results of the treatment are relatively satisfactory—depending on the wood species and the degree of wood degradation, ASE reaches 81–100% after freeze-drying and 47–98% after air-drying (average ASE is about 75%—laboratory tests on small samples) [126,195,197]. However, highly degraded wood tends to warp and collapse due to the treatment and cannot be stabilised sufficiently. In this case, for small artefacts, post-impregnation freeze-drying can increase the treatment effectiveness, but for larger objects, PEG-treatment is recommended instead. In turn, the sucrose method is mainly recommended for bigger and less delicate artefacts for economic reasons [196].

Sucrose can effectively penetrate wood tissue and crystallise within the cell lumina (its penetration capabilities are similar to PEG 300 or 400). It can also bulk the cell walls due to the small size of its molecules. As a result, it can effectively preserve the shape of individual cells. Sucrose presumably interacts with hydroxyl groups of the remaining cellulose and other wood polymers, thus reinforcing the cell walls. It was stated by the author that the reduction in hygroscopicity was due to the blocking of the wood hydroxyl groups [195]. However, since sucrose contains many OH groups, this would not provide an explanation; moreover, the role that OH group concentration has to play in determining sorption properties in wood is not fully understood [155]. Rather, the reduction in hygroscopicity can be attributed to the extra weight due to the added sucrose plus the bulking effect of the sucrose in the pore space of the wood, which is then no longer available for water molecules.

The aesthetic appearance of sucrose-treated wood is generally acceptable [195]. Sometimes the wood darkens, and white crystals or a brown sticky film appear on its surface [126,197]—the latter results from the degradation of the conservation solution by microorganisms [126]. Sucrose solutions are highly susceptible to microbial attack and prone to fermentation, losing their conservation effectiveness. Therefore, the addition of an efficient biocide and careful monitoring of the biocide concentration during the whole impregnation process is necessary [97,126,195,196]. Additionally, the pH of the solution should be adjusted to 7–9, and the bath temperature should not exceed a temperature of 60 °C [97].

The sucrose method also has other drawbacks. This sugar undergoes hydrolysis over time and reabsorbs moisture. Under high humidity conditions exceeding 70–80%, it can leach out from wood, which leads to unaesthetic crystallised deposits on the wood surface and poses a threat of disintegration to unprotected wood due to swelling and shrinkage under humidity changes [97,126,195,197]. Additionally, the treated artefacts require protection against rodents and insects [97,195].

One of the methods to employ sugars in waterlogged wood conservation and eliminate the flaws of sucrose is the application of non-reactive sugars that cannot undergo hydrolysis, such as sucralose, trehalose or sugar alcohols: lactitol, mannitol, sorbitol, xylitol (or mixtures thereof).

#### 5.1.2. Sucralose

Sucralose (a disaccharide composed of 1,6-dichloro-1,6-dideoxyfructose and 4-chloro-4-deoxygalactose) is relatively unreactive compared to sucrose due to the replacement of three hydroxyl groups with chlorine atoms. As confirmed by Kennedy and Pennington [197], its effectiveness in stabilising waterlogged wood dimensions is comparable to

sucralose. The advantage of using this sugar is its long-term stability and better performance at lower concentrations. The impregnation of chemically degraded white birch tongue depressors with 60% sucralose solution (started at 15% and increased by 15% each week) followed by air-drying resulted in the ASE of 63.2% (for sucrose, it was 59%). However, the treated samples were warped and twisted to some degree (which was not seen for samples treated with sucrose and trehalose). This probably results from the substitution of three hydroxyls with chlorine atoms in the sugar molecule that provides sucralose with its stability but also limits its reactivity with wood polymers, thus reducing its reinforcing abilities. On the other hand, the stabilisation effectiveness of sucralose is high. This suggests that the mechanism of stabilisation is different than for sucrose or trehalose and that hydrogen bonding does not play the main role in it.

Considering twisting and warping observed for thin samples, the method is not yet recommended for conservation practice until more knowledge is gained on the effect of sucralose on the structure and mechanical strength of treated wood. It is also worth mentioning that the use of aqueous solutions of sucralose is limited by its solubility. At 60% (*w/v*), sucralose solution is saturated, so it is impossible to use higher concentrations without heating the solution [197].

### 5.1.3. Trehalose

Trehalose is a disaccharide composed of two glucose units joined by a 1–1 alpha bond. Similarly to sucrose, it is relatively unreactive; however, its anhydrous form readily regains moisture to form the dihydrate. Impregnation with trehalose is considered a viable method for waterlogged wood conservation. It is much faster, safer and less expensive than other methods, completely reversible and appropriate even for heavily degraded wood [97,197]. It provides long-term and spectacular stabilisation effects with cross-sectional wood shrinkage below 2% (the ASE values for different wood samples ranged between 86.2 and 98.6%) [97,197–199]. The method, instead of slow air-drying or freeze-drying, uses fast forced air-drying. This is possible because large amounts of trehalose crystallise inside wood tissue immediately after impregnation. The crystallisation removes about 11% of water, turning it into crystal water in the trehalose dihydrate that fills wood tissue. This provides a stabilisation effect to the degraded structure before the actual drying begins. The trehalose crystals prevent the collapse of the cell walls, thus protecting wood against shrinkage, distortion and cracking. Because the strengthening happens first, fast-drying can be applied as the next step, which reduces the conservation time and costs without losing the stabilisation effectiveness [97].

Two types of trehalose methods are used: “cold” and “warm”. The “cold” method is performed at an ambient temperature, with maximum trehalose concentration not exceeding 41%, which is not enough for efficient stabilisation of highly degraded wood. Therefore, this method is recommended for low and medium degraded artefacts. The “warm” method uses higher temperatures (up to 85%) and much higher trehalose concentration (up to about 90%), usually using a stepwise approach as in the methods mentioned above. It is the fastest among all conservation methods available and suitable for wood at all levels of degradation [97].

Trehalose-treated samples have lower hygroscopicity compared to untreated wood (3.9–4.9% vs. 6.9–7.5% for untreated wood) [199]. Their mechanical properties are generally improved, including the modulus of elasticity and the maximum load of samples in the bending test; however, the samples are more brittle than treated with xylitol [199,200]. The treated wood is often slightly darker in colour; its surface can be sometimes covered with a varnish-like coating or crystalline deposits, which can be easily removed with a damp tissue or gentle brushing [12,197,198]. It was shown that sugar crystals fill the cell lumina of fibres and parenchyma cells, leaving the vessels’ lumina empty [198].

#### 5.1.4. Lactitol

Lactitol is chemically more stable and less hygroscopic than sucrose. It is resistant to higher temperatures and alkaline conditions, less susceptible to microbial attack and fermentation, and can be easily removed by dissolving with water providing a reversible treatment. Lactitol-treated wood is not attacked by termites [97].

Similarly to the sucrose and trehalose treatments, there are two methods of wood impregnation using pure lactitol: “cold” and “warm”. The “cold” method is performed at an ambient temperature, with lactitol concentration up to 50–55%. The “warm” impregnation is faster than the “cold” one. It involves higher temperatures (between 50 °C and 80–85 °C), and the concentration of lactitol is limited to 75% at 50 °C, and 85% at 80 °C. Due to the concentration limit, the “cold” method is not suitable for the conservation of highly degraded wood, while the “warm” method is appropriate for wood of all degradation types. It must be remembered that at ambient temperature, pure lactitol tends to crystallise into lactitol trihydrate with large crystals, which would damage the fragile structure of degraded wood. Therefore, to avoid it, wood treated with this sugar has to be dried at 50 °C to promote the formation of much smaller and harmless lactitol dihydrate crystals and provide wood with the expected stabilisation effect [97].

For economic reasons, wood impregnation with a mixture of lactitol and 10% trehalose was proposed: the addition of trehalose prevents the formation of lactitol trihydrate crystals during drying, therefore more cost-efficient air-drying instead of drying at 50 °C can be used. Conservation with this method can be performed at both ambient temperature or using temperature in the range of 50 °C to 80 (85) °C (maximum lactitol concentration at 50 °C is 80% and about 90% at 85 °C). The former method is suitable for low and medium degraded wood, while the latter is applicable for all woods despite the degree of degradation [97]. This method effectively reduces wood shrinkage upon drying (cross-sectional ASE for the treated subfossil waterlogged Scots pine samples was 95%, and for waterlogged oak and beech specimens, it was 91–109%) [131,142,201]. It also significantly decreases wood EMC and sorption hysteresis compared to PEG-treated wood. At high air relative humidity, no abnormal increase in equilibrium moisture content (EMC) is observed like for PEG-treated wood, which increases wood safety when exhibited [142]. The method increases the elastic behaviour of treated wood while the loss factor remains unchanged. However, the increased stiffness of the treated wood together with the reduced strength of highly degraded wood, may pose a risk to the artefact’s integrity. Therefore, the treatment is generally recommended mainly for small and medium-size objects with a low to moderate degree of degradation [202].

#### 5.1.5. Mannitol and Sorbitol

Mannitol and sorbitol were used to impregnate oak samples from the Mary Rose as a potential alternative to trehalose treatment. The samples were soaked in 5, 10 and 20% solutions of individual sugars for one week and then freeze-dried. The best stabilisation effects were obtained for 20% sorbitol solution, resulting in volumetric wood shrinkage of 5.3% and ASE of about 70% (trehalose treatment resulted in 50% ASE). Impregnation with mannitol was less effective, giving wood shrinkage of 12.5% and ASE of 30%; additionally, it left a white crystal covering on the wood surface. The consolidating performance of sorbitol suggests that this method can be more cost-efficient than other sugar-based treatments, shortening the treatment time and reducing the amount of a conservation agent used [12].

Mannitol was also applied to waterlogged wood in a mixture with trehalose. The stabilisation effects were similar to those obtained using lactitol/trehalose mixture, with ASEcs (cs—cross-sectional) reaching 81–103%. Under typical exhibition conditions (RH of 50% and the temperature of 18 °C), the treated wood absorbed less water than wood untreated or treated with lactitol/trehalose mixture [131,201].



### 5.1.6. Xylitol

Xylitol treatment was tried on chemically degraded wooden tongue depressors. The concentration of 40–60% (*w/v*) effectively reduced wood shrinkage (volumetric ASE of 103–106%) without altering wood hygroscopicity and improved its mechanical properties (increasing the maximum load of samples in the bending test). However, the treated wood was prone to fungal degradation. The treatment was more effective than trehalose and lactitol impregnation performed on similar samples [199].

Although the tested sugars generally performed well and some of them have also been applied in conservation practice, extensive research is still required on their long-term stability and the properties of the treated wood before these methods could be proposed as a safer alternative to PEG treatment.

### 5.2. Proteins

Proteins are molecules that, *inter alia*, provide structure to animal cells and organisms. Therefore, they can be considered as potentially useful also for the stabilisation of degraded waterlogged wood.

Proteins have been tried for wood conservation since the beginning of the 2000s. The most promising results were obtained using feather keratin. Keratin belongs to fibrous structural proteins known as scleroproteins and is the main structural component of vertebrate epidermis, hair, nails, horns, feathers, claws, hooves. It is insoluble in water and organic solvents. To apply keratin as a conservation agent, a stable solution is required; therefore, it is usually hydrolysed (using sodium hydroxide) before application on wood. Keratin reduces the surface tension of aqueous solutions. Its pH is 6–7 [203–205].

The best stabilisation results were obtained with hydrolysed duck feather keratin at a final concentration between 30 and 40% (impregnation carried out by stepwise increased concentration, similarly to sugar methods). The higher concentration is not recommended due to the excessive wood swelling leading to its cracking [203]. Depending on the wood species and the degree of wood degradation, ASE between 63.6% and 107.7% was obtained. The treatment turned out to be more effective for less degraded wood [198,203–206]. Goose and chicken feather keratin were less effective in wood stabilisation: the anti-shrink efficiency of 90% and 87.2% were obtained, respectively. It was presumably due to their lower crystalline index and the weaker anti-alkali structures compared to duck feather keratin [203]. To integrate keratin and increase the effectiveness of the treatment, the impregnation was further modified by adding a divalent metal salt (magnesium sulfate) at the end. The obtained results were better than without salt, with ASE over 89%, but for highly degraded wood still not satisfactory—ASE was only 72% [198].

The stabilisation mechanism of keratin is different from PEG [207]. Solid keratin substance has a density similar to the density of the cell wall material (about 1569 kg m<sup>-3</sup>). Its molecules are small enough to quickly diffuse into the wooden tissue and penetrate the cell wall. Keratin adsorbs on the middle lamella, thus reinforcing the cell wall structure and preventing its collapse [198,204,205,207,208]. The remaining open-cell lumina allow for potential retreatment of the samples if necessary [198,207]. The reinforcement of the cell wall translates into improved wood mechanical properties—it was shown in a flexural test that the feather keratin treatment recovers anisotropy of waterlogged wood, as well as the correlation between modulus of rupture (MOR) and modulus of elasticity (MOE) [207].

Keratin treatment maintained the wood colour almost unchanged [198,204,206,207]. The antimicrobial activity of the keratin solution ensured its long-term stability without the addition of any biocides; it also protected the treated wood against bacteria (*E. coli*) and moulds (for more than a year at ambient temperature and moisture content) [204,207]. The treatment also increased wood resistance to UV radiation [204].

However, the keratin-treated wood was highly hygroscopic. Its moisture content and level of swelling were considerably higher than that of PEG-treated samples, which poses a risk of cracking to the wooden object under changeable moisture conditions [207].

Since keratin does not have well defined eutectic temperature, it is not suitable as a pre-treatment followed by freeze-drying [205]. The results by Fejfer et al. [123] confirm much lower stabilising effectiveness of the keratin treatment combined with freeze-drying (ASEtangential about 56%, ASEradial about 46–48%) compared to air-drying (ASEtangential between 30 and 64%, ASEradial between 45 and 85%).

The results obtained so far point out that although the feather keratin treatment can be considered a promising waterlogged wood consolidation method, it should be improved before it can be proposed for practical use. It is not appropriate for the conservation of heavily degraded waterlogged wood, but may be applied as a bulking or stabilisation agent for better-preserved, non-collapsible wood [205]. Interestingly, the method was effective in the conservation of a fragile archaeological waterlogged polypore (about 2600 years old), found at the Neolithic site of Kitashirakawa in Kyoto, Japan [209]. Further research is needed, e.g., on the influence of keratin molecular mass on its stabilising effectiveness, potential additives to improve consolidation of degraded wood, as well as health and safety aspects of keratin's application [205,208].

Hydrolysed silk fibroin has been tried for waterlogged wood stabilisation, although it effectively reduced wood shrinkage, it turned out to be inapplicable due to the low stability of the solution and its tendency to settle even at a concentration of 10% [204].

### 5.3. Cellulose and Its Derivatives

Cellulose is an easily available natural linear polysaccharide composed of hundreds or thousands of  $\beta(1\rightarrow4)$  linked D-glucose units. It is the most abundant polymer in nature and one of the main components of the wood cell wall, which provides it with strength and rigidity. Therefore, different forms of cellulose and its derivatives seem the obvious choice while looking for a consolidation agent for degraded waterlogged wood.

A 5% aqueous suspension of bacterial nanocellulose (nanospheres) obtained by agro-alimentary waste fermentation effectively stabilised dimensions of different waterlogged archaeological hardwoods (ASE of 80–88%), but their effectiveness was more variable for waterlogged softwoods (ASE of 55–94%). The particles penetrated wood tissue, filled most of the cell lumina and formed a compact layer on the cell walls, but their consolidating effects were not satisfactory. The conservation suspension tended to precipitate during impregnation and required constant stirring to prevent this. Despite this, an unaesthetic layer of nanocellulose particles on the wood surface remained after the treatment, but it was relatively easy to remove by gentle brushing. The treatment resulted in yellowing or whitening of wood, which can presumably be avoided by adding an appropriate pigment to the solution. The EMC of the samples remained almost unaltered [210].

Cellulose nanocrystals were less effective than bacterial nanocellulose, giving an ASE in the 37–84% range. They penetrated only about a millimetre inside the wood tissue and coated the cell walls, leaving the cell lumina empty. The impregnation solution turned into gel after a week of treatment, which resulted in the formation of a gel coating on the wood surface (easy to remove by brushing). The colour of the treated samples was similar to the untreated control, and the EMC remained almost unaltered [210].

Wood impregnation with nanocellulose whiskers (rod-like nanoparticles) encountered similar problems with wood penetration and precipitation in the conservation solution. However, it showed that such particles can adhere well to the wood surface and can act as gap-fillers enhancing wood stabilisation [211].

The results of the experiments using different forms of cellulose point to the conclusion that perhaps a better wood stabilisation could be obtained by combining nanoparticles of different shapes—spherical with filamentous ones. This should help fill the voids of different sizes and shapes in the cell walls and create an internal cellulosic network to stabilise the degraded wood. However, the improvement of cellulose penetrability is required first, which could be achieved by adding some surfactants, such as salts or PEG, or by chemical modification of hydroxyl groups present on cellulose particles. Research is also needed to prevent the precipitation or gel formation by nanoparticles in the solution.

It would be highly undesirable to use cellulose whiskers that are produced using sulphuric acid digestion, because the obtained cellulose would be sulphated, and its application as a wood consolidant would result in the same problems we face today with sulphur compounds present in waterlogged artefacts such as Vasa or Mary Rose [210,211].

Crosslinkable cellulose ethers (allyl cellulose, allyl carboxymethyl cellulose, and allyl n-hydroxypropyl cellulose) were also tried for waterlogged wood stabilisation. They were able to penetrate wood samples but only to a limited extent, probably due to the high molecular weight of the ethers or their aggregates present in the conservation solution or due to the limited impregnation time (20 days). The tested cellulose ethers exhibited a high affinity to lignin (the main component of degraded waterlogged wood), but due to crosslinking, the treatment turned out to be irreversible (in contrast to commercial sodium carboxymethyl cellulose, where high reversibility was obtained). Further research is required to improve the effectiveness of this method and evaluate the wood properties treated with cellulose ethers [212]. Klucel (hydroxypropyl cellulose, commonly applied in wood conservation [213]), however, was quite effective in stabilisation of wood dimensions and strengthening its structure, but was also not able to fully penetrate waterlogged wood samples. The EMC of the treated wood was similar to untreated. Optimisation of the conservation process is required, as well as studies on the long-term performance of treated wood [92,214].

Recently, two other cellulose derivatives potentially useful in waterlogged wood conservation have been synthesised and studied: 6-deoxy-6-( $\omega$ -aminoethyl) amino cellulose AEA-1' and its alkyl derivative 6-deoxy-6-( $\omega$ -hydroxyethyl) amino cellulose HEA-1'. The molecular mass of their monomers is in a range of 3.3–5.5 kDa, and they exhibit a protein-like self-associative behaviour. These properties make them suitable to penetrate the degraded wooden tissue and aggregate inside it into larger structures, thus strengthening it and providing stabilisation. The self-association of the chemicals can be partially reversible, which would facilitate the removal of at least part of the polymer from the wood if necessary. The research on the performance of waterlogged wood treated with amino cellulose is in progress [215].

#### 5.4. Lignin and Its Derivatives

Lignin is a natural polymer composed of cross-linked phenolic precursors. It is the second most abundant polymer in the world and a component of the wood cell wall where it provides structural rigidity. Due to its high chemical and biological resistance, it is often the major ingredient remaining in the degraded waterlogged wood and an object of interest as a potential consolidating material.

Lignin nanoparticles obtained from beech wood by the non-solvent dialysis method were used to consolidate different waterlogged wood species. They exhibited only low to moderate stabilisation effectiveness with an ASE of 51–88%. They precipitated at the bottom of the conservation solution, and despite the constant stirring during impregnation, they deposited on the wood surface. The particles were easy to remove by brushing. However, after drying, they were still present on the surface as a fine brown powder, and the colour of the treated wood changed to dark brown. The penetration ability of lignin nanoparticles was poor (about 1 millimetre inside wood tissue), probably due to their hydrophobicity and a tendency to aggregate. They coated the cell walls and filled the cell lumina in the external parts of the treated samples. The equilibrium moisture content of the treated wood remained almost unchanged. A careful selection of lignin sources could help obtain particle colours that match the colour of the treated wood. The impregnation conditions require changes that prevent the precipitation of lignin nanoparticles and facilitate their penetrability into the wood structure [210].

To increase the potential of interactions with wood polymers, different lignin derivatives were synthesised and applied to waterlogged wood. Lignophenol (a polymeric lignin derivative isolated from wood) showed good stabilisation effectiveness for wood differing in the degree of degradation due to hydrophobisation of the cell walls. It also

significantly increased wood hardness in comparison with PEG4000-treated samples [216]. Lignin-like oligomers synthesised from isoeugenol in a 10% ethyl acetate solution fully and evenly penetrated small waterlogged wood samples (1 cm<sup>3</sup>) and coated the cell walls; this shows the potential of these dehydrogenated polymers as consolidants [217]. An in situ polymerisation of isoeugenol monomers inside waterlogged wood has also been tried. It involved wood impregnation with the isoeugenol monomer via bulk addition, and then adding horseradish peroxidase and H<sub>2</sub>O<sub>2</sub> to start polymerisation reactions. As a result, a polymer structure rich in the chemically stable  $\beta$ -5' moiety was formed inside the wood tissue, effectively consolidating wood samples so they could be handled and cross-sections for microscopy imaging could be cut out from them [218]. The preliminary results of these protocols are promising and further research on the consolidation ability of isoeugenol and its derivatives and long-term stability of the treated wood is planned [217,218].

Lignin-silicon hybrids obtained by the reaction of allylated lignin with poly(dimethylsiloane) hydride terminated on both the ends of the silicone chain through a hydrosilylation reaction in the presence of the Karstedt's catalyst were applied to oven-dried waterlogged wood. The impregnation resulted in the increased hydrophobicity and chemical durability of the treated wood. However, the applied chemicals deposited mainly in the external parts of wooden samples, preventing their further penetration into wood tissue. The penetration was also impeded by the steric hindrance of the platinum catalyst necessary in the reaction. The limitations of the proposed conservation method make it hardly applicable for waterlogged wood conservation, but perhaps it could be useful for the consolidation of already dry historical wood. Further study is required to improve the penetrability of the solution and the stabilisation effectiveness of the treatment [219].

### 5.5. Chitosan and Guar

Chitin, a natural mucopolysaccharide consisting of 2-acetamido-2-deoxy- $\beta$ -D-glucose linked by  $\beta$ (1 $\rightarrow$ 4) bonds, is the main component of arthropod exoskeletons. It is the same as cellulose with only a hydroxyl group replaced by an acetamido group. Chitosan is the N-deacetylated derivative of chitin, renewable, biodegradable and non-toxic. Due to its structural functionality, similarity to cellulose, better compatibility with wood than synthetic polymers, and proven antifungal and metal chelating properties, it seems to be a promising multifunctional and "green" consolidant for waterlogged wood conservation [220–223]. The results show that low concentration chitosan solutions (1–2%) can penetrate waterlogged wood tissue (more easily when it is depolymerised) and strengthen it without altering the natural relaxation behaviour of wood, leaving the wood structure open for potential further re-conservation. Chitosan of varying degrees of polymerisation and deacetylation and its tert-butyl dimethylsilyl derivative were also tested as potential consolidants for the already dry degraded archaeological wood giving promising results for future application on fragile alum-treated artefacts such as those from the Oseberg finding [224,225]. Further tests are required on the stabilisation effect of chitosan, as well as the long-term stability and other properties of chitosan-treated waterlogged and archaeological wood [211,220,221,225].

Promising results were also obtained for guar gum. Guar gum is an exo-polysaccharide composed of galactose and mannose, known for its thickening and stabilising properties. Tested as a consolidant for waterlogged wood, it exhibited good penetration ability, great compatibility with wood, and strengthening properties even at a low concentration (only 1%), which illustrates its potential in waterlogged wood conservation [221].

An innovative multi-component supramolecular conservation system based on guar and chitosan has been developed to address three primary needs of waterlogged archaeological wooden artefacts: structural instability upon drying, susceptibility to biodegradation and vulnerability to chemical degradation caused by Fe<sup>3+</sup>-catalysed acidification. Guar and chitosan are safe polymers that provide structural support and do not form acidic by-products on degradation. Chitosan has antimicrobial properties and reactive amino groups available for further functionalisation, while guar can be functionalised through

the diol unit. Guar was enriched with a boronic acid functionalised viologen derivative that provides it with strong biocidal activity. Chitosan was functionalised with naphthol and catechol (the latter enables metal–ligand interactions with  $\text{Fe}^{3+}$  ions). To link polymers, the host–guest chemistry of cucurbit [8] uril was employed. As a result, a dynamic spatial polymer network was formed with three parallel functionalities: structural support (chitosan and guar cross-linked by cucurbit [8] uril), removal of  $\text{Fe}^{3+}$  ions (siderophore activity of catechol) and resistance to biodegradation (chitosan, boronic acid functionalised viologen derivative). The system was tested on degraded waterlogged archaeological oak and was effective in all its three activities (shrinkage reduced to 30% compared to 50% of untreated wood). Although further study on this innovative and reversible system is required, it seems to be a reliable, greener alternative to the methods being in use in the conservation of waterlogged wooden artefacts [226].

### 5.6. Oligoamides

Following the trend of using more “green” compounds, three different water-soluble hydroxylated oligoamides with a chemical structure similar to the main wood polymers were synthesised and tried as consolidants for waterlogged wood: polyethylene-L-tartaramide, polyethylene-D(+)-glucaramide, polyethylene- $\alpha,\alpha'$ -trehaluronamide. They showed high affinity to lignin, usually the main polymer that remains in degraded wood, and good penetrability into wood tissue (much better than cellulose derivatives). They reduced hygroscopicity of the treated wood and reduced wood shrinkage compared to untreated samples (volumetric shrinkage was between 39 and 49% compared to 60% for untreated wood, and the ASE was 18–35%). Although the dimensional stabilisation by oligoamides was beyond the level required by conservation practice (ASE of at least 75%), the chemicals are considered of great interest for the development of the new generation of consolidants waterlogged wood [227].

Experiments that involved four different oligoamides (oligo ethylene-L-tartaramide, oligo esamethylene-L-tartaramide and copolymer between ethylenediamine, adipic and tartaric acids, and allyl  $\alpha,\alpha'$ -trehalose/vinyl alcohol copolymer) applied on waterlogged oak and ash showed their high affinity for lignin, good penetration into wood tissue and effectiveness in the reduction in wood shrinkage upon drying compared to untreated samples. The effectiveness was higher for more degraded ash samples due to its higher porosity, and thus higher permeability for high-molecular consolidants. Oligoamides exhibited higher reversibility than allyl  $\alpha,\alpha'$ -trehalose/vinyl alcohol copolymer [228].

### 5.7. Other Natural Compounds

There is an extensive list of natural substances that have been used to consolidate waterlogged wood. Wood tar and waxes are some of the examples used in the past to protect wooden objects. Beeswax, carnauba wax and paraffin are sometimes still used for small and fragile artefacts and wood/metal composites [127]. The application of other natural compounds is described below.

Colophony is a natural resin obtained from pines and other conifers. It consists mainly of abietic acid (silvic acid), and is commonly used in adhesives, varnishes and sealing wax production. Rosin is chemically modified (esterified) colophony (ester of pentaerythritol).

Colophony and Rosin are applied to waterlogged wood as acetone solutions. This enables the quick distribution of the consolidant inside the wood tissue and reduces drying time. Retention of consolidants is high (weight percent gain at least 70% *w/w*, higher for colophony than its derivatives—a linear relationship was found between the level of retention and molecular weight of consolidants), and the more porous the wood is, the higher the consolidant retention. The consolidants easily penetrate wood tissue. They do not fill all the cell lumina (the largest remained empty) but efficiently encrust the cell wall, thus increasing its volume and strengthening the wood structure. As a result, the shape and dimensions of the treated samples are well maintained, no splitting or cracking is observed. To obtain a more natural colour of treated wood (not too dark), McKerrell et al. proposed

pre-treatment with dilute hydrochloric acid followed by impregnation with rosin in acetone solution [229]. The equilibrium moisture content of the colophony-treated wood remains comparable to that of untreated wood, but treatment with Rosin significantly reduces it. This helps to maintain a good stabilisation effect despite humidity variations and reduces the risk of fungal infestation. Due to the larger size of the molecules and chemical reactivity, Rosin seems more effective in consolidating severely degraded wood. The treatment is appropriate for both softwoods and hardwoods [92,128,229–231]. However, it must be remembered that, similarly to PEG, rosin has a significant plasticising effect on wood. Therefore it seems more suitable for smaller artefacts that do not have a load-bearing function. As a natural substance, rosin is susceptible to ageing, and becomes more brittle in time [202]. The reversibility of colophony/rosin treatment is questionable [58].

Following the trend of searching for bioinspired consolidation materials, recently a new polyhydroxylated monomer was synthesised from  $\alpha$ -pinene (a terpene derived from coniferous trees) and used to obtain a TPA5 polymer through free radical polymerisation. The polymer has an elongated shape, a low molar mass (about 4.5 kDa on average) and a great potential for hydrogen bonding (e.g., with wood polymers and other polymers), which makes it potentially interesting as a consolidant for waterlogged wood [232].

### 5.8. Halloysite Nanotubes

Another approach is the application of Halloysite nanotubes. Halloysite is a natural aluminosilicate clay mineral. Its dominant form is hollow nanotubes (small cylinders) about 0.5–10  $\mu\text{m}$  long, with an inner diameter of 10–60 nm and an outer diameter of 50–300 nm. Nanotubes are made of aluminosilicate sheets rolled up into a layered structure, with an interlayer distance of 0.6 or 1 nm depending on the hydration state of the mineral. The external surface is composed mainly of  $\text{SiO}_2$  and negatively charged, while the inner surface, consisting of  $\text{Al}_2\text{O}_3$ , is charged positively. This allows for the selective modification of inner and outer surfaces with different substances, making Halloysite nanotubes suitable carriers for the sustained release of active molecules and reinforcing fillers for various polymers. Hence the idea to try them as consolidants for waterlogged wood [233–235].

Halloysite nanotubes were mixed with beeswax in acetone and used to consolidate waterlogged wood samples (*Pinus pinaster* Aiton) from the ship Chretienne C (II century, BC) discovered off the coast of Provence. The samples were first dehydrated in acetone, then immersed in the consolidation mixture for three days under magnetic stirring and air-dried. The consolidation resulted in reduced volumetric shrinkage of wood samples from 40.6% for untreated to 6.2% for treated ones, which gives the ASE value of about 85%. The addition of Halloysite nanotubes also enhanced the thermal stability and mechanical properties of beeswax, which makes the applied mixture a potential consolidant for waterlogged wood [236].

The idea was further developed into a new consolidation system—a Pickering emulsion based on Halloysite nanotubes with paraffin wax microparticles as the inner phase of the oil-in-water droplets. Treatment with this organic/inorganic hybrid system reduced volumetric shrinkage of waterlogged wood from the Chretienne C ship from 40% to less than 5% (ASE of 87.5%) by filling the cell lumina and coating the cell walls, thus preventing their collapse upon drying. It also enhanced wood mechanical properties such as stiffness and flexural strength (the elastic modulus and stress at the breaking point increased to the order of magnitude of sound wood of the same species) while it reduced wood elongation capability by 50%. The colour of the treated samples was similar to untreated ones. The results obtained confirm that the organic/inorganic hybrid system composed of Halloysite nanotubes and wax can potentially be used as a consolidant for waterlogged wooden artefacts. It is worth mentioning that the proposed conservation method is environmentally friendly since the components applied are natural and non-toxic, and water was the only solvent used. It then can be scaled up to the requirements necessary for the treatment of large wooden objects [237].

Halloysite nanotubes were also tried for waterlogged wood consolidation in combination with 50% acetone solutions of esterified colophony (Rosin) (wood samples from the above-mentioned ship, an analogical impregnation protocol), and as a composite with Pluronic F108 (Poly(ethylene glycol)-block-poly(propylene glycol)-block-poly(ethylene glycol)). The effectiveness of the former method was lower than that of the Halloysite nanotubes/wax or beeswax mixtures, reaching ASE between 36 and 65% (volumetric wood shrinkage after the treatment was 14–26% compared to 40% for untreated wood). In the latter method, the mixture could only effectively penetrate the wood cell lumina [238,239].

Halloysite was employed as a component of a multifunctional hybrid system for simultaneous consolidation, deacidification and long-term protection of waterlogged wood from chemical degradation under acidic conditions. Wood samples were impregnated in aqueous dispersions of PEG1500 and Halloysite nanotubes loaded with calcium hydroxide as described above. The conservation system successfully penetrated wood tissue, filled the cell lumina and reduced wood porosity, which resulted in significant enhancement of wood mechanical properties (flexural strength and rigidity) in comparison to PEG-treated wood. The treated samples were robust and resistant to crushing. The sustained release of  $\text{Ca}(\text{OH})_2$  from the Halloysite lumen proved effective in neutralising the acidifying effect of PEG degradation by-products measured on the wood surface for 12 months. Moreover, it protected lignin against chemical degradation during artificial ageing under an acidic atmosphere. This makes this “green” conservation system potentially useful also for re-conservation of acidified artefacts previously treated with PEG or alum [240].

There is still much research needed before clay nanotubes can be proposed as a standard conservation method. Information about the anti-shrink efficiency of the method for wood with differing degrees of degradation, its long-term durability, reversibility or retreatability is required, as well as more data about characteristics of the treated wood, including its moisture and aesthetic properties or resistance to biodegradation. However, Halloysite nanotubes seem to have great potential for waterlogged wood conservation—their ability to improve thermo-mechanical performance of various polymers and the possibility for encapsulation of additional molecules of specific functionality (e.g., antifungal, hydrophobising, deacidifying) make them a perfect compound for multi-functional organic/inorganic hybrid systems tailored to the needs of waterlogged wood.

### 5.9. Organosilicon Compounds

Organosilicon compounds can be defined as organometallic compounds containing carbon–silicon bonds. They can be synthesised into various molecular structures, starting with the simplest silanes, through linear or branched siloxanes, to polyhedral silsesquioxanes. Due to their unique chemical reactivity and many potential functionalities, high thermal stability and resistance to external factors, they have been commonly used in many industry sectors, including the wood industry, mainly as adhesives, coatings, sealants and adjuvants. The most common silicon derivatives are organofunctional alkoxy silanes. Owing to the presence of alkoxy groups, alkoxy silanes can polymerise in the sol–gel process. It proceeds through a series of consecutive hydrolysis and polycondensation reactions, leading to the formation of a spatial polymer network. The presence of functional groups provides them with additional specific functionalities [241–243].

In the conservation practice, organosilicon compounds have been sporadically used for waterlogged wood conservation since 1965, when a mixture of PEG, boric acid, borax, and methylpolysiloxane was sprayed over the hull of the Vasa warship. Attempts to use tetraethyl orthosilicate (TEOS) or methacrylate-dimethylsiloxane oligomers for waterlogged wood consolidation were also made [127]. The first fully organosilicon-based conservation method was proposed by C. W. Smith in 1993 and then patented by Klosowski and Smith and Klosowski et al. It employed a primary silicon polymer (silicon oil, polydimethylsiloxane) and a cross-linker (methyltrimethoxysilane, MTMOS) for impregnation of acetone dehydrated wood followed by the addition of a catalyst to ensure the formation of a strengthening three-dimensional polymer network inside the wood

structure [126,244,245]. The method was used to consolidate several waterlogged marine and freshwater artefacts made of wood, bone, ceramic and textiles, including objects from the sunken city of Port Royal, Jamaica, the Uluburun shipwreck and the French shipwreck La Belle. The treatment, however fast and effective for preventing wood shrinkage (the ASE of about 82–90%) and discolouration, is irreversible, and the chemicals used are volatile and toxic. The long-term stability of the treated objects has not been confirmed. The method is suggested to be practical for conserving small waterlogged wooden artefacts [126]. Modification of the method by exchange of acetone with turpentine after wood dehydration and exposure of dry impregnated wood to MTMOS vapours instead of its immersion in the liquid silane improved penetrability of the consolidation mixture inside the wood. The treated samples retained their natural colour and dimensions; no shrinkage or collapse was observed [245]. The treatment did not alter wood mechanical properties, and its stabilising effect seems to result from high retention of the consolidant [202].

The results of more recent research show that the conservation method using organosilicon compounds can be simplified and include the following steps: wood dehydration in ethanol followed by soaking impregnation with an ethanol solution of a selected organosilicon without any catalysts, and finally, slow air-drying [246,247]. Among several tested chemicals, the most effective in stabilising the dimensions of highly degraded (loss of wood substance ca. 70–80%) elmwood were: (3-mercaptopropyl)trimethoxysilane (MPTMS, ASE ca. 98%), (3-aminopropyl)triethoxysilane (APTMS, ASE ca. 91%), 1,3-bis(3-aminopropyl)-1,1,3,3-tetramethyldisiloxane (BAPTMS, ASE ca. 91%), 1,3-Bis-[(diethylamino)-3-(propoxy)propan-2-ol]-1,1,3,3-tetramethyldisiloxane (BDEPPTMS, ASE ca. 90%), 3-(Polyethoxypropyl)1,1,1,3,5,5,5-heptamethyltrisiloxane hydroxyl-terminated (PEGHMTS, ASE ca. 89%), methyltrimethoxysilane (MTMS, ASE ca. 81%) [247]. MTMS turned out to be quite a versatile consolidant, effective for wood differing in the degree of degradation: applied on highly degraded elmwood (with the loss of wood substance (LWS) in the range of 70–64%), it gave the ASE values of 70–95% (higher stabilisation effect was observed for less degraded samples); when used for highly degraded oak sapwood (with LWS ca. 81%), the ASE reached 97–103% (higher values while the oscillating-pressure method was used instead of simple soaking); the lower stabilising effect was observed for better preserved oak heartwood (LWS ca. 25% for outer and 8% for the inner part, respectively) with the ASE of about 68% and 61%, respectively. The lower effectiveness for oak heartwood resulted from much lower permeability of well-preserved wood tissue (the observed weight percent gain after the treatment was about 4 times lower for heartwood than for heavily decayed sapwood) [35,246]. Although at this stage it is impossible to state what makes the organosilicon an effective wood consolidant, it can be concluded that the most effective were the chemicals with small molecules able to penetrate wood tissue easily and potentially bulk the cell wall, and those with other reactive groups allowing for extra interactions with wood polymers. SEM images of the treated wood revealed that organosilicons with smaller molecules (MTMS, MPTMS, APTMS) coat the cell walls or maybe even encrust them, leaving the cell lumina empty, while larger molecules (BAPTMS, BDEPPTMS) both coat the cell walls and fill smaller cell lumina, which suggests different stabilisation mechanisms [35,247,248]. Surface area and porosity measurements confirmed that MTMS could bulk the cell wall of the treated wood, thus stabilising the wood microstructure [91]. Strong chemical interactions between alkoxy groups in alkoxy silanes (MTMS, MPTMS) and hydroxyls in wood polymers or weaker hydrogen bonding between amino groups in BAPTMS and wood, confirmed by Fourier-transform infrared spectroscopy (FT-IR), contribute to the stabilising effect [249].

Apart from amino silicons, the chemicals reduced wood hygroscopicity, which would prevent further potential wood dimensional changes upon changeable moisture conditions [91,247,250,251]. The treatment with MTMS enhanced wood resistance against the brown-rot fungus *Coniophora puteana*, but gave no protection against moulds [251]. Experiments with soaking of the treated wood in 50% ethanol for two weeks showed that the treatment with siloxanes and amino silanes could be reversible, which is in line with



conservation ethics. On the other hand, although the impregnation with hydrophobic alkoxysilanes turned out to be more durable, the chemicals left the cell lumina empty, which potentially allows for further wood re-conservation; the method can then be considered as retreatable [247]. More research on the method is necessary to establish the actual stabilising mechanism, the effect of the treatment on the wood mechanical properties, and the long term stability of the treated wood.

Organosilicon compounds were also used as components in different conservation mixtures used for already dry wood. Methyltrimethoxysilane was successfully applied for re-conservation of PEG-treated sabot, effectively preserving the original dimensions of the object, reducing the feeling of wet and greasy surface, but changing the wood colour to a much lighter hue [252]. New organic/inorganic multi-functional hybrid systems composed of propylene glycol-modified silane, alkaline nanoparticles ( $\text{Ca}(\text{OH})_2$ ), and one of the following compounds: 3-aminopropyl triethoxysilane, trimethylamine, and polydimethylsiloxane hydroxy-terminated proved to be effective deacidifying consolidants in the one-step conservation of the fragile alum-treated wood from the Oseberg find. Application of silane monomer and nanoparticles allowed for efficient penetration of the chemical into the wood structure, where they underwent polymerisation into a three-dimensional network together with lignin that remained in the wood. The treatment increased the robustness and pH of wood without any distortions or shrinkage; it also effectively consolidated wood, reducing its powdering upon handling [253].

#### 5.10. Other Polymers

Several different polymers have been applied to consolidate waterlogged wooden artefacts, such as hydroxyethyl methacrylate, vinyl acetate, poly(vinyl chloride) or poly(acrylamide). However, they were ineffective mainly due to poor penetration into the wood structure resulting in its insufficient stabilisation, shrinkage and excessive cracking [92,101,127,128].

Some other polymers were more promising. One of the examples is phenol-formaldehyde. It has a lignin-like structure but higher resistance to degradation. Although its curing process is irreversible, there was an attempt to use it for the consolidation of wood from waterlogged pillars excavated in China (the remains of an ancient village). Wood was dehydrated in methanol and pre-treated with 2% oxalic acid to reverse its discolouration by bacteria. Then the proper treatment with 20% neutral phenol-formaldehyde in methanol was applied, which prevented wood shrinkage and warping upon drying, increased its strength and stabilised the colour. The treated wood structure remained porous, which, despite the irreversibility of the applied treatment, allows further re-conservation if necessary [254]. An acid-catalysed phenol-formaldehyde (novolac) has also been investigated as a potential consolidant for already dry, extremely fragile alum-treated objects from the Oseberg find. It was shown to thoroughly penetrate wood tissue and undergo in situ polymerisation inside it (at very low pH). The structure of the treated wood was strengthened and remained open owing to phase separation while using acid-catalysed novolacs (based-catalysed resols did not give such good results), allowing re-treatment. The cured consolidant is resistant to acids and ageing. However, the treatment can be inappropriate for highly degraded alum-filled artefacts because the pre-polymer mixture dissolves alum crystals risking disintegration of the wooden object. Further research on larger wood pieces is necessary to assess the actual usefulness of the method, as well as finding more safe solvents to prevent the dissolution of alum crystals during the treatment [211,255].

Melamine formaldehyde is a thermosetting resin of good chemical stability, composed of melamine rings terminated with numerous hydroxyl groups derived from formaldehyde. The small size of its molecules (about 5 Å) and solubility in water allow for its penetration into wood tissue [211,256]. A waterlogged wood consolidation method (also known as the Kauramin method) using melamine formaldehyde has been developed in Germany. It uses low-molecular (400 to 700 g/mol) polymer with low viscosity. The impregnation is carried out under ambient conditions, at a pH of about 7. Depending on the size and the degree of wood degradation, it can take a few weeks up to one year. After impregnation,

the treated wood is oven-dried at 50 °C for 7 to 14 days to ensure resin polymerisation. Compared to PEG-treatment, the Kauramin method is shorter, and the treated artefact is low in weight. However, due to the cross-linkage of the resin upon drying, the treatment is irreversible, which means that the treated object becomes a polymer composite without any possibilities for retreatment [202,211,256,257].

The melamine formaldehyde method provides an excellent dimensional stabilisation, and it is suitable for heavily degraded waterlogged wood. Sometimes deep cross-grain cracks may occur in the treated wood [256,257]. To prevent the formation of an unaesthetic polymer coating on the wood surface, the polymerisation rate of Kauramin should be controlled by careful monitoring of the pH and the turbidity of the solution [256,258]. The changes in wood colour (a much lighter tone) may appear due to wood bleaching by the release of formaldehyde during the thermosetting. To improve wood colour and appearance after the treatment, the wood surface should be treated with wax and darkened with natural oils [202,211,257,259]. It is recommended to add urea to the Kauramin solution to decrease the hazardous effect of free formaldehyde on human health. Additionally, urea increases the penetrability of the solution into wood tissue by decreasing its viscosity [256]. Kauramin imparts high strength to very fragile, highly degraded waterlogged wood and limits its hygroscopicity [259]. Similarly to other curing resins, it contributes significantly to the elastic properties of the treated wood, but only slightly to its viscous behaviour, which results from its polymerisation within wood tissue forming a stable composite material [202]. The addition of triethylene glycol to the melamine-formaldehyde solution increases the flexibility of the treated wood [256].

It must be noted that consolidation of waterlogged wood using melamine-formaldehyde is inconsistent with conservation ethics because of its irreversibility. Despite this, conservators sometimes choose this method due to the particular requirements of the object or exhibition conditions. The Yenikapi shipwreck conservation project in Istanbul, Turkey, is such an example. The conservation method applied was expected to be cost-effective regarding time and resources, and provide a consolidation effectiveness good enough to preserve heavily degraded wooden wrecks and enable their exhibition under uncontrolled environmental conditions. As a result, the Kauramin method was employed as the primary conservation treatment for highly deteriorated elements, in some cases in combination with PEG impregnation. This enabled the salvage of fragile artefacts that would probably not survive any other treatment procedures [122,256,259]. Similarly, part of the Roman-Germanic Central Museum (RGZM) collection in Mainz, Germany, was treated with this method [256]. Further reporting on the performance of Kauramin-treated artefacts is needed to evaluate the actual effectiveness and safety of this conservation method.

Recently, a new method for waterlogged wood stabilisation has emerged, namely, activators regenerated by electron transfer for atom transfer radical polymerization (ARGET ATRP), which uses reducing agents to continuously reduce a deactivator Cu(II) to an activator species Cu(I). In this case, it employs wood modification with 2-bromoisobutryl bromide in  $\text{CH}_2\text{Cl}_2$  to acquire C-Br bonds as initiators, then butyl methacrylate or styrene is introduced into the wood and polymerises there with the use of catalyst ( $\text{CuBr}_2$ ), reductant (ascorbic acid) and ligand ( $\text{N,N,N',N'',N''}$ -pentamethyldiethylenetriamine) in ethanol. Wood samples are then washed and left for natural air drying. The method results in good dimensional stabilisation of waterlogged wood (ASE of 87.8% for polystyrene and 98.5% for polybutylmethacrylate treatment) without collapse or distortions. The polymerisation takes place within cell walls, leaving the cell lumina empty, which allows for potential future wood re-treatment. The method theoretically has great potential due to the possibility of applying different, less toxic and more effective chemicals to obtain even better consolidation results [260]. It has been revised latterly by using less toxic chemicals, including mercaptoethylamine to functionalise waterlogged wood, quinone-based initiators, ascorbic acid 2-glucoside and glucose as reductants and water as a solvent. They obtained a relatively satisfactory ASE of 77.0–85.1% confirms the stabilising potential of the method [261].

A summary of the most important properties of wood treated with new consolidants is presented in Table 2.

**Table 2.** The effects of different conservation methods on wood properties: “+”—improvement, “-”—negative effect, “ncs”—not changed significantly, “...” —not studied; “fd”—freeze-drying, “ad”—air-drying.

Method	ASE [%]	Appearance	Mechanical Properties	Moisture Properties	Resistance to Fungi	Reversibility	Other
Sugars and sugar alcohols							
Sucrose [97, 126,195,197]	81–100 (fd), 47–98 (ad)	darker colour, crystalline deposits, a sticky film of wood surface	...	+ (under RH < 70%)	-	+	cell lumina filled, the cell wall bulked
Sucralose [197]	63	wood warping and twisting	...	...	-	+	long-term stability, reduced reactivity with wood polymers
Trehalose [97,197–199]	86–99	darker colour, crystalline deposits or a coating	+	+	-	+	faster, cheaper and safer than other methods, long-term stabilisation effect, smaller cell lumina filled
Lactitol [97,131, 142,201]	91–109	ncs	+	+	-	+	recommended for small artefacts
Mannitol and sorbitol [12]	70 (sorbitol), 30 (mannitol)	crystalline deposits on the wood surface (mannitol)	...	...	-	+	sorbitol—more cost- and time-efficient than other sugar methods
Xylitol [199]	103–106	ncs	+	ncs	-	+	more effective than trehalose and lactitol treatment
Proteins							
Keratin [204,205,209]	64–108	ncs	+	-	+	potential retreatment	more effective for less degraded wood, cell lumina remain open, reinforcement of the cell wall
Cellulose and its derivatives							
Bacterial nanocellulose [210]	55–94	unaesthetic layer on the surface, wood yellowing or whitening	...	ncs	...	...	cell lumina filled, coated cell walls, non-stable solution
Cellulose nanocrystals [210]	37–84	ncs	...	ncs	...	...	coated cell walls, cell lumina empty, poor wood penetrability, non-stable solution
Nanocellulose whiskers [211]	poor	...	...	...	...	...	poor wood penetrability, non-stable solution
Crosslinkable cellulose ethers [92,212,214]	...	...	...	...	...	-	high affinity to lignin, limited penetrability
6-deoxy-6-( $\omega$ -aminoethyl) amino cellulose, 6-deoxy-6-( $\omega$ -hydroxyethyl) amino cellulose [215]	effective stabilisation	...	+	...	...	partly	improved wood penetrability

Table 2. Cont.

Method	ASE [%]	Appearance	Mechanical Properties	Moisture Properties	Resistance to Fungi	Reversibility	Other
Lignin and its derivatives							
Lignin nanoparticles [210]	51–88	depositions on wood surface, darkened wood colour	...	ncs	...	...	non-stable solution, poor penetrability, coated cell walls and filled cell lumina
Isoeugenol [217,218]	effective stabilisation	...	...	...	...	...	in situ polymerisation
Chitosan and guar							
Chitosan [211, 220,221,225]	effective stabilisation	...	+	...	+	potential re-conservation	good penetrability, cell lumina remain open
Guar [221]	effective stabilisation	...	+	...	...	...	good penetrability,
Chitosan-based supramolecular system [226]	effective stabilisation	...	...	...	...	...	Multifunctional system: stability, chelating Fe ions, protecting against biodegradation
Oligoamides							
polyethylene-L-tartaramide, polyethylene-D(+)-glucaramide, polyethylene- $\alpha,\alpha'$ -trehaluronamide [227]	18–35	...	...	+	...	...	high affinity to lignin, good penetrability
oligo ethylene-L-tartaramide, oligo esamethylene-L-tartaramide, copolymer between ethylenediamine, adipic and tartaric acids, allyl $\alpha,\alpha'$ -trehalose/vinyl alcohol copolymer [228]	effective stabilisation	...	...	...	...	+ (for oligoamides)	high affinity to lignin, good penetrability
Other natural compounds							
Colophony and Rosin [58,92,128,202, 229–231]	effective stabilisation	wood darkening possible	...	+	+	?	good penetrability, cell walls encrusted, cell lumina remain open
Polyhydroxylated monomer synthesised from $\alpha$ -pinene [232]	...	...	...	...	...	...	hydrogen bonding with wood polymers

Table 2. Cont.

Method	ASE [%]	Appearance	Mechanical Properties	Moisture Properties	Resistance to Fungi	Reversibility	Other
Halloysite nanotubes (HNT)							
HNT/beeswax [236]	85	...	...	...	...	...	filled cell lumina
HNT/wax Pickering emulsion [237]	87	ncs	+	...	...	...	filled cell lumina
HNT/Rosin [238,239]	36–65	...	...	...	...	...	filled cell lumina
HNT/PEG/Ca(OH) <sub>2</sub> [240]	...	...	+	...	...	...	filled cell lumina, wood deacidification
Organosilicon compounds							
Silicon polymer + crosslinker + catalyst [126, 202,244,245]	82–90	ncs	ncs	...	...	-	good penetrability
Selected alkoxy-silanes and siloxanes [35,247,248, 251]	81–98	wood colour can change, depending on the chemical	+ (except amino compounds)	...	+	potentially reversible or retreatable, depending on the chemical	good penetrability, smaller molecules bulk the cell wall, bigger fill the cell lumina
Other polymers							
Phenol-formaldehyde [254]	effective stabilisation	ncs	+	...	...	-, retreatable	cell lumina remain open
Melamine formaldehyde (Kauramin) [211,256–259]	excellent dimensional stabilisation	unaesthetic coating on the surface, lighter tone of wood colour	+	+	...	-	time- and cost-efficient method
Activators regenerated by electron transfer for atom transfer radical polymerisation (ARGET ATRP) [260,261]	77–998	slightly lighter wood colour	...	...	...	retreatable	cell lumina remain open

There are plenty of interesting ideas for new consolidants, but extensive research is needed on their effectiveness, reliability, durability and safety before they could be proposed as new methods for conservation practice.

## 6. In Situ Preservation and Reburial

The number of known submerged archaeological sites is enormous, and the development of modern non-invasive searching methods (e.g., airborne laser scanning) results in several new significant sites being discovered every year worldwide. In Denmark alone, there are currently at least 18 sacrificial sites located in water meadows and bogs that were used by the local Iron Age population [45], while in Danish territorial waters, around 20,000 shipwrecks and a similar number of various prehistoric settlements are buried [57]. All of them contain countless waterlogged artefacts made of wood, bone, leather, amber, glass and metal; most of them have not yet been excavated. The funds necessary to excavate, document, properly conserve, store or exhibit all the historical objects buried there are inconceivable and simply impossible to obtain. Then, it becomes a question of whether

it is necessary to excavate all the discovered archaeological sites? Since numerous findings date back to a similar period, perhaps it is more reasonable to leave them as they are, in situ, for future archaeologists [45,57,262]?

Obligation to preserve archaeological sites and underwater cultural heritage and consider their in situ preservation as the first option was legitimised inter alia by the Valletta Convention For the Protection of the Archaeological Heritage of Europe in 1992 [263] and the UNESCO Convention on the Protection of Underwater Cultural Heritage in 2001 [264]. Where it is not possible or when the excavation of an artefact is justified by exceptional historical, scientific or conservation reasons, the recovery may be authorised, or rescue excavation must be undertaken if the object is anyhow endangered.

The recommended long-term protection of waterlogged artefacts in natural environments employs one of the two available techniques: in situ preservation or reburial. “In situ” means that the object will remain on-site, exactly where it was discovered, while reburial allows for its excavation (and possibly a non-destructive examination) and then reburial (in one piece or in parts) in the same or another environment [262]. Complete understanding of the waterlogged environments with all the biological, physical, chemical and geological processes that happen there as well as wood deterioration processes is fundamental to effective in situ preservation of wooden cultural heritage [9,57,262,265].

Waterlogged archaeological wood can survive in the natural environment only under specific conditions that preclude the growth of wood degraders (more details about wood degradation is given in part 2. Degradation of waterlogged wood). In water ecosystems, such conditions are available in anoxic or dysoxic sediments, where wood can be preserved even for hundreds of years, while the exposure to an oxygenated water column limits the time to only a few years (e.g., three years in the Mediterranean Sea). Therefore, for reburial, usually marine or freshwater sediments are used; sometimes, additional cover materials are applied onto the object or the covering sediment layer, including concrete blocks, sandbags, plastic or geotextile, to prevent its re-exposure to oxygenated water [262,265]. In terrestrial habitats, favourable conditions for wood preservation can be found in bogs, wetlands, or highly saturated soil, particularly if they are permanently saturated [8,9,45,266]. The key factor for effective in situ protection is to restore oxygen-free conditions in the environment. It was shown that even heavily degraded wood, almost completely deprived of polysaccharides, can still serve as a substrate for white-rot fungi under oxygenated conditions, e.g., upon desiccation of submerged areas; another threat related to desiccation is a permanent collapse of degraded wood [25,45].

Regardless of whether it is reburial or in situ preservation, a range of specific environmental parameters must be identified before deciding about the place of wood deposition and then carefully monitored to ensure the continuity of preserving conditions. The most important parameters measured are: dissolved oxygen content—based on this parameter, the sites can be classified as oxic ( $>3.0 \text{ mg L}^{-1}$ ), dysoxic ( $0.3\text{--}3.0 \text{ mg L}^{-1}$ ), suboxic ( $0.01\text{--}0.3 \text{ mg L}^{-1}$ ), and anoxic ( $<0.01 \text{ mg L}^{-1}$ ); based on the presence or absence of soft-rot fungi, the environments can be classified as aerobic or anaerobic; oxygen levels below  $0.3 \text{ mL L}^{-1}$  are considered low enough to prevent the growth of any microorganisms, hydrogen-ion concentration (pH)—highly influenced by biodegradation of organic material (can be used as a highlighter of its different phases); extremely high or low pH can accelerate the decomposition of organic matter; most waterlogged environments maintain a neutral or slightly alkaline pH; wood-degrading bacteria generally have a wide range of pH tolerance, redox potential (Eh)—highly influenced by biodegradation of organic matter, anaerobic environments usually have negative redox potentials while aerobic environments have the opposite, the level and duration of saturation—the degree of sediment saturation affects their chemical characteristics and it corresponds to the level of oxygenation; the longer duration of saturation the greater potential for wood preservation, temperature—directly affects microbial activity (low temperatures suppress, and higher temperatures promote it) [8,9,45].

There are also other parameters that can be used to characterise the environment, including the presence of specific reduced or oxidised ion species, salinity or depositional processes. It is important to understand that the mentioned parameters describe different processes that are intertwined and mutually dependent; therefore, they should be considered all together while assessing the preservation potential of a specific site [8,9].

One of the better-researched examples of in situ preservation is the Nydam Mose archaeological site in Denmark [45,267]. Based on the experiences gained from that place, six critical steps to ensure a successful in situ protection have been developed: determination of the area of an archaeological site, identification of the types and the degree of degradation of archaeological materials present, characterisation of the environment on the archaeological site and in the surrounding area, and identification of the most substantial threats to it, development of the best solutions to mitigate deterioration on the site, monitoring of the environment and the state of preservation of artefacts [267].

With proper planning and monitoring, reburial and in situ preservation seem to be an effective way to protect large archaeological sites and artefacts buried there for a long time for reasonable financial investments.

## 7. Discussion and Conclusions

Wooden archaeological artefacts can survive for tens of thousands of years if they are buried in anoxic waterlogged conditions. Under such conditions, bacterial degradation of the holocellulose occurs, but the lignin is largely left intact. The remaining lignified wood structure can give every appearance of being intact, but has very limited mechanical strength and can be easily damaged. The sequence of attack by bacteria and the species involved is not completely understood, although erosion bacteria appear to be the primary degraders. Once degradation begins, a bacterial consortium is formed, which in anoxic conditions will include sulphur reducing bacteria if there is a source of sulphate ions. Where iron is also present, this can result in the deposition of iron sulphides in the wood, which are extremely difficult to remove. This can be a particular problem with large marine artefacts. The bacterial species that are present in the site and their modes of action is poorly understood, as is the influence of site factors, such as pH, redox potential, etc.

Once waterlogged wooden objects are removed from the burial environment they can become susceptible to soft-rot attack and must be stored under appropriate conditions to prevent this from occurring. Soft-rot attack can also occur during burial if the site periodically becomes oxygenated. Once conservation is initiated, it may be necessary to remove contaminating salts by using running water, which can take many years for large objects. If recirculation is used there is a likelihood of microbial contamination occurring and a broad spectrum biocide is normally used to prevent this. As noted, iron sulphides are especially recalcitrant, although other iron salts can be removed using sequestering agents.

We do not have a unified methodology on how to examine degraded wood and the environment from which it is excavated—therefore, we cannot predict/model the degree and pattern of wood degradation (and propose an appropriate conservation method in advance), but every single time we have to measure all the parameters we need. The same relates to the assessment of the effectiveness of the conservation treatment. We measure shrinkage and ASE, but this relates only to the specific wood we are examining, so it is difficult to compare the effectiveness of different types of treatment when it is applied to different woods (different species, degree of degradation, type of degradation, etc.).

Consolidation of waterlogged archaeological wood is undoubtedly a complex and challenging task at the borderline of science and art. It aims to preserve the dimensions and overall appearance of a tangible wooden artefact to make its intangible history and artistic value accessible to the present and future public. Multidisciplinary knowledge is then required to properly maintain wooden artefacts—knowledge about wood as a material, its degree of degradation, degradation processes (including their culprit and the effect on the wood), the impact of different environmental factors, chemistry and physics of

consolidants and consolidated wood, sometimes art and historical context, conservation ethics, health and safety issues during both the treatment and then exhibition.

Thus far, we have not found the perfect consolidant which should be effective in providing wood integrity and dimensional stabilisation, compatible with wood, cheap, inert, easily delivered, resistant to ageing and provide a reversible treatment. There are particular problems with alum, which was one of the first consolidants widely used (especially in Scandinavia). This is being manifested as severe degradation of wooden artefacts, some of which have been destroyed. PEG appeared to be close to providing the best prospects as a consolidant, but it is now realised that this also has problems. The participation of PEG in redox reactions with iron during the conservation process is a disturbing finding, with serious implications for the use of PEG as a consolidant [113]. There are many different consolidants that have been tried and research is continuing in this area. Organosilicon compounds appear to show promise, because they can form inert structures within the wood and there is a wide variety of different chemical structures available. However, polymerisation of organosilicon monomers in the wood is likely to result in polymers that cannot then be subsequently removed. Sugar alcohols continue to be used for smaller objects especially, but do not provide sufficient strength to larger degraded objects in order for them to be self-supporting. The Kauramin method (a melamine-formaldehyde mixture) is undoubtedly successful, but irreversible. However, this would appear to be a very attractive option for artefacts that would be destroyed if they were not treated.

Legacy issues, such as treatment with alum, are causing very serious concerns. Re-treatment of the Oseberg finds is an extremely challenging task. The aims of such treatment would be to provide mechanical integrity as well as de-acidification of the wood. Tests have been conducted using impregnation with PEG solutions, followed by freeze-drying or Kauramin solution followed by air drying. However, many of the more fragile objects do not survive the aqueous immersion process. For such objects, solvent-based consolidation treatments are being studied [95]. Other possibilities to be explored include supercritical CO<sub>2</sub> delivery, or a vapour treatment, combined with in situ polymerisation. If polymerisation within the wood structure is attempted then it must be ensured that the polymerisation process does not result in distortion of the wooden objects.

Regarding the degradation of the Vasa, the crucial questions are: is the degradation reaction an ongoing process or are the oxidative reactions related to the conservation treatment process? Is the degradation linked to a Fenton's reaction, or simply a result of the reaction between iron sulphides and water? If Fenton's was the main reaction responsible for degradation, then it would be expected that oxidation of the lignin content would be occurring, which does not appear to be the case. There are serious challenges involved in removing the already created sulphuric acid from such a large structure, or with ensuring that any treatment involving neutralisation is able to fully penetrate to all the regions where the sulphuric acid is present. Similar issues are being encountered with the Mary Rose and other large marine structures where both iron and sulphur are present. An alternative approach would be to provide an envelope in the wood surface region that prevents oxygen ingress and hence limits oxidation reactions, although this does not deal with the presence of sulphuric acid which is causing damage to the polysaccharide components in the wood.

In the future, will the excavation and display of large timber structures be considered effective, or will new methods of display be used, such as laser scanning combined with virtual reality, or display in situ within immersion chambers? For most sites, once excavation has revealed the necessary information and context, reburial is the only option, with only the smaller objects being subjected to conservation. Sites, such as Must Farm and Flag Fen in Cambridgeshire UK, will be protected by ensuring that the water levels on the sites do not drop to a point where oxygenated conditions are encountered [268].

“Blessed were the ancients, for they had not antiquities”—Italian saying [269].



**Author Contributions:** Conceptualization, C.A.S.H. and M.B.; writing—original draft preparation, M.B. and C.A.S.H.; writing—review and editing, C.A.S.H. and M.B.; visualization, M.B. All authors have read and agreed to the published version of the manuscript.

**Funding:** This research received no external funding.

**Conflicts of Interest:** The authors declare no conflict of interest.

## References

- Grattan, D.W. Waterlogged Wood. *Conserv. Marine Archaeol. Objects* **1987**, *1*, 55–67. [CrossRef]
- Björdal, C.G. Microbial Degradation of Waterlogged Archaeological Wood. *J. Cult. Herit.* **2012**, *13*, S118–S122. [CrossRef]
- Terberger, T.; Zhilin, M.; Savchenko, S. The Shigir Idol in the Context of Early Art in Eurasia. *Quat. Int.* **2021**, *573*, 14–29. [CrossRef]
- Schoch, W.H.; Bigga, G.; Böhner, U.; Richter, P.; Terberger, T. New Insights on the Wooden Weapons from the Paleolithic Site of Schöningen. *J. Hum. Evol.* **2015**, *89*, 214–225. [CrossRef] [PubMed]
- Mcqueen, C.M.A.; Tamburini, D.; Lucejko, J.J.; Braovac, S.; Gambineri, F.; Modugno, F.; Colombini, M.P.; Kutzke, H. New Insights into the Degradation Processes and Influence of the Conservation Treatment in Alum-Treated Wood from the Oseberg Collection. *Microchem. J.* **2017**, *132*, 119–129. [CrossRef]
- Macphail, R.; Bill, J.; Cannell, R.; Linderholm, J.; Rødsrud, C.L. Integrated Microstratigraphic Investigations of Coastal Archaeological Soils and Sediments in Norway: The Gokstad Ship Burial Mound and Its Environs Including the Viking Harbour Settlement of Heimdaljordet, Vestfold. *Quat. Int.* **2013**, *315*, 131–146. [CrossRef]
- Gregory, D.; Jensen, P.; Strætkvern, K. Conservation and in Situ Preservation of Wooden Shipwrecks from Marine Environments. *J. Cult. Herit.* **2012**, *13*, S139–S148. [CrossRef]
- Jordan, B.A. Site Characteristics Impacting the Survival of Historic Waterlogged Wood: A Review. *Int. Biodeterior. Biodegrad.* **2001**, *47*, 47–54. [CrossRef]
- Lillie, M.; Smith, R. The in Situ Preservation of Archaeological Remains: Using Lysimeters to Assess the Impacts of Saturation and Seasonality. *J. Archaeol. Sci.* **2007**, *34*, 1494–1504. [CrossRef]
- Lillie, M.; Smith, R.; Reed, J.; Inglis, R. Southwest Scottish Crannogs: Using in Situ Studies to Assess Preservation in Wetland Archaeological Contexts. *J. Archaeol. Sci.* **2008**, *35*, 1886–1900. [CrossRef]
- Caple, C. Reburial of Waterlogged Wood, the Problems and Potential of This Conservation Technique. *Int. Biodeter. Biodegr.* **1994**, *34*, 61–72. [CrossRef]
- Jones, S.P.P.; Slater, N.K.H.; Jones, M.; Ward, K.; Smith, A.D. Investigating the Processes Necessary for Satisfactory Freeze-Drying of Waterlogged Archaeological Wood. *J. Archaeol. Sci.* **2009**, *36*, 2177–2183. [CrossRef]
- Björdal, C.G.; Nilsson, T.; Daniel, G. Microbial Decay of Waterlogged Archaeological Wood Found in Sweden Applicable to Archaeology and Conservation. *Int. Biodeter. Biodegr.* **1999**, *43*, 63–73. [CrossRef]
- Blanchette, R.A.; Cease, K.R.; Abad, A.; Koestler, R.J.; Simpson, E.; Sams, G.K. An Evaluation of Different Forms of Deterioration Found in Archaeological Wood. *Int. Biodeterior.* **1991**, *28*, 3–22. [CrossRef]
- Han, L.; Tian, X.; Keplinger, T.; Zhou, H.; Li, R.; Svedstrom, K.; Burgert, I.; Yin, Y.; Guo, J. Even Visually Intact Cell Walls in Waterlogged Archaeological Wood Are Chemically Deteriorated and Mechanically Fragile: A Case of a 170 Year-Old Shipwreck. *Molecules* **2020**, *25*, 1113. [CrossRef]
- Pournou, A. Wood Deterioration by Aquatic Microorganisms. In *Biodeterioration of Wooden Cultural Heritage: Organisms and Decay Mechanisms in Aquatic and Terrestrial Ecosystems*; Pournou, A., Ed.; Springer International Publishing: Cham, Switzerland, 2020; pp. 177–260. ISBN 978-3-030-46504-9.
- Blanchette, R.A. A Review of Microbial Degradation Found in Archaeological Wood from Different Environments. *Int. Biodeter. Biodegr.* **2000**, *46*, 189–204. [CrossRef]
- Daniel, G.; Nilsson, T. Developments in the Study of Soft Rot and Bacterial Decay. In *Forest Products Biotechnology*; CRC Press: Boca Raton, FL, USA, 1998; ISBN 978-0-429-07945-0.
- Klaassen, R.K.W.M. Bacterial Decay in Wooden Foundation Piles—Patterns and Causes: A Study of Historical Pile Foundations in the Netherlands. *Int. Biodeterior. Biodegrad.* **2008**, *61*, 45–60. [CrossRef]
- Pedersen, N.B.; Björdal, C.G.; Jensen, P.; Felby, C. Bacterial Degradation of Archaeological Wood in Anoxic Waterlogged Environments. In *Stability of Complex Carbohydrate Structures. Biofuel, Foods, Vaccines, and Shipwrecks*; Harding, I.E., Ed.; The Royal Society of Chemistry: Cambridge, UK, 2013.
- Blanchette, R.A. Microbial Degradation of Wood from Aquatic and Terrestrial Environments. In *Cultural Heritage Microbiology: Fundamental Studies in Conservation Science*; ASM Press: Washington, DC, USA, 2010; pp. 179–190.
- Nilsson, T.; Björdal, C. The Use of Kapok Fibres for Enrichment Cultures of Lignocellulose-Degrading Bacteria. *Int. Biodeterior. Biodegrad.* **2008**, *61*, 11–16. [CrossRef]
- Lukowsky, D.; Keiser, U.; Gohla, A. Strength Properties of Scots Pine from Harbour Piles Degraded by Erosion Bacteria. *Eur. J. Wood Prod.* **2018**, *76*, 1187–1194. [CrossRef]
- Kim, Y.S.; Singh, A.P. Micromorphological Characteristics of Wood Biodegradation in Wet Environments: A Review. *IAWA J.* **2000**, *21*, 135–155. [CrossRef]

25. Huisman, D.J.; Manders, M.R.; Kretschmar, E.I.; Klaassen, R.K.W.M.; Lamersdorf, N. Burial Conditions and Wood Degradation at Archaeological Sites in the Netherlands. *Int. Biodeterior. Biodegrad.* **2008**, *61*, 33–44. [CrossRef]
26. Gelbrich, J.; Kretschmar, E.I.; Lamersdorf, N.; Militz, H. Laboratory Experiments as Support for Development of in Situ Conservation Methods. *Conserv. Manag. Archaeol. Sites* **2012**, *14*, 7–15. [CrossRef]
27. Björdal, C.G.; Daniel, G.; Nilsson, T. Depth of Burial, an Important Factor in Controlling Bacterial Decay of Waterlogged Archaeological Poles. *Int. Biodeterior. Biodegrad.* **2000**, *45*, 15–26. [CrossRef]
28. Lionetto, F.; Quarta, G.; Cataldi, A.; Cossa, A.; Auremma, R.; Calcagnile, L.; Frigione, M. Characterization and Dating of Waterlogged Woods from an Ancient Harbor in Italy. *J. Cult. Herit.* **2014**, *15*, 213–217. [CrossRef]
29. Blanchette, R.A.; Iiyama, K.; Abad, A.R.; Cease, K.R. Ultrastructure of Ancient Buried Wood from Japan. *Holzforschung* **1991**, *45*, 161–168. [CrossRef]
30. Hoffmann, P.; Singh, A.; Kim, Y.S.; Wi, S.G.; Kim, I.-J.; Schmitt, U. The Bremen Cog of 1380—an Electron Microscopic Study of Its Degraded Wood before and after Stabilization with PEG. *Holzforschung* **2004**, *58*, 211–218. [CrossRef]
31. Kim, Y.S. Chemical Characteristics of Waterlogged Archaeological Wood. *Holzforschung* **1990**, *44*, 169–172. [CrossRef]
32. Kretschmar, E.I.; Gelbrich, J.; Militz, H.; Lamersdorf, N. Studying Bacterial Wood Decay under Low Oxygen Conditions—Results of Microcosm Experiments. *Int. Biodeterior. Biodegrad.* **2008**, *61*, 69–84. [CrossRef]
33. Boutelje, J.; Goransson, B. Decay in Wood Constructions below the Ground Water Table. In Proceedings of the 2nd International Biodeterioration Symposium, Lunteren, The Netherlands, 13–18 September 1971; pp. 311–318.
34. Kim, Y.S.; Singh, A.P. Micromorphological Characteristics of Compression Wood Degradation in Waterlogged Archaeological Pine Wood. *Holzforschung* **1999**, *53*, 381–385. [CrossRef]
35. Broda, M.; Mazela, B.; Radka, K. Methyltrimethoxysilane as a Stabilising Agent for Archaeological Waterlogged Wood Differing in the Degree of Degradation. *J. Cult. Herit.* **2019**, *35*, 129–139. [CrossRef]
36. Landy, E.T.; Mitchell, J.I.; Hotchkiss, S.; Eaton, R.A. Bacterial Diversity Associated with Archaeological Waterlogged Wood: Ribosomal RNA Clone Libraries and Denaturing Gradient Gel Electrophoresis (DGGE). *Int. Biodeter. Biodegr.* **2008**, *61*, 106–116. [CrossRef]
37. Nilsson, T.; Björdal, C.; Fällman, E. Culturing Erosion Bacteria: Procedures for Obtaining Purer Cultures and Pure Strains. *Int. Biodeterior. Biodegrad.* **2008**, *61*, 17–23. [CrossRef]
38. Antonelli, F.; Esposito, A.; Galotta, G.; Davidde Petriaggi, B.; Piazza, S.; Romagnoli, M.; Guerrieri, F. Microbiota in Waterlogged Archaeological Wood: Use of Next-Generation Sequencing to Evaluate the Risk of Biodegradation. *Appl. Sci.* **2020**, *10*, 4636. [CrossRef]
39. Singh, A.P. A Review of Microbial Decay Types Found in Wooden Objects of Cultural Heritage Recovered from Buried and Waterlogged Environments. *J. Cult. Herit.* **2012**, *13*, S16–S20. [CrossRef]
40. Nilsson, T.; Singh, A.P. Tunneling Bacteria and Tunneling of Wood Cell Walls. *Access Sci.* **2014**, *7*, 73. [CrossRef]
41. Li, Q.; Cao, L.; Wang, W.; Tan, H.; Jin, T.; Wang, G.; Lin, G.; Xu, R. Analysis of the Bacterial Communities in the Waterlogged Wooden Cultural Relics of the Xiaobaijiao No. 1 Shipwreck via High-Throughput Sequencing Technology. *Holzforschung* **2018**, *72*, 609–619. [CrossRef]
42. Spear, M.J.; Broda, M. Comparison of Contemporary Elm (*Ulmus* Spp.) and Degraded Archaeological Elm: The Use of Dynamic Mechanical Analysis Under Ambient Moisture Conditions. *Materials* **2020**, *13*, 5026. [CrossRef]
43. Björdal, C.G.; Nilsson, T. Observations on Microbial Growth during Conservation Treatment of Waterlogged Archaeological Wood. *Stud. Conserv.* **2001**, *46*, 211–220. [CrossRef]
44. Björdal, C.G.; Nilsson, T. Waterlogged Archaeological Wood—A Substrate for White Rot Fungi during Drainage of Wetlands. *Int. Biodeter. Biodegr.* **2002**, *50*, 17–23. [CrossRef]
45. Gregory, D.; Jensen, P. The Importance of Analysing Waterlogged Wooden Artefacts and Environmental Conditions When Considering Their in Situ Preservation. *J. Wetl. Archaeol.* **2006**, *6*, 65–81. [CrossRef]
46. Muyzer, G.; Stams, A.J.M. The Ecology and Biotechnology of Sulphate-Reducing Bacteria. *Nat. Rev. Microbiol.* **2008**, *6*, 441–454. [CrossRef]
47. Monachon, M.; Albelda-Berenguer, M.; Pele, C.; Cornet, E.; Guilminot, E.; Remazeilles, C.; Joseph, E. Characterization of Model Samples Simulating Degradation Processes Induced by Iron and Sulfur Species on Waterlogged Wood. *Microchem. J.* **2020**, *155*, 104756. [CrossRef]
48. Fors, Y.; Grudd, H.; Rindby, A.; Jalilehvand, F.; Sandstrom, M.; Cato, I.; Bornmalm, L. Sulfur and Iron Accumulation in Three Marine-Archaeological Shipwrecks in the Baltic Sea: The Ghost, the Crown and the Sword. *Sci. Rep.* **2014**, *4*, 4222. [CrossRef] [PubMed]
49. Gibson, G.R. Physiology and Ecology of the Sulphate-Reducing Bacteria. *J. Appl. Bacteriol.* **1990**, *69*, 769–797. [CrossRef]
50. Fors, Y.; Nilsson, T.; Risberg, E.D.; Sandstrom, M.; Torssander, P. Sulfur Accumulation in Pinewood (*Pinus Sylvestris*) Induced by Bacteria in a Simulated Seabed Environment: Implications for Marine Archaeological Wood and Fossil Fuels. *Int. Biodeterior. Biodegrad.* **2008**, *62*, 336–347. [CrossRef]
51. Fagervold, S.K.; Galand, P.E.; Zbinden, M.; Gaill, F.; Lebaron, P.; Palacios, C. Sunken Woods on the Ocean Floor Provide Diverse Specialized Habitats for Microorganisms. *FEMS Microbiol. Ecol.* **2012**, *82*, 616–628. [CrossRef]
52. Fors, Y.; Jalilehvand, F.; Damian Risberg, E.; Björdal, C.; Phillips, E.; Sandström, M. Sulfur and Iron Analyses of Marine Archaeological Wood in Shipwrecks from the Baltic Sea and Scandinavian Waters. *J. Archaeol. Sci.* **2012**, *39*, 2521–2532. [CrossRef]

53. Mortensen, M.N.; Egsgaard, H.; Hvilsted, S.; Shashoua, Y.; Glastrup, J. Tetraethylene Glycol Thermooxidation and the Influence of Certain Compounds Relevant to Conserved Archaeological Wood. *J. Archaeol. Sci.* **2012**, *39*, 3341–3348. [CrossRef]
54. Henrik-Klemens, Å.; Bengtsson, F.; Björdal, C.G. Raman Spectroscopic Investigation of Iron-Tannin Precipitates in Waterlogged Archaeological Oak. *Stud. Conserv.* **2021**, *8*, 1–11. [CrossRef]
55. Fellowes, D.; Hagan, P. Pyrite Oxidation: The Conservation of Historic Shipwrecks and Geological and Palaeontological Specimens. *Stud. Conserv.* **2003**, *48*, 26–38. [CrossRef]
56. Eriksen, A.M.; Gregory, D.J.; Matthiesen, H. The Importance of Cellulose Content and Wood Density for Attack of Waterlogged Archaeological Wood by the Shipworm, *Teredo Navalis*. *J. Cult. Herit.* **2017**, *28*, 75–81. [CrossRef]
57. Eriksen, A.M.; Gregory, D.; Shashoua, Y. Selective Attack of Waterlogged Archaeological Wood by the Shipworm, *Teredo Navalis* and Its Implications for in-Situ Preservation. *J. Archaeol. Sci.* **2015**, *55*, 9–15. [CrossRef]
58. Kaye, B. Conservation of Waterlogged Archaeological Wood. *Chem. Soc. Rev.* **1995**, *24*, 35–43. [CrossRef]
59. Oron, A.; Liphshitz, N.; Held, B.W.; Galili, E.; Klein, M.; Linker, R.; Blanchette, R.A. Characterization of Archaeological Waterlogged Wooden Objects Exposed on the Hyper-Saline Dead Sea Shore. *J. Archaeol. Sci. Rep.* **2016**, *9*, 73–86. [CrossRef]
60. Almkvist, G.; Persson, I. Analysis of Acids and Degradation Products Related to Iron and Sulfur in the Swedish Warship *Vasa*. *Holzforschung* **2008**, *62*, 694–703. [CrossRef]
61. Almkvist, G.; Persson, I. Degradation of Polyethylene Glycol and Hemicellulose in the *Vasa*. *Holzforschung* **2008**, *62*, 64–70. [CrossRef]
62. Pedersen, N.B.; Schmitt, U.; Koch, G.; Felby, C.; Thygesen, L.G. Lignin Distribution in Waterlogged Archaeological *Picea Abies* (L.) Karst Degraded by Erosion Bacteria. *Holzforschung* **2014**, *68*, 791–798. [CrossRef]
63. Pedersen, N.B.; Gierlinger, N.; Thygesen, L.G. Bacterial and Abiotic Decay in Waterlogged Archaeological *Picea Abies* (L.) Karst Studied by Confocal Raman Imaging and ATR-FTIR Spectroscopy. *Holzforschung* **2015**, *69*, 103–112. [CrossRef]
64. Salanti, A.; Zoia, L.; Tolppa, E.-L.; Giachi, G.; Orlandi, M. Characterization of Waterlogged Wood by NMR and GPC Techniques. *Microchem. J.* **2010**, *95*, 345–352. [CrossRef]
65. Pinder, A.P.; Panter, I.; Abbott, G.D.; Keely, B.J. Deterioration of the Hanson Logboat: Chemical and Imaging Assessment with Removal of Polyethylene Glycol Conserving Agent. *Sci. Rep.* **2017**, *7*, 13697. [CrossRef]
66. Modugno, F.; Ribechini, E.; Calderisi, M.; Giachi, G.; Colombini, M.P. Analysis of Lignin from Archaeological Waterlogged Wood by Direct Exposure Mass Spectrometry (DE-MS) and PCA Evaluation of Mass Spectral Data. *Microchem. J.* **2008**, *88*, 186–193. [CrossRef]
67. Zoia, L.; Tamburini, D.; Orlandi, M.; Lucejko, J.J.; Salanti, A.; Tolppa, E.-L.; Modugno, F.; Colombini, M.P. Chemical Characterisation of the Whole Plant Cell Wall of Archaeological Wood: An Integrated Approach. *Anal. Bioanal. Chem.* **2017**, *409*, 4233–4245. [CrossRef]
68. Lucejko, J.J.; Modugno, F.; Ribechini, E.; Tamburini, D.; Colombini, M.P. Analytical Instrumental Techniques to Study Archaeological Wood Degradation. *Appl. Spectrosc. Rev.* **2015**, *50*, 584–625. [CrossRef]
69. Lucejko, J.J.; Modugno, F.; Ribechini, E.; del Rio, J.C. Characterisation of Archaeological Waterlogged Wood by Pyrolytic and Mass Spectrometric Techniques. *Anal. Chim. Acta* **2009**, *654*, 26–34. [CrossRef] [PubMed]
70. Traore, M.; Kaal, J.; Martinez Cortizas, A. Potential of Pyrolysis-GC-MS Molecular Fingerprint as a Proxy of Modern Age Iberian Shipwreck Wood Preservation. *J. Anal. Appl. Pyrolysis* **2017**, *126*, 1–13. [CrossRef]
71. Tamburini, D.; Lucejko, J.J.; Ribechini, E.; Colombini, M.P. Snapshots of Lignin Oxidation and Depolymerization in Archaeological Wood: An EGA-MS Study. *J. Mass Spectrom.* **2015**, *50*, 1103–1113. [CrossRef] [PubMed]
72. Tamburini, D.; Lucejko, J.J.; Ribechini, E.; Colombini, M.P. New Markers of Natural and Anthropogenic Chemical Alteration of Archaeological Lignin Revealed by in Situ Pyrolysis/Silylation-Gas Chromatography-Mass Spectrometry. *J. Anal. Appl. Pyrolysis* **2016**, *118*, 249–258. [CrossRef]
73. Bardet, M.; Foray, M.F.; Maron, S.; Goncalves, P.; Tran, Q.K. Characterization of Wood Components of Portuguese Medieval Dugout Canoes with High-Resolution Solid-State NMR. *Carbohydr. Polym.* **2004**, *57*, 419–424. [CrossRef]
74. Bardet, M.; Gerbaud, G.; Giffard, M.; Doan, C.; Hediger, S.; Le Pape, L. C-13 High-Resolution Solid-State NMR for Structural Elucidation of Archaeological Woods. *Prog. Nucl. Magn. Reson. Spectrosc.* **2009**, *55*, 199–214. [CrossRef]
75. Zoia, L.; Salanti, A.; Orlandi, M. Chemical Characterization of Archaeological Wood: Softwood *Vasa* and Hardwood *Riksapplet* Case Studies. *J. Cult. Herit.* **2015**, *16*, 428–437. [CrossRef]
76. Gelbrich, J.; Mai, C.; Militz, H. Evaluation of Bacterial Wood Degradation by Fourier Transform Infrared (FTIR) Measurements. *J. Cult. Herit.* **2012**, *13*, S135–S138. [CrossRef]
77. Pizzo, B.; Pecoraro, E.; Alves, A.; Macchioni, N.; Rodrigues, J.C. Quantitative Evaluation by Attenuated Total Reflectance Infrared (ATR-FTIR) Spectroscopy of the Chemical Composition of Decayed Wood Preserved in Waterlogged Conditions. *Talanta* **2015**, *131*, 14–20. [CrossRef]
78. Petrou, M.; Edwards, H.G.M.; Janaway, R.C.; Thompson, G.B.; Wilson, A.S. Fourier-Transform Raman Spectroscopic Study of a Neolithic Waterlogged Wood Assemblage. *Anal. Bioanal. Chem.* **2009**, *395*, 2131–2138. [CrossRef] [PubMed]
79. Pecoraro, E.; Pizzo, B.; Alves, A.; Macchioni, N.; Rodrigues, J.C. Measuring the Chemical Composition of Waterlogged Decayed Wood by near Infrared Spectroscopy. *Microchem. J.* **2015**, *122*, 176–188. [CrossRef]
80. Pappas, C.; Rodis, P.; Tarantilis, P.A.; Polissiou, M. Prediction of the PH in Wood by Diffuse Reflectance Infrared Fourier Transform Spectroscopy. *Appl. Spectrosc.* **1999**, *53*, 805–809. [CrossRef]

81. Almkvist, G.; Norbakhsh, S.; Bjurhager, I.; Varmuza, K. Prediction of Tensile Strength in Iron-Contaminated Archaeological Wood by FT-IR Spectroscopy—A Study of Degradation in Recent Oak and Vasa Oak. *Holzforschung* **2016**, *70*, 855–865. [CrossRef]
82. Remazeilles, C.; Tran, K.; Guilminot, E.; Conforto, E.; Refait, P. Study of Fe(II) Sulphides in Waterlogged Archaeological Wood. *Stud. Conserv.* **2013**, *58*, 297–307. [CrossRef]
83. Triantafyllou, M.; Papachristodoulou, P.; Pournou, A. Wet Charred Wood: A Preliminary Study of the Material and Its Conservation Treatments. *J. Archaeol. Sci.* **2010**, *37*, 2277–2283. [CrossRef]
84. Balaban-Ucar, M.; Gonultas, O. Volatile Compounds of Archaeological Wood from the Ancient Harbor Theodosius in Istanbul. *Eur. J. Wood Wood Prod.* **2019**, *77*, 475–481. [CrossRef]
85. Bettazzi, F.; Giachi, G.; Staccioli, G.; Chimichi, S. Chemical Characterisation of Wood of Roman Ships Brought to Light in the Recently Discovered Ancient Harbour of Pisa (Tuscany, Italy). *Holzforschung* **2003**, *57*, 373–376. [CrossRef]
86. Zisi, A.; Dix, J.K. Simulating Mass Loss of Decaying Waterlogged Wood: A Technique for Studying Ultrasound Propagation Velocity in Waterlogged Archaeological Wood. *J. Cult. Herit.* **2018**, *33*, 39–47. [CrossRef]
87. Macchioni, N.; Pecoraro, E.; Pizzo, B. The Measurement of Maximum Water Content (MWC) on Waterlogged Archaeological Wood: A Comparison between Three Different Methodologies. *J. Cult. Herit.* **2018**, *30*, 51–56. [CrossRef]
88. Jensen, P.; Gregory, D.J. Selected Physical Parameters to Characterize the State of Preservation of Waterlogged Archaeological Wood: A Practical Guide for Their Determination. *J. Archaeol. Sci.* **2006**, *33*, 551–559. [CrossRef]
89. Pizzo, B.; Giachi, G.; Fiorentino, L. Evaluation of the Applicability of Conventional Methods for the Chemical Characterization of Waterlogged Archaeological Wood. *Archaeometry* **2010**, *52*, 656–667. [CrossRef]
90. Broda, M.; Curling, S.F.; Frankowski, M. The Effect of the Drying Method on the Cell Wall Structure and Sorption Properties of Waterlogged Archaeological Wood. *Wood Sci. Technol.* **2021**, *9*, 1–19. [CrossRef]
91. Broda, M.; Curling, S.F.; Spear, M.J.; Hill, C.A.S. Effect of Methyltrimethoxysilane Impregnation on the Cell Wall Porosity and Water Vapour Sorption of Archaeological Waterlogged Oak. *Wood Sci. Technol.* **2019**, *53*, 703–726. [CrossRef]
92. Donato, I.D.; Lazzara, G. Porosity Determination with Helium Pycnometry as a Method to Characterize Waterlogged Woods and the Efficacy of the Conservation Treatments. *Archaeometry* **2012**, *54*, 906–915. [CrossRef]
93. Pizzo, B.; Pecoraro, E.; Lazzeri, S. Dynamic Mechanical Analysis (DMA) of Waterlogged Archaeological Wood at Room Temperature. *Holzforschung* **2018**, *72*, 421–431. [CrossRef]
94. Florian, M.-L.E. Scope and History of Archaeological Wood. In *Archaeological Wood; Advances in Chemistry*; American Chemical Society: Washington, DC, USA, 1989; Volume 225, pp. 3–32. ISBN 978-0-8412-1623-5.
95. Braovac, S.; McQueen, C.M.A.; Sahlstedt, M.; Kutzke, H.; Lucejko, J.J.; Klokernes, T. Navigating Conservation Strategies: Linking Material Research on Alum-Treated Wood from the Oseberg Collection to Conservation Decisions. *Herit. Sci.* **2018**, *6*, 77. [CrossRef]
96. Braovac, S.; Kutzke, H. The Presence of Sulfuric Acid in Alum-Conserved Wood—Origin and Consequences. *J. Cult. Herit.* **2012**, *13*, S203–S208. [CrossRef]
97. Morgós, A.; Imazu, S.; Ito, K. Sugar Conservation of Waterlogged Archaeological Finds in the Last 30 Years. In Proceedings of the 2015 Conservation and Digitalization Conference, Gdańsk, Poland, 19–22 May 2015; pp. 15–20.
98. McQueen, C.M.A.; Tamburini, D.; Braovac, S. Identification of Inorganic Compounds in Composite Alum-Treated Wooden Artefacts from the Oseberg Collection. *Sci. Rep.* **2018**, *8*, 2901. [CrossRef] [PubMed]
99. Lucejko, J.J.; La Nasa, J.; Mcqueen, C.M.A.; Braovac, S.; Colombini, M.P.; Modugno, F. Protective Effect of Linseed Oil Varnish on Archaeological Wood Treated with Alum. *Microchem. J.* **2018**, *139*, 50–61. [CrossRef]
100. Christensen, M.; Frosch, M.; Jensen, P.; Schnell, U.; Shashoua, Y.; Nielsen, O.F. Waterlogged Archaeological Wood—Chemical Changes by Conservation and Degradation. *J. Raman Spectrosc.* **2006**, *37*, 1171–1178. [CrossRef]
101. Grattan, D.W. A Practical Comparative Study of Several Treatments for Waterlogged Wood. *Stud. Conserv.* **1982**, *27*, 124–136. [CrossRef]
102. Hocker, E.; Almkvist, G.; Sahlstedt, M. The Vasa Experience with Polyethylene Glycol: A Conservator’s Perspective. *J. Cult. Herit.* **2012**, *13*, S175–S182. [CrossRef]
103. Hoffmann, P. On the Stabilization of Waterlogged Oakwood with PEG. II. Designing a Two-Step Treatment for Multi-Quality Timbers. *Stud. Conserv.* **1986**, *31*, 103–113.
104. Jensen, P.; Jensen, J.B. Dynamic Model for Vacuum Freeze-Drying of Waterlogged Archaeological Wooden Artefacts. *J. Cult. Herit.* **2006**, *7*, 156–165. [CrossRef]
105. Purdy, B.A. *Wet Site Archaeology*; CRC Press: Boca Raton, FL, USA, 2018; ISBN 978-1-351-09465-8.
106. Baird, J.A.; Olayo-Valles, R.; Rinaldi, C.; Taylor, L.S. Effect of Molecular Weight, Temperature, and Additives on the Moisture Sorption Properties of Polyethylene Glycol. *J. Pharm. Sci.* **2010**, *99*, 154–168. [CrossRef]
107. Seborg, R.M.; Inverarity, R.B. Preservation of Old, Waterlogged Wood by Treatment with Polyethylene Glycol. *Science* **1962**, *136*, 649–650. [CrossRef]
108. Stamm, A.J. Dimensional Stabilization of Wood with Carbowaxes. *For. Prod. J.* **1956**, *6*, 201–204.
109. Stamm, A.J. Effect of Polyethylene Glycol on the Dimensional Stability of Wood. *For. Prod. J.* **1959**, *9*, 375–381.
110. Stamm, A.J. Factors Affecting the Bulking and Dimensional Stabilization of Wood with Polyethylene Glycols. *For. Prod. J.* **1964**, *14*, 403–408.

111. Thanh, N.D.; Wakiya, S.; Matsuda, K.; Ngoc, B.D.; Sugiyama, J.; Kohdzuma, Y. Diffusion of Chemicals into Archaeological Waterlogged Hardwoods Obtained from the Thang Long Imperial Citadel Site, Vietnam. *J. Wood Sci.* **2018**, *64*, 836–844. [CrossRef]
112. Jones, A.M.; Rule, M.H. Preserving the Wreck of the Mary Rose. In Proceedings of the 4th ICOM-Group on Wet Organic Archaeological Materials Conference, Bremerhaven, Germany, 20–24 August 1990; pp. 25–48.
113. Preston, J.; Smith, A.D.; Schofield, E.J.; Chadwick, A.V.; Jones, M.A.; Watts, J.E.M. The Effects of Mary Rose Conservation Treatment on Iron Oxidation Processes and Microbial Communities Contributing to Acid Production in Marine Archaeological Timbers. *PLoS ONE* **2014**, *9*, e84169. [CrossRef]
114. Piva, E. Conservation of a Tudor Warship: Investigating the Timbers of the Mary Rose. Ph.D. Thesis, University of Portsmouth, Portsmouth, UK, 2017.
115. Wachsmann, S.; Raveh, K.; Cohen, O. The Kinneret Boat Project Part I. The Excavation and Conservation of the Kinneret Boat. *Int. J. Naut. Archaeol.* **1987**, *16*, 233–245. [CrossRef]
116. Hoffmann, P. To Be and to Continue Being a Cog: The Conservation of the Bremen Cog of 1380. *Int. J. Naut. Archaeol.* **2001**, *30*, 129–140. [CrossRef]
117. Mortensen, M.N.; Egsgaard, H.; Hvilsted, S.; Shashoua, Y.; Glastrup, J. Characterisation of the Polyethylene Glycol Impregnation of the Swedish Warship Vasa and One of the Danish Skuldelev Viking Ships. *J. Archaeol. Sci.* **2007**, *34*, 1211–1218. [CrossRef]
118. Hoffmann, P.; Choi, K.; Kim, Y. The 14th-Century Shinan Ship—Progress in Conservation. *Int. J. Naut. Archaeol.* **1991**, *20*, 59–64. [CrossRef]
119. Ossowski, W. (Ed.) *The Copper Ship: A Medieval Shipwreck and Its Cargo*; Narodowe Muzeum Morskie: Warsaw, Poland, 2014.
120. Millett, M.; McGrail, S.; Creighton, J.D.; Gregson, C.W.; Heal, S.V.E.; Hillam, J.; Holdridge, L.; Jordan, D.; Spencer, P.J.; Stallibrass, S. The Archaeology of the Hasholme Logboat. *Archaeol. J.* **1987**, *144*, 69–155. [CrossRef]
121. Foxon, A.D. The Hasholme Iron Age Logboat: 17 Metres of Trouble! In Proceedings of the 6th ICOM Group on Wet Organic Archaeological Materials Conference, New York, NY, USA, 9–13 September 1996; pp. 547–553.
122. Kocabaş, U. The Yenikapı Byzantine-Era Shipwrecks, Istanbul, Turkey: A Preliminary Report and Inventory of the 27 Wrecks Studied by Istanbul University. *Int. J. Naut. Archaeol.* **2015**, *44*, 5–38. [CrossRef]
123. Fejfer, M.; Matloka, A.; Siepak, J. Spectrophotometric Determination of PEG in Waterlogged Archaeological Wood and Impregnation Solutions. *Stud. Conserv.* **2021**, *66*, 182–189. [CrossRef]
124. Henrik-Klemens, A.; Abrahamsson, K.; Bjordal, C.; Walsh, A. An in Situ Raman Spectroscopic Method for Quantification of Polyethylene Glycol (PEG) in Waterlogged Archaeological Wood. *Holzforschung* **2020**, *74*, 1043–1051. [CrossRef]
125. Kanazawa, Y.; Yamada, T.; Kido, A.; Fujimoto, K.; Takakura, K.; Hayashi, H.; Fushimi, Y.; Kozawa, S.; Koizumi, K.; Okuni, M.; et al. Visualization of Magnetization Transfer Effect in Polyethylene Glycol Impregnated Waterlogged Wood. *Appl. Magn. Reson.* **2017**, *48*, 125–134. [CrossRef]
126. Graves, D.J. A Comparative Study of Consolidants for Waterlogged Wood: Polyethylene Glycol, Sucrose and Silicon Oil. *SSCR J. News Mag. Scott. Soc. Conserv. Restor.* **2004**, *15*, 13–17.
127. Unger, A.; Schniewind, A.; Unger, W. *Conservation of Wood Artifacts: A Handbook*; Springer Science & Business Media: Berlin, Germany, 2001.
128. Giachi, G.; Capretti, C.; Donato, I.D.; Macchioni, N.; Pizzo, B. New Trials in the Consolidation of Waterlogged Archaeological Wood with Different Acetone-Carried Products. *J. Archaeol. Sci.* **2011**, *38*, 2957–2967. [CrossRef]
129. Jiachang, C.; Donglang, C.; Jingen, Z.; Xia, H.; Shenglong, C. Shape Recovery of Collapsed Archaeological Wood Ware with Active Alkali-Urea Treatment. *J. Archaeol. Sci.* **2009**, *36*, 434–440. [CrossRef]
130. Meints, T.; Hansmann, C.; Gindl-Altmutter, W. Suitability of Different Variants of Polyethylene Glycol Impregnation for the Dimensional Stabilization of Oak Wood. *Polymers* **2018**, *10*, 81. [CrossRef]
131. Babinski, L. Dimensional Changes of Waterlogged Archaeological Hardwoods Pre-Treated with Aqueous Mixtures of Lactitol/Trehalose and Mannitol/Trehalose before Freeze-Drying. *J. Cult. Herit.* **2015**, *16*, 876–882. [CrossRef]
132. Babinski, L. Research on Dimensional Stability in Waterlogged Archaeological Wood Dried in a Non-Cooled Vacuum Chamber Connected to a Laboratory Freeze-Dryer. *Drewno* **2012**, *55*, 5–19.
133. Schnell, U.; Jensen, P. Determination of Maximum Freeze Drying Temperature for PEG-Impregnated Archaeological Wood. *Stud. Conserv.* **2007**, *52*, 50–58. [CrossRef]
134. Kaye, B.; Cole-Hamilton, D.J.; Morphet, K. Supercritical Drying: A New Method for Conserving Waterlogged Archaeological Materials. *Stud. Conserv.* **2000**, *45*, 233–252. [CrossRef]
135. Strachan, D.; Skinner, T.; Hall, M.A. The Carpow Bronze Age Logboat: Excavation, Conservation and Display: NOTES. *Int. J. Naut. Archaeol.* **2012**, *41*, 390–397. [CrossRef]
136. Ljungdahl, J.; Berglund, L.A. Transverse Mechanical Behaviour and Moisture Absorption of Waterlogged Archaeological Wood from the Vasa Ship. *Holzforschung* **2007**, *61*, 279–284. [CrossRef]
137. Majka, J.; Zborowska, M.; Fejfer, M.; Waliszewska, B.; Olek, W. Dimensional Stability and Hygroscopic Properties of PEG Treated Irregularly Degraded Waterlogged Scots Pine Wood. *J. Cult. Herit.* **2018**, *31*, 133–140. [CrossRef]
138. Olek, W.; Majka, J.; Stempin, A.; Sikora, M.; Zborowska, M. Hygroscopic Properties of PEG Treated Archaeological Wood from the Rampart of the 10th Century Stronghold as Exposed in the Archaeological Reserve Genius Loci in Poznań (Poland). *J. Cult. Herit.* **2016**, *18*, 299–305. [CrossRef]

139. Chan, K.L.A.; Kazarian, S.G. Visualisation of the Heterogeneous Water Sorption in a Pharmaceutical Formulation under Controlled Humidity via FT-IR Imaging. *Vib. Spectrosc.* **2004**, *35*, 45–49. [CrossRef]
140. Vorobyev, A.; van Dijk, N.P.; Kristofer Gamstedt, E. Orthotropic Creep in Polyethylene Glycol Impregnated Archaeological Oak from the Vasa Ship: Results of Creep Experiments in a Museum-like Climate. *Mech. Time-Depend Mater.* **2019**, *23*, 35–52. [CrossRef]
141. Esteban, L.G.; de Palacios, P.; Garcia Fernandez, F.; Garcia-Amorena, I. Effects of Burial of *Quercus* Spp. Wood Aged 5910 +/- 250 BP on Sorption and Thermodynamic Properties. *Int. Biodeterior. Biodegrad.* **2010**, *64*, 371–377. [CrossRef]
142. Majka, J.; Babinski, L.; Olek, W. Sorption Isotherms of Waterlogged Subfossil Scots Pine Wood Impregnated with a Lactitol and Trehalose Mixture. *Holzforschung* **2017**, *71*, 813–819. [CrossRef]
143. Keating, B.A.; Hill, C.A.S.; Sun, D.; English, R.; Davies, P.; McCue, C. The Water Vapor Sorption Behavior of a Galactomannan Cellulose Nanocomposite Film Analyzed Using Parallel Exponential Kinetics and the Kelvin-Voigt Viscoelastic Model. *J. Appl. Polym. Sci.* **2013**, *129*, 2352–2359. [CrossRef]
144. Hill, C.A.S.; Keating, B.A.; Jalaludin, Z.; Mahrtdt, E. A Rheological Description of the Water Vapour Sorption Kinetics Behaviour of Wood Invoking a Model Using a Canonical Assembly of Kelvin-Voigt Elements and a Possible Link with Sorption Hysteresis. *Holzforschung* **2012**, *66*, 35–47. [CrossRef]
145. Thybring, E.E.; Digaitis, R.; Nord-Larsen, T.; Beck, G.; Fredriksson, M. How Much Water Can Wood Cell Walls Hold? A Triangulation Approach to Determine the Maximum Cell Wall Moisture Content. *PLoS ONE* **2020**, *15*, e0238319. [CrossRef]
146. Gurnev, P.A.; Stanley, C.B.; Aksoyoglu, M.A.; Hong, K.; Parsegian, V.A.; Bezrukov, S.M. Poly(Ethylene Glycol)s in Semidilute Regime: Radius of Gyration in the Bulk and Partitioning into a Nanopore. *Macromolecules* **2017**, *50*, 2477–2483. [CrossRef]
147. Bardet, M.; Gerbaud, G.; Doan, C.; Giffard, M.; Hediger, S.; De Paepe, G.; Tran, Q.-K. Dynamics Property Recovery of Archaeological-Wood Fibers Treated with Polyethylene Glycol Demonstrated by High-Resolution Solid-State NMR. *Cellulose* **2012**, *19*, 1537–1545. [CrossRef]
148. Bardet, M.; Gerbaud, G.; Tràn, Q.-K.; Hediger, S. Study of Interactions between Polyethylene Glycol and Archaeological Wood Components by <sup>13</sup>C High-Resolution Solid-State CP-MAS NMR. *J. Archaeol. Sci.* **2007**, *34*, 1670–1676. [CrossRef]
149. Vorobyev, A.; Almkvist, G.; van Dijk, N.P.; Gamstedt, E.K. Relations of Density, Polyethylene Glycol Treatment and Moisture Content with Stiffness Properties of Vasa Oak Samples. *Holzforschung* **2017**, *71*, 327–335. [CrossRef]
150. Norimoto, M.; Gril, J.; Rowell, R.M. Rheological Properties of Chemically Modified Wood: Relationship between Dimensional and Creep Stability. *Wood Fiber Sci.* **1992**, *24*, 25–35.
151. Afshar, R.; Cheylan, M.; Almkvist, G.; Ahlgren, A.; Gamstedt, E.K. Creep in Oak Material from the Vasa Ship: Verification of Linear Viscoelasticity and Identification of Stress Thresholds. *Eur. J. Wood Prod.* **2020**, *78*, 1095–1103. [CrossRef]
152. Hoffmann, P. On the Long-Term Visco-Elastic Behaviour of Polyethylene Glycol (PEG) Impregnated Archaeological Oak Wood. *Holzforschung* **2010**, *64*, 22. [CrossRef]
153. Vorobyev, A.; Arnould, O.; Laux, D.; Longo, R.; van Dijk, N.P.; Gamstedt, E.K. Characterisation of Cubic Oak Specimens from the Vasa Ship and Recent Wood by Means of Quasi-Static Loading and Resonance Ultrasound Spectroscopy (RUS). *Holzforschung* **2016**, *70*, 457–465. [CrossRef]
154. Wagner, L.; Almkvist, G.; Bader, T.K.; Bjurhager, I.; Rautkari, L.; Gamstedt, E.K. The Influence of Chemical Degradation and Polyethylene Glycol on Moisture-Dependent Cell Wall Properties of Archeological Wooden Objects: A Case Study of the Vasa Shipwreck. *Wood Sci. Technol.* **2016**, *50*, 1103–1123. [CrossRef]
155. Hill, C.; Altgen, M.; Rautkari, L. Thermal Modification of Wood—a Review: Chemical Changes and Hygroscopicity. *J. Mater. Sci.* **2021**, *56*, 6581–6614. [CrossRef]
156. Bjurhager, I.; Ljungdahl, J.; Wallstrom, L.; Gamstedt, E.K.; Berglund, L.A. Towards Improved Understanding of PEG-Impregnated Waterlogged Archaeological Wood: A Model Study on Recent Oak. *Holzforschung* **2010**, *64*, 243–250. [CrossRef]
157. Mortensen, M.N.; Matthiesen, H. Oxygen Consumption by Conserved Archaeological Wood. *Anal. Bioanal. Chem.* **2013**, *405*, 6373–6377. [CrossRef] [PubMed]
158. McQueen, C.M.A.; Mortensen, M.N.; Caruso, F.; Mantellato, S.; Braovac, S. Oxidative Degradation of Archaeological Wood and the Effect of Alum, Iron and Calcium Salts. *Herit. Sci.* **2020**, *8*, 32. [CrossRef]
159. Almkvist, G.; Persson, I. Extraction of Iron Compounds from Wood from the Vasa. *Holzforschung* **2006**, *60*, 678–684. [CrossRef]
160. Bjurhager, I.; Halonen, H.; Lindfors, E.-L.; Iversen, T.; Almkvist, G.; Gamstedt, E.K.; Berglund, L.A. State of Degradation in Archeological Oak from the 17th Century Vasa Ship: Substantial Strength Loss Correlates with Reduction in (Holo)Cellulose Molecular Weight. *Biomacromolecules* **2012**, *13*, 2521–2527. [CrossRef] [PubMed]
161. Almkvist, G.; Persson, I. Fenton-Induced Degradation of Polyethylene Glycol and Oak Holocellulose. A Model Experiment in Comparison to Changes Observed in Conserved Waterlogged Wood. *Holzforschung* **2008**, *62*, 704–708. [CrossRef]
162. Lindfors, E.-L.; Lindstrom, M.; Iversen, T. Polysaccharide Degradation in Waterlogged Oak Wood from the Ancient Warship Vasa. *Holzforschung* **2008**, *62*, 57–63. [CrossRef]
163. Almkvist, G.; Persson, I. Distribution of Iron and Sulfur and Their Speciation in Relation to Degradation Processes in Wood from the Swedish Warship Vasa. *N. J. Chem.* **2011**, *35*, 1491. [CrossRef]
164. Norbakhsh, S.; Bjurhager, I.; Almkvist, G. Impact of Iron(II) and Oxygen on Degradation of Oak—Modeling of the Vasa Wood. *Holzforschung* **2014**, *68*, 649–655. [CrossRef]

165. Fors, Y.; Richards, V. The Effects of the Ammonia Neutralizing Treatment on Marine Archaeological Vasa Wood. *Stud. Conserv.* **2010**, *55*, 41–54. [CrossRef]
166. Fors, Y.; Sandström, M. Sulfur and Iron in Shipwrecks Cause Conservation Concerns. *Chem. Soc. Rev.* **2006**, *35*, 399. [CrossRef] [PubMed]
167. Giorgi, R.; Chelazzi, D.; Baglioni, P. Conservation of Acid Waterlogged Shipwrecks: Nanotechnologies for de-Acidification. *Appl. Phys. A* **2006**, *83*, 567–571. [CrossRef]
168. Poggi, G.; Toccafondi, N.; Chelazzi, D.; Canton, P.; Giorgi, R.; Baglioni, P. Calcium Hydroxide Nanoparticles from Solvothermal Reaction for the Deacidification of Degraded Waterlogged Wood. *J. Colloid Interface Sci.* **2016**, *473*, 1–8. [CrossRef]
169. Schofield, E.J.; Sarangi, R.; Mehta, A.; Jones, A.M.; Smith, A.; Mosselmans, J.F.W.; Chadwick, A.V. Strontium Carbonate Nanoparticles for the Surface Treatment of Problematic Sulfur and Iron in Waterlogged Archaeological Wood. *J. Cult. Herit.* **2016**, *18*, 306–312. [CrossRef]
170. Fors, Y.; Jalilvand, F.; Sandström, M. Analytical Aspects of Waterlogged Wood in Historical Shipwrecks. *Anal. Sci.* **2011**, *27*, 785. [CrossRef]
171. Emery, J.A.; Schroeder, H.A. Iron-Catalyzed Oxidation of Wood Carbohydrates. *Wood Sci. Technol.* **1974**, *8*, 123–137. [CrossRef]
172. Giachi, G.; Bettazzi, F.; Chimichi, S.; Staccioli, G. Chemical Characterisation of Degraded Wood in Ships Discovered in a Recent Excavation of the Etruscan and Roman Harbour of Pisa. *J. Cult. Herit.* **2003**, *4*, 75–83. [CrossRef]
173. Wetherall, K.M.; Moss, R.M.; Jones, A.M.; Smith, A.D.; Skinner, T.; Pickup, D.M.; Goatham, S.W.; Chadwick, A.V.; Newport, R.J. Sulfur and Iron Speciation in Recently Recovered Timbers of the Mary Rose Revealed via X-Ray Absorption Spectroscopy. *J. Archaeol. Sci.* **2008**, *35*, 1317–1328. [CrossRef]
174. Lawson, R.T. Aqueous Oxidation of Pyrite by Molecular Oxygen. *Chem. Rev.* **1982**, *82*, 461–497. [CrossRef]
175. Fengel, D.; Wegener, G. *Wood Chemistry, Ultrastructure, Reactions*; De Gruyter: Berlin, Germany; New York, NY, USA, 1983; ISBN 978-3-11-008481-8.
176. Dedic, D.; Iversen, T.; Ek, M. Cellulose Degradation in the Vasa: The Role of Acids and Rust. *Stud. Conserv.* **2013**, *58*, 308–313. [CrossRef]
177. Arantes, V.; Milagres, A.M.F.; Filley, T.R.; Goodell, B. Lignocellulosic Polysaccharides and Lignin Degradation by Wood Decay Fungi: The Relevance of Nonenzymatic Fenton-Based Reactions. *J. Ind. Microbiol. Biotechnol.* **2011**, *38*, 541–555. [CrossRef] [PubMed]
178. Contreras, D.; Freer, J.; Rodríguez, J. Veratryl Alcohol Degradation by a Catechol-Driven Fenton Reaction as Lignin Oxidation by Brown-Rot Fungi Model. *Int. Biodeterior. Biodegrad.* **2006**, *57*, 63–68. [CrossRef]
179. Zeng, J.; Yoo, C.G.; Wang, F.; Pan, X.; Vermerris, W.; Tong, Z. Biomimetic Fenton-Catalyzed Lignin Depolymerization to High-Value Aromatics and Dicarboxylic Acids. *ChemSusChem* **2015**, *8*, 861–871. [CrossRef] [PubMed]
180. Suzuki, I. Oxidation of Inorganic Sulfur Compounds: Chemical and Enzymatic Reactions. *Can. J. Microbiol.* **1999**, *45*, 97–105. [CrossRef]
181. Albelda Berenguer, M.; Monachon, M.; Jacquet, C.; Junier, P.; Rémazeilles, C.; Schofield, E.J.; Joseph, E. Biological Oxidation of Sulfur Compounds in Artificially Degraded Wood. *Int. Biodeterior. Biodegrad.* **2019**, *141*, 62–70. [CrossRef]
182. Kawai, F.; Kimura, T.; Fukaya, M.; Tani, Y.; Ogata, K.; Ueno, T.; Fukami, H. Bacterial Oxidation of Polyethylene Glycol. *Appl. Environ. Microbiol.* **1978**, *35*, 679–684. [CrossRef]
183. Pele, C.; Guilminot, E.; Labroche, S.; Lemoine, G.; Baron, G. Iron Removal from Waterlogged Wood: Extraction by Electrophoresis and Chemical Treatments. *Stud. Conserv.* **2015**, *60*, 155–171. [CrossRef]
184. Monachon, M.; Albelda-Berenguer, M.; Joseph, E. Biological oxidation of iron sulfides. *Adv. Appl. Microbiol.* **2019**, *107*, 1–27.
185. Rémazeilles, C.; Meunier, L.; Leveque, F.; Plasson, N.; Conforto, E.; Crouzet, M.; Refait, P.; Caillat, L. Post-Treatment Study of Iron/Sulfur-Containing Compounds in the Wreck of Lyon Saint-Georges 4 (Second Century ACE). *Stud. Conserv.* **2020**, *65*, 28–36. [CrossRef]
186. Sandström, M.; Jalilvand, F.; Persson, I.; Gelius, U.; Frank, P.; Hall-Roth, I. Deterioration of the Seventeenth-Century Warship Vasa by Internal Formation of Sulphuric Acid. *Nature* **2002**, *415*, 893–897. [CrossRef]
187. Björdal, C.G.; Fors, Y. Correlation between Sulfur Accumulation and Microbial Wood Degradation on Shipwreck Timbers. *Int. Biodeterior. Biodegrad.* **2019**, *140*, 37–42. [CrossRef]
188. Dedic, D.; Sandberg, T.; Iversen, T.; Larsson, T.; Monica, E.K. Analysis of Lignin and Extractives in the Oak Wood of the 17th Century Warship Vasa. *Holzforschung* **2014**, *68*, 419–425. [CrossRef]
189. Arygyropoulos, V.; Degrigny, C.; Guilminot, E. Monitoring Treatments of Waterlogged Iron-Wood Composite Artifacts Using Hostacor IT-PEG 400 Solutions. *Stud. Conserv.* **2000**, *45*, 253–264. [CrossRef]
190. Li, B.; Liu, A.-H.; He, L.-N.; Yang, Z.-Z.; Gao, J.; Chen, K.-H. Iron-Catalyzed Selective Oxidation of Sulfides to Sulfoxides with the Polyethylene Glycol/O<sub>2</sub> System. *Green Chem.* **2012**, *14*, 130–135. [CrossRef]
191. Hemenway, J.N.; Carvalho, T.C.; Rao, V.M.; Wu, Y.; Levons, J.K.; Narang, A.S.; Paruchuri, S.R.; Stamato, H.J.; Varia, S.A. Formation of Reactive Impurities in Aqueous and Neat Polyethylene Glycol 400 and Effects of Antioxidants and Oxidation Inducers. *J. Pharm. Sci.* **2012**, *101*, 3305–3318. [CrossRef]
192. García-Jimeno, S.; Estelrich, J. Ferrofluid Based on Polyethylene Glycol-Coated Iron Oxide Nanoparticles: Characterization and Properties. *Colloids Surf. A Physicochem. Eng. Asp.* **2013**, *420*, 74–81. [CrossRef]

193. Tamburini, D.; Lucejko, J.J.; Modugno, F.; Colombini, M.P. Combined Pyrolysis-Based Techniques to Evaluate the State of Preservation of Archaeological Wood in the Presence of Consolidating Agents. *J. Anal. Appl. Pyrolysis* **2016**, *122*, 429–441. [CrossRef]
194. Stamm, A.J. Treatment with Sucrose and Invert Sugar. *Ind. Eng. Chem.* **1937**, *29*, 833–835. [CrossRef]
195. Parrent, J.M. The Conservation of Waterlogged Wood Using Sucrose. *Stud. Conserv.* **1985**, *30*, 63–72. [CrossRef]
196. Hoffmann, P. Sucrose for Waterlogged Wood: Not so Simple at All. In Proceedings of the ICOM Committee for Conservation, Edinburgh, Scotland, 1–6 September 1996; pp. 657–662.
197. Kennedy, A.; Pennington, E.R. Conservation of Chemically Degraded Waterlogged Wood with Sugars. *Stud. Conserv.* **2014**, *59*, 194–201. [CrossRef]
198. Nguyen, T.D.; Kohdzuma, Y.; Endo, R.; Sugiyama, J. Evaluation of Chemical Treatments on Dimensional Stabilization of Archeological Waterlogged Hardwoods Obtained from the Thang Long Imperial Citadel Site, Vietnam. *J. Wood Sci.* **2018**, *64*, 436–443. [CrossRef]
199. Liu, L.; Zhang, L.; Zhang, B.; Hu, Y. A Comparative Study of Reinforcement Materials for Waterlogged Wood Relics in Laboratory. *J. Cult. Herit.* **2019**, *36*, 94–102. [CrossRef]
200. Tahira, A.; Howard, W.; Pennington, E.R.; Kennedy, A. Mechanical Strength Studies on Degraded Waterlogged Wood Treated with Sugars. *Stud. Conserv.* **2017**, *62*, 223–228. [CrossRef]
201. Babiński, L.; Fabisiak, E.; Dąbrowski, H.P.; Kittel, P. Study on Dimensional Stabilization of 12,500-Year-Old Waterlogged Subfossil Scots Pine Wood from the Koźmin Las Site, Poland. *J. Cult. Herit.* **2017**, *23*, 119–127. [CrossRef]
202. Pecoraro, E.; Pizzo, B.; Salvini, A.; Macchioni, N. Dynamic Mechanical Analysis (DMA) at Room Temperature of Archaeological Wood Treated with Various Consolidants. *Holzforschung* **2019**, *73*, 757–772. [CrossRef]
203. Endo, R.; Kamei, K.; Iida, I.; Kawahara, Y. Dimensional Stability of Waterlogged Wood Treated with Hydrolyzed Feather Keratin. *J. Archaeol. Sci.* **2008**, *35*, 1240–1246. [CrossRef]
204. Kawahara, Y.; ENDO, P.; Kimura, T. Conservation Treatment for Archaeological Waterlogged Woods Using Keratin from Waste Down. *J. Text. Eng.* **2002**, *48*, 107–110. [CrossRef]
205. Jensen, P.; Christensen, K.V.; Bak, D.; Schnell, U. Keratin as a Bulking and Stabilization Agent for Collapsible Waterlogged Archaeological Wood. In Proceedings of the 11th ICOM-CC Group on Wet Organic Archaeological Materials Conference, Greenville, NC, USA, 20 April 2010; pp. 227–241.
206. Fejfer, M.; Pietrzak, I.; Zborowska, M. Dimensional Stabilization of Oak and Pine Waterlogged Wood with Keratin Aqueous Solutions. In Proceeding of the CONDITION 2015 Conservation and Digitalization Conference, Gdańska, Poland, 19–22 May 2015.
207. Endo, R.; Kamei, K.; Iida, I.; Yokoyama, M.; Kawahara, Y. Physical and Mechanical Properties of Waterlogged Wood Treated with Hydrolyzed Feather Keratin. *J. Archaeol. Sci.* **2010**, *37*, 1311–1316. [CrossRef]
208. Endo, R.; Sugiyama, J. Evaluation of Cell Wall Reinforcement in Feather Keratin-Treated Waterlogged Wood as Imaged by Synchrotron X-Ray Microtomography (MXRT) and TEM. *Holzforschung* **2013**, *67*, 795–803. [CrossRef]
209. Endo, R.; Hattori, T.; Tomii, M.; Sugiyama, J. Identification and Conservation of a Neolithic Polypore. *J. Cult. Herit.* **2015**, *16*, 869–875. [CrossRef]
210. Antonelli, F.; Galotta, G.; Sidoti, G.; Zikeli, F.; Nisi, R.; Davidde Petriaggi, B.; Romagnoli, M. Cellulose and Lignin Nano-Scale Consolidants for Waterlogged Archaeological Wood. *Front. Chem.* **2020**, *8*, 32. [CrossRef]
211. Christensen, M.; Kutzke, H.; Hansen, F.K. New Materials Used for the Consolidation of Archaeological Wood—Past Attempts, Present Struggles, and Future Requirements. *J. Cult. Herit.* **2012**, *13*, S183–S190. [CrossRef]
212. Cipriani, G.; Salvini, A.; Baglioni, P.; Bucciarelli, E. Cellulose as a Renewable Resource for the Synthesis of Wood Consolidants. *J. Appl. Polym. Sci.* **2010**, *118*, 2939–2950. [CrossRef]
213. Broda, M.; Kryg, P.; Ormondroyd, G.A. Gap-Fillers for Wooden Artefacts Exposed Outdoors—A Review. *Forests* **2021**, *12*, 606. [CrossRef]
214. Giachi, G.; Capretti, C.; Macchioni, N.; Pizzo, B.; Donato, I.D. A Methodological Approach in the Evaluation of the Efficacy of Treatments for the Dimensional Stabilisation of Waterlogged Archaeological Wood. *J. Cult. Herit.* **2010**, *11*, 91–101. [CrossRef]
215. Wakefield, J.M.; Hampe, R.; Gillis, R.B.; Sitterli, A.; Adams, G.G.; Kutzke, H.; Heinze, T.; Harding, S.E. Aminoethyl Substitution Enhances the Self-Assembly Properties of an Aminocellulose as a Potential Archaeological Wood Consolidant. *Eur. Biophys. J.* **2020**, *49*, 791–798. [CrossRef] [PubMed]
216. Kataoka, T.; Kurimoto, Y.; Kohdzuma, Y. Conservation of Archaeological Waterlogged Wood Using Lignophenol (II) Adsorption Characteristics of Lignophenol to Hardwood Degraded in Various Degrees, and Surface Hardness and Adsorption/Desorption of Moisture in the Treated Hardwood. *Mokuzai Hozon* **2007**, *33*, 63–72. [CrossRef]
217. McHale, E.; Braovac, S.; Steindal, C.C.; Gillis, R.B.; Adams, G.G.; Harding, S.E.; Benneche, T.; Kutzke, H. Synthesis and Characterisation of Lignin-like Oligomers as a Bio-Inspired Consolidant for Waterlogged Archaeological Wood. *Pure Appl. Chem.* **2016**, *88*, 969–977. [CrossRef]
218. McHale, E.; Steindal, C.C.; Kutzke, H.; Benneche, T.; Harding, S.E. In Situ Polymerisation of Isoeugenol as a Green Consolidation Method for Waterlogged Archaeological Wood. *Sci. Rep.* **2017**, *7*, 46481. [CrossRef]
219. Salanti, A.; Zoia, L.; Zanini, S.; Orlandi, M. Synthesis and Characterization of Lignin–Silicone Hybrid Polymers as Possible Consolidants for Decayed Wood. *Wood Sci. Technol.* **2016**, *50*, 117–134. [CrossRef]



220. Christensen, M.; Larnøy, E.; Kutzke, H.; Hansen, F.K. Treatment of Waterlogged Archaeological Wood Using Chitosan-and Modified Chitosan Solutions. Part 1: Chemical Compatibility and Microstructure. *J. Am. Inst. Conserv.* **2015**, *54*, 3–13. [CrossRef]
221. Walsh, Z.; Janeček, E.-R.; Jones, M.; Scherman, O.A. Natural Polymers as Alternative Consolidants for the Preservation of Waterlogged Archaeological Wood. *Stud. Conserv.* **2017**, *62*, 173–183. [CrossRef]
222. El-Gamal, R.; Nikolaivits, E.; Zervakis, G.I.; Abdel-Maksoud, G.; Topakas, E.; Christakopoulos, P. The Use of Chitosan in Protecting Wooden Artifacts from Damage by Mold Fungi. *Electron. J. Biotechnol.* **2016**, *24*, 70–78. [CrossRef]
223. Broda, M. Natural Compounds for Wood Protection against Fungi—A Review. *Molecules* **2020**, *25*, 3538. [CrossRef] [PubMed]
224. Wakefield, J.M.K.; Gillis, R.B.; Adams, G.G.; McQueen, C.M.A.; Harding, S.E. Controlled Depolymerisation Assessed by Analytical Ultracentrifugation of Low Molecular Weight Chitosan for Use in Archaeological Conservation. *Eur. Biophys. J.* **2018**, *47*, 769–775. [CrossRef]
225. Wakefield, J.M.; Braovac, S.; Kutzke, H.; Stockman, R.A.; Harding, S.E. Tert-Butyldimethylsilyl Chitosan Synthesis and Characterization by Analytical Ultracentrifugation, for Archaeological Wood Conservation. *Eur. Biophys. J.* **2020**, *49*, 781–789. [CrossRef]
226. Walsh, Z.; Janeček, E.-R.; Hodgkinson, J.T.; Sedlmair, J.; Koutsioubas, A.; Spring, D.R.; Welch, M.; Hirschmugl, C.J.; Toprakcioglu, C.; Nitschke, J.R.; et al. Multifunctional Supramolecular Polymer Networks as Next-Generation Consolidants for Archaeological Wood Conservation. *Proc. Natl. Acad. Sci. USA* **2014**, *111*, 17743–17748. [CrossRef]
227. Cipriani, G.; Salvini, A.; Fioravanti, M.; Di Giulio, G.; Malavolti, M. Synthesis of Hydroxylated Oligoamides for Their Use in Wood Conservation. *J. Appl. Polym. Sci.* **2013**, *127*, 420–431. [CrossRef]
228. Papacchini, A.; Dominici, S.; Di Giulio, G.; Fioravanti, M.; Salvini, A. Bio-Based Consolidants for Waterlogged Archaeological Wood: Assessment of the Performance and Optimization of the Diagnostic Protocol. *J. Cult. Herit.* **2019**, *40*, 49–58. [CrossRef]
229. McKerrell, H.; Roger, E.; Varsanyi, A. The Acetone/Rosin Method for Conservation of Waterlogged Wood. *Stud. Conserv.* **1972**, *17*, 111–125. [CrossRef]
230. Donato, D.; Lazzara, G.; Milioto, S. Thermogravimetric Analysis: A Tool to Evaluate the Ability of Mixtures in Consolidating Waterlogged Archaeological Woods. *J. Therm. Anal. Calorim.* **2010**, *101*, 1085–1091. [CrossRef]
231. Bugani, S.; Modugno, F.; Lucejko, J.J.; Giachi, G.; Cagno, S.; Cloetens, P.; Janssens, K.; Morselli, L. Study on the Impregnation of Archaeological Waterlogged Wood with Consolidation Treatments Using Synchrotron Radiation Microtomography. *Anal. Bioanal. Chem.* **2009**, *395*, 1977–1985. [CrossRef]
232. Cutajar, M.; Andriulo, F.; Thomsett, M.R.; Moore, J.C.; Couturaud, B.; Howdle, S.M.; Stockman, R.A.; Harding, S.E. Terpene Polyacrylate TPA5 Shows Favorable Molecular Hydrodynamic Properties as a Potential Bioinspired Archaeological Wood Consolidant. *Sci. Rep.* **2021**, *11*, 1–12. [CrossRef]
233. Lazzara, G.; Cavallaro, G.; Panchal, A.; Fakhrullin, R.; Stavitskaya, A.; Vinokurov, V.; Lvov, Y. An Assembly of Organic-Inorganic Composites Using Halloysite Clay Nanotubes. *Curr. Opin. Colloid Interface Sci.* **2018**, *35*, 42–50. [CrossRef]
234. Cavallaro, G.; Milioto, S.; Lazzara, G. Halloysite Nanotubes: Interfacial Properties and Applications in Cultural Heritage. *Langmuir* **2020**, *36*, 3677–3689. [CrossRef] [PubMed]
235. Cavallaro, G.; Lazzara, G.; Parisi, F.; Riela, S.; Milioto, S. Chapter 8—Nanoclays for Conservation. In *Nanotechnologies and Nanomaterials for Diagnostic, Conservation and Restoration of Cultural Heritage*; Lazzara, G., Fakhrullin, R., Eds.; Advanced Nanomaterials; Elsevier: Amsterdam, The Netherlands, 2019; pp. 149–170. ISBN 978-0-12-813910-3.
236. Cavallaro, G.; Lazzara, G.; Milioto, S.; Parisi, F.; Sparacino, V. Thermal and Dynamic Mechanical Properties of Beeswax-Halloysite Nanocomposites for Consolidating Waterlogged Archaeological Woods. *Polym. Degr. Stabil.* **2015**, *120*, 220–225. [CrossRef]
237. Lisuzzo, L.; Hueckel, T.; Cavallaro, G.; Sacanna, S.; Lazzara, G. Pickering Emulsions Based on Wax and Halloysite Nanotubes: An Ecofriendly Protocol for the Treatment of Archeological Woods. *ACS Appl. Mater. Interfaces* **2021**, *13*, 1651–1661. [CrossRef] [PubMed]
238. Cavallaro, G.; Lazzara, G.; Milioto, S.; Parisi, F.; Ruisi, F. Nanocomposites Based on Esterified Colophony and Halloysite Clay Nanotubes as Consolidants for Waterlogged Archaeological Woods. *Cellulose* **2017**, *24*, 3367–3376. [CrossRef]
239. Parisi, F.; Bernardini, F.; Cavallaro, G.; Mancini, L.; Milioto, S.; Prokop, D.; Lazzara, G. Halloysite Nanotubes/Pluronic Nanocomposites for Waterlogged Archeological Wood: Thermal Stability and X-Ray Microtomography. *J. Therm. Anal. Calorim.* **2020**, *141*, 981–989. [CrossRef]
240. Cavallaro, G.; Milioto, S.; Parisi, F.; Lazzara, G. Halloysite Nanotubes Loaded with Calcium Hydroxide: Alkaline Fillers for the Deacidification of Waterlogged Archeological Woods. *ACS Appl. Mater. Interfaces* **2018**, *10*, 27355–27364. [CrossRef]
241. Brook, M.A. *Silicon in Organic, Organometallic, and Polymer Chemistry*; Brook, M.A., Ed.; John Wiley & Sons: New York, NY, USA, 2000.
242. Hill, C.A.; Farahani, M.M.; Hale, M.D. The Use of Organo Alkoxysilane Coupling Agents for Wood Preservation. *Holzforschung* **2004**, *58*, 316–325. [CrossRef]
243. Mai, C.; Militz, H. Modification of Wood with Silicon Compounds. Inorganic Silicon Compounds and Sol-Gel Systems: A Review. *Wood Sci. Technol.* **2004**, *37*, 339–348. [CrossRef]
244. Hamilton, D.L. *Basic Methods of Conserving Underwater Archaeological Material Culture*; US Department of Defense, Legacy Resource Management Program: Washington, DC, USA, 1996.
245. Kavvouras, P.K.; Kostarelou, C.; Zisi, A.; Petrou, M.; Moraitou, G. Use of Silanol-Terminated Polydimethylsiloxane in the Conservation of Waterlogged Archaeological Wood. *Stud. Conserv.* **2009**, *54*, 65–76. [CrossRef]

246. Broda, M.; Mazela, B. Application of Methyltrimethoxysilane to Increase Dimensional Stability of Waterlogged Wood. *J. Cult. Herit.* **2017**, *25*, 149–156. [CrossRef]
247. Broda, M.; Dąbek, I.; Dutkiewicz, A.; Dutkiewicz, M.; Popescu, C.-M.; Mazela, B.; Maciejewski, H. Organosilicons of Different Molecular Size and Chemical Structure as Consolidants for Waterlogged Archaeological Wood—a New Reversible and Retreatable Method. *Sci. Rep.* **2020**, *10*, 1–13. [CrossRef]
248. Broda, M.; Mazela, B.; Dutkiewicz, A. Organosilicon Compounds with Various Active Groups as Consolidants for the Preservation of Waterlogged Archaeological Wood. *J. Cult. Herit.* **2019**, *35*, 123–128. [CrossRef]
249. Popescu, C.-M.; Broda, M. Interactions Between Different Organosilicons and Archaeological Waterlogged Wood Evaluated by Infrared Spectroscopy. *Forests* **2021**, *12*, 268. [CrossRef]
250. Broda, M.; Majka, J.; Olek, W.; Mazela, B. Dimensional Stability and Hygroscopic Properties of Waterlogged Archaeological Wood Treated with Alkoxysilanes. *Int. Biodeter. Biodegr.* **2018**, *133*, 34–41. [CrossRef]
251. Broda, M. Biological Effectiveness of Archaeological Oak Wood Treated with Methyltrimethoxysilane and PEG against Brown-Rot Fungi and Moulds. *Int. Biodeter. Biodegr.* **2018**, *134*, 110–116. [CrossRef]
252. Smith, C.W.; Wayne, C. Re-Treatment of PEG Treated Composite Artifact | Polyethylene Glycol | Archaeology. Available online: <https://www.scribd.com/document/50291915/Wayne-C-Re-Treatment-of-PEG-Treated-Composite-Artifact> (accessed on 8 June 2021).
253. Andriulo, F.; Giorgi, R.; Steindal, C.C.; Kutzke, H.; Braovac, S.; Baglioni, P. Hybrid Nanocomposites Made of Diol-Modified Silanes and Nanostructured Calcium Hydroxide. Applications to Alum-Treated Wood. *Pure Appl. Chem.* **2017**, *89*, 29–39. [CrossRef]
254. Qiu, J.; Min, R.; Kuo, M. Microscopic Study of Waterlogged Archeological Wood Found in Southwestern China and Method of Conservation Treatment. *Wood Fiber Sci.* **2013**, *45*, 396–404.
255. Christensen, M.; Hansen, F.K.; Kutzke, H. Phenol Formaldehyde Revisited—Novolac Resins for the Treatment of Degraded Archaeological Wood. *Archaeometry* **2015**, *57*, 536–559. [CrossRef]
256. Kiliç, N.; Kiliç, A.G. An Attenuated Total Reflection Fourier Transform Infrared (ATR-FTIR) Spectroscopic Study of Waterlogged Woods Treated with Melamine Formaldehyde. *Vib. Spectrosc.* **2019**, *105*, 102985. [CrossRef]
257. Hoffmann, P.; Wittköpper, M. The Kauramin Method for Stabilizing Waterlogged Wood. In Proceedings of the 7th ICOM-CC Working Group on Wet Organic Archaeological Materials Conference, Grenoble, France, 19–23 October 1998; pp. 163–166.
258. Cesar, T.; Danevčič, T.; Kavkler, K.; Stopar, D. Melamine Polymerization in Organic Solutions and Waterlogged Archaeological Wood Studied by FTIR Spectroscopy. *J. Cult. Herit.* **2017**, *23*, 106–110. [CrossRef]
259. Collis, S. Revisiting Conservation Treatment Methodologies for Waterlogged Archaeological Wood: An Australian Study. *AICCM Bull.* **2015**, *36*, 88–96. [CrossRef]
260. Zhou, Y.; Wang, K.; Hu, D. High Retreatability and Dimensional Stability of Polymer Grafted Waterlogged Archaeological Wood Achieved by ARGET ATRP. *Sci. Rep.* **2019**, *9*, 1–9. [CrossRef]
261. Zhou, Y.; Wang, K.; Hu, D. An Aqueous Approach to Functionalize Waterlogged Archaeological Wood Followed by Improved Surface-Initiated ARGET ATRP for Maintaining Dimensional Stability. *Cellulose* **2021**, *28*, 2433–2443. [CrossRef]
262. Björdal, C.G.; Nilsson, T. Reburial of Shipwrecks in Marine Sediments: A Long-Term Study on Wood Degradation. *J. Archaeol. Sci.* **2008**, *35*, 862–872. [CrossRef]
263. Convention for the Protection of the Archaeological Heritage of Europe (Revised) (Valletta, 1992). Available online: <https://www.coe.int/en/web/culture-and-heritage/valletta-convention> (accessed on 24 June 2021).
264. UNESCO Convention on the Protection of the Underwater Cultural Heritage. Available online: <http://www.unesco.org/new/en/culture/themes/underwater-cultural-heritage/2001-convention/> (accessed on 24 June 2021).
265. Pournou, A. Assessing the Long-Term Efficacy of Geotextiles in Preserving Archaeological Wooden Shipwrecks in the Marine Environment. *J. Archaeol. Sci.* **2018**, *13*, 1–14. [CrossRef]
266. Amendas, G.; McConnachie, G.; Pournou, A. Selective Reburial: A Potential Approach for the in Situ Preservation of Waterlogged Archaeological Wood in Wetland Excavations. *J. Arch. Sci.* **2013**, *40*, 99–108. [CrossRef]
267. Gregory, D.; Matthiesen, H. Nydam Mose: In Situ Preservation at Work. *Conserv. Manag. Archaeol. Sites* **2012**, *14*, 479–486. [CrossRef]
268. Malim, T.; Morgan, D.; Panter, I. Suspended Preservation: Particular Preservation Conditions within the Must Farm—Flag Fen Bronze Age Landscape. *Quat. Int.* **2015**, *368*, 19–30. [CrossRef]
269. Ciferri, O. The Role of Microorganisms in the Degradation of Cultural Heritage. *Stud. Conserv.* **2002**, *47*, 35–45. [CrossRef]



Review

# Sustainability in Heritage Wood Conservation: Challenges and Directions for Future Research

Zarah Walsh-Korb <sup>1,2</sup>

<sup>1</sup> Department of Chemistry, University of Basel, 4058 Basel, Switzerland; zarah.korb@unibas.ch; Tel.: +41-61-207-5960

<sup>2</sup> Department of Biosystems Science and Engineering, ETH Zurich, 4058 Basel, Switzerland

**Abstract:** Conserving the world's cultural and natural heritage is considered a key contributor to achieving the targets set out in the United Nation's Sustainable Development Goals, yet how much attention do we pay to the methods we use to conserve and protect this heritage? With a specific focus on wooden objects of cultural heritage, this review discusses the current state-of-the-art in heritage conservation in terms of sustainability, sustainable alternatives to currently used consolidants, and new research directions that could lead to more sustainable consolidants in the future. Within each stage a thorough discussion of the synthesis mechanisms and/or extraction protocols, particularly for bio-based resources is provided, evaluating resource usage and environmental impact. This is intended to give the reader a better understanding of the overall sustainability of each different approach and better evaluate consolidant choices for a more sustainable approach. The challenges facing the development of sustainable consolidants and recent research that is likely to lead to highly sustainable new consolidant strategies in the future are also discussed. This review aims to contribute to the ongoing discussion of sustainable conservation and highlight the role that consolidants play in truly sustainable heritage conservation.

**Keywords:** heritage wood; conservation; sustainability; bio-based polymers; consolidants



**Citation:** Walsh-Korb, Z.

Sustainability in Heritage Wood Conservation: Challenges and Directions for Future Research.

*Forests* **2022**, *13*, 18. <https://doi.org/10.3390/f13010018>

Academic Editors: Magdalena Broda and Callum A. S. Hill

Received: 1 December 2021

Accepted: 21 December 2021

Published: 23 December 2021

**Publisher's Note:** MDPI stays neutral with regard to jurisdictional claims in published maps and institutional affiliations.



**Copyright:** © 2021 by the author. Licensee MDPI, Basel, Switzerland. This article is an open access article distributed under the terms and conditions of the Creative Commons Attribution (CC BY) license (<https://creativecommons.org/licenses/by/4.0/>).

## 1. Introduction

Wood is an anisotropic, hierarchical material with a three-dimensional fibrous structure composed primarily of cellulose and hemicelluloses, that self-assemble on the nanoscale and are bound into the macroscale structure of wood tissue by lignin [1–3]. It is a widely available natural resource that has been used for centuries to create everything from kitchen utensils to dwellings and transportation. As such, wooden artefacts are common objects in the historical record [3].

Depending on where a wooden artefact is found it will have been subjected to a variety of biotic and abiotic stresses that exert significant influence on the extent and the speed of its degradation [4–7]. All wooden objects will have been exposed to a greater or lesser extent to abiotic factors such as temperature, light, and moisture. Degradation as a function of normal abiotic stress is generally rather slow and such objects can often be displayed or stored with minimal or no active consolidation, although storage in a controlled environment would be recommended to maintain the slow rate of natural degradation [8,9]. At extremes of abiotic stress, particularly moisture, accelerated biotic degradation is often encountered, primarily in the form of wood-decaying fungi and bacteria, although insects and marine borers are also common in certain environments [4]. The action of these organisms can significantly speed up the degradation of wood, through the decomposition of the cellulosic or lignin components, which is highly dependent on the organism. Their action requires mitigation through the use of biocides and/or consolidant treatments to hinder biological activity and maintain the mechanical stability of the artefact. In the majority of cases, the consolidants employed are polymers derived from petrochemical refining.

The Sustainable Development Goals, which form part of the United Nations Agenda for 2030, list strengthening “efforts to protect and safeguard the worlds’ cultural and natural heritage” as a key target to achieving safe, resilient, inclusive and sustainable cities and human settlements (Goal 11) [10]. However, the methods we use to achieve this conservation are not always sustainable themselves. While some natural resins and inorganic minerals are used in wood conservation, many consolidants are petroleum-based. Poly(ethylene glycol) (PEG) [11–15], epoxy-based glues [16], melamine-formaldehyde (MF) resins [17–19] and acrylate or methacrylate copolymers [20,21] are all regularly employed in conservation of wooden objects of cultural importance. As these treatments are by-products of the petroleum industry, their production is inherently unsustainable [22]. The result is that we regularly use highly unsustainable materials, often in large quantities, to ‘sustain’ our cultural heritage.

Currently, only 5–20% of extracted crude oil is refined into chemicals at most refineries [22], with the remainder being used for energy and transportation. This includes the raw materials to produce PEG, MF resins, epoxy, alkoxide (alkoxysilane), methacrylate and acrylate consolidants. With the signing of the Paris Agreement in 2015 [23–28], many countries and institutions pledged to phase out the use of fossil fuels by 2050. What does this mean for the polymers used regularly in the conservation laboratory? One would think that phasing out fossil fuels in the energy sector would reduce the attraction of oil refining and force a switch to more renewable chemical consolidants. Unfortunately, this may not be the case [29]. The reduction in demand for oil for energy and transport means refineries and oil companies are changing their business models and refocusing on petrochemical production [30]. In the coming two decades, petrochemicals will likely make up almost 80% of the products of oil refineries [22]. This significant increase in the availability of non-renewable raw materials for polymers will drive the cost of virgin polymers and plastics down, to the point that it may be more cost-effective to continue using non-renewable consolidants than recyclable or bio-based alternatives [31]. Knowing that cultural institutions often run on very lean budgets [32], the barrier to creating more sustainable conservation methods will increase significantly.

Despite this significant economic driver towards less sustainable conservation practices, the continuation of unsustainable practices across all fields will eventually lead to significant and irreversible damage to our environment with extraordinary economic costs [33], that no amount of cheap petroleum-based products will stem. Thus, there are two strategies we need to enact to ensure a more sustainable conservation practice and do our part to reduce the impact of petroleum-based products on the environment. In the short term, we need to choose sustainable alternatives to current consolidants. This is not a perfect solution, as bio-based alternatives to petroleum-based chemicals are often just as environmentally unfriendly and difficult to dispose of as their fossil-based counterparts [34]. However, their bio-based sourcing does reduce the environmental impact of their production. Unfortunately, commercially available, sustainably sourced alternatives do not exist for all commonly used consolidants. Thus, the longer-term strategy is to explore new bio-inspired alternatives to our current consolidants. This not only requires advances in materials science research but also a mindset shift across all levels of the museum and conservation hierarchy. We must move away from the unsustainable state-of-the-art and embrace sustainable consolidants as a key aspect of the future conservation toolkit, alongside environmentally friendly conservation practices (i.e., use and disposal of gloves and other consumables) and replacement of lighting and ventilation systems with low energy alternatives [35]. Over the following sections, the current state-of-the-art in conservation treatments will be discussed with a specific focus on sustainable alternatives to petroleum-based consolidants and new directions in sustainable consolidant design.

## 2. Consolidants for Wooden Heritage Objects: The Current State-of-the-Art

In the context of wooden objects of cultural importance, there are several commonly used consolidants. These treatments can be broken down into three principal categories:

synthetic, inorganic and bio-based. In the following sections, an overview of the various aspects of consolidant production is given to heighten awareness of the sustainability and environmental impact of the processes involved in their production. This is not a thorough life cycle analysis of each material, which would be outside the scope of this review. However, if we are to increase sustainability in wood conservation, we must be aware of the processes involved in the production of consolidants, to understand whether treatments marked as sustainable alternatives are really an improvement on the state-of-the-art.

Inorganic treatments are the least commonly used in wood conservation, being more heavily exploited in stone and masonry conservation. Those that are used can be divided into two categories—inorganic nanoparticles (INPs) and inorganic polymers. INPs are primarily mined rather than synthesised, thus, their discussion requires a detailed look at the sustainability and practices of the mining industry, which is also too broad a discussion for this review. As such, the discussion of inorganic consolidants will be limited to inorganic polymers that include a petroleum-based component, such as alkoxymethylsilanes. These inorganic polymers are included under the synthetic consolidant section.

### 2.1. Bio-Based Consolidants

Interestingly, the origins of wood consolidation are rather sustainable, insofar as the consolidants have been obtained from renewable resources. Natural resins, oils, and waxes have long been used to preserve and treat wood [36–39]. Waxes (e.g., beeswax obtained from the hives of honey bees (*Apis mellifera* Linnaeus, 1758)), resins (e.g., colophony (rosin) obtained from the sap of various pine (*Pinus* spp.) species) and oils (specifically linseed (from *Linum ussitatissimum* L.) and Tung (from *Vernicia fordii* (Hemsl.) Airy Shaw), have been used to fill cracks, stabilise mechanical properties and enhance the aesthetic qualities of wooden objects for centuries [3]. Their hydrophobicity is also used to improve the water-repellency of wood, reducing susceptibility to bacterial degradation. With the advent of industrial-scale extraction of sucrose for the food industry, sugar conservation also became popular, due to the increased mechanical stability of sugar-conserved wood and its realistic wood-like appearance. Non-reducing sugars and sugar alcohols have also been introduced to the conservation toolkit over the years.

A common misconception is that bio-based consolidants, being obtained from nature, are more sustainable than petroleum-based chemicals. While this is generally true with respect to the renewability of the resource, the methods of cultivation and the processes used to extract and refine these bio-based consolidants into a useable form are often highly damaging to the environment and this must also be taken into consideration. These aspects are discussed in more detail in the following sections.

#### 2.1.1. Oils

Within this class, oils from linseed and tung are the most commonly used. Their relatively low viscosity means that they are used both to enhance the surface aesthetics of the wood by creating a varnished look, as well as penetrate deeper into wooden objects, enhancing the hydrophobicity within their structure [3].

Linseed oil is obtained from flax (*L. ussitatissimum*), an annual crop that exists in two forms, fibre flax and linseed [40]. The former produces high-quality fibres used in the textile industry as linen, while the latter produces lower quality fibres but large quantities of oilseed, from which linseed oil is extracted. With its popularity in the food, textile and automotive industries, it is widely cultivated across North America and large parts of Europe, in areas with cooler temperatures and high rainfall that mean little demand for additional water to maintain crop growth [40]. Otherwise, the cultivation of flax is highly resource-intensive and damaging to the environment. Both flax cultivars have poorly developed root systems and low nutrient uptake, with a low resistance to pests, weeds and disease. Thus, they rely heavily on the use of agrochemicals, derived from petroleum, to sustain high outputs matching demand. High use of agrochemicals combined with soil runoff due to the poor structure of flax roots contributes to eutrophication and degradation of soil quality.

Crop rotations with potatoes and beets, known for their excellent soil structuring and cleaning properties, as well as employing organic manure and natural pest control systems can help reduce the environmental impact of flax leading to more sustainable cultivation and a lower environmental impact [41], however, this is not yet the state-of-the-art. In terms of oil extraction, while cold mechanical pressing is used to obtain food-grade linseed oil [42], warm pressing or solvent extraction is used to retrieve linseed oil for conservation purposes [43]. These techniques lead to greater oil expression but require more input energy or the use of toxic (petroleum-based) solvents, which then require incineration further impacting the environmental footprint of linseed oil. More recently, supercritical and green solvent extraction methods have been explored to extract comparable quantities of oil from oilseeds as their less environmentally friendly counterparts [43,44]. This will hopefully lead to a further reduction of the environmental impact of linseed oil production on the environment. On a positive note, despite their lower fibre quality, fibres from linseed are used as reinforcements in the automotive industry, valorising the waste from oil production and improving the sustainability of crop cultivation, with less material going to waste [40]. A disadvantage of linseed oil as a consolidant is its slow-drying nature, which can lead to softening of the wood during the drying period. This affects the stability of the artefact and has led to much research on improving the drying properties of linseed oil through chemical modifications of the triglyceride structure. An example of this is the epoxidation of linseed oil to create linseed oil-based epoxy resins [45,46], which are discussed in more detail in Section 3.2. While these modifications have significantly enhanced their application in wood conservation, they have impacted the sustainability of linseed oil by reducing the resource efficiency of the consolidant production. Interestingly, while these modifications reduce the sustainability of linseed oil as a consolidant, epoxidised linseed oil is seen as a major improvement to the sustainability of epoxy consolidants, removing a significant amount of the non-renewable component of these adhesives.

Tung oil is obtained from the fruit of the tung tree (*V. fordii*) native to southern China. Tung oil has been used for centuries in China as a wood consolidant and for waterproofing of wooden ships and boats [47]. Its fast-drying nature is an enhancement over the slow-drying properties of linseed oil [48]. This can, however, lead to issues with heterogeneous film formation and incomplete protection of heritage wood, when used alone as a wood consolidant. Thus, combination with thinners is generally recommended to enhance the overall protection of the wood. Interestingly, this fast-drying property led to increased demand for tung oil in the paint industry in the early part of the 20th century to create fast-drying paints with a lower environmental footprint [49,50]. Thus, tung trees were cultivated on an industrial scale to match this new demand. Unlike, the industrial-scale cultivation of linseed, tung trees created a much lower environmental impact. Firstly, tung is a perennial crop, and while it cannot be said that perennials are always more environmentally benign than annual crops due to various dependencies on agrochemicals, the continual growth cycle in comparison to the fragile seedling stage that must be revisited each year does generally reduce overall environmental burden [51]. Perennial crops, combined with low reliance on agrochemicals, are seen as an integral component of sustainable agriculture [52]. Moreover, tung trees have a highly efficient photosynthesis mechanism that leads to initial fruiting, and thus initial oil production, within three years, one of the fastest of all commercial oil crops [53]. The hardy nature of the tung tree reduces the need for extensive agrochemicals, as such, the overall cultivation of tung oil is relatively environmentally friendly. With respect to oil extraction, the same methods are employed with equal environmental concerns as for other oilseeds. However, the advent of green extraction processes, as detailed previously, will likely contribute to further improvement of the overall environmental impact of tung oil, making it one of the most sustainable wood consolidants currently available.

### 2.1.2. Waxes and Resins

In contrast to linseed and tung oil, colophony, and beeswax, due to their high viscosity, have generally been confined to surface treatment [37]. Their major advantages are the ability to fill gaps in the wood surface and bind fragile fragments of the surface, preventing loss and increasing mechanical stability. Their high viscosity, however, means that they often must be heated to penetrate the surface of the wood. Depending on the state of degradation of the wood, the high temperature of the melted treatment can cause darkening of the wood or weakening of the structure if the glass transition temperature of the remaining wood components is exceeded [3].

Looking first at beeswax, produced from the wax secreting glands of the honeybee (*A. mellifera*) [54,55]. The primary function of the wax is to template the formation of the honeycomb that will eventually breed larvae and store pollen and the resulting honey [56]. On a small scale, beeswax is extracted by first warming (35–40 °C) and liquefying the honey. As beeswax melts between 60–65 °C, the wax remains solid and can be filtered from the surface of the liquid honey and then cleaned. This can be melted to form wax cakes that are used for a variety of applications. Bees are not physically harmed by the extraction of the wax from the hive and can continue to thrive after extraction by ‘re-combing’ the hive, thus, it is generally thought that beeswax is a sustainable natural product. However, very little wax is extracted from small apiaries, thus, beeswax is often obtained from industrial beekeeping. The link between industrial beekeeping and monocultures, specifically almond and avocado crops, with respect to the high use of agrochemicals and their environmental impact raises questions about the sustainability of beeswax [57]. The environmental impact of monocultures means we must reconsider the environmental sustainability of beeswax [58–60]. This wax is more commonly extracted using solvent heavy extraction processes involving petroleum-derived dimethylformamide and hexane, to ensure removal of pesticides from the final wax product [61]. Moreover, industrial hives are often sacrificed after the harvest to reduce the cost of sustaining colonies over winter [57], thus, increasing the negative environmental and, for many, the ethical impact of the use of beeswax.

Resin tapping, the process by which colophony is obtained from many species of pine (*Pinus* spp.), is a simple process in which a section of bark is removed, and an incision is made in the outer layers of the tree to encourage resin secretion [62]. A vessel is attached to the tree to collect the expressed resin, a process which is often repeated exhaustively until the tree is felled. Resin tapping is often an integral part of sustainable forestry management for a number of reasons, including the increase in production of resin within the tree as a function of tapping, making it a renewable bio-resource [63]. Moreover, resin tapping increases the profitability of pine stands, creating a sustainable source of income in economically depressed and rural areas [64]. Resin tapping activities also promote increased forest management, often resulting in a lower incidence of forest fires. Many studies have also examined the impact of pine tapping on the wood quality and sensitivity of the trees to climatic and environmental stress [65–68]. While there is often mechanical damage to the wood at the site of tapping, overall, the impact on the quality of the felled wood has been negligible. In fact, some studies have shown that tapped wood is more elastically deformable and less rigid and brittle than untapped wood, contributing to the increased value of the felled wood [69]. Furthermore, it has been observed that tapped trees are no more sensitive to climatic changes and environmental stress than untapped trees, meaning no reduction in stability of forest stands due to resin extraction. Thus, colophony, at least from a sourcing point of view, is an extremely sustainable, environmentally responsible consolidant. Obtaining rosin, and its more valuable counterpart, turpentine, from the tapped resin is a more energy-intensive process known as destructive distillation [70]. Here, the resin is heated to just over 200 °C to distil off phenols and terpenes and degrade unnecessary biological components of the tar (wood shreds, insects, etc.), the remaining gum is the rosin, which is then washed and recrystallised several times using ether and 1% solutions of NaOH to give a pure rosin cake. In comparison to its highly sustainable and



environmentally friendly sourcing, extraction of pure rosin is more energy and resource-intensive. However, advances in green solvent extraction, already discussed with respect to linseed oil extraction could certainly be employed to reduce the environmental impact of the extraction process, increasing the overall sustainability of the final consolidant.

### 2.1.3. Sugars and Sugar Alcohol

Sugars, particularly sucrose obtained from sugarcane (*Saccharum* spp.) and sugar beet (*Beta vulgaris* L.), have also long been employed in the conservation of wooden objects [71]. For conservation, objects are immersed in high concentration solutions that penetrate the wood structure. Controlled drying of the artefact leads to the formation of crystals within the structure that stabilise the wood and enhance mechanical stability [71]. While sucrose is widely available at low cost, due to its use in the food industry, care must be taken during impregnation to avoid bacterial infestations of the wood due to the affinity of bacteria for the sugar solutions and during drying to prevent the formation of excessively large crystals that could rupture the wood cells.

Both sugarcane and beet are cultivated extensively for use in the food industry. In 2020, sugar production reached 187 million tonnes and is set to increase by 3%, to 193 million tonnes, by the end of 2021 [72]. Sugar production has not historically been an environmentally friendly crop, with the tendency to grow sugarcane in extensive monocultures that are highly detrimental to biodiversity and soil quality [73,74]. Monocultures generally require extensive use of agrochemicals to ensure resistance to pests, further damaging soil quality. However, since the mid-2000s, efforts have been made by some of the world's largest sugar producers, particularly in the UK (beet) and Brazil (cane), to improve the environmental impact of both sugar crops. With respect to beet, there is a tendency to grow crops in rotation rather than in monocultures [75] and the advent of green biotechnology has allowed the cultivation of new varieties with greater pest resistance, contributing to a 65% reduction in the use of agrochemicals from 2.0 kg/tonne of beet crop in 1975–80 to 0.7 kg/tonne in 2006 and 2007 [76]. In the UK, this has been reduced even further to total agrochemical usage of 414.5 tonnes in 2018 for a beet production of 6.94 million tonnes, equating to 0.06 kg/tonne [77], a reduction of 97% from 1980s levels. In Brazil, where sugarcane is the primary sugar source, the enhancement of biodiversity on sugar plantations has considerably improved the impact of cane cultivation on the environment. Growing specifically selected complementary crops alongside sugarcane attracts a variety of wildlife and insects that are natural predators of sugarcane pests, thus functioning as natural pest control, reducing or eliminating the need for agrochemicals [78]. One of the best examples of this is the sugarcane plantations of the Balbo group, which alone produces 34% of the world's exported sugar [79]. Their plantation is now exclusively maintained by organic and sustainable agriculture practices improving the environmental impact of sugar cultivation.

Despite significant advances in the enhancement of the sustainability of sugar crops, extraction of sucrose from cane or beet is an energy-intensive process [80], in which the cane is crushed and milled and beet is sliced and diffused to extract the raw juice. This is then followed by heating, liming and clarification (in a different order depending on the starting material), and finally, filtration in the case of beets, to produce the thin juice that is then evaporated and crystallised to give raw sugar. Further refining is carried out to give the white sugar we recognise as table sugar or sucrose [76]. To offset the energy demands of extraction, many sugar refineries are switching to renewable energy to drive these processes, reducing CO<sub>2</sub> emissions in the process. In some cases, this renewable energy is even produced from the by-products of the pulping process, specifically bioethanol and biogas from the fermentation of the beet pulp or sugarcane bagasse, creating a circular system for the extraction of sugar and the valorisation of waste products. Further valorisation of waste products from sugar production includes renewable energy, animal feed, soil enhancers and bio-fertilisers and bioethanol. As such, at many refineries very little of the by-products of the sugar extraction go to waste, creating a more sustainable and circular system with

reduced environmental impact. One of these waste products, sugarcane bagasse [81], is the starting material for bio-glycerol production and will be discussed in more detail in Section 3. Thus, in terms of sustainable consolidants, sucrose is certainly an increasingly environmentally friendly option.

Some alternatives to sucrose have also been explored, specifically lactitol, a sugar alcohol obtained from lactose, and trehalose, a non-reducing sugar found in prokaryotes. While their chemical and environmental stability is much greater than that of sucrose, particularly with respect to bacterial infestation, the dimensional stability of artefacts treated with these alternatives has been observed to be rather inhomogeneous [71]. As such, lactitol and trehalose conservation are rather labour-intensive consolidants in terms of maintaining homogeneity of treated wood, but what of their sustainability?

In the last decade, whey protein has become increasingly interesting as a food additive, improving the texture and nutritional value of a variety of food products [82]. A by-product of whey protein isolate is the milk sugar lactose. The extent of whey protein isolate is such that demand for lactose, a sparsely soluble, low-sweetness sugar, is far outstripped by supply, resulting in large amounts of wastage [82]. Thus, strategies to increase the profitability of lactose by converting it into other high-value products have gained considerable traction. One of these products is lactitol, produced from the catalytic hydrogenation of lactose [82,83]. Lactitol is valued for numerous applications, from low-calorie sweetener to emulsifying agents for polymer and surfactant formulations and, of course, bulking agent and cryo-protective [82], for which it is employed in wood conservation. It is difficult to fully assess the sustainability of lactitol being a by-product of the dairy industry, which can range from very environmentally friendly to highly unsustainable. However, as lactose is a low-value by-product of whey protein isolate, the production of lactitol prevents significant amounts of lactose from being destroyed. As such, it can be considered a positive impact. The catalytic hydrogenation of lactose, or the introduction of hydrogen to the carbonyl group of lactose, currently relies on the use of transition metal catalysts, a finite resource, along with high temperatures (110–200 °C, catalyst dependent), high pressures (10–60 bar) and up to 6 h reaction times. This makes it highly energy and resource-intensive. Moreover, only Ru and Ni catalysts have been shown to produce highly selective hydrogenations (>90%), while Cu (68%) and Pd (30%) have much poorer outcomes [82]. Current manufacturing protocols, thus, impact the overall sustainability of lactitol as a wood consolidant. While not widely used for the hydrogenation of lactose, organocatalytic methods need to be introduced more widely in manufacturing protocols to improve the environmental impact of such waste product valorisation. Organocatalysis relies on the use of small-molecule organic catalysts to promote efficient, low energy and low-temperature transformation, and has revolutionised and improved the environmental impact of catalytic processes in the pharmaceutical and fine chemical industries [84]. Hopefully the recent awarding of the 2021 Nobel prize in Chemistry for organocatalysis [85] will further the uptake of this green methodology in more industrial applications, contributing to lower overall emissions, lower finite resource use and lower energy requirements.

Trehalose, another alternative to sucrose, is a disaccharide consisting of two glucose units with a 1,1- $\alpha$ , $\alpha$ -glycosidic linkage widely found in several prokaryotes, unicellular organisms, of which bacteria are the best-known members. Its role as a bio-protectant, specifically its ability to protect organisms from the effects of desiccation, as well as its resistance to acidic degradation [86], are the principal reasons for its use in wood conservation. Initial attempts to synthesise trehalose focused on chemical glycosylation pathways, however, the unusual 1,1- $\alpha$ , $\alpha$ -glycosidic linkage between the two units of trehalose makes this reaction hard to achieve with high selectivity. A large number of efficient chemoenzymatic trehalose synthesis pathways are known in nature [86], and these have been exploited to make large scale enzymatic synthesis of trehalose a more efficient option for commercial production. In contrast to sucrose, which is extracted, the production of trehalose focuses on enzymatic biotransformation of starch, sucrose, maltose, and maltodextrins. Starch is obtained from the grinding, washing, sieving, and drying of high starch seeds, tubers

and roots like potatoes, corn, wheat, rice and tapioca, in another energy-intensive process, similar to the extraction of sucrose as described previously. Maltose and maltodextrin are obtained from either the acidic or enzymatic degradation of starch, enzymatic methods being the most resource-efficient. Enzymatic pathways to produce trehalose from starch, sucrose, maltose and maltodextrins stemming from fungi and yeasts (phosphorylase), from mesophilic bacteria (glycosyltransferase-hydrolase) and thermophilic bacteria (trehalose synthase) have been reported in the literature [87]. Two of these methods are used to commercially produce trehalose, the glycosyltransferase-hydrolase and the trehalose synthase route. The two-step nature of the phosphorylase route and the low yields of trehalose have made this route commercially non-viable. The one-step trehalose synthase route, relying on extremophilic bacteria, requires a temperature of 75–85 °C and the final yields are up to 85%, thus resulting in a more resource-intensive production route. The glycosyltransferase-hydrolase route is the most environmentally benign, despite the two-step procedure, primarily due to the low temperatures required throughout the procedure (35–45 °C). Furthermore, employing enzymes derived from *Arthrobacter* spp. with corn starch as the substrate, yields of up to 92% have been reported [87]. Despite the energy-efficient final synthesis step, thought must also be given to the cultivation and extraction of the substrates, as in many of the previous cases.

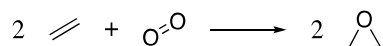
## 2.2. Synthetic Consolidants

Inhomogeneity, or the difficulty in obtaining reproducible treatment standards, has long plagued the use of natural substances as effective consolidants. Thus, when innovations in petroleum refinement and commercial chemical synthesis ushered in the reproducible, large scale, low-cost synthesis of a variety of polymers and polymer precursors in the 1940s, this was seen as a significant benefit to the conservation of heritage wood. While the use of sugars, and oils to a lesser extent, are still popular, the first demonstration of archaeological wood stabilisation using low molecular weight PEG in the late 1950s ushered in a new state-of-the-art for wood conservation. This remains the top choice today, particularly for large artefact conservation. However, methacrylate/acrylate copolymers (e.g., Paraloid B72), melamine-formaldehyde resins (e.g., Kauramin), epoxy resins (e.g., EPO155), and, more recently alkoxysilanes, are also popular. Their various methods of production and their primary applications are discussed below. In comparison to the bio-based consolidants discussed previously, in this section all starting materials are obtained from the petrochemical refining of non-renewable resources and further transformed through synthetic processes to wood consolidants as we are familiar with them.

### 2.2.1. Poly(ethylene glycol), PEG

Poly(ethylene glycol) or PEG is a polyether, a class of polymers in which the repeating unit contains a C–O bond, and by far, the most widely used wood consolidant currently available. Although it was first synthesised in the 1850s, its commercialisation in the 1940s under the name Carbowax was the main driver for its widespread use in applications from cosmetics and personal care products, to medicine and wood conservation [12,88–90], among others. The high solubility of low molecular weight PEG derivatives (under 4000 g/mol) in water means that PEG can effectively penetrate wood cells without precipitation of the chains in the wood cell wall, leading to complete replacement of water with non-volatile PEG retaining the wood structure during drying [13]. Moreover, the high monodispersity associated with the production of PEG means that conservation treatment can consist of several different PEGs penetrating different depths of the wood, offering varying degrees of stabilisation. For example, a low viscosity PEG (200–600 g/mol) is generally used to penetrate deep into a wooden object where degradation is generally lower, but water must still be replaced. Whereas higher molecular weight PEGs (1500–4000 g/mol) with higher viscosity and greater mechanical stability are generally used to conserve the more degraded surface wood.

Synthesis of PEG is carried out on a commercial scale by the ring-opening polymerisation of ethylene oxide (EtO) under cationic or anionic conditions. EtO is industrially produced by the direct oxidation of the petroleum-derived ethylene [91], Scheme 1.



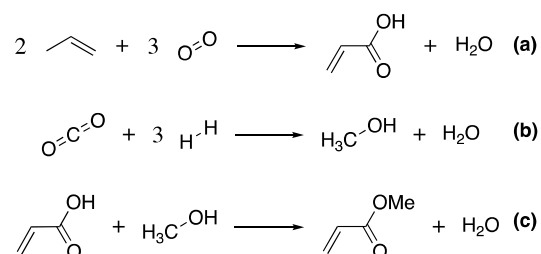
**Scheme 1.** The direct oxidation of ethylene gives ethylene oxide, the starting material for PEG.

The reaction is carried out using high purity O<sub>2</sub> (air is also used in some cases) over a silver catalyst at high temperatures (220–280 °C) and pressures (1–3 MPa) to increase the purity of the yield. On an industrial scale, anionic polymerisations are exploited in which Na, K or Cs alkoxide, hydroxide or carbonates are used to initiate ring-opening of EtO and chain propagation in polar, aprotic solvents (e.g., THF, dioxane and DMSO) [92]. This is a living polymerisation in which no quenching of the reaction occurs. Living polymerisations are characterised by a fast rate of chain initiation with a low rate of chain propagation and no chain termination or chain transfer, meaning a more controlled growth of polymer chains and a less polydisperse chain length distribution [93]. Using this methodology, PEG chains of specific molecule weights can be synthesised. While no external heat is required to start the reaction, the use of toxic, petrochemically obtained starting materials and solvents like THF and dioxane, and the need to dispose of these waste solvents after PEG synthesis, contribute to the negative environmental impact of PEG production.

### 2.2.2. Methacrylate and Acrylate Copolymers

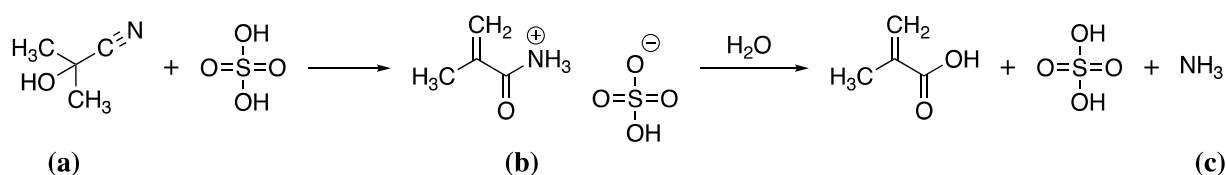
Acrylates and methacrylates are also a variety of polyether known primarily for their use in cosmetics and adhesives. Copolymers of methyl acrylate and ethyl methacrylate are used in wood conservation under the trade name Paraloid B-72 [20]. A range of additional Paraloid variants exist in which the ethyl methacrylate is replaced by methyl methacrylate (B-82), butyl methacrylate (B-66) or isobutyl methacrylate (B-67) [94,95]. These low molecular weight copolymers with high photo and thermal stability are used to improve the dimensional stability of wood and the aesthetic quality of wooden artefacts. Their insolubility in water means they must be applied to wood in organic solvents, most commonly acetone or toluene.

Standard commercial production of methyl acrylate uses acrylic acid as a feedstock, obtained from the oxidation of propylene from petroleum refining, Scheme 2a. This is then esterified with methanol, produced from the energy-intensive catalytic reduction of syngas (Scheme 2b, [96]), under acid conditions (e.g., sulfuric or para-toluenesulfonic acid) at elevated temperatures (Scheme 2c) [96].



**Scheme 2.** The main reactions resulting in the production of methyl acrylate, (a) the synthesis of acrylic acid, (b) the production of methanol and (c) the esterification of acrylic acid.

Methacrylates are prepared from methacrylic acid (MAA) [97]. MAA is produced in a multi-step process involving the reaction of acetone with sodium cyanide at 40 °C to give acetone cyanohydrin (Scheme 3a), which is converted to methacrylamide sulfate (Scheme 3b) by reaction with sulfuric acid at 180 °C and finally hydrolysed to give MAA (Scheme 3c).

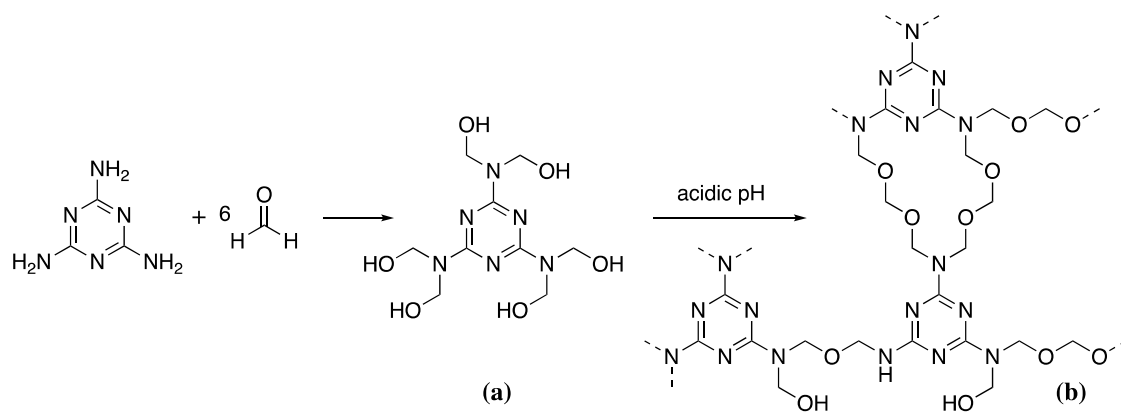


**Scheme 3.** The reaction of acetone cyanohydrin (a) with sulfuric acid to give methacrylamide sulfate (b) as an intermediate which is then hydrolysed to methacrylic acid (c).

This last step can be replaced with an esterification reaction to directly give methyl methacrylate. The production of ethyl, butyl or isobutyl methacrylate requires the further reaction of methacrylic acid with the corresponding alcohol. The preparation of the copolymers that make up the Paraloid B family of consolidants is carried out by free-radical polymerization in a polar solvent using an initiator that generates free radicals upon heating or irradiation with UV light, such as azobisisobutyronitrile (AIBN) or benzoyl peroxide [98]. This initiator generates radicals on the acrylate and methacrylate units by charge transfer allowing chain propagation. This continues until the desired molecular weight has been reached, at which point copolymers are precipitated in a polar solvent terminating the chains. The multi-step nature of the methacrylate production, the high energy input required, as well as the use of large quantities of acid and polar solvents that are produced from finite resources and must be incinerated to dispose of safely makes the production of acrylate-methacrylate copolymers highly resource inefficient. The further requirement to introduce these consolidants into the wood in organic solvents, generally derived from fossil-based resources further increases the negative environmental impact of the use of these consolidants

### 2.2.3. Aminoplasts

Aminoplasts are thermosetting polymers formed by condensation reactions, of which there are two main types-urea-formaldehyde and melamine-formaldehyde resins. Both resins have been used in wood conservation in the past. However, issues with the toxicity of urea-formaldehyde have led to its replacement with the less toxic melamine-formaldehyde, marketed under the name Kauramin [3]. This is one of few commonly used non-reversible wood consolidants. As such it is generally reserved for the most significantly degraded wood requiring consolidants of greater mechanical stability than is provided with standard PEG or bio-based consolidants. The low molecular weight of the monomers means MF consolidants can penetrate deeply into the wood leaving a rigid 3D polymer network after polymerisation. MF resin synthesis requires the pre-synthesis of both melamine and formaldehyde [99]. Commercial melamine production requires urea as a feedstock. Urea is produced by the high temperature (180–210 °C), high pressure (150 bar) reaction of ammonia (NH<sub>3</sub>) and carbon dioxide (CO<sub>2</sub>) forming ammonium carbamate, which is then dehydrated to urea [100]. Urea is then heated to cause decomposition to cyanic acid and ammonia [101]. Cyanuric acid is formed from the polymerisation of cyanic acid, which condenses with the evolved ammonia to form melamine. The off-gas from the melamine production contains such large quantities of ammonia that it is often funnelled off to create feedstock for the further production of urea, helping to reduce the environmental impact of the production cycle, even if only to a small degree. Formaldehyde is produced by the catalytic oxidation of methanol over a silver metal catalyst at 650 °C [102]. Methylolation or the formation of MF pre-polymer is carried out by mixing melamine with formaldehyde in a 1:6 ratio at approximately 60 °C (Scheme 4a) [99].

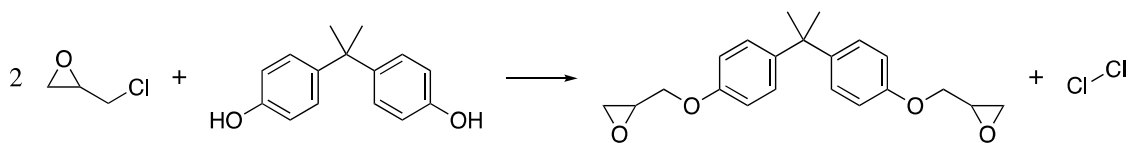


**Scheme 4.** The condensation of melamine and formaldehyde to give the prepolymer (a), followed by polymerisation at acidic pH to give the network structure (b).

This pre-polymer is then infiltrated into the wood over several days/weeks with pH maintained at 8.5 to ensure no unwanted polymerisation of the pre-polymer occurs. This is generally done with triethanolamine. Once the wood has been completely infiltrated, the pH is allowed to drop to acidic pH starting the condensation reaction that produces the MF resin in situ (Scheme 4b). In industrial settings, this would be done by thermal polymerisation to increase reaction efficiency. The entire production process is resource, energy, and labour intensive from the initial preparation of urea to the final MF polymerisation within the wood.

#### 2.2.4. Epoxy Resins

Epoxy resins are another non-reversible treatment, that have primarily been used to repair fragile wood surfaces. Their high viscosity makes infiltration of the wood structure impossible, as such epoxy resins are generally confined to surface work. They are also thermosetting polymers that can be homopolymerised to create pure epoxy resins or cross-linked with a range of curing agents, including polyfunctional amines, acids, acid anhydrides, alcohols, phenols and thiols [103]. The most common system, and the one found in most epoxy resins used in wood conservation, are polyfunctional amines. Thus, heteropolymers of epoxies cross-linked by amine curing agents will be the focus of this discussion. Like MF, epoxy resins are a two-part system containing an epoxy pre-polymer and, typically an amine cross-linking unit. The most commonly used epoxy prepolymer is bisphenol A diglycidyl ether (DGEBA) formed from the reaction of bisphenol A (BPA) and epichlorohydrin (Scheme 5).

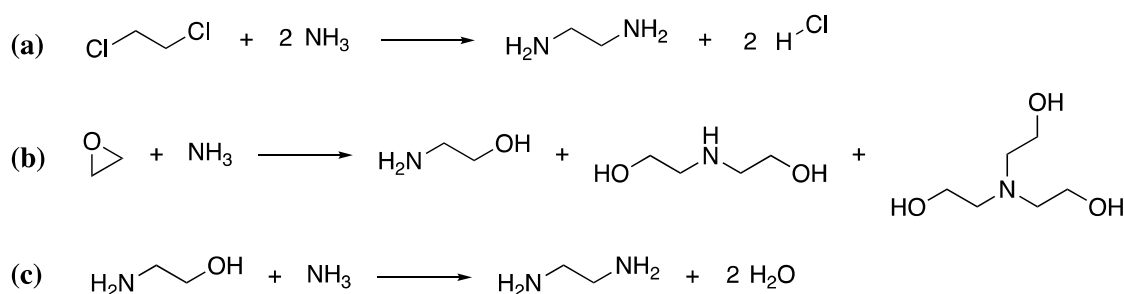


**Scheme 5.** The reaction of bisphenol A with epichlorohydrin to give DGEBA.

Traditionally, allyl chloride is reacted with hypochlorous acid to give two isomeric dichloropropanols, which are treated with NaOH to give epichlorohydrin, salt and water [104]. Allyl chloride is produced from the high-temperature chlorination of propylene from petroleum refining [105]. The reaction must be carried out over 500 °C to produce allyl chloride, lower temperature reactions result in 1,2-dichloropropane as the main reaction product. Hypochlorous acid is produced by the electrolysis of saline solutions [106]. Thus, just to reach the stage of epichlorohydrin production requires a significant amount of inputted energy, in the form of both electricity and heat. The production of BPA involves the condensation of acetone with 2 equivalents of phenol in the presence of a strong acid. Both

acetone and phenol are produced by the cumene process [107], also known as the Hock rearrangement, where benzene is alkylated by propylene, both from petroleum refining, to form isopropylbenzene (cumene) which is then oxidized by air to give acetone and phenol. These are often directly further reacted with a strong acid to produce BPA without further purification. To create the epoxidized DGEBA, BPA is alkylated by epichlorohydrin, this results in the epoxy component of the standard two-barrel resin syringe. In addition to the heavy usage of hazardous chemicals that require specific disposal protocols, and a large energy and resource input, there are significant concerns about the use of BPA. Since the 1990s, BPA has been suspected to be an endocrine disruptor [108,109]. These chemicals disrupt natural hormone production leading to cancers and birth defects, among others. As such, BPA is often replaced by BPS or bisphenol sulfone, in which the starting material for the BP production is a sulfone instead of acetone. However, the process is equally resource-intensive and there are additional health concerns related to the use of BPS which does not significantly improve the impact of the process.

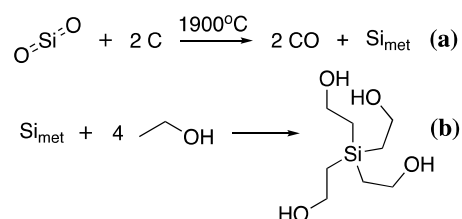
As mentioned previously, polyamines are the most common curing agents for epoxy resins. This family of compounds is extremely large, comprising both aliphatic and aromatic polyamines, of which there are at least 25 commercially available products. Thus, a detailed discussion of their synthesis is not feasible within the context of this review. However, a summary of the basic protocol for some of the simpler aliphatic polyamines will be given to illustrate the process. One common polyamine hardener is triethylenetetramine (TETA), with a curing time of approximately 30 min. It is produced from heating ethylene diamine or mixtures of ethanolamine and ammonia (which react when heated to form ethylene diamine) over a metal oxide catalyst [110]. If the ethylene diamine route is followed, ethylene diamine must be produced by the chlorination of ethylene to produce 1,2-dichloroethane, followed by reaction of the 1,2-dichloroethane with ammonia at 180 °C under pressure in aqueous media (Scheme 6a). Within the second route, ethanolamine must first be formed by the reaction of ethylene oxide with ammonia (Scheme 6b), which is then further reacted with aqueous ammonia to give ethylene diamine (Scheme 6c). Both routes are not completely selective and give a variety of polyfunctional amines. Like that of the epoxidized component, their production also requires significant heat, energy and resources, leaving a significant environmental impact.



**Scheme 6.** The synthesis of ethylenediamine from 1,2-dichloroethane (a) and the ethanolamine (b,c).

#### 2.2.5. Alkoxysilanes

Lastly, alkoxysilanes are a relatively new addition to the wood conservation toolkit but have gained increasing popularity in recent years [111–114]. Alkoxysilanes have already been heavily used in the waterproofing and fire retardancy of construction wood, particularly for external applications, so their transfer into the conservation field is not surprising [115–117]. Moreover, they are a major component of almost all commercially available silicon products, thus the synthesis of these polymers is on an industrial scale [118]. The production of alkoxysilanes is one of the most energy-intensive of all the production processes described so far. Mined sand ( $\text{SiO}_2$ ) is carbothermally reduced at 1900 °C to give pure silicon ( $\text{Si}_{\text{met}}$ ), which is then reacted with the corresponding alcohol to give the desired alkoxysilane [118], Scheme 7.



**Scheme 7.** The synthesis of TEOS from the carbothermal reduction of  $\text{SiO}_2$  (a), followed by reaction of  $\text{Si}_{\text{met}}$  with EtOH (b).

Thus, to produce the commonly used tetraethoxysilane (TEOS), ethanol or ethylene glycol is reacted with  $\text{Si}_{\text{met}}$  with an acidic catalyst. Alcohols for this reaction are either produced from petroleum sources or, in the case of ethylene glycol and ethanol, they can also be produced by fermentation. Alcohols from petroleum refining are produced by acid-catalysed hydration of the corresponding alkene to give the desired alcohol, thus hydration of ethylene produces ethanol. Ethanol can also be produced by fermentation of biomass [119], primarily with the yeast *Saccharomyces cerevisiae*, which breaks down polysaccharides at 35–40 °C releasing ethanol and  $\text{CO}_2$ . The disadvantage of this process is the toxicity of ethanol to yeasts meaning that the overall ethanol content of the fermentation broth cannot exceed 18% by volume. Concentration and distillation must be used to increase overall volume concentrations. Thus, initial savings in energy due to low-temperature fermentations are used to refine the overall product. Currently, the industrial method of choice for ethanol production is country-specific with the US and Brazil favouring biomass-derived ethanol [120], while many other countries favour petroleum refined ethanol. The choice is heavily dependent on the regional costs of oil and grain stocks.

### 3. Sustainable Alternatives to Conventional Treatments

Despite much research in the past decade into new consolidant treatments to replace several state-of-the-art techniques, in particular PEG, there is little uptake of these newer consolidants among heritage institutions. This resistance is, while perhaps frustrating on the part of the conservation scientist, entirely understandable given the one-of-a-kind nature of the wooden objects of interest. New consolidants are often only considered viable alternatives once a large body of data has been collected over many years on the stability, toxicity, and by-products of the process, or when a particular treatment must be replaced due to legislations against its current use.

Due to the long timescale of the transition process, switching to completely new technologies overnight, despite their evident sustainability or other attractive features, is not feasible. As such, the first step in the transition to sustainability is not to switch treatments completely but to search out sustainable alternatives to the treatments currently in use. Thankfully, with more and more interest in the production of bio-based chemicals, there has been a significant increase in the number of commonly used consolidants for which sustainable alternatives exist.

#### 3.1. Poly(ethylene glycol)

One of the most relevant sustainable alternatives is the recent increase in production of PEG from bio-based glycerol, produced from the fermentation of the fibrous waste that remains after the extraction of edible crops (e.g., corn, sugarcane). The ability of various species of yeast (e.g., *S. cerevisiae*) to break down polysaccharides from biomass to produce alcohols has been known for over 150 years [121]. However, in the period after World War II the cost of petroleum refining dropped significantly [122], making the production of alcohols from fermentation a less cost-effective process. Environmental concerns, alongside the desire to valorise the vast amounts of waste from the harvesting of food crops and enhanced yeast variants, have made this approach more attractive in recent decades and has driven a boom in bio-based chemicals, primarily in petroleum poor/agriculturally rich nations, such as Brazil [123].

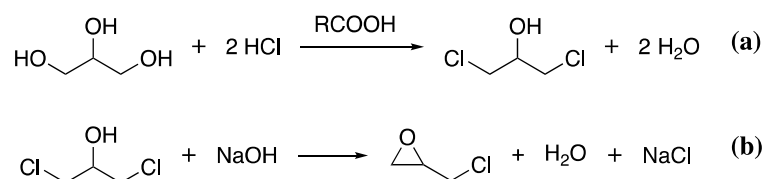


Glycerol, the feedstock required for bio-based PEG, is produced within yeast cells as a reaction to osmotic stress from the environment during fermentation as the concentration of ethanol in the fermentation broth increases. Its production over that of ethanol can be promoted through one of three ways: (1) using more osmotolerant yeast strains that can produce higher quantities of glycerol intercellularly, (2) fermenting at neutral or slightly alkaline pH enhancing the osmotolerance of the yeast or (3) forming complexes that limit ethanol formation. The primary route to option (3) is by promoting reoxidation of nicotinamide adenine dinucleotide (NADH), a coenzyme necessary for metabolism, whose production consumes glycerol as a cytosolic mechanism to maintain redox balance in the yeast cell [124]. As with the production of ethanol described previously, fermentation is carried out around physiological temperature to maintain the best environment for yeast growth. The glycerol can then be used as the raw material to produce any number of bio-based chemicals, including ethylene glycol (EG). Glycerol undergoes a catalytic dehydrogenation over a transition or noble metal catalyst to give ethylene glycol. The polymerisation of EG to give PEG follows the same process as described in Section 2.2.1 [125]. This bio-derived PEG is already commercially available through several suppliers, marketed as sustainable or green or bio-based PEG (bPEG). While the production of the starting material is inherently more environmentally friendly and sustainable than the derivation of PEG from petroleum refining, the catalytic dehydrogenation step that produces the EG is hugely resource-intensive requiring high temperatures, high pressure, and expensive finite catalysts. However, recent publications on the use of enzymatic cascades to produce ethylene glycol through a multi-step process from monosaccharide feedstocks give hope that the environmental footprint of the bPEG production will reduce further in years to come [126]. It must, however, be kept in mind that while the environmental footprint of the production of the PEG is significantly reduced, the disadvantages associated with the use of conventional PEG (non-recyclable, partially biodegradable at low molecular weights, solid-state ion transport and degradation to acidic by-products over time within the wood structure) will continue to be a feature of the bio-based PEG. However, at the very least choosing to employ bio-based PEG (bPEG) over petroleum-based PEG (pPEG) will contribute to improving sustainability in the conservation laboratory.

### 3.2. Epoxies

The widespread use of epoxies in many fields has also led to a significant increase in research in the production of bio-based epoxy resins (bio-epoxies) and resulted in several commercially available products. However, to date, researchers have struggled to produce bio-based epoxies with similar or better mechanical properties than traditional epoxies. Thus, most epoxies marketed as 'bio-based' are a mixture of renewable and non-renewable epoxies up to a total of 70% renewably sourced materials, to maintain the desired mechanical properties of the final product. While the creation of bPEG is almost completely focused on production from bio-glycerol, bio-based epoxies have been derived from bio-glycerol, plant oils and wood biomass. The multi-step nature of the epoxy generation process means that different parts of resin production have been reproduced from different bio-resources.

The most common sustainably produced component of epoxy resins is epichlorohydrin. The widespread availability of biomass feedstock for glycerol production means many chemical companies have transitioned to producing epichlorohydrin from bio-glycerol obtained through the same fermentation process as described for bPEG. To obtain epichlorohydrin, bio-glycerol is treated with hydrochloric acid in the presence of a carboxylic acid catalyst to give 1,3-dichlor-2-propanol, releasing water, Scheme 8a. The 1,3-dichlor-2-propanol is then reacted with NaOH to give epichlorohydrin, Scheme 8b.

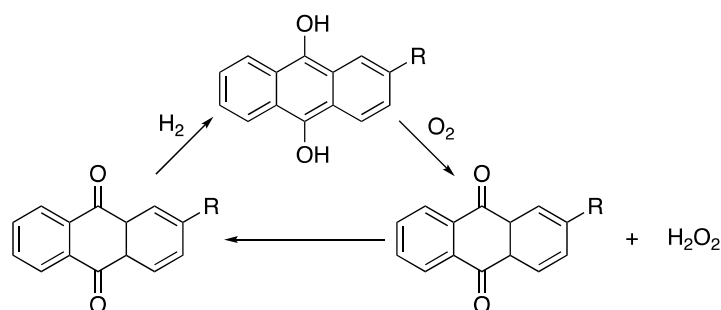


**Scheme 8.** The reaction of bio-glycerol with HCl to give 1,3-dichloro-2-propanol (a), which is further reacted with NaOH to give epichlorohydrin (b).

The use of bio-glycerol feedstock improves the sustainability of the epichlorohydrin production, however, the further synthesis of the DGEBA generally follows the traditional route described above. Thus, the overall improvement in the sustainability of the process is limited. Moreover, methods to reduce the use of chlorine in the process need to be advanced.

Environmental concerns relating to the use of BPA have resulted in various biomass-derived units being explored to replace BPA and any of its derivatives. The most common of these are lignins and tannins. Both lignins and tannins are macromolecules with multiple phenol residues obtained from the valorisation of woody biomass. The presence of the phenol groups means that they can be reacted with (bio)epichlorohydrin in the presence of NaOH in a polar solvent at approx. 50 °C (lignin) [127] or 80 °C (tannin) [128] to give polyfunctional epoxidised monomers. While this eliminates the hazardous BPA component, and the epichlorohydrin can be derived from bio-glycerol, it does not eliminate the use of chlorine and chlorinated intermediates in the epoxide formation.

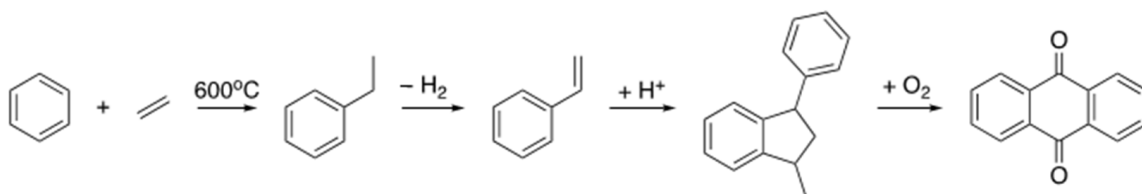
Epoxidising plant and vegetable oils to create polyfunctional epoxide monomers are one of the most explored methods of replacing the entire DGEBA component, removing the need for chlorine gas and chlorinated intermediates [45,129–131]. Suitable candidates for epoxidation require the presence of unsaturated fatty acids, i.e., C=C bonds where the epoxide ring can be formed. Linseed (75–90% oleic, 1 C=C, and linolenic acid, 3 C=C) and soybean oil (~85% oleic, 1 C=C, linoleic, 2 C=C, and linolenic acid, 3 C=C) have significantly high concentrations of fatty acids with multiple C=C bonds to allow cross-linking of epoxidised oils [132,133]. As such, epoxidised linseed oil (ELO) and epoxidised soybean oil (ESBO) are the most explored and commercially available epoxidised oils used in a variety of paints, coatings and resins. Epoxidation of the oils is generally carried out by reacting hydrogen peroxide with the oil, resulting in the addition of an oxygen atom across the C=C creating the epoxide ring. While the renewable sourcing of the oil and the advances in green oil extraction are an improvement on the synthetic DGEBA protocol, the major downside to this process is the production of hydrogen peroxide. H<sub>2</sub>O<sub>2</sub> is prepared by the anthraquinone process [134], Scheme 9.



**Scheme 9.** The anthraquinone process.

This involves the high-temperature reduction of anthraquinone to anthrahydroquinone by hydrogenation over a palladium catalyst. The anthrahydroquinone autoxidizes in the presence of oxygen to regenerate the anthraquinone and transfer the H<sub>2</sub> to the O<sub>2</sub> giving H<sub>2</sub>O<sub>2</sub>. Production of anthraquinone involves the reaction of benzene and ethylene

from petroleum refining to produce ethylbenzene in a Friedel–Craft reaction over a zeolite catalyst. The ethylbenzene is then dehydrogenated using superheated steam (>600 °C) over an iron catalyst to give styrene. This then undergoes acid catalysed dimerization to 1-methyl-3-phenylindane, which is oxidized to anthraquinone [135], Scheme 10. Thus, once again a large amount of resource and energy-intensive processes are used to produce sustainable alternatives to common consolidants.



**Scheme 10.** The multi-step production of anthraquinone from benzene and ethylene.

The final component is the polyamine hardener. This is one of the easiest problems to address given that polyamines are widely found in nature, although they are not yet widely commercialised from bioresources. Until roughly a decade ago little was known about the biosynthetic pathways related to polyamine production, and their low natural abundance made extraction from biomass non-viable from an economic standpoint. However, a better understanding of the biosynthesis of polyamines by bacteria and yeast has led to advances in industrial fermentation of these highly useful molecules and brought their use in bio-based epoxies closer to reality [136]. Several different routes have been explored to engineer the metabolism of bacteria (*Escherichia coli* and *Corynebacterium glutamicum*) and yeast (*S. cerevisiae*) strains that are known to overproduce polyamine precursors (L-arginine, L-lysine and L-ornithine) to directly produce polyamines such as putrescine and cadaverine. These can then be further modified either through biotechnological or chemical means to create a variety of polyamine cross-linkers [137–141]. While the fermentation conditions may differ slightly from bacteria to yeast and depending on the initial feedstock, the clear advantage of this method over the synthetic route is the use of bio-based feedstock and physiological conditions to produce polyamines resulting in a significantly reduced environmental footprint for the process. Although discussed in the literature these advances have not yet made it to the industrial scale for epoxy resin production.

### 3.3. Acrylates and Methacrylates

While no commercially available acrylates or methacrylate currently exist, much research is being carried out to find alternatives to current synthetic procedures. Some of the most promising routes to acrylic acid involve the fermentation of corn starch and vegetable oil to produce glycerol, which is further fermented to lactic acid or 3-hydroxypropionic acid and then dehydrated to give acrylic acid (AA). The disadvantage of this route is the requirement for high-temperature dehydration with heterogeneous or metal oxide catalysts at temperatures approaching 300 °C. Another route to the preparation of bioAA is from poly(3-hydroxybutyrate), which is synthesised bacterially from wastewater and constitutes a waste valorisation route. P3HB can then be pyrolysed to crotonic acid and then metathesised, a reaction in which two hydrocarbons exchange carbon-carbon bonds in the presence of a metal catalyst [142], with (bio-based) ethylene from bio-glycerol to give propene and acrylic acid [143,144].

With respect to bio-based alternatives to MAA production, which can also then be reacted with the appropriate alcohol to give the desired ester, two main commercially viable routes have been described in the literature, although others exist [143]. The first is the decarboxylation of citric acid (CA), found in large quantities in citrus fruits. It is obtained commercially from the fermentation of sugar cane and beet molasses by *Aspergillus niger*. CaOH is added to precipitate the citric acid from the fermentation broth, which must then be neutralised with excess sulfuric acid. The citric acid is then pyrolysed to itaconic anhydride and hydrolysed to itaconic acid. The itaconic acid is then decarboxylated to

methacrylic acid using various supported transition metal catalysts (although some reports also discuss cheaper solid base catalysts) at temperatures ranging from 200–250 °C, and often high pressure. The disadvantages of this protocol are the multiple steps involved, many of which involve high temperature and pressure reactions, as well as the production of large amounts of gypsum waste from the neutralisation of the CaOH precipitant. A less energy-intensive approach is the direct production of itaconic acid from the fermentation of glucose with *Aspergillus terreus* [145]. The itaconic acid is purified by filtration, evaporation, and crystallisation. The drawbacks to this approach are the cost of the substrate and the low yields of itaconic acid compared to the CA approach. However, research is being conducted to investigate cheaper substrates to produce itaconic acid and higher yield, resource-efficient purification techniques. For example, investigations on the use of *Aspergillus oryzae* with lignin biomass as a substrate detailed the highest yield from solid-state fermentation of IA reported to date [146]. This highlights that as interest increases in bio-based methacrylic acid, and of course acrylics, better and more efficient production will be found.

### 3.4. Aminoplasts and Related Consolidants

Limited options exist in the literature for the sustainable production of MF resins, primarily limited by the sustainable production of melamine. One recent publication discusses the replacement of up to 30% of the melamine content with bark extractives (i.e., polyphenols from tannins) in an MF resin to give a mixed phenol-melamine-formaldehyde resin [147]. However, when the total weight % of tannin exceeded 30 wt.% the mechanical properties of the adhesives deteriorated significantly. More promising routes appear to focus on the sustainable production of formaldehyde to improve the overall sustainability of the resins. This generally focuses on the electrolytic production of formaldehyde from seawater and CO<sub>2</sub> [148]. Furthermore, several authors report the replacement of formaldehyde with furfural, which can be obtained from renewable resources and reduces the toxic emissions related to formaldehyde over time. Furfural is a furan-based aldehyde produced from the acid-catalysed hydrolysis and dehydration of pentoses obtained from agricultural waste [149,150]. This has only been reported for urea-formaldehyde (UF) resins to date, however one could envisage the same potential to replace formaldehyde in MF resins. Up to 50% of the formaldehyde could reportedly be replaced before the deterioration in the properties of the materials was observed.

The most promising sustainable alternatives to the use of MF resins in conservation are not actually aminoplasts, but phenol-formaldehyde resins. They were previously investigated in wood conservation but were found to have less desirable properties than MF resins. The wide range of polyphenols that can be obtained from wood biomass, specifically from lignins, tannins and suberins, coupled with the ability to sustainably produce, or replace formaldehyde with bio-derived aldehydes means that there is extraordinary potential for a wide variety of new sustainable alternatives to MF resins. The recent hike in prices on MF by the main producer BASF in response to increasing restrictions on chemicals with a high environmental footprint and no viable sustainable sources will certainly drive research further in this direction [151]. The forerunner in this new category is lignin-formaldehyde resins and several commercially available products exist. A recent study compared the life cycle analysis of three PF resins (with 100% phenol, 40% lignin: 60% phenol and 100% lignin) and both lignin-containing resins showed significantly improved environmental impacts over the traditionally obtained phenol [152], meaning that even the impact of non-sustainable formaldehyde production is balanced by the renewable sourcing of the lignin component. This highlights the fact that even partially sustainably-sourced consolidants show an improved environmental impact compared to the unsustainable consolidants currently in use. Thanks to the sourcing of lignin, tannin and suberin-based resins from woody biomass, compatibility with wooden artefacts would likely not be a significant issue. The major disadvantage here is that, unlike the other proposed alternatives, switching to lignin-phenol-formaldehyde (LPF) resins is not a simple switch from petroleum sourced to a bio-sourced version of the same chemical. Phenol-formaldehyde resins are

not extensively used in wood conservation and LPF resins consist of a completely different phenol structure, as such extensive testing would be necessary before the widespread use of lignin-aldehyde resins could be considered. However, it is certainly a development to monitor in coming years with possible further restrictions, and increased costs, in the manufacture of MF resins.

### 3.5. Alkoxysilanes

While alkoxysilanes are a relatively new addition to the wood conservation toolkit, they are a major component in almost all silicon-based commercial products currently available, as such, they are widely synthesised at industrial levels. Despite their widespread usage and the almost century-long search for an alternative to the standard carbothermal process, few match the yields of the current standard [118]. Recently a bio-based alternative has been found that could match the demand for silicon products. Harvesting of rice for food produces a vast amount of waste in the form of rice husks, this is then generally combusted for energy and the residue remaining after pyrolysis is known as rice husk ash (RHA) [153]. Interestingly RHA contains up to 98% amorphous silica depending on location, rice variety and fertilisers used [154]. This RHA can be depolymerised in a base-catalysed reaction, using 10% NaOH, in the presence of various diols to give distillable spirocyclic alkoxysilanes [118]. Of particular interest is the ability to react RHA with (bio-based) ethylene glycol to produce a bio-based alternative to the most common alkoxysilane TEOS [118].

A report from 2019 states that Indonesia alone, the world's third-biggest rice producer after China and India, can produce 3.2 million tonnes of silica from RHA per year [154]. The global demand for speciality silicas, i.e., SiO<sub>2</sub> used to produce silicon-based polymers, was reported to be 3.9 million tonnes in the same year [155]. Thus, Indonesia alone could satisfy over 80% of the global demand. Assuming the same conversion from rice production to silica for both China and India for the same year [156], results in approximately 28 million tonnes of silica, 7 times the global demand. Thus, bio-based sources of silica can well match global demand for silicon polymers, meaning a sustainable future for the commercial production of alkoxysilanes may soon become a reality.

### 3.6. General Comments

While interest in developing alternatives to petroleum-based polymers for a variety of applications exists, the number of commercially available products is still rather low. Cost-effectiveness over petroleum-based consolidants may still hinder the switch to bio-based consolidants for many institutions. However, the strategy of replacing unsustainable chemicals with sustainable alternatives does not work for all consolidants. It is only possible when considering relatively simple syntheses with easily scalable processes, e.g., the production of PEG, or where the demand across many different fields is so high as to make sustainable synthesis methods a viable commercial option, e.g., bio-based epoxies. For many wood consolidants, this may remain a niche area with a high cost available only to institutions with research laboratories that can create these speciality chemicals on demand for use in limited quantities. Thus, instead of relying on the production of sustainable alternatives to common consolidants that come with the same disposal concerns as their petroleum-based counterparts, we need to start reimagining the entire future of wood consolidation.

## 4. Designing the Sustainable Consolidants of the Future

As mentioned above, simply switching to sustainable alternatives of currently employed consolidants is only part of the solution. While the overall environmental footprint of these bio-derived chemicals is reduced compared to petroleum-based consolidants in terms of production, once produced the bio-based alternatives are just as non-recyclable, toxic and/or non-reparable as the original. Thus, in the long-term, we need to think about the development of more responsible, and circular consolidant solutions, in which none

of the material becomes waste. This translates to the need for consolidants that can be so well-tailored to the specific degradation issues of the wooden object as to adapt to the changing conservation needs of the wood over time negating the need for repetitive treatment and reducing overall consolidant consumption. Furthermore, unused consolidants within the conservation laboratory should be able to be biodegraded under specific conditions or used to create other materials when they are no longer of use, to reduce the quantities of chemicals going to waste. Development of such materials requires us not only to examine the provenance of the consolidant but its compatibility with the wood matrix, the modification strategies used to create the tailored consolidant behaviour, and the impact these modifications have on the environment. Moreover, the energy use and resource efficiency of the abovementioned strategies are also due to their effect on the overall environmental impact and sustainability of the final consolidant.

Moving away from the current state-of-the-art in consolidants is a much longer-term process and requires a significant amount of development. However, there is already plenty of research underway, particularly around responsive consolidants that could adapt to the changing environment within wooden objects overtime reducing or eliminating the need for repetitive conservation. Several ‘new generation’ technologies have appeared in the literature in recent years for the treatment of either archaeological or fresh wood with the potential to significantly impact the future of sustainable consolidants. These fall into one of four different categories; (1) bio-based polymers, (2) bio-based capsules with the sustained or triggered release of cargo, (3) bio-based polymer/inorganic NP composites and (4) bio-based polymers with responsive or targeted bulking of wood structure. Many of these new generations of consolidants are based on polysaccharides, although lignin (and lignin-derived polymers), proteins and waxes are also examined.

#### 4.1. *Polymers Extracted from Biomass*

##### 4.1.1. Proteinaceous Consolidants

Proteinaceous consolidants, particularly collagen, gelatine, and casein, have been extensively used in the conservation of painted works of art. Their ability to form thin, varnish-like films on drying has been exploited in the cleaning and restoration of painted surfaces. Proteinaceous wood consolidants are rarer, apart from keratin, which has recently been extensively investigated for the conservation of waterlogged wood. Keratin is a structural protein that exists in two forms,  $\alpha$ -keratin (soft keratin) which is found in the hair, skin, claws (nails), horns and hooves of all vertebrates and  $\beta$ -keratin (hard keratin) which is found in the feathers and shells of birds and reptiles [157]. Keratin is the third most abundant biopolymer, after cellulose and chitin. Keratin is a significant waste product of the meat-processing industry, with pigskin, for example, containing almost 80% keratin. Thus, the use of keratin as a wood consolidant represents a valorisation of this waste product and an increase in the sustainability of the meat-processing industry. Despite the use of keratin in wood consolidation and other applications reducing waste from the meat processing industry, the methods used for the extraction of keratin are very resource-intensive, with the potential for significant negative impact when considering the quantities of keratin to be processed. The extraction involves three steps, generally performed at 60 °C: (1) urea is commonly used to break the covalent bonds in keratin and allow it to be solubilised, (2) a surfactant like sodium dodecyl sulfate is used to disrupt the intermolecular interactions and (3) followed by treatment with thioglycolic acid or mercaptoethanol to cleave the disulphide bond [158]. Sodium dodecyl sulfate (SDS) is produced from the reaction of the petroleum-derived dodecanol, through the procedures previously mentioned in Section 2.2.1 and reacted with sulfur trioxide (SO<sub>3</sub>), produced by the burning of sulfur or pyrite at 400–600 °C over a silica-supported V<sub>2</sub>O<sub>5</sub> catalyst activated with K<sub>2</sub>O [159]. Reaction with SO<sub>3</sub>, or related derivatives of sulfuric acid, adds a sulfonate group (hydrogen lauryl sulfate), which is then neutralised using NaOH or sodium carbonate [160]. Bio-based SDS can also be produced by hydrolysing plant oils with a high content of C12 fatty acids, e.g., palm or coconut oil, and then hydrogenating to add the

sulfonate group, as described previously [161]. The only disadvantage to this approach is that there is a mixture of fatty acids in all plant oils, thus the resulting SDS is a mixture of various sulfonated fatty acids. The final stage in the extraction of keratin involves the use of mercaptoethanol, produced from the reaction of ethylene oxide (described previously) with hydrogen sulphide in the presence of thiodiglycol. H<sub>2</sub>S, a highly toxic gas, is most commonly obtained from the ‘sweetening’ or refining of natural gas to remove H<sub>2</sub>S and other organosulfurs [162]. This is generally done by amine scrubbing, an acid-base reaction by which solutions of alkylamines (monoethanolamine, diethanolamine or methyldiethanolamine) are used to solubilise H<sub>2</sub>S and CO<sub>2</sub> and remove them from natural gas, due to the higher solubility of dissociated species. The process is carried out using two linked vessels, an absorber to remove the sour gases and release the sweet gas, and a regenerator to collect the sour gases for further use. The absorber uses temperatures of 30–50 °C and pressures of ~200 atm, while the regenerator uses much higher temperatures (115–126 °C) and low pressures of 1.4–1.7 atm, resulting in an energy-intensive process. Thiodiglycol on the other hand is produced from the hydrolysis of bis(2-chloroethyl) sulphide, also known as Mustard gas [163]. Mustard gas is produced by reacting sulphur dichloride, obtained from the high-temperature chlorination of elemental sulphur, with ethylene from petroleum refining. Thus, while the use of keratin is a sustainable method of reducing waste from meat processing, the methods required to extract the keratin have a very high environmental impact. Recent literature reports detail new, more sustainable methods to extract keratin that give hope for less damaging production in the future. This method involves the use of a highly basic industrial degreaser (containing non-ionic surfactants and NaOH) to dissolve the keratin at room temperature within 6 h with constant stirring, followed by filtration to remove larger particles then two rounds of centrifugation, the second with ultrafiltration to give the pure keratin solution. This was also scaled up to an industrial level and required microfiltration in place of the first round of centrifugation and a final reverse osmosis step to ensure pure keratin was obtained at the end. While these processes are still energy-intensive, there are short (20 min) and can be potentially powered by renewable energy. Moreover, they use significantly less toxic chemicals derived from petroleum sources, thus constituting an improvement over current methodologies [164].

#### 4.1.2. Polysaccharides

In addition to proteins, polysaccharides have also been investigated as new consolidants in the past decade, primarily, chitosan and cellulose (and its derivatives). Cellulose, and then chitin (from which chitosan is derived), are the most abundant biopolymers on earth, thus, are considered an infinitely renewable resource (clearly, with proper management of natural resources). As with keratin, despite the bio-sourcing of the consolidant, the commercial methods of extraction are highly unsustainable. We have already seen from the phenol-formaldehyde resin life cycle analysis, the bio-sourcing of the material made a significant effect on the environmental impact of the material to the extent that it negated much of the poor environmental footprint of the use of formaldehyde and the production of epichlorohydrin. Thus, the use of cellulose and chitosan already represents a positive, sustainable direction for conservation science; however, this does not mean we can completely overlook the negative impact of processing.

While various plants have a high cellulose content, and bacteria are also capable of producing cellulose, commercially cellulose is extracted from wood using the Kraft pulping process. The stability of the wood structure means that the extraction of cellulose is a highly intensive process involving high temperatures, pressures, harsh reagents and produces a significant amount of toxic by-products that require resource-intensive neutralisation to minimise damage to the environment [165]. The process starts with the chipping of wood to increase the surface area for extraction. The wood chips are then digested at elevated temperatures and pressures in an aqueous solution of sulphide and sodium hydroxide to remove the alkaline sensitive lignins that bind the cellulose in the wood matrix. The pulp is then washed repeatedly to remove the pulping liquor, pressed, and dried to obtain pure

cellulose. The pulping liquor is collected and concentrated, and then fired to remove the organics and regenerate the sodium sulphide from sodium sulfate. It is from this step that lignin can be recovered for further use. The inorganic chemicals from the pulping process remain as smelt after pyrolysis. These are recovered, resolubilised in water and treated with calcium oxide to regenerate the original 'white' liquor to start the pulping again. The spent CaO (mud) from this step is calcined to regenerate CaO for repeated use. While some energy requirements are met by the heat generated by pyrolysis and calcining steps within the process, the Kraft process relies heavily on additional energy primarily from finite resources. Switching to renewable energy sources would have a positive impact on the overall environmental footprint but there is still significant use of harsh chemicals, high temperatures and pressures that result in a negative environmental impact. The production of large amounts of sulphur-containing compounds that must be treated to prevent emission into the environment, adds to the high cost of this process [165]. Thus, sustainable processing techniques are urgently needed to improve the impact of cellulose extraction.

One alternative is the use of ionic liquids to extract cellulose from sawdust. Ionic liquids are molten salts with a low glass transition temperature (generally lower than 100 °C) [166]. They have many advantages including chemical and thermal stability, environmentally friendly production, and recyclability. Several ILs have been shown to dissolve wood, producing pure cellulose in 3–6 h with the full recovery of the IL after processing under mild conditions [167–174]. With ILs being composed entirely of anions and cations, thus, being good conductors of microwave irradiation, modifications to processing methods to include microwave irradiation of the wood during solubilisation has been shown to reduce processing times from hours to minutes [166]. However, despite the mild dissolution of cellulose and their general perception as environmentally friendly solvents, questions remain about the environmental and health impact of the use of ionic liquids preventing their scale up to commercial applications [173].

A more promising approach is the industrial-scale production of bacterial cellulose (BC). Bacteria from a number of genera have been explored for the production of cellulose from agricultural and industrial waste, specifically, *Gluconacetobacter*, *Aerobacter*, *Rhizobium*, *Sarcina*, *Azotobacter*, *Agrobacterium*, *Pseudomonas* and *Alcaligenes*, of which *G. xylinus* produces the most efficient transition to BC from any number of substrates [175,176]. The biosynthetic production of celluloses from bacteria involves two steps, the intracellular polymerisation of glucose into cellulose polymers (the product of four enzymes catalysed reactions [177,178]), the cellulose polymers are then ejected from the cell and self-assemble into cellulose fibrils [175,179]. Fermentation of BC has already been demonstrated on an industrial scale, and with the potential to use a wide variety of agricultural and industrial waste as feedstocks, vast quantities of BC can be produced, creating a very sustainable source of cellulose that also reduces biological matter waste [180]. More recently, several groups have reported a cell-free enzyme system to produce BC with the potential to generate even higher yields than reported for *G. xylinus*. The cell-free system is developed from the BC producing strains mentioned above, however, enzymes and co-factors are extracted from the bacterial cells and used directly in the fermentation broth. This reduces the loss of cellulose polymers that are not properly expelled from the intracellular matrix, increasing overall yields [181,182]. The only limitation that can be envisaged is that this microbial system produces cellulose nanofibrils (CNFs)/nanocrystals (CNCs) directly after the production of cellulose polymers. In wood conservation, while cellulose polymers and their derivatives have been shown to have great potential, CNCs have not been well studied and in some cases have been shown to achieve poor results due to a filtering effect of the CNCs by the wood structure [183]. As such, they have been primarily used to reinforce the mechanical properties of wood adhesives. Thus, it will be necessary to design methodologies by which the fermentation can be stopped before the assembly of cellulose polymers or by adding additional organisms that inhibit self-assembly to ensure



large quantities of sustainably sourced cellulose polymers can be made available for wood conservation applications from this method.

Another popular polysaccharide derivative is chitosan, derived from chitin. Chitin is found in the exoskeletons of various invertebrates, primarily shellfish and insects, as well as in mushrooms. On a commercial scale, chitin is primarily extracted from the shells of crustaceans as a valorisation of waste from the fishing and food industries. To extract the chitin, shells are subjected to acid treatment with dilute hydrochloric acid to remove the calcium carbonate, this is followed by a neutralisation step with pure water to remove acid before alkaline treatment with dilute NaOH to remove the proteins. Again, the materials must be neutralised by extensive washing with pure water. Depending on the source of the chitin, this might be followed by a decolourisation step to remove pigments remaining in the chitin solution [184,185]. The pure chitin is finally deacetylated by treatment with concentrated NaOH or KOH at high temperatures before copious washing and drying to give chitosan [186]. Despite the natural source of chitosan, the extraction process is quite expensive, uses harsh chemicals and is very water-intensive, as such methods to improve the extraction process are necessary to reduce the environmental impact of chitosan production. While this is the standard commercial extraction procedure, research is already progressing in the development of milder extraction methods to improve the overall sustainability of chitosan extraction. One of the primary alternatives involves microbial bioprocessing [187]. In recent studies, researchers have optimised the activity of two bacterial strains, a protease producing strain to deproteinise the shells, and a lactic acid-producing strain to dissolve calcium carbonate. The processing generally involves the following steps: (1) washing and dehydration of the shells at 60 °C, (2) grinding, (3) enzymatic deproteinization of the shell powder by proteases, and (4) demineralisation of the CaCO<sub>3</sub> by lactic acid, leaving pure chitin. A variety of bacterial strains have been explored including *Alcaligenes faecalis* S3, *Bacillus subtilis*, *B. cereus*, *B. licheniformis*, and *Teredinibacter turnerae* to produce proteases for the removal of proteins [187–192], whereas lactic acid production has been derived from the activity of *Bacillus coagulans* L2, *Lactobacillus plantarum*, *Pseudomonas* spp., *Lactococcus lactis* and *Gluconobacter oxydans* [187,189–192]. Initial attempts at microbial processing reported a two-step procedure involving a deproteinisation step followed by demineralisation. However, several groups have now reported high yields of pure chitin from co-fermentation, further improving the efficiency of the process [188,189,191]. Regardless of the number of steps, the overall energy and water usage related to microbial processing is significantly reduced over the commercial process, highlighting a future method to improve the sustainability of chitin extraction.

#### 4.1.3. Lignin

A final biomass-derived polymer is lignin. Lignin can be obtained from the Kraft pulping process described above by the addition of CO<sub>2</sub> or NaOH at pH 9–10 to the black liquor retained after cellulose is removed. This retrieves 80% of the lignins, which can then be purified into lignin chemicals [193]. This lignin is often heavily sulfonated or otherwise modified during the extraction process [194,195]. Lignin for use in adhesives and varnishes, and thus, wood consolidation, is more commonly obtained through the organosolv process [196]. This produces lignins that maintain more of their original structure with no sulphur content [194,195]. Organosolv lignin is obtained by a two-step treatment of woody biomass with weak and strong acids in organic solvents (generally ethanol/water mixtures) at temperatures up to 200 °C. Examples include mixtures of formic and acetic acid in water for the first step at lower temperatures (50–100 °C) and sulfuric acid/ethanol/water or peroxyformic acid/ peroxyacetic acid/water at higher temperatures (80–200 °C) [197–199]. The organosolv method allows for easier separation of the cellulose and lignin phases, from which the lignin can be extracted by neutralisation and evaporation. The primary uses of these extracted lignins are in the preparation of lignin-based epoxies as described in the previous chapter. However, more recently lignin nanoparticles (LNPs) as consolidants have been investigated in the literature [183]. These were prepared by an ‘anti-

solvent' process in which lignin in a mixed solution of NaOH, dioxane/water and DMSO from the extraction process was dialysed against water to generate LNPs of 40–120 nm diameter [200]. Unfortunately, these LNPs were not found to be particularly successful at infiltrating the wood structure at standard temperature and pressure, managing to penetrate to a depth of just 1 mm. This is similar to the issues observed with consolidation with CNCs. However, these LNPs are interestingly hollow and could be used instead to prepare encapsulated consolidants, with better environmental footprints, as discussed in more detail in the following section.

#### 4.2. Encapsulated Consolidants with Sustained or Triggered Release

One of the first examples of encapsulation of wood treatments was the use of gelatine and, later, chitosan nanocapsules to release fungicides within a wooden structure as a function of compressive stress. While this type of consolidant was employed in the treatment of construction wood, applications in heritage wood conservation are easily envisaged. Biocides are applied in large quantities during the conservation of waterlogged wood to prevent bacterial growth within the treated artefact, particularly with PEG consolidants that are hygroscopic and not naturally resistant to bacterial degradation. To ensure adequate penetration of the biocide within the entire wooden object, it is generally applied in excess. This leads to the use of excessively large quantities of petroleum-based chemical biocides that must be incinerated after use to avoid pollution of waterways, which is in itself a highly unsustainable practice. Moreover, the public health considerations of the leaching of biocides from the treated wood, are also a cause for concern. Thus, systems, such as those proposed by Heiden et al. [201–203], in which biocides are encapsulated within bio-based polymer nanoparticles that can be easily transported deep within the wood due to their small size, are more sustainable, and likely more homogeneous, alternatives to the use of large quantities of biocide, that may or may not penetrate the entire depth of the wood. To date, the proposed systems have been synthetic/bio-based hybrids that continuously release low concentrations of biocide over time, with the release profile tailorable as a function of cross-linking density in the outer capsule wall increasing the sustainability of the use of biocides in wood conservation.

One disadvantage to these systems is the sustained release of the biocide over time which is not triggered by any specific interactions. Thus, a biocide may be released in the wood when and where it is not required, leading to the unnecessary use of, albeit smaller quantities of, biocides. However, the most recent iteration of the encapsulation system employs Kraft lignin to create the nanoparticle structure that contains a fungicide, opening up the possibility of triggered release of the contents of the lignin-nanocapsule by fungal lignase produced in the vicinity of the nanocapsule. This system has already been successfully demonstrated in planta [204,205] and could significantly increase the sustainability of biocide use in heritage wood conservation. Another example of lignin nanocapsules with controlled release based on pH has also recently been described [206]. Such a system could be even more generally useful for the reduction of consolidant usage, contributing to more sustainable conservation practices. As wood degrades, the pH of the environment changes significantly. For example, the pH of fresh oak wood is approximately 4.5, while fresh pine is approximately pH 5.5 [207]. However, as wood degrades the pH can drop to between 0–4, damaging the acid-sensitive chitosan and reducing the mechanical stability of the wood. Moreover, large-scale use of basic treatments can damage the alkaline-sensitive lignin remaining in the wooden object, which often maintains the structural integrity of heavily degraded wooden objects, as cellulose is generally the first part of the wood to be degraded under 'normal' conditions. A bio-based pH-sensitive nanocapsule containing a wood stabilising or deacidification agent could then be tailored to release consolidant only in low pH environments, meaning consolidants are only released into the wood when necessary, reducing the overall use of consolidants and elongating the period over which embedded consolidants are functional. Furthermore, localised use of

neutralisation agents would prevent largescale damage to the structural lignin components enhancing the overall mechanical stability of the artefact.

#### 4.3. Organic-Inorganic Composites

A further development in sustainable consolidants are composite organic/inorganic treatments, using a range of bio-based polymers and resins embedded with halloysite ( $\text{Al}_2\text{Si}_2\text{O}_5(\text{OH})_4$ ) nanotubes (HNTs). Halloysite nanotubes have attracted much attention in recent years in many fields, e.g., the pharmaceutical and construction industries, with their low cost, and high natural abundance in volcanic soils, high mechanical strength, ease of functionalisation and ability to store cargo within their internal cavity. For example, HNTs have been shown to significantly improve the sustainability of concrete production with similar mechanical properties when 10% Portland Cement was replaced with halloysite clay, due to its significantly lower calcining temperature contributing to a reduction in the overall emission of greenhouse gases [208]. Thus, the use of HNTs could be a more sustainable treatment option in comparison with standard inorganic nanoparticles, which are rather energy-intensive in their preparation. Cavallaro, Lazzara and co-workers have been pioneering these natural resin/HNT composites in conservation science for several years and have made great advances [209–213]. Their initial work focused on the use of beeswax/HNT composites to improve the shrinkage upon drying and the mechanical stability of heavily degraded wood. The mechanical strength of the treated objects was found to be independent of temperature at HNT concentrations above 60% and at temperatures below 70 °C ensuring that warming of the wax did not result in a decrease in mechanical properties [209]. This is likely due to the formation of 3D networks of HNTs within the matrix that contribute to excellent mechanical properties. This system has been refined more recently to include examples of esterified colophony, pure paraffin wax and paraffin wax Pickering emulsions as matrices for the HNTs, all with promising results, highlighting their potential to be more extensively exploited in wood conservation [210,211,213–215].

Another interesting aspect of HNTs is that, in a similar way to the bio-based nanocapsules described above, their internal cavities can easily be functionalised to provide sustained or controlled release of molecules over time. This has been demonstrated with a variety of drug molecules stored in the cavity [216–220] and could easily be envisaged for the sustained or controlled release of biocides or additional consolidants within the wood structure. An example of this is the encapsulation of anti-oxidants within the HNTs, which are then embedded in a chitosan/pectin matrix for the conservation of works of art [212]. The success of this method demonstrates the possibility that wood consolidants based on HNTs embedded in a waxy matrix could also be doped with biocides or fungicides as described for the nanocapsules above providing a sustainable mechanical stabiliser that would combat biological activity in the wood over time. Moreover, the cavity can also be functionalised to absorb molecules from the environment, creating an interesting scenario for conservation scientists? Could the internal surface of the HNTs be functionalised to absorb acids from the environment preventing their further action on the already fragile wood structure? However, what happens when the internal cavity is full? Could the internal structure be functionalised in such a way that absorbed molecules could be broken down into non-toxic components and released from the wood, ensuring continued activity over time? Hopefully, an answer to these questions will be possible in the coming years, as such a regenerative consolidant could be a significant boon to sustainable consolidant development.

#### 4.4. Bio-Inspired Consolidants

A major benefit to the future of sustainable consolidants would be the advent of more adaptable, responsive and/or targeted consolidants. These are often referred to as bio-inspired consolidants, replicating some natural function within the consolidant. For example, replicating the ability of siderophores to trap and deactivate catalytic iron to hinder further iron catalysed wood degradation [221]. Consolidants derived from bio-

resources and able to respond to the changing conservation status of an object over time would mean a far reduced environmental footprint to produce these materials and less or no need for retreatment, significantly reducing the quantities of consolidant employed.

One of the first examples of adaptable consolidants was the PolyCatNap hydrogel consolidant [221]. PolyCatNap is a 3D network of multiply functionalised chitosan and guar gum. Guar gum is a galactomannan polysaccharide extracted from the seeds of the guar bean (*Cyamopsis tetragonoloba* L.) by a mechanical process involving roasting, sieving, and polishing [222]. Sieving results in the separation of guar gums of different particle sizes, which result in different viscosity preparations. To create the 3D network, chitosan was covalently modified under room temperature and aqueous conditions with either naphthol or catechol units, while guar was dynamically covalently modified with methyl viologen units. The three polymers were mixed in water, and the addition of the supramolecular host cucurbit[8]uril (CB[8]) allowed the formation of ternary complexes between the naphthol and MV units within the CB[8] cavity creating a basic 3D structure of the network. In wood with a high  $\text{Fe}^{3+}$  concentration, the presence of catechol-functionalised chains provided an additional orthogonal cross-link between 3 catechol functionalised chains and the  $\text{Fe}^{3+}$ , deactivating the catalytic properties of the iron and increasing the mechanical strength of the network. This allows the consolidant to adapt to the changing  $\text{Fe}^{3+}$  concentration in the wood and the possible weakening of the wood over time because of  $\text{Fe}^{3+}$  presence. The consolidant was shown to have no reaction to  $\text{Fe}^{2+}$  in the wood samples, displaying selective cross-linking properties. Clearly, with the synthesis of naphthol, catechol and methyl viologen requiring the use of petroleum-derived starting materials and high energy/resource processes the sustainability of this system is not optimal. Recent developments in this technology have shown, however, that various units could be replaced with bio-derived molecules, enhancing the sustainability of the system. For example, coumarin derivatives that could photo or thermally dimerise to create the basic host-guest cross-links could be employed in place of both naphthol and methyl viologen and dopamine could replace catechol creating a completely bio-based version of this system. What is clear though, is that the advantage of this type of consolidant is that it reacts to the changing chemical environment around it. As  $\text{Fe}^{2+}$  becomes reduced to  $\text{Fe}^{3+}$ , either by chemical or microbial action the resulting  $\text{Fe}^{3+}$  becomes bound within the consolidant preventing additional catalytic action that will further degrade the cellulosic component of the wood. As such, the consolidant can recognise and adapt to changes in the environment, reducing the need for repetitive consolidation as  $\text{Fe}^{3+}$  concentration increases. Such adaptable systems are key to the future of sustainable wood consolidant, assuming we can learn how to also produce them with a minimal environmental footprint.

Interestingly, much of the discussion of alternative consolidants have focused on materials that can replace what is missing from the degraded wood, primarily cellulose, rather than targeting and strengthening what is still there, generally lignin. Lignin is often described as the structural component of the wood. While it generally remains long after celluloses have been degraded, it is often significantly altered [223]. Thus, consolidants that target the lignin component of the wood can be very beneficial to the long-term stability of an artefact, however, such consolidants are quite rare. Several lignin-based consolidants are discussed in previous sections, but their purpose is not specifically to target lignin, rather to reduce the toxicity and improve the sustainability of standard consolidants that are already on the market. However, some work has been done to develop targeted lignin consolidants, which have the potential to significantly improve the stability of heavily degraded wood [224]. Currently, heavily degraded wood is conserved with Kauramin, a highly unsustainable synthetic polymer that irreversibly polymerises in situ and has limited compatibility with the wood structure that often leads to warping and cracking of treated artefacts. McHale et al. [224] propose synthesising lignin-like oligomers that would target and bulk the lignin matrix, as lignin itself is too bulky to effectively penetrate the wood matrix. Using isoeugenol, propenyl-substituted guaiacol similar to the guaiacol sub-unit of lignin, they reported the synthesis of lignin-like oligomers. Isoeugenol is a

major component in the essential oils of cloves, cinnamon or ylang-ylang, among others. The oils are extracted by steam distillation and then treated with NaOH or KOH to recover eugenol and isoeugenol [225]. The polymerisation of isoeugenol was carried out at room temperature for 2 days in the presence of a copper salen catalyst and H<sub>2</sub>O<sub>2</sub> at pH 10. The use of copper catalysts does reduce the sustainability of the system. In follow-up work, the authors showed that the synthesis could be catalysed by horseradish peroxidase (HRP) in place of Cu(salen), significantly improving the environmental impact of the consolidant [226]. Moreover, with this HRP catalyst, a natural producer of H<sub>2</sub>O<sub>2</sub>, the oligomers could be synthesised in situ. The reaction is carried out by immersing the wood in a solution of isoeugenol in ethanol/water. After impregnation of the wood, HRP and H<sub>2</sub>O<sub>2</sub> were added to start polymerisation, which continued over two weeks. The samples were washed to remove ethanol before freeze-drying. Both the infiltration with oligomers and their in situ polymerisation gave promising results for the conservation of heavily degraded wood. The interaction of the guaiacol derivatives with the lignin enhances the specificity of the polymerisation and the compatibility with the matrix, offering a promising alternative to the use of Kauramin for heavily degraded samples.

The most recent example of bio-inspired consolidant is a terpene polyacrylate treatment derived from the  $\alpha$ -pinene, a monoterpene extracted from colophony [227]. While this treatment has only been synthesised and not yet tested on wood, it is certainly an interesting proposition and one that merits further investigation. Terpenes perform a natural protective function in wood [228], as such terpene-based consolidants may provide protective functions to degraded wood that are not exploited in the current conservation toolkit. The only potential disadvantage of this system is the heavy use of petroleum-based solvents and reactants to achieve the final terpene polyacrylate. However, advances in the production of acrylates from bioresources, along with more efficient enzymatic catalysis, as discussed in previous sections, and the drive to develop new bio-based solvents for chemical synthesis [229] means that much of the described reaction process could be replaced with bio-derived chemicals improving the overall sustainability of this novel consolidant.

## 5. Discussion and Conclusions

One of the major challenges to the drive for sustainability in the conservation of wooden objects of cultural importance will most likely be the switch away from fossil fuels as energy. With diminishing demand for fossil fuels for energy production, oil extractors are adapting their portfolios to ensure continued income from fossil fuels, albeit from different sources than in the past. Many oil refineries are planning to increase their petrochemical output from under 20% to between 45–80%, meaning increased production of raw materials for virgin plastics and polymers. Increased production of petrochemicals will also drive down costs, making polymer consolidants derived from biomass less cost-effective. This presents a real barrier to change in a sector that is already under-funded and resistant to move away from state-of-the-art due to the as-yet-unknown potential impacts on artefact conservation.

However, we already know our consumption practices are driving irreversible changes in the dynamics of our planet leading to potentially catastrophic consequences, which will heavily impact the conservation of the world's natural heritage and cultural heritage. Extremes in humidity, in particular, will affect wooden heritage to a significant degree meaning an increase in the number of objects requiring active conservation. Thus, the sooner we can enact new conservation practices that focus on the circularity and sustainability of the entire process from the production of the consolidant to treatment of the artefacts, the greater chance we have to reduce the negative impacts of unsustainable consumption on the planet in general. This will require a significant internal change in the museum and institutional protocols with respect to conservation, however, this is not something unfamiliar in this arena. Museums and cultural institutions are uniquely positioned to significantly impact sustainable development goals. Their role as trusted institutions, in particular centres of formal and informal learning, means that by driving change within,

they can significantly impact change in the wider community. By investing in sustainable conservation practices and making this known to their visitors through awareness and education programmes, they have the potential to influence how their visitors view their own consumption practices. Highlighting the environmental impact of non-sustainable consolidant use and the benefits to the use of bio-based (and preferably dynamic) consolidants that can be reused, recycled, and repaired without significant further resource usage may encourage visitors to examine their own use of sustainable products and effect much wider-reaching change than without such influence from a trusted source. Museums currently do this by choosing renewable energy sources and low-energy ventilation and lighting systems and publicising the use of such, with great effect. What would be the change to petrochemical-based material usage if museums and cultural institutions were to turn their attention to bio-based chemical usage and educate the public about the benefits? Significant testing of long-term stability is required before such circular consolidants are a common part of the conservation toolkit, hence the two-step strategy to achieving truly sustainable conservation processes, but if we do not start now, then when? Alarm bells are already ringing for the future of the planet, the time to make changes for the future and long-term sustainability of conservation practices is now.

**Funding:** This research received no external funding; however, the APC was kindly funded by the Open Access Fund of the University of Basel Library.

**Institutional Review Board Statement:** Not applicable.

**Informed Consent Statement:** Not applicable.

**Data Availability Statement:** Not applicable.

**Acknowledgments:** Z. Walsh-Korb acknowledges financial support from the European Union’s Horizon 2020 research and innovation programme under the Marie Skłodowska-Curie grant agreement No. 842043 [CatchGel].

**Conflicts of Interest:** The author declares no conflict of interest.

## References

1. Fratzl, P. Biomimetic materials research: What can we really learn from nature’s structural materials? *J. R. Soc. Interface* **2007**, *4*, 637–642. [CrossRef]
2. Fratzl, P.; Weinkamer, R. Nature’s hierarchical materials. *Prog. Mater. Sci.* **2007**, *52*, 1263–1334. [CrossRef]
3. Walsh-Korb, Z.; Avérous, L. Recent developments in the conservation of materials properties of historical wood. *Prog. Mater. Sci.* **2019**, *102*, 167–221. [CrossRef]
4. Marais, B.N.; Brischke, C.; Militz, H. Wood durability in terrestrial and aquatic environments—A review of biotic and abiotic influence factors. *Wood Mater. Sci. Eng.* **2020**, *1*–24. [CrossRef]
5. Kirker, G.; Winandy, J. Above Ground Deterioration of Wood and Wood-Based Materials. In *Deterioration and Protection of Sustainable Biomaterials*; Schultz, T.P., Goodell, B., Nicholas, D.D., Eds.; American Chemical Society: Washington, DC, USA, 2014; pp. 113–129. [CrossRef]
6. Jones, J.M.; Heath, K.D.; Ferrer, A.; Brown, S.P.; Canam, T.; Dalling, J.W. Wood decomposition in aquatic and terrestrial ecosystems in the tropics: Contrasting biotic and abiotic processes. *FEMS Microbiol. Ecol.* **2019**, *95*, fty 223. [CrossRef]
7. Kim, Y.; Singh, A.P. Wood as Cultural Heritage Material and its Deterioration by Biotic and Abiotic Agents. In *Secondary Xylem Biology*; Kim, Y.S., Funada, R., Singh, A.P., Eds.; Academic Press: Cambridge, MA, USA, 2016; Chapter 12; pp. 233–257. [CrossRef]
8. Hocker, E. Maintaining a stable environment: Vasa’s new climate-control system. *APT Bull. J. Preserv. Technol.* **2010**, *41*, 3–10.
9. Böhm, C.B.; Zehnder, K.; Domeisen, H.; Arnold, A. Climate Control for the Passive Conservation of the Romanesque Painted Wooden Ceiling in the Church of Zillis (Switzerland). *Stud. Conserv.* **2001**, *46*, 251–268. [CrossRef]
10. United Nations. Transforming Our World: The 2030 Agenda for Sustainable Development. *United Nations: September 2015. Report No.: A/RES/70/1*. Available online: <https://sustainabledevelopment.un.org/content/documents/21252030%20Agenda%20for%20Sustainable%20Development%20web.pdf> (accessed on 22 December 2021).
11. Hocker, E.; Almkvist, G.; Sahlstedt, M. The Vasa experience with polyethylene glycol: A conservator’s perspective. *J. Cult. Herit.* **2012**, *13*, S175–S182. [CrossRef]
12. Stamm, A.J. Dimensional stabilization of wood with carbowaxes. *For. Prod. J.* **1956**, *846*, 1–4.
13. Hoffmann, P. Methods of application of polyethylene glycol. In *Conservation of Archaeological Ships and Boats—Personal Experiences*; Archetype Publications: London, UK, 2013; pp. 43–80.

14. Graves, D.J. A comparative study of consolidants for waterlogged wood: Polyethylene glycol, sucrose and silicon oil. *SSCR J. News Mag. Scott. Soc. Conserv. Restor.* **2004**, *15*, 13–17.
15. Mortensen, M.N.; Egsgaard, H.; Hvilsted, S.; Shashoua, Y.; Glastrup, J. Characterisation of the polyethylene glycol impregnation of the Swedish warship Vasa and one of the Danish Skuldelev Viking ships. *J. Archaeol. Sci.* **2007**, *34*, 1211–1218. [CrossRef]
16. Lionetto, F.; Frigione, M. Effect of novel consolidants on mechanical and absorption properties of deteriorated wood by insect attack. *J. Cult. Herit.* **2012**, *13*, 195–203. [CrossRef]
17. Kiliç, N.; Kiliç, A.G. An attenuated total reflection Fourier transform infrared (ATR-FTIR) spectroscopic study of waterlogged woods treated with melamine formaldehyde. *Vib. Spectrosc.* **2019**, *105*, 102985. [CrossRef]
18. Christensen, M.; Kutzke, H.; Hansen, F.K. New materials used for the consolidation of archaeological wood—Past attempts, present struggles, and future requirements. *J. Cult. Herit.* **2012**, *13*, S183–S190. [CrossRef]
19. Gierlinger, N.; Hansmann, C.; Röder, T.; Sixta, H. Comparison of UV and Confocal Raman Microscopy to Measure the Melamine-Formaldehyde Resin Content within Cell Walls of Impregnated Spruce Wood. *Holzforschung* **2005**, *59*, 210–213. [CrossRef]
20. Crisci, G.M.; La Russa, M.F.; Malagodi, M.; Ruffolo, S.A. Consolidating properties of Regalrez 1126 and Paraloid B72 applied to wood. *J. Cult. Herit.* **2010**, *11*, 304–308. [CrossRef]
21. Traistaru, A.A.T.; Timar, M.C.; Câmpean, M. Studies upon penetration of paraloid B72 into poplar wood by cold immersion treatments. *Bull. Transilvania Univ. Brasov For. Wood Ind. Agric. Food Eng. Ser. II* **2011**, *4*, 81.
22. Yadav, V.G.; Yadav, G.D.; Patankar, S.C. The production of fuels and chemicals in the new world: Critical analysis of the choice between crude oil and biomass vis-à-vis sustainability and the environment. *Clean Technol. Environ. Policy* **2020**, *22*, 1757–1774. [CrossRef]
23. Klein, D.; Carazo, M.P.; Doelle, M.; Bulmer, J.; Higham, A. *The Paris Agreement on Climate Change: Analysis and Commentary*; Oxford University Press: Oxford, UK, 2017.
24. Mathy, S.; Menanteau, P.; Criqui, P. After the Paris Agreement: Measuring the Global Decarbonization Wedges from National Energy Scenarios. *Ecol. Econ.* **2018**, *150*, 273–289. [CrossRef]
25. Sachs, N.M. The Paris Agreement in the 2020s: Breakdown or Breakup. *Ecol. LQ* **2019**, *46*, 865. [CrossRef]
26. Averchenkova, A.; Bassi, S. Beyond the Targets: Assessing the Political Credibility of Pledges for the Paris Agreement; Grantham Research Institute on Climate Change and the Environment, London, UK, 2016. Available online: <http://eprints.lse.ac.uk/65670/> (accessed on 22 December 2021).
27. Bataille, C.; Åhman, M.; Neuhoﬀ, K.; Nilsson, L.J.; Fishedick, M.; Lechtenböhmer, S.; Solano-Rodriguez, B.; Denis-Ryan, A.; Stiebert, S.; Waisman, H.; et al. A review of technology and policy deep decarbonization pathway options for making energy-intensive industry production consistent with the Paris Agreement. *J. Clean. Prod.* **2018**, *187*, 960–973. [CrossRef]
28. Young, O.R. The Paris Agreement: Destined to succeed or doomed to fail? *Polit. Gov.* **2016**, *4*, 124–132. [CrossRef]
29. Ambrose, J.; The Guardian. War on Plastic Waste Faces Setback as Cost of Recycled Material Soars. 13 October 2019. Available online: <http://www.theguardian.com/environment/2019/oct/13/war-on-plastic-waste-faces-setback-as-cost-of-recycled-material-soars> (accessed on 30 November 2021).
30. American Chemical Society. Why the Future of Oil Is in Chemicals, Not Fuels. Available online: <https://cen.acs.org/business/ petrochemicals/future-oil-chemicals-fuels/97/i8> (accessed on 31 May 2021).
31. Tooze, A. Why Central Banks Need to Step Up on Global Warming. 20 July 2019. Available online: <https://foreignpolicy.com/2019/07/20/why-central-banks-need-to-step-up-on-global-warming/> (accessed on 30 November 2021).
32. Feldstein, M. Introduction to “The Economics of Art Museums”. In *The Economics of Art Museums*; Feldstein, M., Ed.; University of Chicago Press: Chicago, IL, USA, 1991; pp. 1–12.
33. Bauer, M.D.; Rudebusch, G.D. The Rising Cost of Climate Change: Evidence from the Bond Market. *Rev. Econ. Stat.* **2021**, 1–45. [CrossRef]
34. Xiao, C. Focus on “Biobased”, “Biodegradable”, & “Compostable” Plastics. Department of Ecology, State of Washington. *Report No.: 14-07-017*. 2014. Available online: <https://www.bpiworld.org/Resources/Documents/Washington%20State%20Biobased%20Fact%20Sheet%20Aug%202014.pdf> (accessed on 22 December 2021).
35. de Silva, M.; Henderson, J. Sustainability in conservation practice. *J. Am. Inst. Conserv.* **2011**, *34*, 5–15. [CrossRef]
36. Unger, A.; Schniewind, A.P.; Unger, W. *Conservation of Wood Artifacts: A Handbook*; Springer: Berlin/Heidelberg, Germany, 2001. [CrossRef]
37. Schönemann, A.; Eisbein, M.; Unger, A.; Dell’mour, M.; Frenzel, W.; Kenndler, E. Historic Consolidants for Wooden Works of Art in Saxony—An Investigation by GC-MS and FTIR Analysis. *Stud. Conserv.* **2008**, *53*, 118–130. [CrossRef]
38. Schönemann, A.; Edwards, H.G.M. Raman and FTIR microspectroscopic study of the alteration of Chinese tung oil and related drying oils during ageing. *Anal. Bioanal. Chem.* **2011**, *400*, 1173–1180. [CrossRef]
39. Schönemann, A.; Frenzel, W.; Unger, A.; Kenndler, E. An Investigation of the Fatty Acid Composition of New and Aged Tung Oil. *Stud. Conserv.* **2006**, *51*, 99–110. [CrossRef]
40. Jacobsson, E. Environmental Impact Analysis of Flax Fibre Cultivation for Composite Reinforcement. MSc Thesis, Mid Sweden University, Sundsvall, Sweden, 2018. Available online: <https://www.diva-portal.org/smash/get/diva2:1262794/FULLTEXT01.pdf> (accessed on 22 December 2021).
41. Heller, K.; Baraniecki, P.; Praczyk, M. Fibre flax cultivation in sustainable agriculture. In *Handbook of Natural Fibres*; Kozłowski, R.M., Ed.; Woodhead Publishing: Sawston, UK, 2012; Chapter 15; pp. 508–531. [CrossRef]

42. Kasote, D.M.; Badhe, Y.S.; Hegde, M.V. Effect of mechanical press oil extraction processing on quality of linseed oil. *Ind. Crops Prod.* **2013**, *42*, 10–13. [CrossRef]
43. Gros, C.; Lanoisellé, J.-L.; Vorobiev, E. Towards an Alternative Extraction Process for Linseed Oil. *Chem. Eng. Res. Des.* **2003**, *81*, 1059–1065. [CrossRef]
44. Kumar, S.P.J.; Prasad, S.R.; Banerjee, R.; Agarwal, D.K.; Kulkarni, K.S.; Ramesh, K.V. Green solvents and technologies for oil extraction from oilseeds. *Chem. Cent. J.* **2017**, *11*, 9. [CrossRef]
45. Supanchaiyamat, N.; Shuttleworth, P.S.; Hunt, A.J.; Clark, J.H.; Matharu, A.S. Thermosetting resin based on epoxidised linseed oil and bio-derived crosslinker. *Green Chem.* **2012**, *14*, 1759–1765. [CrossRef]
46. Panov, D.; Terziev, N. Durability of epoxi-oil modified and alkoxy-silane treated wood in field testing. *Bioresources* **2015**, *10*, 13. [CrossRef]
47. Ciesla, W.M. (Ed.) Fruits. In *Non-Wood Forest Products from Temperate Broad-Leaved Trees*; Food and Agriculture Organization of the United Nations: Rome, Italy, 2002; Chapter 7. Available online: <https://www.fao.org/3/y4351e/y4351e0b.htm> (accessed on 22 December 2021).
48. Armingier, B.; Jaxel, J.; Bacher, M.; Gindl-Altmutter, W.; Hansmann, C. On the drying behavior of natural oils used for solid wood finishing. *Prog. Org. Coat.* **2020**, *148*, 105831. [CrossRef]
49. Tung Oil. *Nature* **1929**, *124*, 272–273. [CrossRef]
50. Tung Oil in the United States. *Nature* **1932**, *130*, 199. [CrossRef]
51. Shultz, E.B. *Fuels and Chemicals from Oilseeds: Technology and Policy Options*; CRC Press: Boca Raton, FL, USA, 2019.
52. Zhang, Y.; Li, Y.; Jiang, L.; Tian, C.; Li, J.; Xiao, Z. Potential of Perennial Crop on Environmental Sustainability of Agriculture. *Proc. Environ. Sci.* **2011**, *10*, 1141–1147. [CrossRef]
53. Li, Z.; Long, H.; Zhang, L.; Liu, Z.; Cao, H.; Shi, M.; Tan, X. The complete chloroplast genome sequence of tung tree (*Vernicia fordii*): Organization and phylogenetic relationships with other angiosperms. *Sci. Rep.* **2017**, *7*, 1–11. [CrossRef]
54. Hepburn, H.R.; Bernard, R.T.F.; Davidson, B.C.; Muller, W.J.; Lloyd, P.; Kurstjens, S.P.; Vincent, S.L. Synthesis and secretion of beeswax in honeybees. *Apidologie* **1991**, *22*, 21–36. [CrossRef]
55. Tinto, W.F.; Elufioye, T.O.; Roach, J. Waxes. In *Pharmacognosy*; Badal, S., Delgoda, R., Eds.; Academic Press: Cambridge, MA, USA, 2017; Chapter 22; pp. 443–455. [CrossRef]
56. Coppock, R.W. Bee products as nutraceuticals to nutraceuticals for bees. In *Nutraceuticals*, 2nd ed.; Gupta, R.C., Lall, R., Srivastava, A., Eds.; Academic Press: Cambridge, MA, USA, 2021; Chapter 47; pp. 813–833. [CrossRef]
57. The Honey Industry. Available online: <https://www.vegansociety.com/go-vegan/why-go-vegan/honey-industry> (accessed on 30 November 2021).
58. Brookfield, H.C. Problems of Monoculture and Diversification in a Sugar Island: Mauritius. *Econ. Geogr.* **1959**, *35*, 25–40. [CrossRef]
59. Lupupa, T.; Mavimbela, S.; Rossi, A.; Laub, R. *From Subsistence Farming to Sugar-Cane Monoculture: Impacts on Agrobiodiversity, Local Knowledge and Food Security*; Food and Agriculture Organization of the United Nations: Rome, Italy, 2008. Available online: <https://www.fao.org/3/aj042e/aj042e00.htm> (accessed on 19 November 2021).
60. Li, X.-F.; Wang, Z.-G.; Bao, X.-G.; Sun, J.-H.; Yang, S.-C.; Wang, P.; Wang, C.-B.; Wu, J.-P.; Liu, X.-R.; Tian, X.-L.; et al. Long-term increased grain yield and soil fertility from intercropping. *Nat. Sustain.* **2021**, *4*, 943–950. [CrossRef]
61. Calatayud-Vernich, P.; VanEngelsdorp, D.; Picó, Y. Beeswax cleaning by solvent extraction of pesticides. *MethodsX* **2019**, *6*, 980–985. [CrossRef]
62. Sharma, S.C.; Prasad, N.; Pandey, S.K. Status of Resin Tapping and Scope of Improvement: A Review. *AMA Agric. Mech. Asia Afr. Lat. Am.* **2018**, *49*, 16–26.
63. Soliño, M.; Yu, T.; Alía, R.; Auñón, F.; Bravo-Oviedo, A.; Chambel, M.R.; de Miguel, J.; Del Río, M.; Justes, A.; Martínez-Jauregui, M.; et al. Resin-tapped pine forests in Spain: Ecological diversity and economic valuation. *Sci. Total Environ.* **2018**, *625*, 1146–1155. [CrossRef]
64. Heinze, A.; Kuyper, T.W.; García Barrios, L.E.; Ramírez Marcial, N.; Bongers, F. Tapping into nature's benefits: Values, effort and the struggle to co-produce pine resin. *Ecosyst. People* **2021**, *17*, 69–86. [CrossRef]
65. Tomusiak, R.; Magnuszewski, M. Effect of Resin Tapping on Radial Increments of Scots Pine (*Pinus sylvestris* L.). In *TRACE: Tree Rings in Archaeology, Climatology, and Ecology, Proceedings of the DENDROSYMPOSIUM 2008, Zakopane, Poland, 27–30 April 2008*; GeoForschungsZentrum: Potsdam, Germany, 2009; Volume 7, pp. 153–157. Available online: [https://gfzpublic.gfz-potsdam.de/rest/items/item\\_16015\\_4/component/file\\_16014/content#page=153](https://gfzpublic.gfz-potsdam.de/rest/items/item_16015_4/component/file_16014/content#page=153) (accessed on 22 December 2021).
66. Papadopoulos, A.M. Resin tapping history of an Aleppo Pine Forest in central Greece. *Open Forensic Sci. J.* **2013**, *6*, 50–53. [CrossRef]
67. Génova, M.; Caminero, L.; Dochao, J. Resin tapping in *Pinus pinaster*: Effects on growth and response function to climate. *Eur. J. For. Res.* **2014**, *133*, 323–333. [CrossRef]
68. van der Maaten, E.; Mehl, A.; Wilmking, M.; van der Maaten-Theunissen, M. Tapping the tree-ring archive for studying effects of resin extraction on the growth and climate sensitivity of Scots pine. *For. Ecosyst.* **2017**, *4*, 1–7. [CrossRef]
69. Silva, M.E.; Loureiro, C.; Pires, J. Influence of Resin Tapping on Wood Characteristics and Properties. Incredible: Innovation Networks for Cork, Resins & Edibles. January 2020. Available online: <https://repository.incredibleforest.net/oppla-factsheet/20255> (accessed on 22 December 2021).



70. Bain, J.P. Resin Acids from Pine Tar. *J. Am. Chem. Soc.* **1942**, *64*, 871. [CrossRef]
71. Hoffmann, P. The Sucrose Method. In *Conservation of Archaeological Ships and Boats—Personal Experiences*; Archetype Publications: London, UK, 2013; Chapter 6.
72. Leading Sugar Producers Worldwide 2020/2021. Available online: <https://www.statista.com/statistics/495973/sugar-production-worldwide/> (accessed on 30 November 2021).
73. Tayyab, M.; Yang, Z.; Zhang, C.; Islam, W.; Lin, W.; Zhang, H. Sugarcane monoculture drives microbial community composition, activity and abundance of agricultural-related microorganisms. *Environ. Sci. Pollut. Res.* **2021**, *28*, 48080–48096. [CrossRef]
74. Beza, S.A.; Assen, M.A. Expansion of sugarcane monoculture: Associated impacts and management measures in the semi-arid East African Rift Valley, Ethiopia. *Environ. Monit. Assess.* **2017**, *189*, 111. [CrossRef] [PubMed]
75. Koch, H.-J.; Trimpler, K.; Jacobs, A.; Stockfisch, N. Crop Rotational Effects on Yield Formation in Current Sugar Beet Production—Results from a Farm Survey and Field Trials. *Front. Plant Sci.* **2018**, *9*, 231. [CrossRef] [PubMed]
76. Hofer, R. *Sustainable Solutions for Modern Economies*; Royal Society of Chemistry: London, UK, 2009.
77. Garthwaite, D.; Ridley, L.; Mace, A.; Parrish, G.; Barker, I.; Rainford, J.; MacArthur, R. Pesticide Usage Survey Report 284: Arable Crops in the United Kingdom 2018. Department for Environment, Food and Rural Affairs; In *Report No.: 284*; 2018. Available online: <https://secure.fera.defra.gov.uk/pusstats/surveys/documents/arable2018.pdf> (accessed on 22 December 2021).
78. Duru, M.; Therond, O.; Martin, G.; Martin-Clouaire, R.; Magne, M.-A.; Justes, E.; Journet, E.P.; Aubertot, J.N.; Savary, S.; Bergez, J.E.; et al. How to implement biodiversity-based agriculture to enhance ecosystem services: A review. *Agron. Sustain. Dev.* **2015**, *35*, 1259–1281. [CrossRef]
79. Regenerating an Ecosystem to Grow Organic Sugar: The Balbo Group. Available online: <https://ellenmacarthurfoundation.org/circular-examples/the-balbo-group> (accessed on 16 November 2021).
80. Singh, R. Hybrid Membrane Systems—Applications and Case Studies. In *Membrane Technology and Engineering for Water Purification*, 2nd ed.; Singh, R., Ed.; Butterworth-Heinemann: Oxford, UK, 2015; Chapter 3; pp. 179–281. [CrossRef]
81. Jiang, L.; Zheng, A.; Zhao, Z.; He, F.; Li, H. Comprehensive utilization of glycerol from sugarcane bagasse pretreatment to fermentation. *Bioresour. Technol.* **2015**, *196*, 194–199. [CrossRef] [PubMed]
82. Cheng, S.; Martínez-Monteagudo, S.I. Hydrogenation of lactose for the production of lactitol. *Asia-Pac. J. Chem. Eng.* **2019**, *14*, e2275. [CrossRef]
83. Martínez-Monteagudo, S.I.; Rathnakumar, K.; Enteshari, M.; Nyuydze, C.; Osorio-Arias, J.C.; Ranaweera, H. Hundred Years of Lactitol: From Hydrogenation to Food Ingredient. In *Lactose and Lactose Derivatives*; Gutiérrez-Méndez, N., Ed.; IntechOpen: Rijeka, Croatia, 2020. [CrossRef]
84. Liu, D.D.; Chen, E.Y.-X. Organocatalysis in biorefining for biomass conversion and upgrading. *Green Chem.* **2014**, *16*, 964–981. [CrossRef]
85. The Nobel Prize in Chemistry 2021. Available online: <https://www.nobelprize.org/prizes/chemistry/2021/press-release/> (accessed on 23 November 2021).
86. O'Neill, M.K.; Piligian, B.F.; Olson, C.D.; Woodruff, P.J.; Swarts, B.M. Tailoring Trehalose for Biomedical and Biotechnological Applications. *Pure Appl. Chem.* **2017**, *89*, 1223–1249. [CrossRef] [PubMed]
87. Schiraldi, C.; Di Lernia, I.; De Rosa, M. Trehalose production: Exploiting novel approaches. *Trends Biotechnol.* **2002**, *20*, 420–425. [CrossRef]
88. Stamm, A.J. The dimensional stability of wood. *For. Prod. J.* **1959**, *9*, 375–381.
89. United States. Patent Office. Official Gazette of the United States Patent Office. U.S. Patent Office. 1940. Available online: <https://play.google.com/store/books/details?id=kmedAAAAMAAJ> (accessed on 22 December 2021).
90. Hoang Thi, T.T.; Pilkington, E.H.; Nguyen, D.H.; Lee, J.S.; Park, K.D.; Truong, N.P. The Importance of Poly(ethylene glycol) Alternatives for Overcoming PEG Immunogenicity in Drug Delivery and Bioconjugation. *Polymers* **2020**, *12*, 298. [CrossRef]
91. Twigg, G.H. The catalytic oxidation of ethylene. *Trans. Faraday Soc.* **1946**, *42*, 284–290. [CrossRef]
92. Herzberger, J.; Niederer, K.; Pohlit, H.; Seiwert, J.; Worm, M.; Wurm, F.R.; Frey, H. Polymerization of Ethylene Oxide, Propylene Oxide, and Other Alkylene Oxides: Synthesis, Novel Polymer Architectures, and Bioconjugation. *Chem. Rev.* **2016**, *116*, 2170–2243. [CrossRef] [PubMed]
93. Grubbs, R.B.; Grubbs, R.H. 50th Anniversary Perspective: Living Polymerization—Emphasizing the Molecule in Macromolecules. *Macromolecules* **2017**, *50*, 6979–6997. [CrossRef]
94. Chiantore, O.; Lazzari, M. Photo-oxidative stability of paraloid acrylic protective polymers. *Polymer* **2001**, *42*, 17–27. [CrossRef]
95. Lazzari, M.; Chiantore, O. Thermal-ageing of paraloid acrylic protective polymers. *Polymer* **2000**, *41*, 6447–6455. [CrossRef]
96. Marlin, D.S.; Sarron, E.; Sigurbjörnsson, Ö. Process Advantages of Direct CO<sub>2</sub> to Methanol Synthesis. *Front. Chem.* **2018**, *6*, 446. [CrossRef]
97. Mahboub, M.J.D.; Dubois, J.-L.; Cavani, F.; Rostamizadeh, M.; Patience, G.S. Catalysis for the synthesis of methacrylic acid and methyl methacrylate. *Chem. Soc. Rev.* **2018**, *47*, 7703–7738. [CrossRef] [PubMed]
98. Norrish, R.G.W.; Smith, R.R. Catalysed polymerization of methyl methacrylate in the liquid phase. *Nature* **1942**, *150*, 336–337. [CrossRef]
99. Merline, D.J.; Vukusic, S.; Abdala, A.A. Melamine formaldehyde: Curing studies and reaction mechanism. *Polym. J.* **2012**, *45*, 413–419. [CrossRef]

100. Urea Production and Manufacturing Process. 4 April 2010. Available online: <https://www.icis.com/explore/resources/news/2007/11/07/9076560/urea-production-and-manufacturing-process/> (accessed on 29 November 2021).
101. Kinoshita, H. Synthesis of Melamine from Urea, II. *Rev. Phys. Chem. Jpn.* **1954**, *24*, 19–27.
102. Bazilio, C.A.; Thomas, W.J.; Ullah, U.; Hayes, K.E. The Catalytic Oxidation of Methanol. *Proc. R. Soc. Lond. Ser. A Math. Phys. Sci.* **1985**, *399*, 181–194.
103. Pham, H.Q.; Marks, M.J. Epoxy Resins. In *Ullmann's Encyclopedia of Industrial Chemistry*; Wiley-VCH Verlag GmbH & Co. KGaA: Weinheim, Germany, 2005. [CrossRef]
104. Lu, Y.; Li, T.; Wang, R.; Luo, G. Synthesis of epichlorohydrin from 1,3-dichloropropanol using solid base. *Chin. J. Chem. Eng.* **2017**, *25*, 301–305. [CrossRef]
105. Stauffer, J.E. Production of Allyl Chloride. European Patent EP 0455644 B1, 5 October 1994.
106. Wang, L.; Bassiri, M.; Najafi, R.; Najafi, K.; Yang, J.; Khosrovi, B.; Hwong, W.; Barati, E.; Belisle, B.; Celeri, C.; et al. Hypochlorous acid as a potential wound care agent: Part I. Stabilized hypochlorous acid: A component of the inorganic armamentarium of innate immunity. *J. Burns Wounds* **2007**, *6*, e5.
107. Luyben, W.L. Design and Control of the Cumene Process. *Ind. Eng. Chem. Res.* **2010**, *49*, 719–734. [CrossRef]
108. Rubin, B.S. Bisphenol A: An endocrine disruptor with widespread exposure and multiple effects. *J. Steroid Biochem. Mol. Biol.* **2011**, *127*, 27–34. [CrossRef]
109. Marqueño, A.; Pérez-Albaladejo, E.; Flores, C.; Moyano, E.; Porte, C. Toxic effects of bisphenol A diglycidyl ether and derivatives in human placental cells. *Environ. Pollut.* **2019**, *244*, 513–521. [CrossRef] [PubMed]
110. Dahmen, K.; Oftring, A.; Hugo, R.; Baumann, K.; Hahn, T.; Melder, J.-P. Triethylenetetraamine Preparation Method. European Patent EP-2114861-B1, 5 September 2012.
111. Broda, M.; Majka, J.; Olek, W.; Mazela, B. Dimensional stability and hygroscopic properties of waterlogged archaeological wood treated with alkoxyxilanes. *Int. Biodeterior. Biodegrad.* **2018**, *133*, 34–41. [CrossRef]
112. Broda, M.; Mazela, B.; Dutkiewicz, A. Organosilicon compounds with various active groups as consolidants for the preservation of waterlogged archaeological wood. *J. Cult. Herit.* **2019**, *35*, 123–128. [CrossRef]
113. Broda, M.; Spear, M.J.; Curling, S.F.; Ormondroyd, G.A. The Viscoelastic Behaviour of Waterlogged Archaeological Wood Treated with Methyltrimethoxysilane. *Materials* **2021**, *14*, 5150. [CrossRef]
114. Broda, M.; Dąbek, I.; Dutkiewicz, A.; Dutkiewicz, M.; Popescu, C.-M.; Mazela, B.; Maciejewski, H. Organosilicons of different molecular size and chemical structure as consolidants for waterlogged archaeological wood—A new reversible and retreatable method. *Sci. Rep.* **2020**, *10*, 1–13. [CrossRef]
115. Saka, S. Wood-inorganic composites prepared by sol-gel processing I. Wood-inorganic composites. *Mokuzai Gakkaishi (J. Jpn. Wood Res. Soc.)* **1992**, *38*, 1043–1049.
116. Saka, S.; Ueno, T. Several SiO<sub>2</sub> wood-inorganic composites and their fire-resisting properties. *Wood Sci. Technol.* **1997**, *31*, 457–466. [CrossRef]
117. Miyafuji, H.; Saka, S. Topochemistry of SiO<sub>2</sub> wood-inorganic composites for enhancing water-repellency. *J. Soc. Mater. Sci. Jpn.* **1999**, *48*, 270–275. [CrossRef]
118. Laine, R.M.; Furgal, J.C.; Doan, P.; Pan, D.; Popova, V.; Zhang, X. Avoiding Carbothermal Reduction: Distillation of Alkoxyxilanes from Biogenic, Green, and Sustainable Sources. *Angew. Chem. Int. Ed.* **2016**, *55*, 1065–1069. [CrossRef]
119. Ethanol Explained—U.S. Energy Information Administration (EIA). Available online: <https://www.eia.gov/energyexplained/biofuels/ethanol.php> (accessed on 1 December 2021).
120. Moncada, J.A.; Versteegen, J.A.; Posada, J.A.; Junginger, M.; Lukszo, Z.; Faaij, A.; Weijnen, M. Exploring policy options to spur the expansion of ethanol production and consumption in Brazil: An agent-based modeling approach. *Energy Policy* **2018**, *123*, 619–641. [CrossRef]
121. Parapouli, M.; Vasileiadis, A.; Afendra, A.-S.; Hatziloukas, E. *Saccharomyces cerevisiae* and its industrial applications. *AIMS Microbiol.* **2020**, *6*, 1–31. [CrossRef] [PubMed]
122. Johnstone, P.; McLeish, C. World wars and the age of oil: Exploring directionality in deep energy transitions. *Energy Res. Soc. Sci.* **2020**, *69*, 101732. [CrossRef]
123. de Souza Abud, A.K.; de Farias Silva, C.E. Bioethanol in Brazil: Status, Challenges and Perspectives to Improve the Production. In *Bioethanol Production from Food Crops*; Ray, R.C., Ramachandran, S., Eds.; Academic Press: Cambridge, MA, USA, 2019; Chapter 21; pp. 417–443. [CrossRef]
124. Wang, Z.X.; Zhuge, J.; Fang, H.; Prior, B.A. Glycerol production by microbial fermentation: A review. *Biotechnol. Adv.* **2001**, *19*, 201–223. [CrossRef]
125. Kandasamy, S.; Samudrala, S.P.; Bhattacharya, S. The route towards sustainable production of ethylene glycol from a renewable resource, biodiesel waste: A review. *Catal. Sci. Technol.* **2019**, *9*, 567–577. [CrossRef]
126. Li, K.; Sun, W.; Meng, W.; Yan, J.; Zhang, Y.; Guo, S.; Lü, C.; Ma, C.; Gao, C. Production of Ethylene Glycol from Glycerol Using an In Vitro Enzymatic Cascade. *Catalysts* **2021**, *11*, 214. [CrossRef]
127. Gioia, C.; Colonna, M.; Tagami, A.; Medina, L.; Sevastyanova, O.; Berglund, L.A.; Lawoko, M. Lignin-Based Epoxy Resins: Unravelling the Relationship between Structure and Material Properties. *Biomacromolecules* **2020**, *21*, 1920–1928. [CrossRef] [PubMed]

128. Shnawa, H.A. Curing and thermal properties of tannin-based epoxy and its blends with commercial epoxy resin. *Polym. Bull.* **2021**, *78*, 1925–1940. [CrossRef]
129. Todorovic, A.; Resch-Fauster, K.; Mahendran, A.R.; Oreski, G.; Kern, W. Curing of epoxidized linseed oil: Investigation of the curing reaction with different hardener types. *J. Appl. Polym. Sci.* **2021**, *138*, 50239. [CrossRef]
130. Tran, T.-N.; Di Mauro, C.; Malburet, S.; Graillot, A.; Mija, A. Dual Cross-Linking of Epoxidized Linseed Oil with Combined Aliphatic/Aromatic Diacids Containing Dynamic S–S Bonds Generating Recyclable Thermosets. *ACS Appl. Bio Mater.* **2020**, *3*, 7550–7561. [CrossRef]
131. Altuna, F.I.; Espósito, L.H.; Ruseckaite, R.A.; Stefani, P.M. Thermal and mechanical properties of anhydride-cured epoxy resins with different contents of biobased epoxidized soybean oil. *J. Appl. Polym. Sci.* **2011**, *120*, 789–798. [CrossRef]
132. Bayrak, A.; Kiralan, M.; Ipek, A.; Arslan, N.; Cosge, B.; Khawar, K.M. Fatty Acid Compositions of Linseed (*Linum Usitatissimum*, L.) Genotypes of Different Origin Cultivated in Turkey. *Biotechnol. Biotechnol. Equip.* **2010**, *24*, 1836–1842. [CrossRef]
133. Clemente, T.E.; Cahoon, E.B. Soybean oil: Genetic approaches for modification of functionality and total content. *Plant Physiol.* **2009**, *151*, 1030–1040. [CrossRef] [PubMed]
134. Chen, Q. Development of an anthraquinone process for the production of hydrogen peroxide in a trickle bed reactor—From bench scale to industrial scale. *Chem. Eng. Process. Process Intensif.* **2008**, *47*, 787–792. [CrossRef]
135. Vogel, A. Anthraquinone. In *Ullmann's Encyclopedia of Industrial Chemistry*; Wiley-VCH Verlag GmbH & Co. KGaA: Weinheim, Germany, 2000. [CrossRef]
136. Igarashi, K.; Kashiwagi, K. Polyamine transport in bacteria and yeast. *Biochem. J.* **1999**, *344*, 633–642. [CrossRef] [PubMed]
137. Schneider, J.; Wendisch, V.F. Biotechnological production of polyamines by bacteria: Recent achievements and future perspectives. *Appl. Microbiol. Biotechnol.* **2011**, *91*, 17–30. [CrossRef] [PubMed]
138. Qin, J.; Krivoruchko, A.; Ji, B.; Chen, Y.; Kristensen, M.; Özdemir, E.; Keasling, J.D.; Jensen, M.K.; Nielsen, J. Engineering yeast metabolism for the discovery and production of polyamines and polyamine analogues. *Nat. Catal.* **2021**, *4*, 498–509. [CrossRef]
139. Ma, W.; Chen, K.; Li, Y.; Hao, N.; Wang, X.; Ouyang, P. Advances in Cadaverine Bacterial Production and Its Applications. *Proc. Est. Acad. Sci. Eng.* **2017**, *3*, 308–317. [CrossRef]
140. Mindt, M.; Walter, T.; Kugler, P.; Wendisch, V.F. Microbial Engineering for Production of N-Functionalized Amino Acids and Amines. *Biotechnol. J.* **2020**, *15*, e1900451. [CrossRef] [PubMed]
141. Ghasemlou, M.; Daver, F.; Ivanova, E.P.; Adhikari, B. Bio-based routes to synthesize cyclic carbonates and polyamines precursors of non-isocyanate polyurethanes: A review. *Eur. Polym. J.* **2019**, *118*, 668–684. [CrossRef]
142. Herndon, J.W. 1.06—Metathesis Reactions. In *Comprehensive Organometallic Chemistry II*; Mingos, D.M.P., Crabtree, R.H., Eds.; Elsevier: Oxford, UK, 2007; pp. 167–195. [CrossRef]
143. Fouilloux, H.; Thomas, C.M. Production and Polymerization of Biobased Acrylates and Analogs. *Macromol. Rapid Commun.* **2021**, *42*, e2000530. [CrossRef] [PubMed]
144. Makshina, E.V.; Canadell, J.; van Krieken, J.; Peeters, E.; Dusselier, M.; Sels, B.F. Bio-acrylates production: Recent catalytic advances and perspectives of the use of lactic acid and their derivatives. *ChemCatChem* **2019**, *11*, 180–201. [CrossRef]
145. Yang, J.; Xu, H.; Jiang, J.; Zhang, N.; Xie, J.; Wei, M.; Zhao, J. Production of Itaconic Acid through Microbiological Fermentation of Inexpensive Materials. *J. Bioresour. Bioprod.* **2019**, *4*, 135–142. [CrossRef]
146. Jiménez-Quero, A.; Pollet, E.; Avérous, L.; Phalip, V. Optimized Bioproduction of Itaconic and Fumaric Acids Based on Solid-State Fermentation of Lignocellulosic Biomass. *Molecules* **2020**, *25*, 1070. [CrossRef]
147. Chai, Y.; Zhao, Y.; Yan, N. Synthesis and Characterization of Biobased Melamine Formaldehyde Resins from Bark Extractives. *Ind. Eng. Chem. Res.* **2014**, *53*, 11228–11238. [CrossRef]
148. Nakata, K.; Ozaki, T.; Terashima, C. High-Yield Electrochemical Production of Formaldehyde from CO<sub>2</sub> and Seawater. *Angew. Chem. Int. Ed.* **2014**, *53*, 871–874. [CrossRef]
149. Ghafari, R.; DoostHosseini, K.; Abdulkhani, A.; Mirshokraie, S.A. Replacing formaldehyde by furfural in urea formaldehyde resin: Effect on formaldehyde emission and physical-mechanical properties of particleboards. *Eur. J. Wood Wood Prod.* **2016**, *74*, 609–616. [CrossRef]
150. Martínez-García, A.; Ortiz, M.; Martínez, R.; Ortiz, P.; Reguera, E. The condensation of furfural with urea. *Ind. Crops Prod.* **2004**, *19*, 99–106. [CrossRef]
151. BASF Increases Prices for Impregnating Resins in Europe. Available online: <https://www.basf.com/global/en/media/news-releases/2018/07/p-18-277.html> (accessed on 15 November 2021).
152. Perederic, O.A.; Mountraki, A.; Papadopoulou, E.; Woodley, J.M.; Kontogeorgis, G.M. Life Cycle Analysis of Phenol—Formaldehyde Resins Substituted with Lignin. In *Computer Aided Chemical Engineering*; Pierucci, S., Manenti, F., Bozzano, G.L., Manca, D., Eds.; Elsevier: Amsterdam, The Netherlands, 2020; pp. 607–612. [CrossRef]
153. Kamari, S.; Ghorbani, F. Extraction of highly pure silica from rice husk as an agricultural by-product and its application in the production of magnetic mesoporous silica MCM-41. *Biomass Convers. Biorefin.* **2021**, *11*, 3001–3009. [CrossRef]
154. Setyawan, N.; Hoerudin, H.; Wulanawati, A. Simple extraction of silica nanoparticles from rice husk using technical grade solvent: Effect of volume and concentration. *IOP Conf. Ser. Earth Environ. Sci.* **2019**, *309*, 012032. [CrossRef]

155. Research, Markets. Global Specialty Silicas Market Report 2019–2025—Precipitated Silica Is the Driving Force for Demand Growth Globally, Which Is Projected to Record a Robust CAGR of 6% between 2019 & 2025. 17 December 2019. Available online: <https://www.globenewswire.com/en/news-release/2019/12/17/1961796/28124/en/Global-Specialty-Silicas-Market-Report-2019-2025-Precipitated-Silica-is-the-Driving-Force-for-Demand-Growth-Globally-which-is-Projected-to-Record-a-Robust-CAGR-of-6-Between-2019-20.html> (accessed on 26 November 2021).
156. Top Countries Based on Production of Milled Rice. Available online: <https://www.statista.com/statistics/255945/top-countries-of-destination-for-us-rice-exports-2011/> (accessed on 30 November 2021).
157. Wang, B.; Yang, W.; McKittrick, J.; Meyers, M.A. Keratin: Structure, mechanical properties, occurrence in biological organisms, and efforts at bioinspiration. *Prog. Mater. Sci.* **2016**, *76*, 229–318. [CrossRef]
158. Kakkar, P.; Madhan, B.; Shanmugam, G. Extraction and characterization of keratin from bovine hoof: A potential material for biomedical applications. *Springerplus* **2014**, *3*, 596. [CrossRef] [PubMed]
159. Ashar, N.G. Chemical and Physical Properties of Sulphur Dioxide and Sulphur Trioxide. In *Advances in Sulphonation Techniques: Liquid Sulphur Dioxide as a Solvent of Sulphur Trioxide*; Ashar, N.G., Ed.; Springer International Publishing: Cham, Switzerland, 2016; pp. 9–19. [CrossRef]
160. Rebello, S.; Asok, A.K.; Mundayoor, S.; Jisha, M.S. Surfactants: Chemistry, Toxicity and Remediation. In *Pollutant Diseases, Remediation and Recycling*; Lichtfouse, E., Schwarzbauer, J., Robert, D., Eds.; Springer International Publishing: Cham, Switzerland, 2013; pp. 277–320. [CrossRef]
161. Bujak, T.; Nizioł-Lukaszewska, Z.; Wasilewski, T. Sodium Lauryl Sulfate vs. Sodium Coco Sulfate. Study of the Safety of Use Anionic Surfactants with Respect to Their Interaction with the Skin. *Tenside Surfactants Deterg.* **2019**, *56*, 126–133. [CrossRef]
162. Shah, M.S.; Tsapatsis, M.; Siepmann, J.I. Identifying Optimal Zeolitic Sorbents for Sweetening of Highly Sour Natural Gas. *Angew. Chem. Int. Ed.* **2016**, *55*, 5938–5942. [CrossRef]
163. Ohsawa, I.; Kanamori-Kataoka, M.; Tsuge, K.; Seto, Y. Determination of thiodiglycol, a mustard gas hydrolysis product by gas chromatography-mass spectrometry after tert-butyl-dimethylsilylation. *J. Chromatogr. A* **2004**, *1061*, 235–241. [CrossRef]
164. Cassoni, A.C.; Freixo, R.; Pintado, A.I.E.; Amorim, M.; Pereira, C.D.; Madureira, A.R.; Pintado, M.M.E. Novel Eco-Friendly Method to Extract Keratin from Hair. *ACS Sustain. Chem. Eng.* **2018**, *6*, 12268–12274. [CrossRef]
165. United States Environmental Protection Agency. Wood Products Industry. In *Compilation of Air Pollutant Emissions Factors (AP-42)*, 5th ed.; USEPA: Washington, DC, USA, 1995. Available online: <https://www3.epa.gov/ttnchie1/ap42/ch10/final/c10s02.pdf> (accessed on 22 December 2021).
166. Wang, X.; Li, H.; Cao, Y.; Tang, Q. Cellulose extraction from wood chip in an ionic liquid 1-allyl-3-methylimidazolium chloride (AmimCl). *Bioresour. Technol.* **2011**, *102*, 7959–7965. [CrossRef]
167. Zhu, S.; Wu, Y.; Chen, Q.; Yu, Z.; Wang, C.; Jin, S.; Ding, Y.; Wu, G. Dissolution of cellulose with ionic liquids and its application: A mini-review. *Green Chem.* **2006**, *8*, 325–327. [CrossRef]
168. Kilpeläinen, I.; Xie, H.; King, A.; Granstrom, M.; Heikkinen, S.; Argyropoulos, D.S. Dissolution of wood in ionic liquids. *J. Agric. Food Chem.* **2007**, *55*, 9142–9148. [CrossRef]
169. Fort, D.A.; Remsing, R.C.; Swatloski, R.P.; Moyna, P.; Moyna, G.; Rogers, R.D. Can ionic liquids dissolve wood? Processing and analysis of lignocellulosic materials with 1-n-butyl-3-methylimidazolium chloride. *Green Chem.* **2007**, *9*, 63–69. [CrossRef]
170. Sun, N.; Rahman, M.; Qin, Y.; Maxim, M.L.; Rodriguez, H.; Rogers, R.D. Complete dissolution and partial delignification of wood in the ionic liquid 1-ethyl-3-methylimidazolium acetate. *Green Chem.* **2009**, *11*, 646–655. [CrossRef]
171. Zavrel, M.; Bross, D.; Funke, M.; Büchs, J.; Spiess, A.C. High-throughput screening for ionic liquids dissolving (ligno-)cellulose. *Bioresour. Technol.* **2009**, *100*, 2580–2587. [CrossRef] [PubMed]
172. Zhang, H.; Wu, J.; Zhang, J.; He, J. 1-Allyl-3-methylimidazolium Chloride Room Temperature Ionic Liquid: A New and Powerful Nonderivatizing Solvent for Cellulose. *Macromolecules* **2005**, *38*, 8272–8277. [CrossRef]
173. Abushammala, H.; Mao, J. A Review on the Partial and Complete Dissolution and Fractionation of Wood and Lignocelluloses Using Imidazolium Ionic Liquids. *Polymers* **2020**, *12*, 195. [CrossRef] [PubMed]
174. Berglund, L.; Anugwom, I.; Hedenström, M.; Aitomäki, Y.; Mikkola, J.-P.; Oksman, K. Switchable ionic liquids enable efficient nanofibrillation of wood pulp. *Cellulose* **2017**, *24*, 3265–3279. [CrossRef]
175. Zhong, C. Industrial-Scale Production and Applications of Bacterial Cellulose. *Front. Bioeng. Biotechnol.* **2020**, *8*, 605374. [CrossRef] [PubMed]
176. Chen, H.-H.; Chen, L.-C.; Huang, H.-C.; Lin, S.-B. In situ modification of bacterial cellulose nanostructure by adding CMC during the growth of *Gluconacetobacter xylinus*. *Cellulose* **2011**, *18*, 1573–1583. [CrossRef]
177. Moniri, M.; Boroumand Moghaddam, A.; Azizi, S.; Abdul Rahim, R.; Bin Ariff, A.; Zuhainis Saad, W.; Navaderi, M.; Mohamad, R. Production and Status of Bacterial Cellulose in Biomedical Engineering. *Nanomaterials* **2017**, *7*, 257. [CrossRef]
178. Portela, R.; Leal, C.R.; Almeida, P.L.; Sobral, R.G. Bacterial cellulose: A versatile biopolymer for wound dressing applications. *Microb. Biotechnol.* **2019**, *12*, 586–610. [CrossRef] [PubMed]
179. Czaja, W.K.; Young, D.J.; Kawecky, M.; Brown, R.M., Jr. The future prospects of microbial cellulose in biomedical applications. *Biomacromolecules* **2007**, *8*, 1–12. [CrossRef]
180. Keshk, S.M.A.S. Bacterial Cellulose Production and Its Industrial Applications. *J. Bioprocess Biotech.* **2014**, *4*, 100150. [CrossRef]
181. Ullah, M.W.; Ul-Islam, M.; Khan, S.; Kim, Y.; Park, J.K. Innovative production of bio-cellulose using a cell-free system derived from a single cell line. *Carbohydr. Polym.* **2015**, *132*, 286–294. [CrossRef] [PubMed]

182. Kim, Y.; Ullah, M.W.; Ul-Islam, M.; Khan, S.; Jang, J.H.; Park, J.K. Self-assembly of bio-cellulose nanofibrils through intermediate phase in a cell-free enzyme system. *Biochem. Eng. J.* **2019**, *142*, 135–144. [CrossRef]
183. Antonelli, F.; Galotta, G.; Sidoti, G.; Zikeli, F.; Nisi, R.; Davidde Petriaggi, B.; Romagnoli, M. Cellulose and Lignin Nano-Scale Consolidants for Waterlogged Archaeological Wood. *Front. Chem.* **2020**, *8*, 32. [CrossRef] [PubMed]
184. Younes, I.; Rinaudo, M. Chitin and chitosan preparation from marine sources. Structure, properties and applications. *Mar. Drugs* **2015**, *13*, 1133–1174. [CrossRef]
185. Ospina Álvarez, S.P.; Ramírez Cadavid, D.A.; Escobar Sierra, D.M.; Ossa Orozco, C.P.; Rojas Vahos, D.F.; Zapata Ocampo, P.; Atehortúa, L. Comparison of Extraction Methods of Chitin from *Ganoderma lucidum* Mushroom Obtained in Submerged Culture. *BioMed Res. Int.* **2014**, *2014*, 169071. [CrossRef]
186. El Knidri, H.; Belaabed, R.; Addaou, A.; Laajeb, A.; Lahsini, A. Extraction, chemical modification and characterization of chitin and chitosan. *Int. J. Biol. Macromol.* **2018**, *120*, 1181–1189. [CrossRef] [PubMed]
187. Rakshit, S.; Mondal, S.; Pal, K.; Jana, A.; Soren, J.P.; Barman, P.; Mondal, K.C.; Halder, S.K. Extraction of chitin from *Litopenaeus vannamei* shell and its subsequent characterization: An approach of waste valorization through microbial bioprocessing. *Bioprocess Biosyst. Eng.* **2021**, *44*, 1943–1956. [CrossRef]
188. Hajji, S.; Ghorbel-Bellaaj, O.; Younes, I.; Jellouli, K.; Nasri, M. Chitin extraction from crab shells by *Bacillus* bacteria. Biological activities of fermented crab supernatants. *Int. J. Biol. Macromol.* **2015**, *79*, 167–173. [CrossRef] [PubMed]
189. Tan, Y.N.; Lee, P.P.; Chen, W.N. Microbial extraction of chitin from seafood waste using sugars derived from fruit waste-stream. *AMB Express* **2020**, *10*, 17. [CrossRef]
190. Harkin, C.; Brück, W.M.; Lynch, C. Isolation & identification of bacteria for the treatment of brown crab (*Cancer pagurus*) waste to produce chitinous material. *J. Appl. Microbiol.* **2015**, *118*, 954–965. [CrossRef] [PubMed]
191. Aytekin, O.; Elibol, M. Cocultivation of *Lactococcus lactis* and *Teredinobacter turnirae* for biological chitin extraction from prawn waste. *Bioprocess Biosyst. Eng.* **2010**, *33*, 393–399. [CrossRef]
192. Liu, P.; Liu, S.; Guo, N.; Mao, X.; Lin, H.; Xue, C.; Wei, D. Cofermentation of *Bacillus licheniformis* and *Gluconobacter oxydans* for chitin extraction from shrimp waste. *Biochem. Eng. J.* **2014**, *91*, 10–15. [CrossRef]
193. Bajpai, P. Wood-Based Products and Chemicals. In *Biermann's Handbook of Pulp and Paper*, 3rd ed.; Bajpai, P., Ed.; Elsevier: Amsterdam, The Netherlands, 2018; Chapter 8; pp. 233–247. [CrossRef]
194. Lobato-Peralta, D.R.; Duque-Brito, E.; Vidales, H.I.V.; Longoria, A.; Sebastian, P.J.; Cuentas-Gallegos, A.K.; Arancibia-Bulnes, C.A.; Okoye, P.U. A review on trends in lignin extraction and valorization of lignocellulosic biomass for energy applications. *J. Clean. Prod.* **2021**, *293*, 126123. [CrossRef]
195. Laurichesse, S.; Avérous, L. Chemical modification of lignins: Towards biobased polymers. *Prog. Polym. Sci.* **2014**, *39*, 1266–1290. [CrossRef]
196. Vishtal, A.G.; Kraslawski, A. Challenges in industrial applications of technical lignins. *BioResources* **2011**, *6*, 3547–3568. [CrossRef]
197. Florian, T.D.M.; Villani, N.; Aguedo, M.; Jacquet, N.; Thomas, H.G.; Gerin, P.; Magali, D.; Richel, A. Chemical composition analysis and structural features of banana rachis lignin extracted by two organosolv methods. *Ind. Crops Prod.* **2019**, *132*, 269–274. [CrossRef]
198. Watkins, D.; Nuruddin Hosur, M.; Tcherbi-Narteh, A.; Jeelani, S. Extraction and characterization of lignin from different biomass resources. *J. Mater. Res. Technol.* **2015**, *4*, 26–32. [CrossRef]
199. Michelin, M.; Liebenritt, S.; Vicente, A.A.; Teixeira, J.A. Lignin from an integrated process consisting of liquid hot water and ethanol organosolv: Physicochemical and antioxidant properties. *Int. J. Biol. Macromol.* **2018**, *120*, 159–169. [CrossRef] [PubMed]
200. Zikeli, F.; Vinciguerra, V.; Taddei, A.R.; D'Annibale, A.; Romagnoli, M.; Mugnozza, G.S. Isolation and characterization of lignin from beech wood and chestnut sawdust for the preparation of lignin nanoparticles (LNPs) from wood industry side-streams. *Holzforschung* **2018**, *72*, 961–972. [CrossRef]
201. Ding, X.; Richter, D.L.; Matuana, L.M.; Heiden, P.A. Efficient one-pot synthesis and loading of self-assembled amphiphilic chitosan nanoparticles for low-leaching wood preservation. *Carbohydr. Polym.* **2011**, *86*, 58–64. [CrossRef]
202. Kashyap, P.L.; Xiang, X.; Heiden, P. Chitosan nanoparticle based delivery systems for sustainable agriculture. *Int. J. Biol. Macromol.* **2015**, *77*, 36–51. [CrossRef]
203. Ela, R.C.A.; Tajiri, M.; Newberry, N.K.; Heiden, P.A.; Ong, R.G. Double-Shell Lignin Nanocapsules Are a Stable Vehicle for Fungicide Encapsulation and Release. *ACS Sustain. Chem. Eng.* **2020**, *8*, 18730–18731.
204. Machado, T.O.; Beckers, S.J.; Fischer, J.; Müller, B.; Sayer, C.; de Araújo, P.H.; Landfester, K.; Wurm, F.R. Bio-Based Lignin Nanocarriers Loaded with Fungicides as a Versatile Platform for Drug Delivery in Plants. *Biomacromolecules* **2020**, *21*, 2755–2763. [CrossRef] [PubMed]
205. Yiamsawas, D.; Beckers, S.J.; Lu, H.; Landfester, K.; Wurm, F.R. Morphology-Controlled Synthesis of Lignin Nanocarriers for Drug Delivery and Carbon Materials. *ACS Biomater. Sci. Eng.* **2017**, *3*, 2375–2383. [CrossRef]
206. Chen, N.; Dempere, L.A.; Tong, Z. Synthesis of pH-Responsive Lignin-Based Nanocapsules for Controlled Release of Hydrophobic Molecules. *ACS Sustain. Chem. Eng.* **2016**, *4*, 5204–5211. [CrossRef]
207. Baglioni, P.; Chelazzi, D.; Giorgi, R. Deacidification of Paper, Canvas and Wood. In *Nanotechnologies in the Conservation of Cultural Heritage: A Compendium of Materials and Techniques*; Baglioni, P., Chelazzi, D., Giorgi, R., Eds.; Springer: Dordrecht, The Netherlands, 2015; pp. 117–144. [CrossRef]

208. Haw, T.T.; Hart, F.; Rashidi, A.; Pasbakhsh, P. Sustainable cementitious composites reinforced with metakaolin and halloysite nanotubes for construction and building applications. *Appl. Clay Sci.* **2020**, *188*, 105533. [CrossRef]
209. Cavallaro, G.; Lazzara, G.; Milioto, S.; Parisi, F.; Sparacino, V. Thermal and dynamic mechanical properties of beeswax-halloysite nanocomposites for consolidating waterlogged archaeological woods. *Polym. Degrad. Stab.* **2015**, *120*, 220–225. [CrossRef]
210. Cavallaro, G.; Lazzara, G.; Milioto, S.; Parisi, F.; Ruisi, F. Nanocomposites based on esterified colophony and halloysite clay nanotubes as consolidants for waterlogged archaeological woods. *Cellulose* **2017**, *24*, 3367–3376. [CrossRef]
211. Cavallaro, G.; Lazzara, G.; Parisi, F.; Riela, S. Nanoclays for Conservation and Nanomaterials. In *Nanotechnologies and Nanomaterials for Diagnostic, Conservation and Restoration of Cultural Heritage*; Lazzara, G., Fakhruddin, R., Eds.; Elsevier: Amsterdam, The Netherlands, 2019; pp. 149–170. [CrossRef]
212. Infurna, G.; Cavallaro, G.; Lazzara, G.; Milioto, S.; Dintcheva, N.T. Bionanocomposite Films Containing Halloysite Nanotubes and Natural Antioxidants with Enhanced Performance and Durability as Promising Materials for Cultural Heritage Protection. *Polymers* **2020**, *12*, 1973. [CrossRef] [PubMed]
213. Lisuzzo, L.; Hueckel, T.; Cavallaro, G.; Sacanna, S.; Lazzara, G. Pickering Emulsions Based on Wax and Halloysite Nanotubes: An Ecofriendly Protocol for the Treatment of Archeological Woods. *ACS Appl. Mater. Interfaces* **2021**, *13*, 1651–1661. [CrossRef]
214. Bettina, G.F.; Giambra, B.; Cavallaro, G.; Lazzara, G. Restoration of a XVII Century's predella reliquary: From Physico-Chemical Characterization to the Conservation Process. *Forests* **2021**, *12*, 345. [CrossRef]
215. Cavallaro, G.; Milioto, S.; Lazzara, G. Halloysite Nanotubes: Interfacial Properties and Applications in Cultural Heritage. *Langmuir* **2020**, *36*, 3677–3689. [CrossRef] [PubMed]
216. Lisuzzo, L.; Cavallaro, G.; Milioto, S.; Lazzara, G. Halloysite nanotubes filled with salicylic acid and sodium diclofenac: Effects of vacuum pumping on loading and release properties. *J. Nanostruct. Chem.* **2021**, *11*, 663–673. [CrossRef]
217. Lisuzzo, L.; Cavallaro, G.; Milioto, S.; Lazzara, G. Halloysite Nanotubes Coated by Chitosan for the Controlled Release of Khellin. *Polymers* **2020**, *12*, 1766. [CrossRef]
218. Dзамukova, M.R.; Naumenko, E.A.; Lvov, Y.M.; Fakhruddin, R.F. Enzyme-activated intracellular drug delivery with tubule clay nanoformulation. *Sci. Rep.* **2015**, *5*, 1–11. [CrossRef]
219. Vikulina, A.; Voronin, D.; Fakhruddin, R.; Vinokurov, V.; Volodkin, D. Naturally derived nano- and micro-drug delivery vehicles: Halloysite, vaterite and nanocellulose. *New J. Chem.* **2020**, *44*, 5638–5655. [CrossRef]
220. Sun, L.; Mills, D.K. Halloysite nanotube-based drug delivery system for treating osteosarcoma. *Conf. Proc. IEEE Eng. Med. Biol. Soc.* **2014**, *2014*, 2920–2923. [CrossRef]
221. Walsh, Z.; Janeček, E.R.; Hodgkinson, J.T.; Sedlmair, J.; Koutsoubas, A.; Spring, D.R.; Welch, M.; Hirschmugl, C.J.; Toprakcioglu, C.; Nitschke, J.R.; et al. Multifunctional supramolecular polymer networks as next-generation consolidants for archaeological wood conservation. *Proc. Natl. Acad. Sci. USA* **2014**, *111*, 17743–17748. [CrossRef]
222. Castro-López, C.; Contreras-Esquivel, J.C.; Martínez-Avila, G.C.; Rojas, R.; Boone-Villa, D.; Aguilar, C.N.; Ventura-Sobrevilla, J.M. Guar gum as a promising hydrocolloid: Properties and industry overview. In *Applied Chemistry and Chemical Engineering*; Apple Academic Press: Cambridge, MA, USA, 2017; pp. 183–205. [CrossRef]
223. Colombini, M.P.; Lucejko, J.J.; Modugno, F.; Orlandi, M.; Tolppa, E.-L.; Zoia, L. A multi-analytical study of degradation of lignin in archaeological waterlogged wood. *Talanta* **2009**, *80*, 61–70. [CrossRef] [PubMed]
224. McHale, E.; Braovac, S.; Steindal, C.C.; Gillis, R.B. Synthesis and characterisation of lignin-like oligomers as a bio-inspired consolidant for waterlogged archaeological wood. *Pure Appl.* **2016**, *88*, 969–977. [CrossRef]
225. Khalil, A.A.; Rahman, U.; Khan, M.R.; Sahar, A.; Mehmood, T.; Khan, M. Essential oil eugenol: Sources, extraction techniques and nutraceutical perspectives. *RSC Adv.* **2017**, *7*, 32669–32681. [CrossRef]
226. McHale, E.; Steindal, C.C.; Kutzke, H.; Benneche, T.; Harding, S.E. In situ polymerisation of isoeugenol as a green consolidation method for waterlogged archaeological wood. *Sci. Rep.* **2017**, *7*, 46481. [CrossRef] [PubMed]
227. Cutajar, M.; Andriulo, F.; Thomsett, M.R.; Moore, J.C.; Couturaud, B.; Howdle, S.M.; Stockman, R.A.; Harding, S.E. Terpene polyacrylate TPA5 shows favorable molecular hydrodynamic properties as a potential bioinspired archaeological wood consolidant. *Sci. Rep.* **2021**, *11*, 7343. [CrossRef]
228. Adamová, T.; Hradecký, J.; Pánek, M. Volatile Organic Compounds (VOCs) from Wood and Wood-Based Panels: Methods for Evaluation, Potential Health Risks, and Mitigation. *Polymers* **2020**, *12*, 2289. [CrossRef] [PubMed]
229. ReSolve Project Developed Bio-Based Alternatives to Replace Toxic Solvents Used in the Chemical Industry. Available online: <https://www.bbi.europa.eu/resolve-project-developed-bio-based-alternatives-replace-toxic-solvents-used-chemical-industry> (accessed on 30 November 2021).



## Article

# Structural Monitoring of a Large Archaeological Wooden Structure in Real Time, Post PEG Treatment

Hugh Collett <sup>1,\*</sup> , Florian Bouville <sup>1</sup>, Finn Giuliani <sup>1</sup> and Eleanor Schofield <sup>2,\*</sup>

<sup>1</sup> Department of Materials Science & Engineering, Imperial College London, Kensington, London SW7 2AZ, UK; f.bouville@imperial.ac.uk (F.B.); f.giuliani@imperial.ac.uk (F.G.)

<sup>2</sup> Mary Rose Trust, College Road, HM Naval Base, Portsmouth PO1 3LX, UK

\* Correspondence: h.collett19@imperial.ac.uk (H.C.); e.schofield@maryrose.org (E.S.)

**Abstract:** Large archaeological wooden structures are potentially at risk of structural failure through deformation and cracking over time if they are left untreated and their structural health is not maintained. This could be in part due to, for example, the shrinkage of waterlogged wood as it dries, or time-dependent creep processes. These dimensional changes are accompanied by associated stresses. However, there are few studies analysing the movement of large wooden structures in real time as they dry, particularly after their conservation treatment. This paper follows the structural monitoring of the *Mary Rose* from after the conservation treatment, where it was sprayed with polyethylene glycol, through to the ship's air-drying process and beyond to assess the effects that drying has had on the displacement of the timbers. A laser-based target system was used to collect displacement data between 2013 and 2020 and the data showed a significant slowing of displacement as the drying reached an equilibrium.

**Keywords:** archaeological wooden structures; structural analysis; geodetic systems; drying process; polyethylene glycol



**Citation:** Collett, H.; Bouville, F.; Giuliani, F.; Schofield, E. Structural Monitoring of a Large Archaeological Wooden Structure in Real Time, Post PEG Treatment. *Forests* **2021**, *12*, 1788. <https://doi.org/10.3390/f12121788>

Academic Editors: Magdalena Broda and Callum A. S. Hill

Received: 19 October 2021

Accepted: 9 December 2021

Published: 16 December 2021

**Publisher's Note:** MDPI stays neutral with regard to jurisdictional claims in published maps and institutional affiliations.



**Copyright:** © 2021 by the authors. Licensee MDPI, Basel, Switzerland. This article is an open access article distributed under the terms and conditions of the Creative Commons Attribution (CC BY) license (<https://creativecommons.org/licenses/by/4.0/>).

## 1. Introduction

Wood has been used as material for building, furniture and ship construction for thousands of years [1–3]. The fact that it is still one of the most widely used building materials is a testament to its suitability and abundance. As a result, there are examples of extant large archaeological wooden structures that we have been able to rediscover/preserve centuries later. Some of these have been discovered underwater, trapped in soil or silt that prevented their degradation over the years [4].

Evaluating the properties and predicting the dimensional change and movement during the drying of large archaeological wooden structures is very challenging for a number of reasons. Firstly, the properties of archaeological wood depend on multiple conditions, including age, wood species, use and the conditions the artefact has been buried in. Large structures may also be composed of wood from several different trees. Secondly, wood is an anisotropic and heterogeneous material [5]. Properties vary within the same piece and with different orientations. The properties of wood and its response to load vary over time and are dependent on the amount of degradation and any changes in moisture content [6]. Finally, to ensure the long-term stability of the structure, a conservation process is generally carried out. This aims to compensate for lost material, achieve dimensional stability and reduce shrinkage of the marine archaeological wood during drying. This process alters the chemical composition and mechanical properties of the wood, adding to the complexity of understanding it.

Previous research studies provide us with an understanding of how changes in moisture content affect the properties and dimensions of large archaeological wooden structures [7,8]. However, there are very few studies into the structural changes that occur in large archaeological wooden objects in real time as they reach their drying equilibrium.



Wood is hygroscopic and the moisture content of archaeological oak can be as high as approximately 700%, with the loss of wood substance as high as approximately 80%, a key indicator of degradation [9]. The moisture content of wood is defined as the ratio of the total mass of moisture within the wood to the mass of the dry wood, and hence moisture contents of wood that are greater than 100% are possible. After removal from the burial site, the migration of moisture during drying can thus cause severe dimensional changes [10]. In anaerobic conditions, wood can survive for thousands of years due to limited degradation because of the reduced development of decay fungi [11]. Once extracted, however, these structures need to be dried, which, if not performed properly, can lead to cracking due to the shrinkage associated with the removal of water, and the voids created by degradation [12].

There are several different methods for stabilising recovered waterlogged archaeological wooden objects [13]. Older, obsolete treatments, such as the application of alum salts, suffer from severe deterioration [14]. Polyethylene glycol (PEG) impregnation is still the most common treatment for conserving waterlogged archaeological wood. The advantages of PEG are its low cost and straightforward methodology [15]. However, we do now know that PEG can cause issues for the wood, e.g., acid production and creep [16].

An important example of a PEG-treated, large archaeological wooden ship is the *Mary Rose*, which will be the focus of this study. The *Mary Rose* is the oldest extant Tudor warship and was the flagship of Henry VIII's fleet. The ship was sunk in 1545 and raised from the seabed 437 years later in 1982. Between 1994 and 2004 the ship was sprayed with low molecular PEG 200, which was administered in an aqueous solution with concentration levels of up to 40%. The PEG concentration was increased incrementally in 5–10% increments. From 2004 until April 2013, the ship was sprayed with higher concentrations of high molecular PEG 2000. Immediately after spraying was completed, the ship's environment was controlled at 50–58% relative humidity with temperatures of 18–20 °C, which has been kept consistent ever since [17]. The moisture content of sections of the ship has been determined using the gravimetric method since the spraying was ceased. The analysis has shown that the ship is now predominantly dry and that only limited movement due to drying should now be occurring [18]. Moisture content studies have been carried out since the onset of drying, but, due to the high variability of wood, there is corresponding variability in the moisture content value as a function of depth and location around the hull. However, in 2016, the surface in all of the locations studied on the ship was found to have a moisture content below 15%, and core samples displayed a MC% of between 10–20% [18]. It was therefore at this point determined to be predominantly dry, with only minimal moisture left to migrate out.

As discussed, large archaeological wooden structures, such as the *Mary Rose*, are complex to monitor and understand. While shrinkage in the direction of the growth ring is generally limited to 7–8% in recent wood, it can be around 60% in deteriorated archaeological wood [19]. This is compounded by the difference in drying shrinkage associated with different species and orientations, and it is complicated to assess the health of large wooden structures and predict changes in their structural integrity. It is, however, possible to measure the displacement and distortion of these large wooden structures in real time during drying to better understand the drying process. The monitoring should also alert the conservator to any major changes that need swift intervention. Non-contact geodetic measurements, such as theodolites, photogrammetry and terrestrial laser scanners, have all been used extensively in cultural heritage [20–22]. Many constraints limit the scanning systems that can be used to obtain the three-dimensional coordinates of the structure in question. These include the size and shape of the object, the surface material of the object (e.g., reflectance) and the cost, ease of use, etc. [23].

This paper analyses the displacement undergone by the *Mary Rose* shipwreck during conservation and the procedure undertaken to collect geodetic measurements of this large wooden structure. As a result of the anaerobic environment of the seabed, the ship remained in good condition. The conservation treatment consisted of spraying with

two molecular weights of polyethylene glycol (PEG) before undergoing a controlled air-drying procedure [24]. The PEG conservation treatment was similar to the treatment of the *Vasa* shipwreck, however there was limited real-time/live monitoring of displacement throughout the *Vasa* drying process [25]. From the geodetic measurements collected continuously over the years, the aim of this study is to analyse the changes in displacement and displacement rate over the years 2013–2020 to identify any major structural changes in the timbers and to provide a greater understanding of the drying process of large wooden structures that are impregnated with PEG. While the displacement analysis will help to identify any immediate and long-term concerns regarding the structural stability of the *Mary Rose*, the findings and methodology will also be applicable to other similar large wooden structures worldwide.

## 2. Methods and Measuring Systems

The methods section briefly summarises the systems used to monitor displacement at points on the *Mary Rose*'s hull by comparing current positions with a reference point.

A total station (TS), Leica NOVA TS50, Germany, was installed in September 2013 (approximately 4 months after drying commenced) to observe the global and local movements of the ship. The geodetic monitoring system, with an accuracy of 0.6 mm in distance measurements and  $0.0001^\circ$  in angle measurement, is located on the port side. The total station recorded the position of targets on the ship at 08:00, 16:00 and 00:00 every day since late 2013. However, there are some gaps in recordings due to conservation work on the ship during this time.

Total stations work according to the phase-shift principle. A signal is sent from the total station towards the targets and the phase of the returning signal is compared to the phase of the emitted signal. The electromagnetic signals are fired at targets of cooperative materials. A typical total station is able to measure distances of up to 1500 m with an accuracy of 1.5 mm [26]. The total station data are obtained from the machine automatically as X, Y and Z coordinates, and have been processed in Python using a Jupyter Notebook.

The data were processed as follows:

- Errors in the total station data, such as a sudden and constant shift in the Z direction data of more than 10 mm that was stable over a long period of time, were removed. The source of this shift has not been conclusively proven, but is likely to be a hardware error since the recording returned to normal after some time and the oscillation desisted of its own accord.
- For the total displacement plots, a scatter graph was plotted showing the total displacement against time for each target in each direction.
- For the displacement rate plots, a curve of best fit was plotted on each target's dataset. The fitted curve was then differentiated to find the rate of change.

In total there are 35 targets on the ship that are scanned by the total station (c.f., Figure 1) and the name of each target was chosen as follows. The first number increases moving from bow to stern. The second number describes which deck the target is located on: 01 indicates the target is on the orlop deck, 02 indicates the main deck, 03 the upper deck and 04 the castle deck. Taking the target labelled 01.01 as an example, the first 01 denotes that the target is the closest to the bow on that deck. The second 01 indicates that the target is located on the orlop deck.

The X direction is positive from stern to bow. The Y direction is positive from port to starboard and the Z direction is positive from the ground up.

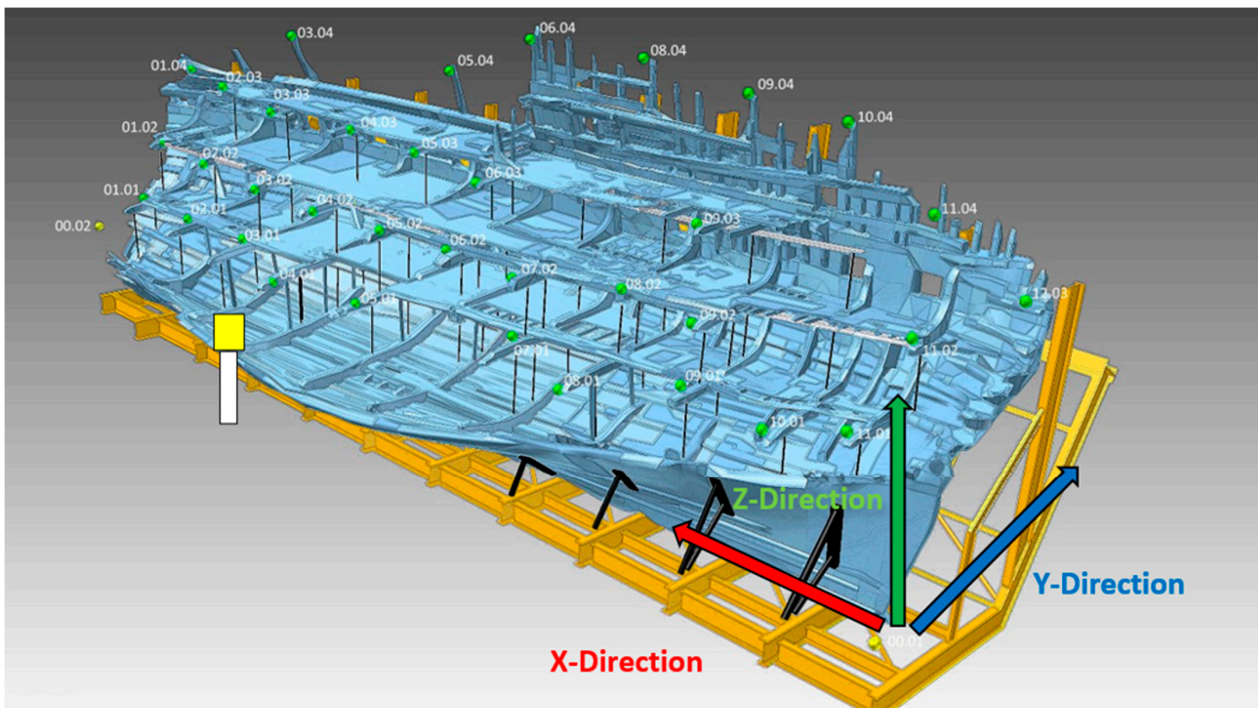


**Figure 1.** Schematic of the *Mary Rose* showing the location of the laser targets on the ship and the laser scanner.

### 3. Results and Discussion

#### 3.1. Total Displacement of the TS Targets in the X, Y and Z Directions Respresented on the Ship

The position of each target on the ship and the displacement measured from the September 2013 to March 2020 is shown in Figure 2. The green arrows are proportional to the displacement's magnitude in the Z direction, the blue arrows the Y direction and the red arrows the X direction. One conclusion that can be drawn from this Figure is that the displacement increases moving higher up the ship. For instance, the average X, Y and Z displacement in the orlop deck is 60 mm, 20 mm and 40 mm, respectively, whereas, in the castle deck the values are 55 mm, 140 mm and 180 mm, respectively.

Focusing on the Z direction, the whole ship experienced downward displacement, as would be expected. The Z displacement is around 1.3, 2.2 and 4.3 times larger on average in the castle deck than in the upper, main, and orlop decks, respectively. This is the effect of the cumulative deformation of the decks below. In addition, the castle deck has the least support and the targets are attached to more independent sections of wood, as opposed to the beams in the lower sections that are more interconnected with the original ship structure and which had subsequent supports installed.

The displacement along the Y direction is predominantly from starboard to port throughout, i.e., negative. In contrast, the displacement along the X direction switches on alternate decks, creating a shear-like movement. The largest displacements in any one direction are approximately 250 mm. These occurred in the castle deck in the Y and Z directions and only in two targets.

#### 3.2. Cumulative Displacement of the TS Targets in the X, Y and Z Directions over the Time Period (2013–2020)

By looking at the displacement of each deck separately over time, we found that the movement of the majority of the positions was slowing down over time, independent of direction. Figure 3 displays the displacement along the X direction over time between September 2013 (Year 0) and March 2020 (Year 6.5). The few positions where the rate of displacement was near constant over the time period of September 2013–March 2020 were displacing at a slow rate.

**Total Station and Displacement Targets:**

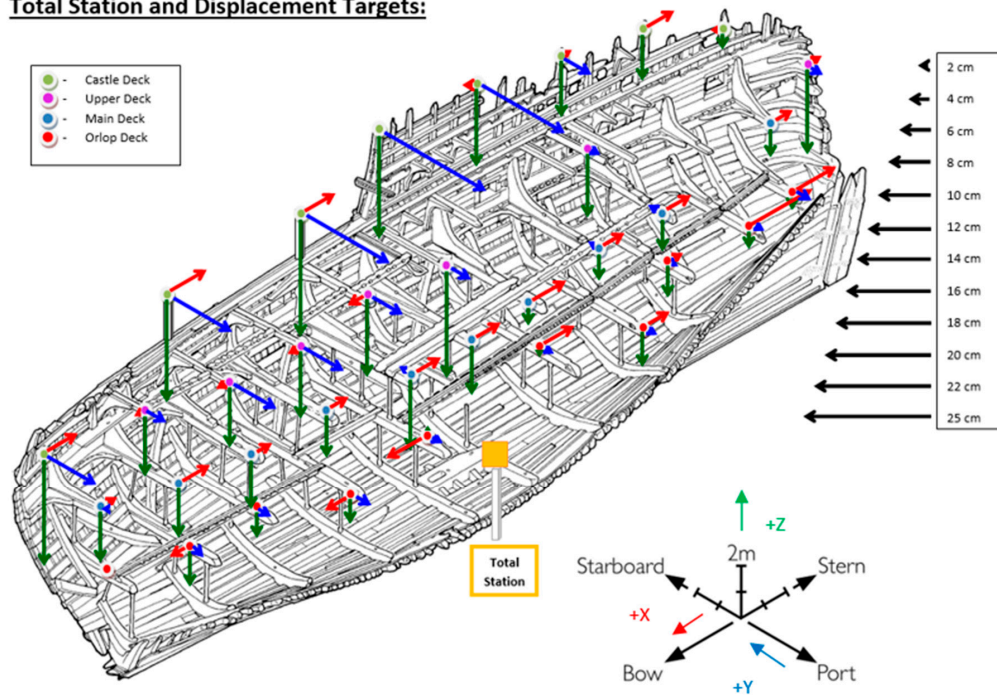


**Figure 2.** Shows the total displacement of the targets between 2013 and 2020 in the X (red arrows), Y (blue arrows) and Z (green arrows) directions. The scale bar on the right is a reference for the magnitude of the displacements.

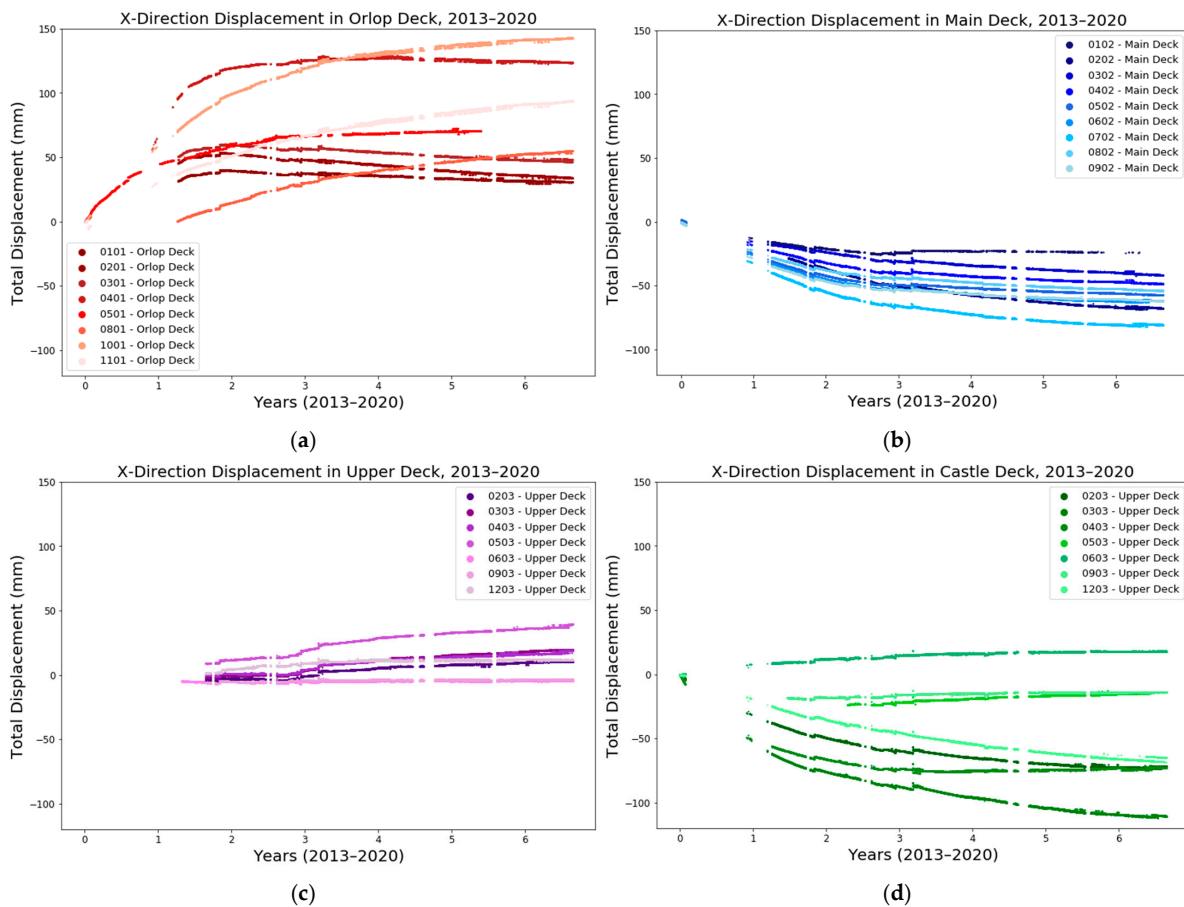


**Figure 3.** X direction displacement of the TS targets in the (a) orlop, (b) main, (c) upper and (d) castle decks plotted against time for the period between September 2013 and March 2020.

The displacement along the X direction in the ship experienced a concertina motion as the direction of the displacement flipped between each deck. The direction of displacement in the X direction is consistent across each deck, with an average of  $+60 \pm 40$  mm for the orlop deck,  $+20 \pm 9$  mm for the upper deck,  $-60 \pm 20$  mm for the main deck and  $-60 \pm 30$  mm for the castle deck. The orlop deck and the castle deck have displaced further than the main and upper decks. This is potentially because the orlop deck does not have the titanium support beams that the other decks have, and the castle level is the least interconnected.

Displacement in the Y direction is shown in Figure 4. The displacement along Y averaged at approximately  $-20 \pm 10$  mm in the orlop deck,  $+10 \pm 10$  mm in the main deck,  $-60 \pm 30$  mm in the upper deck and  $-150 \pm 80$  mm in the castle deck. The target with the greatest displacement between 2013 and 2020 is the 06.04 target, towards the centre of the castle deck, which has displaced by 250 mm.

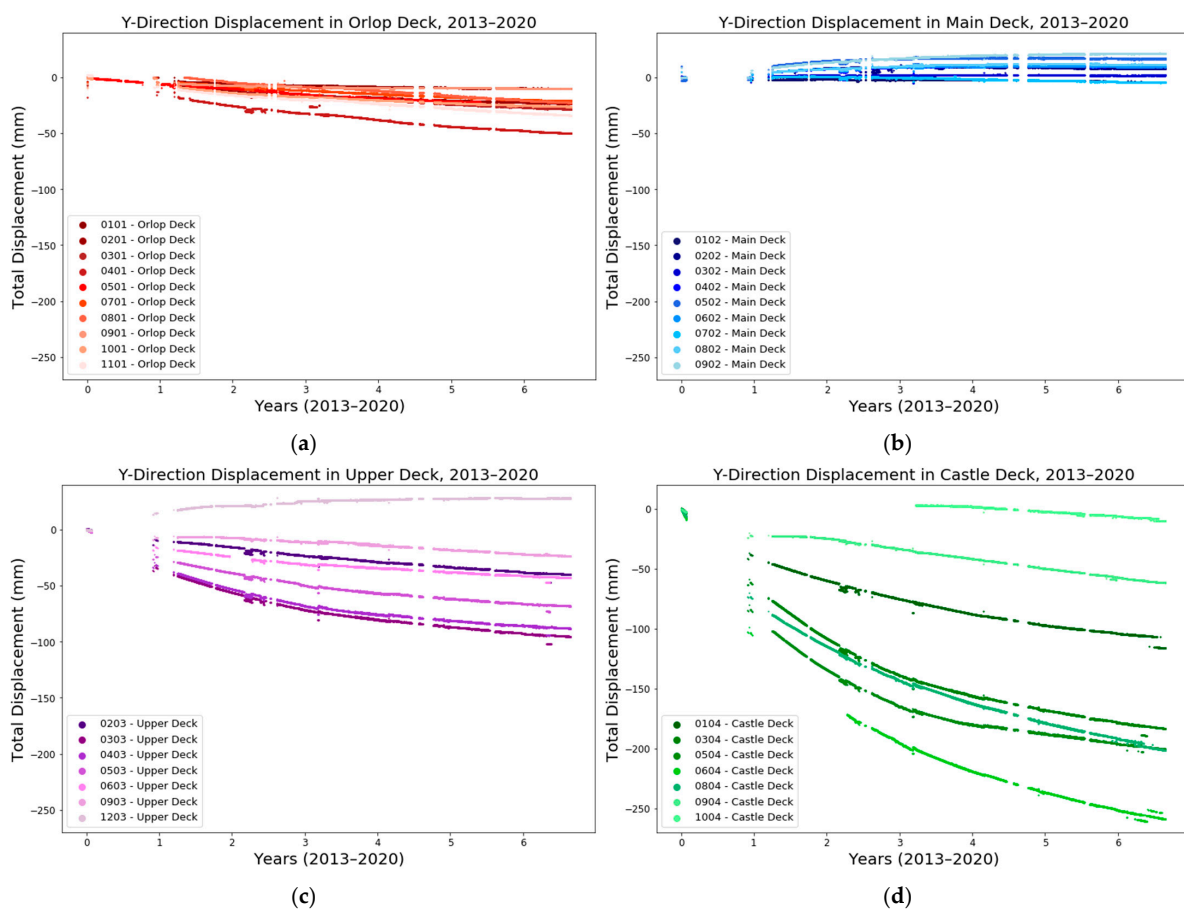


**Figure 4.** Y direction displacement of the TS targets in the (a) orlop, (b) main, (c) upper and (d) castle decks plotted against time for the period between September 2013 and March 2020.

Similarly to the displacement along the X direction, some targets display negative Y displacement and some positive, i.e., some targets were displaced from starboard to port and others port to starboard (c.f., Figure 2). This could create a shearing motion in the ship, although the majority of Y displacement is from starboard to port. In total, 26 of the targets moved in the negative Y direction and eight in the positive direction. The sum of total negative displacement of all the targets in the Y direction is 1500 mm, whereas the total movement in the positive Y direction, i.e., from port to starboard, is 170 mm. The targets were displaced far more from starboard to port than port to starboard.

Comparisons across the four decks in Figure 5 show that the total displacement in the Z direction increased in each higher deck. The average displacement in the Z direction

in the orlop deck was  $-40 \pm 20$  mm, in the main deck it was  $-90 \pm 30$  mm, in the upper deck it was  $-150 \pm 30$  mm and in the castle deck it was  $-190 \pm 50$  mm. The greatest total displacement of 260 mm occurred in the castle deck. This means that the 05.04 target, which is around halfway along the castle deck of the ship (c.f., Figure 2), has displaced more than any other target in the Z direction.

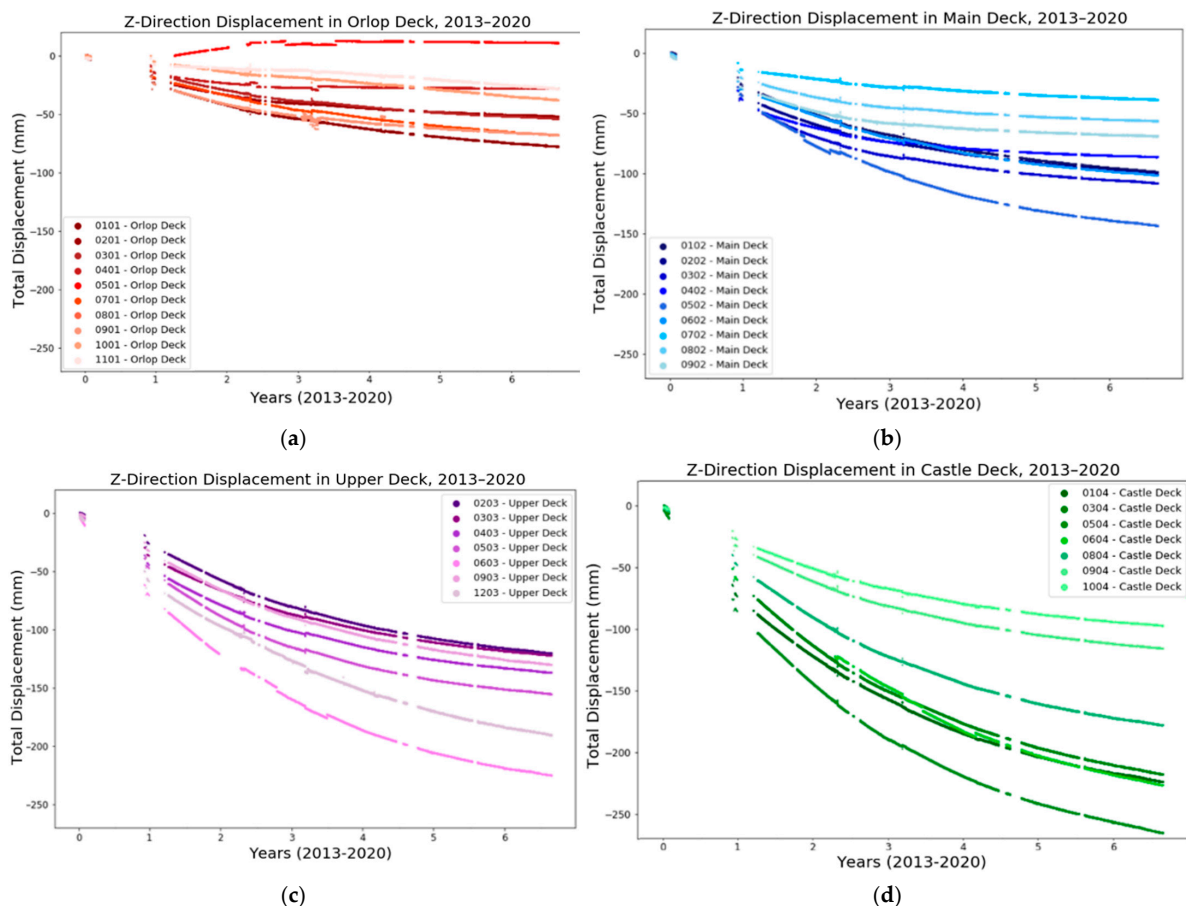


**Figure 5.** Z direction displacement of the TS targets in the (a) orlop, (b) main, (c) upper and (d) castle decks plotted against time for the period between September 2013 and March 2020.

Unlike the trends moving up the ship's decks in the Z direction, the trends moving across the ship from stern to bow are less clear. However, the largest displacement in each deck occurred in the targets 02.01, 05.02, 06.03 and 06.04. From this, one conclusion could be that the Z displacement is greatest in the middle of the ship, i.e., a relatively equal distance between bow and stern.

Fortunately, all the targets slowed in their displacement, as evidenced by the decay in magnitude for all of the displacements measured, regardless of the direction and position on the ship.

### 3.3. Displacement Rate of the TS Targets in the X, Y and Z Directions over the Time Period (2013–2020)

Notable amongst the X direction displacement rate plots in Figure 6, the 04.01 target displayed a high initial rate of 165 mm/year in the first 2 weeks of recording. However, the rate of displacement for this target slowed to a similar level to all other targets after the first year. The issue with the 04.01 target can be explained by the damage to the hull at the point where this target was attached, which had to be repaired in November 2013, with scaffolding support being inserted. This was then reinforced up to the main deck in September 2014.

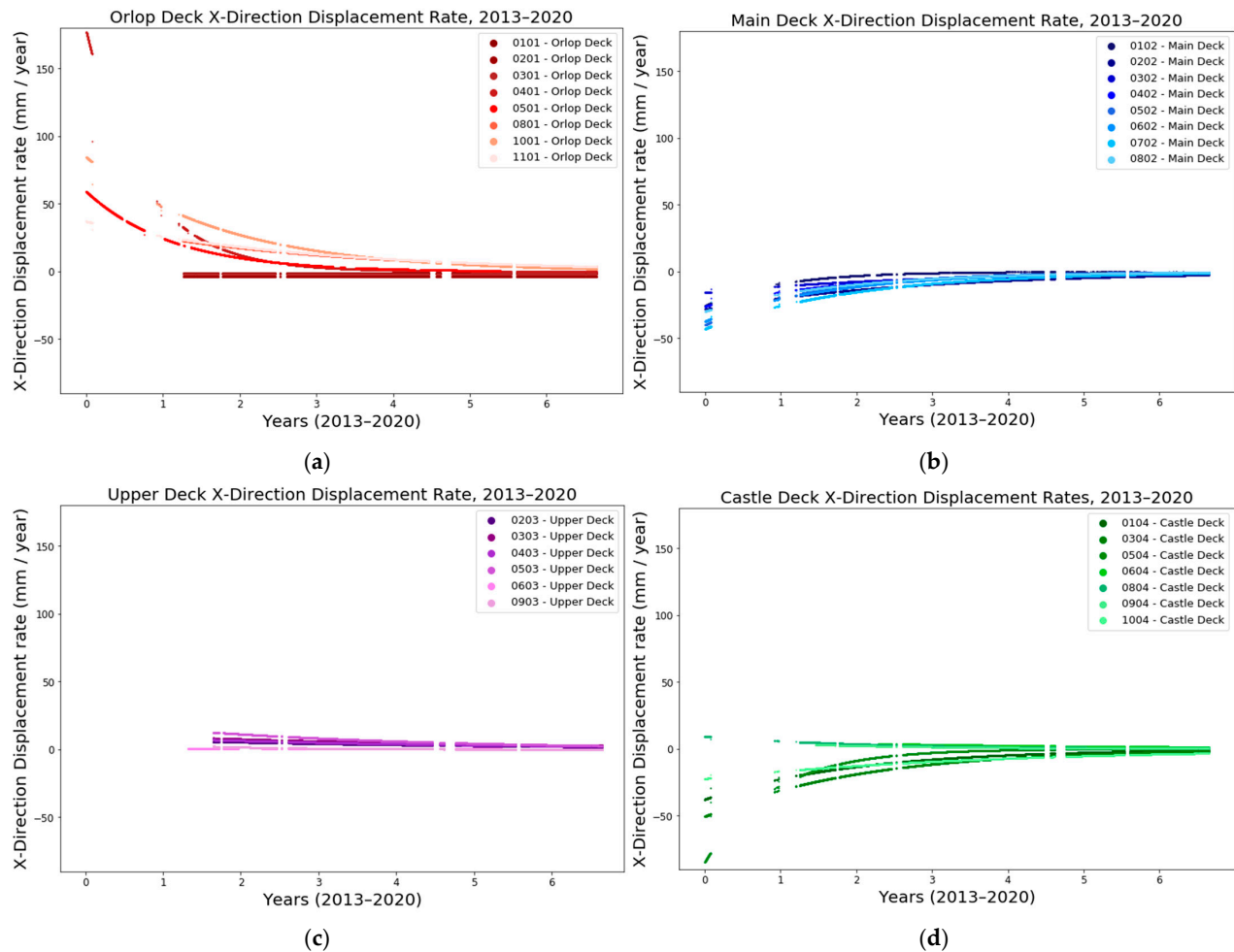


**Figure 6.** Rate of the X displacement of the TS targets in the (a) orlop, (b) main, (c) upper and (d) castle decks plotted against time for the period between September 2013 and March 2020.

The most recent X direction displacement rates are similar, and relatively slow, across the four decks and across the length of the ship, too, with an average of  $+2 \pm 1$  mm/year in the orlop deck,  $-1.0 \pm 0.6$  mm/year in the main deck,  $+2.0 \pm 1.6$  mm/year in the upper deck and  $1 \pm 1$  mm/year in the castle deck. The displacement rates across all targets show promising signs of slowing in the X direction.

The Y displacement rates in Figure 7 show a similar pattern of slowing as they do along the X direction. While there was some variance of the initial displacement rate, with the value going from 110 mm/year in the fastest displacing target in 2013, which was 06.04, as of 2020, all the displacement rate magnitudes were below 20 mm/year. For instance, 06.04 was approximately 110 mm/year and, as of 2020, was approximately 7 mm/year, whereas the 09.04 target was approximately 8 mm/year and became 7 mm/year.

The average most recent Y direction displacement rates are  $2 \pm 1$  mm/year in the orlop deck,  $0.2 \pm 0.2$  mm/year in the main deck,  $3 \pm 1$  mm/year in the upper deck and  $5 \pm 2$  mm/year in the castle deck. The most recent average rate of X direction displacement is highest in the castle deck.

Figure 8 presents the displacement rates along the Z direction of the targets in each separate deck. Similarly to the two other directions, the rate of displacement was reducing in all targets over the 6.5 years since September 2013.

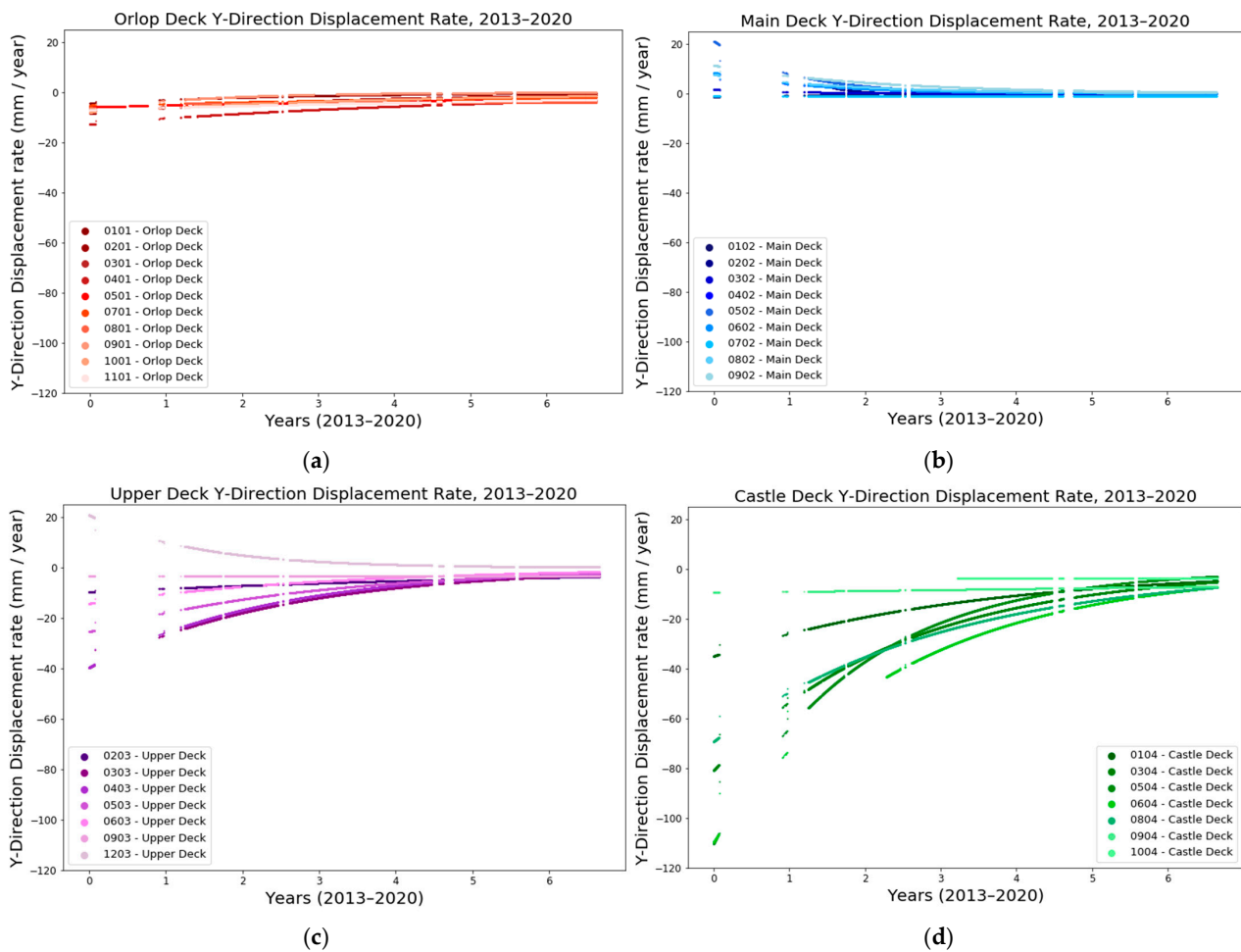


**Figure 7.** Rate of the Y displacement of the TS targets in the (a) orlop, (b) main, (c) upper and (d) castle decks plotted against time for the period between September 2013 and March 2020.

The faster initial rates of displacement of the upper and castle decks could be expected from the discussion in the previous total displacement section. The most recent displacement rates are still higher in the upper decks, even though they have reduced and are now all below 20 mm/year.

The most recent average displacement rates in the Z direction for targets in each deck are:  $2 \pm 2$  mm/year in the orlop deck,  $3 \pm 2$  mm/year in the main deck,  $7 \pm 2$  mm/year in the upper deck and  $9 \pm 3$  mm/year in the castle deck. If the targets continue to follow the same Z displacement trends, then the Z displacement rates should approach zero.

The most recent rates of displacement of each target are shown in Figure 9a–c. The ship is currently moving most in the Z direction across all four decks. In addition, the most recent displacement rate is highest in the upper two decks and increases moving up the ship. Since the ship is predominantly dry, according to the moisture content recordings, the most recent limited movement is from other structural considerations, such as interconnectivity, or lack of, within the ship.

As a rough selection process for identifying problematic sections, we could investigate any targets currently displacing faster than 10 mm/year. From the graphs, the sections with greater than 10 mm/year displacement are 03.04, 05.04 and 06.04. These should be monitored carefully moving forward to ascertain if they will slow down in accordance with the other sections.



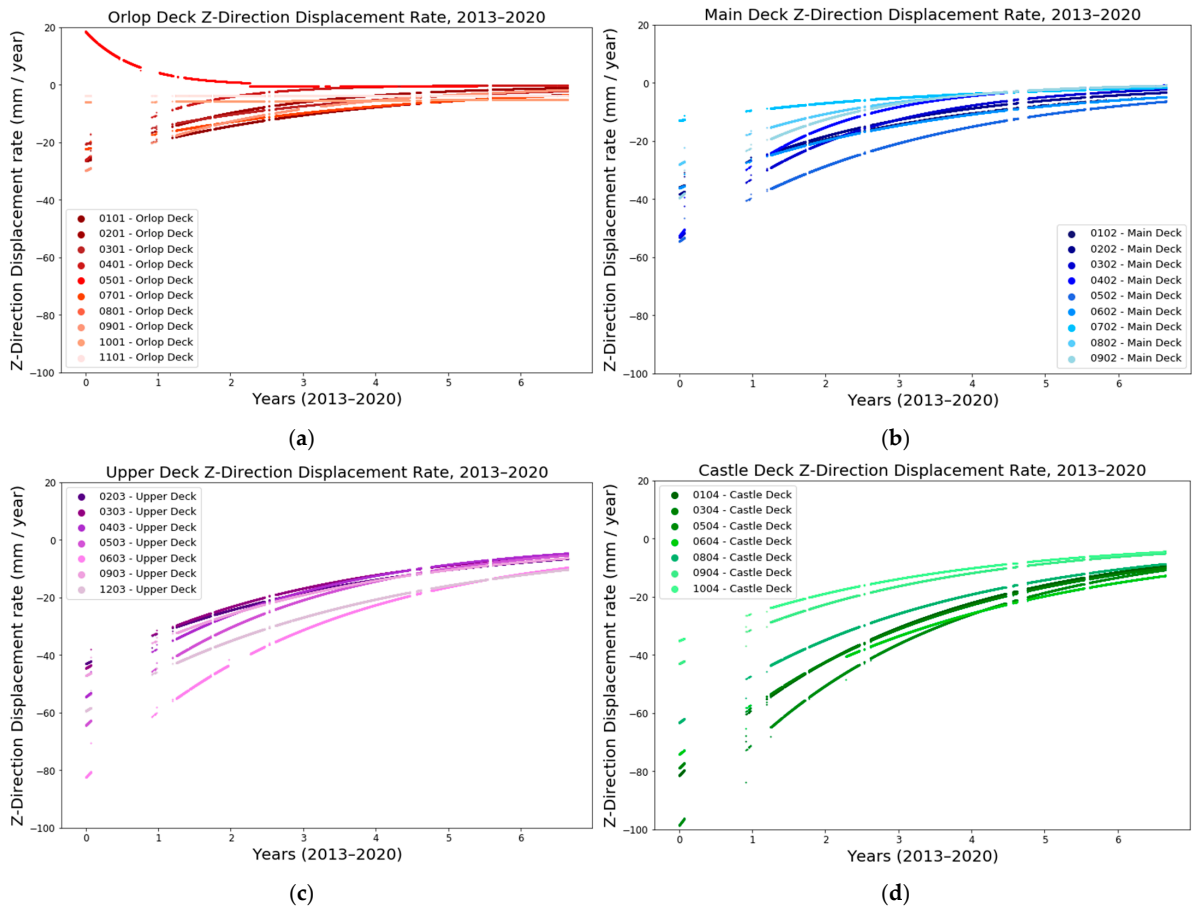


**Figure 8.** Rate of the Z displacement of the TS targets in the (a) orlop, (b) main, (c) upper and (d) castle decks plotted against time for the period between September 2013 and March 2020.

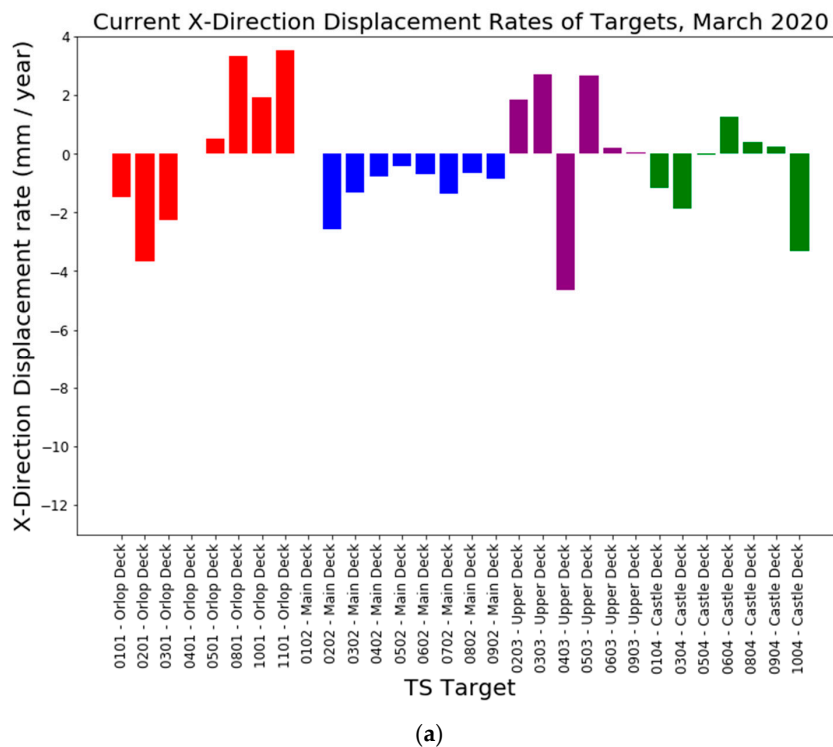


**Figure 9.** Cont.

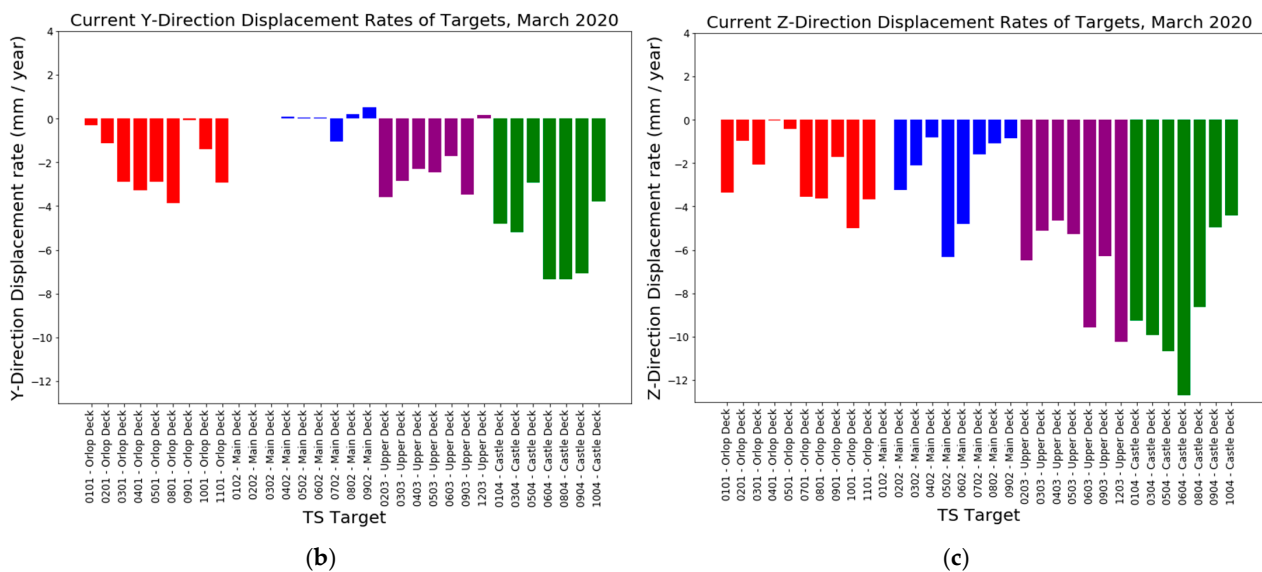


**Figure 9.** Most recent (2020) displacement rates in the (a) X, (b) Y and (c) Z directions. The colour of the bars denotes the deck on which the target is located: red—orlop, blue—main, purple—upper, green—castle.

#### 4. Conclusions

In this study on the *Mary Rose*, we've illustrated how a laser-based target system can be used to measure the displacement of a large archaeological wooden structure, in real time, during the air-drying process after PEG treatment. The displacements since the drying process began were significant in the early stage of drying, but have since slowed considerably.

- In the first year of drying, in the X, Y and Z directions, the highest displacement rates were 70, 110 and 100 mm/year, respectively, whereas after 6.5 years the highest displacement rates are an order of magnitude slower, at 5, 7 and 12 mm/year respectively. Evidently, the displacement rates have reduced significantly, which is a positive finding, indicating the stabilisation of the hull.
- This slower rate of displacement corresponds to an average displacement of the targets in the X, Y and Z directions between the period of recording (2013–2020) of approximately 50, 60 and 110 mm, respectively.
- Average displacement rates as of 2020 across all targets in the X, Y and Z directions are approximately 1.6, 2.3 and 5 mm/year respectively. The displacement rates are now reasonably small when considered in context of the approximately 30 m long ship.
- Finally, as a first analysis of current displacement rates to identify critical sections in need of intervention, the work conducted here alleviates any fears of significant further displacement.

**Author Contributions:** Conceptualization, E.S., F.B., F.G. and H.C.; methodology, E.S., F.B., F.G. and H.C.; software, E.S.; validation, E.S.; formal analysis, E.S., F.B., F.G. and H.C.; investigation, E.S., F.B., F.G. and H.C.; resources, H.C.; data curation, E.S., F.B., F.G. and H.C.; writing—original draft preparation, E.S., F.B., F.G. and H.C.; writing—review and editing, E.S., F.B., F.G. and H.C.; visualization, H.C., E.S., F.B. and F.G.; supervision, E.S., F.B., F.G. All authors have read and agreed to the published version of the manuscript.

**Funding:** H.C. received funding for a Ph.D. by the EPSRC Centre for Doctoral Training in the Advanced Characterisation of Materials (CDT-ACM)(EP/L015277/1).

**Institutional Review Board Statement:** Not applicable.

**Informed Consent Statement:** Not applicable.

**Data Availability Statement:** Not applicable.

**Conflicts of Interest:** The authors declare no conflict of interest.

## References


- Varga, T.; Pauliny, P. Timber-traditional material history or vision in architectural design? In *Advanced Materials Research*; Trans Tech Publications Ltd.: Freienbach, Switzerland, 2014; Volume 899, pp. 460–465.
- Namichev, P.; Petrovski, M. Wood as a primary selection of material for furniture production. *J. Process. Manag. New Technol.* **2019**, *7*, 6–12. [CrossRef]
- Laures, F.F. The evolution of antique ship construction in the Mediterranean: A hypothesis. *Int. J. Naut. Archaeol.* **1984**, *13*, 323–325. [CrossRef]
- Majka, J.; Zborowska, M.; Fejfer, M.; Waliszewska, B.; Olek, W. Dimensional stability and hygroscopic properties of PEG treated irregularly degraded waterlogged Scots pine wood. *J. Cult. Herit.* **2018**, *31*, 133–140. [CrossRef]
- Eriksen, A.M.; Gregory, D.J.; Villa, C.; Lynnerup, N.; Botfeldt, K.B.; Rasmussen, A.R. The effects of wood anisotropy on the mode of attack by the woodborer *Teredo navalis* and the implications for underwater cultural heritage. *Int. Biodeterior. Biodegrad.* **2016**, *107*, 117–122. [CrossRef]
- Nagao, K.; Fujii, S. Effect of Moisture Content and Temperature on the Mechanical Properties of Food Models for Examining Thermal Conduction. *J. Home Econ. Jpn.* **2004**, *55*, 573–580.
- Vorobyev, A.; van Dijk, N.P.; Gamstedt, E.K. Orthotropic creep in polyethylene glycol impregnated archaeological oak from the Vasa ship: Results of creep experiments in a museum-like climate. *Mech. Time-Depend. Mater.* **2019**, *23*, 35–52. [CrossRef]
- Dionisi-Vici, P.; Allegretti, O.; Braovac, S.; Hjulstad, G.; Jensen, M.; Storbekk, E. The Oseberg ship. Long-term physical-mechanical monitoring in an uncontrolled relative humidity exhibition environment. Analytical results and hygromechanical modelling. In Proceedings of the Climate for Collections Standards and Uncertainties, Munich, Germany, 7–9 November 2012.
- Broda, M.; Mazela, B.; Królikowska-Pataraja, K.; Hill, C.A.S. The use of FT-IR and computed tomography non-destructive technique for waterlogged wood characterisation. *Wood Res.* **2015**, *60*, 707–722.
- Thybring, E.E.; Glass, S.V.; Zelinka, S.L. Kinetics of water vapor sorption in wood cell walls: State of the art and research needs. *Forests* **2019**, *10*, 704. [CrossRef]
- Björdal, C.G.; Nilsson, T. Waterlogged archaeological wood—A substrate for white rot fungi during drainage of wetlands. *Int. Biodeterior. Biodegrad.* **2002**, *50*, 17–23. [CrossRef]
- Kowalczyk, J.; Rachocki, A.; Broda, M.; Mazela, B.; Ormondroyd, G.A.; Tritt-Goc, J. Conservation process of archaeological waterlogged wood studied by spectroscopy and gradient NMR methods. *Wood Sci. Technol.* **2019**, *53*, 1207–1222. [CrossRef]
- Broda, M.; Hill, C.A.S. Conservation of waterlogged wood—Past, present and future perspectives. *Forests* **2021**, *12*, 1193. [CrossRef]
- McQueen, C.M.A.; Steindal, C.C.; Narygina, O.; Braovac, S. Temperature- and humidity-induced changes in alum-treated wood: A qualitative X-ray diffraction study. *Herit. Sci.* **2018**, *6*, 1–11. [CrossRef]
- Wagner, L.; Almkvist, G.; Bader, T.K.; Bjurhager, I.; Rautkari, L.; Gamstedt, E.K. The influence of chemical degradation and polyethylene glycol on moisture-dependent cell wall properties of archeological wooden objects: A case study of the Vasa shipwreck. *Wood Sci. Technol.* **2016**, *50*, 1103–1123. [CrossRef]
- Preston, J.; Smith, A.D.; Schofield, E.J.; Chadwick, A.V.; Jones, M.A.; Watts, J.E.M. The effects of Mary Rose conservation treatment on iron oxidation processes and microbial communities contributing to acid production in marine archaeological timbers. *PLoS ONE* **2014**, *9*, e84169. [CrossRef] [PubMed]
- Jones, M.; Schofield, E.J.; McConnachie, G. Air drying of the Mary Rose hull'. In Proceedings of the 12th ICOM-CC Group on Wet Organic Archaeological Materials Conference, Istanbul, Turkey, 13–17 May 2013.
- Piva, E. *Conservation of a Tudor Warship: Investigating the Timbers of the Mary Rose*; Portsmouth University: Portsmouth, UK, 2017.
- Nguyen, T.D.; Sakakibara, K.; Imai, T.; Tsujii, Y.; Kohdzuma, Y.; Sugiyama, J. Shrinkage and swelling behavior of archaeological waterlogged wood preserved with slightly crosslinked sodium polyacrylate. *J. Wood Sci.* **2018**, *64*, 294–300. [CrossRef]
- El-Hakim, S.; Beraldin, J.-A.A.; Picard, M.; Cournoyer, L. Surface Reconstruction of Large Complex Structures from Mixed Range Data—The Erechtheion Experience. *Int. Arch. Photogramm. Remote Sens. Spat. Inf. Sci.* **2008**, *37*, 1077–1082. Available online: [https://www.researchgate.net/profile/J-A-Beraldin/publication/44054006\\_Surface\\_Reconstruction\\_of\\_Large\\_Complex\\_Structures\\_from\\_Mixed\\_Range\\_Data\\_-\\_The\\_Erechtheion\\_Experience/links/00463521d20bbbe45e000000/Surface-Reconstruction-of-Large-Complex-Structures-](https://www.researchgate.net/profile/J-A-Beraldin/publication/44054006_Surface_Reconstruction_of_Large_Complex_Structures_from_Mixed_Range_Data_-_The_Erechtheion_Experience/links/00463521d20bbbe45e000000/Surface-Reconstruction-of-Large-Complex-Structures-) (accessed on 20 September 2021).
- Neubauer, W.; Doneus, M.; Studnicka, N.; Riegl, J.; Systems, L.M.; Documentation, D. Combined High Resolution Laser Scanning and Photogrammetrical Documentation of the Pyramids at Giza. *Security* **2005**, 470–475.
- Vorobyev, A.; Garnier, F.; van Dijk, N.P.; Hagman, O.; Gamstedt, E.K. Evaluation of displacements by means of 3D laser scanning in a mechanically loaded replica of a hull section of the Vasa ship. *Digit. Appl. Archaeol. Cult. Herit.* **2018**, *11*, e00085. [CrossRef]
- Wujanz, D.; Neitzel, F.; Hebel, H.P.; Linke, J.; Busch, W. Terrestrial radar and laser scanning for deformation monitoring: First steps towards assisted radar scanning. *ISPRS Ann. Photogramm. Remote Sens. Spat. Inf. Sci.* **2013**, *2*, 325–330. [CrossRef]
- McConnachie, G. *Air Drying Behavior of Waterlogged Archaeological Woods from the Tudor Warship Mary Rose*; Portsmouth University: Portsmouth, UK, 2005.

25. Van Dijk, N.P.; Gamstedt, E.K.; Bjurhager, I. Monitoring archaeological wooden structures: Non-contact measurement systems and interpretation as average strain fields. *J. Cult. Herit.* **2016**, *17*, 102–113. [CrossRef]
26. Leica Flexline TS02/06/09 (Datasheet for model TS06). 2008. Available online: [https://leica-geosystems.com/-/media/files/leicageosystems/products/datasheets/leica\\_viva\\_ts16\\_ds.ashx?la=en&hash=2746A736346652C1C8CF15B5371AD534](https://leica-geosystems.com/-/media/files/leicageosystems/products/datasheets/leica_viva_ts16_ds.ashx?la=en&hash=2746A736346652C1C8CF15B5371AD534) (accessed on 28 August 2021)



## Article

# Effect of Polyethylene Glycol Treatment on Acetic Acid Emissions from Wood

Sarah Hunt <sup>1,\*</sup>, Josep Grau-Bove <sup>2</sup>, Eleanor Schofield <sup>3,\*</sup> and Simon Gaisford <sup>1</sup> <sup>1</sup> UCL School of Pharmacy, University College London, London WC1N 1AX, UK; s.gaisford@ucl.ac.uk<sup>2</sup> Institute for Sustainable Heritage, University College London, London WC1H 0NN, UK; josep.grau.bove@ucl.ac.uk<sup>3</sup> Mary Rose Trust, Portsmouth PO1 3GW, UK

\* Correspondence: sarah.hunt.15@ucl.ac.uk (S.H.); E.Schofield@maryrose.org (E.S.)

**Abstract:** Acetic acid is known to be emitted from sound wood and can accelerate damage to heritage materials, particularly metals. However, few studies have investigated the extent of acetic acid emissions from archaeological wood. This research utilised Solid-Phase-Micro-Extraction (SPME) GC–MS and lead coupon corrosion to identify volatile emissions from polyethylene glycol (PEG)-treated archaeological wood from the *Mary Rose* collection and assess if they could cause accelerated damage. In addition, the effect of PEG treatment on acetic acid emissions was investigated using sound wood samples. For sound wood, the PEG treatment acted as a barrier to acetic acid emissions, with higher-molecular-weight PEGs preventing more emissions. Archaeological wood, despite its age and high-molecular-weight PEG treatment, still emitted detectable concentrations of acetic acid. Moreover, they emitted a wider array of compounds compared to sound wood, including carbon disulphide. Like sound wood, when the archaeological wood samples were in a sealed environment with lead coupons, they caused accelerated corrosion to lead. This evidences that archaeological wood can emit high enough concentrations of volatile compounds to cause damage and further investigation should be performed to evaluate if this can occur inside museum display cases.

**Keywords:** waterlogged wood; PEG treatment; acetic acid; volatile emissions; GC–MS



**Citation:** Hunt, S.; Grau-Bove, J.; Schofield, E.; Gaisford, S. Effect of Polyethylene Glycol Treatment on Acetic Acid Emissions from Wood. *Forests* **2021**, *12*, 1629. <https://doi.org/10.3390/f12121629>

Academic Editors: Magdalena Broda and Callum A. S. Hill

Received: 20 October 2021

Accepted: 22 November 2021

Published: 25 November 2021

**Publisher's Note:** MDPI stays neutral with regard to jurisdictional claims in published maps and institutional affiliations.



**Copyright:** © 2021 by the authors. Licensee MDPI, Basel, Switzerland. This article is an open access article distributed under the terms and conditions of the Creative Commons Attribution (CC BY) license (<https://creativecommons.org/licenses/by/4.0/>).

## 1. Introduction

Sound wood emits acetic acid, which is known to accelerate damage to a range of heritage materials [1–3]. Hence, it is accepted that uncoated wood should not be used in the construction or decoration of museum display cases, as, due to their low air exchange rate, unacceptable concentrations of damaging volatile emissions can be observed [4]. Moreover, modern design display cases favour a low air exchange rate as this allows better humidity control. However, because of this, volatile compounds emitted from within the display case will dissipate slower, and therefore other sources of potential emissions inside display cases should be investigated.

In contrast to sound wood, much less research has been performed on acetic acid emissions from wooden artefacts [5]. In addition, these are often more complex materials than sound wood due to degradation and the requirement of a consolidant. Polyethylene glycol (PEG), which is often used to consolidate archaeological organic objects, is known to affect molecular permeation transport properties of materials [6]. Therefore, it is likely that the application of PEG into and onto wood will affect the emission rate of volatile compounds. Additionally, PEG can also emit volatile compounds—previous work identified formic acid as a marker for PEG degradation but found limited formic acid in PEG-treated archaeological wood samples from the *Vasa*, the *Skuldelev* Viking ships and the *Bremen Cog*, concluding that the extent of PEG degradation was thought to be minimal approximately 45 years after it was applied [7]. However, whilst the concentration emitted might be minimal with respect to PEG degradation, the volatile formic acid emitted could

have a negative impact on other heritage materials if allowed to concentrate inside display cases over time. Additionally, it could lower the pH of the wood and hence accelerate hydrolysis of wood cellulose fibre [8].

This paper uses SPME-GC-MS to identify the emissions from PEG-treated archaeological wood from the *Mary Rose* collection—a collection which contains the wooden hull and contents of the *Mary Rose*, an English Tudor warship. These emissions included acetic acid and carbon disulphide, which are known to damage some heritage materials. To investigate this, lead coupon corrosion experiments were also used to evaluate if the volatile emissions accelerated damage to lead. Lead was chosen due to its sensitivity towards acetic acid [2]. Additionally, the effect of PEG treatment on acetic acid emissions from sound wood was investigated, which was found to reduce acetic acid emissions.

## 2. Materials and Methods

### 2.1. Samples

To imitate standard conservation treatments on archaeological wood, modern cubes of oak (*Quercus robur* L.) wood, 1.5 cm<sup>3</sup>, were soaked in 40% solutions of either 200-, 400- or 600-molecular-weight PEG for approximately three years. Prior to analysis, they were dried at room temperature. Additionally, cubes of untreated wood and PEG 600-treated wood were soaked in 50 mL of distilled water for four days and then air dried at room temperature prior to analysis in order to evaluate the effects of washing on the acetic acid emissions.

Four PEG-treated archaeological artefacts were obtained from the *Mary Rose* collection—a collection of 16th-century objects from Henry VIII's flagship, including the hull of the ship which was excavated in 1982—and PEG treatment started in 2004. The age of the PEG treatment of the other artefacts varies, with some conserved as soon as they were raised in the 1970s and 1980s. Three of these (Artefact 1–3) were PEG treated at the same time as each other, using the same method—soaking in 10% PEG 600, 20% PEG 600, 30% PEG 4000, followed by freeze drying and surface treatment with PEG 4000 where required. The only exception is Artefact 4, which was sprayed with 40% PEG 200, then 65% PEG 2000 followed by controlled air drying. The treatment of the woods used in this study is summarised in Table 1. The approximate surface areas of Artefact 1, 2, 3 and 4 were 0.10, 0.08, 0.05 and 0.05 m<sup>2</sup>, respectively.

### 2.2. SPME GC-MS Analysis

Treated and untreated sound wood samples (sound wood 1–4) were sealed for nine days in 20 mL headspace sample vials (Thermo Scientific Chromacol, Waltham, MA, USA) with screw caps and silicone/PTFE liners. For sterilisation, all sample vials, caps and seals were heated in an oven at 150 °C for at least 24 h prior to use.

The PEG-treated archaeological artefacts (Artefacts 1–4) were placed inside 5 L Tedlar sample bags with a single polypropylene fitting (SKC, Blandford Forum, UK). The sample bag was then resealed using a packer poly heat sealer. A vacuum pump was used to evacuate the air, which was then replaced with nitrogen (minimum 99.998% purity). The artefacts were sealed for nine days.

The SPME-GC-MS method used in this study was developed by Curran et al. [9]. A Divinylbenzene/Carboxen/Polydimethylsiloxane SPME fibre was exposed to the headspace of the vials and Tedlar bags for one hour at room temperature. It was then heated in the injection port of a gas chromatograph (Perkin Elmer Clarus 500, Beaconsfield, UK) at 250 °C in splitless mode for one minute. A 60 m in length and 0.25 mm in diameter column (VOCOL Sigma-Aldrich, St. Louis, MO, USA) was used. The GC was coupled to a Perkin Elmer Clarus 560D mass spectrometer. Mass spectra were collected under electron ionisation mode at 70 eV and recorded from  $m/z$  45 to 300.

The separation method was such that acetic acid eluted between 11.3 and 11.7 min. The extracted-ion chromatogram obtained from the intensity of the signal at a mass to charge ratio of 60 was used to estimate the acetic acid peak intensity. To account for

instrument day-to-day variation, the acetic acid peak was divided by that of the doublet peak in the MISA Group 17 Non-Halogen Organic Mix standard (Supelco, Bellefonte, PA, USA) which eluted at 21 min.

**Table 1.** Summary of samples used in this study. Artefacts 1 to 4 are pre-treated wood from the *Mary Rose* collection. The collection reference number is indicated between brackets when available. The samples “sound wood” 1 to 4 have been treated during this research.

Sample	Species	Treatment
Artefact 1 (83A0637)	Oak ( <i>Quercus robur</i> )	10% PEG 600, 20% PEG 600, 30% PEG 4000, freeze dried, surface PEG 4000 treatment
Artefact 2 (90A0049)	Ash ( <i>Fraxinus excelsior</i> L.)	10% PEG 600, 20% PEG 600, 30% PEG 4000, freeze dried, surface PEG 4000 treatment
Artefact 3 (87A0068)	Elm ( <i>Ulmus procera</i> Salisb.) or Beech ( <i>Fagus sylvatica</i> L.)	10% PEG 600, 20% PEG 600, 30% PEG 4000, freeze dried, surface PEG 4000 treatment
Artefact 4	Oak ( <i>Quercus robur</i> )	Sprayed with 40% PEG 200, then 65% PEG 2000, air dried.
Sound wood 1	Oak ( <i>Quercus robur</i> )	No treatment
Sound wood 1W	Oak ( <i>Quercus robur</i> )	Sound wood 1, washed and air dried
Sound wood 2	Oak ( <i>Quercus robur</i> )	40% PEG 200, air dried
Sound wood 3	Oak ( <i>Quercus robur</i> )	40% PEG 400, air dried
Sound wood 4	Oak ( <i>Quercus robur</i> )	40% PEG 600, air dried
Sound wood 4W	Oak ( <i>Quercus robur</i> )	Sound wood 4, washed and air dried

Analysis of empty vials and Tedlar bags was performed. No acetic acid was detected from the sealed Tedlar bags, including one which was sealed for 17 weeks. However, a small acetic acid peak was detected from the blank headspace vials. Nine measurements of the empty vials were used to estimate the limit of detection (LOD) for acetic acid measurements from Chromacol headspace vials.

### 2.3. Lead Coupon Exposure

Lead foil, approximate thickness 0.25 mm and >99.96% purity, purchased from Merck Millipore, was mechanically prepared by grinding with a glass bristle brush. It was then cut into strips, approximately 10 by 20 mm and degreased in acetone. The lead strips were exposed in custom holders, made from a clear polymethyl methacrylate. An electronic microbalance (4401 MP8, Sartorius, Goettingen, Germany) with a sensitivity of 10 µg was used to weigh the metal strips before and after exposure. All weight measurements were performed in triplicate. The initial mass was used to calculate the surface area and the mass change per lead surface area calculated.

The sound wood samples (sound wood 1–4) were sealed in 70 mL screw top amber vials with polyethylene lids for 15 weeks. Additionally, a vial containing 5 mL of saturated sodium bromide solution was used as a control for the sound wood. Two lead coupons were placed in each vial. The average conditions outside the vials were 25 °C and 37% RH, which was recorded using an EasyLog USB logger (LASCAR electronics, Salisbury, UK). The artefacts (Artefacts 1–4) were sealed inside 5 L Tedlar bags with three lead coupons for 17 weeks. Additionally, coupons were placed in an empty 5 L Tedlar bag as a control for the artefacts. The average temperature and RH outside the Tedlar bags were 21 °C and 36%, which was recorded using an EasyLog USB logger (LASCAR electronics, Salisbury, UK).



### 3. Results and Discussion

HS-SPME-GC-MS analysis of sound wood 1 identified volatile acetic acid, toluene, hexanal, furfural, alpha-pinene, octanal, nonanal and decanal in the HS above the sample, with acetic acid being the dominant peak as shown in Figure 1. The two intense peaks in Figure 1 are siloxanes and are not thought to be from the sample, but rather contamination from the SPME fibre, injection port, or column. The literature also reports similar emission profiles from oak, with high acetic acid emissions, which is due to the hydrolysis of acetyl groups in hemicellulose [10]. Furan derivative compounds, such as furfural, are cellulose degradation products and hence could be used as an indicator of cellulose degradation [11], whereas the aldehydes detected are thought to be formed by oxidation of unsaturated fatty acids within the wood [10].

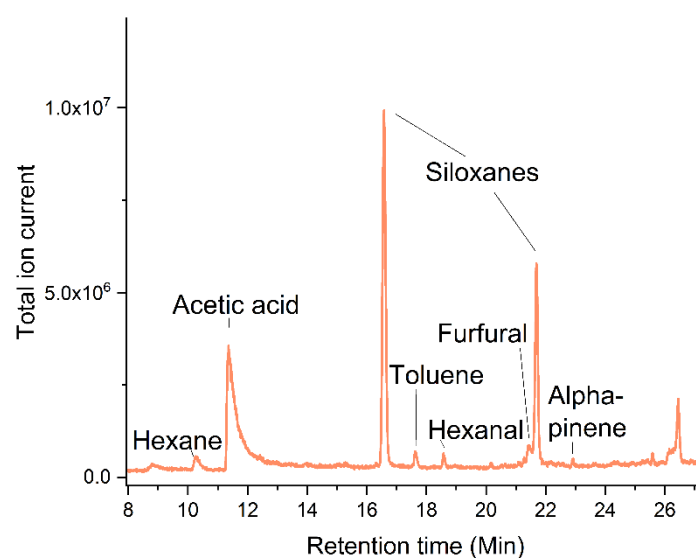


**Figure 1.** HS-SPME-GC-MS chromatogram of untreated sound wood (sound wood 1). The siloxanes peaks are highly unlikely to be from the sample, but rather a contaminant from the SPME fibre, GC-MS inlet and/or column.

Terpene compounds, such as alpha pinene, are present in woods as natural oils [12]. No formic acid was detected from the untreated wood as the lowest detectable mass to charge ratio in this study was 45, whereas the main ion in the mass spectrum of formic acid is 29. Additionally, the SPME fibre used has a poor affinity for small polar molecules, such as formic acid. Therefore, this analysis cannot provide information on formic acid emissions as the sensitivity for this compound is likely to be low. Whilst oak is expected to emit formic acid, the concentration emitted has been reported to be around thirty times smaller compared to acetic acid [1]. Therefore, a different method would have to be used to detect low concentrations of formic acid—SPME fibres have been previously used to detect formic acid in air samples. However, to achieve this, a polyacrylate-coated fibre was used which is more suitable for polar compounds.

In comparison to the untreated wood, the PEG-treated wood samples (sound wood 2, 3 and 4), had lower emissions, particularly after treatment with PEG 400 and 600 molecular weight, with only alphapinene and toluene being consistently detected. No other intense peaks were detected from the PEG-treated samples, and hence the PEG is not believed to be significantly off-gassing compared to the wood. Therefore, there was no evidence to suggest that the recent PEG treatment increased the variety or concentration of emissions from sound wood. Rather, the recently applied PEG treatment appears to reduce emissions dramatically. Therefore, as the PEG was only recently applied to the sound wood samples used in this study, and they are unlikely to contain iron compounds, which are postulated to accelerate PEG degradation in archaeological wood, minimal PEG degradation products are expected in the samples [13].

### 3.1. Acetic Acid Emissions and Effect of Washing

The concentration of volatile acetic acid in the vial for the PEG-treated samples (sound wood 2–4) is reduced compared to the untreated sample (sound wood 1). The samples treated with 400- and 600-molecular-weight PEG have acetic acid peak areas below the limit of detection. This reduction could be explained by the presence of PEG or by other steps in the conservation treatment, such as the washing of the samples. To explore further this possibility, volatile emissions from washed samples were measured. As shown in Figure 2, acetic acid emissions from the washed untreated sample (sound wood 1W) were approximately 80% lower compared to the unwashed sample (sound wood 1). This is due to free acetic acid being removed by aqueous washing, which is a major source of volatile acetic acid from wood. This is further supported by pH measurements of the washings, which were pH 3.5. Moreover, all detected volatile compounds also decreased after washing.

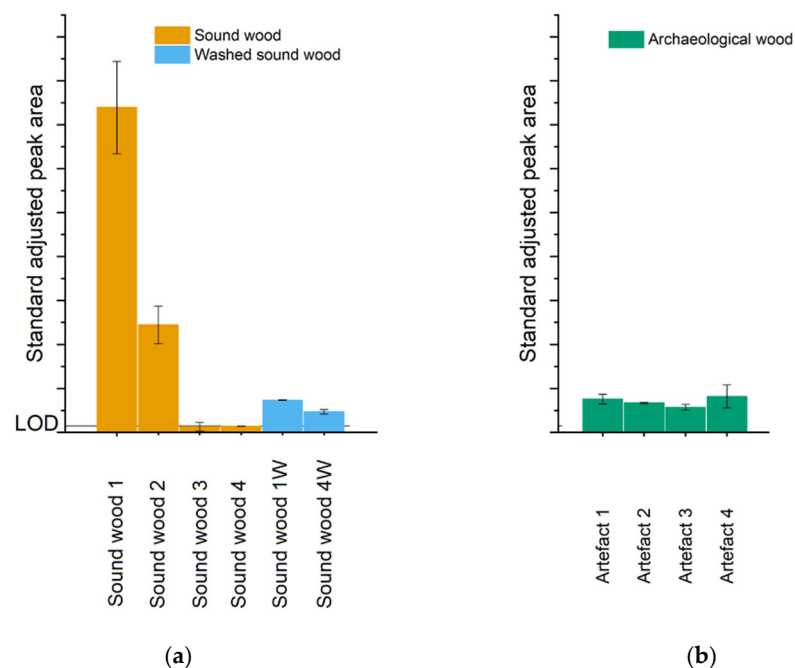


**Figure 2.** Acetic acid peak areas detected by SPME GC–MS analysis for sound wood and washed sound wood (a) and archaeological wood (b).

Conversely, after washing the PEG 600-treated sample (sound wood 4W), the acetic acid emissions increased. We hypothesise that, as aqueous washing partially removes the PEG treatment, the PEG is acting as an impenetrable barrier for acetic acid emissions. Hence, when this barrier is removed, emissions increase. Whilst 600-molecular-weight PEG will penetrate into archaeological wood, very little PEG can be accommodated within sound wood [14]. Therefore, it could reside predominantly on the surface of the wood and act as an efficient barrier to volatile compounds. In contrast, PEG 200 will penetrate more easily deeper into the core of the wood, due to its smaller size, and hence may not form as efficient a barrier on the wood surface [14]. Additionally, lower-molecular-weight PEGs have lower viscosities which will aid transportation from solution to the bulk of the sample.

Whilst washing dramatically decreases acetic acid emissions from treated sound wood, it is thought that over time, due to the hydrolysis of the acetyl groups in the wood, the free acetic acid content will increase, and hence acetic acid emissions will increase again [1]. Whilst this factor could partially explain why PEG-treated sound wood has lower acetic acid emissions, due to the wood being recently soaked in aqueous PEG solutions during treatment, it cannot explain why additional washing of PEG-treated wood increases acetic

acid emissions. It is therefore believed increased acetic acid emissions are the result of PEG removal during washing.

### 3.2. Emissions from Archaeological Wood

In comparison to sound wood, emissions from the archaeological samples were much more complex—a wider array of compounds was detected as shown in Figure 3. Despite the increased complexity of the emissions, there was good agreement between the four artefacts, with similar compounds being detected but with varying intensity, as shown in Figure 3b. Similar to the sound wood, no glycol compounds were detected, and hence it is again concluded that it is the wood, rather than the PEG treatment that is contributing to the volatile emissions the archaeological woods. The PEG treatment does not appear to almost eliminate emissions as it did for sound oak. However, no untreated archaeological wood was available to be tested, it is not known what effect the PEG treatment has on emissions.

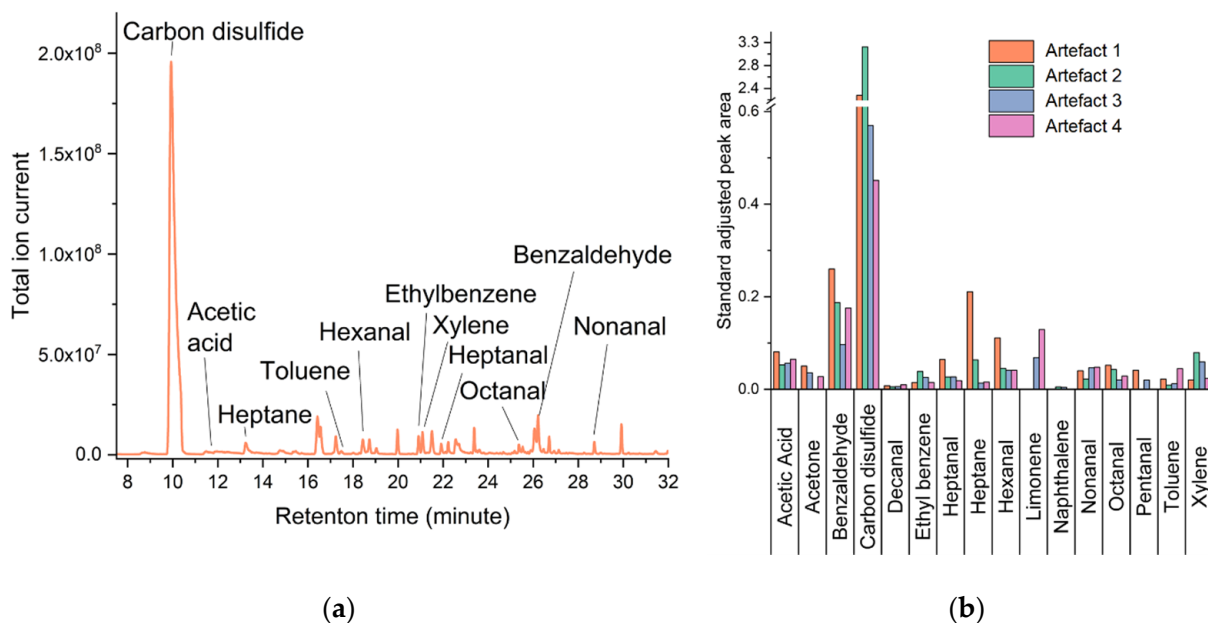


**Figure 3.** Compounds detected by HS-SPME-GC-MS analysis from *Mary Rose* wooden artefacts after 48 days inside a Tedlar bag. Right, (a) Chromatogram of Artefact 1 (87A0068). Left, (b) standard adjusted peak areas of Artefacts 1 to 4.

All the PEG-treated archaeological artefacts had similar acetic acid peak areas. It should be noted that the acetic acid peak areas for sound and archaeological wood cannot be directly compared due to the different sample setup. As archaeological wood is likely to have a significantly reduced free acetic acid content compared to sound wood, further washing is unlikely to significantly decrease its acetic acid emissions significantly. However, the barrier properties of PEG could influence emissions—high-molecular-weight PEGs are commonly applied as surface treatments and could therefore also act as barriers for volatile emissions from the wood. Whilst this study could not compare acetic acid emissions from PEG-treated and untreated archaeological wood, due to the difficulty in obtaining the latter, it was found that PEG-treated archaeological artefacts did emit acetic acid, and therefore, unlike sound wood, the PEG treatment does not completely prevent emissions.

In addition to a reduced acetic acid peak area and a greater number of aromatic and carbonyl compounds detected, the most significant difference compared to sound oak is the presence of an intense peak attributed to carbon disulphide. The *Mary Rose* wood, as well as other shipwreck timbers, are known to contain hydrogen sulphide, which is produced by bacteria [15]. This compound can react with lignin to form thiols, which further oxidise to sulphate esters and sulphonates. However, disulphides, such as carbon disulphide, have been identified as intermediate compounds [16,17].

### 3.3. Corrosion Caused to Lead by Sound and Archaeological Wood

Emissions from sound and archaeological wood were found to accelerate lead corrosion compared to the control environment, as shown in Figure 4. The lead coupon results for sound and archaeological wood are not directly comparable due to differences in other parameters, such as size and shape of the object, temperature and humidity. However, these results highlight that, despite the wood's age and likely reduced acetyl content, archaeological wood can cause a similar magnitude of damage to lead as sound wood.

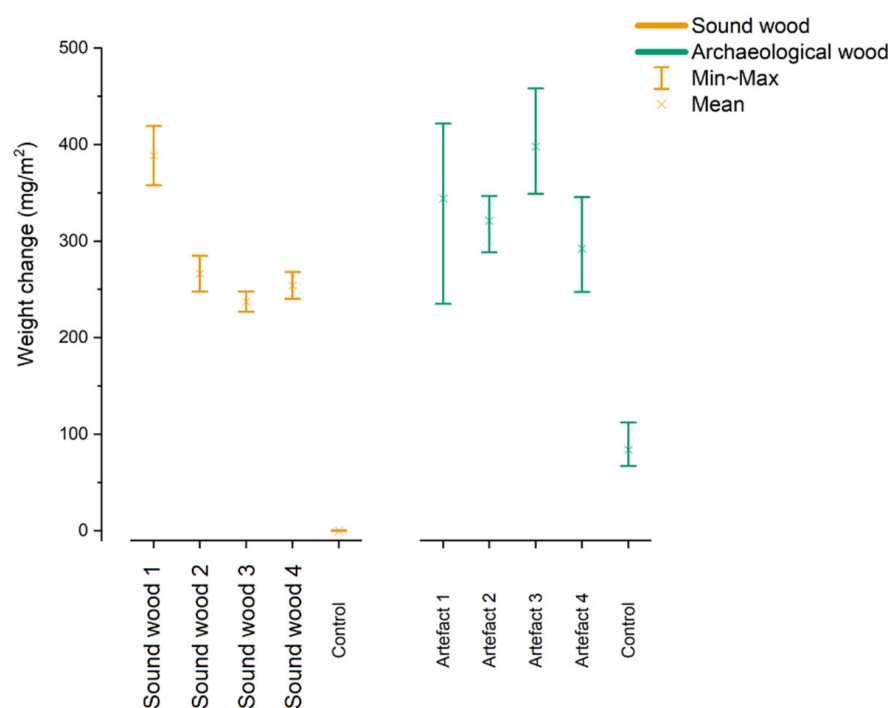


**Figure 4.** Lead coupon weight change after exposure to sound wood 1–4 in sealed vials for 15 weeks, and archaeological wood (Artefacts 1–4) sealed inside Tedlar bags for 17 weeks.

Raman spectra of the lead coupons exposed to sound wood 1 and 2 had the same peaks as spectra of lead coupons after exposure to acetic acid. In contrast, no detectable peaks were observed for the sound woods treated with higher-molecular-weight PEGs (sound wood 3 and 4). This is further evidence that higher-molecular-weight PEG treatment reduces acetic acid emissions compared to untreated wood and wood treated with PEG 200.

## 4. Conclusions

The treatment of sound wood with PEG was found to reduce the amount of volatile acetic acid emitted. This is postulated to be due to the PEG treatment acting as a sealant and trapping in the acetic acid. In the case of archaeological wood, despite its age and high-molecular-weight PEG treatment, artefacts from the *Mary Rose* collection were found to emit acetic acid, causing lead corrosion. This highlights that, independently of its age, archaeological wood has the potential to emit acetic acid, which could be a concern when materials susceptible to acid damage are stored in the same environment. Future research should take steps towards quantifying emission rates in order to assess the potential accumulation of acetic acid in enclosures.

**Author Contributions:** Conceptualisation, S.H., J.G.-B., E.S. and S.G.; methodology, S.H., J.G.-B. and E.S.; formal analysis, S.H.; investigation, S.H.; resources, S.H., J.G.-B., E.S. and S.G.; writing—original draft preparation, S.H., J.G.-B. and E.S.; writing—review and editing, S.H., J.G.-B., E.S. and S.G.; supervision, J.G.-B., E.S. and S.G. All authors have read and agreed to the published version of the manuscript.

**Funding:** This project has been funded by EPSRC Grant EP/L016036/1.


**Conflicts of Interest:** The authors declare no conflict of interest.

## References

- Gibson, L.T.; Watt, C.M. Acetic and formic acids emitted from wood samples and their effect on selected materials in museum environments. *Corros. Sci.* **2010**, *52*, 172–178. [CrossRef]
- Tétreault, J.; Sirois, J.; Stamatopoulou, E. Studies of lead corrosion in acetic acid environments. *Stud. Conserv.* **1998**, *43*, 17–32. [CrossRef]
- Tétreault, J. *Airborne Pollutants in Museums, Galleries, and Archives: Risk Assessment, Control Strategies, and Preservation Management*; Canadian Conservation Institute: Ottawa, QC, Canada, 2003.
- Tétreault, J.; Cano, E.; van Bommel, M.; Scott, D.; Dennis, M.; Barthés-Labrousse, M.-G.; Minel, L.; Robbiola, L. Corrosion of copper and lead by formaldehyde, formic and acetic acid vapors. *Stud. Conserv.* **2003**, *48*, 237–250. [CrossRef]
- Allen, N.S.; Edge, M.; Appleyard, J.H.; Jewitt, T.S.; Horie, C.V.; Francis, D. Degradation of historic cellulose triacetate cinematographic film: The vinegar syndrome. *Polym. Degrad. Stab.* **1987**, *19*, 379–387. [CrossRef]
- Chakrabarty, B.; Ghoshal, A.K.; Purkait, M.K. Effect of molecular weight of PEG on membrane morphology and transport properties. *J. Membr. Sci.* **2008**, *309*, 209–221. [CrossRef]
- Mortensen, M.N. *Stabilization of Polyethylene Glycol in Archaeological Wood*; Technical University of Denmark: Lyngby, Denmark, 2009.
- Dupont, A.-L.; Tétreault, J.; Tetreault, J. Cellulose Degradation in an Acetic Acid Environment. *Stud. Conserv.* **2000**, *45*, 201. [CrossRef]
- Curran, K.; Aslam, A.; Ganiaris, H.; Hodgkins, R.; Moon, J.; Moore, A.; Ramsay, L. Volatile Organic Compound (VOC) emissions from plastic materials used for storing and displaying heritage objects. In Proceedings of the ICOM-CC 18th Triennial Conference Preprints, Copenhagen, Denmark, 4–8 September 2017.
- Risholm-Sundman, M.; Lundgren, M.; Vestin, E.; Herder, P. Emissions of acetic acid and other volatile organic compounds from different species of solid wood. *European. J. Wood Wood Prod.* **1998**, *56*, 125–129. [CrossRef]
- Gu, X.; Ma, X.; Li, L.; Liu, C.; Cheng, K.; Li, Z. Pyrolysis of poplar wood sawdust by TG-FTIR and Py-GC/MS. *J. Anal. Appl. Pyrolysis* **2013**, *102*, 16–23. [CrossRef]
- Jensen, L.K.; Larsen, A.; Mølhav, L.; Hansen, M.K.; Knudsen, B. Health Evaluation of Volatile Organic Compound (VOC) Emissions from Wood and Wood-Based Materials. *Arch. Environ. Health* **2001**, *56*, 419. [CrossRef] [PubMed]
- Almkvist, G.; Persson, I. Fenton-induced degradation of polyethylene glycol and oak holocellulose. A model experiment in comparison to changes observed in conserved waterlogged wood. *Holzforschung* **2008**, *62*, 704–708. [CrossRef]
- Hoffmann, P.; Singh, A.; Kim, Y.S.; Wi, S.G.; Kim, I.J.; Schmitt, U. The Bremen Cog of 1380—An electron microscopic study of its degraded wood before and after stabilization with PEG. *Holzforschung* **2004**, *58*, 211–218. [CrossRef]
- Jalilehvand, F.; Damian, E.; Fors, Y.; Gelius, U.; Jones, M.; Salome, M. Sulfur accumulation in the timbers of King Henry VIII's warship Mary Rose: A pathway in the sulfur cycle of conservation concern. *Proc. Natl. Acad. Sci. USA* **2005**, *102*, 14165–14170.
- Schofield, E.J.; Sarangi, R.; Mehta, A.; Jones, A.M.; Mosselmans, F.J.; Chadwick, A.V. Nanoparticle de-acidification of the mary rose. *Mater. Today* **2011**, *14*, 354–358. [CrossRef]
- Fors, Y.; Jalilehvand, F.; Sandström, M. Analytical aspects of waterlogged wood in historical shipwrecks. *Anal. Sci. Int. J. Jpn. Soc. Anal. Chem.* **2011**, *27*, 785. [CrossRef] [PubMed]

## Article

# Numerical Modelling of Moisture Loss during Controlled Drying of Marine Archaeological Wood

Gabriel Lipkowitz <sup>1,\*</sup>, Karoline Sofie Hennem <sup>2,3</sup> , Eleonora Piva <sup>4</sup> and Eleanor Schofield <sup>3,\*</sup><sup>1</sup> Department of Mechanical Engineering, Stanford University, Stanford, CA 94305, USA<sup>2</sup> Department of Conservation, University of Oslo, Frederiks Gate 3, 0164 Oslo, Norway; karolinesofiehennem@gmail.com<sup>3</sup> Mary Rose Trust, 1.10 College Road, HM Naval Base, Portsmouth PO1 3LX, UK<sup>4</sup> School of Civil Engineering & Surveying, University of Portsmouth, Portland Building, Portsmouth PO1 3AH, UK; piva.eleonora@gmail.com

\* Correspondence: gel19@stanford.edu (G.L.); e.schofield@maryrose.org (E.S.)

**Abstract:** If left to dry uncontrollably following excavation, marine archaeological wood suffers significant and irreparable damage. Conservation treatments are required to consolidate degraded wood and to remove residual water. Drying must be controlled to eliminate erratic and heterogeneous water removal. Monitoring and understanding the drying process progression is invaluable information to garner real-time knowledge to correlate with chemical and physical material properties, and to develop future conservation strategies. Here, polyethylene glycol (PEG) consolidated marine archaeological wood was periodically sampled during drying to determine the moisture content as a function of location, time, and sample depth. The heterogeneous nature of the material leads to significant noise across spatial and temporal measurements, making it challenging to elucidate meaningful conclusions from visual observation of the raw data. Therefore, the spatiotemporal data was computationally analysed to produce a representative model of the ship's drying, illustrated by a dynamic simulation. From this we can quantitatively predict the drying rate, determine the depth-dependence of drying, and estimate the resulting equilibrium moisture content. This is the first time such simulations have been carried out on this material and conservation process, demonstrating the power of applying numerical modelling to further our understanding of complex heritage data.

**Keywords:** marine archaeological wood; moisture content; polyethylene glycol; computational modelling; *Mary Rose*; predictive model



**Citation:** Lipkowitz, G.; Hennem, K.S.; Piva, E.; Schofield, E. Numerical Modelling of Moisture Loss during Controlled Drying of Marine Archaeological Wood. *Forests* **2021**, *12*, 1662. <https://doi.org/10.3390/f12121662>

Academic Editors: Callum A. S. Hill and Magdalena Broda

Received: 26 October 2021

Accepted: 24 November 2021

Published: 30 November 2021

**Publisher's Note:** MDPI stays neutral with regard to jurisdictional claims in published maps and institutional affiliations.



**Copyright:** © 2021 by the authors. Licensee MDPI, Basel, Switzerland. This article is an open access article distributed under the terms and conditions of the Creative Commons Attribution (CC BY) license (<https://creativecommons.org/licenses/by/4.0/>).

## 1. Introduction

Prior to excavation, marine archaeological wood can experience chemical decay, cellulose hydrolysis and bacterial cellulose consumption [1]. Upon excavation, the wood's capillaries and microcapillaries, both naturally occurring and due to degradation, are saturated with water [2–4]. If left to dry uncontrollably without prior consolidation to compensate for lost wood components, it will likely suffer from extensive dimensional changes that can cause severe structural collapse and irreparable damage [3]. To prevent this, marine archaeological wood often requires a carefully designed, and often bespoke, conservation treatment. Of particular concern are wooden shipwrecks, which due to their size and the interconnectivity and reliance of one timber on another for structural integrity, require a considered approach to their conservation. The absence of one, will lead to catastrophic failure.

One of the first waterlogged shipwrecks to undergo conservation was the Viking age *Oseberg*, which was surface-treated with linseed oil and creosote at the beginning of the 20th century [4]. In April 1962, the Swedish Warship *Vasa* in Stockholm was the first larger shipwreck to be sprayed with a different chemical, polyethylene glycol (PEG). It has subsequently become a popular consolidation treatment and has been used for conserving

the *Skuldelev* Viking ships in Denmark, the *Bremen cog* in Germany [5] and Tudor warship *Mary Rose* [6]. However, the conservation treatment of marine archaeological wood is not complete until it has been dried to remove any residual water, usually by freezing-drying [7], or controlled air-drying [8]. The drying method selected is usually dictated by the item's size and ability to fit within a freeze dryer as a whole, or the ease of dismantling the structure.

During air-drying, it is essential to carefully monitor the progression of water removal to prevent the wood from drying too quickly. If allowed to happen, this can cause shrinkage, fracture, and collapse. Equally, upon reaching an equilibrium moisture content, and when the drying is considered complete, the monitoring of such structures must continue. Adsorption, and desorption, is a constant concern due to its effect on weight and subsequent impact on the structural stability. This is highlighted by ongoing efforts to monitor and understand structural movement at *Vasa* [9–11], *Mary Rose* [12] and *Bremen Cog* [13].

The *Mary Rose* sank during the Battle of the Solent in 1545, and remained submerged for 437 years, until the remaining starboard side was excavated in 1982 [14]. The *Mary Rose* comprises species including oak, poplar, and pine. However, the vast majority is oak, and all the samples used in this study were this type of wood. For twelve years following its salvage, the *Mary Rose* was sprayed with fresh water as a temporary measure, to prevent the shipwreck drying out and to reduce bacterial activity [3]. For ten years thereafter, it was sprayed with PEG-200, until the solution concentration reached 40% *w/v*, and for the remaining nine years it was sprayed with PEG-2000, until the solution concentration reached 60% *w/v*. For drying thereafter, common methods such as atmospheric pressure freeze drying and vacuum freeze drying, the latter being used for smaller artefacts, were not possible for the *Mary Rose*, due to its size and reluctance to disassemble the structure. Therefore, controlled air drying was chosen, with temperature, relative humidity, air velocity and light levels in a sealed enclosure tightly monitored. This ensured that we minimised the possibility of shrinking or cracking and differential drying rates, which would likely result in damage.

In 2013, air-drying of the hull began, following computational fluid dynamics (CFD) modelling of air flow around the hull, and carefully positioned air ducts were placed to deliver the appropriate air, in terms of velocity, relative humidity and temperature. The entire ship was subjected to the same air relative humidity of 54% RH  $\pm$  4% and temperature of 18 and 20  $\pm$  1 °C, kept in controlled light levels [12,15]. The entire ship was subjected to this same air relative humidity, temperature, and velocity during drying and even to this day whilst on display.

The drying of the *Mary Rose* offered an unprecedented opportunity to understand, real-time, the drying process of a large salvaged shipwreck following a consolidation treatment. Determining the moisture content of archaeological wood can be used to assess the degradation levels of marine archaeological wood prior to any consolidation treatment (maximum moisture content, MCM%) or to monitor and determine the drying rates following consolidation treatment (moisture content, MC%) [16]. The MCM% values for a variety of *Mary Rose* woods are documented in [15]. In the case of the *Mary Rose* moisture content data was also gathered to monitor the progression of the drying of the hull, post consolidation. While there are many ways to measure moisture content, such as with a resistance meter or by monitoring shrinkage by inserting pins or nails into the surface of the wood [17], a gravimetric method was used. To that end, throughout the drying process from 2013 to 2017 samples were taken periodically at representative locations around the hull, from which moisture content was determined.

The moisture content data were qualitatively analysed [18] as the process progressed, which offered general observations of how the wood was drying. However, this analysis lacked detail in terms of correlating different areas of the ship, different time stamps, and how the drying was progressing into the depth of the timbers. This was due to the heterogeneity of the data, often encountered with complex heritage materials, and the associated noise observed. This meant that whilst the data could be used to look simply at

how much water had been removed, it was impossible to recognise trends, and furthermore impossible to correlate the data with other measurable processes which are impacted by the level of moisture present, e.g., chemical changes [19,20] and physical movement [20].

To clarify trends through such noise, many scientific fields make successful use of mathematical modelling. Here, mathematical formulae, often implemented in computational models, were employed to optimally describe the observed data. Functions were selected to fit the data, and thus mitigate the influence of outliers, while at the same time having the smallest deviations from the real-world data. The aim was to produce a predictive quantitative model, taking advantage of the spatially and temporally comprehensive, albeit noisy, moisture content data collected real-time from the *Mary Rose*. Thus, identifying genuine drying patterns in conserved marine archaeological wood, and allowing a more comprehensive understanding of the drying process itself, which in turn can be correlated with observed chemical and physical changes.

## 2. Materials and Methods

### 2.1. Observational Measurements

During controlled air-drying of the *Mary Rose* (Figure 1a), moisture content changes were recorded periodically until 1092 days had passed. This time stamp represented significant moisture loss and an associated difficulty in removing samples from the hull. Core samples were retrieved using an incremental borer from locations chosen to give a representation of the entire hull (Figure 1b,c). Sample codes indicate the level of the ship from which cores were taken, e.g., Hold (H), Orlop (O), Main (M) and Upper (U), which represents the ascending order from the base of the ship. Cores were sectioned every 5 mm up to a depth of 30 and 10 mm thereafter. This process was completed more frequently in the initial changes, in order to capture when the most significant moisture loss was expected to happen. A gravimetric method was used to determine the moisture content [18], using the following formula:

$$M = \frac{m_{wet} - m_{dry}}{m_{dry}} \times 100 \quad (1)$$

where  $M$  is moisture content percent,  $m_{wet}$  the mass of the wet sample, and  $m_{dry}$  the mass of the oven-dried sample (24 h drying at 100 °C).

### 2.2. Computational Modelling

Moisture content data from the *Mary Rose* was numerically analysed using a custom script written in *Python*, to take advantage of that language's in-built function libraries for data analysis and plotting (*pandas* and *matplotlib*, respectively). To fit the theoretical moisture content model to the observational data collected from both the internal and external samples, an exponential decay function was used:

$$M_d(t) = ae^{-bt} + c \quad (2)$$

where  $M_d$  is moisture content (%) at depth  $d$  (mm),  $t$  is time (days), and  $a$ ,  $b$ , and  $c$  are model-fitted constants. Differentiated with respect to time, this produces the simple ordinary differential equation (ODE) describing the rate of change of drying as:

$$\frac{dM_d(t)}{dt} = -abe^{-bt} \quad (3)$$

The optimal selection of the parameters  $a$ ,  $b$ , and  $c$  was accomplished using the curve fitting capabilities of *Python SciPy* library, which takes as input the aforementioned inverse exponential with three parameters, along with data, here *Mary Rose* moisture content



measurements, and outputs parameter values, here,  $a$ ,  $b$ , and  $c$ , which minimise the sum of the squared residuals between the curve and data for that location in the ship, expressed as:

$$a_d^*, b_d^*, c_d^* = \operatorname{argmin}_{a,b,c} \sum_{k=0}^{n_s} \sum_{t=0}^{t_{max}} ((ae^{-bt} + c) - M_d^{k,t}) \quad (4)$$

where  $a_d^*$ ,  $b_d^*$ , and  $c_d^*$  are the optimized parameters for the function describing drying at depth  $d$ ;  $n_s$  is the total number of sample measurements for depth  $d$ ;  $t$  is time in days;  $t_{max}$  is the maximum timepoint; and  $M_d^{k,t}$  is the moisture content value measurement at location  $k$  and at time  $t$ , for depth  $d$ .

To produce a holistic simulation of the drying process (i.e., estimate moisture content values for every day, at all depths from 0 to 70 mm deep in the ship), moisture content values at 0.1 mm depth intervals were inferred by linear interpolation between model estimates at those 5 or 10 mm intervals where measurements were taken, for every day during the drying process.

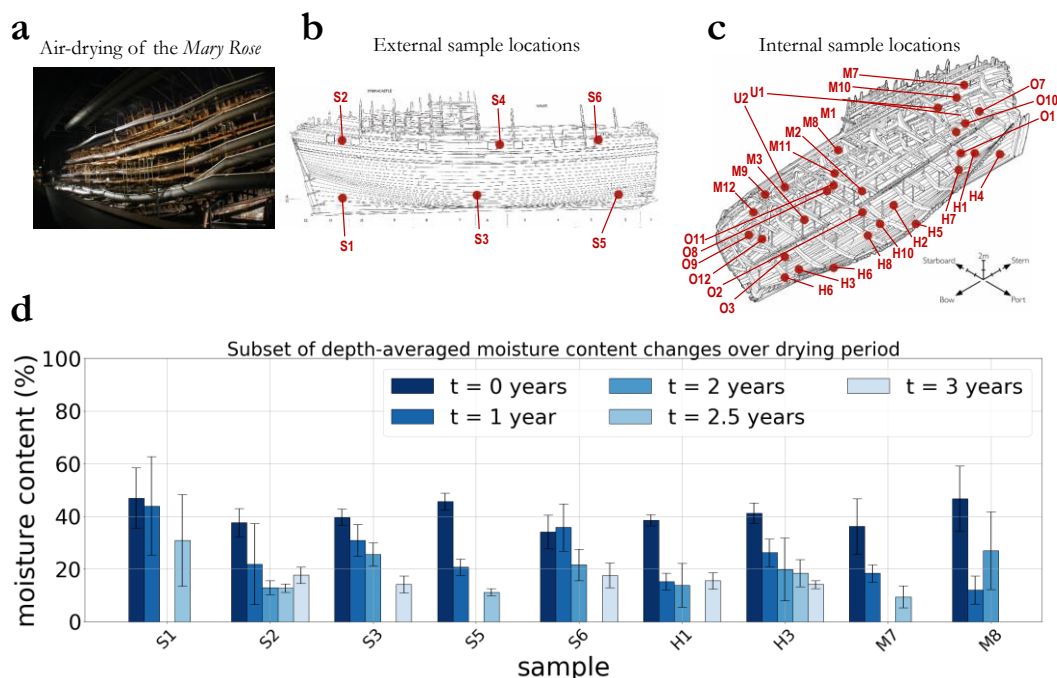


**Figure 1.** Overview of the treatment and drying of the *Mary Rose*. (a) The *Mary Rose* during controlled air-drying ©*Mary Rose Trust*. (b,c) Core sampling locations, from both the external side (b) and internal side of the hull (c), with nomenclature defined in Supplementary Table S1. (d) Moisture contents for 9 locations, averaged over all depths from 0 to 220 mm, at the onset of drying and subsequent yearly intervals. Error bars denote  $\pm 1$  standard deviation from the mean.

### 3. Results and Discussion

#### 3.1. Raw Data Describing the Drying of the *Mary Rose*

A summary of the moisture content measurements taken at a representative sample of locations is shown in Figure 1d. The time stamp  $t = 0$  years indicates the starting point of the drying process. Across all sample locations, and over all depths, at the onset of drying the average moisture content ranged between 37% and 52%, with a global average of 41% and a standard deviation of 5%. After 4 years of drying, the average moisture content ranged between 11% and 38% across sample locations, with a global average of 23% (i.e., approximately half that at the beginning of drying) and a standard deviation of 8%. Overall, these demonstrate that significant drying of the ship did indeed occur over the period, and in the set environmental conditions, as expected [21].

These averages, however, mask significant variability in the data. Some samples showed overall markedly lower moisture content levels during the entire drying process. For instance, core samples M7, M8 and M9, retrieved from internal side planks on the main deck, from the stern end, centre, and bow end, respectively, never had a moisture content above 30%. By contrast, the core sample O7, also retrieved from internal side planks but from the orlop deck below, showed significantly higher moisture content values, over 40%, during the drying period. There was not only significant variation in absolute moisture content values; there was also substantial variability in their changes over time. The overall drop of moisture content for depth-averaged samples ranged between 4 and 34%. For instance, core samples H4 and M12 only saw an average drop of moisture content of approximately 4%, whereas core samples S3, S5, H9, O7, and M7 saw a drop of moisture content higher than 25%.

Similar trends, but with similarly high variability, were observed when moisture contents at varying depths were averaged over all sample locations. Here, analysis was limited to depths up to 70 mm, as beyond that point the wood was visually observed to be of a qualitatively different, and better, preservation state. The raw data (Figure 2a,b) do suggest differences in the drying process by depth, with shallower samples appearing to dry more quickly than deeper ones. In Figure 2c,d, averages from the same raw data suggest the depth-dependence of drying; once again, though, there is great variability. As one example, at day 135 of drying MC% appears to drop precipitously across sample locations, followed by an equally rapid recovery by the next timepoint.

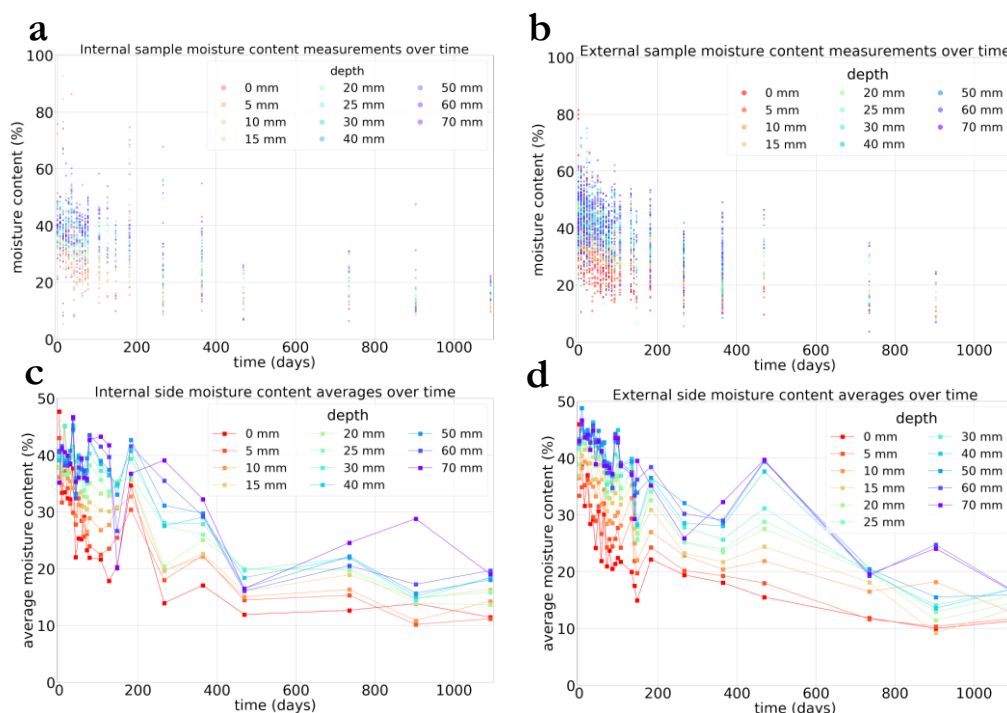


**Figure 2.** Depth resolved moisture content data for external and internal sides of the hull during drying. (a,b) Raw moisture content data for wood samples at depths of 0–70 mm, taken at 27 distinct timepoints over 1092 days; warmer colours indicate shallower depths, and cooler colours deeper depths. (c,d) Averages from the above raw data, with a similar colour scheme as in (a,b).

It is important to note that this variability in the raw data is not necessarily surprising, for a number of reasons. Fresh wood itself is a highly heterogeneous material, varying significantly throughout its structure depending on factors such as the degree of cell wall decomposition [22]. Adding to this natural variation is the heterogeneity of degradation in marine archaeological wood before treatment, with the outer wooden layers of the hull less well-preserved than the drier inner layers. Previous studies determined the basic

density of the inner parts of the *Mary Rose* wood to be  $0.67 \text{ g/cm}^3$  (using the formula  $R = W_{\text{dry}}/V_{\text{wat}}$ , where  $W_{\text{dry}}$  is the weight of sample after oven drying, and  $V_{\text{wat}}$  is the volume of waterlogged sample) which is comparable to values obtained for fresh wood. However, when looking at the degradation across a sample, moisture content was shown to vary drastically indicating a range of degradation, with a preserved inner core and degraded outer area [23]. Any subsequent variation in their conservation treatment could also have introduced further variability. As the *Mary Rose* had to be sprayed with PEG, rather than immersed in PEG baths, penetration will have differed throughout the wood structure, where different orientations of timbers are exposed. It is also expected that the higher grade PEG is concentrated closer to the surfaces than in the inner layers [15]. Finally, the potentially non-negligible weight of PEG itself, likely distributed heterogeneously throughout the samples, could have exacerbated the widespread in the raw data, given moisture content measurements were obtained using a gravimetric approach as described above. All these factors, and others, contribute to the observed spread in the moisture content measurements, and corroborate findings at *Vasa*, where drying patterns were found to be dependent on the temperature, relative humidity and the nature of the PEG impregnation [24].

While to a certain degree unavoidable, this variation does make determining drying rates and predicting the kinetics of drying from just the raw data difficult, if not impossible. For instance, the seemingly simple question of how quickly the waterlogged archaeological wood dried would be answered differently depending upon which sample in the dataset is considered; one starboard sample, S1, suggests that barely any drying occurs in the first year, whereas a different starboard sample, S5, indicates that >50% drying occurred in that time. One common, simple way of seeing trends through noisy data is through averaging, but as the above analysis makes clear, even multiple different averaging techniques do not yield reliable or useful trends.

### 3.2. Numerical Modelling of the Drying of the *Mary Rose*

To overcome this analytical hurdle, a computational model was implemented to predict wood drying kinetics. The results of the numerical modelling are shown in Figure 3a,b. Despite the significant noise present in the raw data described above, this modelling successfully yielded mathematical functions that revealed a clear and consistent trend: for each sample depth, an inverse exponential drying rate over time. Such a drying curve is not unexpected for marine archaeological wood; indeed, small ( $1 \text{ cm}^3$ ) specimens of PEG consolidated *Mary Rose* wood which were air dried to determine the optimal drying conditions for the hull structure, were found to display similar exponential decay [15]. Notably in the present study, however, in situ data on the drying process was collected not only for surface samples, but for deeper ones too, differences between which this modelling revealed with great clarity. Surface samples consistently displayed the sharpest exponential decay in moisture content, and earliest on, whereas deeper samples display much shallower decays, and later on. Notably, this trend was remarkably consistent; every incremental increase in sample depths brought an incrementally slower drying time.

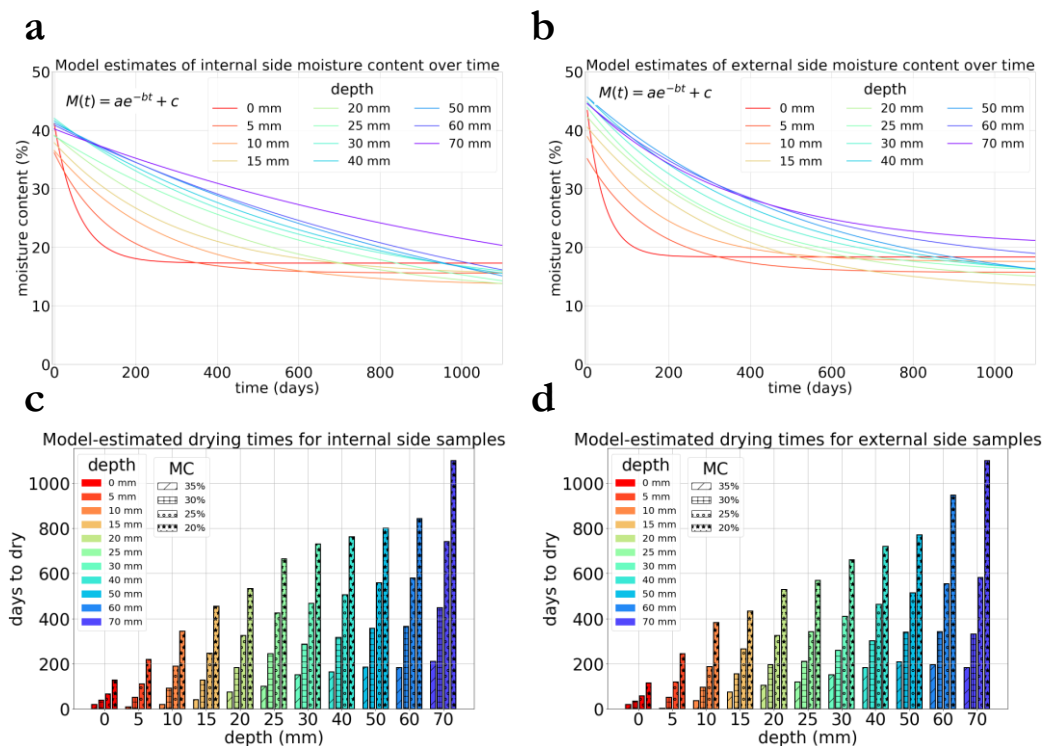


**Figure 3.** Modelling of *Mary Rose* moisture content data. (a,b) Exponential decay curves fitted to the data in Figure 2, describing the change in moisture content at varying depths (colour-coded as in Figure 2), over time, for (a) internal, and (b) external samples. (c,d) Estimates, derived from the curves in (a,b), of the time for samples at varying depths to dry to four moisture contents: 35%, 30%, 25%, and 20%. Here, colour again indicates depths, while hatching indicates the level of drying for the given estimate.

The most intuitive explanation for the more rapid drying of surface samples is their higher degree of atmospheric exposure; indeed, these results accord well with recent reports that kinetically studied the drying of marine archaeological wood using sorption isotherms, which revealed extremely rapid evaporation and geometric distortion even at high environmental relative humidity levels [25]. Others have noted that under high humidity, marine archaeological wood can leach PEG from the surface [15], which may also help explain these differential drying rates compared with the interior. Another potential explanation may stem from the spatially inhomogeneous distribution of different molecular weight PEG in the waterlogged wood. It has been observed that in such a 2-step treatment, lower molecular weight PEG impregnates firmly in the better-preserved interior, whereas higher molecular weight PEG remains limited to the more degraded outer surfaces [26]. As this is the case for the *Mary Rose*, with the interiors more stably impregnated by PEG-200 than the exterior surfaces, this could also exacerbate the differences in drying time. In short, the more rapid drying of the *Mary Rose* surface samples is not entirely unexpected, taking into account the fundamental chemical investigations of similar samples carried out previously.

These depth-dependent drying trends clarified by the model were quantified as drying time estimates in Figure 3c,d, which were obtained directly from the curves in Figure 3a,b. These quantitatively describe how much more quickly our model predicts that samples closer to the surface dry compared with deeper samples. A sample 50 mm deep, for instance, is predicted to dry to half its original moisture content (to ~20%), in about two years. Surface samples, on the other hand, are predicted to take less than half a year to dry to that level. In general, these drying times exceeded those found for small *Mary Rose* samples in the aforementioned study; in that instance 1 cm<sup>3</sup> samples treated with PEG 200/1500 took on the order of 10 days to dry to a new moisture content of half its original point, whereas surface samples obtained in situ in this study required on the order of

100 days to do so, and deeper samples even longer. This is not surprising though, and in fact may be expected, due to scale differences: whereas the previous study examined samples with a depth of 1 cm, this in situ study considers those with 10 cm depths.

To further clarify these moisture content trends suggested by the modelling in Figure 3, a dynamic, temporal simulation was produced estimating how the moisture content of the *Mary Rose* changed at all depths, and at all times. These model estimates were based on those measured moisture content values at select depths and timepoints, as shown in Figure 2a,b, and the mathematical and computational details of how this simulation was achieved are described in the Supplementary Materials. The results of this further modelling are described statically in Figure 4, while the simulation can be viewed dynamically as Supplementary Figure S1 and Video S1.

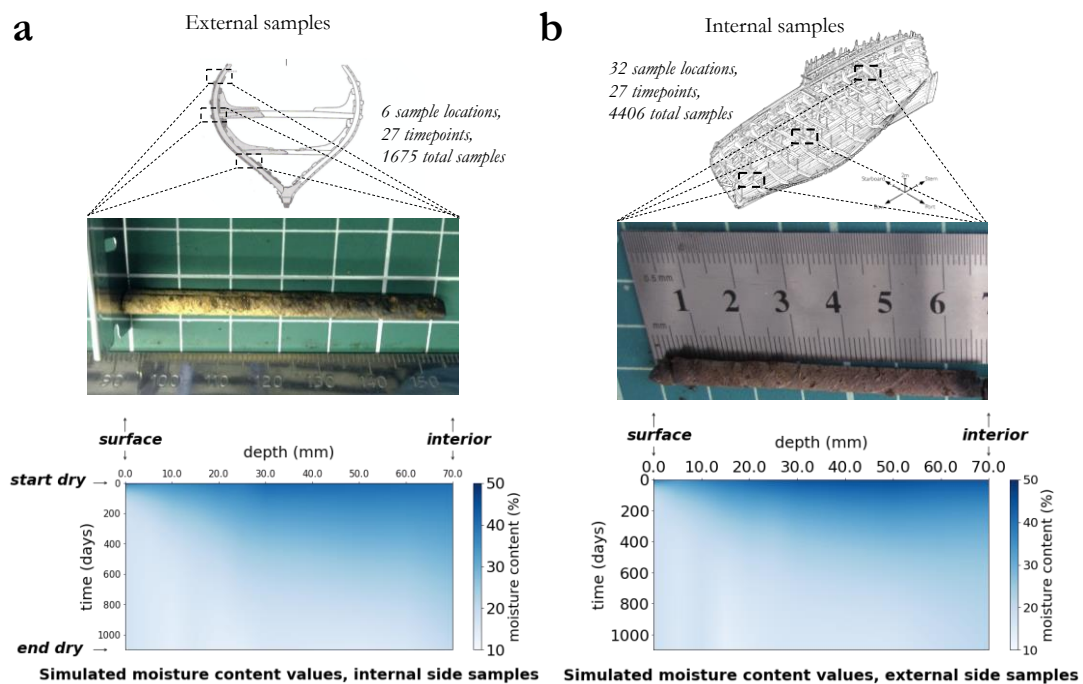


**Figure 4.** Spatiotemporal model description of the *Mary Rose* drying process. (a,b) At top and in middle, images describing which parts of the ship the model describes. Below, model results are shown for these external and internal samples, respectively. Depth is indicated on the horizontal axis (with shallower depths to the left), time on the vertical axis (with  $t = 0$  days on top), and moisture content for a particular depth and time is described by the colour bar, with whiter colours describing drier conditions. Model results are produced at a resolution of every 0.1 mm from 0 to 70 mm, and for every day from 0 to 1092 days.

At the start of drying, the model predicts that all samples have roughly the same moisture content, as expected, of around 40%; in the simulation space, this is indicated by dark blue at all depths for the initial timepoint. The first samples to dry (reflected by simulation space colour lightening) are the shallowest, and the region of most rapid drying can be seen to migrate through the wood depth at a rate of approximately 75 nanometres per day, or about 30 millimetres per year. In the simulation space, this is the slope of the line describing the boundary where the change in moisture content in the sample is steepest; physically, this can be interpreted as the estimated water particle velocity in the waterlogged archaeological wood during the drying process. Eventually, between two and three years after drying starts, the model predicts that a rough new equilibrium is reached, with consistently lower moisture content values throughout the wood samples.

Three major lessons can be learned from this study's analysis of the moisture content changes undergone in the *Mary Rose* throughout its air-drying following PEG treatment. First, this study presents the first quantitative verification of the two-step PEG treatment

approach for marine archaeological wood. In the past, it has been theorised that by first immersing marine archaeological wood in a low molecular weight PEG (MW = 200), and then in a higher molecular weight PEG (MW = 2000), all sections of the wood are successfully impregnated; thus, moisture loss should occur evenly without major structural damage. The observational results presented here, understood with the aid of novel computational modelling approaches, provide perhaps the first empirical validation of this mechanistic theory, further suggesting it as a standard conservation treatment for marine archaeological wood.

A second lesson from the study is that this drying process with such consolidants can in fact be accurately predicted. This has been a notoriously difficult process to predict, using even the most advanced experimental techniques. Some recent studies have attempted to predict the spatial diffusion of polymer consolidants like PEG in waterlogged archaeological wood using methods such as in situ Raman spectroscopy, but these have struggled to identify consistent patterns, perhaps not surprisingly given the aforementioned heterogeneity of the material [27]. This study suggests, however, that with the use of computational modelling, it may not be strictly necessary to do so to reveal consistent drying trends over time. PEG may be distributed stochastically throughout the wood structure, but this study's empirically validated models still show that drying in the aggregate follows a predictable course.

The trajectory this course of drying takes is a final important lesson from the study. Namely, while the predictions it makes—that moisture loss occurs first, and most rapidly, at the surface, with drying of the deeper layers occurring later, and more slowly—may seem intuitive, it is important to emphasise that this mechanism need not necessarily be the case. After all, many alternative drying scenarios for marine archaeological wood may take place; for instance, only drying of the surface could have occurred, or drying could have occurred simultaneously for all depths. Only with the data and modelling presented in this study can these alternative scenarios be disproven, and it be shown that the entire wood sample dries, and in a diffusive manner at that. Additionally, it is only with this information that we can start to correlate the drying process to other observed changes in the wood. For instance, the evolution of sulphur deposits as a function of drying time and depth into the wood have been observed alongside quantifying the resulting wood degradation, via a combination of synchrotron-based (XANES and XRF imaging) and analytical techniques (FTIR and XRF elemental line scans) [28]. Further, chemical and physical data exists that can now be systematically analysed against these new, clear findings on the moisture removal from the wood, to give a clear oversight of the current status of the wood and ship structure as a whole.

#### 4. Conclusions

This study presents moisture content data collected from a wide range of locations on the *Mary Rose* over three years of its controlled drying, and a computational model, built from those data, to describe the drying of consolidated marine archaeological wood generally. In doing so, it helps to explain the notoriously difficult drying behaviour of consolidated and dried marine archaeological wood, a heterogeneous material where sharp transitions exist between preserved and degraded areas in the timber. The *Mary Rose* was no exception; while its timber was impregnated with PEG to help stabilise the wood, there were high variations in moisture content in the wood, which affected the drying rates. As such, it would have been very difficult, if not impossible, to predict how quickly different regions and depths of marine archaeological wood will dry, without data, and modelling. This study, the first empirical and computational analysis of its kind, addresses that difficulty by using longitudinal data over multiple depths and locations. The numerical model was verified against real world moisture content data, and good agreement was found between the two. This provides knowledge on the material state at select time intervals, which now can be correlated to other associated datasets such as physical movement and chemical changes, thereby developing a deeper understanding of

this unique piece of cultural heritage. Only by gathering and correlating all this data can the status be understood, and appropriate strategies be developed to safeguard it for years to come.

**Supplementary Materials:** The following are available online at <https://www.mdpi.com/article/10.3390/f12121662/s1>, Table S1, Location of all core samples. Figure S1, Dynamic drying simulation. Video S1, Moisture Content over time for depths 0–90 mm.

**Author Contributions:** Conceptualization, E.S. and G.L.; methodology, E.S., G.L., E.P. and K.S.H.; formal analysis, G.L. and E.S.; investigation, E.S., G.L., E.P., K.S.H.; data curation, E.S., G.L. and K.S.H.; writing—original draft preparation, E.S., G.L. and K.S.H.; writing—review and editing, E.S., G.L. and K.S.H.; supervision, E.S. All authors have read and agreed to the published version of the manuscript.

**Funding:** This research received no external funding.

**Institutional Review Board Statement:** Not applicable.

**Informed Consent Statement:** Not applicable.

**Data Availability Statement:** Not applicable.

**Acknowledgments:** The authors thank the *Mary Rose* Trust conservation and maintenance teams for collecting samples from the hull for analysis. The authors would like to thank David Begg, Nikos Nanos and Susan Braovac for their input to this study and useful discussions. Eleonora Piva thanks the *Mary Rose* Trust for funding at the University of Portsmouth. Karoline Sofie Hennem thanks Erasmus+ for sponsoring her placement with the *Mary Rose* Trust. Gabriel Lipkowitz thanks the US/UK Fulbright Commission for supporting his studies at Imperial College London.

**Conflicts of Interest:** The authors declare no conflict of interest.

## References

1. Caple, C. *Conservation Skills—Judgement, Method and Decision Making*; Routledge: Abingdon, UK, 2000.
2. Grattan, D.W. Waterlogged Wood. In *Conservation of Marine Archaeological Objects*; Pearson, C., Ed.; Butterworths Heinemann: Oxford, UK, 1987.
3. Florian, M.E. Scope and History of Archaeological Wood. In *Archaeological Wood—Properties, Chemistry and Preservation*; Advances in Chemistry Series; American Chemical Society: Washington, DC, USA, 1990; Volume 225.
4. Rosenqvist, A.M. The Stabilizing of Wood Found in the Viking Ship of Oseberg: Part I. *Stud. Conserv.* **1959**, *4*, 13–22. [CrossRef]
5. Hoffmann, P. To Be and to Continue Being a Cog: The Conservation of the Bremen Cog of 1380. *Int. J. Naut. Archaeol.* **2001**, *30*, 129–140. [CrossRef]
6. Jones, M.A. *For Future Generations: Conservation of a Tudor Maritime Collection*; Mary Rose Trust: Portsmouth, UK, 2011; ISBN 1-78570-155-X.
7. Ambrose, W.R. Application of Freeze-Drying to Archaeological Wood. In *Archaeological Wood—Properties, Chemistry and Preservation*; Advances in Chemistry Series; Rowell, R.M., Barbou, R.J., Eds.; American Chemical Society: Washington, DC, USA, 1990; Volume 225.
8. Håfors, B. *Conservation of the Swedish Warship Vasa from 1628*; The Vasa Museum: Stockholm, Sweden, 2000.
9. Vorobyev, A.; Almkvist, G.; van Dijk, N.P.; Gamstedt, E.K. Relations of Density, Polyethylene Glycol Treatment and Moisture Content with Stiffness Properties of Vasa Oak Samples. *Holzforschung* **2017**, *71*, 327–335. [CrossRef]
10. Vorobyev, A.; van Dijk, N.P.; Kristofer Gamstedt, E. Orthotropic Creep in Polyethylene Glycol Impregnated Archaeological Oak from the Vasa Ship: Results of Creep Experiments in a Museum-like Climate. *Mech. Time-Depend. Mater.* **2019**, *23*, 35–52. [CrossRef]
11. van Dijk, N.P.; Gamstedt, E.K.; Bjurhager, I. Monitoring Archaeological Wooden Structures: Non-Contact Measurement Systems and Interpretation as Average Strain Fields. *J. Cult. Herit.* **2016**, *17*, 102–113. [CrossRef]
12. Schofield, E.J.; McConnachie, G.; Jones, M. *Air Drying of the Mary Rose Hull*; ICOM-CC: Paris, France, 2013.
13. Hoffmann, P. On the Long-Term Visco-Elastic Behaviour of Polyethylene Glycol (PEG) Impregnated Archaeological Oak Wood. *Holzforschung* **2010**, *64*, 725–728. [CrossRef]
14. Marsden, P. Understanding the Mary Rose. In *Mary Rose: Your Noblest Shippe. Anatomy of a Tudor Warship*; Mary Rose Trust: Portsmouth, UK, 2009; Volume 2, ISBN 0-9544029-2-8.
15. McConnachie, G. Air Drying Behaviour of Waterlogged Archaeological Woods from the Tudor Warship Mary Rose. Ph.D. Thesis, University of Portsmouth, Portsmouth, UK, 2005.
16. Macchioni, N.; Pecoraro, E.; Pizzo, B. The Measurement of Maximum Water Content (MWC) on Waterlogged Archaeological Wood: A Comparison between Three Different Methodologies. *J. Cult. Herit.* **2018**, *30*, 51–56. [CrossRef]

17. Håfors, B.; Persson, U. Monitoring Changes in Water Content of the Vasa Wood with a Resistance Meter. In Proceedings of the 6th ICOM Group on Wet Organic Archaeological Materials Conference, York, UK, 9–13 September 1996; Schiffahrtsmuseum: Bremerhaven, Germany, 1997; pp. 35–45.
18. Piva, E. *Conservation of a Tudor Warship: Investigating the Timbers of the Mary Rose*; Mary Rose Trust: Portsmouth, UK, 2017.
19. Schofield, E.J. Illuminating the Past: X-ray Analysis of Our Cultural Heritage. *Nat. Rev. Mater.* **2018**, *3*, 285–287. [CrossRef]
20. Piva, E. Structural Conservation of the Tudor Warship Mary Rose. Ph.D. Thesis, University of Portsmouth, Portsmouth, UK, 2017.
21. Hocker, E.; Almkvist, G.; Sahlstedt, M. The Vasa Experience with Polyethylene Glycol: A Conservator's Perspective. *J. Cult. Herit.* **2012**, *13*, S175–S182. [CrossRef]
22. Babiński, L.; Izdebska-Mucha, D.; Waliszewska, B. Evaluation of the State of Preservation of Waterlogged Archaeological Wood Based on Its Physical Properties: Basic Density vs. Wood Substance Density. *J. Archaeol. Sci.* **2014**, *46*, 372–383. [CrossRef]
23. McConnachie, G. A Re-Evaluation of the Use of Maximum Moisture Content Data for Assessing the Condition of Waterlogged Archaeological Wood. *e-Preserv. Sci.* **2008**, *5*, 29–35.
24. Håfors, B. The Drying Pattern of the Outer Planking of the Wasa Hull. In Proceedings of the 2nd ICOM Waterlogged Wood Working Group Conference, Grenoble, France, 28–31 August 1984; Centre d'Étude et de Traitement des Bois Gorgés d'Eau: Grenoble, France, 1984; pp. 313–326.
25. Klügl, J.; Di Pietro, G. The Interaction of Water with Archaeological and Ethnographic Birch Bark and Its Effects on Swelling, Shrinkage and Deformations. *Herit. Sci.* **2021**, *9*, 3. [CrossRef]
26. Walsh, Z.; Janeček, E.-R.; Jones, M.; Scherman, O.A. Natural Polymers as Alternative Consolidants for the Preservation of Waterlogged Archaeological Wood. *Stud. Conserv.* **2017**, *62*, 173–183. [CrossRef]
27. Henrik-Klemens, Å.; Abrahamsson, K.; Björdal, C.; Walsh, A. An In Situ Raman Spectroscopic Method for Quantification of Polyethylene Glycol (PEG) in Waterlogged Archaeological Wood. *Holzforschung* **2020**, *74*, 1043–1051. [CrossRef]
28. Aluri, E.R.; Reynaud, C.; Bardas, H.; Piva, E.; Cibir, G.; Mosselmans, J.F.W.; Chadwick, A.V.; Schofield, E.J. The Formation of Chemical Degraders during the Conservation of a Wooden Tudor Shipwreck. *ChemPlusChem* **2020**, *85*, 1632–1638. [CrossRef] [PubMed]





## Article

# Chemical Properties and Microbial Analysis of Waterlogged Archaeological Wood from the Nanhai No. 1 Shipwreck

Yeqing Han <sup>1,†</sup>, Jing Du <sup>2,†</sup>, Xinduo Huang <sup>1</sup>, Kaixuan Ma <sup>1</sup>, Yu Wang <sup>1</sup>, Peifeng Guo <sup>1</sup>, Naisheng Li <sup>2</sup>, Zhiguo Zhang <sup>2</sup> and Jiao Pan <sup>1,\*</sup>

- <sup>1</sup> Ministry of Education Key Laboratory of Molecular Microbiology and Technology, Department of Microbiology, College of Life Sciences, Nankai University, Tianjin 300071, China; 2120191000@mail.nankai.edu.cn (Y.H.); 2120191084@mail.nankai.edu.cn (X.H.); makaixuan16@163.com (K.M.); 2120201036@mail.nankai.edu.cn (Y.W.); Gary19981114@163.com (P.G.)
- <sup>2</sup> National Center of Archaeology, Beijing 100020, China; ldusts@163.com (J.D.); lineas@126.com (N.L.); zzwgws@126.com (Z.Z.)
- \* Correspondence: panjiaonk@nankai.edu.cn
- † These authors contribute equal to this work.

**Abstract:** The Nanhai No. 1 was a wooden merchant ship of the Southern Song Dynasty, which wrecked and sank in the South China Sea, Yangjiang City, Guangdong Province, China. The Nanhai No. 1 shipwreck was salvaged as a whole in 2007 and began to be excavated in 2013. During the archaeology excavation, some of the hull wood fell off the hull. These waterlogged archaeological woods (WAW) were immersed in the buffer containing EDTA-2Na and isothiazolinone K100 for moisture stabilization, preliminary desalination, and microbial inhibition. We evaluated the properties of these WAW through testing the chemical components (including lignin, holocellulose, and ash content) of the wood, and monitoring the iron element content, anion and cation content in the buffer. At the same time, the microbial composition in the desalination buffer was also detected. The results showed that the holocellulose content in these WAW were much lower than in fresh wood. The ash content in these WAW decreased after desalination treatment. The iron element content, anion and cation content in the buffer were high and kept at a certain level after desalination treatment. At the same time, the problem of biodegradation in the buffer should be paid attention to. The comprehensive protection of WAW requires to combine wood properties and microbial problems. This study provides a reference for the protection of WAW from the Nanhai No. 1 shipwreck and other similar historical wood.

**Keywords:** Nanhai No. 1 shipwreck; waterlogged archaeological wood (WAW); wood properties; microbial composition



**Citation:** Han, Y.; Du, J.; Huang, X.; Ma, K.; Wang, Y.; Guo, P.; Li, N.; Zhang, Z.; Pan, J. Chemical Properties and Microbial Analysis of Waterlogged Archaeological Wood from the Nanhai No. 1 Shipwreck. *Forests* **2021**, *12*, 587. <https://doi.org/10.3390/f12050587>

Academic Editors: Magdalena Broda and Callum A. S. Hill

Received: 15 April 2021

Accepted: 6 May 2021

Published: 8 May 2021

**Publisher's Note:** MDPI stays neutral with regard to jurisdictional claims in published maps and institutional affiliations.



**Copyright:** © 2021 by the authors. Licensee MDPI, Basel, Switzerland. This article is an open access article distributed under the terms and conditions of the Creative Commons Attribution (CC BY) license (<https://creativecommons.org/licenses/by/4.0/>).

## 1. Introduction

The Nanhai No. 1 shipwreck was a wooden merchant ship of the Southern Song Dynasty (1127 to 1279 AD), which sank in the South China Sea in Guangdong province, China. After the Nanhai No. 1 shipwreck was salvaged as a whole out of the sea, it was placed in the Maritime Silk Road Museum [1]. Many precious cultural relics had been unearthed from the Nanhai No. 1 shipwreck. Among all the cultural relics from the Nanhai No. 1 shipwreck, the wooden hull cultural relic was the most precious and the most difficult to protect, not only because the Nanhai No. 1 shipwreck is huge in volume, but also because the corrosion degree of the hull was uneven. The excavation of the wooden hull cultural relics ran through the excavation of the Nanhai No. 1 shipwreck since 2013. Maritime wooden cultural relics had been immersed in seawater for a long time, and their preservation environment was closed, at a constant temperature, constant pressure, high salt, and oxygen deficient environment. When they were excavated, the preservation environment changed into an open environment where the temperature,

humidity and air circulation were not easy to control. Moreover, the control of oxidation, corrosion, microorganism biodegradation and other diseases would become extremely difficult. In order to maintain the stability of wooden cultural relics and control or delay the breeding and development of diseases, protection measures such as cleaning, moisturizing, desalination, reinforcement and anticorrosion and so on are usually taken. A series of scientific on-site protection measures laid the foundation for the transition from on-site protection of cultural relics to laboratory protection and restoration. During the excavation of the Nanhai No. 1 shipwreck, a large number of scattered individual pieces of wood were unearthed. After excavation, this hull wood was usually immersed in deionized water containing the metal chelating agent EDTA-2Na [2] and the antimicrobial agent isothiazolinone [3] for moisture stabilization, preliminary desalination, and microbial inhibition. At the same time, it is necessary to regularly monitor the water temperature, pH, concentration of main ions, conductivity, and microbial composition of the desalination buffer, and replace the desalination buffer regularly. The above treatment lays a solid foundation for the overall desalination, reinforcement, and protection of the hull in the later stage.

Wooden cultural relics are a carrier of ancient human civilization and represent a valuable material for the study of ancient history, art, science and technology, economy, and so on. Wooden cultural relics exist in many cultural sites, usually in the form of houses, tombs, hulls, decorations, and so on [4]. Wooden cultural relic can be divided into dry type and waterlogged type. In the original environment, the cellulose in the cell wall of waterlogged wooden cultural relics has been partially or completely degraded by bacteria or fungi. After the loss of degradation products, the structure of the cell wall becomes loose and even produces a large number of holes, and the original place of the cell wall is filled with water. This makes the moisture content of waterlogged archaeological wood (WAW) much higher than ordinary wood [5,6]. Generally, the moisture content of ordinary fresh wood is about 20%, while that of WAW can reach more than 500% [7,8]. The texture of WAW is fragile, so it is difficult to maintain a good condition after excavation. In general, WAW will be preserved in water after being excavated, and the temperature and humidity of the preservation environment will be as stable as possible. One is to maintain the moisture in the wood, so as to maintain the waterlogged state of the wooden cultural relic; the other is to cut off the air and avoid the further reproduction of aerobic microorganisms. The maritime wooden cultural relic is a kind of classic WAW. Due to long-term immersion in seawater, the intracellular electrolytes of maritime WAW have reached a full balance with seawater, and the wood contains a lot of salt. After the maritime WAW is excavated, many physical and chemical reactions will occur due to the change of environmental temperature and humidity, leading to the corrosion of wood. A high concentration of salts can degrade the fibers in WAW. When the environmental temperature and humidity change, some salts may crystallize and dissolve repeatedly, which will lead to fiber degradation and fracture. In addition, there are insoluble salts such as sulfur iron compounds in maritime WAW that easily oxidize into sulfuric acid during long-term exposure, leading to wood acidification and corrosion [2,9]. For example, in the protection of the Swedish warship *Vasa*, the problem of the acidity of wood and iron compounds in wood was highly apparent [10–12]. Research on the impact of biological pathways of iron and sulfur oxidation on the protection of the *Mary Rose* was also being studied [13]. At the same time, due to the large volume of maritime WAW, the desalination process is very slow. Therefore, it is necessary to carry out a long-term desalination treatment for maritime WAW to reduce its salt content.

During the preservation of maritime WAW, a variety of disease problems may occur. Therefore, it is necessary to regularly monitor the properties of wood, the nature of the desalination buffer, and microbial biodegradation, and replace the desalination buffer regularly. Once maritime WAW is excavated, it will come into contact with the surrounding environment, which may cause biodegradation problems. Biodegradation is mainly caused by microbial activities, mainly including bacteria and fungi, whose rapid growth and

secretion of secondary metabolites may lead to damage to cultural relics [14]. Wood is an excellent organic substrate for the growth of microorganisms [15]. There are many bacteria and fungi that can produce cellulolytic enzymes and ligninolytic enzymes [16–18]. Some researchers analyzed the bacterial community in 108 samples of WAW from different ages and identified a variety of bacteria [19]. The main disease microorganisms of the “Xiaobaijiao No. 1” shipwreck were erosion bacteria (EB) and tunneling bacteria (TB) [15]. EB and soft rot fungi were found to be active in WAW [20]. Therefore, it is necessary to comprehensively consider wood properties and microbial problems, in order to better solve various diseases of WAW.

## 2. Materials and Methods

### 2.1. Sample Collection

In this study, we mainly monitored monitoring tank 8 (NH.W2) in the archaeological excavation site of the Nanhai No. 1 shipwreck. The average annual temperature of the site is 25.6 °C and the average annual humidity is 84.1% [21]. The NH.W2 had a capacity of one cubic meter, and contained about 20 pieces of scattered wood of different sizes from the hull. Identified by archaeologists, the hull wood of the Nanhai No. 1 shipwreck was mainly *Pinus latteri* [22]. The scattered wood unearthed during the excavation were washed to remove the surface sea mud, and then gradually put into NH.W2 for preliminary desalination. In NH.W2, deionized water with 10mmol/LEDTA-2Na and 0.5% isothiazolinone K100 was used as the desalination buffer. The wood properties of the WAW in NH.W2 were detected in April and July 2019. The iron content of the desalination buffer in NH.W2 was detected in August and September 2019. The anion and cation content of the desalination buffer in NH.W2 was detected in May, June and October 2019. The microbial composition of the desalination buffer in NH.W2 was detected in November 2019 (Figure 1). In November 2019, the pH of the desalination buffer in NH.W2 was 4.83, and the water temperature was 20.8 °C. The desalination buffer was collected by 50 mL aseptic centrifuge tubes, then cryopreserved and transported to the laboratory.



**Figure 1.** Sampling picture of monitoring tank 8 (NH.W2) in November 2019.

### 2.2. Detection of Chemical Components in the Wood

The same piece of wood in NH.W2 was sampled in April and July 2019 to detect chemical components (including lignin, holocellulose, and ash content) in the wood. Then, the degradation degree and ash content of the WAW were evaluated by comparing with the content of lignin, holocellulose and ash in fresh *Pinus* wood. The content of lignin in wood was determined according to the method specified in the national standard GB/T 2677.8-94 (fibrous raw material—determination of acid-insoluble lignin) [23]. The content of holocellulose in wood was determined according to the method specified in national standard GB/T 2677.10-1995 (fibrous raw material—determination of holocellulose) [24]. The ash content of wood was determined according to the method specified in the national standard GB/T 2677.3-1993 (fibrous raw material—determination of ash) [25]. GB/T refers to the national standard of the people’s Republic of China.

### 2.3. Detection of Iron Element Content in the Buffer

The iron content of the desalination buffer in NH.W2 was detected in August and September 2019 to evaluate the removal effect of insoluble salts mainly composed of sulfur iron compounds. The iron content was detected by inductively coupled plasma mass spectrometer (ICP-MS) (Elan 9000, PerkinElmer, Waltham, MA, USA). Due to the high iron element in the desalination buffer, the sample needed to be pretreated. The water sample was diluted 1000 times with ultrapure water and filtered to prepare 2% HNO<sub>3</sub> aqueous solution for testing. The specific parameters were as follows: the scanning was performed 20 times, repeating three times; the sample injection washing time was 45 s with a reading delay time of 15 s, sample residence time of 50 ms in detector, sample injection pump speed of 26 r/min; the sample chamber vacuum was less than  $2 \times 10^{-7}$  PA; the protective gas was argon, gas pressure  $415 \pm 7$  kPa; the cooling water pressure was 45 to 65 kPa and the temperature was  $20 \pm 2$  °C.

### 2.4. Detection of Anion and Cation Content in the Buffer

The anion and cation content of the desalination buffer in NH.W2 were detected in May, June and October 2019 to evaluate the removal effect of soluble salts. The anion and cation ions include Na<sup>+</sup>, Cl<sup>-</sup>, and SO<sub>4</sub><sup>2-</sup>. The detection of anion and cation content used ion chromatography (IC) (HIC-10A super IC, Kyoto, Japan). Due to the high anion and cation content in the desalination buffer, the sample needed to be pretreated. The water sample was diluted 100 times with ultrapure water, filtered and injected for determination. The anion test conditions were as follows: eluent: 0.35 mmol/L Na<sub>2</sub>CO<sub>3</sub> solution, column temperature 45 °C, flow rate 0.8 mL/min, column pressure 11 MPa, injection volume 60 µL. The cation test conditions were as follows: eluent: 0.70 mmol/L H<sub>2</sub>SO<sub>4</sub> solution, column temperature 40 °C, flow rate 1.0 mL/min, column pressure 3.7 MPa, injection volume 60 µL. The standard samples of Na<sup>+</sup>, Cl<sup>-</sup>, and SO<sub>4</sub><sup>2-</sup> were all 100 mg/L. Na<sub>2</sub>CO<sub>3</sub> and H<sub>2</sub>SO<sub>4</sub> were both analytically pure.

### 2.5. Total DNA Extractions and High-Throughput Sequencing

The microbial composition of the desalination buffer in NH.W2 was detected in November 2019 to evaluate the biodegradation problem in the desalination buffer. The water sample total DNA was extracted using DNeasy PowerWater Kit (QIAGEN, Hilden, Germany). The total DNA was sent to Novogene Genome Sequencing Company for high-throughput sequencing. We analyzed the 16SV4 region (bacteria) and ITS1-5F region (fungi) to comprehensively detect the microbial composition in the desalination buffer.

## 3. Results

### 3.1. Analysis of Chemical Components in the Wood

The contents of lignin, holocellulose and ash are shown in Table 1. According to literature reports, in fresh *Pinus* wood, the lignin content is generally about 25%, the holocellulose content is generally about 75%, and the ash content is generally less than 1% [26,27]. Through comparison, it can be found that the holocellulose content was much lower than that of fresh wood, while the ash content was higher than that of fresh wood. Since most of the cellulose had been degraded and lignin is difficult to degrade, the percentage of lignin in the wood has increased to 63%. Therefore, the wood degradation degree of WAW from the Nanhai No. 1 shipwreck was high, and the ash content of the WAW was high. In addition, the changes of lignin and holocellulose contents in April and July 2019 were not obvious, indicating that the degradation of the WAW became slow during the desalination. The ash content in July 2019 was significantly lower than that in April 2019, indicating that some inorganic salt ions were slowly removed after immersion in desalination buffer.

**Table 1.** Lignin, holocellulose, and ash content of WAW in NH.W2 in April and July 2019.

	Lignin Content (%)	Holocellulose Content (%)	Ash Content (%)
20 April 2019	61.32	4.72	13.02
12 July 2019	64.96	4.43	3.86
Mean Value	63.14	4.575	8.44

### 3.2. Analysis of Iron Element Content in the Buffer

The iron contents of the desalination buffer are shown in Table 2. We found that the iron content in the desalination buffer increased significantly after one month of the desalination treatment. The results showed that some insoluble salts mainly composed of sulfur iron compounds in WAW could be removed slowly after soaking in desalination treatment.

**Table 2.** Iron element content of the desalination buffer in NH.W2 in August and September 2019.

	Iron Element Content (g/L)
1 August 2019	127.23
10 September 2019	611.47

### 3.3. Analysis of Anion and Cation Content in the Buffer

The anion and cation content of the desalination buffer are shown in Table 3. In the original desalination buffer,  $\text{Cl}^-$  and  $\text{SO}_4^{2-}$  did not exist. The  $\text{Na}^+$  in the original desalination buffer mainly existed in EDTA-2Na, and the content of original  $\text{Na}^+$  was 460 mg/L. We found that after immersion in the desalination buffer, the contents of  $\text{Na}^+$ ,  $\text{Cl}^-$  and  $\text{SO}_4^{2-}$  in the desalination buffer were significantly higher than those in the original desalination buffer. Moreover, the contents of  $\text{Na}^+$ ,  $\text{Cl}^-$  and  $\text{SO}_4^{2-}$  tended to be stable after a period of desalination treatment. The results showed that the soluble salt in WAW was gradually removed after immersion in the desalination buffer.

**Table 3.** Anion and cation content of the desalination buffer in NH.W2 in May, June and October 2019.

	$\text{Na}^+$ Content (mg/L)	$\text{Cl}^-$ Content (mg/L)	$\text{SO}_4^{2-}$ Content (mg/L)
29 May 2019	786.30	386.12	162.23
28 June 2019	745.33	512.67	219.22
22 October 2019	786.30	396.81	170.95

### 3.4. Microbial Diversity Analysis by High-Throughput Sequencing

We detected the microbial composition of the desalination buffer in NH.W2 in November 2019. Figure 2a,b show the composition and proportion of bacteria in NH.W2 desalination buffer. Figure 2a represents the distribution of the bacteria at the phylum level. The results show that at the phylum level, Proteobacteria accounts for the largest proportion, accounting for 71.95%. This is followed by Firmicutes and Actinobacteria, accounting for 13.90% and 10.04%, respectively. Figure 2b and Table 4 represent the distribution of the bacteria at the genus level. We found that at the genus level, the most abundant bacteria is *Pseudomonas*, accounting for 34.06%. Followed by *Methylobacillus* and *Pandoraea*, accounting for 11.33% and 7.25%, respectively. In addition, there are unidentified *Mitochondria*, *Microbacterium*, *Agromyces*, *Leifsonia*, and *Escherichia-Shigella*. Figure 2c,d show the composition and proportion of fungi in NH.W2 desalination buffer. Figure 2c represents the distribution of the fungi at the phylum level. The results show that at the phylum level, Basidiomycota accounts for the largest proportion, accounting for 99.63%, followed by Ascomycota, accounting for 0.25%. Figure 2d and Table 4 represent the distribution of the fungi at the genus level. We found that at the genus level, the most abundant fungi is *Cutaneotrichosporon*, accounting for 99.59%, followed by *Fusarium* and *Cryptococcus*, accounting for 0.18% and 0.03%, respectively.

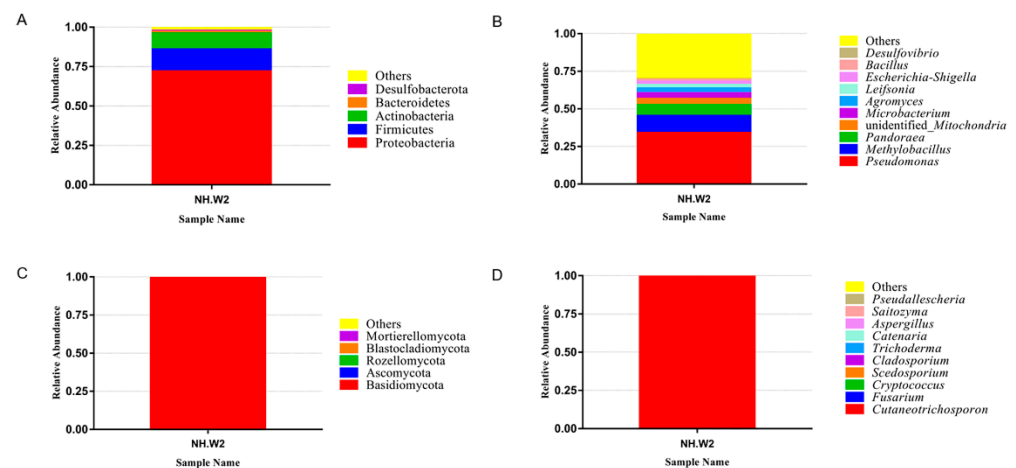


**Figure 2.** The relative abundance of microbial communities in monitoring tank 8 (NH. W2). The relative abundance is shown as a percentage. Phylum and genera are colored according to the legend on the right. (A) Relative abundance of bacteria at phylum level. (B) Relative abundance of bacteria at genera level. (C) Relative abundance of fungi at phylum level. (D) Relative abundance of fungi at genera level.

**Table 4.** Relative abundance of dominant bacteria and dominant fungi of the desalination buffer in the NH.W2 at the genus level.

Dominant Bacteria Genus (%)		Dominant Fungi Genus (%)	
<i>Pseudomonas</i>	34.06	<i>Cutaneotrichosporon</i>	99.59
<i>Methylobacillus</i>	11.33	<i>Fusarium</i>	0.18
<i>Pandoraea</i>	7.25	<i>Cryptococcus</i>	0.03
unidentified_Mitochondria	3.99	<i>Scenedosporium</i>	0.01
<i>Microbacterium</i>	3.75	<i>Cladosporium</i>	0.01
<i>Agromyces</i>	3.12	<i>Trichoderma</i>	0.01
<i>Leifsonia</i>	2.53	<i>Catenaria</i>	0.01
<i>Escherichia-Shigella</i>	2.09	<i>Aspergillus</i>	0.01
<i>Bacillus</i>	1.18	<i>Saitozyma</i>	0.01
<i>Desulfovibrio</i>	0.42	<i>Pseudallescheria</i>	0.00
Others	30.28	Others	0.16

#### 4. Discussion

The Nanhai No. 1 shipwreck is a complex organism, and its excavation and protection represent a great challenge. In this study, we monitored monitoring tank 8 (NH.W2), where the scattered wood was stored in the archaeological excavation site of the Nanhai No. 1 shipwreck. It mainly included the chemical components (including lignin, holocellulose, and ash content) of the wood, the iron element content, anion and cation content in the desalination buffer, and the microbial composition in the desalination buffer. Through the analysis of the above data, a preliminary evaluation is made on the preservation status of WAW from the Nanhai No. 1 shipwreck, which provides data support for the protection of the No. 1 shipwreck in the later stage.

Through the detection, we have drawn the following conclusions: (1) compared with fresh wood, the degradation degree of cellulose in WAW was higher, and the ash content in WAW was higher. The degradation of WAW became slow during the desalination treatment. After immersion in desalination buffer, some inorganic salt ions in WAW were removed slowly. (2) After immersion in the desalination buffer, the iron content in the desalination buffer increased significantly. It showed that some insoluble salts mainly composed of iron compounds in WAW could be removed slowly after soaking in desalination treatment. (3) After immersion in the desalination buffer, the contents of  $\text{Na}^+$ ,  $\text{Cl}^-$  and  $\text{SO}_4^{2-}$  in the desalination buffer were significantly higher than those in the original desalination buffer.

Moreover, the contents of  $\text{Na}^+$ ,  $\text{Cl}^-$  and  $\text{SO}_4^{2-}$  tended to be stable after a period of the desalination treatment. The results showed that the soluble salt in WAW was gradually removed after immersion in desalination buffer. (4) The high-throughput sequencing results of the desalination buffer showed that at the bacteria phylum level, Proteobacteria accounts for the largest proportion, accounting for 71.95%. At the bacteria genus level, the most abundant bacteria is *Pseudomonas*, accounting for 34.06%. At the fungi phylum level, Basidiomycota accounts for the largest proportion, accounting for 99.63%. At the fungi genus level, the most abundant fungi is *Cutaneotrichosporon*, accounting for 99.59%.

At the initial stage of the excavation of the Nanhai No. 1 shipwreck, archaeologists carried out a preliminary test on the wood properties of the Nanhai No. 1 shipwreck. The Nanhai No. 1 shipwreck used different species of wood in each part of the hull, and it was found that the main wood was *Pinus latteri* [22]. The average moisture content of wood was 300 to 700%, which indicated moderate and severe corrosion. After analyzing the chemical composition of the wood, it was found that the content of cellulose and hemicellulose in the wood was much lower than that in fresh wood, which indicated that the degree of decay of the wood was high. The ash content in the wood was much higher than that in normal wood, indicating that the salt content in the wood was higher. The salt composition in the hull wood was analyzed, and it was found that there were soluble salts mainly composed of NaCl and insoluble salts mainly composed of sulfur iron compounds, and the content of  $\text{Na}^+$ ,  $\text{Cl}^-$  and  $\text{SO}_4^{2-}$  were high. The pH of hull wood was between 6 and 7, which belonged to neutral and weak acidity. Combined with the results of this research, we can preliminarily evaluate the preservation status of WAW from the Nanhai No. 1 shipwreck. By storing the WAW in the desalination buffer, the progress of wood degradation may be slowed down to a certain extent, and most of the soluble salt and a small part of the slightly soluble salt can be removed slowly.

In this study, we detected the microbial composition in the desalination buffer. The pH of the desalination buffer was 4.83 and the water temperature was 20.8 °C. *Pseudomonas* and *Cutaneotrichosporon* were the most abundant bacteria and fungi in NH.W2 desalination buffer, respectively. *Pseudomonas* is a common bacterium; it likes to live in humid environments, it grows well in acidic environments [28], and has a high salt tolerance [29]. *Pseudomonas* may participate in the metabolism of sulfur and iron [30,31] and has the ability to degrade cellulose and lignin [32]. *Cutaneotrichosporon* is a kind of yeast with a wide living environment [33] and is often isolated from clinical samples [34]. *Cutaneotrichosporon* has a certain resistance to antifungal drugs, and has a certain acid resistance, high salt tolerance and metal tolerance [35–37]. The ability of microorganisms to destroy wood is determined by a variety of parameters, including the interaction between various organisms, as well as environmental temperature and humidity and other factors [38–40]. Therefore, the biodegradation problem of wooden cultural relics needs to be paid great attention.

## 5. Conclusions

To sum up, the preservation status of WAW from the Nanhai No. 1 shipwreck was comprehensively analyzed and evaluated through the detection of the properties of WAW and the detection of the desalination buffer. This study provides data support for the overall protection of the Nanhai No. 1 shipwreck in the later stage and provides a reference for the protection of other WAW.

**Author Contributions:** Conceptualization, J.P.; Data curation, J.D., X.H., K.M., Y.W. and P.G.; Resources, N.L. and Z.Z.; Writing—original draft, Y.H.; Writing—review and editing, J.P. All authors have read and agreed to the published version of the manuscript.

**Funding:** This research was funded by Natural Science Foundation of Tianjin (19JCZDJC33700) and National Key R&D Program of China [2020YFC1521800].

**Institutional Review Board Statement:** Not applicable.

**Informed Consent Statement:** Not applicable.



**Data Availability Statement:** The raw high-throughput sequencing data can be downloaded at the NCBI Sequence Read Archive (SRA) with the study accession number PRJNA721031.

**Acknowledgments:** We gratefully acknowledge the assistance of Dawa Shen from Chinese Academy of Cultural Heritage.

**Conflicts of Interest:** The authors declare no conflict of interest. The funders had no role in the design of the study; in the collection, analyses, or interpretation of data; in the writing of the manuscript, or in the decision to publish the results.

## References

- Wei, J. 2007 whole salvage of “Nanhai No. 1”. *China Cult. Herit.* **2007**, *4*, 21–30.
- Zhang, Z.; Li, N.; Tian, X.; Liu, J.; Shen, D. Research on the removal of the iron sulfides in the Qing Dynasty marine shipwreck, Ningbo Xiaobaijiao No. 1. *Sci. Conserv. Archaeol.* **2014**, *26*, 30–38.
- Ji, H.; Zhang, L.; Liu, J.; Wang, F. Progress on Analytical Method for Isothiazolinone Derivatives Used as Industrial Biocides. *Chem. Reag.* **2016**, *38*, 523–527.
- Zheng, L.; He, Y.; Wang, Y. Study of the Restoration of Rotten Handed-down Wooden Cultural Relics. *Huaxia Archaeol.* **2012**, *003*, 136–140.
- Björdal, C.G.; Nilsson, T.; Daniel, G. Microbial decay of waterlogged archaeological wood found in Sweden-Applicable to archaeology and conservation. *Int. Biodeterior. Biodegrad.* **1999**, *43*, 63–73. [CrossRef]
- Capretti, C.; Macchioni, N.; Pizzo, B.; Galotta, G.; Giachi, G.; Giampaola, D. The characterization of waterlogged archaeological wood: The three roman ships found in Naples (Italy). *Archaeometry* **2008**, *50*, 855–876. [CrossRef]
- Chen, H. Research on the correlation between water content and basic density of waterlogged wooden cultural relics. *Identif. Apprec. Cult. Relics* **2017**, *11*, 86–88.
- Li, G.; Zeng, L.; Chen, C. Study on the equilibrium water content of three kinds of hull wood of Song Dynasty ships in Quanzhou Bay and 14 kinds of modern wood in Quanzhou area. *J. Fujian Coll. For.* **1984**, *1*, 49–59.
- Hocker, E. From the Micro- to the Macro-: Managing the Conservation of the Warship, Vasa. *Macromol. Symp.* **2010**, *238*, 16–21. [CrossRef]
- Chelazzi, D.; Giorgi, R.; Baglioni, P. Nanotechnology for Vasa Wood De-Acidification. *Macromol. Symp.* **2010**, *238*, 30–36. [CrossRef]
- Giorgi, R.; Chelazzi, D.; Baglioni, P. Conservation of acid waterlogged shipwrecks: Nanotechnologies for de-acidification. *Appl. Phys. A* **2006**, *83*, 567–571. [CrossRef]
- Almkvist, G.; Persson, I. Extraction of iron compounds from wood from the Vasa. *Holzforschung* **2006**, *66*, 1125–1684. [CrossRef]
- Joanne, P.; Smith, A.D.; Schofield, E.J.; Chadwick, A.V.; Jones, M.A.; Watts, J.E.M. The Effects of Mary Rose Conservation Treatment on Iron Oxidation Processes and Microbial Communities Contributing to Acid Production in Marine Archaeological Timbers. *PLoS ONE* **2014**, *9*, 1–8. [CrossRef]
- Sterflinger, K.; Guadalupe, P. Microbial deterioration of cultural heritage and works of art—Tilting at windmills? *Appl. Microbiol. Biotechnol.* **2013**, *97*. [CrossRef] [PubMed]
- Gao, M.; Zhang, Q.; Jin, T.; Luo, P.; Li, Q.; Xu, R. Observation and damage assessment of microbial diseases in some wooden cultural relics from the ancient marine shipwreck, Ningbo Xiaobaijiao No. 1. *Sci. Conserv. Archaeol.* **2017**, *29*, 102–111.
- Lee, R.L.; Paul, J.W.; Willem, H.v.Z.; Isak, S. Pretorius. Microbial Cellulose Utilization: Fundamentals and Biotechnology. *Microbiol. Mol. Biol. Rev.* **2002**, *66*, 506–577. [CrossRef]
- Sánchez, C. Lignocellulosic residues: Biodegradation and bioconversion by fungi. *Biotechnol. Adv.* **2009**, *27*, 185–194. [CrossRef]
- OSMAN, M.E.-S.; EL-SHAPHY, A.A.E.-N.; MELIGY, D.A.; AYID, M.M. Survey for fungal decaying archaeological wood and their enzymatic activity. *Int. J. Conserv. Sci.* **2014**, *5*, 295–308.
- Eleanor, T.L.; Julian, I.M.; Hotchkiss, S.; Eaton, R.A. Bacterial diversity associated with archaeological waterlogged wood: Ribosomal RNA clone libraries and denaturing gradient gel electrophoresis (DGGE). *Int. Biodeterior. Biodegrad.* **2008**, *61*, 106–116. [CrossRef]
- Björdal, C.G. Microbial degradation of waterlogged archaeological wood. *J. Cult. Herit.* **2012**, *13S*, S118–S122. [CrossRef]
- Liu, Z.; Fu, T.; Hu, C.; Shen, D.; Macchioni, N.; Sozzi, L.; Chen, Y.; Liu, J.; Tian, X.; Ge, Q.; et al. Microbial community analysis and biodeterioration of waterlogged archaeological wood from the Nanhai No. 1 shipwreck during storage. *Sci. Rep.* **2018**, *8*, 7170. [CrossRef] [PubMed]
- Li, N.; Chen, Y.; Shen, D. *Study on the Protection of the Excavation Site of the Nanhai No. 1 Shipwreck (2014–2016)*; Science Press: Beijing, China, 2017; pp. 124–133.
- Chen, Y.; Zhang, X.; Lei, Y.; Shi, X. Microstructure and chemical composition of wheat straw. *J. Northwest. A&F Univ.* **2015**, *2*, 179.
- Jiao, S. Study on the Quality of Timber and Bamboo Wood by Chemometrics and Near Infrared Spectroscopy Methods. Master’s Thesis, Capital Normal University, Beijing, China, 2009; p. 5.
- Ministry of Light Industry of the People’s Republic of China. Fibrous Raw Material—Determination of Ash GB/T 2677.3-1993. 1 March 1993. Available online: <http://www.csres.com/detail/64292.html> (accessed on 10 April 2021).
- Kim, B. Chemical Characteristics of Waterlogged Archaeological Wood. *Holzforschung* **1990**, *44*, 169–172. [CrossRef]

27. Passialis, C.N. Physico-Chemical Characteristics of Waterlogged Archaeological Wood. *Holzforschung* **1997**, *51*, 111–113. [CrossRef]
28. Dejsirilert, S.; Kondo, E.; Chiewsilp, D.; Kanai, K. Growth and survival of *Pseudomonas pseudomallei* in acidic environments. *Jpn. J. Med. Sci. Biol.* **1991**, *44*, 63. [CrossRef]
29. Kawaguchi, A.; Akazawa, T.; Sakai, M.; Kanazawa, S. Role of Ca Resistance in Competitive Survival of Fluorescent *Pseudomonads* in Soil with High Salinity. *J. Fac. Agric.-Kyushu Univ.* **2003**, *48*, 113–119. (In Japanese) [CrossRef]
30. Zhao, R.; Zhao, S.; He, H. Factors influencing production of siderophore from *Pseudomonas* C-12. *Guizhou Agric. Sci.* **2013**, *41*, 112–114.
31. Sultan, S.; Faisal, M. Isolation and Characterization of Iron and Sulfur Oxidizing Bacteria from Coal Mines. *J. Environ. Earth Sci.* **2016**, *6*, 153–157.
32. Yang, C.; Yue, F.; Cui, Y.; Xu, Y.; Shan, Y.; Liu, B.; Zhou, Y.; Lü, X. Biodegradation of lignin by *Pseudomonas* sp. Q18 and the characterization of a novel bacterial DyP-type peroxidase. *J. Ind. Microbiol. Biotechnol.* **2018**, *45*, 913–927. [CrossRef]
33. Hofmeyer, T.; Hackenschmidt, S.; Nadler, F.; Thürmer, A.; Daniel, R.; Kabisch, J. Draft Genome Sequence of *Cutaneotrichosporon curvatus* DSM 101032 (Formerly *Cryptococcus curvatus*), an Oleaginous Yeast Producing Polyunsaturated Fatty Acids. *Genome Announc.* **2016**, *4*, e00362-16. [CrossRef]
34. Tjomme, V.D.B.; Anna, K.; Bart, T.; Kwakkel-Van, E.J.M.; Bert, A.; Teun, B. *Cutaneotrichosporon* (*Cryptococcus*) *cyanovorans*, a basidiomycetous yeast, isolated from the airways of cystic fibrosis patients. *Med. Mycol. Case Rep.* **2018**, *22*, 18–20. [CrossRef]
35. Pagani, D.M.; Heidrich, D.; Paulino, G.V.B.; Alves, K.D.O.; Dalbem, P.T.; Oliveira, C.F.D.; Andrade, Z.M.M.; Sliva, C.; Correia, M.D.; Scroferneker, M.L.; et al. Susceptibility to antifungal agents and enzymatic activity of *Candida haemulonii* and *Cutaneotrichosporon dermatitis* isolated from soft corals on the Brazilian reefs. *Arch. Microbiol.* **2016**. [CrossRef] [PubMed]
36. Liu, S.; Chen, Y.; Hong, W.; Wu, Q.; Lu, C.; Liu, A. Screening and identification of an oxytetracycline degradation strain resistant to Cu<sup>2+</sup> and Zn<sup>2+</sup> and its characteristics. *J. South. China Agric. Univ.* **2020**, *41*, 56–62.
37. Su, J.; Feng, X.; Gulsimay, A.; Erkin, R.; Muhtar, A. Examination of pH Tolerance Test of Two Alkalitolerant Yeasts. *Microbiology* **2007**, *6*, 11.
38. Setälä, H.; Mclean, M.A. Decomposition rate of organic substrates in relation to the species diversity of soil saprophytic fungi. *Oecologia* **2004**, *139*, 98–107. [CrossRef]
39. Hunt, D. Properties of wood in the conservation of historical wooden artifacts. *J. Cult. Herit.* **2012**, *13*, S10–S15. [CrossRef]
40. Pietikäinen, J.; Marie, P.; Bååth, E. Comparison of temperature effects on soil respiration and bacterial and fungal growth rates. *FEMS Microbiol. Ecol.* **2004**, *1*, 49–58. [CrossRef]



## Article

# Interactions between Different Organosilicons and Archaeological Waterlogged Wood Evaluated by Infrared Spectroscopy

Carmen-Mihaela Popescu <sup>1,2</sup>  and Magdalena Broda <sup>3,4,\*</sup> 

- <sup>1</sup> Petru Poni Institute of Macromolecular Chemistry of Romanian Academy, 700487 Iasi, Romania; mihapop@icmpp.ro
- <sup>2</sup> Centre of Wood Science and Technology, Edinburgh Napier University, Edinburgh EH11 4BN, UK
- <sup>3</sup> Department of Wood Science and Thermal Techniques, Faculty of Forestry and Wood Technology, Poznań University of Life Sciences, Wojska Polskiego 38/42, 60-637 Poznań, Poland
- <sup>4</sup> BioComposites Centre, Bangor University, Deiniol Road, Bangor, Gwynedd LL57 2UW, UK
- \* Correspondence: magdalena.broda@up.poznan.pl

**Abstract:** The goal of the study was to characterise chemical interactions between waterlogged archaeological wood and organosilicon compounds applied for its conservation to shed lights on the mechanism of wood dimensional stabilisation by the chemicals. Two alkoxysilanes (methyltrimethoxysilane and (3-mercaptopropyl) trimethoxysilane) and a siloxane (1,3-bis(diethylamino)-3-propoxypropanol)-1,1,3,3-tetramethyldisiloxane) were selected for the research since they already have been proven to effectively stabilise waterlogged wood upon drying. Fourier transform infrared spectroscopy was used for structural characterisation of the degraded wood and evaluation of reactivity of the applied chemicals with polymers in the wooden cell wall. The results obtained clearly show much stronger interactions in the case of alkoxysilanes than the siloxane, suggesting a different mechanism of wood stabilisation by these compounds. The results of this study together with other data obtained in our previous research on stabilisation of waterlogged archaeological wood with organosilicon compounds allow the conclusion that the mechanism of waterlogged wood stabilisation by the used alkoxysilanes is based on bulking the cell wall by silane molecules and wood chemical modification, while in the case of the applied siloxane, it builds upon filling the cell lumina.

**Keywords:** archaeological wood; degraded wood; silane; FT-IR; alkoxysilanes; wood-silane interactions; wood stabilisation; wood conservation; silane treatment



**Citation:** Popescu, C.-M.; Broda, M. Interactions between Different Organosilicons and Archaeological Waterlogged Wood Evaluated by Infrared Spectroscopy. *Forests* **2021**, *12*, 268. <https://doi.org/10.3390/f12030268>

Academic Editor: Angela Lo Monaco

Received: 2 February 2021

Accepted: 22 February 2021

Published: 26 February 2021

**Publisher's Note:** MDPI stays neutral with regard to jurisdictional claims in published maps and institutional affiliations.



**Copyright:** © 2021 by the authors. Licensee MDPI, Basel, Switzerland. This article is an open access article distributed under the terms and conditions of the Creative Commons Attribution (CC BY) license (<https://creativecommons.org/licenses/by/4.0/>).

## 1. Introduction

Organosilicon compounds are chemicals containing a silicon atom and carbon–silicon bonds. Differing in the molecular weight, size and shape of molecules as well as the type of the side chain, they have found numerous applications in a broad range of industries, including the pharmaceutical, cosmetic, medical, chemical, food, agricultural, building, automobile, textile or paper industries. Most common are binding agents and adhesives, sealants, adjuvants, coatings or surface modifiers produced from organosilicons [1–6].

Due to the specific chemical structure and the resulting properties, the alkoxysilanes (particularly trialkoxysilanes) are the most frequently used organosilicon compounds. They are bifunctional chemicals containing alkoxy groups and organic groups (i.e., alkyl, fluoroalkyl, aminoalkyl, phenyl, thiol, hydroxyl, hydrogen, vinyl) which provide the specific functionality [3,7]. Alkoxy groups are easily hydrolysed in the presence of water. The resulting silanols are very reactive and condense readily, forming new covalent Si–O–Si bonds between silane monomers. A series of subsequent hydrolysis and condensation reactions, called the sol-gel process, leads to the formation of linear or spatial polymers [8,9]. Silanols can not only crosslink with the neighbouring molecules, but also react with hydroxyl groups of wood components by establishing siloxy bonds (Si–O–C) [10,11]. All

the above features make alkoxysilanes very useful for modification of wood and wood-based products. They have so far been applied to increase wood durability against fungi and termites, limit leachability of other wood preservatives, improve wood weathering performance, reduce its flammability and hydrophilicity, or as coupling agents to improve bonding strength in various composites [12–17]. They have also proved to penetrate and bulk the cell wall, forming a three-dimensional network of polysiloxane and wood polymers which improves dimensional wood stability [8,13,18]. Therefore, they were also tried for archaeological waterlogged wood conservation, and some of them proved effective in stabilisation of wood dimensions upon drying, which is one of the most crucial issues related to conservation of this type of wood [19–22]. However, the method still requires further study, e.g., on the mechanical properties of the treated wood, the influence of the chemicals on wood colour, gloss and texture, or their long-term effect on wood before it could be proposed as a reliable conservation method.

The results of the research by Broda et al. [21,22] clearly showed that the stabilisation effect on waterlogged wood depends mainly on the type of an organic group attached to a silicon atom in organosilicons. Great dimensional stabilisation of waterlogged wood was obtained among other things due to methyltrimethoxysilane (MTMS), (3-mercaptopropyl) trimethoxysilane (MPTES) and 1,3-bis(diethylamino)-3-propoxypropanol-1,1,3,3-tetramethyldisiloxane (DEAPTMS) treatment, reaching anti-shrink efficiency values of about 81%, 98% and 90%, respectively. The chemicals applied vary in the effectiveness of wood stabilisation, as well as in the chemical structure. But in general, they represent two groups of organosilicons tested in our research on waterlogged wood stabilisation: alkoxysilanes (MTMS and MPTES) and siloxanes (DEAPTMS). Therefore, as representative and the most effective ones, they were selected for further study on their reactivity with wood as this is considered one of the factors presumably affecting their stabilisation efficiency. Gaining this knowledge is the first step towards understanding the full mechanism of waterlogged wood stabilisation by organosilicon compounds, and it will be necessary to explain the results of different ongoing and future mechanical tests performed on untreated and treated wood.

Fourier transform infrared spectroscopy (FT-IR) is a fast, simple and sensitive method for the structural characterisation of many different materials, including wood. It has already been used for qualitative and quantitative evaluation of main wood components [23] or to study chemical and structural changes in wood polymers during biodegradation and weathering [24–26]. As the method requires only a small amount of the studied material, the technique proved to be useful for research on historical wooden objects. It allows, i.e., the evaluation of the extent of archaeological wood deterioration, the effectiveness of penetration and potential reactivity of conservation agents with wood or the monitoring of the impregnation agent polymerisation during the conservation process [27–31].

The aim of the present study is to characterise the reactivity of three organosilicon compounds differing in the chemical structure and type of the organic groups (methyltrimethoxysilane, (3-mercaptopropyl) trimethoxysilane and 1,3-bis(diethylamino)-3-propoxypropanol-1,1,3,3-tetramethyldisiloxane) with archaeological waterlogged elm wood by using the infrared spectroscopy method in order to understand better their ability to stabilise dimensions of waterlogged wood upon drying. Moreover, the evaluation of the chemical composition of the waterlogged elm was performed to assess the extent of its degradation.

## 2. Materials and Methods

### 2.1. Materials

Waterlogged archaeological elm (*Ulmus* spp.) wood, dated back to the 10–11th centuries (Figure 1), along with fresh-cut elm wood as a reference, were used in this study. The archaeological elm log was excavated from the Lednica Lake (Greater Poland Voivodeship, Poland), where it was buried in the bottom sediments near the remains of the medieval bridge named “Poznań” connecting the medieval stronghold on the Ostrów Lednicki island with a road leading to Poznań city. The degree of wood degradation was severe, with

maximum wood moisture content ( $MC_{max}$ ) of 425%, the wood basic density of  $160 \text{ kg/m}^3$ , loss of wood substance calculated to be 70%, and cellulose content reduced to about 5% (calculated as a percentage of the oven-dried mass of wood before degradation) [20].



**Figure 1.** Waterlogged elm (*Ulmus* spp.) wood excavated from the Lednica Lake (dated back to the 10–11th centuries).

For the present study, small cuboid samples with dimensions of  $20 \times 20 \times 10 \text{ mm}^3$  (in the tangential, radial and longitudinal direction, respectively) were cut out from the log, dehydrated in 96% ethanol for four weeks and divided into four sets (five specimens for each set). One set remained untreated, while the other three were treated with different organosilicon compounds: methyltrimethoxysilane (MTMS-1), (3-mercaptopropyl)trimethoxy silane (MPTES-2) and 1,3-bis(diethylamino)-3-propoxypropanol)-1,1,3,3-tetramethyldisiloxane (DEAPTMS-3) (Figure 2), using the oscillated vacuum–pressure method as described before [20].

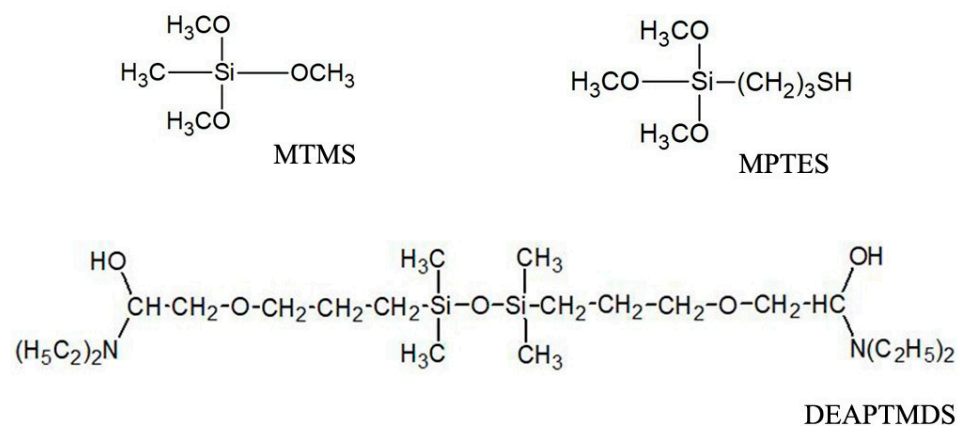


**Figure 2.** Chemical structure of organosilicons selected for the research.

All the samples (treated and untreated) were air-dried for two weeks, then powdered and sieved, and the fraction with an average diameter less than 0.2 mm was retained for further analyses.

## 2.2. Methods

### 2.2.1. Scanning Electron Microscopy

The microstructure of untreated and treated wood was analysed using a scanning electron microscope (SEM) JEOL 7001F (Tokyo, Japan) with a Secondary Electron Imaging (SEI) detector (JEOL, Tokyo, Japan). The samples were air-dried, cut into smaller pieces and thoroughly cleaned from remaining dust and wooden particles by purging with nitrogen. Such prepared specimens were then coated for 240 s with a thin layer of chromium, mounted in the specimen holder and analysed. Imaging was performed at 1 kV or 5 kV accelerating voltage, depending on a wood sample.

### 2.2.2. Fourier Transform Infrared Spectroscopy

The infrared spectra of fresh-cut elm, untreated and treated archaeological elm wood samples, as well as for pure silanes were recorded in KBr tablets on a Bruker ALPHA FT-IR spectrometer (Bruker, Billerica, MA, USA), with a resolution of  $4\text{ cm}^{-1}$  using the  $4000\text{--}400\text{ cm}^{-1}$  spectral range. The concentration in the tablets was constant: 2 mg of powdered sample and 200 mg KBr. For spectral processing, the Grams 9.1 software (Thermo Fisher Scientific, Waltham, MA, USA) was used. Five recordings were performed for each analysed sample, and the average spectrum obtained was used for the evaluation.

Principal component analysis (PCA) is a multivariate statistical technique which is usually used to extract the systematic variance in a data set. The outputs are represented by the PC scores and PC loadings. To perform PCA the pre-processed infrared spectra of the untreated contemporary and archaeological as well as treated wood were used.

## 3. Results and Discussion

### 3.1. Structural Evaluation of Archaeological Elm Wood

Infrared spectra and their second derivatives for the reference (fresh cut elm wood) and archaeological elm samples are presented in Figure 3. The spectra generally present two main regions:  $3800\text{--}2700\text{ cm}^{-1}$  (Figure 3a) assigned to  $\text{--OH}$  groups involved in inter- and intramolecular hydrogen bonds, as well as free  $\text{--OH}$  groups and methyl, methylene groups stretching vibrations, and  $1830\text{--}800\text{ cm}^{-1}$  (Figure 3b), assigned to different stretching and deformation vibrations of the groups related to the main wood components, also called the fingerprint region.

From Figure 3a, the differences between the control and archaeological wood are observable, especially in the second derivative spectra. The bands from  $3522/3520\text{ (1) cm}^{-1}$ ,  $3070\text{ (2) cm}^{-1}$ ,  $3017/3010\text{ (3) cm}^{-1}$ ,  $2926/2932\text{ (4) cm}^{-1}$ ,  $2884/2881\text{ (5) cm}^{-1}$  and  $2853/2844\text{ (6) cm}^{-1}$  increase in intensity in the spectrum of the archaeological sample. These bands are assigned to free OH(6) and OH(2) in cellulose, weakly absorbed water, but also to the intramolecular hydrogen bond in a phenolic group (in lignin), to the multiple formation of an intermolecular hydrogen bond between biphenol and other phenolic groups in lignin, and to the symmetric and antisymmetric stretching vibration of methyl and methylene groups. There is also a strong shifting of the band from  $3431$  to  $3419\text{ cm}^{-1}$  assigned to the  $\text{O(2)H} \dots \text{O(6)}$  intramolecular hydrogen bonds and this comes from the crystalline regions in cellulose.

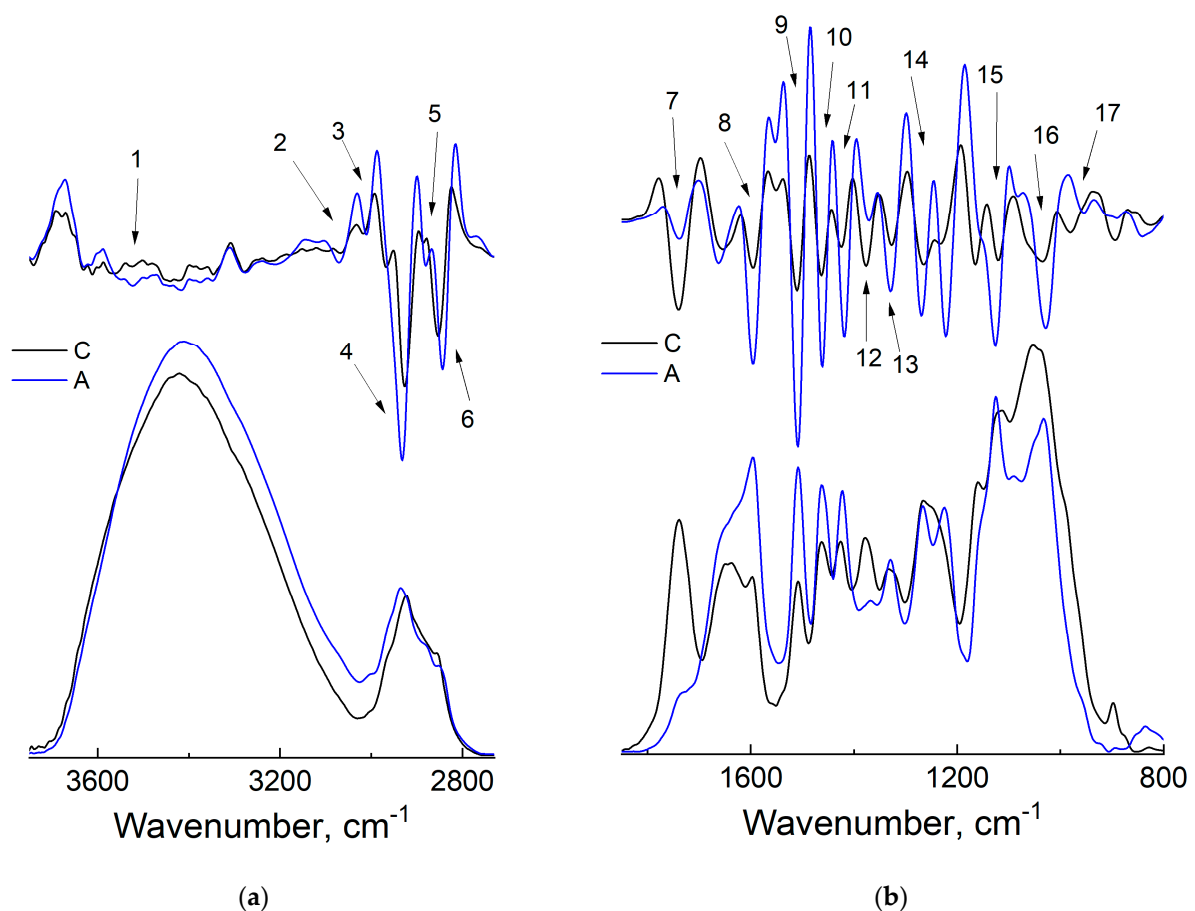


**Figure 3.** Infrared spectra and their derivatives for the control (C) and the archaeological (A) elm wood samples in 3750–2750 cm<sup>-1</sup> (a) and 1850–800 cm<sup>-1</sup> (b) regions.

In Figure 3b, there is a strong decrease of the intensity of the band from 1742/1740 (7) cm<sup>-1</sup>, 1377/1369 (12) cm<sup>-1</sup> and 987/984 (17) cm<sup>-1</sup> assigned to C=O stretching vibrations in acetyl, carbonyl and carboxyl groups (of carbohydrate origin), C–H deformation vibration in carbohydrates, and C–O stretching vibration in carbohydrates, and increase of the intensity of the bands from 1593 (8) cm<sup>-1</sup>, 1510 (9) cm<sup>-1</sup>, 1464 (10) cm<sup>-1</sup>, 1426/1421 (11) cm<sup>-1</sup>, 1332/1328 (13) cm<sup>-1</sup>, 1268 (14) cm<sup>-1</sup>, 1125 (15) cm<sup>-1</sup> and 1031/1029 (16) cm<sup>-1</sup> assigned to C=C stretching of the aromatic ring of lignin, C–H deformation in lignin and carbohydrates, C–H vibration in cellulose and C<sub>1</sub>–O vibration in syringyl derivatives—condensed structures in lignin, C–O stretching in lignin, C–O ester stretching vibrations in methoxyl and β–O–4 linkages in lignin, and C–O–C and C–O stretching vibration in crystalline regions in cellulose. A new band was observed in archaeological wood at 1188 cm<sup>-1</sup> which is assigned to C–O bonds in lignin.

The strong reduction in the intensity of the bands associated to carbohydrates (especially the amorphous ones), as well as an increase in intensity and shifting of the maxima for the bands associated to lignin and crystalline regions in cellulose, indicate the degradation of amorphous carbohydrates during the time of burial in the lake sediments. It is known that under severe environmental conditions (i.e., biodegradation or moisture), the most susceptible to degradation are the hemicelluloses and amorphous cellulose, the degradation taking place via hydrolysis reactions followed by breakdown of the components in lower molecular compounds. These results are in line with the information mentioned before that the excavated elm wood showed a significant degree of degradation and a high percent of mass loss.

The SEM image of archaeological elm (A), presented in Figure 4, confirms its bad state of preservation. The wood cells are flattened, of irregular shape, which indicates a



high degree of shrinkage during drying, characteristic for degraded wood. In comparison with sound, contemporary elm (C in Figure 4), the cell walls of archaeological wood are significantly thinner, full of smaller and bigger holes, which result from microbial attack. Their layers are peeled-off from middle lamellae in some places. Additionally, fungal hyphae can be visible in some cells (marked with “^”), which suggests fungal decay and explains the degradation of amorphous carbohydrates showed by FT-IR measurements.

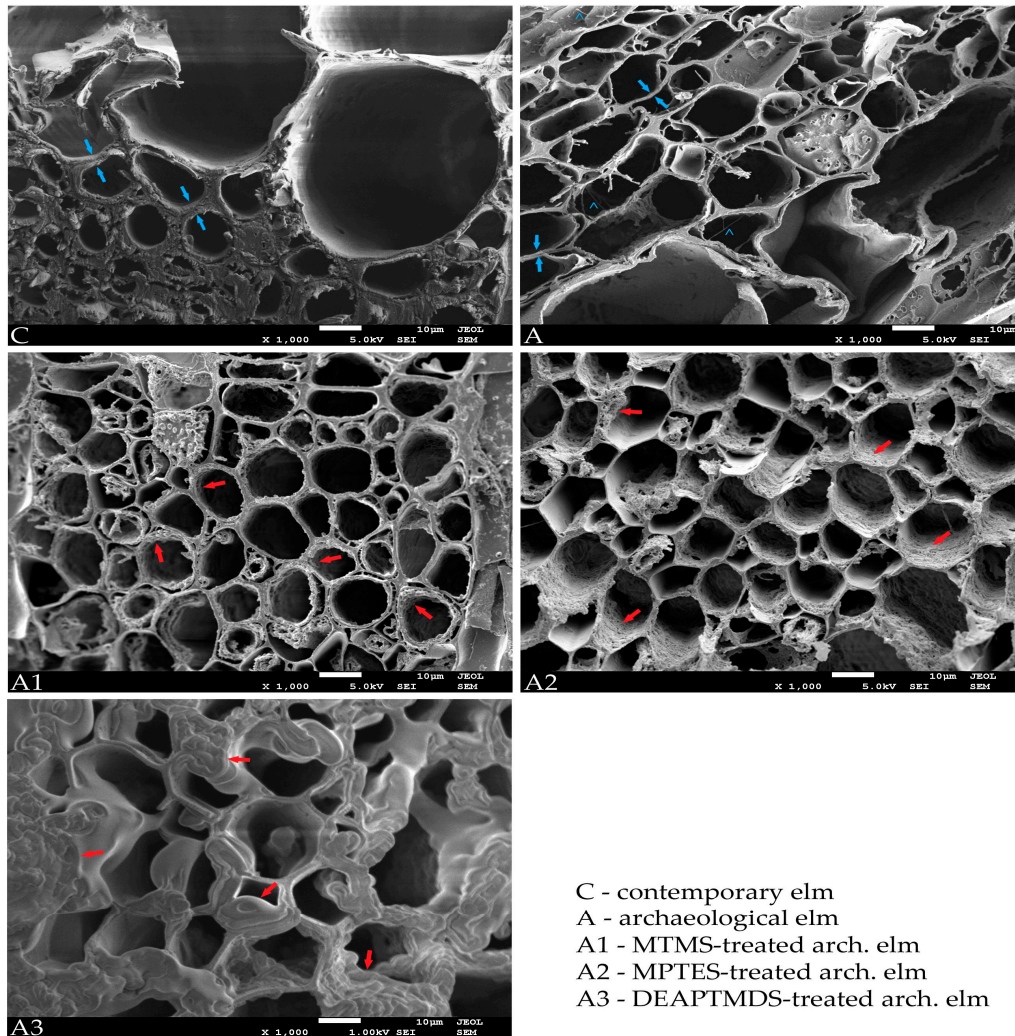


**Figure 4.** Scanning electron microscope (SEM) images of untreated (C, A) and treated (A1, A2, A3) elm; blue arrows point to the thickness of the cell walls of non-degraded (C) and degraded (A) wood, red arrows indicate organosilicon layers on the cell wall of treated archaeological elm (A1, A2, A3), ^ indicate fungal hyphae.

### 3.2. Interactions between Organosilicons and Archaeological Elm

In order to preserve waterlogged archaeological elm and stabilise its dimensions upon drying, treatment with the use of three different organosilicons (MTMS, MPTES and DEAPTMDs) was applied. After the wood impregnation, the weight percent gain (WPG) for the samples treated with MTMS (A1), MPTES (A2) and DEAPTMDs (A3) was about  $242 \pm 6.6\%$ ,  $148 \pm 12.0\%$  and  $230 \pm 8.4\%$ , respectively [22]. Reduction in the shrinkage of the treated wood in comparison with the untreated control, expressed as anti-shrink efficiency (ASE), was  $81 \pm 2.6\%$  for A1,  $98 \pm 1.3\%$  for A2 and  $90 \pm 7.8\%$  for A3, which indicates high stabilising effectiveness of the applied chemicals [22]. However, comparison of SEM images of the treated wood revealed significant differences in the deposition of particular compounds in the wood structure. In the case of MTMS-treated wood (A1

in Figure 4), the cells have a more regular shape in comparison with untreated wood, the cell lumina are empty, and a cobweb-like polymer network is visible on the cell wall surface (red arrows). The structure of MPTES-treated wood (A2 in Figure 4) looks similar. However, for the DEAPTMS-treated elm (A3 in Figure 4), the image is different. The layers of siloxane look different. They are thicker and not only cover the cell walls, but also fill the cell lumina. The observation suggests then that alkoxy silanes applied can incrust or coat the cell walls, while the siloxane is present not only as a coating on the cell walls but also inside the cell lumina.

The aforementioned results indicate a different mechanism of wood stabilisation by various organosilicons, hence the decision to conduct the infrared spectroscopy study to shed some light on the issue.

The spectrum of untreated archaeological elm wood sample was compared with the spectra of the treated samples, as well as their derivatives. As in the previous case, the spectra were divided into two regions, presented in Figure 5a,b, respectively.

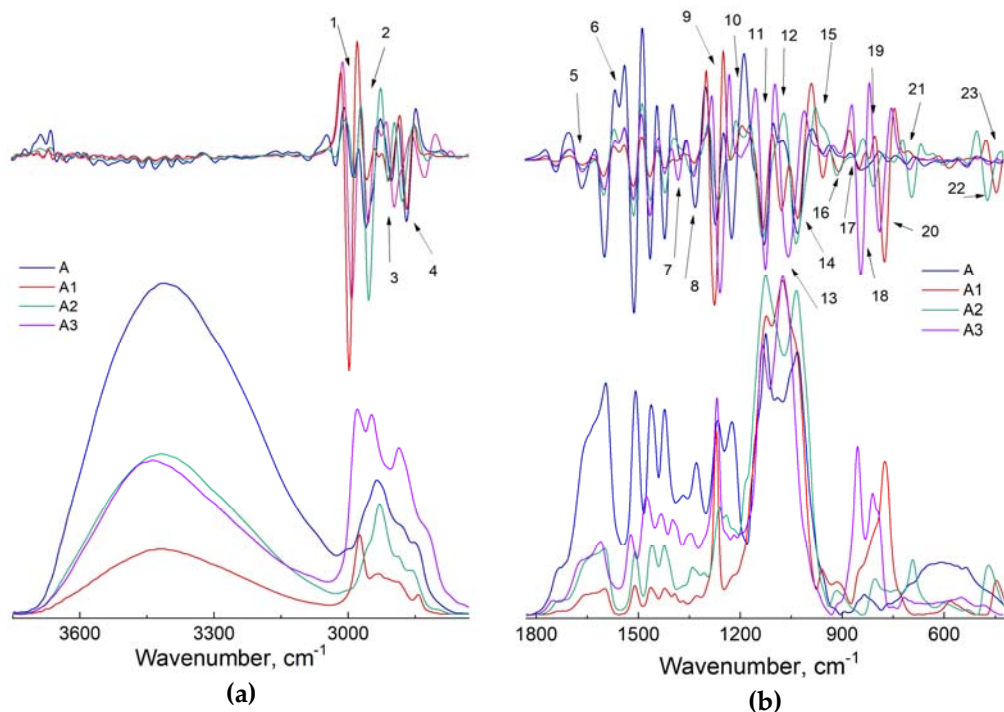


**Figure 5.** Infrared spectra and their derivatives for the untreated archaeological elm wood (A) and silane-treated samples (A1, A2, A3, respectively) in 3750–2750 cm<sup>-1</sup> (a) and 1800–400 cm<sup>-1</sup> (b) regions.

Compared to the control (A) sample spectrum, the spectra of treated samples with organosilicons (A1–A3) present (aside from the bands present in the wood material) bands that are expected to appear due to the presence of chemical bonds from silanes and the bands that appear after the interactions between the wood and organosilicon compounds. A detailed list of the bands' position and their assignments according to the literature [24,32–38] is presented in Table 1.

**Table 1.** Band assignments and their position [24,32–40].

Bands Assignment	Bands Position, $\text{cm}^{-1}$			
	A	A1	A2	A3
symmetric stretching vibration of C–H bonds in $\text{CH}_3$ groups in wood and <i>silanes/siloxanes</i>	2966	2974	2961	2968
asymmetric stretching vibration of C–H bonds in $\text{CH}_3$ groups in wood and <i>silanes/siloxanes</i>	2935	2933	2929	2932
symmetric stretching vibration of C–H bonds in $\text{CH}_2$ groups in wood and <i>silanes/siloxanes</i>	2877	2883	2885	2882
asymmetric stretching vibration of C–H bonds in $\text{CH}_2$ groups in wood and <i>silanes/siloxanes</i>	2842	2841	2853	2843
C=O stretching vibration of carbonyl, carboxyl and acetyl groups	1738	1738	1736	1738
conjugated C–O in quinines coupled with C=O stretching of various groups; <i>N-H bending vibration</i>	1663	1661	1659	1660
C=C stretching of aromatic skeletal (lignin)	1595	1598	1598	1594
conjugated C–O; <i>C-N stretching vibration in secondary amines</i>	1552	1552	1551	1554
C=C stretching of aromatic skeletal (lignin)	1509	1510	1509	1511
C–H deformation in lignin and carbohydrates <i>C–H deformation in -CH<sub>2</sub>-CH<sub>3</sub></i>	1462	1462	1460	1462
C–H deformation in lignin and carbohydrates; <i>C–H deformation in -CH<sub>2</sub>-CH<sub>3</sub></i>	1417	1419	1418	1419
C–H deformation in cellulose and hemicellulose; <i>C–H asymmetric deformation in Si-R</i>	1371	1382	—	1380
C–H vibration in cellulose and $\text{C}_1\text{–O}$ vibration in syringyl derivatives—condensed structures in lignin; <i>CH<sub>2</sub> deformation vibration and C-N stretching vibration in primary amines</i>	1329	1333	1338	1333
<i>-CH<sub>2</sub> groups twisting</i>	—	—	1307	1299
C–O stretching in lignin; <i>Si-C stretching vibration in Si-CH<sub>3</sub></i>	1268	1272	1260	1256
C–O–C stretching mode of the pyranose ring; <i>asymmetric stretching vibration of Si-O-C</i>	1222	1224	1229	—
			1187	1189
C–O stretching; <i>Si-O-C asymmetric stretching vibration</i>	1126	1131	1131	1123
glucose ring stretching vibration; <i>asymmetric stretching vibration of Si-O-Si</i>	1082	1075	—	1056
C–O ester stretching vibrations in methoxyl and $\beta\text{–O–4}$ linkages in lignin; <i>Si-O-C asymmetric stretching vibration</i>	1027	1027	1031	—
<i>Si-O in-plane stretching vibration of the silanol Si-OH groups</i>	955	954	—	974
				946
<i>Si-O-C bending vibration</i>	—	906	913	904
<i>Si-C and Si-O-C symmetric stretching vibration</i>	840	848	865	842
<i>Si-O-Si bonds stretching vibration</i>	—	818	806	
<i>-Si-C rocking in -SiCH<sub>3</sub></i>	—	773	745	787
<i>Si-O-Si bonds symmetric stretching vibration</i>	—	715	700	700
<i>C-S stretching vibration</i>	—		645	
<i>Si-O stretching vibration</i>	—	582	597	—
<i>O-Si-O deformation vibration</i>	—	497	470	467
		444		

From Figure 5a, it can be observed that the band assigned to hydroxyl groups from  $3600$  to  $3100\text{ cm}^{-1}$  tend to decrease in intensity for the treated wood compared to the untreated one, indicating that these groups are less available due to their reaction with silanol groups from the organosilicons. The decrease of the available hydroxyl groups was also evidenced by dynamic water sorption experiments [41,42] showing that wood treatment caused a reduction in the equilibrium moisture content and the sorption hysteresis and limited access of water molecules to primary sorption sites in comparison with untreated wood.

Higher differences can be observed appearing in the 3100–2700  $\text{cm}^{-1}$  region (Figure 5a), assigned to antisymmetric and symmetric stretching vibration of C–H bonds in  $-\text{CH}_3$ , and  $-\text{CH}_2$  groups from wood and silanes structure. Both band intensities and their maxima vary for each spectrum. This is due to the position of the methyl or methylene groups in the silane/siloxane structure, as well as due to the surrounding groups which allow or hinder their free vibration. The A1 spectrum present higher intensity of the band from 2974  $\text{cm}^{-1}$  (1). At the same time, the maximum is shifted to higher wavenumber, compared to the same band in the A spectrum (at 2966 (1)  $\text{cm}^{-1}$ ). The A2 spectrum present higher intensity for the band from 2934 (2)  $\text{cm}^{-1}$  compared to similar bands from the other spectra, while in A3 both 2969 (1) and 2931 (2)  $\text{cm}^{-1}$  have higher intensities comparing to other spectra. Because A1 has in its structure only  $-\text{CH}_3$  groups, the bands from 2883 (3) and 2842 (4)  $\text{cm}^{-1}$  are mostly due to the groups from the wood structure (A). By contrast, A2 and A3 have in their structure  $-\text{CH}_2$  groups, and in consequence, we observe higher intensities and also shifting of the maxima to higher/lower wavenumber values.

The fingerprint region (Figure 5b) is more sensitive; in this region, stretching and bending vibrations of all groups from the wood and organosilicons structures can be observed, presenting unique features specific to each component. Therefore, here the presence of several new bands as well as increased intensity or shifting of the bands which may be assigned to silane/siloxane structures could be identified.

The wood sample treated with silane 1 (A1) shows the presence of strong absorption bands at 1271 (9), 1169 (10), 1128 (11), 1075 (12), 959 (15), 811 (19), 772 (20) and 449 (23)  $\text{cm}^{-1}$  (see assignments in Table 1).

The samples of wood treated with silane 2 (A2) present most informative bands at 1340 (8) and 1308 (8)  $\text{cm}^{-1}$  assigned to deformation of  $-\text{CH}_2$  groups present in the spectra due to existence of a larger number of these groups in the solid network. Furthermore, similarly to A1, were observed bands at 1187 (10), 1130 (11), 1030 (14), 1004 (14), 918 (16), 861 (17), 807 (19), 768 (20), 692 (21), and 474 (22)  $\text{cm}^{-1}$  (see assignments in Table 1).

The A3 treated wood sample shows new bands at 1662 (5), 1552 (6), 1371 (7), 1329 (8), and at 1056 (13)  $\text{cm}^{-1}$ . All these bands are overlapped with the bands present in the wood spectrum (A), but for the treated wood, compared to the reference one, they present higher intensities.

In order to identify the possible interactions between the organosilicons and the wood substrate, spectra of the pure chemicals were recorded, and their second derivatives were plotted against the second derivatives of the archaeological wood and the treated wood (see Figure 6).

Analysing the first set of spectra (A, A1 and 1) for the MTMS silane, differences can be observed as follows: the bands from the 1444 (1) and 1406 (2)  $\text{cm}^{-1}$  in spectrum of the silane are not observable in the spectrum of treated wood, due to the overlapping of these bands with the bands from the wood structure at 1462 (1) and 1417 (2)  $\text{cm}^{-1}$ . The same behaviours show bands from 1278 (4), 1139 (5), 945 (7), and 854 (9)  $\text{cm}^{-1}$  in the silane spectrum, which are overlapped with the bands from the 1268 (4), 1126 (5), 955 (7) and 840 (9)  $\text{cm}^{-1}$  in the wood spectrum and are shifted towards each other in the spectrum of the A1 (1272 (4), 1131 (5), 954 (7) and 848 (9)  $\text{cm}^{-1}$ ). The bands from 1357 (3) and 674 (11)  $\text{cm}^{-1}$  (observable in the silane spectrum) are not observable in the treated wood spectrum (A1), while the band from 448 (13)  $\text{cm}^{-1}$  decreases in intensity in the spectrum of the treated wood sample. These bands are assigned to C–H asymmetric deformation and Si–O stretching vibration in silanes and to deformation vibration of the O–Si–O bonds. At the same time, new bands at 1382 (3) and 497 (12)  $\text{cm}^{-1}$  are observed in the spectrum of the silane treated wood sample. They are assigned to C–H asymmetric deformation in Si–R groups, as well as to Si–O–C stretching vibration. The observed differences in the analysed spectra indicate changes in the silane monomers due to their condensation with other monomers or wood polymers.

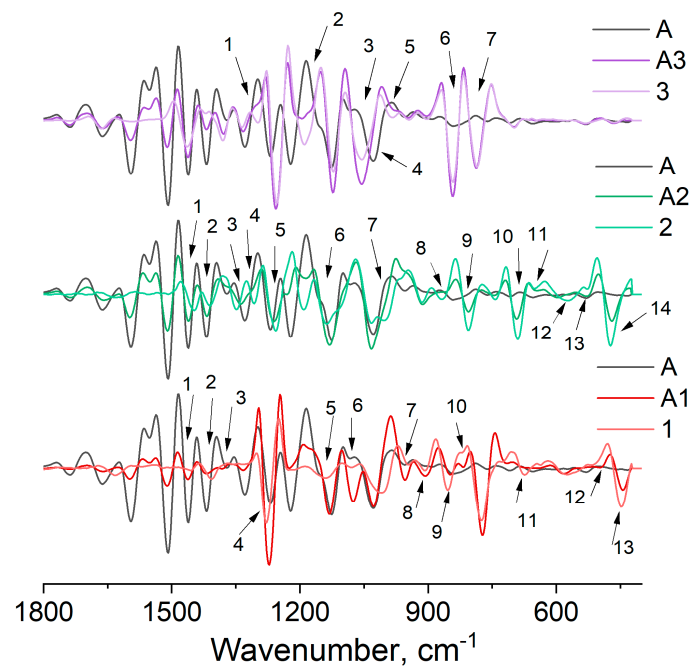


**Figure 6.** Second derivative spectra in the 1800–400  $\text{cm}^{-1}$  region for the untreated archaeological elm wood (A), wood samples treated with particular organosilicons (A1, A2, A3) and pure silanes and siloxane (1, 2, 3).

Other differences can be observed for the band from 1080 (6)  $\text{cm}^{-1}$  (in the spectrum of silane) and from 1083  $\text{cm}^{-1}$  (in the spectrum of wood), which are of low intensity, but increase drastically in the spectrum of the treated wood (A1) and is shifted to 1076 (6)  $\text{cm}^{-1}$ . This band is assigned to asymmetric stretching vibration of Si–O–Si groups, indicating the presence of condensation reactions between silane monomers via alkoxy groups.

The bands from 947 (7) and 907 (8)  $\text{cm}^{-1}$  (from the silane spectrum) increase in the spectrum of the treated wood and are shifted to 955 (7) and 909 (8)  $\text{cm}^{-1}$ . Furthermore, the band from 821 (10)  $\text{cm}^{-1}$  which is observable as a small shoulder in the silane spectrum, appear as a well-defined band at 818 (10)  $\text{cm}^{-1}$  in silane treated wood sample (A1). These three bands are assigned to in-plane stretching vibration of the Si–O in silanol Si–OH groups, bending vibration of Si–O–C groups, and stretching vibration of the Si–O–Si bonds.

The aforementioned increase in the intensity of the bands assigned to Si–O in silanol, Si–O–C and Si–O–Si bonds confirms that the sol-gel process took place between the silane and wood polymers, in which through a series of hydrolysis and condensation reactions, silane monomers can not only polymerise into a spatial polymer network (observed by Si–O–Si bonds), but can also react with –OH groups present on all the main wood components, forming a wood–silane composite and establishing siloxy bonds (Si–O–C) [7]. Moreover, the disappearance or decrease in intensity of the bands assigned to C–H asymmetric deformation and Si–O stretching vibration in silanes and to deformation vibration of the O–Si–O bonds, indicate the reduction of the Si–O and O–Si–O bonds, confirming the effectiveness of the sol-gel process.

Furthermore, analysing the second series of spectra (A, A2, 2), belonging to archaeological wood, treated wood with MPTES and the pure silane spectra, differences mainly in the fingerprint region can be observed as in the previous case. Thus, the bands from 1448 (1), 1410 (2), 1256 (5) and 1138 (6)  $\text{cm}^{-1}$  (in the spectrum of pure silane) are overlapped with the bands from the wood from 1462 (1), 1418 (2), 1269 (5) and 1127 (6)  $\text{cm}^{-1}$ . These bands are assigned to C–H deformation in lignin and carbohydrates and in –CH<sub>2</sub>–CH<sub>3</sub> in silane, C–O stretching in lignin and Si–C stretching vibration in Si–CH<sub>3</sub> in silane and to C–O stretching in wood and Si–O–C asymmetric stretching vibration in silane.

The band from 1348 (3)  $\text{cm}^{-1}$  in the spectrum of silane (2) is shifted to 1338 (3)  $\text{cm}^{-1}$  in the spectrum of the silane treated wood (A2) and is merged with the band from 1329 (3)  $\text{cm}^{-1}$  from the wood spectrum (A). This band is assigned to C–H vibration in cellulose and C<sub>1</sub>–O vibration in syringyl derivatives, condensed structures in lignin, and to –CH<sub>2</sub> deformation vibration in silane. The bands from 1306 (4), 1002 (7), and 869 (8)  $\text{cm}^{-1}$  seen in the spectrum of the silane are not identified in the spectrum of the wood treated with silane. These bands are assigned to –CH<sub>2</sub> groups twisting vibration, Si–O–Si stretching vibration, and Si–O stretching vibration in silane and indicate changes in silane structure due to its reactivity with other silane monomers or wood hydroxyls.

The bands from 573 (12) and 530 (13)  $\text{cm}^{-1}$  from the silane spectrum increase in intensity in the spectrum of the treated wood samples, while the bands from 805 (9) and 473 (14)  $\text{cm}^{-1}$  decrease in intensity. They are assigned to stretching vibration of the Si–O–C and Si–O bonds.

The bands from 692 (10) and 645 (11)  $\text{cm}^{-1}$  (assigned to C–S stretching vibration) in the spectrum of pure silane are shifted to higher wavenumber and decrease in intensity in the spectrum of treated wood, indicating that these bands participate to interactions with wood.

As in the previous case, the modifications observed in the spectra of the silane-treated wood compared to pure silane and wood spectra indicate interactions taking place between the silane and the wood substrate, as well as the formation of bonds after the condensation of the silane on the surface of the wood.

The last series of spectra (A, A3, and 3), belonging to archaeological wood, DEAPTMDS-treated wood as well as pure siloxane are also presented in Figure 6. In this case, smaller differences were observed; thus, the bands from 1299 (1) and 985 (5)  $\text{cm}^{-1}$  from the pure siloxane spectrum are not observed in the siloxane-treated wood spectrum. These bands are assigned to –CH<sub>2</sub> groups twisting vibration and stretching vibration of the Si–O in silanol groups. The band from 1055 (3)  $\text{cm}^{-1}$  can be identified in the siloxane-treated wood spectrum, and the band from 1028 (4)  $\text{cm}^{-1}$  from the wood spectrum is not identified in the A3 spectrum. The band from the wood spectrum is assigned to stretching vibration of the C–O in methoxyl groups in lignin, indicating a possible contribution of these groups to the interactions with siloxane. The band from 1055 (3)  $\text{cm}^{-1}$  is assigned to the asymmetric stretching vibration of Si–O–Si in siloxane structure and confirms the presence of the siloxane in the treated wood.

Furthermore, the band from 1190 (2)  $\text{cm}^{-1}$  from the siloxane spectrum is shifted to higher wavenumber, at 1195 (2)  $\text{cm}^{-1}$  in the A3 spectrum. This band also presents the lower intensity and higher width in the spectrum of treated wood, and it is assigned to the asymmetric stretching vibration of Si–O–C groups. The band from 843 (6)  $\text{cm}^{-1}$  observed in the siloxane spectrum decreases in intensity in the spectrum of treated wood, while the band from 787 (7)  $\text{cm}^{-1}$  presents similar intensities in both spectra. Both bands could not be identified in the wood spectrum. The modification of intensity, band width and wavenumber maximum may indicate interactions taking place between the siloxane and wood structure.

The PCA analysis (Figure 7) illustrated by PC scores (Figure 7a) and PC loadings (Figure 7b) clearly show the differences appearing between the analysed spectra.

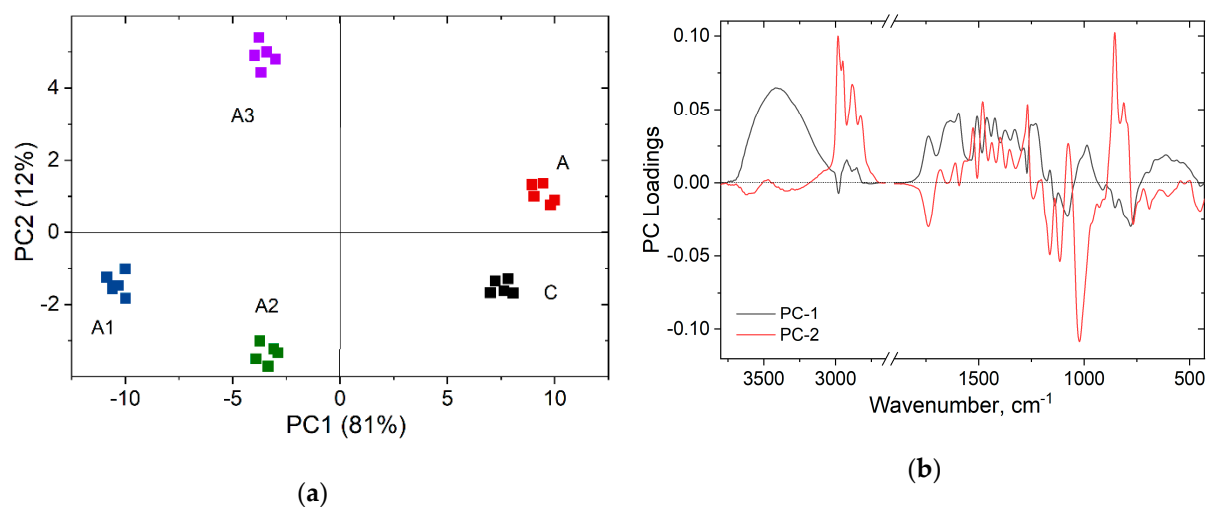


**Figure 7.** Principal component (PC) scores (a) and principal component (PC) loadings (b) calculated for the studied samples.

The principal component factor 1 (PC1) describes 81% and principal component factor 2 (PC2) describes 12% of data variance, so 93% of the variances were captured using these two dimensions instead of the initial data (see Figure 7a). Therefore, the PC1 presents positive values for both untreated wood samples (C and A) and negative ones for the treated samples (A1, A2 and A3). At the same time, PC2 differentiates the samples according to control and archaeological, as well as the samples treated with the two silanes and the sample treated with the siloxane. Both PCs are indicative to indicate modifications in the wood structure according to state of preservation and type of treatment.

The PC loading plot (see Figure 7b) gives information about the chemical features which are responsible for grouping the samples along the PC1 and PC2. The PC1 loading presents positive bands mainly assigned to wood structure and negative ones assigned to the polymers used, while PC2 loading presents positive bands mainly assigned to the siloxane compound and negative ones assigned mainly to wood and silane compounds.

The modifications observed in all three series of samples indicate the interactions between the silane/siloxane and wood substrate (primarily via hydroxyl groups) through silylation or condensation reactions (as mentioned above). In Figure 8 are represented the possible interactions taking place between the wood structure and the organosilicon compounds structure as observed through infrared spectroscopy.

Comparing the three organosilicons, higher interactions with wood were observed in the case of silanes 1 and 2, i.e., MTMS and MPTES, which have relatively short alkyl chain and reactive alkoxy groups than for DEAPTMDs (3) with a much longer chain and amino groups of different reactivity. Alkoxysilanes can react not only with wood hydroxyls, but also condense with their own molecules. As a result, a potential spatial network can be formed on the surface or inside the cell wall which would bind together wood polymers and thus stabilise the structure of wood. Moreover, a reactive thiol group in the MPTES molecule enables an extra bond with wood hydroxyls, additionally strengthening interactions between the chemical and wood polymers.

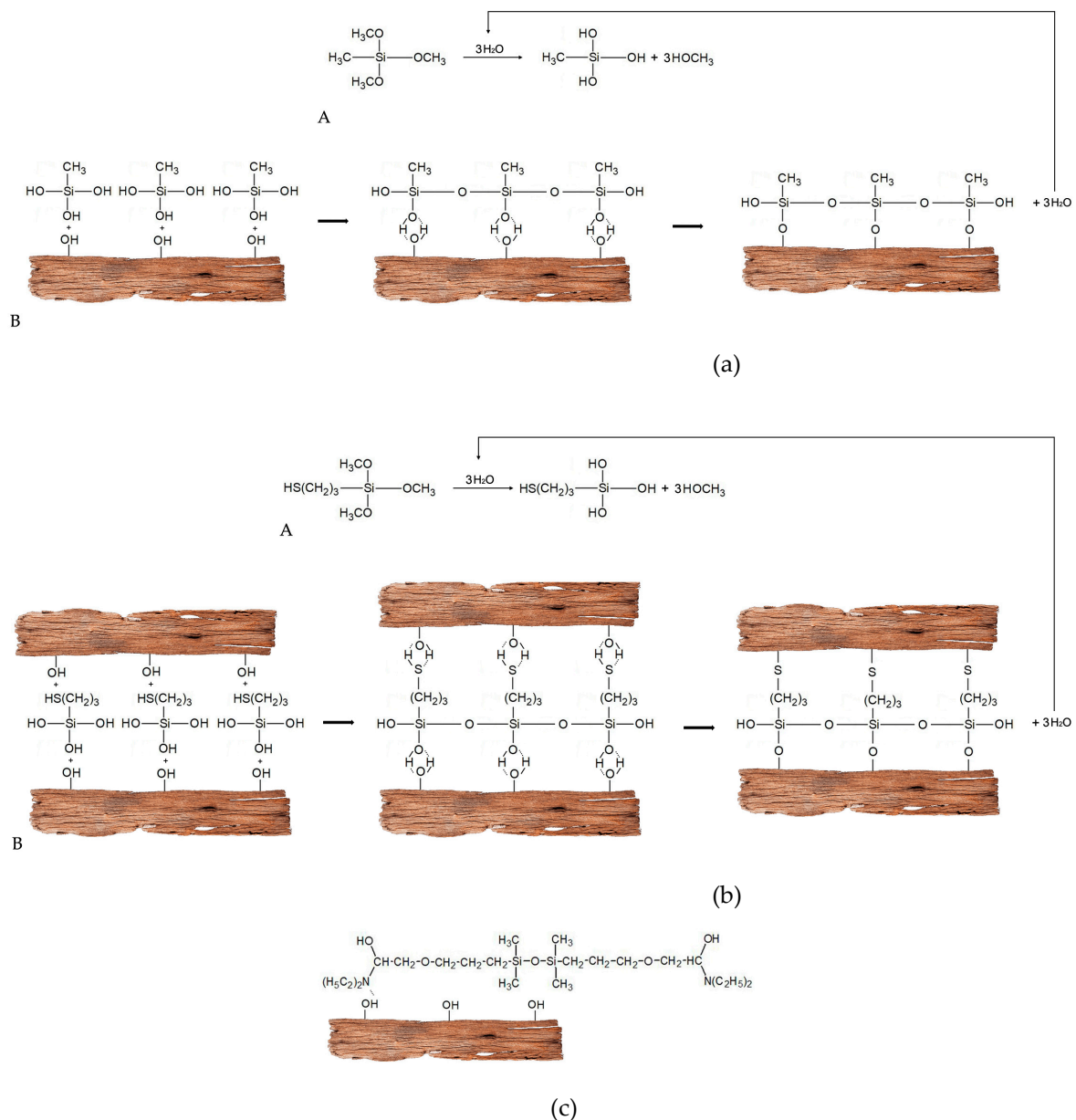


**Figure 8.** Schematic illustration of possible interactions taking place between the wood structure (hydroxyl groups present in the cell wall polymers) and the organosilicon compounds used (a–c); (A) hydrolysis of silane, (B) a set of consecutive steps of a condensation reaction.

Although Figure 8 is just a schematic drawing, it captures the idea of the interactions between organosilicons and the cell wall polymers. It shows clearly that the number and the strength of the possible interactions are different. Therefore, although all the three chemicals are effective in stabilisation of wood dimensions upon drying, the stabilising mechanism must involve much more than only the chemical structure and reactivity of a conservation agent applied.

#### 4. Conclusions

The presence of chemical interactions between organosilicons and the cell wall polymers of waterlogged archaeological wood were clearly shown through infrared spectroscopy. The reactivity depends on the chemical structure and varies between the applied chemicals, indicating a higher number of interactions between the alkoxy silanes (MTMS and MPTES) and wood, than in the case of the tested siloxane (DEAPTMS). In the case



of alkoxysilanes, the highly reactive alkoxy groups (3 per a silane molecule) are involved in interactions with hydroxyls present on wood polymers. For MPTES, an additional chemical reaction between the thiol group and wood hydroxyls occurs, which strengthens silane–wood interactions and can be involved in auxiliary stabilisation of wood dimensions. The chemical structure of the tested siloxane allows it only to react with wood polymers via hydrogen or ionic bonds, in which amino groups are involved. SEM images of the treated wood also revealed a different pattern of organosilicons deposition on wood microstructure. Alkoxysilanes seem to form coatings on the cell walls and, perhaps, also encrust them, while the siloxane covers the cell walls, but also fills the cell lumina. Different deposition of organosilicons in the wood structure may result from the differences in their chemical composition (the presence of particular reactive groups) and molecular weight—the biggest DEAPTMDS is probably too large to encrust the cell wall. All these results and observations suggest a different mechanism of wood stabilisation by various organosilicon compounds.

The results of our previous research on dimensional stabilisation of waterlogged archaeological wood with organosilicon compounds showed the reduction in EMC of wood treated with MTMS and MPTES in comparison with untreated wood and lower MC of wood treated with MPTES and MTMS (2.6% and 5%, respectively) in comparison with DEAPTMDS-treated or untreated (7.9% and 6.6%, respectively). Additionally, the cell wall bulking by MTMS was shown by porosity measurements. The results of this study together with all the aforementioned data allow the conclusion that the mechanism of waterlogged wood stabilisation by the used alkoxysilanes can involve bulking the cell wall by silane molecules and wood chemical modification, while in the case of the applied siloxane, it builds upon filling the cell lumina. However, the topic is not closed yet and some more structural and mechanical experiments performed in the nano-scale could reveal more details about the stabilisation mechanism.

**Author Contributions:** Conceptualisation, M.B. and C.-M.P.; methodology, C.-M.P. and M.B.; investigation, C.-M.P. and M.B.; writing—original draft preparation, C.-M.P. and M.B.; writing—review and editing, M.B. and C.-M.P.; visualisation, M.B. and C.-M.P. All authors have read and agreed to the published version of the manuscript.

**Funding:** This research was funded by the Polish Ministry of Science and Higher Education through National Grant 2bH 15 0037 83 and by the COST Action FP1303 (COST-STSM-FP1303-37557).

**Institutional Review Board Statement:** Not applicable.

**Informed Consent Statement:** Not applicable.

**Data Availability Statement:** The data presented in this study are available on request from the corresponding author. The data are not publicly available due to the ongoing study in this field.

**Acknowledgments:** The authors would like to express their thanks to the Directorate of the Museum of the First Piasts at Lednica for sharing the research material—waterlogged elm, and to Mikołaj Grzeszkowiak and Roksana Markiewicz from Adam Mickiewicz University in Poznań, NanoBioMedical Centre for their help in SEM imaging.

**Conflicts of Interest:** The authors declare no conflict of interest. The funders had no role in the design of the study; in the collection, analyses, or interpretation of data; in the writing of the manuscript, or in the decision to publish the results.

## References





1. Cai, Y.; Hou, P.; Duan, C.; Zhang, R.; Zhou, Z.; Cheng, X.; Shah, S. The use of tetraethyl orthosilicate silane (TEOS) for surface-treatment of hardened cement-based materials: A comparison study with normal treatment agents. *Constr. Build. Mater.* **2016**, *117*, 144–151. [CrossRef]
2. Kregiel, D. Advances in biofilm control for food and beverage industry using organo-silane technology: A review. *Food Control* **2014**, *40*, 32–40. [CrossRef]
3. Mojsiewicz-Pieńkowska, K.; Jamrógiewicz, M.; Szymkowska, K.; Krenczkowska, D. Direct Human Contact with Siloxanes (Silicones)—Safety or Risk Part 1. Characteristics of Siloxanes (Silicones). *Front. Pharmacol.* **2016**, *7*, 132. [CrossRef]

4. Onar, N.; Mete, G.; Aksit, A.; Kutlu, B.; Celik, E. Water-and oil-repellency properties of cotton fabric treated with Silane, Zr, Ti based nanosols. *Int. J. Text. Sci.* **2015**, *4*, 84–96.
5. Szymanowski, H.; Olesko, K.; Kowalski, J.; Fijalkowski, M.; Gazicki-Lipman, M.; Sobczyk-Guzenda, A. Thin SiNC/SiOC Coatings with a Gradient of Refractive Index Deposited from Organosilicon Precursor. *Coatings* **2020**, *10*, 794. [CrossRef]
6. Wang, M.; Hao, X.; Wang, W. Reinforcing Behaviors of Sulfur-Containing Silane Coupling Agent in Natural Rubber-Based Magnetorheological Elastomers with Various Vulcanization Systems. *Materials* **2020**, *13*, 5163. [CrossRef]
7. Donath, S.; Militz, H.; Mai, C. Wood modification with alkoxysilanes. *Wood Sci. Technol.* **2004**, *38*, 555–566. [CrossRef]
8. Mai, C.; Militz, H. Modification of wood with silicon compounds. Inorganic silicon compounds and sol-gel systems: A review. *Wood Sci. Technol.* **2004**, *37*, 339–348. [CrossRef]
9. Levy, D.; Zayat, M. (Eds.) *The Sol-Gel Handbook: Synthesis, Characterization and Applications*; 3-Volume Set; John Wiley & Sons Inc.: Hoboken, NJ, USA, 2015.
10. Panov, D.; Terziev, N. Study on some alkoxysilanes used for hydrophobation and protection of wood against decay. *Int. Biodeter. Biodegr.* **2009**, *63*, 456–461. [CrossRef]
11. Xie, Y.; Hill, C.A.S.; Xiao, Z.; Militz, H.; Mai, C. Silane coupling agents used for natural fiber/polymer composites: A review. *Compos. Part A Appl. Sci. Manuf.* **2010**, *41*, 806–819. [CrossRef]
12. Hill, C.A.S.; Farahani, M.M.; Hale, M.D. The use of organo alkoxysilane coupling agents for wood preservation. *Holzforschung* **2004**, *58*, 316–325. [CrossRef]
13. De Vetter, L.; Van den Bulcke, J.; Van Acker, J. Impact of organosilicon treatments on the wood-water relationship of solid wood. *Holzforschung* **2010**, *64*, 463–468. [CrossRef]
14. Kartal, S.N.; Yoshimura, T.; Imamura, Y. Modification of wood with Si compounds to limit boron leaching from treated wood and to increase termite and decay resistance. *Int. Biodeter. Biodegr.* **2009**, *63*, 187–190. [CrossRef]
15. Giudice, C.A.; Alfieri, P.V.; Canosa, G. Decay resistance and dimensional stability of *Araucaria angustifolia* using siloxanes synthesized by sol-gel process. *Int. Biodeter. Biodegr.* **2013**, *83*, 166–170. [CrossRef]
16. Liu, Y.; Guo, L.; Wang, W.; Sun, Y.; Wang, H. Modifying wood veneer with silane coupling agent for decorating wood fiber/high-density polyethylene composite. *Constr. Build. Mater.* **2019**, *224*, 691–699. [CrossRef]
17. Dodangeh, F.; Dorraji, M.S.; Rasoulifard, M.H.; Ashjari, H.R. Synthesis and characterization of alkoxy silane modified polyurethane wood adhesive based on epoxidized soybean oil polyester polyol. *Compos. B Eng.* **2020**, *187*, 107857. [CrossRef]
18. Canosa, G.; Alfieri, P.V.; Giudice, C.A. Low Density Wood Impregnation with Water-Repellent Organosilicic Compounds. *MSCE* **2018**, *6*, 39. [CrossRef]
19. Smith, C.W.; Hamilton, D.L. Treatment of Waterlogged Wood Using Hydrolyzable, Multi-Functional Alkoxysilane Polymers. In Proceedings of the 8th ICOM Group on Wet Organic Archaeological Materials Conference, Stockholm, Sweden, 11–15 June 2001; pp. 614–615.
20. Broda, M.; Mazela, B. Application of methyltrimethoxysilane to increase dimensional stability of waterlogged wood. *J. Cult. Herit.* **2017**, *25*, 149–156. [CrossRef]
21. Broda, M.; Dąbek, I.; Dutkiewicz, A.; Dutkiewicz, M.; Popescu, C.-M.; Mazela, B.; Maciejewski, H. Organosilicons of different molecular size and chemical structure as consolidants for waterlogged archaeological wood—a new reversible and retreatable method. *Sci. Rep.* **2020**, *10*, 2188. [CrossRef]
22. Broda, M.; Mazela, B.; Dutkiewicz, A. Organosilicon compounds with various active groups as consolidants for the preservation of waterlogged archaeological wood. *J. Cult. Herit.* **2019**, *35*, 123–128. [CrossRef]
23. Popescu, M.-C.; Popescu, C.-M.; Lisa, G.; Sakata, Y. Evaluation of morphological and chemical aspects of different wood species by spectroscopy and thermal methods. *J. Mol. Struct.* **2011**, *988*, 65–72. [CrossRef]
24. Popescu, C.-M.; Popescu, M.-C.; Vasile, C. Characterization of fungal degraded lime wood by FT-IR and 2D IR correlation spectroscopy. *Microchem. J.* **2010**, *95*, 377–387. [CrossRef]
25. Gelbrich, J.; Mai, C.; Militz, H. Evaluation of bacterial wood degradation by Fourier Transform Infrared (FTIR) measurements. *J. Cult. Herit.* **2012**, *13*, S135–S138. [CrossRef]
26. Tolvaj, L.; Popescu, C.-M.; Molnar, Z.; Preklet, E. Dependence of the Air Relative Humidity and Temperature on the Photodegradation Processes of Beech and Spruce Wood Species. *BioResources* **2016**, *11*, 296–305.
27. Łucejko, J.J.; Modugno, F.; Ribechini, E.; Tamburini, D.; Colombini, M.P. Analytical instrumental techniques to study archaeological wood degradation. *Appl. Spectrosc. Rev.* **2015**, *50*, 584–625. [CrossRef]
28. Traoré, M.; Kaal, J.; Cortizas, A.M. Application of FTIR spectroscopy to the characterization of archeological wood. *Spectrochim. Acta A Mol. Biomol. Spectrosc.* **2016**, *153*, 63–70. [CrossRef]
29. Cesar, T.; Danevčič, T.; Kavkler, K.; Stopar, D. Melamine polymerization in organic solutions and waterlogged archaeological wood studied by FTIR spectroscopy. *J. Cult. Herit.* **2017**, *23*, 106–110. [CrossRef]
30. McHale, E.; Steindal, C.C.; Kutzke, H.; Benneche, T.; Harding, S.E. In situ polymerisation of isoeugenol as a green consolidation method for waterlogged archaeological wood. *Sci. Rep.* **2017**, *7*, 46481. [CrossRef] [PubMed]
31. Kiliç, N.; Kiliç, A.G. An attenuated total reflection Fourier transform infrared (ATR-FTIR) spectroscopic study of waterlogged woods treated with melamine formaldehyde. *Vib. Spectrosc.* **2019**, *105*, 102985. [CrossRef]
32. Popescu, M.-C.; Froidevaux, J.; Navi, P.; Popescu, C.-M. Structural modifications of *Tilia cordata* wood during heat treatment investigated by FT-IR and 2D IR correlation spectroscopy. *J. Mol. Struct.* **2013**, *1033*, 176–186. [CrossRef]

33. Al-Oweini, R.; El-Rassy, H. Synthesis and characterization by FTIR spectroscopy of silica aerogels prepared using several Si (OR)<sub>4</sub> and R'' Si (OR')<sub>3</sub> precursors. *J. Mol. Struct.* **2009**, *919*, 140–145. [CrossRef]
34. Benmouhoub, C.; Gauthier-Manuel, B.; Zegadi, A.; Robert, L. A Quantitative Fourier Transform Infrared Study of the Grafting of Aminosilane Layers on Lithium Niobate Surface. *Appl. Spectrosc.* **2017**, *71*, 1568–1577. [CrossRef] [PubMed]
35. Pasteur, G.A.; Schonhorn, H. Interaction of Silanes with Antimony Oxide to Facilitate Particulate Dispersion in Organic Media and to Enhance Flame Retardance. *Appl. Spectrosc.* **1975**, *29*, 512–517. [CrossRef]
36. Kavale, M.S.; Mahadik, D.B.; Parale, V.G.; Wagh, P.B.; Gupta, S.C.; Rao, A.V.; Barshilia, H.C. Optically transparent, superhydrophobic methyltrimethoxysilane based silica coatings without silylating reagent. *Appl. Surf. Sci.* **2011**, *258*, 158–162. [CrossRef]
37. Latthe, S.S.; Imai, H.; Ganesan, V.; Rao, A.V. Porous superhydrophobic silica films by sol–gel process. *Microporous Mesoporous Mater.* **2010**, *130*, 115–121. [CrossRef]
38. Lin, J.; Chen, H.; Fei, T.; Zhang, J. Highly transparent superhydrophobic organic–inorganic nanocoating from the aggregation of silica nanoparticles. *Colloids Surf.* **2013**, *421*, 51–62. [CrossRef]
39. Robles, E.; Csóka, L.; Labidi, J. Effect of reaction conditions on the surface modification of cellulose nanofibrils with aminopropyl triethoxysilane. *Coatings* **2018**, *8*, 139. [CrossRef]
40. Pacaphol, K.; Aht-Ong, D. The influences of silanes on interfacial adhesion and surface properties of nanocellulose film coating on glass and aluminum substrates. *Surf. Coat. Technol.* **2017**, *320*, 70–81. [CrossRef]
41. Broda, M.; Majka, J.; Olek, W.; Mazela, B. Dimensional stability and hygroscopic properties of waterlogged archaeological wood treated with alkoxysilanes. *Int. Biodeter. Biodegr.* **2018**, *133*, 34–41. [CrossRef]
42. Broda, M.; Curling, S.F.; Spear, M.J.; Hill, C.A.S. Effect of methyltrimethoxysilane impregnation on the cell wall porosity and water vapour sorption of archaeological waterlogged oak. *Wood Sci. Technol.* **2019**, *53*, 703–726. [CrossRef]

## Article

# Evaluation of Soda Lignin from Wheat Straw/Sarkanda Grass as a Potential Future Consolidant for Archaeological Wood

Jeannette J. Lucejko<sup>1,2</sup> , Anne de Lamotte<sup>1</sup> , Fabrizio Andriulo<sup>1</sup>, Hartmut Kutzke<sup>1</sup>, Stephen Harding<sup>1,3</sup> , Mary Phillips-Jones<sup>1,3</sup>, Francesca Modugno<sup>1,2</sup>, Ted M. Slaghek<sup>1,4</sup> , Richard J. A. Gosselink<sup>1,4</sup> and Susan Braovac<sup>1,\*</sup>

- <sup>1</sup> Museum of Cultural History, University of Oslo, PB 6762 St. Olavs Plass, 0130 Oslo, Norway; jeannette.lucejko@unipi.it (J.J.L.); annedelam@hotmail.fr (A.d.L.); fabrizio.andriulo@khm.uio.no (F.A.); hartmut.kutzke@khm.uio.no (H.K.); steve.harding@nottingham.ac.uk (S.H.); mary.phillips-jones@nottingham.ac.uk (M.P.-J.); francesca.modugno@unipi.it (F.M.); ted.slaghek@wur.nl (T.M.S.); richard.gosselink@wur.nl (R.J.A.G.)
- <sup>2</sup> Department of Chemistry, University of Pisa, Via G. Moruzzi 13, 56124 Pisa, Italy
- <sup>3</sup> National Centre for Macromolecular Hydrodynamics (NCMH), School of Biosciences, University of Nottingham, Sutton Bonington LE12 5RD, UK
- <sup>4</sup> Wageningen Food & Biobased Research, Bornse Weiland 9, 6708WG Wageningen, The Netherlands
- \* Correspondence: susan.braovac@khm.uio.no



**Citation:** Lucejko, J.J.; de Lamotte, A.; Andriulo, F.; Kutzke, H.; Harding, S.; Phillips-Jones, M.; Modugno, F.; Slaghek, T.M.; Gosselink, R.J.A.; Braovac, S. Evaluation of Soda Lignin from Wheat Straw/Sarkanda Grass as a Potential Future Consolidant for Archaeological Wood. *Forests* **2021**, *12*, 911. <https://doi.org/10.3390/f12070911>

Academic Editors: Magdalena Broda and Callum A. S. Hill

Received: 6 June 2021

Accepted: 9 July 2021

Published: 13 July 2021

**Publisher's Note:** MDPI stays neutral with regard to jurisdictional claims in published maps and institutional affiliations.



**Copyright:** © 2021 by the authors. Licensee MDPI, Basel, Switzerland. This article is an open access article distributed under the terms and conditions of the Creative Commons Attribution (CC BY) license (<https://creativecommons.org/licenses/by/4.0/>).

**Abstract:** This work is part of a larger study, which aims to use soda lignin from straw as the starting point for a non-aqueous consolidant for highly degraded archaeological wood from the Oseberg collection. This wood was treated with alum salts in the early 1900s, is actively degrading and exists in varying states of preservation. Non-aqueous consolidants are an option to stabilize this wood mechanically in cases where it is too deteriorated to undergo aqueous-based retreatments, for example using polyethylene glycol. The aim of this study was to compare the extent of penetration of two soda lignin preparations in low- to medium-degraded archaeological pine. The soda lignins were dissolved in ethyl acetate and had two molecular weight groups: P1000 (molecular weight Mw of ~3 kDa) and the ethyl acetate fraction FB01 (Mw of ~1 kDa). Penetration after immersion was evaluated by infrared spectroscopy and analytical pyrolysis. Treated specimens were also evaluated using weight and dimensional change and scanning electron microscopy. Both lignins penetrated into sample cores, but P1000 did not penetrate as well as FB01. This may be due to differences in their molecular weights, but also differences in polarity due to the presence of different functional groups.

**Keywords:** soda lignin; penetration; archaeological wood; infrared spectroscopy (ATR-FTIR); pyrolysis gas chromatography mass spectrometry (Py-GC/MS); scanning electron microscopy (SEM)

## 1. Introduction

From the mid-1800s to ca 1950-60s, alum salts (either pure  $KAl(SO_4)_2 \cdot 12 H_2O$  or mixtures with  $NH_4Al(SO_4)_2 \cdot 12H_2O$ ) were used to treat highly deteriorated archaeological waterlogged wood before drying to prevent their destruction [1–5]. However, this method is now known to cause chemical deterioration due to the presence of sulphuric acid in the wood [6–8]. The sulphuric acid was generated during the alum treatment and absorbed by the wood [9]. Due to the absorbed sulphuric acid, the pH of alum-treated wood is very low, ranging from 0 to 3.5, and high acidity is considered to be the main reason for the observed deterioration. Aluminium salts (aluminium chlorate, aluminium sulphate) have been reported to catalyse the degradation processes of polysaccharides [10–12]. Evidence of aluminium-catalysed hydrolysis of cellulose in paper treated with aluminium salts has also been found [13–15]. Generally, alum-treated wood has a highly degraded holocellulose fraction and an altered, partially depolymerized lignin structure [16]. To preserve alum-treated wood for future generations, the main strategy is to reconserve it [17–19]. The

general approach has relied on an aqueous method, where re-immersion in water removes alum salts and acidic products. The wood is then strengthened by impregnation with PEG 2000 or 3000 and, finally, freeze-dried. This produces a wood with pH of ca 5, which is strong enough for 'museum use', such as study and display.

A significant proportion of the wooden objects from the Viking Age Oseberg burial finds have been treated with alum salts from 1905 to ca 1912–1913 [4,20]. Aqueous retreatment is suitable for some of these objects, but for others, the wood would risk irreparable damage if re-conserved using the PEG freeze-dry method. This is because wooden objects may now be too deteriorated to withstand immersion in water or have previous damage from this treatment, which includes deep cracks, voids and collapse that would make an object fall apart if re-immersed. Furthermore, many of the objects have been restored using glue, plaster fills, new wood and metal hardware (screws, pins, iron bars, etc.) [21]. These objects also may have features that may be damaged during immersion or freeze-drying, such as fine surface carvings and tool marks. For such objects, we must find alternative retreatment strategies that are not water-based. The research project Saving Oseberg (2015–2020) was established to carry out investigations for this purpose.

This consideration has led us to try different types of non-aqueous consolidants, either commercially bought or developed within the Saving Oseberg project. One of the potential consolidants under investigation is based on lignin. Lignin is a major side product from the pulp and paper industry, which has high potential for further use. As it is a biopolymer derived from plants, it has relevant properties to potentially act as a consolidant for archaeological wood preservation. These include its binding and antimicrobial properties as well as its relative hydrophobicity compared to cellulose [22–25].

A soda lignin from mixed wheat straw/Sarkanda grass (P1000) was selected as a non-sulphur containing technical lignin, which is commercially available [22,26]. As the molar mass distribution could be a limiting factor for impregnation into the core of the wood, an ethyl acetate-fraction from the soda lignin was also studied [27].

The main aim of this work was to determine eventual differences in extent of penetration of the two lignins in archaeological wood after immersion in non-aqueous solutions using ethyl acetate as the solvent.

Methods used to evaluate penetration include pyrolysis gas-chromatography/mass spectrometry (Py-GC/MS) and attenuated total reflectance Fourier transform infrared spectroscopy (ATR-FTIR). We also investigated cellular morphology after treatment using scanning electron microscopy (SEM).

## 2. Materials and Methods

### 2.1. Wood Specimens

Discarded archaeological wood (identified as pine by light microscopy) recently excavated from Medieval Oslo in 2018 were donated from NIKU (Norsk institutt for kulturminneforskning). This was received as logs with diameter of ca 30 cm. The outermost 10 cm were more degraded than wood deeper below the surface. They were received in the waterlogged state and shortly afterwards were cut into  $2 \times 2 \times 2$  cm<sup>3</sup> cubes and freeze-dried. Specimens contained heartwood, sapwood or both. The cubes were then acclimatized to 50% RH and 20 °C.

A total of 23 archaeological specimens were chosen for these experiments: 13 for impregnation and 5 for density and maximum moisture content measurements (Table 1). Due to the variability in wood condition, both well-preserved and less well-preserved wood were mixed for each group. Sound pine was used as reference wood for density measurements (6 specimens) relative to 50% RH, 20 °C, as well as for ATR-FTIR, Py-GC/MS and SEM analyses.

**Table 1.** Specimens in each polymer, solvent or control group. Analysis methods are also indicated for each specimen.

Polymer/Solvent	Sample	Analysis		
		FTIR	Py-GC/MS	SEM
30% P1000 ( <i>w/v</i> )	9	x	x	x
	10	x	x	
	11	x	x	
	12	x	x	
30% FB01 ( <i>w/v</i> )	21	x	x	x
	22	x	x	
	23	x	x	
	24	x	x	
ethyl acetate control	37	x	x	x
	38	x		
	39			
	40			
	41	x		
no treatment, control	47	x	x	
	48	x		
	49	x		
	50	x		
	51	x		
oven-dry for characterization	52	x		
	53	x		
	54	x		
	55	x		
	56	x		

## 2.2. Density and Maximum Moisture Content Measurements

For density and maximum moisture content measurements, 5 archaeological cubes were re-waterlogged (specimens 52–56) by submerging cubes in water under low vacuum pressure. After waterlogging, the specimens were weighed, and their volumes were measured by water displacement. After measurements, the specimens were oven-dried to constant weight (105 °C). The basic density was calculated by dividing the oven-dried weight by the waterlogged volume. For specimens acclimatized to 50% RH and 20 °C (specimens 47–51 and sound pine, specimens 60, 70, 80, 90, 99, 100), density was based on the weight at 50% RH and volume based on direct measurement.

## 2.3. Materials Used for Impregnation

A commercially available soda lignin from mixed wheat straw/Sarkanda grass (P1000) was obtained from GreenValue (US/India). Lignin isolation by the soda method is described by Browning [28]. A lower molar mass fraction (FB01) was obtained by fractionating P1000 in ethyl acetate, using the procedure described by Gosselink, Putten and Van Es [27]. After collection of the solubilized lignin in ethyl acetate, the solvent was removed by rotary evaporation under reduced pressure. The recovered lignin fraction (FB01) was finally dried at 30 °C.

Chemical composition of both P1000 and FB01 were determined using wet chemical methods, where the lignin content was determined after a two-step hydrolysis as Klason lignin, the acid-insoluble fraction (AIL) and acid-soluble lignin (ASL). The carbohydrates were quantified by high performance anion exchange chromatography with pulsed amperometric detection (HPAEC-PAD) in the hydrolysate as previously described by Gosselink, van Dam, de Jong, Scott, Sanders, Li and Gellerstedt [29]. P1000 contained 83.5% AIL, 4.8% ASL, 1.9% Ash and 2.8% carbohydrates. FB01 contained 76.5% AIL, 5.8% ASL and 0.4% carbohydrates.

The chemical composition of P1000 and FB01 was also determined by Py-GC/MS in order to be able to properly evaluate the results obtained for the specimens after treatment. The results of this analysis are presented in Supplementary Materials, while the pyrolysis products deriving exclusively from these lignins have been highlighted in red in Table 2.

**Table 2.** Pyrolysis products identified by Py-GC/MS. Fragment ions' mass-over-charge ratios (m/z) are also shown, where the m/z in bold indicates the main ion. Compounds were categorized, where H—holocellulose, L—lignin, lignin units: p-hydroxyphenyl (H-lignin), guaiacyl (G-lignin) and syringyl (S-lignin). Lignin pyrolysis products in red script were identified in lignin preparations (P1000, FB01). These were either very low or absent in archaeological pine and were used to evaluate lignin penetration in test specimens.

	Compound	Fragment Ions (m/z)	Category	Origin
1	1,2-dihydroxyethane (2TMS)	73, 103, <b>147</b> , 191	small molecules	H/L
2	2-hydroxymethylfuran (TMS)	53, 73, <b>81</b> , 111, 125, 142, 155, 170	furan	H
3	phenol (TMS)	75, <b>151</b> , 166	short chain	H-lignin
4	2-hydroxypropanoic acid (2TMS)	73, 117, <b>147</b> , 190	small molecules	H/L
5	2-hydroxyacetic acid (2TMS)	73, <b>147</b> , 177, 205	small molecules	H/L
6	1-hydroxy-1-cyclopenten-3-one (TMS)	53, 73, 81, 101, 111, 127, <b>155</b> , 169	cyclopentenone	H
7	3-hydroxymethylfuran (TMS)	53, 75, <b>81</b> , 111, 125, 142, 155, 170	furan	H
8	o-cresol (TMS)	73, 91, 135, 149, <b>165</b> , 180	short chain	H-lignin
9	2-furancarboxylic acid (TMS)	73, 95, <b>125</b> , 169, 184	furan	H
10	unknown I	73, <b>152</b> , 167	small molecules	H
11	m-cresol (TMS)	73, 91, <b>165</b> , 180	short chain	H-lignin
12	2-hydroxy-1-cyclopenten-3-one (TMS)	53, 73, 81, 101, 111, 127, <b>155</b> , 170	cyclopentenone	H
<b>13</b>	<b>p-cresol (TMS)</b>	<b>73, 91, 165, 180</b>	<b>short chain</b>	<b>H-lignin</b>
14	3-hydroxy-(2H)-pyran-2-one (TMS)	75, 95, 125, 151, <b>169</b> , 184	pyran	H
15	unknown II	59, 73, 85, 101, 115, <b>131</b> , 159	small molecules	H
16	unknown III	59, <b>73</b> , 85, 103, 115, 129, 145, 173, 188	small molecules	H

Table 2. Cont.

	Compound	Fragment Ions (m/z)	Category	Origin
17	Z-2,3-dihydroxy-cyclopent-2-enone (TMS)	59, 73, 115, 143, 171, 186	cyclopentenone	H
18	E-2,3-dihydroxy-cyclopent-2-enone (TMS)	75, 101, 143, 171, 186	cyclopentenone	H
19	1,2-dihydroxybenzene (TMS)	75, 91, 136, 151, 167, 182	hydroxybenzene	H/L
20	3-hydroxy-(4H)-pyran-4-one (TMS)	75, 95, 139, 151, 169, 184	pyran	H
21	5-hydroxy-2H-pyran-4(3H)-one (TMS)	59, 75, 101, 129, 143, 171, 186	pyran	H
22	2-hydroxymethyl-3-methyl-2-cyclopentenone (TMS)	73, 103, 129, 173, 183, 198	cyclopentenone	H
23	1-hydroxy-2-methyl-1-cyclopenten-3-one (TMS)	73, 97, 125, 139, 169, 184	cyclopentenone	H
24	1-methyl-2-hydroxy-1-cyclopenten-3-one (TMS)	73, 97, 125, 139, 169, 184	cyclopentenone	H
25	1,3-dihydroxyacetone (2TMS)	73, 103, 147, 189, 219	small molecules	H/L
26	guaiacol (TMS)	73, 151, 166, 181, 196	short chain	G-lignin
27	ethyl phenol TMS	73, 135, 179, 194	short chain	H-lignin
28	3-hydroxy-6-methyl-(2H)-pyran-2-one (TMS)	73, 109, 139, 168, 183, 198	pyran	H
29	vinyl phenol (TMS)	73, 151, 177, 192	short chain	H-lignin
30	2-methyl-3-hydroxy-(4H)-pyran-4-one (TMS)	73, 101, 153, 183, 198	pyran	H
31	2-methyl-3-hydroxymethyl-2-cyclopentenone (TMS)	73, 103, 129, 173, 183, 198	cyclopentenone	H
32	2,3-dihydrofuran-2,3-diol (2TMS)	73, 147, 231, 246	furan	H
33	2-furyl-hydroxymethylketone (TMS)	73, 81, 103, 125, 183, 198	furan	H
34	5-hydroxymethyl-2-furaldehyde (TMS)	73, 81, 109, 111, 139, 169, 183, 198	furan	H



Table 2. Cont.

	Compound	Fragment Ions (m/z)	Category	Origin
35	4-methylguaiacol (TMS)	73, 149, <b>180</b> , 195, 210	short chain	G-lignin
36	1,2-dihydroxybenzene (2TMS)	<b>73</b> , 151, 239, 254	hydroxybenzene	H/L
37	2-hydroxymethyl-2,3-dihydropyran-4-one (TMS)	73, 142, 170, 185, 200	pyran	H
38	1,4:3,6-dianhydro- $\alpha$ -D-glucopyranose (TMS)	<b>73</b> , 103, 129, 155, 170, 171, 186	anhydrosugars	H
39	Z-2,3-dihydroxy-cyclopent-2-enone (2TMS)	73, 147, 230, <b>243</b> , 258	cyclopentenone	H
<b>40</b>	<b>p-hydroxy benzaldehyde TMS</b>	<b>73, 151, 179, 194</b>	<b>carbonyl</b>	<b>H-lignin</b>
41	4-methylcatechol (2TMS)	<b>73</b> , 180, 253, 268	demethylated	G-lignin
42	4-ethylguaiacol (TMS)	73, 149, 179, <b>194</b> , 209, 224	short chain	G-lignin
<b>43</b>	<b>syringol (TMS)</b>	<b>73, 153, 181, 196, 211, 226</b>	<b>short chain</b>	<b>S-lignin</b>
44	1,4-dihydroxybenzene (2TMS)	73, 112, <b>239</b> , 354	hydroxybenzene	H/L
45	arabinofuranose (4TMS)	73, 147, <b>217</b> , 230		H
46	4-vinylguaiacol (TMS)	73, 162, 177, <b>192</b> , 207, 222	short chain	G-lignin
47	3-hydroxy-2-hydroxymethyl-2-cyclopentenone (2TMS)	73, 147, <b>257</b> , 272	cyclopentenone	H
48	E-2,3-dihydroxy-cyclopent-2-enone (2TMS)	73, 147, <b>243</b> , 258	cyclopentenone	H
49	4-ethylcatechol (2TMS)	<b>73</b> , 147, 179, 231, 267, 282	demethylated	G-lignin
50	3-hydroxy-2-(hydroxymethyl) cyclopenta-2,4-dienone (2TMS)	73, 147, <b>255</b> , 270	cyclopentenone	H
51	eugenol (TMS)	73, 147, 179, <b>206</b> , 221, 236	long chain	G-lignin
<b>52</b>	<b>4-methylsyringol (TMS)</b>	<b>73, 167, 210, 225, 240</b>	<b>short chain</b>	<b>S-lignin</b>
53	3-methoxy-1,2-benzenediol (2TMS)	<b>73</b> , 153, 254, 269, 284	demethylated	G-lignin
54	3,5-dihydroxy-2-methyl-(4H)-pyran-4-one (2TMS)	73, 128, 147, 183, <b>271</b> , 286	pyran	H
55	1,6-anhydro-beta-D-glucopyranose (TMS at position 4)	73, 103, 117, <b>129</b> , 145, 155, 171	anhydrosugars	H

Table 2. Cont.

	Compound	Fragment Ions (m/z)	Category	Origin
56	1,6-anhydro-beta-D-glucopyranose (TMS at position 2)	73, 101, 116, 129, 132, 145, 155, 171	anhydrosugars	H
57	Z-isoeugenol (TMS)	73, 179, 206, 221, 236	long chain	G-lignin
58	vanillyl alcohol (2TMS)	73, 151, 210, 253, 268, 283, 298	long chain	G-lignin
59	vanillin (TMS)	73, 194, 209, 224	carbonyl	G-lignin
60	methyl 4-hydroxy-3,5-dimethoxybenzoate TMS	73, 223, 254, 269, 284	ester	S-lignin
61	1,2,3-trihydroxybenzene (3TMS)	73, 133, 147, 239, 327, 342	hydroxybenzene	H
62	4-ethylsyringol (TMS)	73, 191, 209, 224, 239, 254	short chain	S-lignin
63	E-isoeugenol (TMS)	73, 179, 206, 221, 236	long chain	G-lignin
64	1,4-anhydro-D-galactopyranose (2TMS)	73, 101, 116, 129, 145, 155, 171, 217	anhydrosugars	H
65	1,6-anhydro-D-galactopyranose (2TMS)	73, 101, 116, 129, 145, 161, 189, 204, 217	anhydrosugars	H
66	2-hydroxymethyl-5-hydroxy-2,3-dihydro-(4H)-pyran-4-one (2TMS)	73, 129, 147, 155, 183, 273, 288	pyran	H
67	4-vinylsyringol (TMS)	73, 179, 222, 237, 252	short chain	S-lignin
68	1,4-anhydro-D-glucopyranose (2TMS at position 2 and 4)	73, 101, 116, 129, 155, 191, 204, 217	anhydrosugars	H
69	1,2,4-trihydroxybenzene (3TMS)	73, 133, 147, 239, 327, 342	hydroxybenzene	H
70	acetovanillone (TMS)	73, 193, 208, 223, 238	carbonyl	G-lignin
71	4-hydroxy benzoic acid (2TMS)	73, 147, 193, 223, 267, 282	acid	H-lignin
72	1,6-anhydro-beta-D-glucopyranose (2TMS at position 2 and 4)	73, 101, 116, 129, 155, 191, 204, 217	anhydrosugars	H
73	propenyl-syringol (TMS)	73, 205, 236, 251, 266	long chain	S-lignin
74	1,4-anhydro-D-galactopyranose (3TMS)	73, 129, 147, 157, 191, 204, 217, 243, 332	anhydrosugars	H

Table 2. Cont.

	Compound	Fragment Ions (m/z)	Category	Origin
75	syringaldehyde (TMS)	73, 224, 239, 254	carbonyl	S-lignin
76	2,3,5-trihydroxy-4H-pyran-4-one (3TMS)	73, 133, 147, 239, 255, 270, 330, 345, 360	pyran	H
77	1,6-anhydro-beta-D-glucopyranose (3TMS)	73, 103, 129, 147, 191, 204, 217, 243, 333	anhydrosugars	H
78	1,4-anhydro-D-glucopyranose (3TMS)	73, 103, 129, 147, 191, 204, 217, 243, 332	anhydrosugars	H
79	<i>E</i> -propenylsyringol (2TMS)	73, 205, 236, 251, 266	long chain	S-lignin
80	1,6-anhydro-beta-D-glucofuranose (3TMS)	73, 103, 129, 147, 191, 204, 217, 243, 319	anhydrosugars	H
81	vanillic acid (2TMS)	73, 253, 282, 297, 312	acid	G-lignin
82	acetosyringone (TMS)	73, 223, 238, 253, 268	carbonyl	S-lignin
83	vanillylpropanol (2TMS)	73, 179, 206, 221, 236, 311, 326	long chain	G-lignin
84	<i>Z</i> -coniferyl alcohol (2TMS)	73, 204, 252, 293, 309, 324	monomer	G-lignin
85	coumaryl alcohol (2 TMS)	73, 189, 205, 267, 279, 294	monomer	H-lignin
86	coniferylaldehyde (TMS)	73, 192, 220, 235, 250	carbonyl	G-lignin
87	syringic acid (2TMS)	73, 253, 297, 312, 327, 342	acid	S-lignin
88	<i>E</i> -coniferyl alcohol (2 TMS)	73, 204, 252, 293, 309, 324	monomer	G-lignin
89	3,4-dihydroxy cinnamyl alcohol (3TMS)	73, 205, 293, 355, 382	demethylated	G-lignin
90	<i>E</i> -synapyl alcohol (2TMS)	73, 234, 323, 339, 354	monomer	S-lignin
91	Ferulic acid (2TMS)	73, 249, 308, 323, 338	acid	G-lignin

P1000 has a (weight average) molecular weight  $M_w$  of  $(3.0 \pm 0.1)$  kDa, and FB01 has an  $M_w$  of  $(1.0 \pm 0.1)$  kDa as characterized by sedimentation equilibrium in the analytical ultracentrifuge reinforced by size exclusion chromatography measurements, which determined 2242 Daltons for P1000 and 1272 Daltons for FB01 [30]. Both lignin preparations had oblate disc-like conformations [30].

Ethyl acetate was purchased from Sigma-Aldrich.

#### 2.4. Impregnation Set-Up

The investigation presented here was part of a larger study which involved more specimens, treated at different lignin concentrations (5%, 10% and 30%). The data obtained

for concentrations lower than 30% were less clear both from the point of view of penetration and deposition. This led to the final choice of a 30% solution of lignin preparation.

Table 1 gives an overview of the impregnation systems used here and which analytical methods were used on each specimen.

Pre-immersion: wood specimens were saturated with ethyl acetate.

Impregnation: After solvent saturation, the specimens were immersed in 30% (weight/volume) concentrations of each lignin, made up to 100 mL using volumetric flasks. Immersion took place under normal atmospheric pressure. The lignin concentration is only approximate, as we did not know the exact solubility of lignin in ethyl acetate, and there was undissolved lignin residue in the volumetric flask.

There were four specimens tested for each lignin preparation. Five control specimens were immersed in ethyl acetate only (specimens 37–41). Five specimens remained completely untreated (specimens 47–51) and were stored in a climate chamber set to 50% RH and 20 °C.

Immersion time was two weeks, as previous experience has shown that the specimen size used here allows for full penetration of archaeological wood using polyethylene glycol (PEG 2000).

Drying: After removal from lignin solutions, the specimens were slowly air-dried for four days before they were placed in a climate chamber at 50% RH and 20 °C. Drying was monitored by weight change. Constant weight was reached after 21 days at 50% RH and 20 °C.

Before and after treatment, photographs were taken of each treatment group.

### 2.5. Change in Dimensions and Weight

Dimensions after each step of the treatment (dry state, after solvent saturation, after lignin impregnation and after drying) were measured based on reference pins placed into the cross-section of the wood in both radial and tangential orientations. Here, we report dimensions before and after treatment only. Dimensional changes in treated woods after acclimatization to 50% RH and 20 °C were compared against that measured at the start, when wood was dry, yet acclimatized to 50% RH and 20 °C. Equation (1) shows how % linear dimensional change was calculated.

$$\% \text{ linear dimensional change} = \frac{\left( \text{Dimension After}_{(\text{Rad or Tan})} - \text{Dimension Before}_{(\text{Rad or Tan})} \right)}{\text{Dimension Before}_{(\text{Rad or Tan})}} \times 100\% \quad (1)$$

Weight was measured using a 4-decimal balance before treatment, after each treatment step mentioned above as well as after acclimatization at 50% RH and 20 °C. Note, however, that weights measured in the ‘wet’ state are not reported here, as they were only valid to 1–2 decimal places due to the rapid evaporation of ethyl acetate during weighing.

### 2.6. Chemical Characterization and Distribution

After treatment, penetration and distribution of polymers within wood cells was assessed by weight gain, by SEM, PY-GC/MS and by ATR-FTIR.

Morphological analyses of cross-sections of selected specimens were undertaken by scanning electron microscopy (SEM).

#### 2.6.1. SEM

Morphological analyses were performed using a FEI Quanta 450 Scanning Electron Microscope, using low vacuum mode to avoid charging and a voltage of 8 kV. The spot size was 4.5–5, chamber pressure 90–100 Pa, and the working distance between detector and sample was 10–13mm, depending on the sample.

### 2.6.2. ATR-FTIR

Fourier transform infrared spectroscopy of untreated and treated archaeological pine and reference samples (sound pine and pure lignins) were carried out in the attenuated total reflection (ATR) mode on a Thermo Fischer FTIR spectrometer (Nicolet iS50), with range 4000–400  $\text{cm}^{-1}$ . Each spectrum was acquired with 32 scans and 4  $\text{cm}^{-1}$  resolution. Three spectra were taken of each sample and averaged. For each specimen, infrared spectra were taken at four depths: outer surface, inner surface (the underside of the surface sample), core edge and core centre (Figure 1). Averaged spectra at each depth were baseline corrected and normalized to the band maximum in the range 1027–1032  $\text{cm}^{-1}$ . To assess the extent of penetration of P1000 and FB01 lignins in archaeological wood, spectral band heights were then measured at ca 1328  $\text{cm}^{-1}$  at each depth for each treated specimen. Band heights from the same depth for each treatment group were then averaged. For example, for P1000 lignin, all ‘outer surface’ spectra were averaged. This was repeated for each depth analysed, for each P1000 and FB01 lignin treatments.

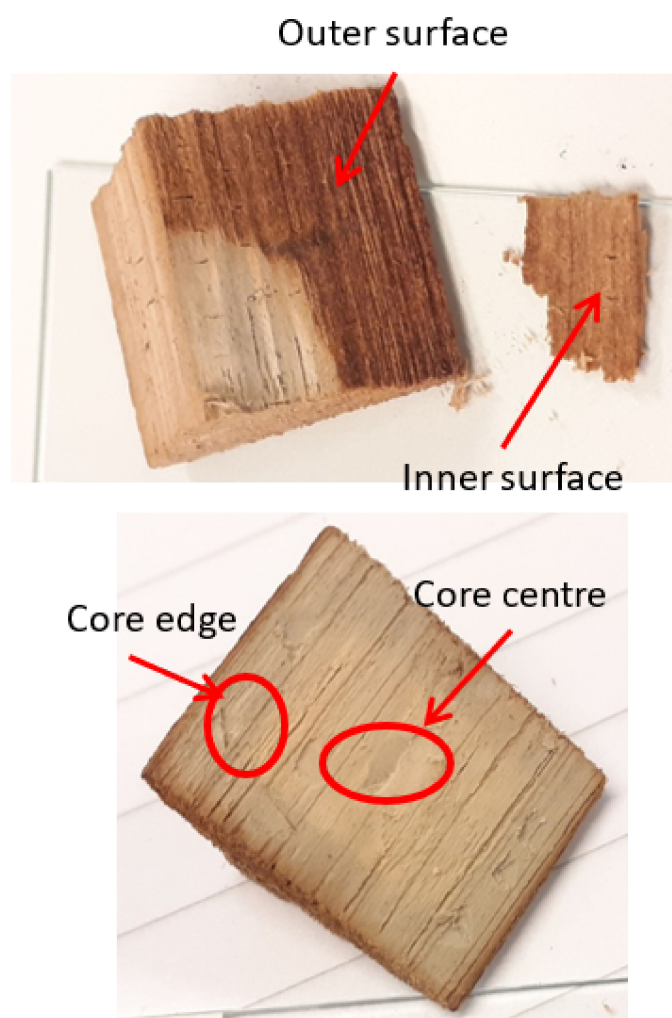


**Figure 1.** Areas sampled for infrared analyses: ‘outer surface’, ‘inner surface’, ‘core edge’ and ‘core centre’. For Py-GC/MS, only ‘inner surface’ and ‘core centre’ were analysed. These depths were used to evaluate penetration of the polymer.

### 2.6.3. Analytical Pyrolysis Py-GC/MS

Analytical pyrolysis was performed at 550 °C for 0.2 min in the presence of 1,1,1,3,3,3-hexamethyldisilazane (HMDS, chemical purity 99.9%, Sigma Aldrich Inc., St. Louis, MO, USA) for the thermally assisted silylation of pyrolysis products. A micro-furnace of

Multi-Shot Pyrolyzer EGA/Py-3030D (Frontier Lab) was coupled to a gas chromatograph 6890 Agilent Technologies (USA) equipped with an HP-5MS fused silica capillary column (stationary phase 5% diphenyl—95% dimethyl-polysiloxane, 30 m × 0.25 mm i.d., Hewlett Packard, USA) and with a deactivated silica pre-column (2 m × 0.32 mm i.d., Agilent J&W, USA). The GC was coupled with an Agilent 5973 Mass Selective Detector operating in electron impact mode (EI) at 70 eV. Approximately 80 µg of sample and 2 µL HMDS were inserted into a stainless steel cup and placed in the micro-furnace. Before analysis, all the samples were oven-dried for 24 h at 40–50 °C to remove residual water. Samples were analysed in triplicate.

Ninety-one pyrolysis products were identified by comparing their mass spectra with spectra reported in the Wiley and NIST08 libraries and in the literature [31,32] and reported in Table 2. Deconvolution and integration of chromatographic peaks derived from lignin and holocellulose pyrolysis products were carried out by AMDIS software (automated mass spectral deconvolution and identification system by NIST). Semi-quantitative calculations were performed using chromatographic areas: peak areas were normalised with respect to the sum of the peak areas of all the pyrolysis products identified, and the data were averaged and expressed as percentages. The percentage areas were used to calculate the relative abundances of wood pyrolysis products divided into categories on the base of their chemical structure as described in [33]. Lignin pyrolysis products were sorted into six groups: monomers, long chain, short chain, demethylated, carbonyl and acid, while holocellulose pyrolysis products into five categories: furans, cyclopentenones, pyranones, hydroxybenzenes and anhydrosugars.

Samples analysed by Py-GC/MS were taken from the ‘inner surface’ and ‘core centre’, as shown in Figure 1.

### 3. Results and Discussion

#### 3.1. Characterization of Wood Specimens before Treatment

##### 3.1.1. Macroscopic Observations

Annual rings were not perfectly aligned with cut faces. Specimens were composed of both well-preserved and more degraded wood, related to where they originated from the log. Some specimens contained defects, such as knots and cracks (Figure 2). It is very difficult to obtain flawless sampling material from archaeological wood.

##### 3.1.2. Density and Maximum Moisture Content

The basic density of archaeological specimens (52–56) showed a variation in the state of preservation of the archaeological wood, ranging from 0.210 g/cm<sup>3</sup> to 0.443 g/cm<sup>3</sup> (Table 3). Specimens 52 and 53 were much better preserved than specimens 54, 55 and 56. For comparison, sound pine has a density of about 0.5 g/cm<sup>3</sup>, based on our own measurements of oven-dried sound pine. The maximum moisture content of the archaeological specimens ranged from 140–410%. The wood specimens may, thus, be considered to be low (52, 53) to medium degraded (54, 55, 56), see for example Grattan and Clarke [34]. This variation in condition is common in archaeological wood, due to uneven degradation in the soil. As degradation during burial proceeds from the surface to the inner core, surfaces are generally more degraded than cores.

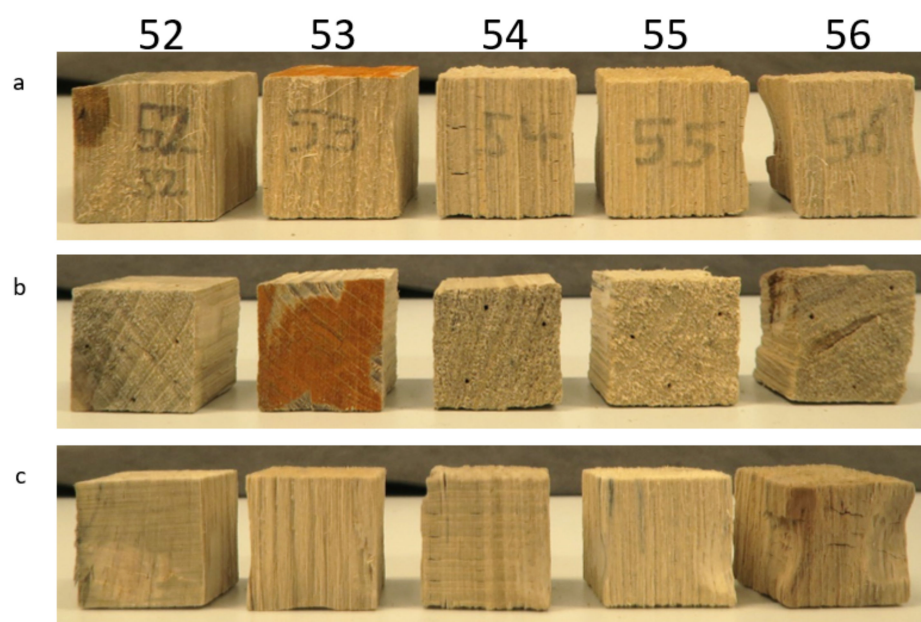


**Figure 2.** Samples used for wood characterization after oven-drying. Images show variability in samples: (a) nr. 52 has a knot (dark spot on upper left corner), 54 shows cross-grained cracking after freeze-drying or oven-drying. (b) nr. 53 has orange staining on its transverse section, possibly iron compounds. Additionally, note that the annual rings are not aligned with sample sides. (c) nr. 56 shows cross-grained cracking after freeze- or oven-drying.

**Table 3.** Characterization of wood specimens by density and maximum moisture content. For the oven-dried specimens, density is based on oven-dried weight and waterlogged volume. For the specimens acclimatized to 50% RH and 20 °C, the density is based on weight at 50% RH and volume at 50% RH.

Specimen Nr.	Density (g/cm <sup>3</sup> )	Max MC, %
Archaeological pine, oven-dried		
52	0.443	140
53	0.431	153
54	0.217	393
55	0.225	381
56	0.210	410
Archaeological pine, freeze-dried, acclimatized to 50% RH, 20 °C		
47	0.258	
48	0.237	
49	0.361	
50	0.244	
51	0.381	

The density of freeze-dried archaeological pine specimens (47–51) acclimatized to 50% RH and 20 °C were also measured (Table 3). Again, there are relatively large differences in densities among archaeological wood specimens (range: 0.237–0.381 g/cm<sup>3</sup>). Specimens 49 and 51 are best preserved.

### 3.1.3. Analytical Pyrolysis (Py-GC/MS)

Sound untreated pine, archaeological untreated pine and archaeological wood immersed in ethyl acetate are considered reference specimens. Seventy-four pyrolysis products deriving from holocellulose and lignin were identified and their peaks integrated. Pine is a conifer, and its lignin is mainly composed of guaiacyl units. The semi-quantitative analysis results show that the archaeological pine is composed of about 50% of polysaccharides and 50% of lignin (Table 4), showing that it is well preserved when compared with undegraded reference sound wood.

**Table 4.** Percentage composition of pine reference woods determined by Py-GC/MS, collected from external and internal parts of the cubes. H = holocellulose, L = lignin, H/L = ratio of holocellulose over lignin.

	Sound Pine	Archaeological Pine Untreated	Archaeological Pine Ethyl Acetate Treated
Specimen	/	47	37
H%	60.7	49.9	40.1
L%	39.3	50.1	59.9
H/L	1.54	1	0.67

As expected, the polysaccharide fraction in the archaeological specimen is preferentially degraded, resulting in H/L indices lower than those of fresh wood. Differences between specimens of untreated and solvent-treated archaeological woods (47 and 37, respectively), are also apparent, demonstrating not only the heterogeneity of the wood specimens, likely related to variability in the initial state of preservation but also the extractive capacity of the solvent. According to polysaccharide content, nr. 37 is not as well preserved as nr. 47. Further details of reference specimens are given in the Supplementary Materials.

### 3.1.4. Infrared Spectroscopy (ATR-FTIR)

The chemical state of preservation of all control specimens were investigated by infrared spectroscopy and compared to spectra from sound pine. Variability in archaeological wood substrates was noted in infrared analyses. Figure 3 shows the spectrum from a representative untreated, medium-degraded specimen (nr. 47), an ethyl acetate-treated control (nr. 37) and sound pine. Table 5 gives an overview of the band assignments referred to here. Specimens 37 and 47 showed a decrease in signals from hemicellulose (1733, 1242  $\text{cm}^{-1}$ ). Signals originating from cellulose (1370, 1156, 896  $\text{cm}^{-1}$ ) were present in both nrs. 37 and 47, but have lower absorbances than sound pine. In other archaeological specimens, we observed these signals as well, but with varying strength, decreasing with increasing degradation. For nrs. 37 and 47, lignin signals (at 1592, 1508, 1264 and 1217  $\text{cm}^{-1}$ ) are enhanced due to reduction in signals from hemicellulose and cellulose. We also see that both nrs. 37 and 47 are more oxidized (1605  $\text{cm}^{-1}$ ). These observations are confirmed by Py-GC/MS, although pyrolysis does not distinguish cellulose from hemicellulose. For both sound pine and archaeological woods, the band with greatest absorbance occurs at 1028  $\text{cm}^{-1}$ , which is a combined C-O stretch band containing signals predominantly from carbohydrates (cellulose and hemicellulose). Spectra also show that the untreated specimen (nr. 47) and that which had been treated with ethyl acetate (nr. 37) are very similar to each other. The differences at ca. 1600  $\text{cm}^{-1}$  may be either due to removal of extractive compounds by ethyl acetate or due to natural variability.



**Table 5.** Overview of band assignments for infrared spectroscopy.

Band Position (cm <sup>-1</sup> )	Assignment	Reference
1738–1709	C=O stretch in unconjugated ketones, carbonyls and in ester groups, frequently of carbohydrate origin; conjugated aldehydes and carboxylic acids absorb around and below 1700 cm <sup>-1</sup>	[35]
1646	conjugated C=O groups, mainly originating from lignin	[36]
1635	adsorbed water	[35]
1605–1593	aromatic skeletal vibrations plus C=O stretch	[35]
1515–1505	aromatic skeletal vibrations	
1375–1374	CH deformation vibration (cellulose)	
1326	syringyl plus guaiacyl ring condensed	[37]
1270–1266	G ring plus C=O stretch	
1235–1225	OH plane deformation, also COOH	[35]
1230–1221	C-C plus C-O plus C=O stretch; G-condensed > G-etherified	
1162–1125	C-O-C asymmetric valence vibration (cellulose)	
1151	C-O-C asymmetric valence vibration in cellulose and hemicelluloses	[38]
1110–1107	ring asymmetric valence vibration	[35]
1024	C-O stretch in cellulose and hemicelluloses; C-O of primary alcohol	[38]
892	C-H deformation in cellulose; C1 group frequency in cellulose and hemicelluloses	
835–834	C-H out-of-plane in position 2 and 6 of S and in all positions of H units	[39]
832–817	C-H out-of-plane in positions 2, 5 and 6 of G units	

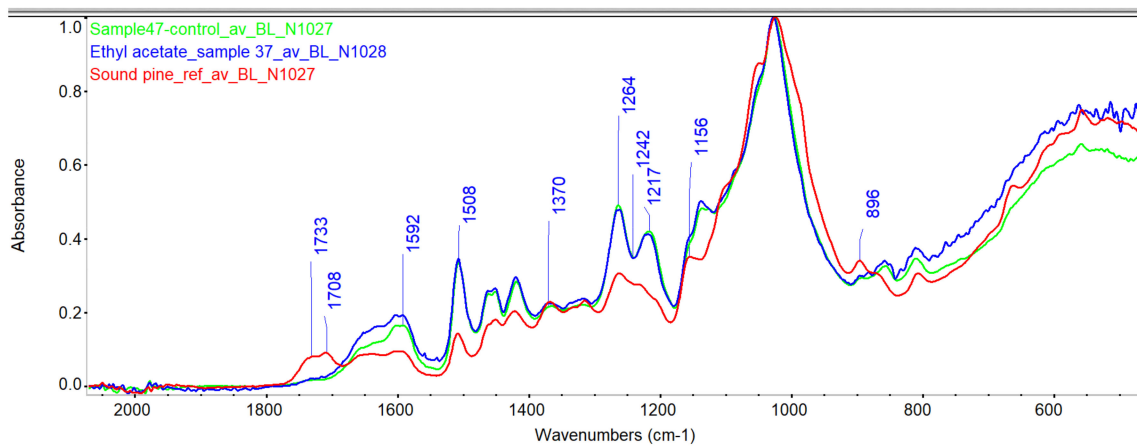


**Figure 3.** Infrared spectra of archaeological wood, untreated specimen nr. 47 (green curve), ethyl acetate-treated control nr. 37 (blue curve) and sound pine (red curve). Main differences are highlighted at indicated bands.

### 3.2. After Treatment

Specimens treated with ethyl acetate, P1000 and FB01 are shown in Figure 4. It is obvious that the introduction of lignin has caused darkening. Different faces of the same specimen cube were unevenly coloured after treatment. The figure also shows the inner wood from specimens 12, 24 and 37. It is clear that P1000 treated wood is much lighter in colour than that treated with FB01, suggesting that the larger P1000 has penetrated less into the specimens.

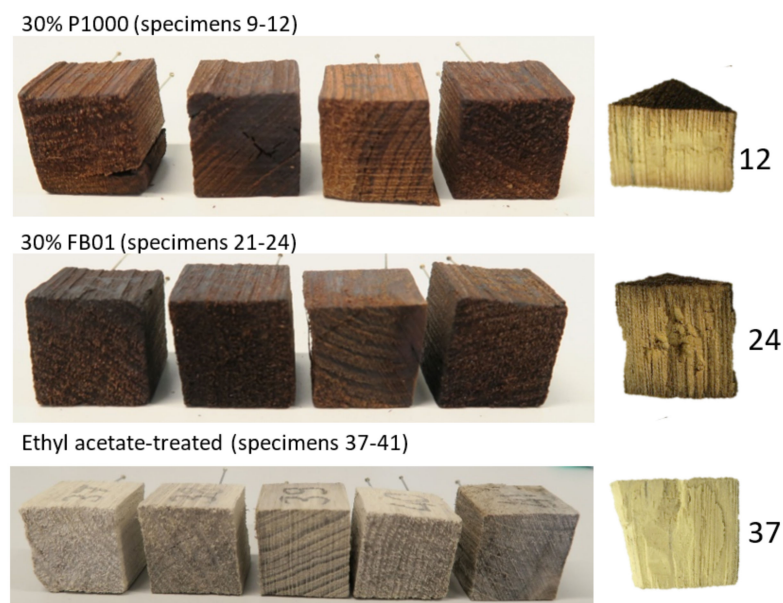


**Figure 4.** Specimens treatment with 30% lignins P1000, FB01 (*w/v*) and the control (ethyl acetate-immersed) after air-drying. Specimens 12, 24 and 37 are also shown after they were cut in half for sampling.

In many cases such a darkening as seen on surfaces of the lignin-treated specimens would be unacceptably high for objects. However, acceptable colour change depends on the benefits of a particular consolidant and the colour of the starting material. For alum-treated wood from Oseberg, many are very dark to start with, and the colour change may not be unduly large if treated with lignin.

### 3.2.1. Weight Gain

Both lignin treatments increased weight of specimens (Table 6). It was expected that some weight loss in ethyl acetate controls would occur during immersion due to dissolution of wood resins (which turned the solvent a pale yellow). Weight losses of up to 1.5% were recorded. However, one specimen (41) lost more than 10% of its initial weight after immersion in ethyl acetate. This was due to the loss of material from the knot region during immersion.

P1000 lignin, which has a MW of 4000, had lower weight gain (from 13–19%) compared to FB01 (MW 1000), which ranged from 61–68% (Table 6). However, specimen 11 (P1000 treated) had only 10% weight gain, and specimen 23 (FB01 treated) had 23% weight gain. Both specimens had markedly greater initial weights, indicating better preservation. Thus, more lignin uptake occurred in samples that were in worse condition. Wood with greater degradation has lost more of its polymers, which increases porosity, allowing for more uptake of lignin. This is visible in SEM images, shown in Section 3.2.3.

Mechanical tests were not undertaken in these experiments, but observations during preparation of some specimens for infrared and SEM analyses were noted. The treatment with lignin made some specimens ‘harder to cut’ than those that were untreated (see Comments in Table 6). This was surprising, as the lignin is not a film-forming material on its own, it is a powder, and as such, we did not expect it to increase the specimens’ cutting resistance. However, an increase in hardness is very likely due to non-covalent interactions between the lignin and wood.

### 3.2.2. Dimensional Changes

Table 7 and Figure 5 show linear shrinkages for all specimens, expressed as % dimensional change in the tangential and radial directions relative to before treatment, including both oven-dried and the ethyl acetate-treated controls. Untreated controls were measured as well, even though they did not undergo treatment.

For sound pine, one would expect most dimensional change in the radial direction, especially in the larger and thinner earlywood cells. This is because in pine, the tangential direction is more physically reinforced than in the radial direction, due to the low area of overlap between rays and tracheids, which is much lower than in many other woods, such as oak or birch [40]. Furthermore, the shape of cells also plays a role. In pine, thin-walled earlywood cells are elongated in the radial direction, while thick-walled latewood cells are elongated in the tangential direction. This makes earlywood cells more susceptible to compression in the radial direction.

**Table 6.** Changes in weight relative to start weight.

Polymer/Solvent	Sample	Before Treatment (g) *	After Treatment (g) *	% Change Relative to Start	Comment
30% P1000 ( <i>w/v</i> )	9	2.1580	2.4369	12.9	
	10	2.2111	2.6099	18.0	hard to cut
	11	3.5335	3.8734	9.6	hard to cut
	12	2.1890	2.6101	19.2	
30% FB01 ( <i>w/v</i> )	21	2.1147	3.5541	68.1	
	22	2.3584	3.8057	61.4	very hard to cut
	23	3.7985	4.6819	23.3	very hard to cut
	24	2.1844	3.6044	65.0	
ethyl acetate control	37	2.2583	2.2555	−0.1	easy to cut
	38	2.5720	2.5306	−1.6	easy to cut
	39	4.2203	4.1607	−1.4	orange end grain (corrosion)
	40	2.1703	2.1559	−0.7	easy to cut
	41	5.1835	4.5726	−11.8	knot

\* weight after freeze-drying and conditioning at 50% RH, 20 °C.

**Table 7.** Dimensional change in samples relative to before treatment. ‘Rad’ is the distance in the radial direction, and ‘Tan’ is the distance in the tangential direction on the transverse face.

Polymer/Solvent	Sample	Before Treatment (Dry State)		After Impregnation and Drying		% Change Relative to Start	
		(mm)		(mm)		Rad	Tan
		Rad	Tan	Rad	Tan		
30% P1000 ( <i>w/v</i> )	9	7.97	8.74	8.04	8.86	0.9	1.4
	10	8.99	10.39	9.06	10.44	0.8	0.5
	11	6.19	10.25	6.20	10.31	0.2	0.6
	12	8.77	10.66	8.86	10.68	1.0	0.2
30% FB01 ( <i>w/v</i> )	21	7.64	12.49	7.68	12.48	0.5	−0.1
	22	9.12	10.76	9.15	10.71	0.3	−0.5
	23	9.40	10.19	9.40	10.14	0.0	−0.5
	24	9.00	9.67	9.54	8.97	6.0	−7.2
ethyl acetate control	37	7.06	11.65	7.20	11.68	2.0	0.3
	38	6.50	8.53	6.45	8.41	−0.8	−1.4
	39	8.26	7.36	8.33	7.39	0.8	0.4
	40	9.30	11.40	9.31	11.45	0.1	0.4
	41	8.72	4.58	8.74	5.59	0.2	22.1
no treatment, control	47	9.28	9.53	9.38	9.55	1.1	0.2
	48	10.40	11.17	10.38	11.26	−0.2	0.8
	49	5.10	7.91	5.15	7.89	1.0	−0.3
	50	6.12	10.40	6.15	10.34	0.5	−0.6
	51	11.17	13.72	11.08	13.36	−0.8	−2.6
oven-dry for characterization	52	12.28	13.01	11.65	12.16	−5.1	−6.5
	53	9.09	15.03	8.39	13.96	−7.7	−7.1
	54	10.32	13.04	9.96	12.38	−3.5	−5.1
	55	10.44	15.36	9.98	14.30	−4.4	−6.9
	56	13.92	14.83	13.54	14.28	−2.7	−3.7

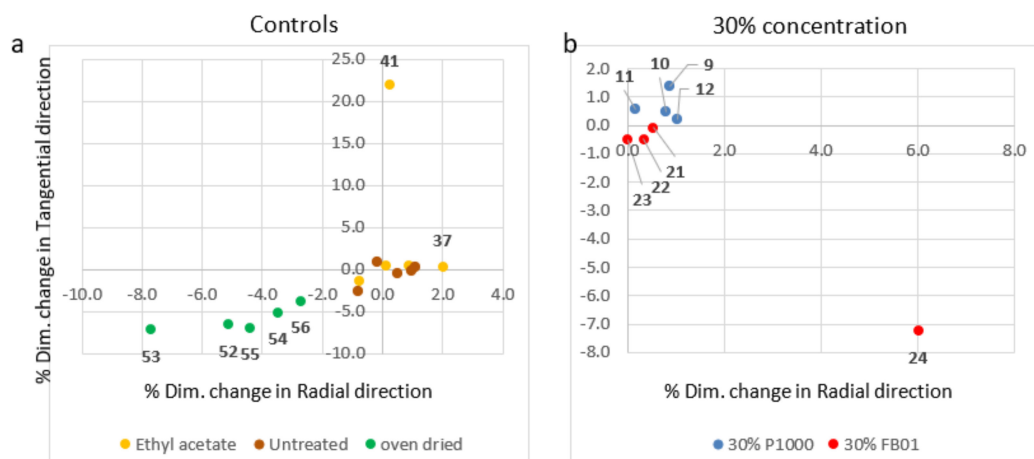


**Figure 5.** % Dimensional change plotted as % tangential change (*y*-axis) vs. % radial change (*x*-axis). (a) Controls, where only data points with largest changes are labelled; (b) 30% concentrations of P1000 and FB01 lignins. Data points are labelled with specimen number.

In these experiments, changes in one direction did not predominate over the other. This is likely related to the bacterial degradation the substrates have undergone. For instance, oven-dried specimens (nrs. 52–56) used to characterize the wood had very similar shrinkage values, ranging from −7.7% to −2.7%, in both directions (Figure 5a).

The untreated controls (nrs. 47–51) should theoretically have no dimensional change, as they were kept in the climate chamber during the experiments. Small dimensional changes were, however, measured, ranging from  $-2.6\%$  to  $1.1\%$ , Figure 5a. For these specimens, the changes measured are, therefore, due to the experimental error of the ‘pin method’. This method of measuring dimensional change is affected by the angle of the caliper relative to the pins, such that ‘before’ and ‘after’ dimensions may not be measured in exactly the same way. Different measurement angles can give slightly different distances between pins. Thus, more certain evaluation of change would have been possible to achieve if several repeat measurements were recorded and then averaged. In this experiment, we consider that changes within the error range spanning  $-2.6\%$  to  $1.1\%$  are not significant.

Dimensional changes in ethyl acetate-treated control specimens (nrs. 37–41) are also shown in Figure 5a. For specimen nr. 41, there are very large dimensional changes measured, which are most likely attributable to cracks that had formed during treatment, which were located in the pin measurement area. This specimen had a knot in it, which may have led to cracking. Otherwise, very little dimensional change was measured with ethyl acetate-immersed controls, which ranged between  $-0.8\%$  and  $2\%$ . Low % dimensional change is likely related to ethyl acetate’s low surface tension (similar to ethanol), which reduces the risk of collapse due to capillary forces during evaporation.

Figure 5b shows % dimensional changes for treated specimens. Most dimensional changes were within the range of  $-0.5\%$  to  $+2.5\%$ , which is within the measurement limits of the method used, and are, therefore, not significant. However specimen 24 had very high changes (up to  $7\%$ ), which is most likely due to manual errors in measurement, due to another factor than the error range for the pin method, since this specimen was very similar to nrs. 21 and 22, which showed only  $\pm 0.5\%$  change.

### 3.2.3. Morphology

Wood cellular morphology of untreated controls were compared to sound pine (Figure 6) and treated specimens using the scanning electron microscope (SEM). Figures 7 and 8 show images of 30% concentrations of P1000 and FB01. Images taken from the outer edge are compared to the core of the same specimen.

Comparing the ethyl acetate-treated archaeological pine to sound pine, it was easier to discern morphological differences in the latewood than in the earlywood, likely because there is simply more secondary wall material in latewood (Figure 6). The latewood cells in the archaeological pine are somewhat distorted in shape and have an airy, spongy secondary wall. In sound pine latewood, cells are very regularly shaped and contain very thick, compact walls. Both Py-GC/MS and infrared analyses showed that the archaeological pine mainly suffered from losses in hemicellulose; this loss is likely visualized in the SEM images by this spongy texture.

It is difficult to distinguish organic polymers within another organic material such as wood in the electron microscope. Nonetheless, it was possible to observe slight changes in cell morphology after treatment. For instance, we noted the extent of ‘clogging’ of the typical airy, spongy secondary cell wall material of the latewood after treatment. For 30% P1000, more clogging of the spongy cells are visible on the surface of specimen 9 (Figure 7). The core is similar to the solvent-treated specimen (Figure 6), indicating little or no polymer. This is also reflected in both Py-GC/MS and infrared analyses, discussed in the next section.

In contrast, specimen 21, treated with 30% FB01, the secondary cell walls in both surfaces and cores do not appear as spongy as the control, likely due to the presence of polymer (Figure 8). This was supported by Py-GC/MS and infrared analyses (discussed in the next section), which indicated better penetration of FB01.

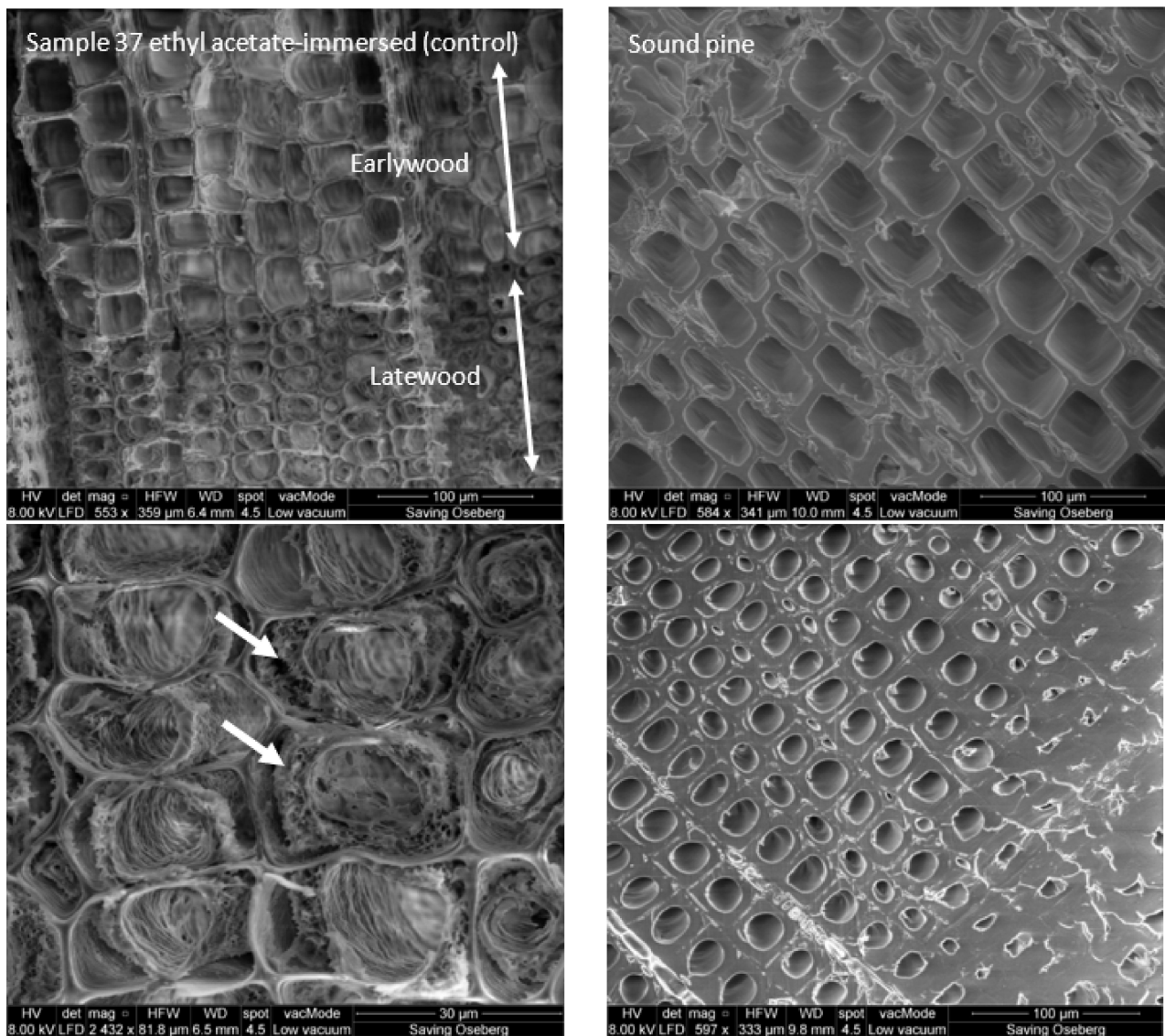
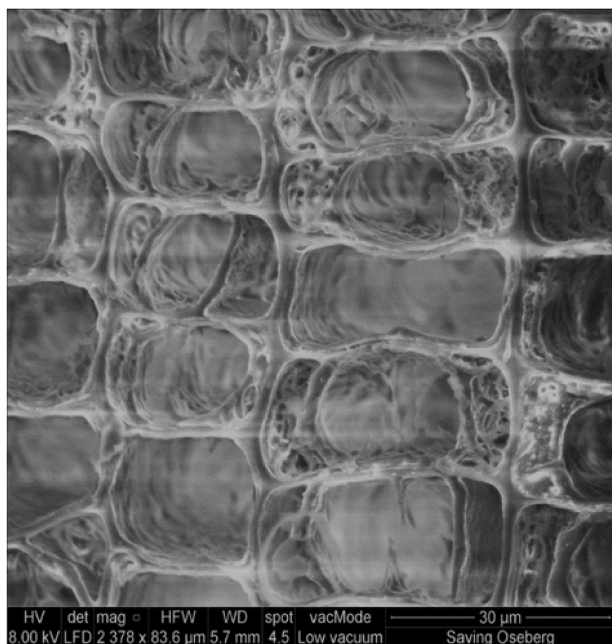


**Figure 6.** SEM images of the transverse faces of ethyl acetate-immersed sample 37 (control) on the left panel and of sound pine on the right panel. The upper right image shows the earlywood of sound pine, and the bottom right shows latewood cells of sound pine. The lower left image, which magnifies a region of latewood, shows the spongy nature of the secondary walls (arrows) in the archaeological sample.

#### 3.2.4. Extent of Penetration of Soda Lignins in Treated Specimens

Weight gain informs about the uptake of polymers, but it does not tell us about their distribution within a specimen. Two analytical methods were used to evaluate extent of penetration of the soda lignins: infrared spectroscopy (ATR-FTIR) and Py-GC/MS. Infrared spectra of samples were compared from four different depths of the specimen: from the surface to the core: outer surface, inner surface, core edge and core centre. Py-GC/MS compared two depths: inner surface and core centre (see Figure 1).

Sample 9 outer edge, latewood



Sample 9 core, latewood

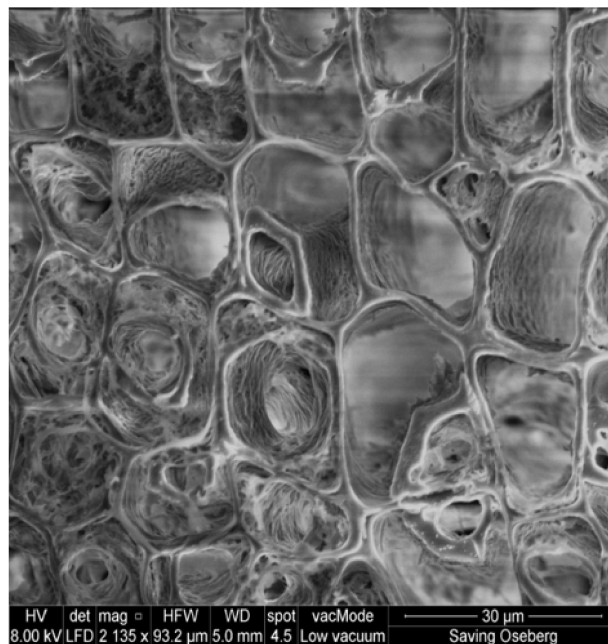
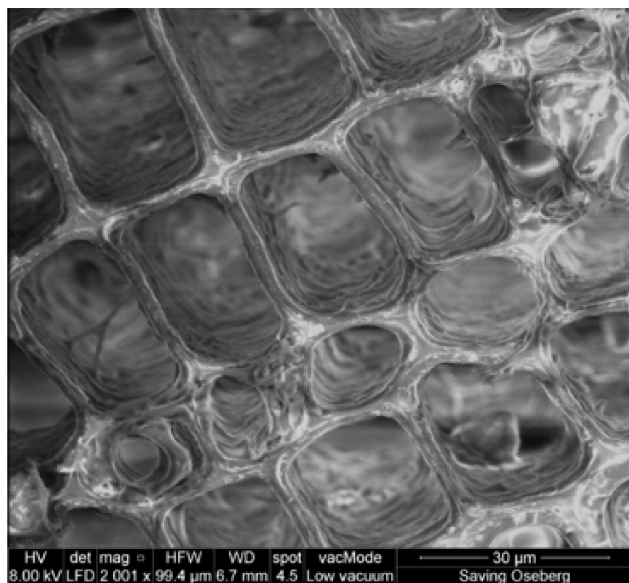


**Figure 7.** SEM images of the transverse faces of 30% P1000-treated sample 9. The left image is taken from the outer edge and the right image from the core of the sample. The spongy nature of the secondary walls appears to be reduced in the surface and only slightly reduced in the core, compared to the untreated reference shown in Figure 6. This may be attributed to the polymer within the cell walls in the surface.

Sample 21 outer edge, latewood



Sample 21 core, latewood

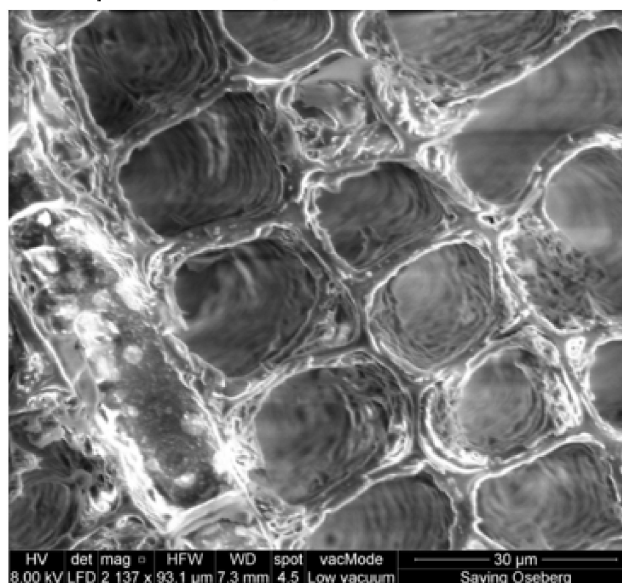


**Figure 8.** SEM images of the transverse faces of 30% FB01-treated sample 21. The left image is taken from the outer edge and the right image from the core of the sample. The spongy nature of the secondary walls appears to be reduced in both the surface and core, compared to the untreated reference shown in Figure 6. This may be attributed to the polymer within the cell walls.

### Evaluation of Penetration by Py-GC/MS

Wood samples were collected from inner surfaces and core centres of specimens treated with 30% concentrations of P1000 and FB01. Figure 9 shows the chromatographic profiles obtained for wood treated with 30% FB01 (specimen 22) and that obtained for the ethyl acetate-treated reference archaeological wood (specimen 37). Here, we observe an increase in the number and intensity of peaks in the treated wood, due to the presence of compounds formed during pyrolysis of FB01. The pyrolysis products that are written in red script in Table 2 were used to evaluate the penetration effectiveness of the soda lignins.

The semi-quantitative calculations and the composition of the woods treated with lignin materials are shown in Table 8. As expected, the contribution of the added soda lignin results in a lower relative abundance of polysaccharide pyrolysis products. Therefore, higher overall percentages of lignin indicate presence of soda lignin. Surface samples have greater relative abundances of lignin than core samples, due to more accumulation of soda lignin on surfaces.

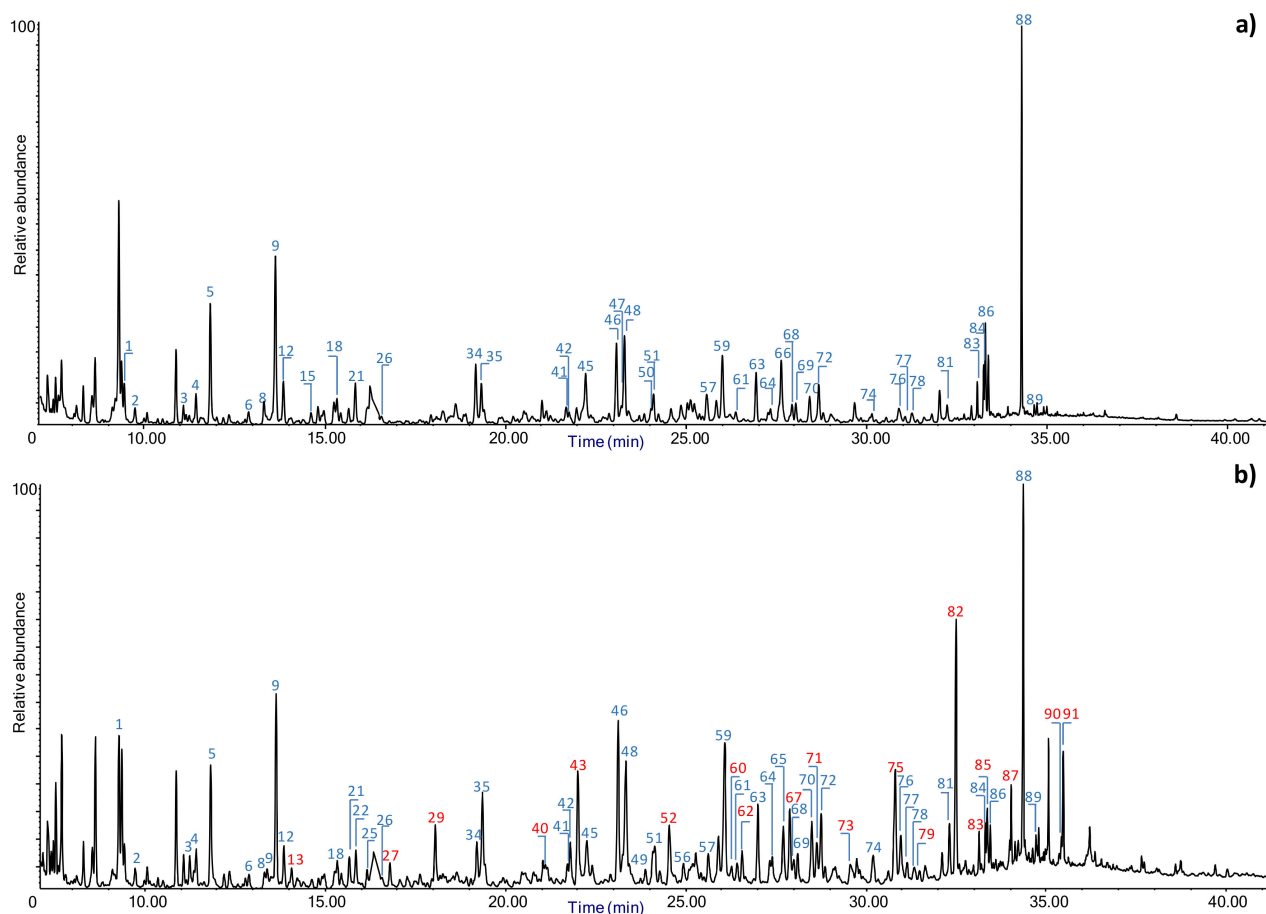


**Figure 9.** Chromatographic profiles obtained by Py(HMDS)-GC/MS (a) archaeological pine (specimen 47) and (b) archaeological pine treated with FB01 (specimen 22). Lignin pyrolysis products, which were very low or absent in archaeological pine, were used to evaluate lignin penetration in test specimens. These are labelled in red script. Peak numbers refer to Table 2.



**Table 8.** Percentage composition of pine determined by Py-GC/MS. The average values were obtained from four specimens analysed for each P1000 and FB01. Here, the percentages are based on total pyrolysis products identified, including those from the impregnating materials.

	Specimens Treated with P1000		Specimens Treated with FB01	
	Core Centre	Inner Surface	Core Centre	Inner Surface
H%	41.3	35.5	33.6	25.9
L%	58.7	64.5	66.4	74.1
H/L	0.7 ± 0.13	0.6 ± 0.09	0.5 ± 0.03	0.4 ± 0.04
H-lignin	6.8	8.3	10.8	13.7
S-lignin	12.3	21.9	26.6	34.1
G-lignin	81.0	69.8	62.6	52.1
S/G	0.2 ± 0.01	0.3 ± 0.04	0.4 ± 0.07	0.7 ± 0.10

Pine is a conifer, and its lignin is mainly composed of guaiacyl units. Thus, syringyl (S)-based pyrolysis products are observed only in specimens treated with FB01 and P1000. In treated specimens, it was, thus, possible to calculate the S/G ratio and exploit it as an index of the effectiveness of penetration, where higher S/G ratios indicate greater amounts of S lignin are present. As expected, S/G ratios are higher on the outside (inner surface) than the inside (core centre) parts of the lignin-treated specimens. However this parameter cannot be used to compare extent of penetration between P1000 and FB01, since their S/G ratios are different to begin with; P1000 has an S/G ratio of 1.51, and FB01 has an S/G ratio of 1.80 (Table S1). To see which lignin penetrated better, we must consider % syringyl units.

All lignin pyrolysis products identified in specimens treated with P1000 and FB01 were divided into syringyl (S-lignin), guaiacyl (G-lignin) and p-hydroxyphenyl (H-lignin) units. Figure 10a shows the total relative abundances of lignin units from wood specimens and soda lignins, expressed as a % of total wood. The archaeological pine reference specimen (ethyl acetate treated, 37) is richest in G units. Compounds deriving from H-lignin units are only present in low abundances (2.2% of the total units detected) and products derived from S-lignin units are almost absent in the reference pine specimen (0.4% of the total units detected). In specimens treated with soda lignins, we observe an increase in both H-lignin and S-lignin units and a relative decrease in G-lignin units. This indicates that both lignins P1000 and FB01 were deposited in the cores of treated specimens. However, higher percentages of especially S units, which are almost absent in the reference pine, are present in the cores of FB01 treated specimens. This indicates better penetration than in P1000 treated specimens. Thus, despite the fact that P1000 has a greater % of S type lignin than FB01, the greater percentage of S lignin in cores of FB01-treated specimens indicates that it penetrated much better than the P1000.

The reasons for FB01's better impregnation may be due to its significantly lower molecular weight (ca. 1000 versus ca. 3000 g/mol), but differences in polarity (functional groups) of the two lignins may also have affected extent of penetration. Therefore, another evaluation of the penetration effectiveness may be based on observing the types of pyrolysis products from the soda lignins, which are present in surfaces and cores. Products which are either absent or are only found in very low amounts in pine (products in red script in Table 2) mainly derive from syringyl and p-hydroxyphenyl lignin, but also include ferulic acid units derived from G-lignin. Figure 10b shows in more detail compounds from the H-lignin and S-lignin groups in treated specimens. Here, we exclude ferulic acid, a G-lignin, as it is only present in low amounts in soda lignin. The relative abundances of carbonyl compounds in both soda lignins increase considerably in the cores of samples treated with both P1000 and FB01. However, greater amounts of carbonyl compounds were found in FB01-treated specimens. As FB01 is more polar, as shown in Figure S2, its better penetration in the specimens may also be due to its greater polarity. Therefore, the extent

of penetration in specimens may have been affected by differences in their chemistries, in addition to differences in their molecular weights.

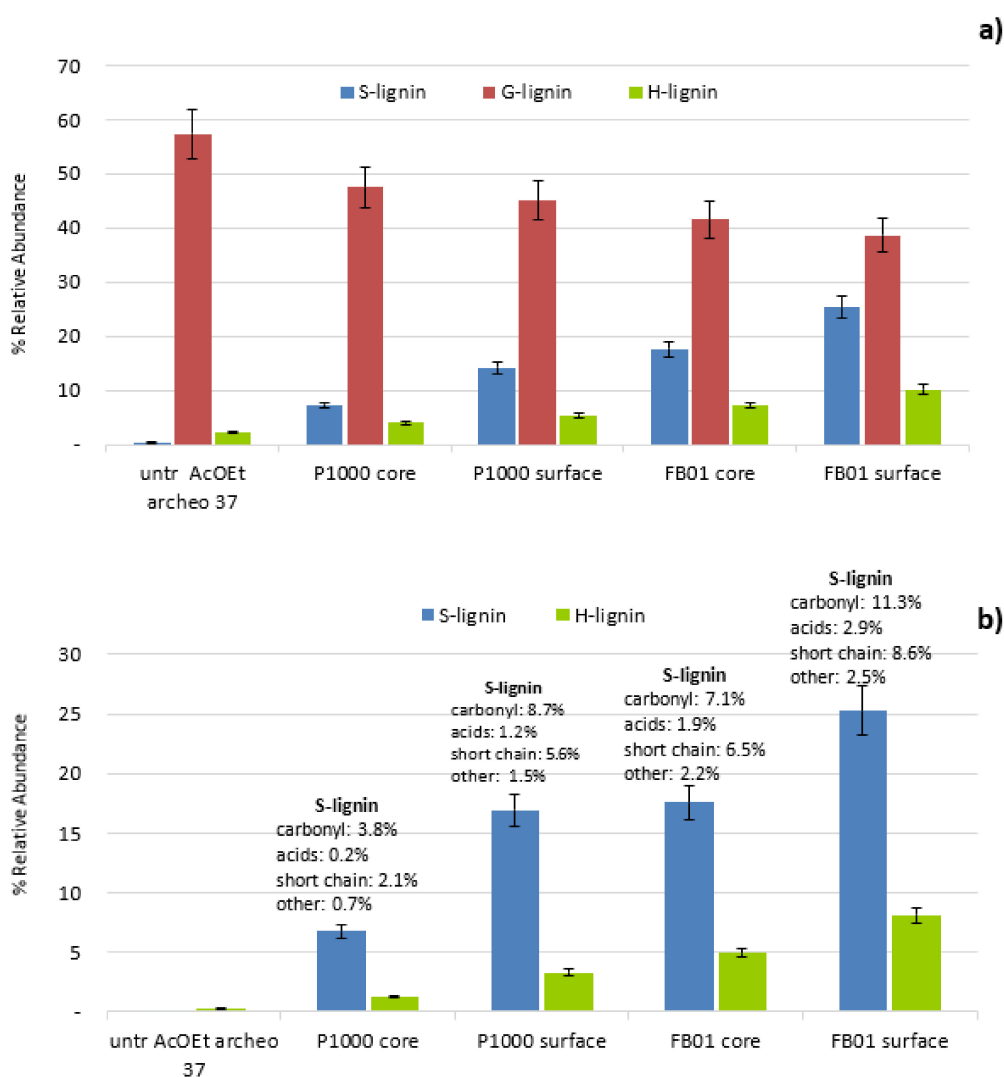
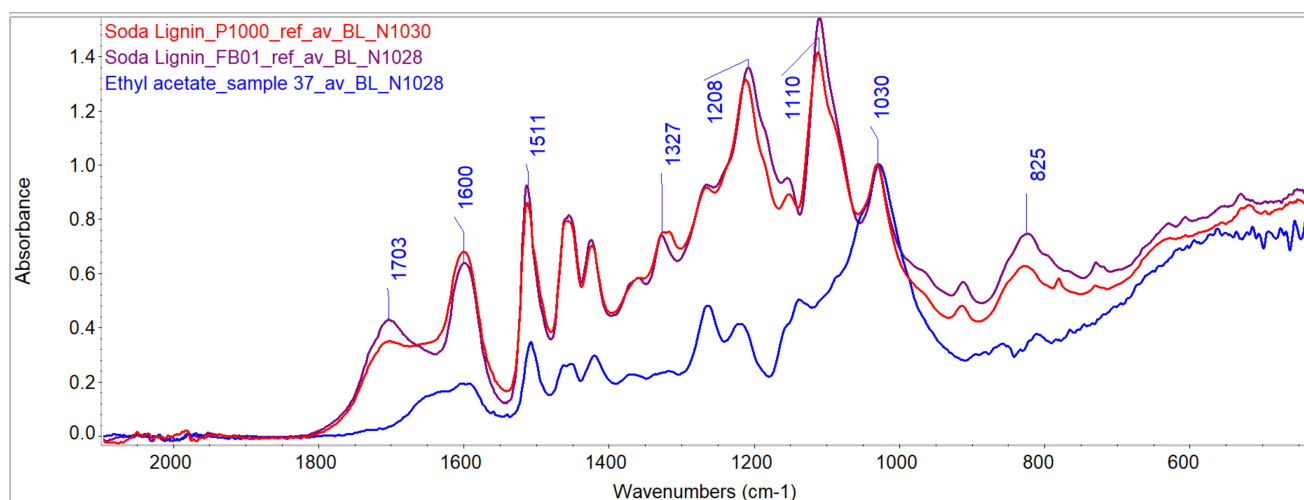


**Figure 10.** Distribution of (a) S-, G- and H-lignin units as percentages of lignin pyrolysis products identified in archaeological pine specimens treated with ethyl acetate (archeo AcOEt) and with P1000 and FB01 lignins, (b) S-lignin and H-lignin units as percentages of lignin pyrolysis products determined in P1000 and FB01 treated specimens are very low or absent in archaeological pine (products in red script in Table 2). Relative abundance is expressed as a percentage of total wood.

To summarize, Py-GC/MS showed that both soda lignins, P1000 and FB01, penetrated into cores of archaeological pine specimens, but better penetration was achieved with FB01. This was likely due to the lower MW of this lignin, but penetration may also have been enhanced by FB01's greater polarity.

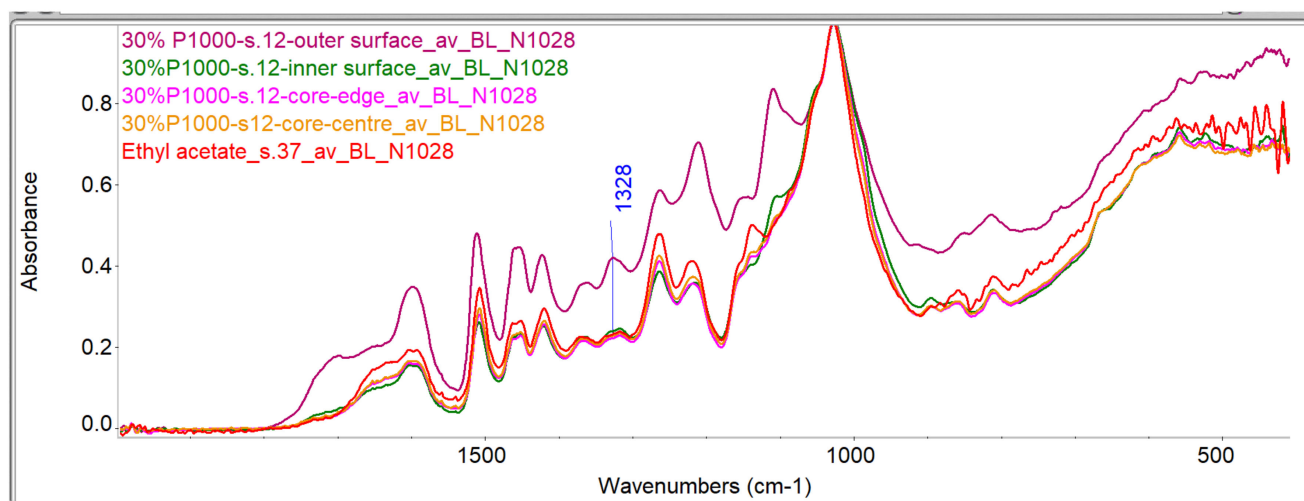
#### Evaluation of Penetration by ATR-FTIR

Table 5 gives an overview of the infrared band assignments used here. Spectra were baseline corrected and normalized at  $1030\text{ cm}^{-1}$ , the same band used to normalize spectra of wood specimens. Both lignins have almost the same bands, with similar intensities (Figure 11). The main difference occurs at  $1703\text{ cm}^{-1}$ , which is higher in FB01 than in P1000. This band is assigned to carbonyl and carboxylic groups and, thus, confirms Py-GC/MS analyses, which indicated greater relative abundances of 'oxidized' lignin groups.



**Figure 11.** Comparing lignins to ethyl acetate-treated archaeological wood (nr. 37). Infrared spectra of lignin P1000 (red curve), FB01 (purple curve) and of wood (blue curve) were baseline corrected and normalized at  $1028\text{ cm}^{-1}$ . The band height used to measure extent of penetration of lignins into the wood samples is shown at  $1327\text{ cm}^{-1}$ .

Figure 11 shows the infrared spectrum of an ethyl acetate-treated reference specimen with medium degradation (nr. 37). Infrared spectra of wood contain many bands, which overlap with signals from the soda lignins. However, we can see that the band at  $1327\text{ cm}^{-1}$  is much more distinct in the soda lignins than in the ethyl acetate-treated wood specimen. This band is due to both S-ring and G-ring condensed vibrations [37]. This band is very low in pine, since S-lignin is present in very low amounts, as shown by Py-GC/MS. Therefore, this band was used as a ‘marker’ for soda lignin in the wood substrate, where greater absorbance indicates more soda lignin is present (Figures 12 and 13). The extent of penetration of soda lignin was evaluated by measuring heights of this band at four depths in each specimen. Band heights from corresponding depths were then averaged from specimens in the same treatment group and are shown in Table S2 and Figure 14.



**Figure 12.** Comparing infrared spectra of 30% P1000-treated specimen 12 from different depths. Bands at  $1328\text{ cm}^{-1}$  were measured. The ethyl acetate-treated control is shown in the red curve (nr. 37). The image shows ‘outer surface’ (purple), ‘inner surface’ (green), ‘core edge’ (pink) and ‘centre core’ (orange). All spectra were baseline corrected and normalized to  $1028\text{ cm}^{-1}$ .

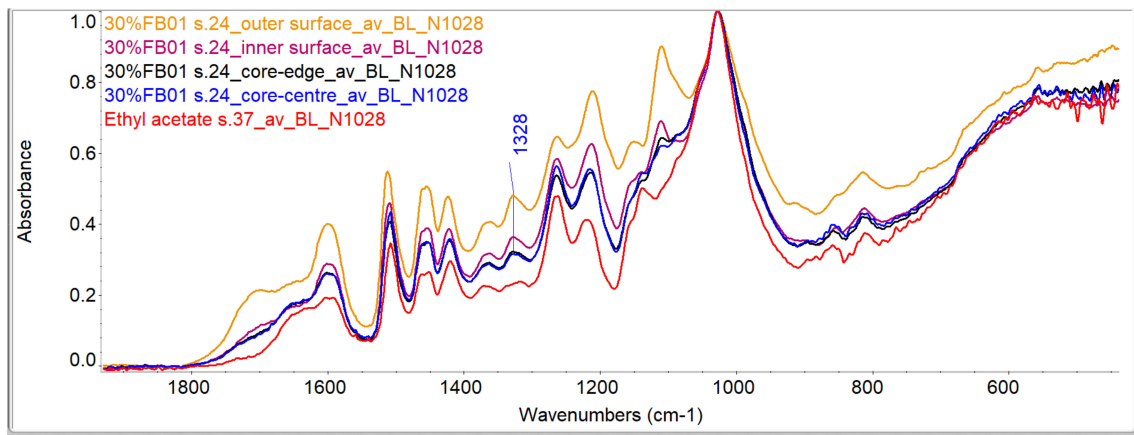


**Figure 13.** Comparing infrared spectra of 30% FB01-treated specimen 24 from different depths to assess penetration from outside to inner core by measuring band heights at  $1328\text{ cm}^{-1}$ . The ethyl acetate-treated control (nr. 37) is shown in the red curve. The image shows ‘outer surface’ (orange), ‘inner surface’ (purple), ‘core edge’ (black) and ‘core centre’ (blue). All spectra were baseline corrected and normalized to  $1028\text{ cm}^{-1}$ .

Both soda lignins have similar absorbances at  $1327\text{ cm}^{-1}$ , but it is slightly greater (24%) in FB01 than in P1000. In order to compare the extent of penetration of P1000 against that of FB01, it is necessary to ensure that the absorbance at  $1327\text{ cm}^{-1}$  is the same. This was accomplished by multiplying the absorbance at  $1327\text{--}1328\text{ cm}^{-1}$  by 1.24 for P1000-treated specimens. This is shown as ‘corrected band heights for P1000’ in Figure 14 and Table S2.

Wood specimens treated with 30% FB01 showed greater band heights at  $1327\text{--}1328\text{ cm}^{-1}$  at all depths compared to reference specimens, indicating that this polymer reached the cores of the specimens (Table S2 and Figure 14). For specimens treated with 30% P1000, the outer and inner surfaces had strong signals (higher band heights), but at depths below the surface, signals were markedly lower. However, the P1000 polymer is likely present, since the band heights are still greater than that for untreated specimens.

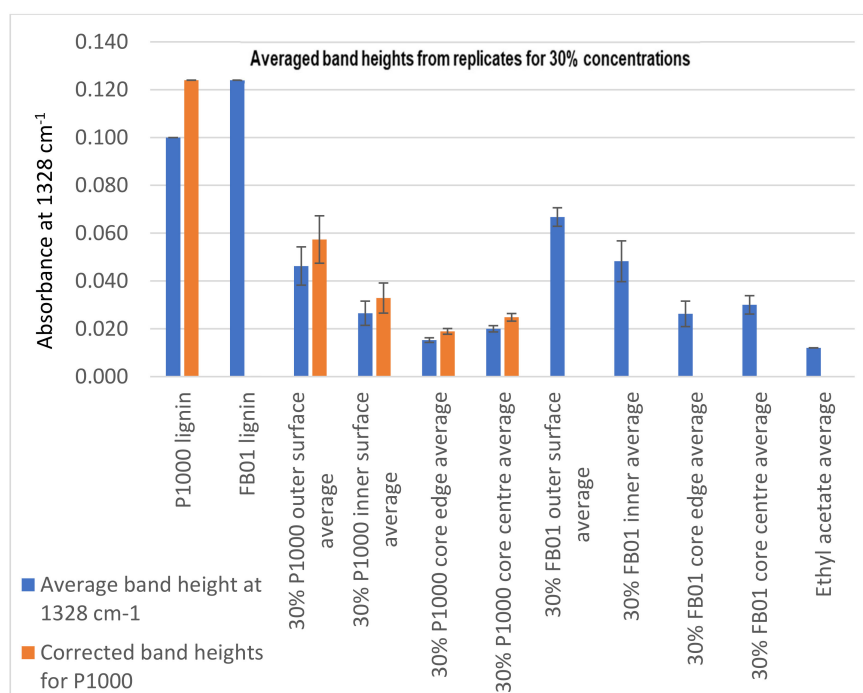


**Figure 14.** Comparing band heights measured from infrared spectra for 30% concentrations. The band heights from each depth were averaged for each treatment group (4 replicates): ‘outer surface’, ‘inner surface’, ‘core edge’ and ‘core centre’.

These results show the same trends as Py-GC/MS analyses.

In summary, detecting the presence of soda lignin in wood by chemical analyses was straightforward due to the choice of pine as the substrate in these experiments. This is because lignins derived from straw, such as P1000 and FB01, contain units that are not usually present in significant amounts in conifers, such as syringyl, p-hydroxyphenyl and ferulic acid residues. Here, syringyl units could, therefore, be used as 'markers' for detection of soda lignin presence.

#### 4. Conclusions and Perspectives

Lignin treatments caused large colour changes in surfaces of treated specimens relative to controls. However, if the starting archaeological wood is very dark, as is, for example, highly degraded alum-treated wood, this colour change may not be as noticeable.

Linear dimensional changes after treatment were small (within 2.5% for most specimens) and did not have preferred radial or tangential directions. Due to the errors involved in the 'pin method', changes between  $-2.6\%$  and  $1.1\%$  were not considered as significant.

Specimens treated with FB01 (Mw~1 kDa) gained significantly more weight than those treated with P1000 (Mw~3 kDa). SEM images showed presence of FB01 in cores, but it was difficult to assess the presence of P1000 at the same depth, likely because there was relatively little material. Py-GC/MS and infrared analyses showed that both soda lignins penetrated the cores of  $2 \times 2 \times 2 \text{ cm}^3$  specimens, but P1000 to a lesser extent than FB01.

The better penetration of FB01 in the wood core compared to P1000 was likely mainly due to its lower molecular weight; however, other factors, such as polymer-solvent interactions or the lignin's chemical interactions with wood polymers, may also have played a role [41]. For instance, Py-GC/MS showed that lignins richer in products with carbonyl functionalities penetrated more easily, which may partially explain FB01's better penetration. This should be kept in mind when evaluating penetration.

The great variability in archaeological wood specimens used here has been highlighted throughout the results, as it is another important factor that can affect penetration and dimensional changes. For example, our results were affected by the initial state of preservation of the wood specimens (based on density measurements) and the presence of knots. Pith, juvenile wood and reaction wood also may affect experimental results. This is the challenge when using archaeological wood as test substrate. On the other hand, archaeological wood is the best substrate for testing materials aimed at preserving it. This is because the slow bacterial decay it undergoes during burial produces wood, which has particular degradation patterns that are difficult to reproduce in the laboratory. Furthermore, objects are not made from 'perfect' wood, so it is important to know how defects will react to a treatment.

Based on these experiences, we suggest that experiments designed during the development of new materials for archaeological wood would benefit from several testing phases, with a step-wise increase in specimen number. For example, lower specimen numbers can be used to investigate initial questions about penetration, as in this case, as it would direct further work on polymer development. The next phase would involve larger sample numbers where trends based on measurements (such as dimensional change, weight gain, colour, interaction with moisture) can be understood with better certainty. It is, thus, very important to standardize a testing regime as for example described in Kavvouras, Kostarelou, Zisi, Petrou and Moraitou [42]. This, however, may be difficult to achieve if large amounts of archaeological wood are not available.

Greater numbers of test specimens require that sufficient amounts of polymer are available for testing. Therefore, in the design of new polymers, a scaling-up phase for polymer production is of vital importance to plan, as large-scale production may not be as straightforward as it is at smaller scales.

Finally, if lignin-based treatments prove to be promising, it is our considered opinion that they should be tested on real test objects of alum-treated wood from the Oseberg collection.

**Supplementary Materials:** The following are available online at <https://www.mdpi.com/article/10.3390/f12070911/s1>, Figure S1: Distribution of categories of (a) holocellulose and (b) lignin pyrolysis products for sound pine wood, untreated and soaked in ethyl acetate archaeological pine wood specimens. Table S1: Holocellulose(H) and Lignin (L) relative abundances from soda lignins used in the experiments expressed as percentages of all holocellulose and lignin pyrolysis products. Figure S2. Distribution of lignin pyrolysis products from soda lignin P1000 and FB01, shown as % relative abundances of the total lignin pyrolysis products obtained by Py-GC/MS. Table S2. Band heights averaged from each depth analyzed by FTIR.

**Author Contributions:** Conceptualization, methodology H.K., R.J.A.G., T.M.S., S.B. and J.J.L.; writing—original draft preparation, S.B. and J.J.L.; formal analysis, S.B., A.d.L. and J.J.L.; writing—review and editing, S.B., J.J.L., A.d.L., F.A., H.K., S.H., M.P.-J., F.M., T.M.S., R.J.A.G. All authors have read and agreed to the published version of the manuscript.

**Funding:** This work was carried out as part of the Saving Oseberg project, funded by the Norwegian Ministry of Education and Research and University of Oslo. The EU Erasmus+ program funded Anne de Lamotte’s 3-month traineeship in Oslo. The authors also gratefully acknowledge the contribution of COST Action LignoCOST (CA17128), supported by COST (European Cooperation in Science and Technology), in promoting interaction, exchange of knowledge and collaborations in the field of lignin valorisation.

**Acknowledgments:** Jacqueline Donkers and Jacinta van der Putten (Wageningen Food and Biobased Research) are gratefully acknowledged for the fractionation work for the soda lignin and the performed analytical characterisation of the lignins using wet chemical methods.

**Conflicts of Interest:** The authors declare no conflict of interest.

## References

- Herbst, C.F. Om bevaring af oldsager af træ fundne i törvemoser. In *Antiquarisk Tidsskrift*; Det Kongelige Nordiske Oldskriftselskab: Kjøbenhavn, Danmark, 1861; pp. 174–176.
- Speerschneider, C.A. Behandling af oldsager af træ, som ere fundne i moser for at bevare dem i deres oprindelige form og farve. In *Antiquarisk Tidsskrift*; Det Kongelige Nordiske Oldskrift-Selskab: Kjøbenhavn, Danmark, 1861; pp. 176–178.
- Christensen, B.B. *The Conservation of Waterlogged Wood in the National Museum of Denmark: With a Report on the Methods Chosen for the Stabilization of the Timbers of the Viking Ships from Roskilde Fjord, and a Report on Experiments Carried out in Order to Improve upon These Methods*; The National Museum of Denmark: Copenhagen, Denmark, 1970; Volume 1.
- Rosenqvist, A.M. The Stabilizing of Wood Found in the Viking Ship of Oseberg: Part I. *Stud. Conserv.* **1959**, *4*, 13–22.
- Eaton, J.W. The preservation of wood by the alum process. *Fla. Anthropol.* **1962**, *XV*, 115–117.
- McQueen, C.M.A.; Tamburini, D.; Braovac, S. Identification of inorganic compounds in composite alum-treated wooden artefacts from the Oseberg collection. *Sci. Rep.* **2018**, *8*, 2901. [CrossRef]
- McQueen, C.M.A.; Tamburini, D.; Łucejko, J.J.; Braovac, S.; Gambineri, F.; Modugno, F.; Colombini, M.P.; Kutzke, H. New insights into the degradation processes and influence of the conservation treatment in alum-treated wood from the Oseberg collection. *Microchem. J.* **2017**, *132*, 119–129. [CrossRef]
- Braovac, S.; Tamburini, D.; Łucejko, J.J.; McQueen, C.M.A.; Kutzke, H.; Colombini, M.P. Chemical analyses of extremely degraded wood using analytical pyrolysis and inductively coupled plasma atomic emission spectroscopy. *Microchem. J.* **2016**, *124*, 368–379. [CrossRef]
- Braovac, S.; Kutzke, H. The presence of sulfuric acid in alum-conserved wood—Origin and consequences. *J. Cult. Herit.* **2012**, *13*, S203–S208. [CrossRef]
- Wang, C.; Zhang, L.; Zhou, T.; Chen, J.; Xu, F. Synergy of Lewis and Brønsted acids on catalytic hydrothermal decomposition of carbohydrates and corn cob acid hydrolysis residues to 5-hydroxymethylfurfural. *Sci. Rep.* **2017**, *7*, 40908. [CrossRef]
- Zhou, L.; Zou, H.; Nan, J.; Wu, L.; Yang, X.; Su, Y.; Lu, T.; Xu, J. Conversion of carbohydrate biomass to methyl levulinate with Al<sub>2</sub>(SO<sub>4</sub>)<sub>3</sub> as a simple, cheap and efficient catalyst. *Catal. Commun.* **2014**, *50*, 13–16. [CrossRef]
- Brazdauskas, P.; Paze, A.; Rizhikovs, J.; Puke, M.; Meile, K.; Vedernikovs, N.; Tupciauskas, R.; Andzs, M. Effect of aluminium sulphate-catalysed hydrolysis process on furfural yield and cellulose degradation of *Cannabis sativa* L. shives. *Biomass Bioenergy* **2016**, *89*, 98–104. [CrossRef]
- Chamberlain, D. Anion mediation of aluminium-catalysed degradation of paper. *Polym. Degrad. Stab.* **2007**, *92*, 1417–1420. [CrossRef]
- Baty, J.; Minter, W.; Lee, S. The role of electrophilic metal ions aluminum (III) and magnesium (II) in paper degradation and deacidification. In American Institute for the Conservation of Historic and Artistic Works. In Proceedings of the 38th Annual Meeting, Milwaukee, WI, USA, 11–14 May 2010.

15. Baty, J.; Sinnott, M.L. Efficient electrophilic catalysis of 1,5-anhydrocellobiitol hydrolysis by AlIII; implications for the conservation of ?rosin-alum? sized paper. *Chem. Commun.* **2004**, *2004*, 866–867. [CrossRef] [PubMed]
16. Łucejko, J.J.; McQueen, C.M.A.; Sahlstedt, M.; Modugno, F.; Colombini, M.P.; Braovac, S. Comparative chemical investigations of alum treated archaeological wood from various museum collections. *Herit. Sci.* **2021**, *9*, 69. [CrossRef]
17. Häggström, C.; Sandström, T.; Lindahl, K.; Sahlstedt, M. *Alum-Treated Archaeological Wood: Characterization and Re-Conservation*; Riksantikvarieämbetet: Gotland, Sweden, 2013; p. 131.
18. Bojesen-Koefoed, I.M. Re-conservation of wood treated with alum in the 1920s—Challenges and strategies. In Proceedings of the 11th ICOM Group on Wet Organic Archaeological Materials Conference, Greenville 2010, Greenville, NC, USA, 20 April 2012; Strætkvern, K., Williams, E., Eds.; Springer: Berlin/Heidelberg, Germany, 2012; pp. 497–502.
19. Braovac, S.; Wittköpper, M.; Sahlstedt, M. Retreatment testing of alum-treated woods from the Oseberg collection—Results from first trials. In Proceedings of the 14th ICOM-CC Wet Organic Archaeological Materials Conference, Portsmouth, UK, 20–23 May 2019.
20. Brøgger, A.W.; Shetelig, H.; Falk, H. *Osebergfundet*; Den norske Stat: Kristiania, Norge, 1917.
21. Braovac, S.; McQueen, C.M.A.; Sahlstedt, M.; Kutzke, H.; Łucejko, J.J.; Klokkernes, T. Navigating conservation strategies: Linking material research on alum-treated wood from the Oseberg collection to conservation decisions. *Herit. Sci.* **2018**, *6*, 77. [CrossRef]
22. Lora, J. Chapter 10-Industrial Commercial Lignins: Sources, Properties and Applications. In *Monomers, Polymers and Composites from Renewable Resources*; Elsevier: Amsterdam, The Netherlands, 2008; pp. 225–241.
23. Ang, A.F.; Ashaari, Z.; Lee, S.H.; Tahir, P.M.; Halis, R. Lignin-Based Copolymer Adhesives for Composite Wood Panels—A Review. *Int. J. Adhes. Adhes.* **2019**, *95*, 102408. [CrossRef]
24. Ghaffar, S.H.; Fan, M. Lignin in straw and its applications as an adhesive. *Int. J. Adhes. Adhes.* **2014**, *48*, 92–101. [CrossRef]
25. Vachon, J.; Assad-Alkhateb, D.; Baumberger, S.; van Haveren, J.; Gosselink, R.J.A.; Monedero, M.; Bermudez, J.M. Use of lignin as additive in polyethylene for food protection: Insect repelling effect of an ethyl acetate phenolic extract. *Compos. Part. C Open Access* **2020**, *2*, 100044. [CrossRef]
26. Lora, J.H. Characteristics, Industrial Sources, and Utilization of Lignins from Non-Wood Plants. In *Chemical Modification, Properties, and Usage of Lignin*; Springer Science and Business Media LLC: Boston, MA, USA, 2002; pp. 267–282.
27. Gosselink, R.J.A.; Putten, J.C.; van Es, D.S. Fractionation of Technical Lignin. Patent WO2015 178771, 26 November 2015.
28. Browning, B.L. *Methods of Wood Chemistry*; Interscience Publishers: New York, NY, USA, 1967; Volume I–II.
29. Gosselink, R.J.A.; Van Dam, J.E.G.; de Jong, E.; Scott, E.L.; Sanders, J.P.M.; Li, J.; Gellerstedt, G. Fractionation, analysis, and PCA modeling of properties of four technical lignins for prediction of their application potential in binders. *Holzforschung* **2010**, *64*, 193–200. [CrossRef]
30. Lu, Y.; Joosten, L.; Donkers, J.; Andriulo, F.; Slaghek, T.M.; Phillips-Jones, M.K.; Gosselink, R.J.A.; Harding, S.E. Characterisation of mass distributions of solvent-fractionated lignins using analytical ultracentrifugation and size exclusion chromatography methods. *Sci. Rep.* **2021**, *11*, 1–12. [CrossRef]
31. Tamburini, D.; Łucejko, J.J.; Zborowska, M.; Modugno, F.; Cantisani, E.; Mamoňová, M.; Colombini, M.P. The short-term degradation of cellulosic pulp in lake water and peat soil: A multi-analytical study from the micro to the molecular level. *Int. Biodeterior. Biodegrad.* **2017**, *116*, 243–259. [CrossRef]
32. Tamburini, D.; Łucejko, J.J.; Ribechini, E.; Colombini, M.P. New markers of natural and anthropogenic chemical alteration of archaeological lignin revealed by in situ pyrolysis/silylation-gas chromatography-mass spectrometry. *J. Anal. Appl. Pyrolysis* **2016**, *118*, 249–258. [CrossRef]
33. Tamburini, D.; Łucejko, J.J.; Zborowska, M.; Modugno, F.; Prądzyński, W.; Colombini, M.P. Archaeological wood degradation at the site of Biskupin (Poland): Wet chemical analysis and evaluation of specific Py-GC/MS profiles. *J. Anal. Appl. Pyrolysis* **2015**, *115*, 7–15. [CrossRef]
34. Grattan, D.W.; Clarke, R.W. Conservation of Waterlogged wood. In *Conservation of Marine Archaeological Objects*; Pearson, C., Ed.; Butterworth-Heinemann: Oxford, UK, 1987; pp. 164–206.
35. Schwanninger, M.; Rodrigues, J.; Pereira, H.; Hinterstoisser, B. Effects of short-time vibratory ball milling on the shape of FT-IR spectra of wood and cellulose. *Vib. Spectrosc.* **2004**, *36*, 23–40. [CrossRef]
36. Faix, O.; Bremer, J.; Schmidt, O.; Stevanovic, T.J. Monitoring of chemical changes in white-rot degraded beech wood by pyrolysis—Gas chromatography and Fourier-transform infrared spectroscopy. *J. Anal. Appl. Pyrolysis* **1991**, *21*, 147–162. [CrossRef]
37. Boeriu, C.; Bravo, D.; Gosselink, R.J.A.; van Dam, J.E.G. Characterisation of structure-dependent functional properties of lignin with infrared spectroscopy. *Ind. Crop. Prod.* **2004**, *20*, 205–218. [CrossRef]
38. Mohebbi, B. Attenuated total reflection infrared spectroscopy of white-rot decayed beech wood. *Int. Biodeterior. Biodegrad.* **2005**, *55*, 247–251. [CrossRef]
39. Faix, O. Classification of Lignins from Different Botanical Origins by FT-IR Spectroscopy. *Holzforschung* **1991**, *45*, 21–28. [CrossRef]
40. Blomberg, J.; Persson, B.; Bexell, U. Effects of semi-isostatic densification on anatomy and cell-shape recovery on soaking. *Holzforschung* **2006**, *60*, 322–331. [CrossRef]
41. Horie, V. *Materials for Conservation: Organic Consolidants, Adhesives and Coatings*, 2nd ed.; Butterworth-Heinemann: Oxford, UK, 2010.
42. Kavvouras, P.K.; Kostarelou, C.; Zisi, A.; Petrou, M.; Moraitou, G. Use of Silanol-Terminated Polydimethylsiloxane in the Conservation of Waterlogged Archaeological Wood. *Stud. Conserv.* **2009**, *54*, 65–76. [CrossRef]

## Article

# Chemical Characterization of Waterlogged Charred Wood: The Case of a Medieval Shipwreck

Eirini Mitsi <sup>1</sup>, Stamatis Boyatzis <sup>2</sup> and Anastasia Pournou <sup>2,\*</sup>

<sup>1</sup> Department of History, Archaeology and Cultural Resources Management, University of the Peloponnese, 24100 Kalamata, Greece; eir.mitsi@gmail.com

<sup>2</sup> Department Conservation of Antiquities & Works of Art, University of West Attica, Ag. Spyridonos Str., Aegaleo, 12243 Athens, Greece; sboyatzis@uniwa.gr

\* Correspondence: pournou@uniwa.gr

**Abstract:** In 2008, a medieval wooden shipwreck was discovered at the port of Rhodes, Greece. The shipwreck was partly burned, presenting a challenge for conservators, as uncharred, semi-charred and charred waterlogged wood were often encountered on the same piece of timber. In seeking the most appropriate conservation method for this unusual material, its chemical characterization was considered necessary. This study examined the chemistry of the three dominant wood conditions found in the wreck. Fourier transform infrared spectroscopy and X-ray diffraction analysis were implemented in comparison to reference samples. Energy dispersive analysis was also used for assessing the inorganic composition of each condition. Moreover, for charred and semi-charred wood, proximate analysis was undertaken. Results obtained regarding the organic moieties of the waterlogged archaeological material, demonstrated that charred samples were chemically comparable to charcoals, semi-charred material showed similarity to thermally modified wood, whereas uncharred waterlogged wood was proven to have an analogous chemistry to biodeteriorated wood. Elemental analysis results also diversified among the three shipwreck's conditions. Sulfur, iron, and oxygen decreased in charred areas, whereas carbon increased. Proximate analysis showed that ash and fixed carbon content increased with charring, whereas volatile matter decreased. This work proved major chemical differences among shipwreck timbers' conditions owing to different degree of charring. These are anticipated to influence not only conservation methods' efficacy, but also the post-treatment behavior of the material. Further investigation is needed for correlating the chemistry of the archaeological material to its physical properties in order to contribute to practical aspects of conservation.

**Keywords:** medieval shipwreck; waterlogged wood; charred wood; chemical analysis; EDS; FTIR; XRD; proximate analysis



**Citation:** Mitsi, E.; Boyatzis, S.; Pournou, A. Chemical Characterization of Waterlogged Charred Wood: The Case of a Medieval Shipwreck. *Forests* **2021**, *12*, 1594. <https://doi.org/10.3390/f12111594>

Academic Editors: Magdalena Broda and Callum A. S. Hill

Received: 9 October 2021

Accepted: 17 November 2021

Published: 19 November 2021

**Publisher's Note:** MDPI stays neutral with regard to jurisdictional claims in published maps and institutional affiliations.



**Copyright:** © 2021 by the authors. Licensee MDPI, Basel, Switzerland. This article is an open access article distributed under the terms and conditions of the Creative Commons Attribution (CC BY) license (<https://creativecommons.org/licenses/by/4.0/>).

## 1. Introduction

During a routine survey in 2008, a late-12th-century ship was discovered at the commercial port of Rhodes by the Greek Ephorate of Underwater Antiquities [1,2]. The shipwreck lay at a maximum depth of 13–14 m and was found half-buried in muddy sediment [1].

In 2013, a partial excavation of the shipwreck revealed that it was a merchant ship loaded with a cargo of amphorae and made apparent that a fire event took place before the vessel sunk [1]. Extensive or superficial traces of burning were recorded on many constructional elements of the ship, such as frames, ceiling planking, and stringers, and almost on every artifact recovered [1,2].

Excavated wooden hull members, identified as *Pinus halepensis* Mill. or *Pinus brutia* Ten. [1], showed a varied preservation state, as the degree and depth of charring was not homogenous among ship timbers due to the fire progression [3]. The coexistence of uncharred, semi-charred, and charred wood, often encountered on the same timber,



poses a great challenge for the ship's future conservation as wood responds differently to impregnation and drying, depending on its charring degree [3]. However, literature on the conservation of waterlogged charred wood is scarce and there are no studies associating the conservation requirements with material's physical and chemical properties. Nonetheless, it is well known that thermal decomposition of wood is accompanied by major chemical changes in hygroscopicity, viscosity, cell wall structure, color, density, and loss of mass and strength [4–8]. Moreover, it is also documented that these alterations depend on variables related not only on the wood, such as density, moisture content, permeability, species, size, grain direction, and surface protection [7,9], but also on the heating scenario, which incorporates the heat flux (temperature and duration) and the environment surrounding the wood like the oxygen concentration [7,9–13]. All these factors which influence pyrolysis, combustion, and the charring rate of wood justify the coexistence of charred, semi-charred, and uncharred wood in the shipwreck.

Preliminary experiments undertaken for the conservation of this material with polyethylene glycol followed by air or freeze drying have demonstrated a very dissimilar response to consolidation [3]. This was rather anticipated because as wood reaches elevated temperatures, the thermally degraded structural and chemical components affect greatly its behavior [4–6,12,14].

Therefore, this study was set to characterize the chemistry of this dissimilarly charred material in order to help understand its behavior and provide insights towards the development of a successful conservation method.

## 2. Materials and Methods

Waterlogged wood examined in this study belonged to a wreck's frame made of *Pinus halepensis* Mill. (Aleppo pine) or *Pinus brutia* Ten. (Turkish pine) [1]. Part of the frame was retrieved in 2013, and was kept waterlogged at 5 °C until sampling. The material presented a varied degree of charring, as its outer surface was charred, its inner core was uncharred, and layers in between were semi-charred [3]. Samples used for the chemical characterization were taken from the surface inwards, at least 50 annual rings away from the pith, to correspond to the sapwood of the mature pine, and contained all three charring conditions.

### 2.1. Energy Dispersive Analysis (EDS)

Uncharred and semi-charred waterlogged archaeological samples were cut in subsamples using a double-edged razor blade, whereas charred samples were fractured. Subsamples were then dehydrated in a series of ethanol solutions of increasing concentrations until water-free alcohol was reached and left to air-dry in a desiccator. They were then mounted on aluminum stubs using a double coated carbon conductive tape and energy dispersive X-ray spectroscopy (EDS) was performed at an acceleration voltage of 20 kV under low vacuum (33 Pa) using a JEOL JSM-6510LV scanning electron microscope, equipped with an Inca x-act silicon drift detector (SDD) with PentaFET<sup>®</sup> Precision (Oxford Instruments, Oxford, UK). The analytical data were obtained with Inca<sup>®</sup> analysis software. Bulk analysis was applied on every wood condition, whereas line scans and mapping were applied on samples where all conditions coexisted.

### 2.2. Fourier Transform Infrared Spectroscopy (FTIR)

Uncharred, semi-charred, and charred waterlogged archaeological wood was air-dried, and along with sapwood of sound wood of mature *Pinus halepensis* Mill. and *Pinus brutia* Ten. were finely grounded manually with the use of an agate mortar and pestle to ~100 µm (No 140-mesh size). Wood powder was then mixed with potassium bromide powder (KBr, Merck), and pressed into 13 mm discs with a hydraulic press. Disc samples were placed in the FTIR system sample chamber for analysis.

All samples were analyzed with a Perkin Elmer Spectrum GX spectrometer, equipped with DTGS (deuterated diglycine sulfate) detector. Spectra were recorded and edited with the Perkin Elmer Spectrum v.5.3.1 software.

### 2.3. X-Ray Diffraction Analysis (XRD)

Air-dried uncharred, semi-charred, and charred, waterlogged archaeological samples along with sapwood of sound wood of mature *Pinus halepensis* Mill. and *Pinus brutia* Ten. were finely grounded manually with the use of an agate mortar and pestle to ~100 µm (No 140 mesh size).

X-ray diffraction spectra of wood powdered samples were recorded with the help of InXitu BTX II Benchtop X-ray Diffraction/X-ray Fluorescence hybrid system using a Cobalt source ( $K\alpha_1$  1.78897 Å). All spectra were recorded in duplicate after the completion of >1200 scan cycles from 5 to 50 degrees  $2\theta$ .

The crystallinity index (CrI) was calculated based on the method developed by Segal et al. in 1959 [15] using the height ratio between the crystalline intensity, expressed as the difference ( $I_{200} - I_{am}$ ) and the total intensity ( $I_{200}$ ), Equation (1). Diffractograms were baseline-corrected with the X Powder software and consequently analyzed using the Perkin Elmer Spectrum v.5.3.1 software with no further processing of peak heights at the (200) plane and at the amorphous region. The total intensity that corresponds to both crystalline and amorphous material ( $I_{200}$ ), is assigned at  $2\theta \sim 25.60^\circ$ , whereas the amorphous intensity ( $I_{am}$ ) is assigned at  $2\theta \sim 20.60^\circ$ , angles corresponding to Cobalt source radiation.

$$\%CrI = \frac{I_{(200)} - I_{am}}{I_{(200)}} \times 100 \quad (1)$$

The apparent crystallite size  $L$  (in nm) was estimated using the Scherrer Equation (2) [16], where  $K$  is the Scherrer constant, for which, the value of 0.94 was typically adopted;  $\lambda$  is the X-ray wavelength (1.78897 Å for Co  $K\alpha_1$  radiation);  $\beta$  is the full width at half maximum (FWHM) of the diffraction band calculated after curve deconvolution using the Thermo GRAMS suite v.9.0 at the ~11–30.5  $2\theta$  range using a 1:1 Gaussian-Lorentzian profile; and  $\theta$  is the Bragg angle corresponding to the (200) plane.

$$L = \frac{K \times \lambda}{\beta \times \cos\theta} \quad (2)$$

### 2.4. Proximate Analysis

Proximate analysis was implemented on charred and semi-charred wood samples according to ASTM D1762-84. Samples were air-dried to a constant weight at 21 °C and 65% RH. They were then grounded manually with the use of an agate mortar and pestle, to ~100 µm (No 140-mesh size). Determination of moisture, ash, volatile matter, and fixed carbon was duplicated.

For moisture, approximately 1 g of each condition was placed in a porcelain crucible and weighed to the nearest 0.1 mg. Crucibles and covers were previously dried in a muffle furnace at 750 °C for 10 min and cooled in a desiccator for 1 h. Crucibles containing grounded samples were then placed uncovered in an oven at 105 °C for 2 h. Dried samples were cooled covered in a desiccator for 1 h and weighed. Samples were considered oven-dried when the decrease in weight was  $\leq 0.0005$  g. Succeeding drying periods were 1 h. Moisture content was calculated based on Equation (3).

$$\text{Moisture}\% = [(A - B)/A] \times 100 \quad (3)$$

where  $A$  = grams of air-dry sample used, and  $B$  = grams of sample after drying at 105 °C.

For volatile matter, crucibles with lids in place and containing the samples used for moisture determination were placed in a muffle furnace heated to 950 °C. They were first positioned, with the furnace door open, for 2 min on the outer ledge of the furnace (300 °C),

then for 3 min on the edge of the furnace (500 °C) and finally to the rear of the furnace for 6 min with the muffle door closed. Samples were then cooled in a desiccator for 1 h and weighed. The percentage of volatile matter in the sample was calculated based on the Equation (4)

$$\text{Volatile matter}\% = [(B - C)/B] \times 100 \quad (4)$$

where C = grams of sample after drying at 950 °C.

For ash, lids and uncovered crucible used for the volatile matter determination containing the samples were placed in a muffle furnace at 750 °C for 6 h. Samples were cooled with lids in place covered in a desiccator for 1 h and weighed. Samples were repeatedly burned with succeeding 1-h periods until results showed loss of less than 0.0005 g.

The percentage of ash content was calculated based on the Equation (5)

$$\text{Ash}\% = (D/B) \times 100 \quad (5)$$

where D = grams of residue.

Fixed carbon was calculated on a dry basis according to ASTM E870–82 based on the Equation (6).

$$\text{Fixed Carbon}\% = 100 - [\text{Volatile Matter}\% + \text{Ash}\%] \quad (6)$$

### 3. Results and Discussion

#### 3.1. EDS

Bulk analysis of uncharred, semi-charred, and charred material (Figure 1a,b) showed the presence of aluminum (Al), calcium (Ca), magnesium (Mg), and silica (Si) (Figure 1c). Moreover, both sulfur (S) and iron (Fe) concentrations were shown to decrease in charred areas. This is more likely owed to the different porosity/permeability of the material, which is charring-dependent [17] and that did not allow Fe found in the burial environment [18,19] and S produced by the action of sulfate-reducing bacteria [18] to penetrate into the material uniformly.

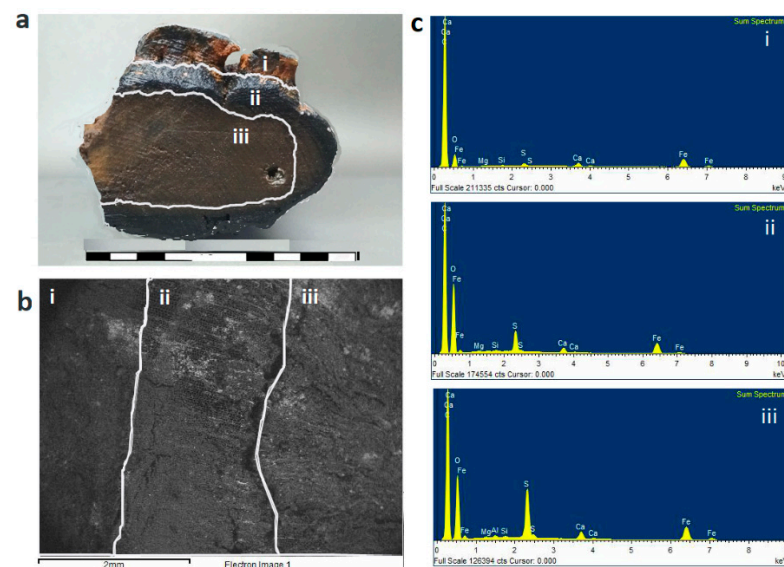


**Figure 1.** Macroscopic image (a) and SEM micrograph (b) of a sample where charred (i), semi-charred (ii), and uncharred (iii) material coexisted; (c) EDS spectrum of each condition.

Elemental mapping and line scans on samples where all conditions coexisted (Figure 2) also confirmed that the presence of S and Fe is more intense in uncharred areas. Moreover, mapping revealed the coexistence of S and Fe in some spots, which possibly indicates their co-occurrence in the same compound [20,21]. This concurrent presence of S and

Fe in the material is expected to cause severe post-excavation and post-conservation problems [20–23].

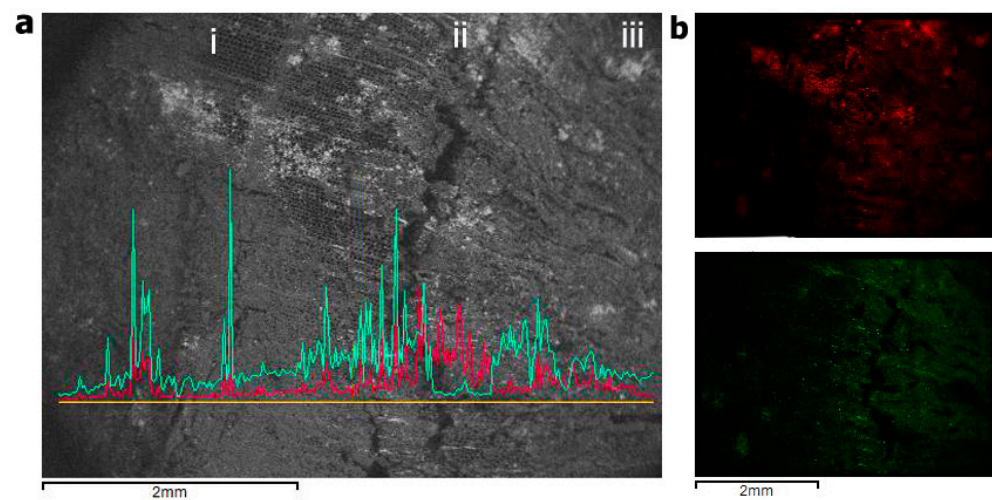


**Figure 2.** EDS line-scan and mapping of a sample where all conditions coexisted. (a) Line scan of Fe (red) and S (green) (left to right the transition from charred to uncharred, i–iii); (b) mapping of Fe (red) and S (green).

Another find revealed by EDS was the different concentration of carbon (C) and oxygen ( $O_2$ ) due to charring (Figure 3). As expected, C percentage increases in charred material [17,24,25] while O decreases [17,24]. The increase/decrease rate of C and O is dependent on both temperature and heating duration [17]. Moreover, the relative concentrations of these two elements (Figure 3a) showed that in charred material carbon is much higher than oxygen, indicating that oxygen-containing organic moieties such as polysaccharides and lignin are depleted [26,27]. In contrast, in uncharred areas the ratio of O to C is constant but relatively low, indicating the presence of organic matter, most likely lignin [27], which is in accordance with FTIR results.

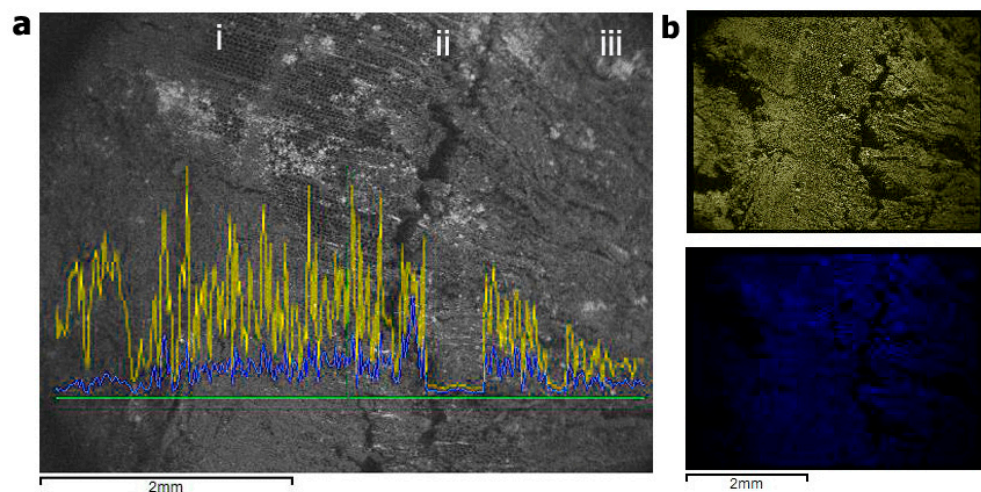


**Figure 3.** EDS Line-scan and mapping of a sample where all conditions coexisted. (a) Line scan of carbon (yellow) and oxygen (blue) (left to right the transition from charred to uncharred, i–iii); (b) mapping of carbon (yellow) and oxygen (blue).

### 3.2. FTIR

Spectra obtained from uncharred, semi-charred, and charred archaeological samples along with reference spectra of *Pinus halepensis* and *Pinus brutia* are presented in Figure 4.

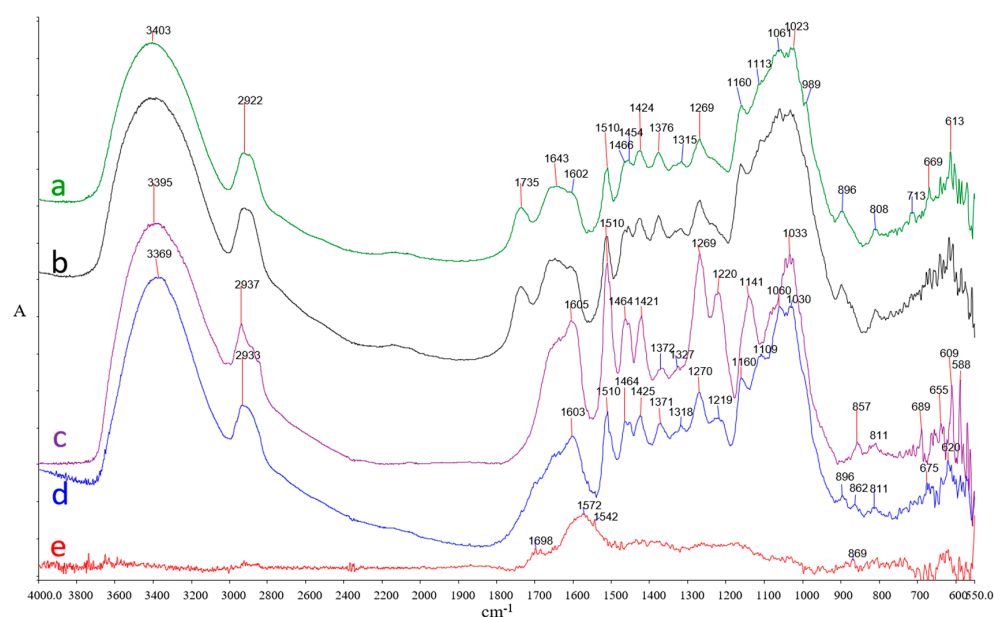


**Figure 4.** Spectra obtained for reference samples, (a) *Pinus halepensis* and (b) *Pinus brutia* (c) uncharred (d) semi-charred, and (e) charred archaeological samples.

The charred archaeological sample infrared spectrum (Figure 4e) appears typical to charcoals where the broad band at  $3400\text{--}3320\text{ cm}^{-1}$  representing the  $\text{--OH}$  stretching vibration of water and the peaks at  $3000\text{--}2800\text{ cm}^{-1}$ , due to aliphatic C-H stretching vibration derived from methyl, methylene, and methine group, are absent, as these bands decrease in intensity with increasing temperature [11,13,28,29]. Moreover, specific bands assigned to wood components such as hemicelluloses ( $\sim 1737\text{ cm}^{-1}$ ), lignin ( $\sim 1510$  and  $1269\text{ cm}^{-1}$ ) and cellulose ( $1026$  and  $\sim 898\text{ cm}^{-1}$ ) [23] and generally all bands in the “fingerprint” region  $1500\text{--}900\text{ cm}^{-1}$  [23,28] are absent, displaying the chemical changes caused by pyrolysis as well [29]. Nonetheless, the charred sample spectrum presents broad bands at  $\sim 1708\text{ cm}^{-1}$ , due to the acidic C=O groups, characteristic of low temperature charcoals’ spectra [11,13] and a broad band at  $1610\text{--}1590\text{ cm}^{-1}$  due to lignin aromatic C=C skeletal vibrations, which have been also reported to increase in intensity with increasing charring [29].

Semi-charred material spectrum appears comparable to spectra of thermally modified wood. The intensity of hemicelluloses ester carbonyl peak at  $1737\text{ cm}^{-1}$  is evidently decreased, as most of the xylan-linked acetyl groups are expected to be cleaved with increasing temperature and time during the burning of wood [30–34]. The cellulose peak at  $\sim 895\text{ cm}^{-1}$  due to C-H deformations at the glycosidic linkage was also decreased, which has been reported to occur when wood is exposed to heat [32,33,35]. It should be mentioned though, that part of carbohydrates’ reduction could be owed to abiotic or biotic processes occurring in the marine environment during the service life of the ship or during burial [36–38]. Other carbohydrate bands at  $\sim 1371$ ,  $\sim 1160$ , and  $1110\text{ cm}^{-1}$  showed no significant difference in intensity. Similarly, the major lignin bands, approximately at  $1603$ ,  $1510$ ,  $1464$ ,  $1425$ ,  $1371$ ,  $1316$ ,  $1269$ , and  $1223\text{ cm}^{-1}$  showed no intensity differences as reported for thermally modified wood [33] whereas the slight rise observed for some ( $1603$ ,  $1510$ , and  $1425\text{ cm}^{-1}$ ) is mainly due to the increase in relative lignin content [35]. Nonetheless, an increase in absorption at  $1030$  and  $1060\text{ cm}^{-1}$  has been observed indicating respectively the pronounced aromatic nature of the semi-charred wood, since this absorption band also indicates aromatic in-plane C-H deformation and changes in cellulose structure [34,35] along with the formation of aliphatic alcohols during heating [31,35].

The spectrum of uncharred waterlogged wood appears typical of biodeteriorated waterlogged wood, where significantly pronounced lignin bands  $1605$ ,  $1510$ ,  $1269$ , and  $1220\text{ cm}^{-1}$  appear with a corresponding decrease in the intensities of carbohydrate bands at  $1737$ ,  $1370$ ,  $1158$ , and  $895\text{ cm}^{-1}$ . More specifically, it is indicated that shipwreck timbers

have been deteriorated by erosion bacteria or/and soft-rot fungi, which thrive in the marine environment [37]. Erosion bacteria decay has been often reported to be associated with lignin bands' increment and carbohydrates bands' decrement [38,39]. Soft-rotters also degrade carbohydrates in preference to lignin [37] and most of them are unable to degrade guaiacyl lignin, found predominantly in softwoods, with the exception of the cavity-forming species [40]. This probably explains the new band developed at  $\sim 1140\text{ cm}^{-1}$ , which in combination with the decrease in the intensity at  $1060$  and the increase at  $1030\text{ cm}^{-1}$ , may be attributable to the guaiacyl lignin relative increase compared to carbohydrates [41] (C–H deformation in the guaiacyl unit, with C–O deformation in primary alcohol). This is also in accordance with another band present in uncharred wood sample at  $\sim 855\text{ cm}^{-1}$  that is associated with the C–H out-of-plane vibrations in guaiacyl lignin [42].

### 3.3. XRD

Diffractograms regarding the  $(1\bar{1}0)$ ,  $(110)$ ,  $(102)$ ,  $(200)$ , and  $(004)$  reflections of the two reference samples (*P. halepensis* and *P. brutia*) along with charred, semi-charred, and uncharred archaeological waterlogged samples are shown in Figure 5. Both reference samples and semi-charred diffractograms showed all peaks typical of reflection planes of wood cellulose [43–45]. In contrast, the uncharred sample diffractogram showed a considerably flattened line-shape; nonetheless, it showed a more prominent peak on the  $(200)$  plane reflection with respect to the  $(1\bar{1}0)$  and  $(110)$ . The charred sample diffractogram, as reported by other researchers [46], appeared also flattened with a weak and broad peak regarding the  $(200)$  reflection plane, with a shifted vague maximum at  $\sim 30^\circ$ .

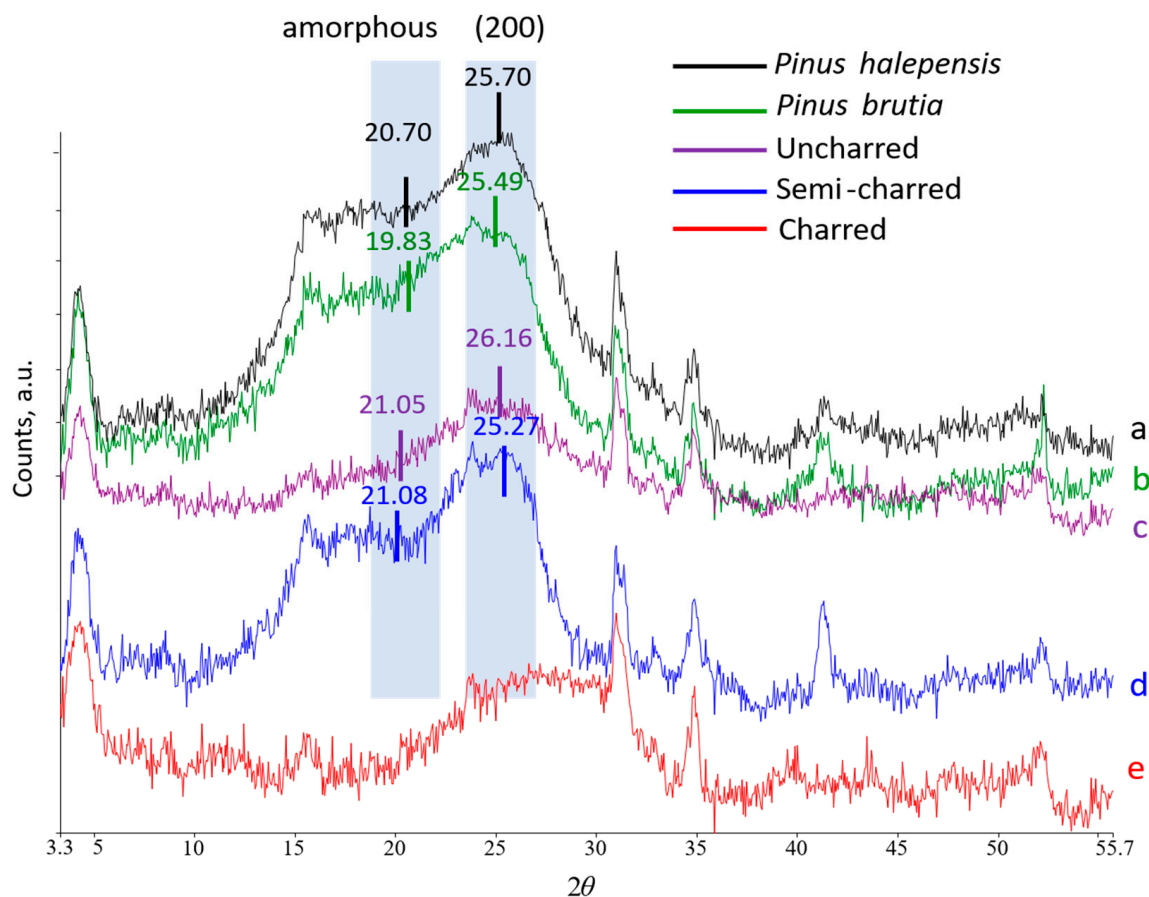


**Figure 5.** X-ray diffraction pattern of (a) *Pinus halepensis* and (b) *Pinus brutia* reference samples in comparison with (c) uncharred, (d) semi-charred, and (e) charred waterlogged samples. The  $2\theta$  values correspond to Cobalt source reflections.

Crystallinity index (CrI) of the material examined varied greatly depending on the charring degree (Table 1). The higher cellulose CrI value was calculated for the uncharred material, and followed by semi-charred wood and by controls. However, CrI values were not in accordance with the respective crystallite sizes ( $L$ ), as for the uncharred material,  $L$  presented the lowest value.

**Table 1.** Band positions of the maximum total intensity ( $I_{200}$ ) and the minimum intensity of the amorphous cellulose ( $I_{am}$ ). CrI represents the crystalline index based on Segal's method and  $L$  correspond to the crystallite size.

Sample	$2\theta$ ( $I_{200}$ ) <sup>a</sup>	$2\theta$ ( $I_{am}$ ) <sup>a</sup>	CrI	$L$ (nm)
<i>Pinus brutia</i>	25.49	19.83	41.7%	2.29
<i>Pinus halepensis</i>	25.70	20.70	41.8%	2.51
Semi-charred	25.27	21.08	47.4%	2.75
Uncharred	26.16	21.05	53.2%	1.10
Charred <sup>b</sup>	-	-	-	-

<sup>a</sup>  $2\theta$  values are expressed as Co-source. <sup>b</sup> CrI was not calculated as no cellulose is expected to be preserved with charring above 400 °C.

The considerably high CrI of uncharred material was not anticipated, as in archaeological wood the crystallinity usually decreases with decay [23,47–49]. Nonetheless, crystallinity's increase has been reported by other authors in initial stages of degradation due to the dramatic loss of amorphous cellulose regions [23,48,50]. It is believed though that this explanation does not justify the high CrI values of uncharred material as the diffractogram line-shape, the FTIR results and the lowest crystallite size ( $L$ ) recorded point out to a material in which cellulose is probably completely destroyed. Therefore, it appears that the Segal method for CrI calculation cannot successfully apply to severely deteriorated material. This could be due to several reasons related to the deficiency of the Segal method [44,51,52]; nonetheless, it is considered that is principally owed to the highly depleted cellulose fraction. It is recommended for this type of material to use other methods such as the two-dimensional X-ray diffraction.

The relative higher CrI of semi-charred material compared to references is considered that is due to amorphous cellulose degradation, which occurs during the initial stages of heating and progresses as the heat temperature rises [53–55]. This is in accordance with the high  $L$  value that corresponds to relatively larger crystal that the other materials examined. Moreover, indicates that the charring temperature for semi-charred material was lower than ~300 °C as above this threshold, cellulose crystalline part is expected to degrade severely [46,56].

### 3.4. Proximate Analysis

Proximate analysis' results on moisture content, volatile matter, ash content and fixed carbon are presented in Table 2 for both semi-charred and charred conditions. For the moisture content, no difference was recorded among samples. As it was anticipated, the volatile matter was lower in fully charred material as it is negatively correlated with temperature [57–59]. Similar values for volatile matter have been recorded by Dias Junior et al. (2020) [59] indicating combustion at/over 450 °C. The difference of volatile matter between the two conditions can be attributed to the barrier role of charred layer over the inner areas [60,61].

**Table 2.** Proximate analysis results for charred and semi-charred samples. Percentages values of moisture content, volatile matter, ash content and fixed carbon are the average of 2 replicates. Fixed carbon was calculated on dry basis.

Sample	Moisture Content	Volatile Matter	Ash Content	Fixed Carbon
Semi-charred	6.53	75.07	1.87	16.51
Charred	6.71	24.16	3.53	65.59

Ash content appears to increase with combustion as expected [57,58]. Likewise, fixed carbon content appears to increase as combustion progresses and it is in accordance with results of other researchers [57–59] and with the EDS results obtained in the present study. This increase is suggested to be a result of pyrolytic process which favors the volatile removal and consequently the elevation of ash-minerals and carbon [57].

#### 4. Conclusions

This work demonstrated major chemical differences among shipwreck timbers' due to charring. Three distinct conditions, consisting of uncharred, semi-charred, and charred wood, were documented which were directly related to the fire heat flux (temperature and duration) and the surrounding oxygen concentration.

Regarding the organic chemistry of the archaeological material, charred samples showed an analogous profile to charcoals, where both polysaccharides and lignin were almost absent due to pyrolysis. Semi-charred material showed a chemical similarity to thermally modified wood, where hemicelluloses were reduced, cellulose crystallinity was increased, and lignin showed no large differences compared to sound wood. Uncharred waterlogged wood chemistry was analogous to biodeteriorated wood, as carbohydrates were dramatically depleted, and the relative lignin content appeared increased.

The inorganic chemistry of the archaeological wood, based on elements' concentrations and topography also varied among the three conditions. Sulfur and iron concentrations were found increased in uncharred areas and their topochemistry indicated their possible co-existence in the same compounds. This concurrent presence of S and Fe it is considered that has the potential to cause severe post-excavation problems.

Finally, proximate analysis also demonstrated differences among conditions, as ash content and fixed carbon was higher in charred compared to semi-charred samples.

All chemical differences documented are awaited to be taken into consideration when developing the conservation plan of this shipwreck, as it is anticipated to influence not only conservation methods' efficacy but also the post-treatment behavior of the material.

It is believed, however, that further investigation is required in order to correlate this diverse chemistry to physical properties such as porosity, permeability, density, and shrinkage, in order to provide a more practical contribution to the shipwreck conservation.

**Author Contributions:** Conceptualization: A.P.; data curation: E.M., S.B. and A.P.; formal analysis: E.M. and S.B.; investigation: E.M., S.B. and A.P.; methodology: E.M., S.B. and A.P.; Supervision: A.P. All authors have read and agreed to the published version of the manuscript.

**Funding:** This research received no external funding.

**Acknowledgments:** The authors would like to thank G. Koutsouflakis, for providing the archaeological material and A. Karabotsos for his assistance with the SEM-EDS analysis.

**Conflicts of Interest:** The authors declare no conflict of interest.



## References

- Koutsouflakis, G.; Rieth, E. A late-12th-century byzantine shipwreck in the port of Rhodes A preliminary report. In *Under the Mediterranean I Studies in Maritime Archaeology*; Demesticha, S., Blue, L., Eds.; Sidestone Press: Leiden, The Netherlands, 2021.
- Koutsouflakis, G. Three shipwrecks of the medieval era in the commercial port of Rhodes. In *Proceedings of the Archeological Work in Aegean Islands, Lesbos, Greece, 27 November–1 December 2013*; Birtacha, K., Triantaphyllidis, P., Sarantidis, K., Eds.; pp. 477–500.
- Mitsi, E.; Pournou, A. Conserving a charred medieval shipwreck: A preliminary study. In *Proceedings of the 14th ICOM-CC WOAM Conference, Portsmouth, UK, 20–24 May 2019*.
- Stamm, A.J. Thermal degradation of wood and cellulose. *Ind. Eng. Chem.* **1956**, *48*, 413–417. [CrossRef]
- Shafizadeh, F. The chemistry of pyrolysis and combustion. *Adv. Chem.* **1984**, *207*, 489–529.
- Meincken, M.; Smit, N.H.; Steinmann, D. Physical properties of burnt timber, with special focus on the drying performance. *Eur. J. Wood Wood Prod.* **2015**, *68*, 455–461. [CrossRef]
- Bartlett, A.I.; Hadden, R.M.; Bisby, L.A. A review of factors affecting the burning behaviour of wood for application to tall timber construction. *Fire Technol.* **2019**, *55*, 1–49. [CrossRef]
- Kollmann, F.F.; Côté, W.A. *Principles of Wood Science and Technology. Vol. I. Solid Wood*; Springer: Berlin/Heidelberg, Germany, 1968; ISBN 9783642879302.
- Friquin, K.L. Material properties and external factors influencing the charring rate of solid wood and glue-laminated timber. *Fire Mater.* **2011**, *35*, 303–327. [CrossRef]
- Liu, Q.; Wang, S.R.; Fang, M.X.; Luo, Z.Y.; Cen, K.F.; Chow, W.K. Bench-scale studies on wood pyrolysis under different environments. *Fire Saf. Sci.* **1994**, *7*, 94.
- Guo, Y.; Bustin, R. FTIR spectroscopy and reflectance of modern charcoals and fungal decayed woods: Implications for studies of inertinite in coals. *Int. J. Coal Geol.* **1998**, *37*, 29–53. [CrossRef]
- White, R.H.; Dietersberger, M. Wood products: Thermal degradation and fire. *Encycl. Mater. Sci. Technol.* **2001**, 9712–9716. [CrossRef]
- Constantine, M.; Mooney, S.; Hibbert, B.; Marjo, C.; Bird, M.; Cohen, T.; Forbes, M.; Mcbeath, A.; Rich, A.; Stride, J. Science of the Total Environment Using charcoal, ATR FTIR and chemometrics to model the intensity of pyrolysis: Exploratory steps towards characterising fire events. *Sci. Total Environ.* **2021**, *783*, 147052. [CrossRef]
- Hill, C.A.S. Modifying the properties of wood. In *Wood Modification: Chemical, Thermal and Other Processes*; John Wiley & Sons: Hoboken, NJ, USA, 2006; pp. 19–44. ISBN 9780470021729.
- Segal, L.; Creely, J.J.; Martin, A.E., Jr.; Conrad, C.M. An empirical method for estimating the degree of crystallinity of native cellulose using the X-ray diffractometer. *Text. Res. J.* **1959**, *29*, 786–794. [CrossRef]
- Scherrer, P.; Debye, P. Bestimmung der grösse und der inneren struktur von kolloidteilchen mittels röntgensahlen [determination of the size and internal structure of colloidal particles using X-rays]. *Nachr. Ges. Wiss. Göttingen Math.-Physik. Kl.* **1918**, *2*, 101–120.
- Rutherford, D.; Wershaw, R.; Cox, L. *Changes in Composition and Porosity Occurring during the Thermal Degradation of Wood and Wood Components: U.S. Geological Survey Scientific Investigations Report 2004-5292*; U.S. Geological Survey: Reston, VA, USA, 2005; Volume 79.
- Sandström, M.; Jalilehvand, F.; Persson, I.; Fors, Y.; Damian, E.; Gelius, U.; Hall-Roth, I.; Dal, L.; Richards, V.L.; Godfrey, I. The sulphur threat to marine archaeological artefacts: Acid and iron removal from the Vasa. In *Proceedings of the Conservation Science 2002, Edinburgh, UK, 22–24 May 2002*; pp. 79–87.
- Monachon, M.; Albelda-Berenguer, M.; Pelé, C.; Cornet, E.; Guilminot, E.; Rémazeilles, C.; Joseph, E. Characterization of model samples simulating degradation processes induced by iron and sulfur species on waterlogged wood. *Microchem. J.* **2020**, *155*, 104756. [CrossRef]
- Fors, Y. Sulfur-Related Conservation Concerns for Marine Archaeological Wood. Ph.D. Thesis, Stockholm University, Stockholm, Sweden, 2008.
- Remazeilles, C.; Tran, K.; Guilminot, E.; Conforto, E.; Refait, P. Study of Fe (II) sulphides in waterlogged archaeological wood. *Stud. Conserv.* **2013**, *58*, 297–307. [CrossRef]
- Fors, Y.; Nilsson, T.; Risberg, E.D.; Sandström, M.; Torssander, P. Sulfur accumulation in pinewood (*Pinus sylvestris*) induced by bacteria in a simulated seabed environment: Implications for marine archaeological wood and fossil fuels. *Int. Biodeterior. Biodegrad.* **2008**, *62*, 336–347. [CrossRef]
- High, K.E.; Penkman, K.E.H. A review of analytical methods for assessing preservation in waterlogged archaeological wood and their application in practice. *Herit. Sci.* **2020**, *8*, 1–34. [CrossRef]
- Valenzuela-Calahorra, C.; Bernalte-García, A.; Gómez-Serrano, V.; Bernalte-García, M.J. Influence of particle size and pyrolysis conditions on yield, density and some textural parameters of chars prepared from holm-oak wood. *J. Anal. Appl. Pyrolysis* **1987**, *12*, 61–70. [CrossRef]
- Todaro, L.; Rita, A.; Cetera, P.; D’Auria, M. Thermal treatment modifies the calorific value and ash content in some wood species. *Fuel* **2015**, *140*, 1–3. [CrossRef]
- Inari, G.N.; Petrisans, M.; Lambert, J.; Ehrhardt, J.J.; Gérardin, P. XPS characterization of wood chemical composition after heat-treatment. *Surf. Interface Anal.* **2006**, *38*, 1336–1342. [CrossRef]

27. Kocaefe, D.; Huang, X.; Kocaefe, Y.; Boluk, Y. Quantitative characterization of chemical degradation of heat-treated wood surfaces during artificial weathering using XPS. *Surf. Interface Anal.* **2013**, *45*, 639–649. [CrossRef]
28. Poletto, M.; Zattera, A.J.; Santana, R.M.C. Structural differences between wood species: Evidence from chemical composition, FTIR spectroscopy, and thermogravimetric analysis. *J. Appl. Polym. Sci.* **2012**, *126*, E336–E343. [CrossRef]
29. Tintner, J.; Preimesberger, C.; Pfeifer, C.; Soldo, D.; Ottner, F.; Wriessnig, K.; Rennhofer, H.; Lichtenegger, H.; Novotny, E.H.; Smidt, E. Impact of pyrolysis temperature on charcoal characteristics. *Ind. Eng. Chem. Res.* **2018**, *57*, 15613–15619. [CrossRef]
30. Tjeerdsmas, B.F.; Militz, H. Chemical changes in hydrothermal treated wood: FTIR analysis of combined hydrothermal and dry heat-treated wood. *Holz Roh-Und Werkst.* **2005**, *63*, 102–111. [CrossRef]
31. Popescu, M.-C.; Froidevaux, J.; Navi, P.; Popescu, C.-M. Structural modifications of *Tilia cordata* wood during heat treatment investigated by FT-IR and 2D IR correlation spectroscopy. *J. Mol. Struct.* **2013**, *1033*, 176–186. [CrossRef]
32. Esteves, B.; Marques, A.V.; Domingos, I.; Pereira, H. Chemical changes of heat treated pine and eucalypt wood monitored by FTIR. *Maderas. Cienc. Tecnol.* **2013**, *15*, 245–258. [CrossRef]
33. Özgenç, Ö.; Durmaz, S.; Boyacı, İ.H.; Eksi-Koçak, H. ATR-FTIR spectroscopic analysis of thermally modified wood degraded by rot fungi. *Drewno* **2018**, *61*. [CrossRef]
34. Kubovsk, I.; Ka, D. Structural changes of oak wood main components caused by thermal modification. *Polymers* **2020**, *12*, 485. [CrossRef]
35. Kotilainen, R.A.; Toivanen, T.-J.; Alén, R.J. FTIR monitoring of chemical changes in softwood during heating. *J. Wood Chem. Technol.* **2000**, *20*, 307–320. [CrossRef]
36. Kim, Y.S. Short note: Chemical characteristics of waterlogged archaeological wood. *Holzforschung* **1990**, *44*, 169–172. [CrossRef]
37. Pournou, A. Wood deterioration by aquatic microorganisms. In *Biodeterioration of Wooden Cultural Heritage: Organisms and Decay Mechanisms in Aquatic and Terrestrial Ecosystems*; Pournou, A., Ed.; Springer International Publishing: Cham, Switzerland, 2020; pp. 177–260. ISBN 978-3-030-46504-9.
38. Pedersen, N.B.; Gierlinger, N.; Thygesen, L.G. Bacterial and abiotic decay in waterlogged archaeological *Picea abies* (L.) Karst studied by confocal Raman imaging and ATR-FTIR spectroscopy. *Holzforschung* **2015**, *69*, 103–112. [CrossRef]
39. Gelbrich, J.; Mai, C.; Militz, H. Chemical changes in wood degraded by bacteria. *Int. Biodeterior. Biodegrad.* **2008**, *61*, 24–32. [CrossRef]
40. Nilsson, B.T.; Daniel, G.; Kirk, T.K.; Obst, J.R.; Service, F. Chemistry and microscopy of wood decay by some higher ascomycetes. *Holzforschung* **1989**, *43*, 11–18. [CrossRef]
41. Pandey, K.; Pitman, A. FTIR studies of the changes in wood chemistry following decay by brown-rot and white-rot fungi. *Int. Biodeterior. Biodegrad.* **2003**, *52*, 151–160. [CrossRef]
42. Traoré, M.; Kaal, J.; Cortizas, A.M. Differentiation between pine woods according to species and growing location using FTIR-ATR. *Wood Sci. Technol.* **2018**, *52*, 487–504. [CrossRef] [PubMed]
43. Andersson, S.; Wikberg, H.; Pesonen, E.; Maunu, S.L.; Serimaa, R. Studies of crystallinity of Scots pine and Norway spruce cellulose. *Trees* **2004**, *18*, 346–353. [CrossRef]
44. Park, S.; Baker, J.O.; Himmel, M.E.; Parilla, P.A.; Johnson, D.K. Cellulose crystallinity index: Measurement techniques and their impact on interpreting cellulase performance. *Biotechnol. Biofuels* **2010**, *3*, 10. [CrossRef]
45. Agarwal, U.P.; Reiner, R.R.; Ralph, S.A.; Forest, A.; Gi, O.; Drive, P. Estimation of cellulose crystallinity of lignocelluloses using near-IR. *J. Agric. Food Chem.* **2013**, *61*, 103–113. [CrossRef]
46. Kwon, S.-M.; Kim, N.-H.; Cha, D.-S. An investigation on the transition characteristics of the wood cell walls during carbonization. *Wood Sci. Technol.* **2009**, *43*, 487–498. [CrossRef]
47. Giachi, G.; Bettazzi, F.; Chimichi, S.; Staccioli, G. Chemical characterisation of degraded wood in ships discovered in a recent excavation of the Etruscan and Roman harbour of Pisa. *J. Cult. Herit.* **2003**, *4*, 75–83. [CrossRef]
48. Popescu, C.-M.; Larsson, P.T.; Tibirna, C.M.; Vasile, C. Characterization of fungal-degraded lime wood by X-ray diffraction and cross-polarization magic-angle-spinning <sup>13</sup>C-nuclear magnetic resonance spectroscopy. *Appl. Spectrosc.* **2010**, *64*, 1054–1060. [CrossRef]
49. Zhou, Y.; Wang, K.; Hu, D. Degradation features of archaeological wood surface to deep inside a case study on wooden boards of marquis of Haihun’s outer coffin. *Wood Res.* **2018**, *63*, 419–430.
50. Howell, C.; Hastrup, A.C.S.; Goodell, B.; Jellison, J. Temporal changes in wood crystalline cellulose during degradation by brown rot fungi. *Int. Biodeterior. Biodegrad.* **2009**, *63*, 414–419. [CrossRef]
51. Thygesen, A.; Oddershede, J.; Lilholt, H.; Thomsen, A.B.; Ståhl, K. On the determination of crystallinity and cellulose content in plant fibres. *Cellulose* **2005**, *12*, 563–576. [CrossRef]
52. French, A.D.; Cintron, M.S. Cellulose polymorphism, crystallite size, and the segal crystallinity index. *Cellulose* **2013**, *20*, 583–588. [CrossRef]
53. Sivonen, H.; Maunu, S.L.; Sundholm, F.; Jämsä, S.; Viitaniemi, P. Magnetic resonance studies of thermally modified wood. *Holzforschung* **2002**, *56*, 648–654. [CrossRef]
54. Esteves, B.M.; Pereira, H.M. Wood modification by heat treatment: A review. *BioResources* **2009**, *4*, 370–404. [CrossRef]
55. Tarmian, A.; Mastouri, A. Changes in moisture exclusion efficiency and crystallinity of thermally modified wood with aging. *iFor.-Biogeosci. For.* **2019**, *12*, 92–97. [CrossRef]

56. Wang, S.; Dai, G.; Ru, B.; Zhao, Y.; Wang, X.; Xiao, G. Influence of torrefaction on the characteristics and pyrolysis behavior of cellulose. *Energy* **2017**, *120*, 864–871. [CrossRef]
57. Fuwape, J.A. Effects of carbonisation temperature on charcoal from some tropical trees. *Bioresour. Technol.* **1996**, *57*, 91–94. [CrossRef]
58. Ruiz-aquino, F.; Ruiz-ángel, S.; Sotomayor-castellanos, J.R. Energy characteristics of wood and charcoal of selected tree species in Mexico. *Wood Res.* **2019**, *64*, 71–82.
59. Dias Junior, A.F.; Esteves, R.P.; Da Silva, Á.M.; Sousa Júnior, A.D.; Oliveira, M.P.; Brito, J.O.; Napoli, A.; Braga, B.M. Investigating the pyrolysis temperature to define the use of charcoal. *Eur. J. Wood Wood Prod.* **2020**, *78*, 193–204. [CrossRef]
60. Mikkola, E. Charring of Wood Based Materials. *Fire Saf. Sci.* **1991**, *3*, 547–556. [CrossRef]
61. Lowden, L.A.; Hull, T.R. Flammability behaviour of wood and a review of the methods for its reduction. *Fire Sci. Rev.* **2013**, *2*, 4. [CrossRef]

## Article

# A Modelling Approach for the Assessment of Climate Change Impact on the Fungal Colonization of Historic Timber Structures

Petros Choidis <sup>1,\*</sup> , Dimitrios Kraniotis <sup>1</sup> , Ilari Lehtonen <sup>2</sup>  and Bente Hellum <sup>1</sup>

<sup>1</sup> Department of Civil Engineering and Energy Technology, Oslo Metropolitan University—OsloMet, St. Olavs Plass 4, N-0130 Oslo, Norway; dimkra@oslomet.no (D.K.); bente.hellum@oslomet.no (B.H.)

<sup>2</sup> Finnish Meteorological Institute, Weather and Climate Change Impact Research, Erik Palménin Aukio 1, PB 503, 00101 Helsinki, Finland; Ilari.Lehtonen@fmi.fi

\* Correspondence: petrosch@oslomet.no; Tel.: +47-4772-6478

**Abstract:** Climate change is anticipated to affect the degradation of the building materials in cultural heritage sites and buildings. For the aim of taking the necessary preventive measures, studies need to be carried out with the utmost possible precision regarding the building materials of each monument and the microclimate to which they are exposed. Within the present study, a methodology to investigate the mold risk of timber buildings is presented and applied in two historic constructions. The two case studies are located in Vestfold, Norway. Proper material properties are selected for the building elements by leveraging material properties from existing databases, measurements, and simulations of the hygrothermal performance of selected building components. Data from the REMO2015 driven by the global model MPI-ESM-LR are used in order to account for past, present, and future climate conditions. In addition, climate data from ERA5 reanalysis are used in order to assess the accuracy the MPI-ES-LR\_REMO2015 model results. Whole building hygrothermal simulations are employed to calculate the temperature and the relative humidity on the timber surfaces. The transient hygrothermal condition and certain characteristics of the timber surfaces are used as inputs in the updated VTT mold model in order to predict the mold risk of certain building elements. Results show a significant increase of the mold risk of the untreated timber surfaces due to climate change. The treated surfaces have no mold risk at all. It is also observed that the most significant increase of the mold risk occurs in the north-oriented and the horizontal surfaces. It is underlined that the mold risk of the timber elements is overestimated by the MPI-ES-LR\_REMO2015 model compared to ERA5 reanalysis. The importance of considering the surface temperature and humidity, and not the atmospheric temperature and humidity as boundary conditions in the mold growth model is also investigated and highlighted.

**Keywords:** hygrothermal performance; timber buildings; cultural heritage; numerical simulations; monitoring and sensors; climate models; fungi identification; mold growth modelling



**Citation:** Choidis, P.; Kraniotis, D.; Lehtonen, I.; Hellum, B. A Modelling Approach for the Assessment of Climate Change Impact on the Fungal Colonization of Historic Timber Structures. *Forests* **2021**, *12*, 819. <https://doi.org/10.3390/f12070819>

Academic Editors: Magdalena Broda and Callum Hill

Received: 28 May 2021  
Accepted: 19 June 2021  
Published: 22 June 2021

**Publisher's Note:** MDPI stays neutral with regard to jurisdictional claims in published maps and institutional affiliations.



**Copyright:** © 2021 by the authors. Licensee MDPI, Basel, Switzerland. This article is an open access article distributed under the terms and conditions of the Creative Commons Attribution (CC BY) license (<https://creativecommons.org/licenses/by/4.0/>).

## 1. Introduction

Historic constructions constitute an integral part of the human cultural heritage and they play a significant role to the economies of the areas where they are located. Thus, we need to ensure their existence on a long-term horizon. Recent research underlines that an additional burden that the historic constructions have to deal with is climate change [1–7]. The impact of climate change on the tangible cultural heritage have been investigated in several projects, with the most known ones being the Noah's Ark [1] and the Climate for Culture [3]. Within the Noah's Ark project, data from climate models have been used as inputs in damage functions in order to examine the climate change impact on the deterioration of the building materials in cultural heritage sites. In the project Climate for Culture, the methodology that was followed included some additional steps in order to examine the impact of climate change on artifacts that are located in interior environments. Specifically, there were data used from climate models, material properties for the elements

of the building cell, and the heat, air, and moisture (HAM) loads in the interior of certain rooms in order to calculate the air temperature and air relative humidity inside them. Then, by using appropriate standards and models describing the deterioration of the valuable tangible cultural heritage, the result of the action of certain deterioration mechanisms was investigated. The current research is conducted in the framework of the HYPERION EU project [8], which aims to create an online platform for the assessment of the resilience of historic areas by taking into account several different hazards. One of the examined hazards is climate change. In the framework of this project, specific buildings of high cultural significance are modelled in detail in order to be able to investigate their risks in a building component level. This detailed investigation is important, especially for the managers of the cultural heritage buildings, who mainly focus their conservation strategy on the material level and are also interested in examining the effectiveness of different conservation strategies. The focus of the current study is to investigate the mold risk of two timber historic buildings located in southern Norway.

In many studies, the impact of climate change on the mold risk of timber elements has been investigated [9–12] by using the biohygrothermal model [13]. In [9,10,12], the mold risk of historically significant artifacts that are made of timber was investigated, while in [11], the focus was placed on the investigation of the mold growth risk on the log walls of a historic timber construction. The biohygrothermal model accounts for the temperature and relative humidity on the surface of interest, and also for different substrate categories in order to calculate the mold growth in millimeters. One disadvantage of the biohygrothermal model is the limited number of the substrate categories that does not allow for defining of the different mold risks among different wood species, or between a rough and a planed wood surface. In addition, the biohygrothermal model does not account for the reduction of the mold risk under unfavorable conditions and, thus, it is not appropriate for the assessment of the mold risk for periods of several years. Considering the inputs, outputs, and applicability of several different mold growth models reviewed in [14–16], it was concluded that the assessment of the mold growth risk on the timber building elements can be most effectively employed by using the updated Technical Research Centre of Finland (VTT) mold growth model [17]. The updated VTT mold model, apart from the temperature and the relative humidity on the surface of interest, takes into account the wood species (hardwood or softwood), the type of surface (planed or rough), four different sensitivity classes, and four different material classes, according to which it can be parametrized in order to account for different final surfaces, e.g., untreated sapwood, surface treated with tar, etc. The updated VTT mold model also accounts for the decrease of the mold level during unfavorable growth periods.

The temperature and the relative humidity on both the exterior and the interior surfaces of the building components should be defined in order to be used as inputs in the mold growth model. Their calculation can be done by using whole building heat, air, and moisture (HAM) tools, given the outdoor climate, the material properties of the building components, the type of use (e.g., visitors, interior sources of moisture), and the operating heating, ventilation, and air conditioning (HVAC) systems. The HAM tools available for such applications have been reviewed in [18]. According to the conclusions of the Climate for Culture project [3], the software that are more appropriate to be used for applications related to historic buildings are the WUFI® Plus [19] and the HAMBase [20]. The studies [9,10,12,21–25] are relevant applications employed within the project ‘Climate for Culture’.

Then, the input material properties should be defined for the components of the buildings under investigation. Within the studies [9,10,12,21–25], the material properties have been selected from existing databases. In the current research, the material properties should be defined with greater accuracy. For this purpose, a methodology to select the proper material properties for the simulated building components is proposed. Within this method, material properties from existing databases, measurements, and simulations of the hygrothermal performance of selected building components are used. The hygrothermal

models suitable to be used in such applications, as well as the input material properties that they take into account, have been reviewed in [26].

In addition, climate data from climate models are used in order to account for the past, present, and future conditions. The focus is to investigate the climate change impact on the mold growth of various building components and how it may vary based on the different exposure environment, i.e., differences between indoors and outdoors and differences among different orientations. Moreover, climate data from ERA5 reanalysis for the present conditions are used in order to assess the accuracy of the results deriving from the climate models. Finally, the importance of assessing the mold growth on the building components by taking into account the surface temperature and the surface relative humidity, and not the atmospheric temperature and the atmospheric relative humidity is also investigated. It should be highlighted that the calculation of the temperature and the relative humidity on the exterior and the interior surfaces of the building elements indicates the computationally demanding process of the employment of whole-building hygrothermal simulations, given the material properties of the building cell and the outdoor climate.

## 2. Materials and Methods

The study consists of an experimental part and numerical simulations.

The experimental part is focused on:

- Description of the case studies;
- Determination of the presence of fungal colonization in aerosol and on the material surface, and identification of the microfungi in the laboratory;
- Mapping the geometry and different building materials in the two case studies;
- Monitoring of the hygric and thermal performance of selected building elements in order to validate, on a later stage, respective numerical simulations.

The numerical simulations are focused on:

- Using measurements from the sensors, material properties from existing databases, and a one-dimensional hygrothermal simulation tool in order to select appropriate material properties for the components of the two buildings;
- Synthesis of climate files that will be used in order to assess the climate change impact on the hygric and thermal performance of the building components;
- Employment of whole building hygrothermal simulations in order to define the temperature and relative humidity on the surface of the building components (both exterior and interior) under the considered climate excitations;
- Use of a mold growth model that accounts for the transient hygrothermal conditions of the building elements in order to assess their mold risk.

At this point, it is noteworthy that the hygrothermal building simulation software WUFI® provides an extensive database with material properties relevant to the building materials of the current study. In addition, the software packages WUFI®Pro 5.3 by Fraunhofer Institute for Building Physics (IBP), Germany [27], WUFI®Plus V.3.2.0.1 by Fraunhofer IBP, Germany [28], and WUFI Mould Index VTT 2.1 by Technical Research Centre of Finland and Fraunhofer IBP, Germany [29] can be used for the one-dimensional hygrothermal simulations, whole building hygrothermal simulations, and mold risk assessment, respectively. This is the main reason why this specific software family has been selected in the current research. The WUFI® software is a numerical solver of a moisture transfer and an energy transfer equation, which are coupled. More information on the governing transport equations and the calculation procedure can be found at [30].

### 2.1. Experimental Part

#### 2.1.1. Study Site

In this research, the focus has been placed in the county of Vestfold, Norway, which hosts the highest number of timber historic buildings in the country. Specifically, in the city of Tønsberg, there are several historic timber buildings which have been moved there

from various regions around Vestfold, and they are currently property of the Slottsfjell museum. The effect of the buildings' displacement on their hygrothermal performance was insignificant. That is because the climatic conditions in their former and current location—both in the county of Vestfold—are similar. In addition, the traditional techniques of wood preservation were respected in any rehabilitation project employed by the Slottsfjell museum. The two buildings selected to be investigated in the current research are the Fadum storehouse (Figure 1a), having a characteristic design that is found only in the examined area, and the Heierstad loft (Figure 1b), which is the oldest building in the area. Both buildings owe their names to the region that they originally come from.



**Figure 1.** Photographs of (a) the Fadum storehouse and (b) the Heierstad loft taken from south-west.

The Fadum storehouse is a two-storey building and is dated back to 1820. In 1958, it was moved to its current location at the Slottsfjellet hill. It has a rectangular plan, with its major axis east–west oriented. Its entrance is in the southern façade. Its unique design features are the pillars or stumps upon which it stands and the shed or coating that surrounds the main body of the building. It also has openings in the eastern and western façade, both in the ground and upper floor. The stumps contribute to keeping the lower part of the construction dry, since they protect it from the ground rising damp, and they also allow the wind to flow under the main body of the construction. The coating-shed protects the outer walls from rain, wind, and solar radiation. Finally, the openings in the smaller facades of the building ensure adequate natural ventilation to its interior. The Heierstad loft is also a two-storey building. Its ground level is dated back to 1407, while its upper level was reconstructed in 1957, when the building was moved to the Slottsfjellet hill. The building is not directly based on the ground, but it stands on rocks. It has openings in its upper floor, in three out of four facades, and a turf roof that was reconstructed in 2019. The main body of both constructions is built of horizontal logs notched at the corners. The log walls are made of softwood, most likely Scotch pine (*Pinus sylvestris*) or Norway Spruce (*Picea abies*), treated with tar on their outer surface.

#### 2.1.2. Fungi Sampling Strategy and Microscopy Analysis

Fungal growth was detected on some building components of the two constructions and, thus, it was decided to examine it thoroughly. Fungal colonization, both in aerosol and on the surface of the building elements, was investigated. Active sampling was performed outdoors, in the ground, and in the upper level of the two buildings in order to detect fungal cells and spores. A portable Surface Air System (SAS) sampler with a flow rate of 180 L/min was used for active sampling. In all sampling positions, both malt and dichloran glycerol (DG-18 without hyphen) agar were used as the growth media in the plates. The fungal colonies were counted three days after the sample collection and the fungal identification took place ten days after the sample collection. Regarding the fungal

colonies on the building material surfaces, samples were collected in malt agar plates by using a pocketknife and the fungal species on them were identified in the laboratory ten days later. The morphology of fungi isolated colonies was observed by an optical microscope. In particular, conidiophores and conidia fungal structures were examined after methylene blue staining.

### 2.1.3. Monitoring Strategy and Sensors

The building elements of the examined constructions are made of different types of timber and have a different age. For that reason, the building components were grouped into homogeneous categories, and representative building elements from each category were selected in order to monitor their hygrothermal performance by using sensors (Figure 2). The sensors monitor the air temperature ( $\theta$ ) and the air relative humidity ( $\varphi$ ) every 5 min on both sides of the building element, the moisture content inside the building element ( $u$ ) every 4 h, and, in one case, the temperature inside the timber component ( $\theta_{timber}$ ) every 5 min. The measurement of the temperature inside the timber prerequisites drilling a hole of 5 mm in diameter and 10 mm in depth in order to fit the sensor inside. The irreversible damage on the log wall in order to install this certain type of sensor is the reason why only one of them was used.

In more detail (Figure 2), three sensors monitoring the air temperature and the air relative humidity were placed in the Fadum storehouse. One sensor was placed in the upper floor (sensor A), the second in the ground floor (sensor C), and the third one under the coating (sensor F). Moreover, sensors monitoring the moisture content at the interior side of the south-oriented wall of the upper level (sensor B) and the ground level (sensor D) were installed. Finally, one sensor was installed to monitor the temperature inside the timber at the interior side of the south-oriented wall of the ground level (sensor E).

At the Heierstad loft, three sensors monitoring the air temperature and the air relative humidity were installed, one at the opening of the northwest façade of the upper floor (sensor G), another at the bigger room of the upper floor (sensor I), and the last one at the ground floor (sensor K). In addition, the moisture content at the interior side of the northwest-oriented log walls of the upper and ground level were monitored by the sensors H and J, respectively.

It is worth mentioning that the installation depth of the sensor monitoring the temperature inside the wood was 10 mm, and its measurements corresponded to the average temperature along the installation depth. In addition, the moisture content sensors measured the electrical resistance between two electrodes and converted it to water content units based on Equation (1). The electrodes were installed at the depth of 10 mm, and the distance between them was 20 mm. The measurements of the sensors corresponded to the average moisture content along the installation depth. The moisture content values estimated from Equation (1), together with the temperature measurements from the nearest temperature sensor, were used to calculate the temperature-corrected moisture content values with Equation (2).

The sensors installed in the Fadum storehouse have been operating since 22 November 2019, while the sensors installed in the Heierstad loft have been operating since 12 February 2020. For the aims of this study, measurements until 4 April 2020 were processed. An annual monitoring schedule would have provided a complete view of the hygrothermal performance and the moisture- and temperature-related damage on the timber components. Nevertheless, the selected period is still useful in order to assess the hygrothermal performance of the buildings and validate relevant numerical models.

$$u = \frac{1.005 - \log(\log(R + 1))}{0.040} \quad (1)$$

$$u_c = \frac{u + 0.567 - 0.0260 \times (\theta_{timber} + 2.8) + 0.000051 \times (\theta_{timber} + 2.8)^2}{0.881 \times (1.0056)^{(\theta_{timber} + 2.8)}} \quad (2)$$



where:

$u$ : equilibrium moisture content (-);

$R$ : electrical resistance ( $M\Omega$ );

$u_c$ : temperature corrected moisture content (-);

$\theta_{timber}$ : temperature in wood or close to the surface of wood ( $^{\circ}C$ ).

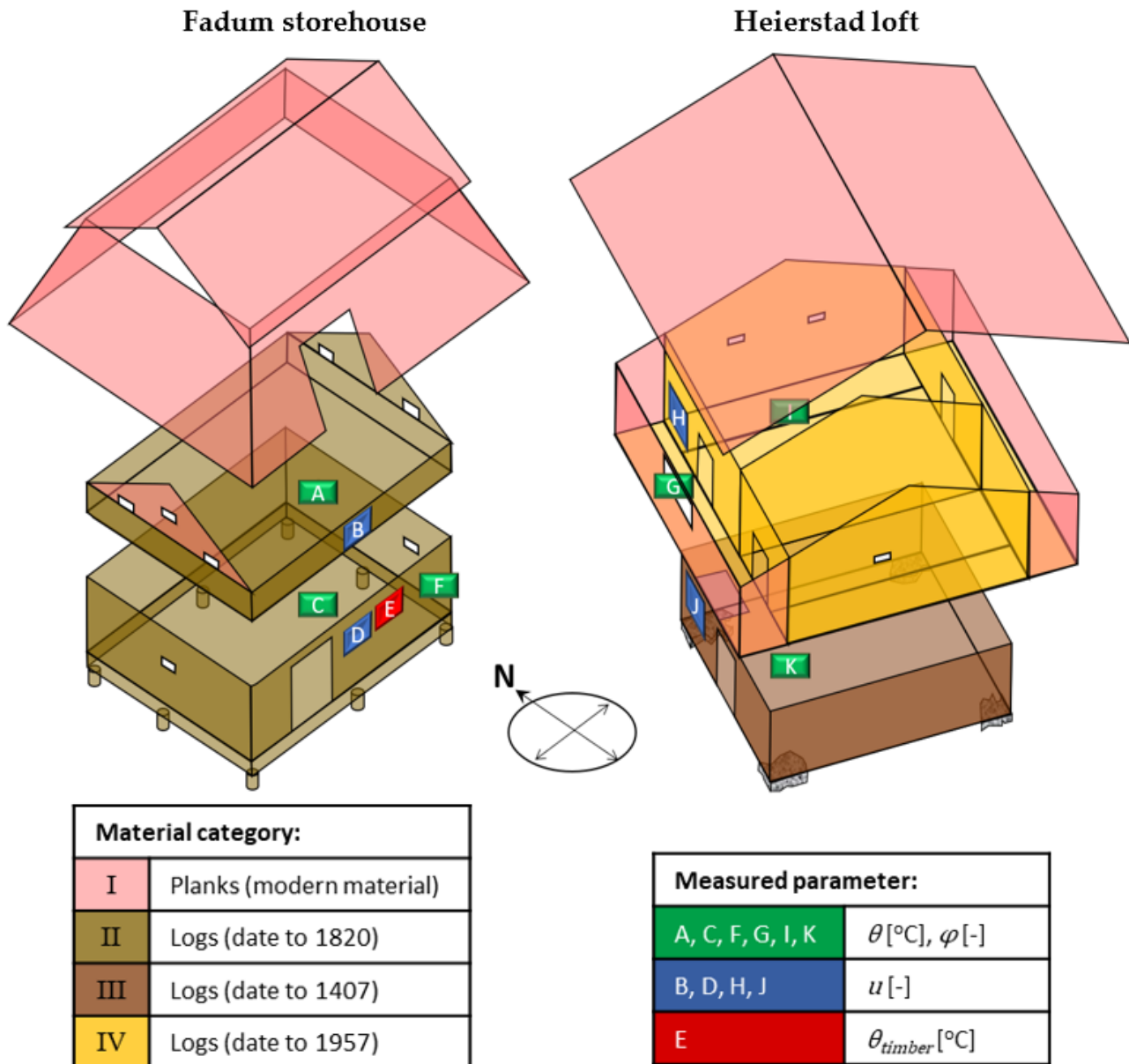


**Figure 2.** The building components have been grouped in four homogeneous categories, highlighted with different colors, based on the type and age of wood that they are made of. The positions of the installed sensors are also highlighted with green color for the air temperature and humidity sensors (A, C, F, G, I, K), blue color for the moisture content sensors (B, D, H, J), and red color for the sensor monitoring the temperature inside the timber (E).

## 2.2. Numerical Simulations

### 2.2.1. Selection of Building Material Properties

Based on the information about the building components provided by the historic buildings' curator (Slottsfjells museum), the planks are modern material (Figure 2) and have been replaced several times throughout the years, e.g., the planks of the coating of the Fadum storehouse were replaced in 2012 and the roof of the Heierstad loft was

reconstructed in 2019. The material properties for these building elements were derived from another research on one of the two buildings [11] and coincides with the Softwood (by Fraunhofer-IBP) from the database of WUFI<sup>®</sup>Pro [27].

For the logs that form the main body of buildings, it is known that they have local origin and they are either Scots' pine or Norway Spruce. In addition, all logs at the Fadum storehouse are of the same tree species and date back to 1820 (Figure 2). All logs of the ground level of the Heierstad loft are of the same tree species and are dated back to 1407 (Figure 2). Finally, all logs of the upper level of the Heierstad loft are of the same tree species and are dated back to 1957 (Figure 2). Representative logs from each category were selected in order to both monitor and simulate their hygrothermal performance (Table 1) by taking into account different sets of material properties and, finally, select the properties that provide the best fit between measurements and simulations (Equation (3)). The sets of material properties were derived from the built-in database of WUFI<sup>®</sup>Pro 5.3, and they are: (a) Softwood (by Fraunhofer-IBP, Germany), (b) Spruce, radial (by Fraunhofer-IBP, Germany), (c) Spruce, tangential (by LTH Lund University, Sweden), (d) Scandinavian spruce transverse direction (by Norwegian University of Science and Technology 'NTNU'), (e) Pine transverse direction (by NTNU), and (f) Spruce (University of Technology Vienna, Austria). The different tree species have different hygric performance, which can be depicted in their moisture storage functions (Figure 3). For example, as can be seen in Figure 3, for an extended period of relative humidities, around 85% of the moisture content of the:

1. Pine transverse direction (by NTNU) is approximately  $142 \text{ kg/m}^3$  or 27.8%, given that its bulk density ( $\rho$ ) is  $510 \text{ kg/m}^3$ ;
2. Scandinavian spruce transverse direction (by NTNU) is approximately  $95 \text{ kg/m}^3$  or 22.7%, given that  $\rho = 420 \text{ kg/m}^3$ ;
3. Spruce, radial (by Fraunhofer-IBP) is approximately  $90 \text{ kg/m}^3$  or 19.8%, given that  $\rho = 455 \text{ kg/m}^3$ ;
4. Spruce, tangential (by LTH Lund University, Sweden) is approximately  $89 \text{ kg/m}^3$  or 20.6%, given that  $\rho = 430 \text{ kg/m}^3$ ;
5. Softwood (by Fraunhofer-IBP) is approximately  $74 \text{ kg/m}^3$  or 18.5%, given that  $\rho = 400 \text{ kg/m}^3$ ;
6. Spruce (University of Technology Vienna, Austria) is approximately  $79 \text{ kg/m}^3$  or 13.1%, given that  $\rho = 600 \text{ kg/m}^3$ .

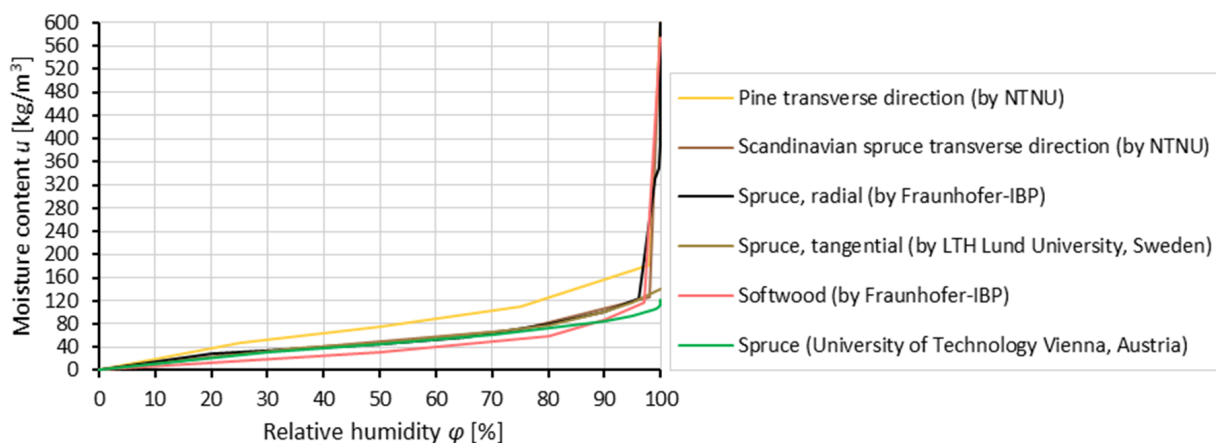


**Figure 3.** Moisture storage functions of the wood species that were tested for the selection of proper material properties for the two case studies. The data derive from the WUFI<sup>®</sup> database.

**Table 1.** Inputs, outputs, and origin of the measurements to validate the outputs of the simulated hygrothermal performance of selected building components.

Group	1D Hygrothermal Simulations			Output	Origin of Measurements to Validate the Output
	Component	Input Climate			
		Interior $\theta, \varphi$	Exterior $\theta, \varphi$		
II	Log at the southern wall of the ground level of the Fadum storehouse	Sensor C	Sensor F	$\theta_{timber}^1$ $u^1$	Sensor E Sensor D
	Log at the southern wall of the upper level of the Fadum storehouse	Sensor A	Sensor F	$u^1$	Sensor B
III	Log at the northwest wall of the ground level of the Heierstad loft	Sensor K	Sensor G	$u^1$	Sensor J
IV	Log at the northwest wall of the upper level of the Heierstad loft	Sensor I	Sensor G	$u^1$	Sensor H

<sup>1</sup> The simulated outputs of  $\theta_{timber}$  (temperature inside the timber) and  $u$  (moisture content) were calculated as the average values along a depth of 10 mm from the inner surface of the building components.

The 1D hygrothermal model [27] that was used to simulate the performance of the building components takes into account (i) heat transport via thermal conduction and enthalpy flow through moisture movement with phase change, (ii) vapor transport via vapor diffusion and solution diffusion, and (iii) liquid transport via capillary conduction and surface diffusion.

The agreement between measurements and simulated outputs was examined by using the goodness of fit (Equation (3)). The set of properties for which measurements and simulations had the highest fit were considered as the appropriate ones to be further used within the study.

$$fit = \left( 1 - \frac{\sqrt{\sum_{i=1}^N (x_{i,meas} - x_{i,sim})^2}}{\sqrt{\sum_{i=1}^N (x_{i,sim} - \bar{x}_{i,meas})^2}} \right) \cdot 100 \quad (3)$$

where:

$x_{i,meas}$ : measured value of the hygrothermal parameter ( $u$  or  $\theta_{timber}$ ) at the time step  $i$ ;

$x_{i,sim}$ : simulated value of the hygrothermal parameter at the time step  $i$ ;

$N$ : total number of points across the studied period of time;

$\bar{x}_{meas}$ : the average of the measured values of the hygrothermal parameter during the studied time period.

#### 2.2.2. Climate Data

Climate files including data about all climate parameters affecting the hygrothermal performance of the buildings were synthesized. Specifically, the following climate parameters were used:

- Air temperature  $\theta$  (°C);
- Air relative humidity  $\varphi$  (%);
- Precipitation  $rr$  (mm);
- Wind speed  $ff$  (m/s);
- Wind direction  $dd$  (°);
- Cloud cover  $N_c$  (oktas);
- Atmospheric long-wave counter-radiation incident on a horizontal surface  $G_{Lin}$  (W/m<sup>2</sup>);
- Global short-wave radiation incident on a horizontal surface  $I_H$  (W/m<sup>2</sup>);
- Diffusive short-wave radiation incident on a horizontal surface  $I_{dH}$  (W/m<sup>2</sup>);
- Direct short-wave radiation incident on a horizontal surface  $I_{DH}$  (W/m<sup>2</sup>).

In order to account for climate change, hourly climate data of 0.11 degrees spatial resolution were synthesized for three ten-year periods: 1960–1969 (past), 2010–2019 (current) under representative concentration pathway (RCP) 8.5, and 2060–2069 (future) under RCP8.5. The RCP8.5 represents a high-end emission scenario leading to accelerated global

warming during the ongoing century [31]. The climate data used were produced with the latest hydrostatic version of the REgional MOdel REMO (version REMO2015), driven by the global model MPI-ESM-LR. The REMO [32] is a three-dimensional regional atmosphere model developed at the Max Planck Institute for Meteorology, Germany, and is currently maintained at the Climate Service Center Germany (GERICS). The MPI-ESM-LR is the low-resolution version of the Max Planck-Institute Earth System Model (MPI-ESM) [33]. The model data were acquired from the EURO-CORDEX project [34] data archive. Some additional calculations were employed in order to produce the wind direction, and diffuse and direct shortwave radiation data. Specifically, the hourly wind direction data were produced by combining files of northward and eastward wind speed having a 6 h temporal resolution and assuming constant wind direction during the whole 6 h period. In addition, the direct and diffuse shortwave radiation data were calculated by using the ENLOSS model introduced by Taesler and Andersson [35]. A brief description of the steps that were followed is provided below:

1. Calculation of the solar altitude ( $a$ ) and the zenith angle ( $z$ ) for the sites' position with an hourly timestep;
2. Calculation of the airmass ( $m$ ), given the  $z$ , by using the Young formula;
3. Calculation of the saturation pressure of water vapor ( $p_{vs}$ ), given the  $\theta$ , by using the relations found at [36];
4. Calculation of the vapor partial pressure ( $p_v$ ), given the  $p_{vs}$  and the  $\varphi$ ;
5. Calculation of the absorption of radiation by water vapor ( $F$ ), given the  $p_v$  and the  $m$ ;
6. Calculation of the intensity of direct radiation in the direction of normal ( $I'_{DN}$ ), given (i) the coefficient of turbidity ( $\beta$ ), (ii) the spectral distribution of solar radiation outside the atmosphere  $i_0$  ( $\lambda$ ) in the wavelength ( $\lambda$ ) region 0.115–50 nm, (iii) the  $m$ , and (iv) the  $N_c$ ;
7. Calculation for each day of the year of the correction factor ( $k_e$ ) that takes into account the eccentricity of the Earth's orbit around the Sun;
8. Calculation of the direct normal radiation ( $I_{DN}$ ), given the  $F$ , the  $I'_{DN}$ , and the  $k_e$ ;
9. Calculation of the  $I_{DH}$ , given the  $I_{DN}$  and the  $a$ ;
10. Calculation of the  $I_{dH}$ , given the  $I_{DH}$  and the  $I_H$ .

More information about each individual step can be found at [37]. By comparing climate data that derive from the same model and refer to different periods (past, present, and future), it is possible to detect the signal of climate change, i.e., quantify the change of each individual climate parameter throughout the years. In order to assess how much the modelled climate deviates from the actual one, a fourth climate file was prepared containing data from ERA5 reanalysis [38] for the period 2010–2019 (current conditions). ERA5 is the latest climate reanalysis produced by the European Centre for Medium-Range Weather Forecasts (ECMWF). Climate reanalyses combine past observations with models to generate consistent time series of multiple climate variables. The ERA5 data have been used because there were no applicable observations available near the study site for many of the parameters that should be taken into account. The spatial resolution of the ERA5 data is 0.25 degrees. The climate data from ERA5 are representative of the study site, given the minor topographic differences within the grid cell in ERA5, which includes the study site.

Once again, not all climate parameters that were needed could be directly downloaded. Relative humidity is not archived directly in ERA datasets, but the archive contains near-surface temperature ( $\theta$ ) and dew point temperature ( $\theta_d$ ), from which the relative humidity can be calculated from the equation:

$$\varphi = 100 \cdot \frac{e_s(\theta_d)}{e_s(\theta)} \quad (4)$$

where  $e_s$  is the saturation pressure, defined with respect to water for temperatures over 0 °C and ice for temperatures below 0 °C as described in [36].

A comparison between air temperature, air relative humidity, and precipitation data derived from a weather station 5 km from the study site [39] and ERA5 reanalysis is presented in Figure 4a–c, respectively. It is verified that the data derived from ERA5 reanalysis can well describe the climate conditions in the study site. The most notable difference seems to be that the coldest temperatures are warmer in ERA5 in each month, but particularly in winter.

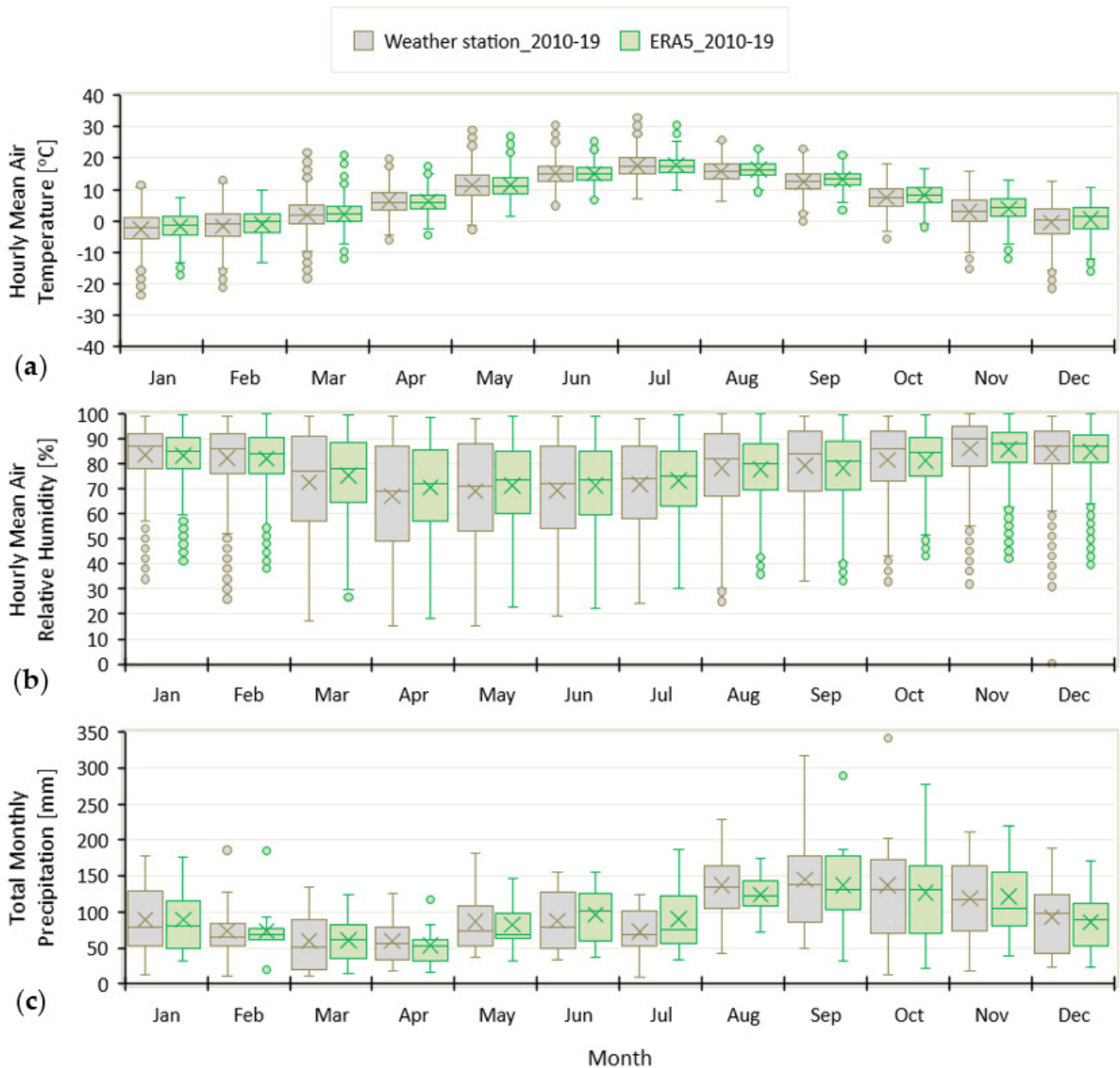


**Figure 4.** Comparison between (a) air temperature, (b) air relative humidity and (c) precipitation data derived from the Melsom weather station that is located 5 km from the study site, and from the ERA5 reanalysis. In the boxplots the box shows 50% of the data, with median represented as a horizontal bar and the average value highlighted with the ‘x’ symbol. The whisker extends to two standard deviations of the data and the circles represent the outliers.

### 2.2.3. Whole-Building Hygrothermal Simulations

The selected material properties of the building components and the prepared climate data were used as an input in whole-building hygrothermal simulations using the software WUFI® Plus V.3.2.0.1 [28] (Figure 5). Within the employed models, the heat

transport mechanisms that were taken into account were: thermal conduction, enthalpy flow through moisture movement with phase change, short-wave solar radiation, and night-time long-wave radiation cooling. The vapor transport mechanisms that were taken into account included vapor diffusion and solution diffusion. The considered liquid transport mechanisms were capillary conduction and surface diffusion. Moreover, the employed models incorporated calculations of explicit radiation balance on external surfaces shading calculations with hourly time step, wind dependent heat transfer on external surfaces, rain load calculation on external surfaces, and air flow calculation.

The buildings have no HVAC systems or transparent components. Within the airflow model the openings of the two buildings were modelled as orifices. Special attention was paid to consider within the simulations that the buildings are not directly based on the ground, but there is free air flow down below them. For that purpose, an additional zone was considered under the buildings which has the same length and width as the ground floor of each construction, and a height of 50 cm in the case of the Fadum store house and 30 cm in the case of the Heierstad loft. All vertical sides of this zone were considered as orifices within the simulations.

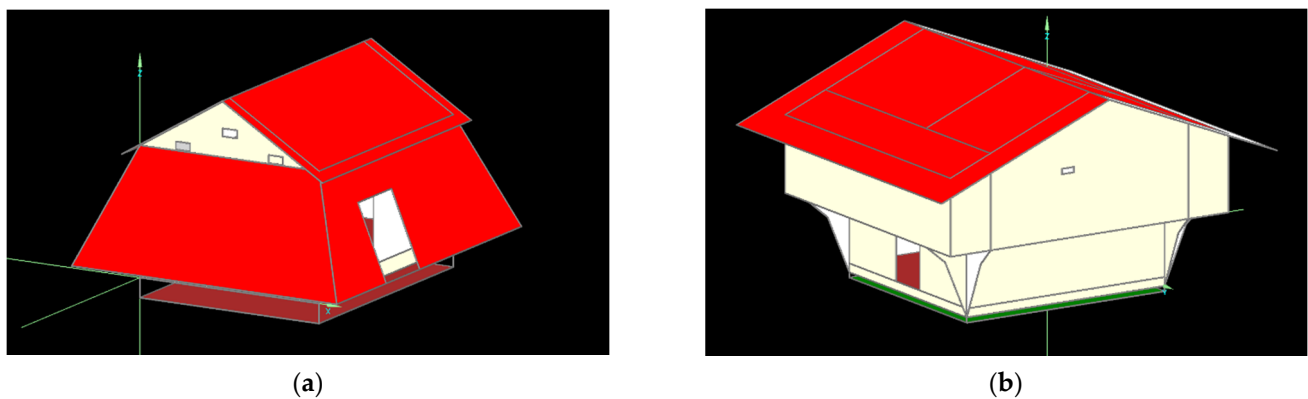


**Figure 5.** The whole-building simulation models of (a) the Fadum storehouse and (b) the Heierstad loft.

#### 2.2.4. Mold Growth Model

In the current study, the WUFI Mold Index VTT 2.1 software [29] was used to calculate the mold growth on the building components according to the updated VTT mold model [17]. The updated VTT model is an empirical mold growth prediction model, which is based on regression analysis of a set of measured data [40,41]. The mold growth development is expressed by the mold index ( $M$ ), which can range between 0 and 6 (Table 2). The mold index can be used as a design criterion, e.g., often  $M = 1$  is defined as the maximum tolerable value, given that the germination process starts from the particular point.

**Table 2.** Description of the mold growth index [41].

Index	Growth Rate	Description
0	No growth	Spores not activated
1	Small amounts of mold on surface (microscope)	Initial stages of growth
2	<10% coverage of mold on surface (microscope)	-
3	10–30% coverage of mold on surface (visual)	New spores produced
4	30–70% coverage of mold on surface (visual)	Moderate growth
5	>70% coverage of mold on surface (visual)	Plenty of growth
6	Very heavy and tight growth	Coverage around 100%

Compared to the other mold growth models, the features of the updated VTT mold model that render it more appropriate for the aims of the current research are the following:

- Accounts for surface temperature, surface relative humidity, different types and qualities of the substrate timber;

- Estimation of growth and not just an indication of start;
- Decrease of mold level during unfavorable growth periods;
- Appropriate for application to extended periods of time (10-year periods in the current research).

The mold growth intensity in the updated VTT mold model is based on Equation (5) [17]:

$$\frac{dM}{dt} = \frac{k_1 \cdot k_2}{7 \cdot e^{(-0.68 \cdot \ln \theta - 13.9 \cdot \ln \varphi + 0.14 \cdot W - 0.33 \cdot SQ + 66.02)}} \quad (5)$$

where:

$M$ : mold index (-)

$t$ : time (h). The numerical simulation carried out using one-hour time steps (climate data intervals).

$\theta$ : temperature (°C)

$\varphi$ : relative humidity (%)

$W$ : coefficient that depends on the timber species. It is equal to 1 for hardwood and 0 for softwood and nontimber materials.

$SQ$ : coefficient that depends on surface quality. It is equal to 1 for rough surfaces and 0 for planed surfaces and nontimber materials.

$k_1$ : coefficient that expresses the intensity of the mold growth and depends on the growth level. It is used to scale the equation for different substrate materials, e.g., a surface treated with tar and an untreated sapwood surface.

$k_2$ : coefficient to limit the growth to a maximum possible index level. It is also used to scale the equation for different substrate materials, and is calculated by Equation (6):

$$k_2 = \max \left[ 1 - e^{[2.3 \cdot (M - M_{max})]}, 0 \right] \quad (6)$$

where:

$M_{max}$ : the maximum mold index on a specific substrate material, given by Equation (7):

$$M_{max} = A + B \cdot \frac{\varphi_{crit} - \varphi}{\varphi_{crit} - 100} - C \cdot \left( \frac{\varphi_{crit} - \varphi}{\varphi_{crit} - 100} \right)^2 \quad (7)$$

where:

$A, B, C$ : coefficients that have been determined experimentally and categorized into four sensitivity classes by [17], and they are dependent on the substrate material.

$\varphi_{crit}$ : The lowest relative humidity value where mold growth is possible when the material is exposed to it for a long enough period, and it is given by (Equation (8)):

$$\varphi_{crit} = \begin{cases} -0.0026 \cdot \theta^3 + 0.160 \cdot \theta^2 - 3.13 \cdot \theta + 100, & \text{when } \theta \leq 20 \\ \varphi_{min}, & \text{when } \theta > 20 \end{cases} \quad (8)$$

where  $\varphi_{min}$  is 80% for wood-based products and 85% for materials that are more resistant to mold growth, e.g., the surfaces treated with tar in the case studies of the current research.

The updated VTT mold model takes into account the decrease in the mold index level when the conditions (relative humidity or temperature) are outside the favorable conditions for mold growth. For this reason, the mold decline intensity for a reference material (re-sawn pine wood) is first calculated, and then multiplied by an appropriate scaling factor  $C_{mat}$  to adjust the mold decline intensity to the actual substrate material. More details about the updated VTT mold model can be found at [17].

As can be seen in Table 3, the model was parametrized accordingly in order to account for all different types of surfaces existing in the two case studies.

**Table 3.** Parametrization of the updated VTT mold model based on the features of the examined surfaces.

Surface Description	W	SQ	$k_1$		$k_2 (M_{max})$				$C_{mat}$
			$M < 1$	$M \geq 1$	A	B	C	$\varphi_{min}$ [%]	
Log/plank treated with tar	0	0	0.072	0.097	0.0	5	1.5	85	1
Log without treatment	0	0	1.000	2.000	1.0	7	2.0	80	1
Plank without treatment	0	0	0.578	0.386	0.3	6	1.0	80	1
Degraded surface (positions with cracks, splits, etc.)	0	1	1.000	2.000	1.0	7	2.0	80	1

### 3. Results and Discussion

#### 3.1. Mapping and Identification of Fungi

The exterior side of the building components that is treated with tar was not colonized by mold. In contrast, at the untreated planks of the coating/shed of the Fadum storehouse colonization was observed. As can be seen in Figure 6, the north-oriented side of the coating was the most aggravated. Moreover, fungal growth was detected at the interior of the two buildings. In the Fadum storehouse, brown-rot fungi (*Coniophora puteana*) was detected in the north-oriented side of both the roof and the coating (Figure 7a). The fungus was identified based on its fruiting body. *Coniophora puteana* is a wood-destroying fungus that breaks down the hemicellulose and cellulose [42]. The rotting fungus grew in positions with leaks in which the rainwater had penetrated. The infected building elements were untreated planks. These planks were replaced immediately by the historic buildings' curator. In the Heierstad loft, fungal growth was detected at the inner side of the northeast-oriented wall of the upper level and on the ceiling of the ground floor (Figure 7). The infected surfaces were untreated logs.



**Figure 6.** At the Fadum storehouse, the growth of biological organisms is more intense on (a) the north façade than on (b) the south façade.

Apart from the fungi grown on the building components, samples of airborne fungal spores were also collected. In Figure 8, the position from which the aerosol samples were collected, as well as the fungi colonies grown three days after the samples collection, are shown. As has already been mentioned in Section 2.1.2, two different growth media were used in the plates. This is because some species of fungi grow favorably on malt agar, while others on DG-18 agar. Moreover, quantitative microbial concentrations were estimated for the culturable fungi colonies as colony forming units per air volume (CFU/m<sup>3</sup>) (Figure 9). As can be seen in Figures 8 and 9, the smallest fungal concentration was observed outdoors. According to the same figures, in the ground level of the Fadum storehouse, the concentration of the airborne fungal spores was at acceptable levels, with values lower than 500 CFU/m<sup>3</sup>, which is the threshold defined by the World Health Organization (WHO) for noncontaminated indoor air [43]. On the upper level of the Fadum storehouse, on the ground level of the Heierstad loft, and on the upper level of the Heierstad loft, the concen-



tration of the airborne fungal spores was extremely high, exceeding by far the maximum acceptable limit of the WHO (Figure 9).

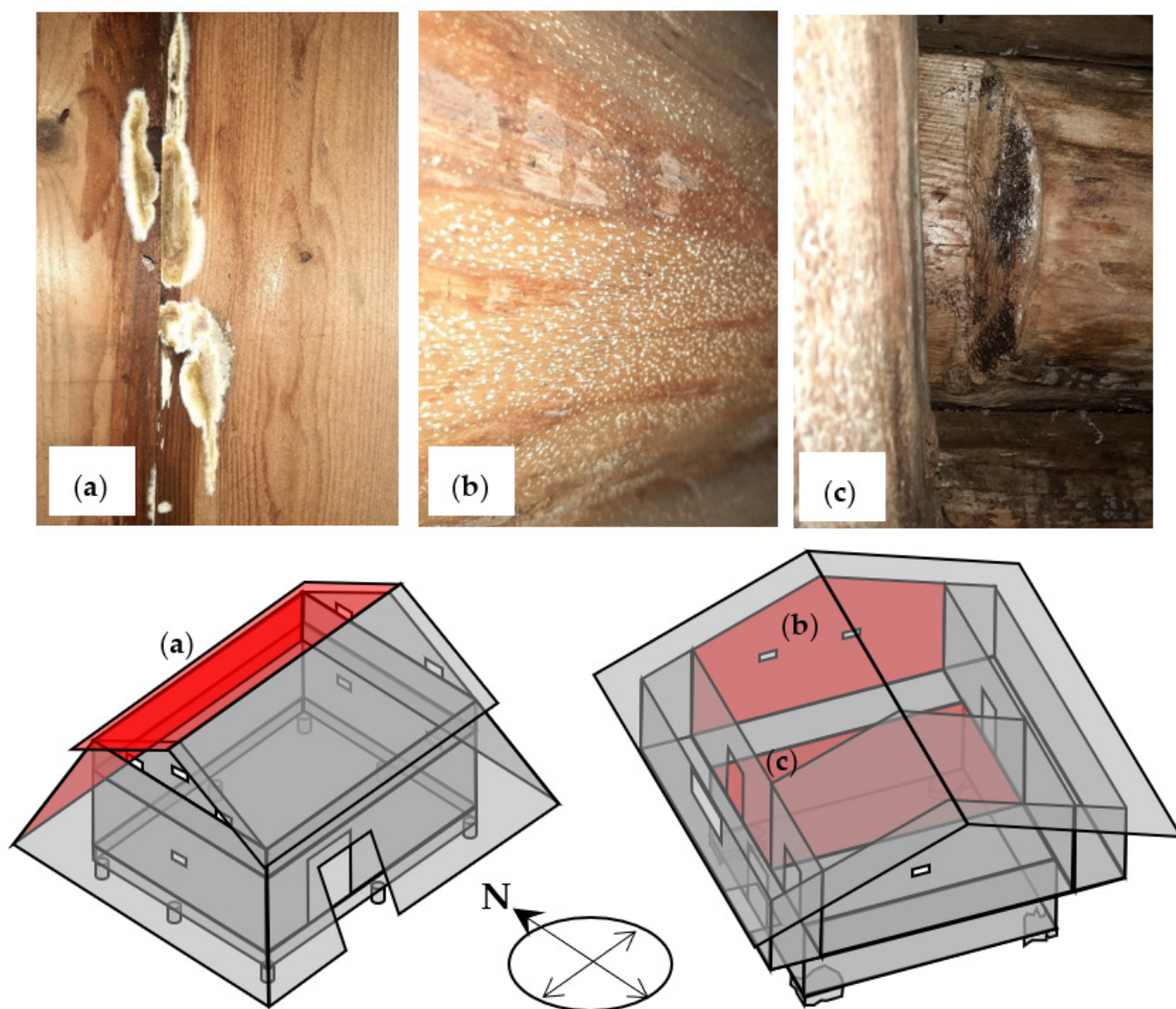


**Figure 7.** (a) Brown-rot fungi (*Coniophora puteana*) detected at the positions highlighted with red color at the Fadum storehouse. (b) *Scopulariopsis* colonies and (c) *Myxomycetes* detected at the positions highlighted with red color at the Heierstad loft.

In addition, identification of microfungi grown on the plates was performed by using optical microscopy (Figure 10). In Table 4, the microfungi species found in each of the two buildings are presented. The identified microfungi (Figure 10 and Table 4) in the concentrations that were found (Figure 8) can cause irritation of the eyes and respiratory tract, headache, drowsiness, skin rash, and itching of the skin, or even allergies and more adverse human diseases [44].

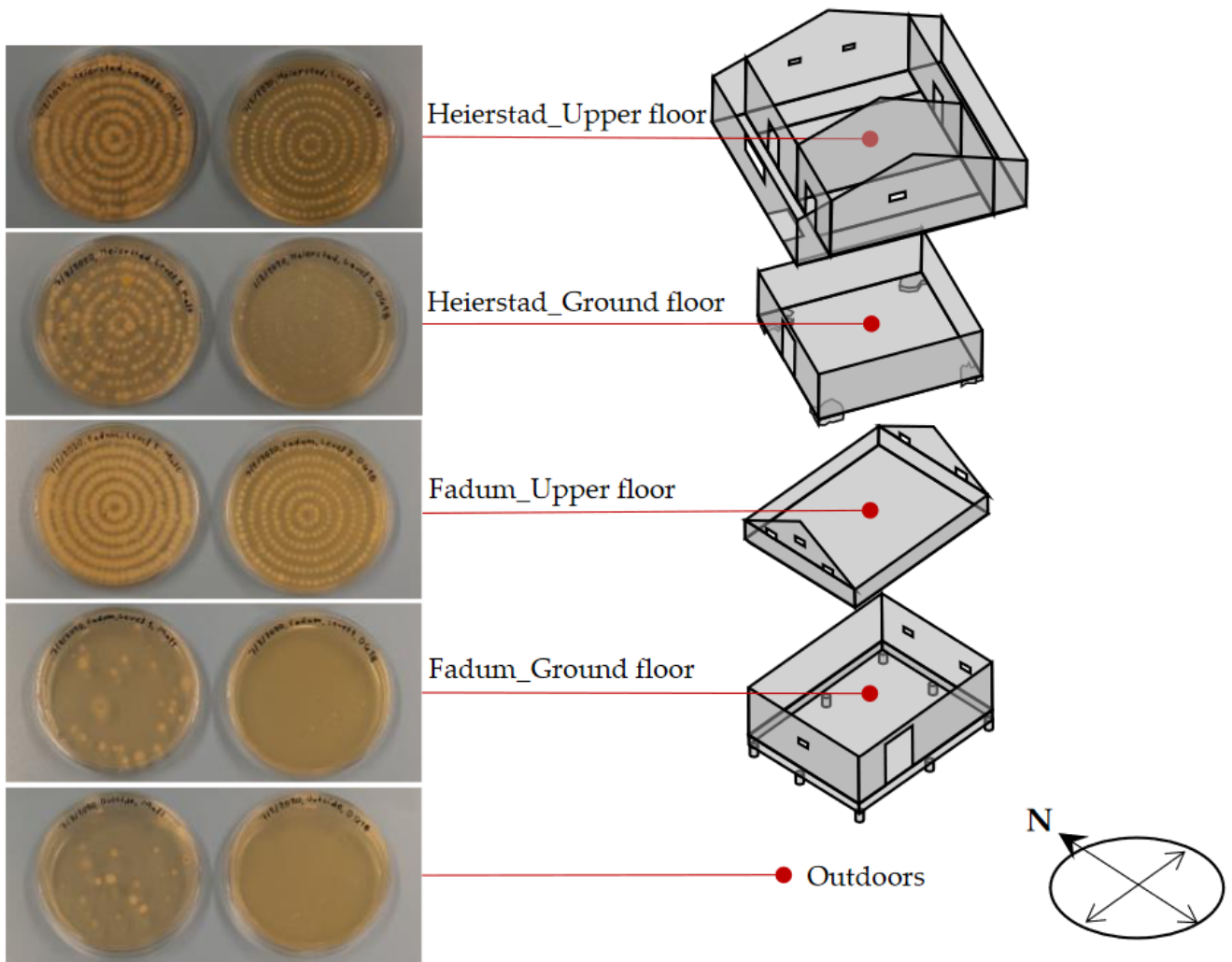


**Figure 8.** Positions of aerosol sampling and fungi colonies grown after 3 days at 25 °C on malt agar (plates on the left side of the pictures) and on DG-18 agar (plates on the right side of the pictures).

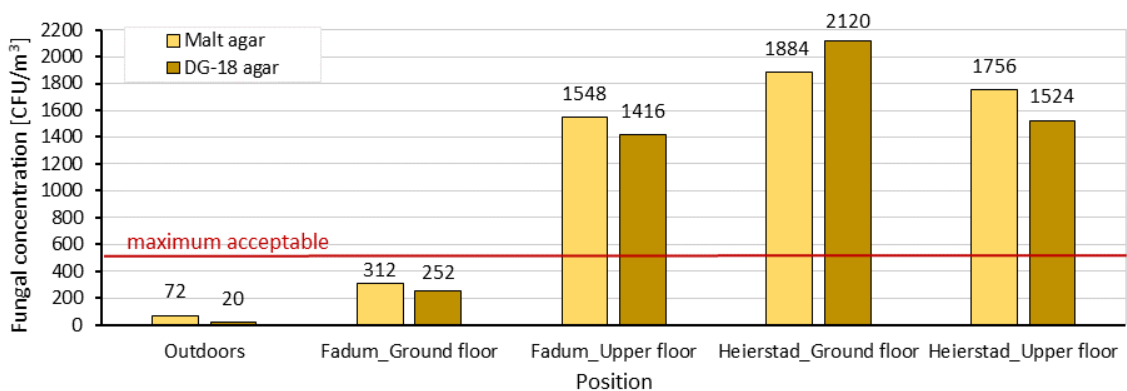


**Figure 9.** Fungal concentration in the two case studies considering the number of colony forming units found on the plates. The maximum acceptable value of 500 CFU/m<sup>3</sup> for noncontaminated indoor environments [43] is highlighted with the red line.

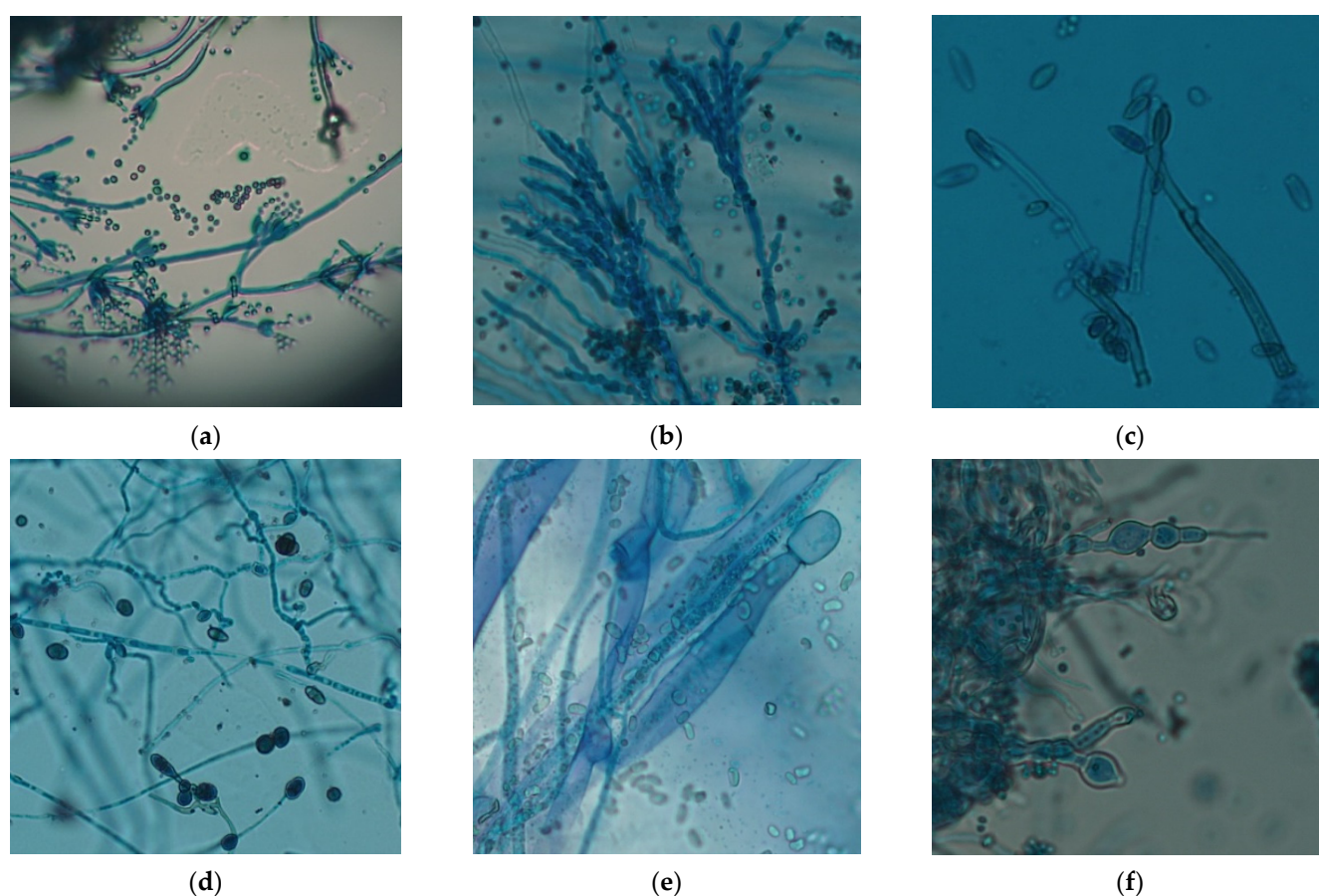


**Figure 10.** Fungal structures of (a) *Penicillium* spp., (b) *Aureobasidium* spp., (c) *Cladosporium* spp., (d) *Alternaria* spp., (e) *Mucor* spp., and (f) *Scopulariopsis* spp. after methylene blue staining.

**Table 4.** Fungi genera identified from the samples collected from the two case studies.

Fungi Genera	Fadum Storehouse	Heierstad Loft
<i>Penicillium</i> spp.	✓	✓
<i>Aureobasidium</i> spp.	✓	✓
<i>Cladosporium</i> spp.	✓	✓
<i>Alternaria</i> spp.	✓	✓
<i>Scopulariopsis</i> spp.	✓	✓
<i>Mucor</i> spp.	✓	

It was suggested to the administrators of the historic timber buildings (i) to clean the rooms of the two buildings in order to remove the dust and organic materials that constitute proper medium for the spores to germinate, (ii) to open the doors of the two buildings during the working hours of the museum for better natural ventilation, and (iii) temporarily to not use the Heierstad loft and the upper level of the Fadum storehouse, since they constitute a threat for human health due to contaminated indoor air. A systematic air sampling strategy was also proposed in order to monitor the indoor air quality and adjust the measures that should be taken accordingly. Finally, it was highlighted that, in case of rot-fungi detection, the infected building element should be replaced immediately.

### 3.2. Material Selection, Measured and Simulated Hygrothermal Performance

The goodness of fit between measured and simulated test parameters of the hygrothermal performance of selected building components in the two case studies was calculated (Table 5). Five different sets of material properties were examined within the simulations.

According to the results (Table 5), the Fadum storehouse and the ground level of the Heierstad loft are most probably made of spruce logs. The upper level of the Heierstad loft, which was reconstructed in 1957, is most probably built of pine logs (Table 5). It is noteworthy that the measurements do not cover the whole range of the hygrothermal performance of the components during a year (Figure 11). In addition, they include incidents within the capillary region where the actual performance of the logs cannot be accurately simulated (Figure 11b,d). Hence, a longer period of measurements, e.g., one year, would provide more robust results. During the summer period, the material temperatures are expected to be significantly higher than the ones presented in Figure 11c, while the moisture content is expected to produce lower values than the ones depicted in Figure 11d. For the certain study site, the periods that the temperature and humidity conditions are favorable for mold growth and, thus, it would be interesting to have measurements for are typically from March to May and from August to October [11].

In regard to the monitored temperatures (Figure 11a,c) and the air relative humidity (Figure 11b), there are no significant differences between the indoors and outdoors environments. This is because the buildings have openings without transparent elements and they do not have HVAC systems. Among the different interior environments, the ground level of the two buildings is the one with the more stable conditions.

The monitored moisture content of the log walls is at very high levels, exceeding the values that are considered critical for mold growth. The low temperatures during the same period are the main reason that the conditions are unfavorable for mold or other wood-destroying microorganisms to grow.

**Table 5.** Selection of material properties for the logs of the two case studies by examining the goodness of fit between measured and simulated hygrothermal performance.

Group	Group Description	Test Component	Test Parameter	Goodness of Fit				
				a <sup>1</sup>	b <sup>1</sup>	c <sup>1</sup>	d <sup>1</sup>	e <sup>1</sup>
II	Logs forming the walls and floors of the Fadum storehouse	Log at the southern wall of the ground level	$\theta_{timber}$	92.9	92.9	93.5	94.1	90.2
		Log at the southern wall of the upper level	$u$	44.5	31.1	57.4	24.5	1.74
III	Logs forming the walls and floors of the ground level of the Heierstad loft	Log at the southern wall of the upper level	$u$	56.9	17.7	57.2	38.7	4.3
		Log at the northwest wall of the ground level	$u$	28.3	20.7	43.0	44.2	7.7
IV	Logs forming the walls and floors of the upper level of the Heierstad loft	Log at the northwest wall of the upper level	$u$	7.2	0.3	8.29	13.2	48.3

<sup>1</sup> The materials are derived from WUFI database and they can be found under the names: (a) Softwood (by Fraunhofer-IBP), (b) Spruce, radial (by Fraunhofer-IBP), (c) Spruce, tangential (by LTH Lund University, Sweden), (d) Scandinavian spruce transverse direction (by NTNU), (e) Pine transverse direction (by NTNU).

### 3.3. Past, Present, and Future Climate Conditions

Climate data for three different decades, i.e., 1960–1969 (referred to as past), 2010–2019 (referred to as present), and 2060–2069 (referred to as future), derived from the MPI-ES-LR\_REMO2015 model were used for the examination of the climatic changes occurring throughout the years. A fourth climate file with data derived from the ERA5 reanalysis for the period 2010–2019 (current) was used in order to examine the accuracy of the climate model data. The climate parameters that mostly affect the hygrothermal performance of the building components are presented in Figure 12.

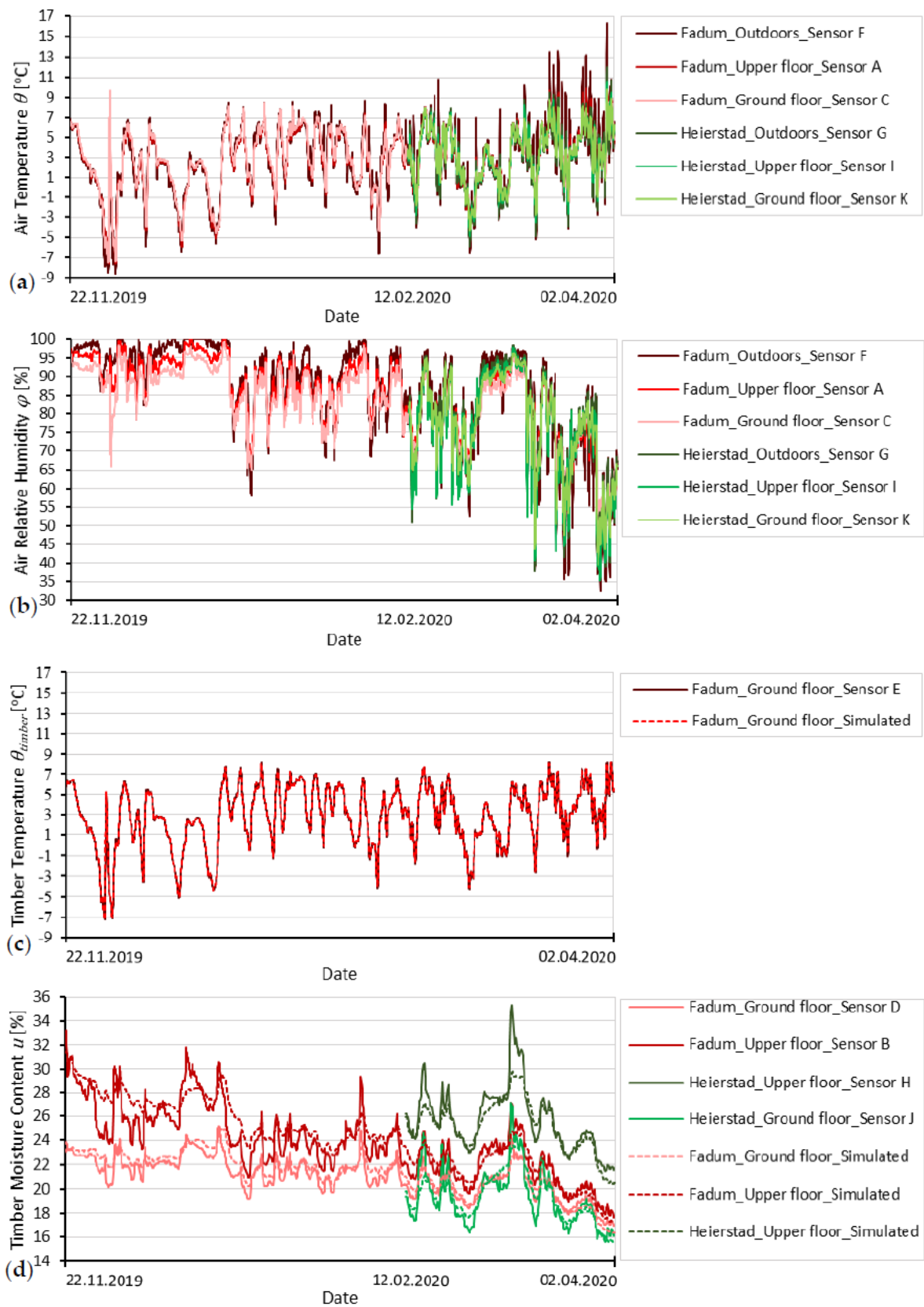


**Figure 11.** Measurements of the (a) air temperature and (b) relative humidity, which have been used as boundary conditions in the hygrothermal models, and both measured and simulated (c) temperature and (d) moisture content in the timber building components.

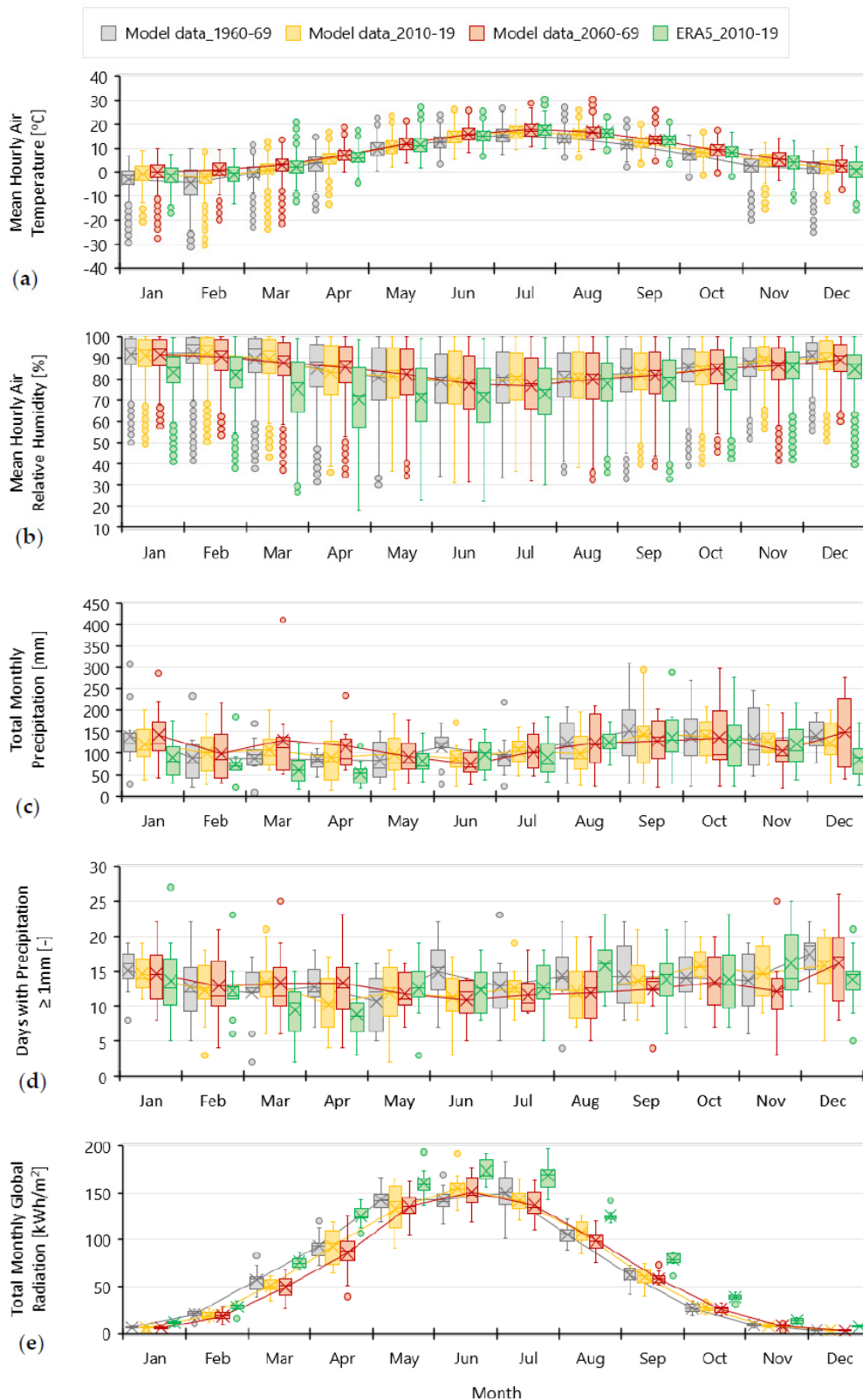


**Figure 12.** Comparison among (a) air temperature, (b) air relative humidity, (c,d) precipitation and (e) radiation data derived from the MPI-ESM-LR\_REMO2015 model and ERA5 reanalysis. In the boxplots the box shows 50% of the data, with median represented as a horizontal bar and the average value highlighted with the ‘x’ symbol. The whisker extends to two standard deviations of the data and the circles represent the outliers.

The signal of climate change in terms of the air temperature (Figure 12a) is an average increase of 1.6 °C from past to current conditions, and 1.2 °C from current to potential future conditions. The air temperatures are slightly underestimated in the model data, showing an average difference of 0.3 °C compared to the ERA5 reanalysis.

According to the climate model data, the air relative humidity remains at the same levels under past, current, and potential future conditions, with an average value of approximately 85% (Figure 12b). The air relative humidity is overestimated significantly by the climate model data since, according to the ERA5 reanalysis dataset, its average value is 78%.

In some months, the precipitation levels seem to decrease slightly from past to current conditions and to increase from current to future conditions (Figure 12c). However, precipitation levels vary considerably between different years in the region so, based on 10-year periods, it is hard to consistently detect any trends and the results might be different based on a continuous data series. Nevertheless, in winter, from December to April, the highest precipitation level is projected for the latest period 2060–2069. This agrees with most of climate model simulations, indicating increasing wintertime precipitation in Southern Norway, and in Northern Europe in general, while only small changes are usually projected for summer precipitation [45,46]. At the same time, the number of days with precipitation (greater than 1 mm) is projected to change little in winter and spring, and decrease slightly in summer and autumn (Figure 12d). The climate model data overestimate significantly the precipitation. The number of days with precipitation is overestimated by the climate model for the period from December to April, while it is underestimated during the summer period.

The global radiation incident on a horizontal surface shows a slight decrease throughout the years, while it is underestimated according to the climate model data.

### 3.4. Hygrothermal Performance of Building Elements

The surface temperature and the surface relative humidity of selected exterior surfaces of the two buildings are presented in Figure 13. Significant differences are observed on the range of the surface temperature and the surface relative humidity according to the exposure environment. The greatest range is observed at the south-oriented surfaces and the smallest one at the surfaces that are protected under the coating/shed of the Fadum storehouse. Moreover, substantive differences are observed among the average values of the surface temperature and the surface relative humidity according to the environment of exposure. The greatest differences are noticed at the coating of the Fadum storehouse. Specifically, pursuant to the data derived from the ERA5 reanalysis, the average value of the surface temperature of the south-oriented side of the coating is 3.18 °C higher than the respective one at the north-oriented side. In addition, according to the data derived from the ERA5 reanalysis, the surface relative humidity at the south-oriented side of the coating is 8% lower than the respective one at the north side. Thus, it is apparent that, for a given period of time, the surface temperature and the surface relative humidity vary significantly based on the orientation.

The surface temperatures simulated with the climate model data were underestimated, while the surface relative humidities were overestimated. Moreover, the differences among different orientations, and especially between south and north, were underestimated significantly based on the data derived from the used climate model. This was mainly due to the underestimation of the incident solar radiation (Figure 12).

The signal of climate change for all surfaces shows an increase of the surface temperature and a slight decrease of the surface relative humidity. The signal of climate change is more intense in the case of north-oriented surfaces and less intense in the case of south-oriented surfaces. The most important changes are observed in the case of the coating of the Fadum storehouse. Specifically, the average value of the surface temperature increases from the past to the future conditions as follows: 2.7 °C at the south and 2.8 °C at the north. Moreover, the average value of the surface relative humidity from the past

to future conditions shows a decrease of 0.5% at the south and 1.0% at the north. It is also observed that the differences among all the cardinal orientations become smaller throughout the years.

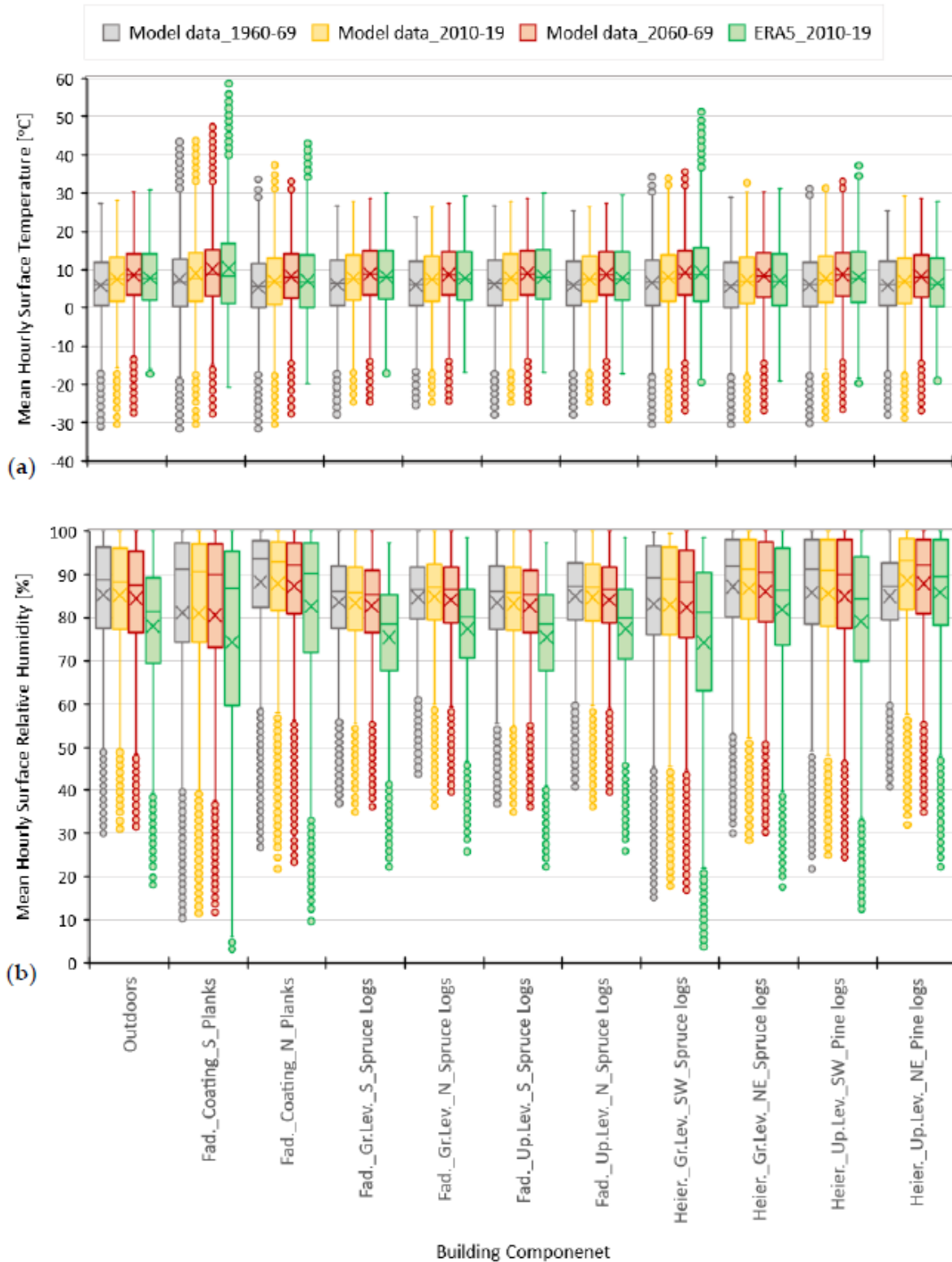


**Figure 13.** Distribution of (a) hourly surface temperature and (b) hourly surface relative humidity for the exterior surface of selected building components. In the boxplots the box shows 50% of the data, with median represented as a horizontal bar and the average value highlighted with the ‘x’ symbol. The whisker extends to two standard deviations of the data, and the circles represent the outliers.



### 3.5. Mold Risk

The type of wood (i.e., softwood or hardwood), the type of surface (i.e., planed or rough), the sensitivity of the surface to mold growth (i.e., different sensitivity classes by taking into account that the final surface is sapwood, heartwood, or tar treatment), the surface temperature, and the surface relative humidity were taken into account for the calculation of the mold index of the building components. The four different climate excitations described in the previous chapters were taken into account. The different types of surfaces found at the two case studies, in ascending order regarding their sensitivity to mold growth, are: (i) the exterior surfaces treated with tar, (ii) the surfaces of the planks that have no treatment, (iii) the surfaces of logs that have no treatment, and (iv) the exterior degraded surfaces (due to weathering, checks, and splits). For the assessment of the mold risk of the building components, it is taken into account that mold indices ( $M$ ) from 0 to 1 do not constitute a threat for the decay of the components. That is because the germination process starts at  $M = 1$ . Mold indices from 1 to 3 are considered as a risk for the decay of the building elements. The mold index  $M = 3$  is the threshold over which mold can be detected by the naked eye and new mold fungi spores are produced. Mold indices above 3 are considered as significant decay risk. Considering the aforementioned categorization of the mold index values, in Figure 14, the mold indices from 0 to 1 are depicted with different shades of green, the mold indices from 1 to 3 are depicted with different shades of yellow, and the mold indices from 3 to 6 are depicted with different shades of red.

#### 3.5.1. Current Conditions

First and foremost, the current conditions of the two case studies based on the climate data derived from the ERA5 reanalysis will be discussed. According to the results of the mold growth model, all exterior surfaces treated with tar have no mold risk at all ( $M = 0$ ). The untreated planks that are exposed to the exterior environment, i.e., the exterior surfaces of the coating of the Fadum storehouse, have a different mold risk depending on their orientation. These differences are depicted in Figure 14d, in which the average values of the annually maximum mold index of the exterior surfaces of the coating are presented. The surface with the highest mold risk is the north-oriented one, with a maximum mold index of 1.3 for the period 2010–19. In contrast, the surface with the lowest mold risk is the south-oriented one, with a maximum mold index of 0.6 during the same period. The untreated planks exposed to the interior environment, i.e., the planks at the roof of the two buildings, and at the walls of the northwest and southeast cantilevers of the Heierstad loft (Figure 14d), are not threatened by mold. In addition, the interior untreated surfaces of the logs are not threatened by mold (Figure 14d). The degraded exterior surfaces (positions with extreme weathering, checks, and splits) that are exposed to rain and solar radiation have significant mold risk. In these cases, the maximum annual mold index fluctuates between 4.5 and 6. This observation underlines the importance of the immediate cleaning and treatment of the damaged surfaces. The degraded exterior surfaces of the floors of the two buildings, which are not exposed to rain and solar radiation, have a maximum mold index of 1.5 during the period 2010–19 and, thus, their decay risk is not significant. Finally, the degraded exterior surfaces that are protected under the coating of the Fadum storehouse have mold indices lower than 1 and, thus, they are not threatened by mold.

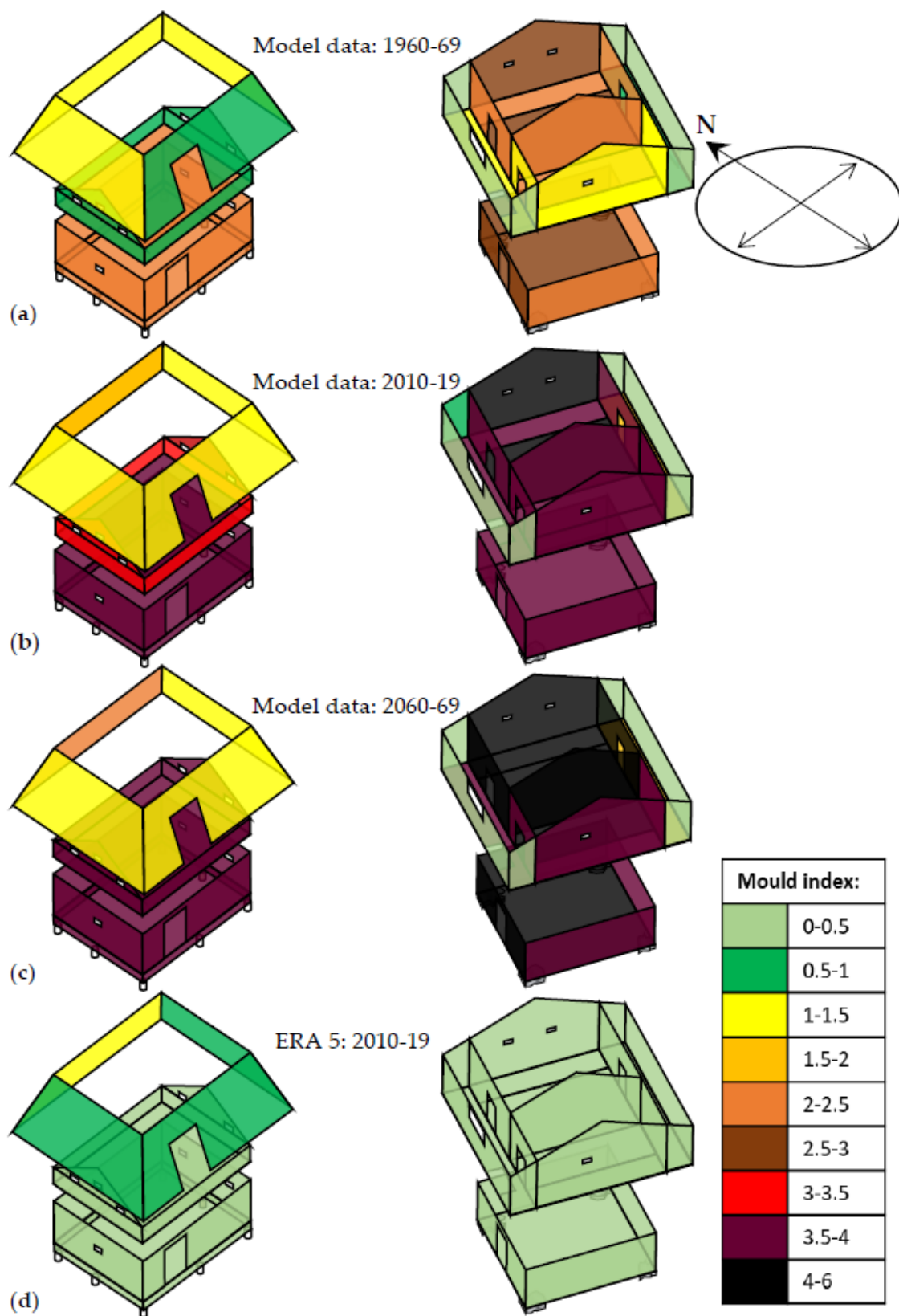


**Figure 14.** Average values of annually maximum mold indices under (a) past, (b) current, and (d) future climate conditions, considering climate data from MPI-ESM-LR\_REMO2015 model. (d) Respective results for the current conditions by considering climate data from the ERA5 reanalysis. The results refer to the interior surfaces of the building components, with the exception of the coating of the Fadum storehouse where the exterior side is taken into account.

### 3.5.2. Impact of Climate Change

The mold risk of the surfaces of the two buildings is clearly overestimated by the climate model data. However, the results from the climate model are useful to highlight future changes in sensitivity to mold growth, even though the effect is exaggerated. The exterior surfaces treated with tar are not threatened by mold. Specifically, the maximum mold index occurring on a surface of this category is  $M = 0.1$ . The untreated planks that are exposed to the exterior environment have an increase of their decay risk due to climate change. In Figure 14a–c, it can be seen that the increase of the mold index of the exterior surfaces of the coating of the Fadum storehouse depends on their orientation. The increase of the mold index is greater in the case of the north-oriented surface. The mold risk of the untreated planks that are exposed to the interior environment, i.e., the planks at the roof of the two buildings and at the walls of the northwest and southeast cantilevers of the Heierstad loft, do not change due to the climate change (Figure 14a–c). The interior untreated surfaces of the logs of the two buildings have an increase of their mold risk due to climate change. This increase is even more significant from the past to the current conditions. In addition, in both buildings, the interior surfaces of the north-oriented log walls are at a higher mold risk (Figure 14a–c). Finally, all exterior degraded surfaces have significant mold risk under past, current, and future conditions that is intensified due to climate change.

At a given room, very similar mold indices are observed among the interior surfaces of the same surface category (Figure 14). This observation indicates that the air temperature and the air relative humidity of the room can be used instead of the surface temperature and the surface relative humidity as a simplification. At this point, it is worth mentioning that, in Figure 14, the floor of the upper level in both buildings and the log walls of the Heierstad loft that are exposed in both sides to the interior environment are represented by their surface with the highest mold risk. At the Fadum storehouse, the surfaces at the ground level have higher mold risk than the upper level. At the Heierstad loft, higher mold risk occurs at the surfaces of the ground level, secondly at the upper level at the northeast-oriented room, thirdly at the southwest-oriented room, fourthly at the northwest-oriented cantilever, and lastly at the southeast-oriented cantilever. It is worth mentioning that the most aggravated surfaces of the Heierstad loft according to the numerical simulations results (Figure 14) are the same as those where fungal growth was detected in reality (Figure 7). In the case of the Fadum storehouse, both simulations (Figure 14) and reality (Figures 6 and 7) underline that the north-oriented surfaces are more vulnerable to fungal colonization.

### 3.5.3. Surface vs. Air Temperature and Relative Humidity

The calculation of the surface temperature and the surface relative humidity of the building components, given the outdoor climate from the models, is important for the production of accurate and robust assessment of their mold risk. However, it is a computationally demanding process. In addition, considering that the buildings have openings without transparent elements, are not occupied, and do not have HVAC systems, their indoor and outdoor conditions do not differ significantly. For these reasons, it was examined whether the atmospheric temperature and the relative humidity could be effectively used for the assessment of the decay risk instead of the surface air temperature and the surface air relative humidity. The results (Table 6) show that this simplification is not appropriate for the description of the mold risk at the exterior untreated planks of the coating of the Fadum storehouse (Figure 14). That is because both the mold risk of the surfaces at a given period and the signal of climate change in terms of the mold risk vary significantly based on the orientation. Additionally, this simplification is not appropriate for the interior surfaces of the untreated logs and planks, since it overestimates significantly their mold risk and cannot reproduce the differences occurring among the different rooms (Figure 14 and Table 6).

**Table 6.** Average values of annually maximum mold indices by taking into account all different substrate surfaces of the case studies, the atmospheric temperature, and the relative humidity under four different climatic excitations.

Surface Description	Climate Model Data			ERA5
	1960–69	2010–19	2060–69	2010–19
Log/plank treated with tar	0.0	0.0	0.0	0.0
Log without treatment	5.7	5.7	5.8	1.1
Plank without treatment	1.1	1.3	1.5	0.2
Degraded surface (positions with cracks)	5.8	5.8	5.9	4.5

#### 4. Conclusions

The focus of the current research is on investigating the impact of climate change on the mold risk of two historic timber buildings located in the county of Vestfold, Norway. Climate data from REMO2015 driven by the global model MPI-ESM-LR were used in order to take into account the climate change. The climate data refer to the past, present, and potential future climate conditions. After selecting proper material properties for the building components of the two constructions, and given the outdoors climate, whole-building hygrothermal simulations were employed in order to calculate the temperature and the relative humidity on the surface of the building elements. Given the transient hygrothermal conditions and certain characteristics of the timber surfaces, the updated VTT mold model was used in order to calculate their mold index.

Based on the climate data from the MPI-ES-LR\_REMO2015 model, it is concluded that there is an increased mold risk of the two timber constructions due to climate change. This impact of climate change is more severe in the case of the untreated logs exposed, either in the outdoors or the indoors environment. It is also significant in the case of the untreated planks which are exposed to the outdoors environment, e.g., the planks of the coating/shed of the Fadum storehouse. The surfaces which are treated are not threatened by mold risk due to climate change. In addition, the untreated surfaces of the planks which are exposed to the indoors environment are not threatened by mold due to climate change. It was also observed that the increase of the mold risk due to climate change is more intense in the case of the horizontal surfaces, i.e., ceilings and floors, and the north-oriented vertical or inclined surfaces. According to the employed numerical simulations, the ceiling at the ground level of the Heierstad loft and the northeast-oriented wall at the upper level of the same building are the most aggravated ones in terms of the mold risk due to climate change. These same surfaces are the ones on which fungal colonization was detected on site.

The results derived from the MPI-ES-LR\_REMO2015 model overestimate significantly the mold risk of the two buildings compared to results derived from ERA5 reanalysis. This is mainly attributed to the fact that the MPI-ES-LR\_REMO2015 model overestimates significantly the relative humidity and the precipitation compared to the ERA5 reanalysis.

The importance of using the surface temperature and the surface relative humidity as inputs in the updated VTT mold model, and not the atmospheric temperature and the atmospheric relative humidity, is also underlined. The mold risk of the interior surfaces is significantly lower than the respective one that is calculated based on the temperature and the relative humidity of the outdoor air. In the opposite direction, the mold risk of the north-oriented exterior surfaces is higher than the respective risk that is calculated based on the temperature and the relative humidity of the outdoor air.

According to the onsite inspection and the numerical simulation results based on the ERA5 reanalysis climate data, the two buildings are in good condition. The only surfaces that have significant mold risk are the exterior degraded surfaces—which have lost their tar treatment—that are exposed to rain and solar radiation. At this point, it is highlighted that the exterior surfaces should be treated systematically in order for the vulnerable positions that occur due to weathering, checks, and splits to not be exposed to rain and solar radiation. In case of extensive degradation, the building elements should be

replaced. Moreover, there is moderate mold risk of the untreated wood surfaces with north orientation that are exposed to the outdoors environment. This observation highlights that the orientation of the untreated timber surfaces influences their mold risk.

It is also worth mentioning that the mold risk of wooden cultural heritage is considered vital, as it involves health hazards, aesthetic problems, and implications on other wood deteriorogens' niches. It is possible that, in the near future, proper cleaning from mold growth will be needed for the untreated logs in the interior of the historic buildings on a periodic basis.

**Author Contributions:** Conceptualization, P.C. and D.K.; methodology, P.C., D.K., I.L., and B.H.; software, P.C.; validation, P.C.; formal analysis, P.C.; investigation, P.C. and D.K.; resources, P.C., D.K., and I.L.; data curation, P.C.; writing—original draft preparation, P.C.; writing—review and editing, P.C., D.K., I.L., and B.H.; visualization, P.C.; supervision, D.K.; project administration, P.C. and D.K.; funding acquisition, P.C., D.K., and I.L. All authors have read and agreed to the published version of the manuscript.

**Funding:** This work is a part of the HYPERION project. HYPERION has received funding from the European Union's Framework Program for Research and Innovation (Horizon 2020) under grant agreement no. 821054. The content of this publication is the sole responsibility of Oslo Metropolitan University and the Finnish Meteorological Institute and does not necessarily reflect the opinion of the European Union.

**Institutional Review Board Statement:** Not applicable.

**Informed Consent Statement:** Not applicable.

**Data Availability Statement:** The climate data that support the findings of this study are derived from the online databases of the Norwegian Center for Climate Services (NCCS), the Copernicus climate change service, the Earth System Grid Federation (ESGF), and they are openly available from [39,47,48], respectively.

**Acknowledgments:** We would like to thank Jørgen Solstad, consultant at Vestfold county culture department, and the personnel of the Slottsfjell museum for providing information and access to the two historic timber buildings examined in the current research.

**Conflicts of Interest:** The authors declare no conflict of interest.

## References





1. Sabbioni, C.; Brimblecombe, P.; Cassar, M. *The Atlas of Climate Change Impact on European Cultural Heritage: Scientific Analysis and Management Strategies*; Anthem Press: London, UK; New York, NY, USA, 2010.
2. Fatorić, S.; Seekamp, E. Are cultural heritage and resources threatened by climate change? A systematic literature review. *Clim. Chang.* **2017**, *142*, 227–254. [CrossRef]
3. Leissner, J.; Kilian, R.; Kotova, L.; Jacob, D.; Mikolajewicz, U.; Broström, T.; Ashley-Smith, J.; Schellen, H.L.; Martens, M.; van Schijndel, J. Climate for Culture: Assessing the impact of climate change on the future indoor climate in historic buildings using simulations. *Herit. Sci.* **2015**, *3*, 38. [CrossRef]
4. Brimblecombe, P. Refining climate change threats to heritage. *J. Inst. Conserv.* **2014**, *37*, 85–93. [CrossRef]
5. Howard, A.J.; Knight, D.; Coulthard, T.; Hudson-Edwards, K.; Kossoff, D.; Malone, S. Assessing riverine threats to heritage assets posed by future climate change through a geomorphological approach and predictive modelling in the Derwent Valley Mills WHS, UK. *J. Cult. Herit.* **2016**, *19*, 387–394. [CrossRef]
6. Kaslegard, A.S. *Climate Change and Cultural Heritage in the Nordic Countries*; Nordic Council of Ministers: Copenhagen, Sweden, 2011.
7. Kelman, I.; Haugen, A.; Mattsson, J. Preparations for climate change's influences on cultural heritage. *Int. J. Clim. Chang. Strateg. Manag.* **2011**. [CrossRef]
8. The Hyperion Project. Available online: <https://www.hyperion-project.eu/> (accessed on 25 May 2021).
9. Huijbregts, Z.; Schellen, H.; Martens, M.; van Schijndel, J. Object damage risk evaluation in the European project Climate for Culture. *Energy Procedia* **2015**, *78*, 1341–1346. [CrossRef]
10. Huijbregts, Z.; Kramer, R.; Martens, M.; Van Schijndel, A.; Schellen, H. A proposed method to assess the damage risk of future climate change to museum objects in historic buildings. *Build. Environ.* **2012**, *55*, 43–56. [CrossRef]
11. Choidis, P.; Tsikaloudaki, K.; Kraniotis, D. Hygrothermal performance of log walls in a building of 18th century and prediction of climate change impact on biological deterioration. *E3S Web Conf.* **2020**, *172*, 15006. [CrossRef]

12. Rajčić, V.; Skender, A.; Damjanović, D. An innovative methodology of assessing the climate change impact on cultural heritage. *Int. J. Archit. Herit.* **2018**, *12*, 21–35. [CrossRef]
13. Sedlbauer, K. Prediction of Mould Fungus Formation on the Surface of/and Inside Building Components. Ph.D. Thesis, University of Stuttgart, Fraunhofer Institute for Building Physics, Stuttgart, Germany, 2001.
14. Lepage, R.; Glass, S.V.; Knowles, W.; Mukhopadhyaya, P. Biodeterioration models for building materials: Critical review. *J. Archit. Eng.* **2019**, *25*, 04019021. [CrossRef]
15. Vereecken, E.; Roels, S. Review of mould prediction models and their influence on mould risk evaluation. *Build. Environ.* **2012**, *51*, 296–310. [CrossRef]
16. Gradeci, K.; Labonnote, N.; Köhler, J.; Time, B. Mould models applicable to wood-based materials—a generic framework. *Energy Procedia* **2017**, *132*, 177–182. [CrossRef]
17. Ojanen, T.; Viitanen, H.; Peuhkuri, R.; Lähdesmäki, K.; Vinha, J.; Salminen, K. Mold growth modeling of building structures using sensitivity classes of materials. In Proceedings of the 11th International Conference on Thermal Performance of the Exterior Envelopes of Whole Buildings, Buildings XI, Clearwater, FL, USA, 4–9 December 2010.
18. Woloszyn, M.; Rode, C. Tools for performance simulation of heat, air and moisture conditions of whole buildings. *Build. Simul.* **2008**, *1*, 5–24. [CrossRef]
19. Lengsfeld, K.; Holm, A. Entwicklung und Validierung einer hygrothermischen Raumklima-Simulationssoftware WUFI®-Plus. *Bauphysik* **2007**, *29*, 178–186. [CrossRef]
20. De Wit, M. *Hambase: Heat, Air and Moisture Model for Building and Systems Evaluation*; Technische Universiteit Eindhoven: Eindhoven, Germany, 2006.
21. Antretter, F.; Schöpfer, T.; Kilian, R. An approach to assess future climate change effects on indoor climate of a historic stone church. In Proceedings of the 9th Nordic Symposium on Building Physics, Tampere, Finland, 29 May–2 June 2011.
22. Leissner, J.; Kilian, R.; Antretter, F.; Holm, A. Modelling climate change impact on cultural heritage the European project climate for culture. In *Urban Habitat Constructions Under Catastrophic Events: Proceedings of the COST C26 Action Final Conference*; CRC Press: London, UK, 2010; p. 45.
23. Antretter, F.; Kosmann, S.; Kilian, R.; Holm, A.; Ritter, F.; Wehle, B. Controlled Ventilation of Historic Buildings: Assessment of Impact on the Indoor Environment via Hygrothermal Building Simulation. In *Hygrothermal Behavior, Building Pathology and Durability*; de Freitas, V., Delgado, J., Eds.; Springer: Berlin/Heidelberg, Germany, 2013; Volume 1, pp. 93–111. [CrossRef]
24. Coelho, G.B.; Silva, H.E.; Henriques, F.M. Calibrated hygrothermal simulation models for historical buildings. *Build. Environ.* **2018**, *142*, 439–450. [CrossRef]
25. Erhardt, D.; Antretter, F. Applicability of regional model climate data for hygrothermal building simulation and climate change impact on the indoor environment of a generic church in Europe. In Proceedings of the 2nd European Workshop on Cultural Heritage Preservation EWCHP-2012, Kjeller, Norway, 23–26 September 2012; pp. 99–105.
26. Delgado, J.; Ramos, N.M.; Barreira, E.; De Freitas, V.P. A critical review of hygrothermal models used in porous building materials. *J. Porous Media* **2010**, *13*. [CrossRef]
27. Zirkelbach, D.; Schmidt, T.; Kehrer, M.; Künzle, H. *Wufi®Pro-Manual*; Fraunhofer Institute: Munich, Germany, 2007.
28. Antretter, F.; Winkler, M.; Fink, M.; Pazold, M.; Radon, J.; Stadler, S. *WUFI® Plus 3.1-Manual*; Fraunhofer Institute: Munich, Germany, 2017.
29. WUFI®Mold Index VTT. Available online: <http://wufi.de/en/software/wufi-add-ons/> (accessed on 25 May 2021).
30. Karagiozis, A.; Künzle, H.; Holm, A. WUFI-ORN/IBP—A North American hygrothermal model. In Proceedings of the 8th International Conference on Thermal Performance of the Exterior Envelopes of Whole Buildings, Buildings VIII, Clearwater Beach, FL, USA, 2–7 December 2001; pp. 2–7.
31. Riahi, K.; Rao, S.; Krey, V.; Cho, C.; Chirkov, V.; Fischer, G.; Kindermann, G.; Nakicenovic, N.; Rafaj, P. RCP 8.5—A scenario of comparatively high greenhouse gas emissions. *Clim. Chang.* **2011**, *109*, 33–57. [CrossRef]
32. Jacob, D.; Podzun, R. Sensitivity studies with the regional climate model REMO. *Meteorol. Atmos. Phys.* **1997**, *63*, 119–129. [CrossRef]
33. Giorgetta, M.A.; Jungclaus, J.; Reick, C.H.; Legutke, S.; Bader, J.; Böttinger, M.; Brovkin, V.; Crueger, T.; Esch, M.; Fieg, K. Climate and carbon cycle changes from 1850 to 2100 in MPI-ESM simulations for the Coupled Model Intercomparison Project phase 5. *J. Adv. Modeling Earth Syst.* **2013**, *5*, 572–597. [CrossRef]
34. Jacob, D.; Petersen, J.; Eggert, B.; Alias, A.; Christensen, O.B.; Bouwer, L.M.; Braun, A.; Colette, A.; Déqué, M.; Georgievski, G. EURO-CORDEX: New high-resolution climate change projections for European impact research. *Reg. Environ. Chang.* **2014**, *14*, 563–578. [CrossRef]
35. Taesler, R.; Andersson, C. A method for solar radiation computations using routine meteorological observations. *Energy Build.* **1984**, *7*. [CrossRef]
36. Handbook, A. *Fundamentals*. Atlanta, Ga; American Society of Heating, Refrigerating and Air Conditioning Engineers, Inc.: Norcross, GA, USA, 2001.
37. Nik, V.M. *Climate Simulation of an Attic Using Future Weather Data Sets-Statistical Methods for Data Processing and Analysis*; Chalmers University of Technology: Göteborg, Sweden, 2010; Available online: <https://core.ac.uk/download/pdf/70582877.pdf> (accessed on 21 June 2021).

38. Hersbach, H.; Bell, B.; Berrisford, P.; Hirahara, S.; Horányi, A.; Muñoz-Sabater, J.; Nicolas, J.; Peubey, C.; Radu, R.; Schepers, D. The ERA5 global reanalysis. *Q. J. R. Meteorol. Soc.* **2020**, *146*, 1999–2049. [CrossRef]
39. Norwegian Climate Service Center: Observations and Weather Statistics. Available online: <https://seklima.met.no/observations/> (accessed on 25 May 2021).
40. Hukka, A.; Viitanen, H. A mathematical model of mould growth on wooden material. *Wood Sci. Technol.* **1999**, *33*, 475–485. [CrossRef]
41. Viitanen, H.; Ojanen, T. Improved model to predict mold growth in building materials. In Proceedings of the 10th International Conference on Thermal Performance of the Exterior Envelopes of Whole Buildings, Buildings X, Clearwater Beach, FL, USA, 2–7 December 2007.
42. Schmidt, O.; Grimm, K.; Moreth, U. Molecular identity of species and isolates of the Coniphora cellar fungi. *Holzforschung* **2002**, *56*, 563–571. [CrossRef]
43. Heseltine, E.; Rosen, J. *WHO Guidelines for Indoor Air Quality: Dampness and Mould*; World Health Organization Regional Office for Europe: Copenhagen, Denmark, 2009.
44. Baxi, S.N.; Portnoy, J.M.; Larenas-Linnemann, D.; Phipatanakul, W.; Barnes, C.; Baxi, S.; Grimes, C.; Horner, W.E.; Kennedy, K.; Larenas-Linnemann, D. Exposure and health effects of fungi on humans. *J. Allergy Clin. Immunol. Pract.* **2016**, *4*, 396–404. [CrossRef]
45. Lehtonen, I.; Ruosteenoja, K.; Jylhä, K. Projected changes in European extreme precipitation indices on the basis of global and regional climate model ensembles. *Int. J. Climatol.* **2014**, *34*, 1208–1222. [CrossRef]
46. Räisänen, J.; Ylhäisi, J.S. CO<sub>2</sub>-induced climate change in northern Europe: CMIP2 versus CMIP3 versus CMIP5. *Clim. Dyn.* **2015**, *45*, 1877–1897. [CrossRef]
47. Copernicus Climate Change Service: ERA5 Hourly Data on Single Levels from 1979 to Present. Available online: <https://cds.climate.copernicus.eu/cdsapp#!/dataset/reanalysis-era5-single-levels?tab=form> (accessed on 25 May 2021).
48. NCI ESGF Node. Available online: <https://esgf.nci.org.au/search/esgf-nci/> (accessed on 25 May 2021).

## Article

# Restoration of a XVII Century's *predella reliquary*: From Physico-Chemical Characterization to the Conservation Process

Giuseppina Fiore Bettina <sup>1</sup>, Belinda Giambra <sup>1</sup>, Giuseppe Cavallaro <sup>2</sup>, Giuseppe Lazzara <sup>2,\*</sup>,  
Bartolomeo Megna <sup>3</sup>, Ramil Fakhrullin <sup>4</sup>, Farida Akhatova <sup>4</sup> and Rawil Fakhrullin <sup>4,\*</sup>

<sup>1</sup> Restorer at Laurea Magistrale in Conservazione e Restauro per i Beni Culturali, Università degli Studi di Palermo, Viale delle Scienze pad 17, 90128 Palermo, Italy; giuseppina.fb@gmail.com (G.F.B.); info@belindagiambra.it (B.G.)

<sup>2</sup> Dipartimento di Fisica e Chimica Emilio Segre, Università degli Studi di Palermo Viale delle Scienze, pad. 17, 90128 Palermo, Italy; giuseppe.cavallaro@unipa.it

<sup>3</sup> Dipartimento di Ingegneria, Università degli Studi di Palermo Viale delle Scienze, pad. 6, 90128 Palermo, Italy; bartolomeo.megna@unipa.it

<sup>4</sup> Institute of Fundamental Medicine and Biology, Kazan Federal University, Kremlyurami 18, 420008 Kazan, Republic of Tatarstan, Russia; ramilfakhrullin@gmail.com (R.F.); akhatovaf@gmail.com (F.A.)

\* Correspondence: giuseppe.lazzara@unipa.it (G.L.); kazanbio@gmail.com (R.F.)

**Abstract:** We report on the restoration of a XVII century's *predella reliquary*, which is a part of a larger setup that includes a wall reliquary and a wooden crucified Christ, both belonging to the church of "Madre Maria SS. Assunta", in Polizzi Generosa, Sicily, Italy. The historical/artistic and paleographic research was flanked successfully by the scientific objective characterization of the materials. The scientific approach was relevant in the definition of the steps for the restoration of the artefact. The optical microscopy was used for the identification of the wood species. Electron microscopy and elemental mapping by energy-dispersive X-ray (EDX) was successful in the identification of the layered structure for the gilded surface. The hyperspectral imaging method was successfully employed for an objective chemical mapping of the surface composition. We proved that the scientific approach is necessary for a critical and objective evaluation of the conservation state and it is a necessary step toward awareness of the historical, liturgical, spiritual and artistic value. In the second part of this work, we briefly describe the conservation protocol and the use of a weak nanocomposite glue. In particular, a sustainable approach was considered and therefore mixtures of a biopolymer from natural resources, such as funori from algae, and naturally occurring halloysite nanotubes were considered. Tensile tests provided the best composition for this green nanocomposite glue.

**Keywords:** reliquary; electron microscopy; wood; restoration; halloysite nanotubes



**Citation:** Bettina, G.F.; Giambra, B.; Cavallaro, G.; Lazzara, G.; Megna, B.; Fakhrullin, R.; Akhatova, F.; Fakhrullin, R. Restoration of a XVII Century's *predella reliquary*: From Physico-Chemical Characterization to the Conservation Process. *Forests* **2021**, *12*, 345. <https://doi.org/10.3390/f12030345>

Academic Editor: Magdalena Broda

Received: 23 February 2021

Accepted: 11 March 2021

Published: 15 March 2021

**Publisher's Note:** MDPI stays neutral with regard to jurisdictional claims in published maps and institutional affiliations.



**Copyright:** © 2021 by the authors. Licensee MDPI, Basel, Switzerland. This article is an open access article distributed under the terms and conditions of the Creative Commons Attribution (CC BY) license (<https://creativecommons.org/licenses/by/4.0/>).

## 1. Introduction

Among tangible cultural heritage, wooden artworks are very common due to the availability and workability of this material and its suitability for generating tools or decorative elements.

Wood conservation represents an open task for scientists and conservators to work synergistically to properly solve a specific issue. An advanced physico-chemical approach can be very helpful in the evaluation of the conservation state [1–5], as well as to formulate new materials used in restoration protocols that, nowadays, are tailored to specific artworks [6–13].

Knowledge of the physico-chemical state of the object, and particularly of any visible alteration products that form during display or in storage environments, is also essential to preventive conservation.

This article is about the restoration work of a XVII century *predella reliquary* and of four reliquary busts that date back to the XVII century from an unknown artist (Figure 1).



These goods belong to the church of “Madre Maria SS. Assunta”, in Polizzi Generosa in Sicily (Italy).



**Figure 1.** Photos of the *predella reliquary* and four busts from the church of “Madre Maria SS. Assunta”, in Polizzi Generosa, Sicily, Italy.

The exact year of the *predella reliquary*'s completion is not known. However, the priest Giovanni Malatucca prepared a detailed drawing showing the complete reliquary setup, including this *predella*, before his death in 1722. Thus, it is likely this artwork was completed no later than the end of the 1600s. The work is a Baroque ornament sumptuously carved with flowers, leaves and repetitive geometric patterns, typical of this period.

With respect to the four busts, their creation dates, their artists and their original positions are unknown. The four busts are also contained in some wooden shrines. According to their technique with which they were made, these shrines were probably realized for a larger structure, such as, for example, a wall reliquary, into which every shrine was a kind of moving drawer.

However, they should be dated back to the XVII century, which is the same period of *predella reliquary*.

Here, we report the identification of wood species, as well as a detailed view of the surface treatment and materials used for decoration. Electron microscopy with elemental mapping (energy-dispersive X-ray; EDX) will be used for the investigation of the layered structure in the gilded surface while hyperspectral imaging will provide an objective view of the conservation state and execution technique, providing the necessary information for a conservation action and for a correct historical interpretation of this artwork. Microscopy is a powerful tool in cultural heritage and historical studies, allowing for investigation of minute features [14]. In addition, image processing software was employed for the enhancement of historical drawings and engravings [15].

Moreover, we investigate the application of an advanced nanocomposite glue system based on Halloysite nanotubes and Funori. Both components can be considered sustainable materials, bringing a novel approach to the conservation protocol. Halloysite is a nanotubular clay with the chemical structure of kaolinite and a rolled-up morphology that is considered an emerging material in a wide range of application [16–25]. It should be noted that halloysite exhibits low toxicity as proved by *in vitro* and *in vivo* tests [26,27]. The characteristic sizes are 20–100 nm for diameter and up to 2  $\mu\text{m}$  for the length and depend on the deposit [28,29]. The anisotropic shape typically enhances the mechanical performances of bionanocomposites and it can also function as a smart container for bioactive

species [30–34]. Funori is a polysaccharide mucilage from algae, extracted from seaweed, composed primarily of galactose, used as a weak water-soluble adhesive [35]. Although the adhesive strength of funori is far below that for synthetic adhesives, its use is justified in conservation protocols due to the reversibility of the application. We believe that the combination of the polysaccharide and halloysite nanotubes can show synergistic effects in mechanical materials, as well as glue composite materials, similar to other nanocomposite systems [36,37]. With this in mind, tensile measurements have been carried out to evaluate the best biopolymer/halloysite nanotubes ratio based on the adhesive strength. It should also be noted that natural product-based binders, such as polysaccharides, could be subjected to biological attack; therefore, the addition of hollow nanotubular fillers can be further evaluated for biocide vehiculation with slow release.

## 2. Materials and Methods

Halloysite nanotubes were purchased from Sigma-Aldrich (Italy). Funori was obtained from CTS srl (Italy).

*Tensile Analysis:* Tensile properties of glued wood samples were determined by means of a DMA Q800 instrument (TA Instruments, Milan, Italy). Tensile tests were performed on rectangular samples obtained by gluing two identical pieces (length  $\times$  width  $\times$  thickness, ca.  $10 \times 5 \times 3$  mm; glued surface:  $5 \times 3$  mm) under a stress ramp of  $1 \text{ MPa min}^{-1}$  at  $25.0 \pm 0.5$  °C. We determined the stress at which the material fractures (or) and the corresponding maximum deformation from the stress vs. strain curves. The reproducibility was assessed by repeating the experiment at least three times.

*Identification of wooden species:* wood species were identified by means of a dichotomous keys method, by observing the microscopic anatomical features of the samples using a Leica DMLM stereoscopic microscope equipped with a DinoLite DinoEye camera using Dinoscope software. Wood sections were prepared by cutting wood slides directly from the artworks by hand, using a razor blade after the surface had been softened by wetting (see figure in supporting information). This was carried out in order to minimize the amount of material required for identification.

*SEM-EDX:* Scanning electron microscopy (SEM) was performed using an Auriga CrossBeam microscope (Carl Zeiss, Jena, Germany), as described elsewhere [14]. The specimens were coated with ca. 20 nm carbon layer using a Quorum Q150T ES sputter-coater. SEM images were obtained in secondary electron imaging mode (20 kV, 700 pA). For energy-dispersive X-ray (EDX) spectroscopy data and elemental surface mapping, an INCA X-Max EDS-spectrometer (Oxford Instruments, High Wycombe, UK) was used.

*Hyperspectral images:* Bright-field reflected light microscopy images and reflected light spectra in visible-near infrared range were obtained using an Olympus BX51 (Olympus) upright microscope equipped with a 150 W Fibre-Lite DC-950 halogen light source (Dolan-Jener) and a ProScan III motorized stage (JH Technologies, Fremont, CA, US) [38]. Optical images were obtained using Exponent 7 (Dage-MTI) image acquisition software [39]. Spectra were recorded using a Specim V10E spectrometer (Spectral Imaging LTD) and a Pixelfy.usb CCD camera (PCO) in 400–1000 nm range. Hyperspectral data were analyzed using ENVI v. 4.8 software (Harris Geospatial Solutions, Broomfield, CO, USA) [40]. All HSI data obtained were corrected for the spectral contribution of the light source.

*Preparation of nanocomposite glue:* The funori solution was prepared by adding ca. 40 g of Funori to 500 g of water and was kept at 80 °C under magnetic stirring for 2 h. A yellowish viscous solution was obtained that was vacuum filtered through a 0.45  $\mu\text{m}$  cellulosic filter. The final funori concentration in the stock solution was  $7.3 \pm 0.2$  wt% (estimated from gravimetric method after solvent evaporation at 120 °C).

The funori/halloysite nanotube (HNT) composite glue was prepared by adding varying amounts of HNTs to 10 g of funori stock solution. The glue composition is expressed in terms of halloysite mass percentage referring to the funori + halloysite total dried mass.

### 3. Results and Discussion

This work reports on the characterization of the XVII century *predella reliquary* and four reliquary busts. Firstly, the identification of wood taxon and the finishing layers are reported. The rigorous physico-chemical characterization of the artefacts helps to define the degradation level, design the conservation protocol, but also contributes to the understanding of the early technologies. Secondly, the conservation action, with a particular focus on the use of an advanced nanocomposite glue that was designed in our laboratories, is described.

#### 3.1. Identification of the Wood Species and Microscopy Analysis

The external *predella* wooden sample was observed by optical microscopy (Figure 2). The images indicate a coniferous wood without resin canals. Tangential and radial sections highlight that the tracheid walls have no spiral thickenings. The rays are homogeneous with small pits in the cross-fields, and are without tracheids. Based on the observed characteristics, one can identify the wood species belonging to the *Abies* genus. According to the literature, it is impossible to distinguish between the different species of this genus [41]. The identification of this genus could indicate the use of the species *Abies nebrodensis*. Nowadays, this is classified as critically endangered by the International Union for Conservation of Nature, but was widespread in Sicily in the past as an endemic species [42].

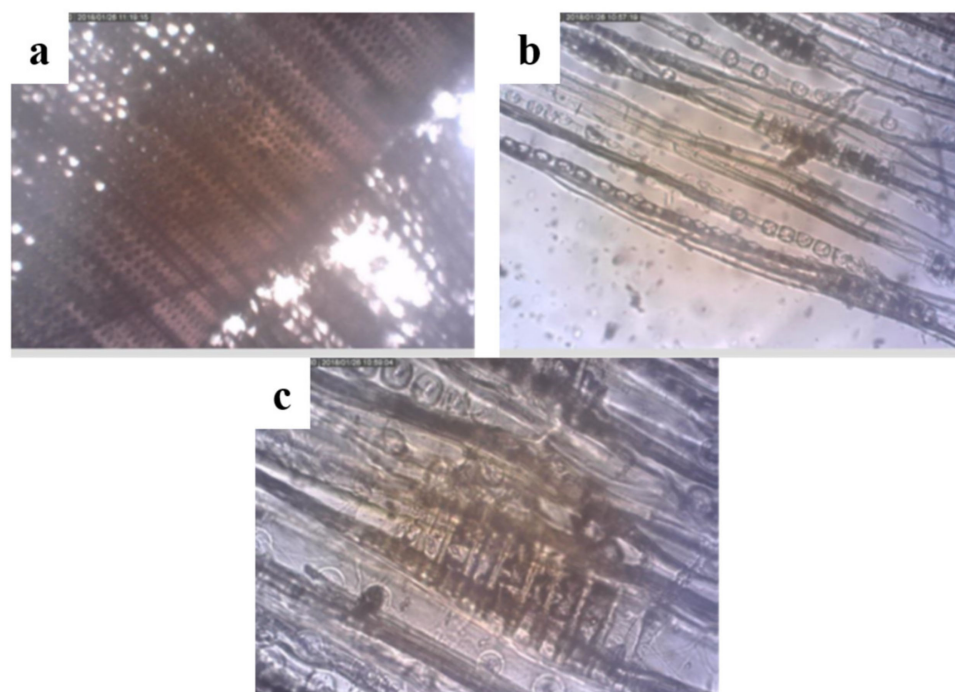


**Figure 2.** Optical images of the cross-section (a), tangential section (b) and subradial section (c) of the wood constituting the external structure of the *predella reliquary*.

The little frame structure is a hardwood with diffuse porosity and multiseriate homogeneous rays (Figure 3), two to four cells wide, with vessels showing spiral thickenings. Rays flare along growth ring boundaries. It can be concluded that it is lime wood, specifically *Tilia cordata* Mill.

As the busts are fully gilded, only tangential sections have been observed due to the sampling. The observable features—spiral thickening of the vessels, multiseriate homogeneous rays—further indicate that the wooden species is likely to be lime wood.

The bases of the busts consist of different wood species. Microscopic observation of tangential sections, the only available for sampling, revealed homogeneous uniseriate rays,

vessels with simple perforation and without spiral thickenings (Figure 4). According to these features, the most likely wood species is poplar, *Populus nigra* L.

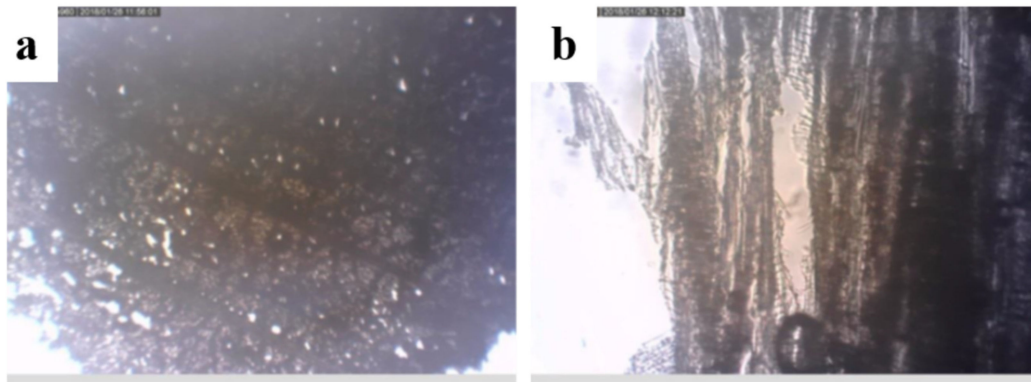


**Figure 3.** Optical image of the cross-section (a), tangential section (b) of the wood constituting the little frame structure of the *predella reliquary*.

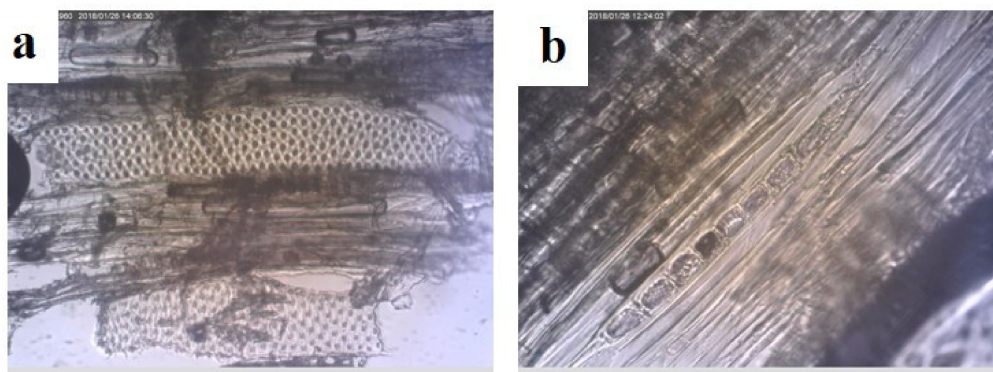


**Figure 4.** Optical image of the tangential section: (a) vessel and (b) rays of the wood, constituting the basements of the busts.

Mixing several wood species in a single work is not peculiar. In fact, the carvers knew very well the materials they used and the selection was based on the physico-chemical characteristics. For example, lime wood, having a fine texture and a low degree of hardness, was more suitable for carving as an excellent degree of detail could be achieved. Poplar has a strong tendency to chip, but being available at low cost, it is more suitable for parts that do not require carving.

Concerning the preparation layer and decorative surface, from the optical micrographs one can already see evidence of red bole (a soft fine clay typically with a reddish-brown color also used as a pigment) layers appearing below a gilded surface. To shed more light on this aspect, SEM imaging and EDX mapping have been carried out on the *predella reliquary* (Figure 5). The elemental analysis clearly identified the gold layer of ca. 7  $\mu\text{m}$  (Figure 5d,h). It should be noted that modern gold leaf is very thin (below 200 nm) [43] and therefore we might conclude that this is an original gilded surface. The preparation layer located between the gold foil and the wood has a thickness of ca. 40  $\mu\text{m}$  and it is composed of O (34%), Si (23%), Fe (17%), Al (16%) and Ca (10%). The obtained composition is consistent with red bole clay [44]. The use of clay in the preparation layer to paste a gold leaf was largely used by Italian artists and it is also reported for gilded wooden artworks from Giotto [43].

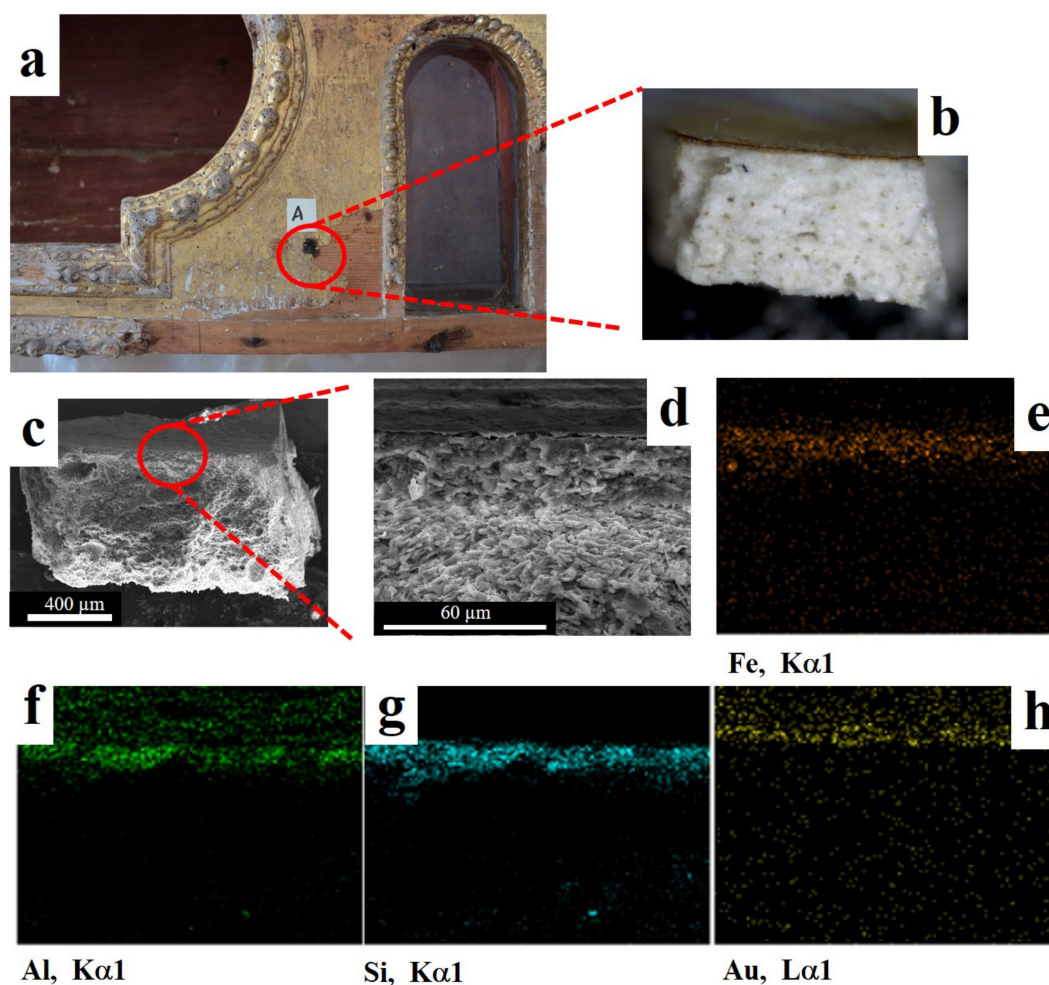


**Figure 5.** Optical photo of the sampling area (a) and optical microscopy (b) of the cross-section for the decorative surface. Scanning electron microscopy (SEM) images (c,d) and elemental mapping (e–h) for the same cross-section from the *predella reliquary*.

The decorative surface was also imaged by means of hyperspectral microscopy. This methodology is based on full spectrum collection from the specimen surface, providing more detailed chemical information on the surface composition. The reflected light microscopy images and spectra are shown in Figure 6. The spectra obtained from the “lacuna” and the gilded surface are very different. In particular, the surface plasmon resonance (SPR) peaks at the characteristic wavelengths for gold thin layers are evidenced [45]. On this basis, the reflected light hyperspectral mapping can be used as a valuable tool to clearly identify the gold lacuna on an analytical basis. Moreover, as the surface plasmon resonance peaks is sensitive to the gold layer thickness, it should be efficient in evidencing modern gold leaf from recent restorations.

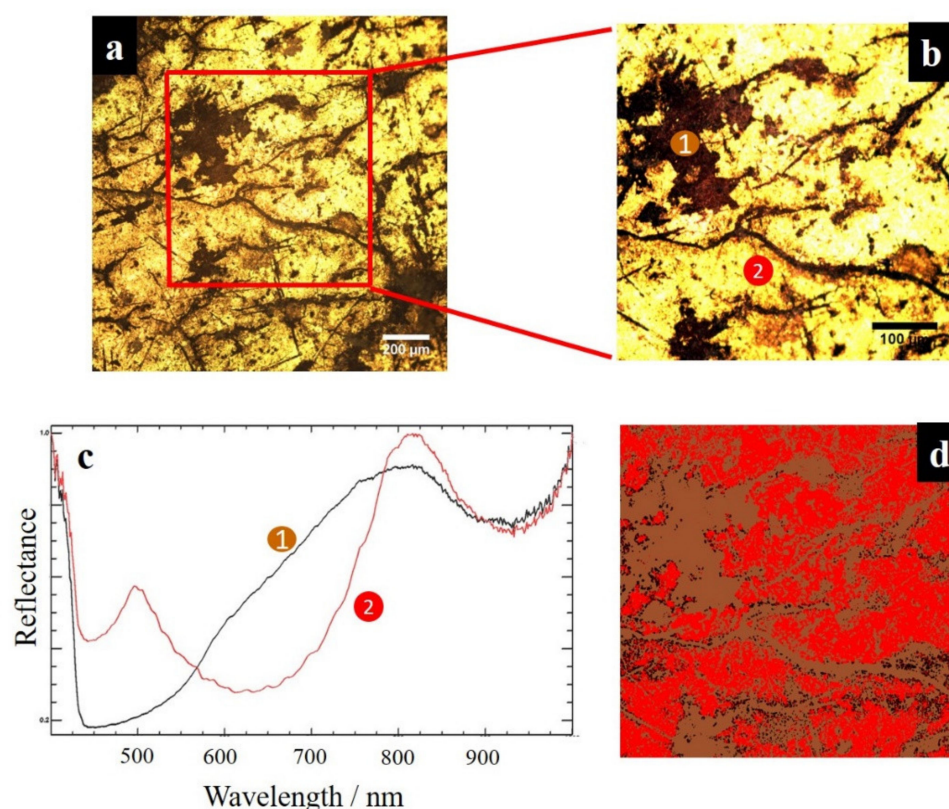


**Figure 6.** Reflected light optical microscopy images sampling area at lower (a) and higher magnification (b) of the surface for the decorative surface. Reflected light spectra (c) and spectral mapping (d) for the same sample from the *predella reliquary*.

### 3.2. Application of an Advanced Nanocomposite Glue

The restoration was carried out with a conservation approach aimed at restoring the cultural aesthetic harmony. The treatments were based on the principle of minimal intervention not to predominate with respect to “normal” aging. Diagnostic investigations, with the aim to recognizing the woody species of the support, the materials of the preparatory and pictorial layers and the stratigraphy have allowed us to study the cultural asset in its totality. Although a full description is out of the scope of this manuscript, herein we provide a brief outline of the work. The restoration was carried out in several steps: dusting with the aid of microaspirator and brushes with soft bristles; disinfestation of the support with an insecticide based on permethrin; consolidation of the support was carried out with an acrylic resin; restoration of the mechanical capacities of the structure; restoration of wooden inserts using Balsa wood; grouting of erosions with cellulose pulp and cellulose ether; treatment of metal parts, with rust converter. After this, we moved on to the process of the preparatory layers and gilding consolidation, a thermoplastic polymer (poly (2-ethyl-2-Oxazoline),  $M_w = 500 \text{ kg mol}^{-1}$ ), applied punctually and sintered with the aid of slight heating. Then, we progressed to cleaning with a water in oil emulsion at neutral pH and to the reconstruction of the missing frames, with two-component epoxy-based putty after making the casts with silicone rubber. We then proceeded to the intermediate painting with retouching paint using watercolors.

During the restoration it was necessary to fix some fragments that had become detached. Within this issue, we investigated the possibility of using a weak water-based glue (based on funori) in combination with natural nanotubes (halloysite HNTs). Therefore, the adhesion was tested by measuring the stress vs. strain curves of glued wooden samples (Figure 7). A systematic trend was observed by increasing the percentage of halloysite nanotubes in the HNT/funori mixture ( $C_{\text{HNT}}$ ) and, in particular, the response appears more rigid to deformation in the geometry that is sketched in Figure 7.

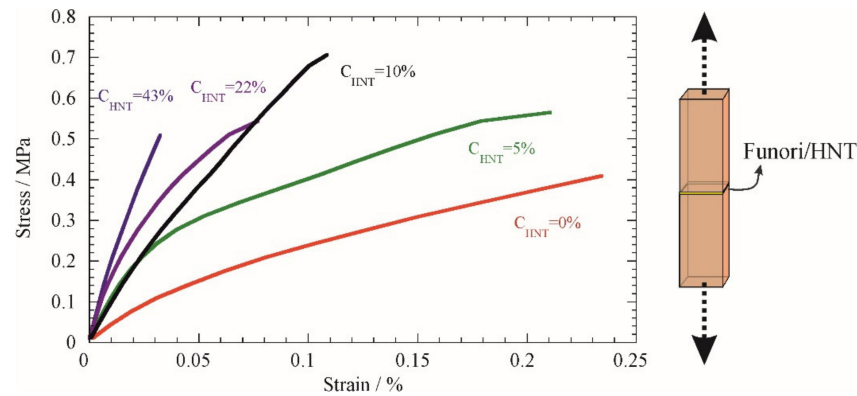


**Figure 7.** Stress–strain curves for funori/halloysite nanotube glue at variable composition. The scheme shows the geometry for the carried tensile tests.

For a quantitative assessment, the ultimate stress and deformation at detaching, as well as the slope of the linear deformation region (Young’s modulus) were calculated and are provided in Figure 8 for the wood glued with pure funori and funori with increasing percentages of HNTs ( $C_{\text{HNT}}$ ). The ultimate stress was improved by halloysite nanotubes up to a concentration of 10%; additional nanotubes did not further improve this parameter. This behavior could be explained considering the percolation threshold that predicts clustering effects above 10% of halloysite in polymeric matrices [32]—namely, at ca. 10% the contact distance between nanotubes is approached and clustering effects might reduce the efficacy as reinforcing agents. Furthermore, the ultimate elongation and elastic modulus reports a monotonic change with the increase in halloysite nanotube contents. In particular, the glue appears more rigid (increase in the modulus and decrease in the ultimate deformation) in the presence of halloysite. Based on the above arguments, we considered the mixture at  $C_{\text{HNT}} = 10\%$  as the best compromise for the actual application.

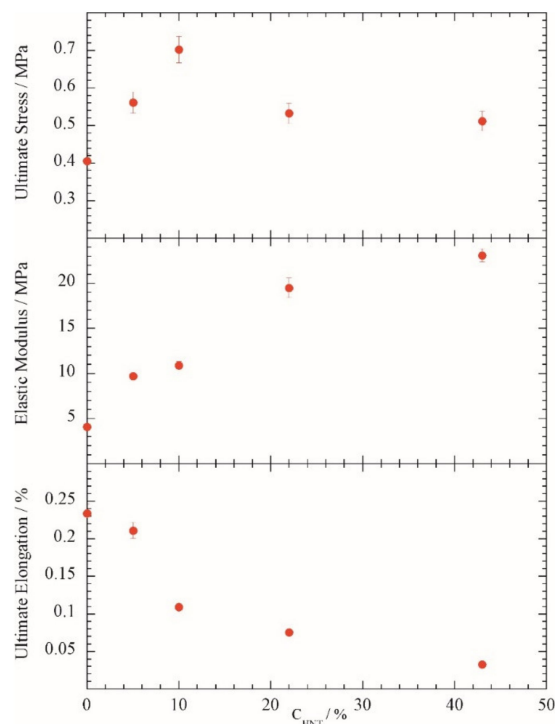


**Figure 8.** Tensile parameters for funori/halloysite nanotubes glue at variable composition.

#### 4. Conclusions

In this work, we briefly report on the characterization and restoration of a number of wooden artifacts. We used advanced imaging methods for the evaluation of the conservation conditions as a preliminary step toward the restoration protocol and for a comprehensive understanding of the ancient methodology and material selection.

Finally, a nanocomposite glue has been designed by using natural nanotubular particles and a biopolymer extract from algae, funori. We, therefore, report a sustainable approach for the preparation of consolidant materials with a functional nanoarchitecture that can be further developed to target specific needs such as biocide or smart responsive features by filling the nanotubular lumen with proper active molecules.

**Author Contributions:** Conceptualization, G.L. and G.C.; methodology, G.F.B. and B.G.; investigation, R.F. (Ramil Fakhrullin), F.A. and R.F. (Rawil Fakhrullin); data curation, G.F.B. and B.G.; writing—original draft preparation, G.C., G.L. and B.M.; funding acquisition, G.L. and R.F. (Rawil Fakhrullin). All authors have read and agreed to the published version of the manuscript.

**Funding:** G.C., G.L. and B.M. thank University of Palermo for financial support. This work was funded by the subsidy allocated to Kazan Federal University for the state assignment in the sphere of scientific activities (0671-2020-0058). Rawil Fakhrullin acknowledges funding by Russian Federation presidential grant MD-2153.2020.3.

**Institutional Review Board Statement:** Not applicable.

**Informed Consent Statement:** Not applicable.

**Data Availability Statement:** Data are available upon request to corresponding authors.

**Acknowledgments:** We thank Ilvina Safina for technical help with SEM. We thank Giovanni Silvestri as priest of the church of “Madre Maria SS. Assunta” in Polizzi Generosa (Italy).

**Conflicts of Interest:** The authors declare no conflict of interest.

#### References

1. Cavallaro, G.; Agliolo Gallitto, A.; Lisuzzo, L.; Lazzara, G. Comparative Study of Historical Woods from XIX Century by Thermogravimetry Coupled with FTIR Spectroscopy. *Cellulose* **2019**, *26*, 8853–8865. [CrossRef]
2. Bernabei, M.; Macchioni, N.; Pizzo, B.; Sozzi, L.; Lazzari, S.; Fiorentino, L.; Pecoraro, E.; Quarta, G.; Calcagnile, L. The Wooden Foundations of Rialto Bridge (Ponte Di Rialto) in Venice: Technological Characterisation and Dating. *J. Cult. Herit.* **2019**, *36*, 85–93. [CrossRef]
3. Babiński, L.; Izdebska-Mucha, D.; Waliszewska, B. Evaluation of the State of Preservation of Waterlogged Archaeological Wood Based on Its Physical Properties: Basic Density vs. Wood Substance Density. *J. Archaeol. Sci.* **2014**, *46*, 372–383. [CrossRef]
4. Čufar, K.; Merela, M.; Erič, M. A Roman Barge in the Ljubljanica River (Slovenia): Wood Identification, Dendrochronological Dating and Wood Preservation Research. *J. Archaeol. Sci.* **2014**, *44*, 128–135. [CrossRef]
5. Guo, J.; Zhang, M.; Liu, J.; Luo, R.; Yan, T.; Yang, T.; Jiang, X.; Dong, M.; Yin, Y. Evaluation of the Deterioration State of Archaeological Wooden Artifacts: A Nondestructive Protocol Based on Direct Analysis in Real Time—Mass Spectrometry (DART-MS) Coupled to Chemometrics. *Anal. Chem.* **2020**, *92*, 9908–9915. [CrossRef]
6. Cavallaro, G.; Lazzara, G.; Milioto, S.; Parisi, F.; Ruisi, F. Nanocomposites Based on Esterified Colophony and Halloysite Clay Nanotubes as Consolidants for Waterlogged Archaeological Woods. *Cellulose* **2017**, *24*, 3367–3376. [CrossRef]
7. Cavallaro, G.; Milioto, S.; Parisi, F.; Lazzara, G. Halloysite Nanotubes Loaded with Calcium Hydroxide: Alkaline Fillers for the Deacidification of Waterlogged Archeological Woods. *ACS Appl. Mater. Interfaces* **2018**, *10*, 27355–27364. [CrossRef]
8. Broda, M.; Dąbek, I.; Dutkiewicz, A.; Dutkiewicz, M.; Popescu, C.-M.; Mazela, B.; Maciejewski, H. Organosilicons of Different Molecular Size and Chemical Structure as Consolidants for Waterlogged Archaeological Wood—A New Reversible and Retreatable Method. *Sci. Rep.* **2020**, *10*, 2188. [CrossRef]
9. Broda, M.; Mazela, B.; Dutkiewicz, A. Organosilicon Compounds with Various Active Groups as Consolidants for the Preservation of Waterlogged Archaeological Wood. *J. Cult. Herit.* **2019**, *35*, 123–128. [CrossRef]
10. Antonelli, F.; Galotta, G.; Sidoti, G.; Zikeli, F.; Nisi, R.; Davide Petriaggi, B.; Romagnoli, M. Cellulose and Lignin Nano-Scale Consolidants for Waterlogged Archaeological Wood. *Front. Chem.* **2020**, *8*, 32. [CrossRef]
11. Poggi, G.; Toccafondi, N.; Chelazzi, D.; Canton, P.; Giorgi, R.; Baglioni, P. Calcium Hydroxide Nanoparticles from Solvothermal Reaction for the Deacidification of Degraded Waterlogged Wood. *J. Colloid Interface Sci.* **2016**, *473*, 1–8. [CrossRef] [PubMed]
12. Broda, M. Natural Compounds for Wood Protection against Fungi—A Review. *Molecules* **2020**, *25*, 3538. [CrossRef] [PubMed]
13. Lisuzzo, L.; Hueckel, T.; Cavallaro, G.; Sacanna, S.; Lazzara, G. Pickering Emulsions Based on Wax and Halloysite Nanotubes: An Ecofriendly Protocol for the Treatment of Archeological Woods. *ACS Appl. Mater. Interfaces* **2021**, *13*, 1651–1661. [CrossRef]



14. Khranchenkova, R.; Safina, I.; Drobyshev, S.; Batasheva, S.; Nuzhdin, E.; Fakhrullin, R. Advanced Microscopy Techniques for Nanoscale Diagnostic of Cultural Heritage. In *Nanotechnologies and Nanomaterials for Diagnostic, Conservation and Restoration of Cultural Heritage*; Elsevier: Amsterdam, The Netherlands, 2019; pp. 1–23. ISBN 978-0-12-813910-3.
15. Aidarova-Volkova, G.N.; Fakhrullin, R.F.; Kees, B. Historical-Architectural Analysis of the Panoramic Image of Kazan by Cornelis de Bruijn. *Vestn. Spbsu. Hist.* **2020**, *65*, 566–583. [CrossRef]
16. Papoulis, D. Halloysite Based Nanocomposites and Photocatalysis: A Review. *Appl. Clay Sci.* **2019**, *168*, 164–174. [CrossRef]
17. Lvov, Y.M.; Shchukin, D.G.; Mohwald, H.; Price, R.R. Halloysite Clay Nanotubes for Controlled Release of Protective Agents. *ACS Nano* **2008**, *2*, 814–820. [CrossRef]
18. Yendluri, R.; Otto, D.P.; De Villiers, M.M.; Vinokurov, V.; Lvov, Y.M. Application of Halloysite Clay Nanotubes as a Pharmaceutical Excipient. *Int. J. Pharm.* **2017**, *521*, 267–273. [CrossRef]
19. Joussein, E.; Petit, S.; Churchman, G.J.; Theng, B.; Righi, D.; Delvaux, B. Halloysite Clay Minerals—A Review. *Clay Miner.* **2005**, *40*, 383–426. [CrossRef]
20. Panchal, A.; Fakhrullina, G.; Fakhrullin, R.; Lvov, Y. Self-Assembly of Clay Nanotubes on Hair Surface for Medical and Cosmetic Formulations. *Nanoscale* **2018**, *10*, 18205–18216. [CrossRef] [PubMed]
21. Cavallaro, G.; Milioto, S.; Lazzara, G. Halloysite Nanotubes: Interfacial Properties and Applications in Cultural Heritage. *Langmuir* **2020**, *36*, 3677–3689. [CrossRef]
22. Zhang, Y.; Bai, L.; Cheng, C.; Zhou, Q.; Zhang, Z.; Wu, Y.; Zhang, H. A Novel Surface Modification Method upon Halloysite Nanotubes: A Desirable Cross-Linking Agent to Construct Hydrogels. *Appl. Clay Sci.* **2019**, *182*, 105259. [CrossRef]
23. Cheng, C.; Gao, Y.; Song, W.; Zhao, Q.; Zhang, H.; Zhang, H. Halloysite Nanotube-Based H<sub>2</sub>O<sub>2</sub>-Responsive Drug Delivery System with a Turn on Effect on Fluorescence for Real-Time Monitoring. *Chem. Eng. J.* **2020**, *380*, 122474. [CrossRef]
24. Taroni, T.; Cauteruccio, S.; Vago, R.; Franchi, S.; Barbero, N.; Licandro, E.; Ardizzone, S.; Meroni, D. Thiahelicene-Grafted Halloysite Nanotubes: Characterization, Biological Studies and PH Triggered Release. *Appl. Surf. Sci.* **2020**, *520*, 146351. [CrossRef]
25. Barman, M.; Mahmood, S.; Augustine, R.; Hasan, A.; Thomas, S.; Ghosal, K. Natural Halloysite Nanotubes /Chitosan Based Bio-Nanocomposite for Delivering Norfloxacin, an Anti-Microbial Agent in Sustained Release Manner. *Int. J. Biol. Macromol.* **2020**, *162*, 1849–1861. [CrossRef] [PubMed]
26. Long, Z.; Wu, Y.-P.; Gao, H.-Y.; Zhang, J.; Ou, X.; He, R.-R.; Liu, M. In Vitro and in Vivo Toxicity Evaluation of Halloysite Nanotubes. *J. Mater. Chem. B* **2018**, *6*, 7204–7216. [CrossRef]
27. Wang, X.; Gong, J.; Gui, Z.; Hu, T.; Xu, X. Halloysite Nanotubes-Induced Al Accumulation and Oxidative Damage in Liver of Mice after 30-Day Repeated Oral Administration. *Environ. Toxicol.* **2018**, *33*, 623–630. [CrossRef] [PubMed]
28. Cavallaro, G.; Chiappisi, L.; Pasbakhsh, P.; Gradzielski, M.; Lazzara, G. A Structural Comparison of Halloysite Nanotubes of Different Origin by Small-Angle Neutron Scattering (SANS) and Electric Birefringence. *Appl. Clay Sci.* **2018**, *160*, 71–80. [CrossRef]
29. Pasbakhsh, P.; Churchman, G.J.; Keeling, J.L. Characterisation of Properties of Various Halloysites Relevant to Their Use as Nanotubes and Microfibre Fillers. *Appl. Clay Sci.* **2013**, *74*, 47–57. [CrossRef]
30. Bugatti, V.; Brachi, P.; Viscusi, G.; Gorrasi, G. Valorization of Tomato Processing Residues Through the Production of Active Bio-Composites for Packaging Applications. *Front. Mater.* **2019**, *6*, 34. [CrossRef]
31. Gorrasi, G. Dispersion of Halloysite Loaded with Natural Antimicrobials into Pectins: Characterization and Controlled Release Analysis. *Carbohydr. Polym.* **2015**, *127*, 47–53. [CrossRef] [PubMed]
32. Lisuzzo, L.; Cavallaro, G.; Milioto, S.; Lazzara, G. Effects of Halloysite Content on the Thermo-Mechanical Performances of Composite Bioplastics. *Appl. Clay Sci.* **2020**, *185*, 105416. [CrossRef]
33. Lisuzzo, L.; Cavallaro, G.; Milioto, S.; Lazzara, G. Layered Composite Based on Halloysite and Natural Polymers: A Carrier for the PH Controlled Release of Drugs. *New J. Chem.* **2019**, *43*, 10887–10893. [CrossRef]
34. Tarasova, E.; Naumenko, E.; Rozhina, E.; Akhatova, F.; Fakhrullin, R. Cytocompatibility and Uptake of Polycations-Modified Halloysite Clay Nanotubes. *Appl. Clay Sci.* **2019**, *169*, 21–30. [CrossRef]
35. Swider, J.R.; Smith, M. Funori: Overview of a 300-Year-Old Consolidant. *J. Am. Inst. Conserv.* **2005**, *44*, 117–126. [CrossRef]
36. Zhao, X.; Zhou, C.; Liu, M. Self-Assembled Structures of Halloysite Nanotubes: Towards the Development of High-Performance Biomedical Materials. *J. Mater. Chem. B* **2020**, *8*, 838–851. [CrossRef]
37. Bertolino, V.; Cavallaro, G.; Milioto, S.; Lazzara, G. Polysaccharides/Halloysite Nanotubes for Smart Bionanocomposite Materials. *Carbohydr. Polym.* **2020**, *245*, 116502. [CrossRef]
38. Fakhrullin, R.; Nigamatzyanova, L.; Fakhrullina, G. Dark-Field/Hyperspectral Microscopy for Detecting Nanoscale Particles in Environmental Nanotoxicology Research. *Sci. Total Environ.* **2021**, *772*, 145478. [CrossRef] [PubMed]
39. Nigamatzyanova, L.; Fakhrullin, R. Dark-Field Hyperspectral Microscopy for Label-Free Microplastics and Nanoplastics Detection and Identification in Vivo: A Caenorhabditis Elegans Study. *Environ. Pollut.* **2021**, *271*, 116337. [CrossRef] [PubMed]
40. Akhatova, F.; Danilushkina, A.; Kuku, G.; Saricam, M.; Culha, M.; Fakhrullin, R. Simultaneous Intracellular Detection of Plasmonic and Non-Plasmonic Nanoparticles Using Dark-Field Hyperspectral Microscopy. *Bull. Chem. Soc. Jpn.* **2018**, *91*, 1640–1645. [CrossRef]
41. Schweingruber, F.H. *Microscopic Wood Anatomy*; Fluck-Wirth: Teufen, Switzerland, 1982.
42. Rivers, M. *European Red List of Trees*; IUCN, International Union for Conservation of Nature: Grand, Switzerland, 2019; ISBN 978-2-8317-1985-6.

43. Eveno, M.; Ravaud, E.; Calligaro, T.; Pichon, L.; Laval, E. The Louvre Crucifix by Giotto—Unveiling the Original Decoration by 2D-XRF, X-Ray Radiography, Emissiography and SEM-EDX Analysis. *Herit. Sci.* **2014**, *2*, 17. [CrossRef]
44. Barata, C.; Rocha, F.; Cruz, A.J.; Andrejkovičová, S.; Reguer, S. Synchrotron X-ray Diffraction of Bole Layers from Portuguese Gilded Baroque Retables. *Appl. Clay Sci.* **2015**, *116–117*, 39–45. [CrossRef]
45. Rai, V.N.; Srivastava, A.K.; Mukherjee, C.; Deb, S.K. Surface Enhanced Absorption and Transmission from Dye Coated Gold Nanoparticles in Thin Films. *Appl. Opt.* **2012**, *51*, 2606. [CrossRef] [PubMed]



## Article

# Assessment of Wooden Foundation Piles after 125 Years of Service

Miha Humar <sup>\*</sup>, Angela Balzano , Davor Kržišnik  and Boštjan Lesar 

Biotechnical Faculty, University of Ljubljana, SI1000 Ljubljana, Slovenia; angela.balzano@bf.uni-lj.si (A.B.); davor.krzisnik@bf.uni-lj.si (D.K.); bostjan.lesar@bf.uni-lj.si (B.L.)

\* Correspondence: miha.humar@bf.uni-lj.si

**Abstract:** Buildings on piles have been constructed in Ljubljana since the Bronze Age. The piles were made of different types of wood. In the present study, piles that were erected about 125 years ago were investigated. Investors tend to renovate a building; therefore, the piles were analysed to assess the structural condition of the building. The building showed no signs of damage. To gain access to the piles, a 2 m thick layer of soil was removed. On-site, the following analyses were carried out: drilling resistance with a resistograph and a screw withdrawal test. Part of the piles was isolated and light microscopy, scanning electron microscopy, infrared spectroscopy, dynamic vapour sorption, density analysis, and chemical analysis were performed. Microscopic analysis revealed that the piles were made from the wood of Scots pine (*Pinus sylvestris*). The results indicate that the wood was severely degraded, mainly by soft-rot fungi and bacteria, resulting in a significant deterioration of its mechanical properties.

**Keywords:** piles; waterlogged wood; soft rot; decay; microscopy



**Citation:** Humar, M.; Balzano, A.; Kržišnik, D.; Lesar, B. Assessment of Wooden Foundation Piles after 125 Years of Service. *Forests* **2021**, *12*, 143. <https://doi.org/10.3390/f12020143>

Academic Editors: Magdalena Broda and Callum A. S. Hill

Received: 28 December 2020

Accepted: 22 January 2021

Published: 26 January 2021

**Publisher's Note:** MDPI stays neutral with regard to jurisdictional claims in published maps and institutional affiliations.



**Copyright:** © 2021 by the authors. Licensee MDPI, Basel, Switzerland. This article is an open access article distributed under the terms and conditions of the Creative Commons Attribution (CC BY) license (<https://creativecommons.org/licenses/by/4.0/>).

## 1. Introduction

Wood is one of the most important building materials that has been used for several thousand years [1]. Similar to other building applications, the use of wood for piles has a long history. In the Alpine region, this construction technique has been used for about 7000 years [2]. Among other regions, Ljubljana and its surroundings are recognised as one of the places with the longest tradition of using wooden piles [3]. The southern part of Ljubljana has been built on piles since Roman times, while pilings in Ljubljana Moor have their origin in Bronze Age. Traditionally, pilings were made by hammering down wooden stakes vertically into the marsh soil at even intervals. For this purpose, piles with dimensions between 25 cm and 35 cm are commonly used to support the foundations and to transfer the load more in-depth into the soil [4]. In the Bronze Age, the Ljubljana Moor piles were mainly made of oak (*Quercus robur*, *Q. petraea*, *Q. cerris*) and ash (*Fraxinus excelsior* and *F. ornus*). At the same time, the wood of *Sorbus aucuparia* (rowan), *Carpinus betulus* (hornbeam), *Alnus glutinosa* (black alder), and *Corylus avellana* (hazel) were less frequently used [5]. Afterwards, timber logs of softwood species (pine, spruce or larch) were frequently used for foundation piles [6]. In the recent periods, the pilings in Ljubljana are predominately made of Scots pine (*Pinus sylvestris*), sweet chestnut (*Castanea sativa*), and black alder. In the Bronze Age, pilings were made for building shelters above the water or moor. Still later, this construction technique was used to reclaim marshes and settle wastelands [6,7]. Thus, the use of piles somehow enables constructions even on unstable soil.

Wooden piles in waterlogged conditions have a long service life [8,9]. Many historical cities near rivers, waterfronts, and the sea still stand on the original wooden piles [6], such as Stockholm, Hamburg, Amsterdam, Trondheim, Venice, Saint Petersburg, Ljubljana, etc. [10]. In recent decades, biological damage to a considerable number of wooden foundations across Europe has been identified. Therefore, it is of great importance to

understand the performance of waterlogged wood to enable safe homes for citizens and predict the future performance of buildings.

Submerged wood was once considered safe from any form of fungal decay due to the absence of oxygen [8]. However, it has been known for decades that wood in below-ground applications is exposed to a variety of the decay organisms [11,12]. The prevalent type of decay in the ground contact is soft rot. Soft-rot organisms preferentially attack hemicellulose and cellulose in the S2 layer of the secondary cell wall, forming longitudinal cavities (Type 1) or eroding the wood cell wall from the lumen surface in hardwoods (Type 2) or the S2 in conifers. Fungi that cause soft rot are taxonomically classified into Ascomycota and Deuteromycota [13]. Soft rot was initially characterised as a soft, decayed surface of the wood in contact with excessive moisture [14]. Common fungi that cause soft rot include *Chaetomium globosum* and *Alternaria alternata* [15]. Soft-rot fungi colonise wood under conditions that are too cold, too hot, or too moist for white or brown rot fungi. Soft-rot fungi are less aggressive decomposers than white- and brown-rot fungi; therefore, decomposition is slower under soil conditions than above ground or in the air-soil transition zone [16]. In addition to fungi, some bacteria are also known to cause decay in soil by causing tunneling, erosion, or cavitation [17]. Bacterial decomposition in soil and above ground is slower than decomposition caused by fungi in similar applications [18].

Various techniques have been developed to assess the condition of waterlogged wood [19]. The basic principles are based on visual assessments and the use of simple tools such as needles and a knife [20]. The mechanical properties of piles in situ can also be assessed using resistance drilling and penetrometers such as the pylodine. These techniques are concerned with wood density, which is closely related to porosity and maximum water content [21]. There are numerous reports on the use of a wide range of analytical techniques, from pH measurements [22] to thermogravimetric techniques (TGA, DSC, DMA) [23,24] to X-ray-based measurements (XRD) and spectroscopic and chromatographic methods (FTIR, HPLC, GCMS) [25,26]. Some of the classical tools in wood analysis are different types of microscopy (SEM, confocal, light microscopy) and imaging techniques (MRI) [25]. The choice of technique depends on the expected results and the hypothesis. Moreover, it should be taken into account that the research object is a cultural heritage; therefore, less invasive techniques are preferred.

The respective manuscript aims to analyse the properties of wooden piles installed 125 years ago. During the period in question, many buildings were built or reconstructed in Ljubljana, as Ljubljana was affected by a devastating earthquake that destroyed several buildings. Thus, the respective case study could serve as an assessment of the state of other piles in Ljubljana. Moreover, many of these buildings are considered part of the cultural heritage, and therefore the protection of wooden piles is important to protect objects of cultural significance.

## 2. Materials and Methods

### 2.1. Material

An 1895 building (old school) (Figure 1) was analysed in detail before renovation. Due to the soft terrain, the building was constructed on wooden foundation piles. The piles were 2 m below ground level and were constantly wet. After 125 years, the top layer (2 m deep) of soil was removed, and five piles were examined in several locations (at the edges) of the building. The water level was about 50 cm above the piles at the time of the measurements. Pieces of wood were cut from the piles with an axe and knife. Multiple samples (2–3) per pile were isolated to represent the pile conditions. Isolated samples were put in plastic bags with an excess of water to prevent drying. Samples were stored at 5 °C approximately 2 h after isolation and kept in the fridge until the analysis. Samples were of uneven shape. The volume varied between 2 cm<sup>3</sup> to 10 cm<sup>3</sup>. For comparison, the sapwood of Scots pine (*Pinus sylvestris*) was used.



**Figure 1.** Old school in Ljubljana prior to renovation.

### 2.2. Resistograph and Screw Withdrawal Measurements

The structural condition of the wooden foundation piles was quantified by resistograph measurements (PD 500, IML, Wiesloch, Germany). The resistograph analysis was carried out in October 2020. A resistograph is a high-resolution needle-drill resistance measuring device. A thin, steel needle is driven into the wood. During drilling, the energy required is measured as a function of the depth of the needle. The resistograph instrument provides a high linear correlation between the readings and the wood's density being drilled through. Even internal decay can be easily detected. A 1.5 mm diameter drilling needle with a needle tip diameter of 2.0 mm was used [27,28]. Multiple measurements were taken on five piles. On the same piles, screw withdrawal measurements were also performed using a Fakopp instrument (Fakopp Enterprise Bt, Agfalva, Hungary). The screw size was 4 mm in diameter, and the length of the threads was 18 mm. Since the withdrawal force depends slightly on the test speed, a speed of 0.5 mm/s was used. At the end of the measurement, the maximum force was determined [29]. For comparison, measurements were performed on wet Scots pine wood as well.

### 2.3. Density and DVS Analysis

The envelope density of oven-dry wood was determined using GeoPyc 1365 (Micromeritics, Unterschleissheim, Germany). The envelope density was measured on 15 wood samples (average dry mass 0.7 g). The GeoPyc is a dry and void-filling method using a free-flowing solid, compression, and a displacement measurement technique. Instead of Hg, a free-flowing solid Dry Flo (registered trademark, Micromeritics Instrument Corporation) was used. First, the sample chamber was filled with Dry Flo only; under rotating movement and the desired pressure, the volume of sand was calculated. Second, the sample was positioned in Dry Flo, and the sand was agitated and gently consolidated around the sample. The envelope volume of the sample was calculated from the difference in volume between the two measurements. A 19.1 mm inner diameter chamber was chosen to perform the envelope density determination of the wooden samples. A recommended consolidation force of 28 N and a conversion factor of  $0.1284 \text{ cm}^3/\text{mm}$  was used for this chamber. As recommended by the operating manual, this force was low enough not to damage the wood structure [30,31].

The sorption isotherms of the pile sample were determined using a DVS Intrinsic instrument (DVS Intrinsic, Surface Measurement Systems Ltd., London, UK). Before the experiment, the sample was conditioned for at least 24 h at  $20 \pm 0.2 \text{ }^\circ\text{C}$  and  $1 \pm 1\% \text{ RH}$ . For analysis, a small amount (approximately 40 mg) of the milled sample was placed on the sample holder and suspended in a microbalance within a sealed, thermostatically controlled chamber in which a constant flow of dry compressed air was passed over the sample at a flow rate of  $200 \text{ cm}^3/\text{s}$  and a temperature of  $25 \pm 0.1 \text{ }^\circ\text{C}$  throughout the RH

range. The DVS method was set to 20 steps of 5% between 0% and 95% RH for both the sorption and desorption steps. Two full isothermal runs were performed to capture the material's sorption behaviour fully; however, only one cycle is presented in the respective study. The instrument held a constant target RH until the rate of change of sample moisture content ( $dm/dt$ ) was less than 0.002% per minute for 10 min. The run time, target RH, actual RH, and sample weight was recorded every 20 s throughout the isothermal run. Sorption and desorption isotherms were constructed by plotting the change in equilibrium moisture content (EMC) against relative humidity (RH). Additionally, the drying dynamics were determined for the water-saturated sample. A small piece of wet wood (approximately 45 mg) was placed on the sample holder and exposed in the chamber with the conditions described above. The only difference was that in this case the sample was passed over with compressed air of 0% RH until the rate of change of the sample moisture content ( $dm/dt$ ) was less than 0.002% per minute over a period of 10 min.

#### 2.4. Chemical Analysis

Diffuse reflectance infrared Fourier transform spectra (DRIFT) were recorded between  $4000\text{ cm}^{-1}$  and  $450\text{ cm}^{-1}$  with a PerkinElmer FTIR Spectrum Two spectrometer (Waltham, MA, USA) using diamond ATR (PerkinElmer, Waltham, MA, USA). The spectra were recorded at a resolution of  $1\text{ cm}^{-1}$  and 16 scans. FTIR spectra were normalised based on the lignin peak at  $1505\text{ cm}^{-1}$  [32].

For the determination of Klason lignin, 1 g of the sample was used. The sample was placed in a 50 mL beaker and mixed with 72%  $\text{H}_2\text{SO}_4$ . After 2 h, the mixture was diluted with distilled water to obtain a 3% aqueous  $\text{H}_2\text{SO}_4$  solution and heated for another 4 h. The next day, the solution was filtered through filter paper. The filter paper containing the lignin was dried at  $103 \pm 2\text{ }^\circ\text{C}$  for 24 h and weighed. Then, the lignin content was calculated [33,34]. The lignin content was determined on three parallel samples from three poles.

The pH of the wood was determined by an extraction method. Wood samples (2 g) were ground into sawdust that could pass through a 40-mesh sieve. The sawdust was then immediately added to 50 mL of boiling deionised water (pH = 6.5) and stirred for 5 min in an Erlenmeyer flask with reflux. The mixture stood in the closed Erlenmeyer flask for 30 min and was then rapidly cooled to room temperature. The extract was then filtered, and the pH of the solution was measured using a glass electrode [35]. The experiment was carried out in three parallel measurements.

#### 2.5. Microscopic Analysis

Light microscopy was performed on specimens oriented in all three anatomical planes and containing at least one tree ring. The specimens were dehydrated in a graded ethanol series (70, 90, 95, and 100%), cleaned with D-limonene, and embedded in paraffin blocks (tissue processor Leica TP1020-1, Nussloch, Germany). Thin sections (9  $\mu\text{m}$  thick) were cut using a semi-automatic rotary microtome RM 2245 (Leica, Nussloch, Germany), stained with a safranin and astra blue solution and mounted in Euparal (Gladwick St, Compton, CA 90220, USA). Slides were observed under a Nikon Eclipse 800 light microscope and photomicrographs were taken by a digital camera (DS-Fi1) connected to a NISElements BR 3 image analysis system (Melville, NY, USA).

Scanning electron microscopy (SEM) was performed to reveal detailed anatomical features of the three-dimensional structure of the wood. Specimens were cut into  $1\text{ cm}^3$  cubes, ensuring that they were oriented in all three anatomical planes. The surfaces were planed using a sliding microtome equipped with a new disposable blade. Specimens were dried and coated with gold (Q150R ES Coating System Quorum technologies, Laughton, UK) for 30 s at 20 mA intensity. SEM micrographs were then taken at high vacuum and low voltage (between 5 and 12.5 kV). A large field detector (LFD) and a concentric backscatter detector (CBS) were used in an FEI Quanta 250 SEM microscope (Hillsboro, OR, USA). Observations were performed at a working distance between 8 and 10 mm. Energy-

dispersive X-ray spectroscopy (EDX) analysis was made using a TEAM EDS analysis system (EDAX, AMETEK Inc., Berwyn, PA, USA). The point analysis, performed at a voltage of 20 kV, allowed the identification of the elements present on the sample surface, in particular, we detected calcium (by X-ray energy  $K\alpha$  at 3.69 keV), sulfur (by X-ray energy  $K\alpha$  at 2.30 keV), and iron (by X-ray energy  $K\alpha$  at 6.39 keV).

### 3. Results and Discussion

The soil in the vicinity of the piles was classified as histosol and humic gleysol on clay. The layer from which samples were isolated was moist, unstructured, smeary, clayey, mineral, strongly carbonate (type 5Y4/1). The pH was about 8 [36]. It should be noted that the soil layers in the marginal areas were mixed during construction and remediation works. Therefore, this layer contained more organic material (peat) and construction debris than the surrounding soil. The average temperature at 100 cm depth varied from 3.7 °C (February) to 20.1 °C (August) (Figure 2).

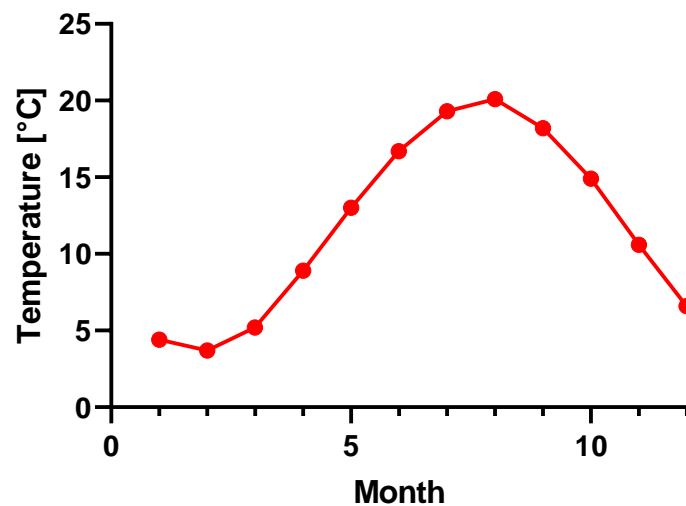


**Figure 2.** Average soil temperature 100 cm below the layer in Ljubljana in the period between 1961–2016 [37].

The structural health of the piles was assessed with resistograph and screw withdrawal force measurements. These measurements were carried out in situ. Resistance drilling is frequently used for decay assessment, but in the respective study, data were linked to chemical composition as well. It should be taken into account that the wood was saturated with water. It is well known that wood's mechanical properties are significantly affected by moisture content (MC) [38]. However, increased MC is not the only reason for a decrease in mechanical properties. The blue curve in Figure 3 represents the typical resistograph curve. This reference curve was determined on a freshly cut Scots pine (*Pinus sylvestris*) representative beam [39]. MC of this beam was above fibre saturation to have comparable moisture conditions with wooden piles. The annual rings and the pith were resolved in the respective curves. The red curves in Figure 3 represent measurements taken on the piles. Three typical measurements are shown. Measurement one (Figure 3, pile 1) shows the pile where one part of the pile was severely degraded while the other part was less degraded. Although the heartwood of Scots pine has better durability than sapwood [40,41], no difference was found between the degradation rate of sapwood and heartwood. However, as shown in the other resistograph measurements (Figure 3, piles 1 and 2), all piles' parts were significantly degraded. As can be seen from resistograph measurements, pile 3 was less degraded. As the piles were located in comparable conditions, we could not determine the reasons for this difference. The key reason is presumably heterogeneity of the wood used and variations in micro-locations. It should be considered that piles were not in direct contact with each other.



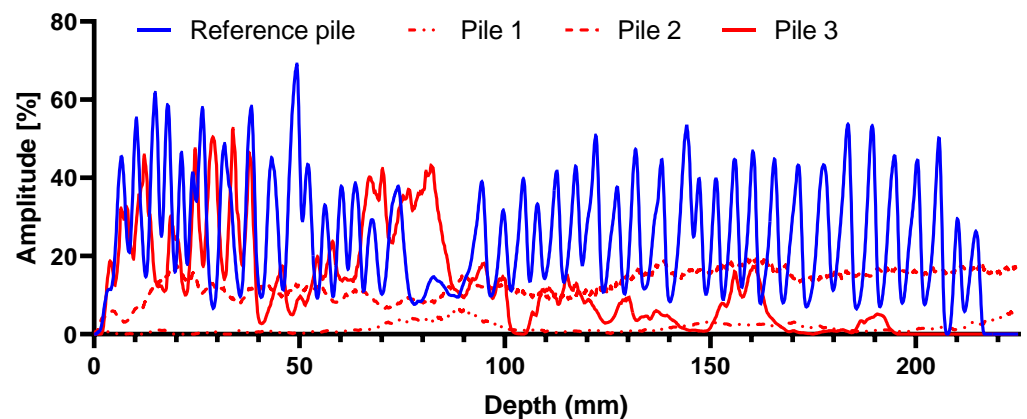


Figure 3. Resistograph analysis of pine piles and reference Scots pine trunk.

Resistograph measurements were in line with the screw withdrawal force (SWF) measurements. The SWF determined on the reference pine beam was 2060 N, while the SWF determined on wooden piles was only 272 N (Figure 4). This value was about 13% of the value determined on fresh wood. Both methods, resistograph and SWF, indicate that the wood was significantly degraded. However, it should be considered that the measurements were made on the upper part of the wooden piles. Literature data indicate that the upper parts are more exposed to biodegradation than the part of the piles deeper in the soil [6]. It can therefore be assumed that the worst part of the piles was analysed.

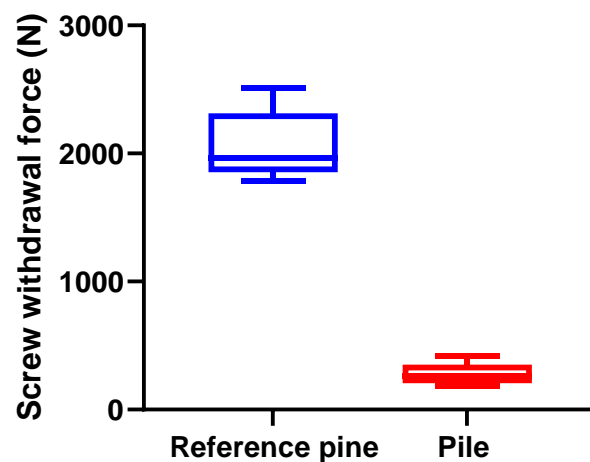
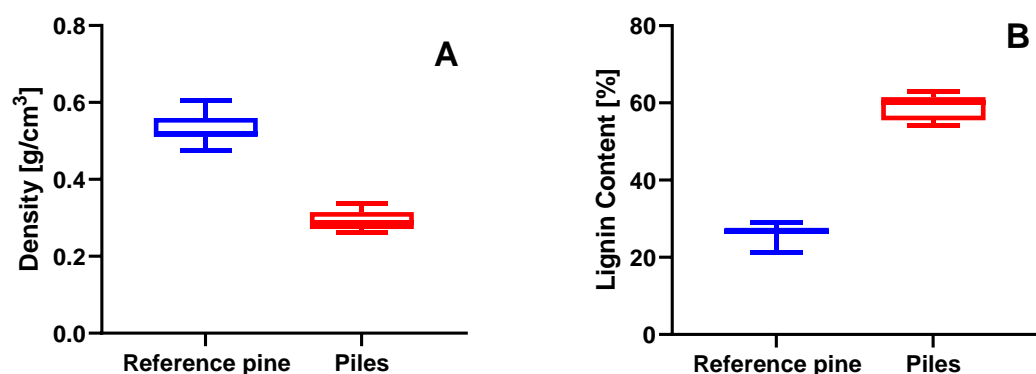


Figure 4. Screw withdrawal force measurements on pine pile and reference Scots pine trunk.

The decay of the piles was also confirmed visually. When isolated, the colour of the wood was white, and after a few minutes, it became grey. The wood had a fibrous, spongy texture, with no distinct odour. Cutting was easy, and the wood did not present much resistance. Decay is usually reflected in density, especially since the wood was saturated with water and carefully dried to prevent collapse before densities were determined. The density of the reference pine was  $532 \text{ kg/m}^3$ . This value is in line with literature data [42]. However, the density of the wood from the piles was significantly lower. The average density of the wood from the piles was  $296 \text{ kg/m}^3$  (Figure 5A). This confirms that the piles were highly degraded. Chemical analysis confirmed the results obtained by the other methods of investigation. The lignin content in the pinewood was 26.7% (Figure 5B). However, due to the general depletion of cellulose and hemicelluloses [13], the piles' relative lignin content increased (58.8%). These values are still slightly lower than the lignin content in the Bronze Age piles from a nearby location. The lignin content in 4500- to 5700-year-old Bronze Age piles ranged from 63.8% to 70.3% [43]. The pH of the degraded wood was 7.1 and corresponded with the pH of the surrounding soil [36]. On the other

hand, the pH of reference Scots pine sapwood (pH = 4.68) and heartwood (pH = 5.02) was considerably lower. Scots pine pH values were in line with literature data [44].



**Figure 5.** The density (A) and lignin content (B) of oven-dried pine pile and reference Scots pine sapwood.

The degradation of cellulose and hemicelluloses was also reflected in the FTIR spectra (Figure 6). The most notable change was the disappearance of the  $1725\text{ cm}^{-1}$  peak, which was assigned to C=O stretching in hemicelluloses [32]. Additionally, changes were also observed in other peaks assigned to cellulose and hemicelluloses, namely:  $1453\text{ cm}^{-1}$ ,  $1230\text{ cm}^{-1}$ ,  $1160\text{ cm}^{-1}$ ,  $1050\text{ cm}^{-1}$ , and  $895\text{ cm}^{-1}$  [45,46]. Peaks assigned to lignin were less affected (Figure 6). This is in line with the lignin content and typical patterns of soft-rot decay [47].

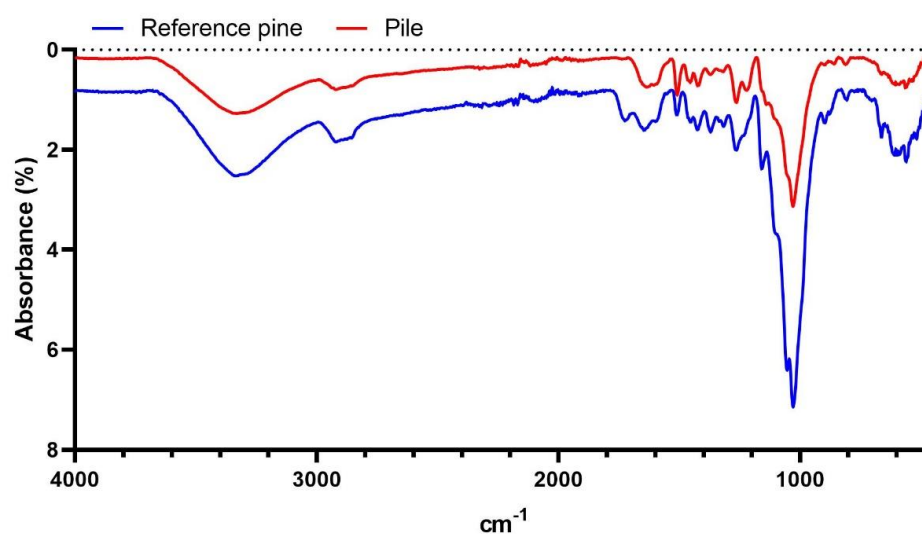


**Figure 6.** FTIR spectra of pine pile and reference Scots pine sapwood.

The moisture content of waterlogged wood was very high. DVS analysis showed that the MC of waterlogged wood ranged from 450% to 500% (Figure 7B). This is typical of water-saturated wood as it decomposes and reduces density (Figure 5). Similar high MCs are also reported in the literature [8,43]. As shown in Figure 7B, the mass loss during drying in the DVS device was linear, indicating that the water was not bound in the wood. Drying slowed down below fibre saturation. The wooden piles' chemical changes were reflected in the increased equilibrium moisture content during both sorption and desorption cycles. For example, the reference pine's EMC at 95% RH was 25.93%, while the EMC of the pile at the same RH was 23.79%. Similar differences were also observed at other RH (Figure 7A). This phenomenon has been reported previously [12,48] and may be attributed to partial depolymerisation of lignin, greater amorphous cellulose content, and consequent greater availability of OH groups [49].

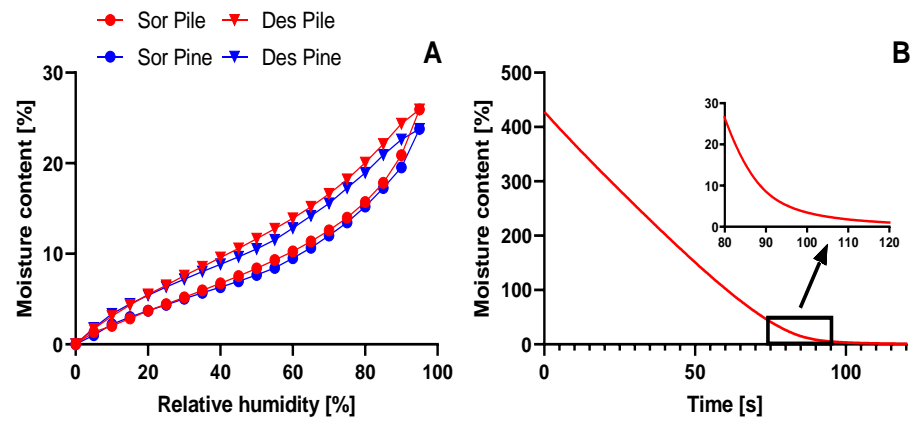


**Figure 7.** (A) Sorption (Sor) and desorption (Des) curves of pine pile and reference Scots pine sapwood. (B) Drying pattern of the fresh pile sample.

Finally, the degradation of the wood was confirmed by light and scanning electron microscopy. Light microscopy analysis confirmed that the piles were made of Scots pine (Figure 8). Predominantly in the latewood cells, the typical soft-rot decay pattern can be seen as described previously [17]. The S2 layer was absent in most of the tracheids, except for a very few latewood tracheids.

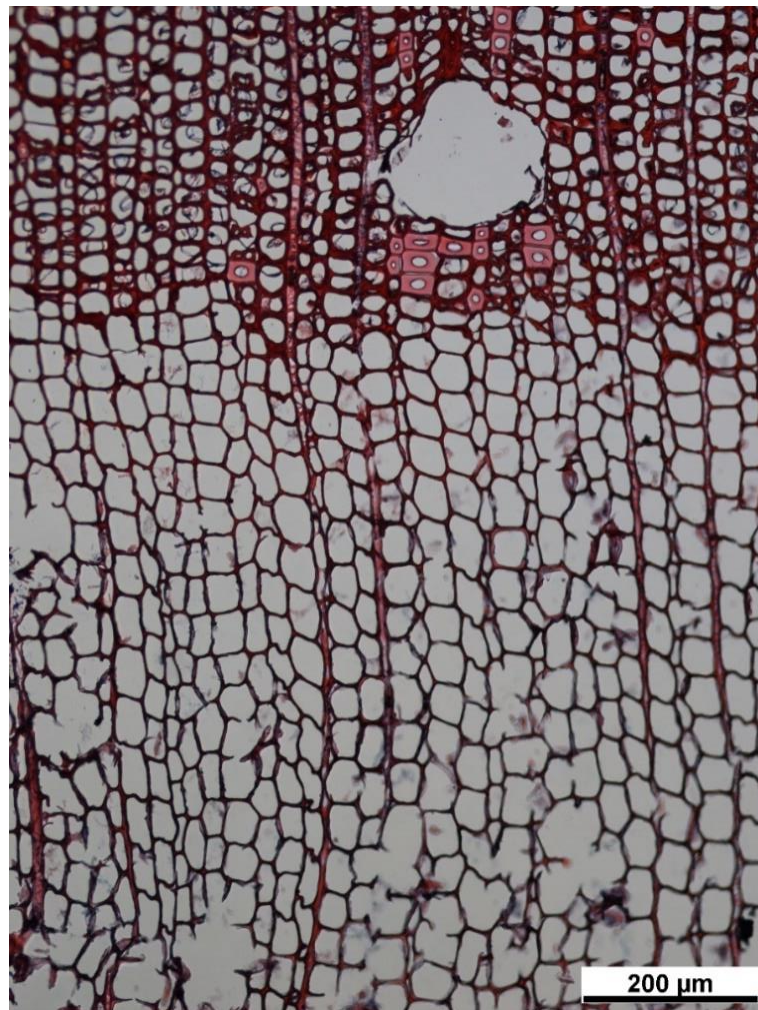


**Figure 8.** Light microscope image of the cross-section of a 125-year-old wooden pile.

The SEM analysis proved the typical soft-rot decay, as can be seen in Figures 9 and 10. The S2 layer in the tracheids of the latewood cells of the wooden pile was wholly decayed. In contrast, the middle lamellas were less affected. This was consistent with the chemical analysis. Middle lamellas were predominately lignin, whereas more cellulose was present in the S2 layer of tracheids [44]. The S2 layer was too degraded to distinguish between Type I and Type II soft rot.

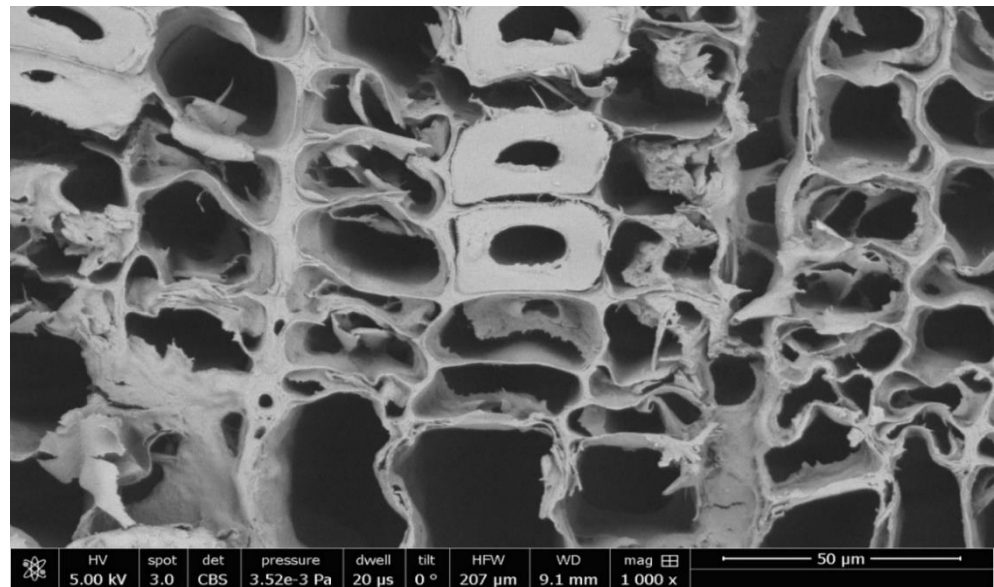


**Figure 9.** Scanning electron microscopy image of the cross-section of the latewood cells of the wooden pile.

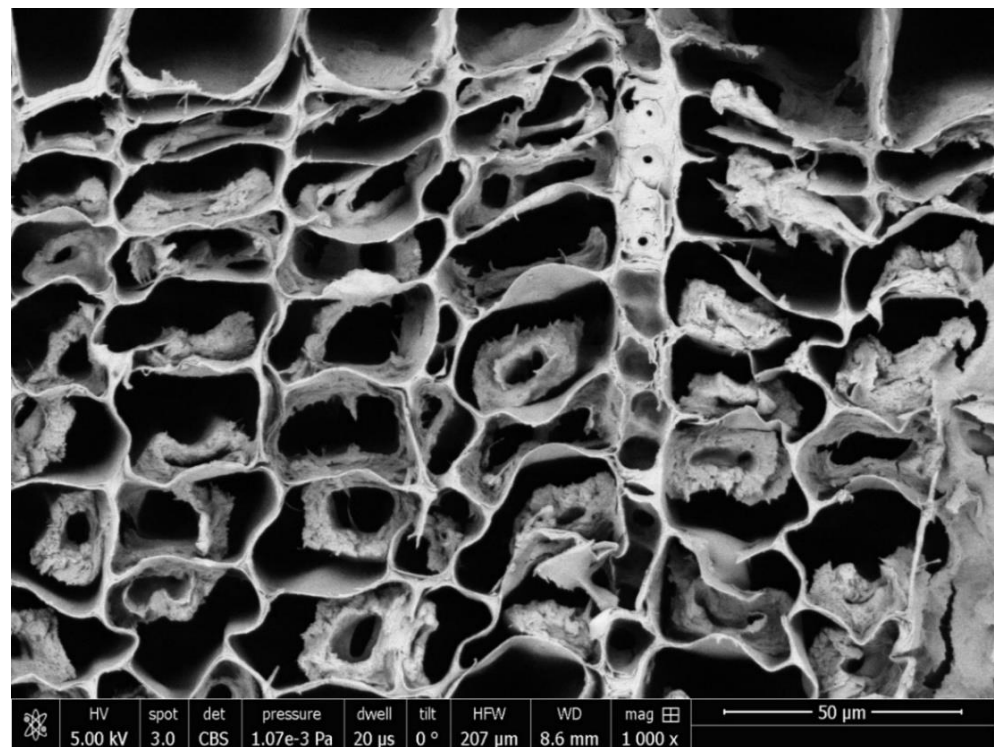


**Figure 10.** Scanning electron microscopy image of the cross-section of the latewood cells of the wooden pile.

Although no bacteria were detectable in the degraded wood, we noted several spherical structures in the wood cell walls (Figure 11). EDX analysis of the crystals confirmed

the presence of sulfur, iron, and calcium. Chemical analysis of the crystals showed that these structures could be of bacterial origin [50]. This process is known as biomineralisation, the chemical alteration of an environment by microbial activity leading to minerals' precipitation. The most important bacteria associated with biomineralisation belong to the *Bacillus* sp. and *Lysinibacillus* sp. More than 60 different biological minerals have been reported as a result of biomineralisation [51]. However, these minerals are not an explicit confirmation of bacterial decay, but an indication that the bacteria were somehow involved in the respective piles' degradation.

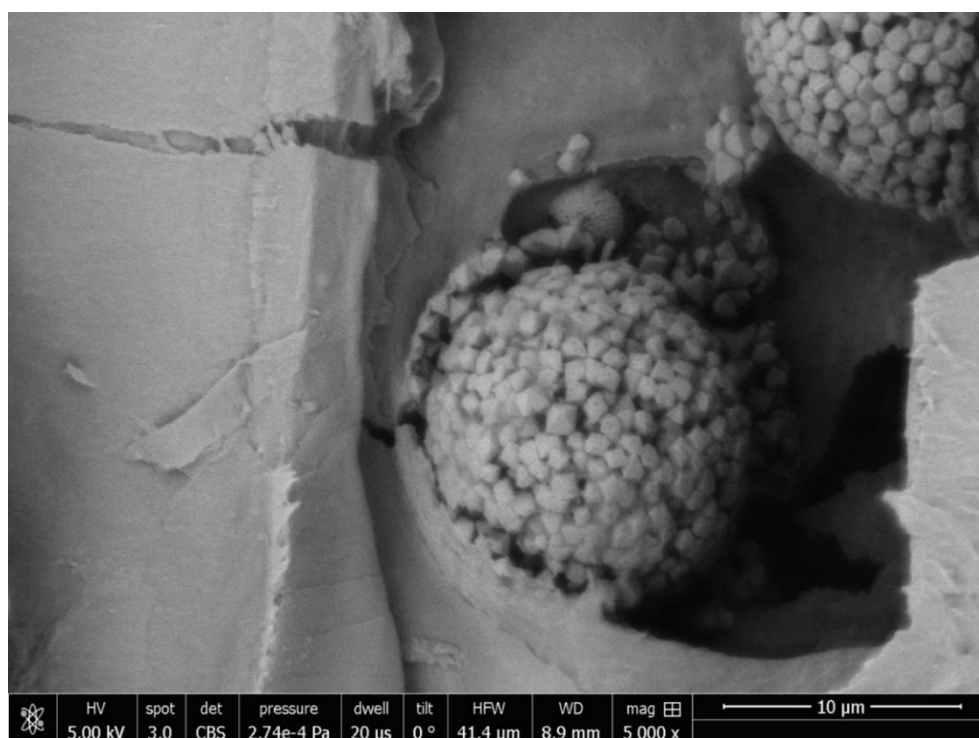


**Figure 11.** Scanning electron microscopy image of the spherical form in the wood cells.

It has been reported in the literature that artificial mineralization of wood yields materials with improved mechanical properties compared to natural wood when mineralization is carried out to a higher degree [52]. Wood modification processes have been developed that take advantage of this principle and are used to consolidate building materials [53]. However, in waterlogged piles, mineralization does not appear to be sufficient enough to lead to significantly improved mechanical properties. However, further studies could clarify the role of deposited crystals on the mechanical properties of waterlogged wood. On the other hand, the bacteria associated with mineralization to strengthen the wood could be increased with the biological mechanisms. The consolidation of a foundation is a challenging task. Different strategies have been developed depending on the historical value and quality of the structure. First, the mass of a building should not be increased, which should be considered during renovation. If necessary, concrete beams should be placed under the building and new piles should be installed under the beams to support the building.

#### 4. Conclusions

One hundred and twenty-five years of exposure of Scots pine piles to waterlogged conditions in Ljubljana resulted in severe degradation. The waterlogged wood became saturated with water. SEM and light microscopy confirmed that soft rot was the main cause of wood decay in the buried piles. Soft rot is typical for waterlogged wood, but the decay of the piles in question was more rapid than reported in some of the previous case

studies. The decay resulted in reduced density, a relative increase in lignin content, and a loss of mechanical properties. Chemical and morphological changes resulted in increased hygroscopicity. Due to the degradation of the piles, special attention should be paid to the reconstruction of the building. Only low-density material should be used, and the piles should be consolidated somehow.

Based on the analysis performed, we can conclude that resistance drilling provides useful insight into waterlogged piles. Microscopy and FTIR could serve as an additional method of validation. Suppose the measurements cannot be made by resistance drilling. In this case, screw withdrawal could be used as a partial alternative, as the results reflect only the properties of the outer parts of the piles.

In Ljubljana and its surroundings, there are about 10,000 buildings constructed in the corresponding period. Approximately 30% of them were built on piles. It can be assumed that these buildings face the same problems as the corresponding case study.

**Author Contributions:** Conceptualisation, M.H.; methodology, M.H.; validation, M.H., D.K., and B.L.; formal analysis, A.B., D.K., and B.L.; investigation, A.B., D.K., and B.L.; resources, M.H.; data curation, M.H.; writing—original draft preparation, M.H.; writing—review and editing, A.B., D.K., and B.L.; visualisation, M.H.; supervision, M.H.; project administration, M.H. and B.L.; funding acquisition, M.H. All authors have read and agreed to the published version of the manuscript.

**Funding:** The authors acknowledge the financial support of the Slovenian Research Agency (ARRS) within research program P4-0015 (Wood and lignocellulosic composites) and the infrastructural centre (IC LES PST 0481-09). Part of the published research was also supported by project Durasoft, founded in the frame of the program Interreg Italia-Slovenija 2014–2020.

**Institutional Review Board Statement:** Not applicable.

**Informed Consent Statement:** Not applicable.

**Data Availability Statement:** Data are available at repository of University of Ljubljana, upon request.

**Acknowledgments:** Authors would like to acknowledge the technical support during chemical and density analysis of Andreja Žagar, Blaž Jemec, and Samo Grbec.

**Conflicts of Interest:** The authors declare no conflict of interest.

## References

- Shabani, A.; Kioumars, M.; Plevris, V.; Stamatopoulos, H. Structural vulnerability assessment of heritage timber buildings: A methodological proposal. *Forests* **2020**, *11*, 881. [CrossRef]
- Heumüller, M. Erosion and archaeological heritage protection in lake constance and lake zurich: The interreg iv project “erosion und denkmalschutz am bodensee und zürichsee”. *Consero. Manag. Archaeol. Sites* **2012**, *14*, 48–59.
- Cufar, K.; Levanic, T.; Veluscek, A.; Kromer, B. First chronologies of the Eneolithic pile dwellings from the Ljubljana moor, Slovenia. *Dendrochronologia* **1997**, *15*, 39–50.
- Klaassen, R.K.W.M. Bacterial decay in wooden foundation piles—Patterns and causes: A study of historical pile foundations in the Netherlands. *Int. Biodeterior. Biodegrad.* **2008**, *61*, 45–60. [CrossRef]
- Jeraj, M.; Velušček, A.; Jacomet, S. The diet of Eneolithic (Copper Age, Fourth millennium cal b.c.) pile dwellers and the early formation of the cultural landscape south of the Alps: A case study from Slovenia. *Veg. Hist. Archaeobot.* **2009**, *18*. [CrossRef]
- Elam, J.; Björdal, C. A review and case studies of factors affecting the stability of wooden foundation piles in urban environments exposed to construction work. *Int. Biodeterior. Biodegrad.* **2020**, *148*, 104913. [CrossRef]
- Curtis, D.R.; Campopiano, M. Medieval land reclamation and the creation of new societies: Comparing Holland and the Po Valley, c.800–c.1500. *J. Hist. Geogr.* **2014**, *44*, 93–108. [CrossRef]
- Fejfer, M.; Majka, J.; Zborowska, M. Dimensional Stability of Waterlogged Scots Pine Wood Treated with PEG and Dried Using an Alternative Approach. *Forests* **2020**, *11*, 1254. [CrossRef]
- Humar, M.; Lesar, B.; Kržišnik, D. Tehnična in estetska življenjska doba lesa. *Acta Silvae et Ligni* **2020**, *121*, 33–48. [CrossRef]
- Klaassen, R.K.W.M.; Creemers, J.G.M. Wooden foundation piles and its underestimated relevance for cultural heritage. *J. Cult. Herit.* **2012**, *13*, 123–128. [CrossRef]
- Terziev, N.; Nilsson, T. Effect of soluble nutrient content in wood on its susceptibility to soft rot and bacterial attack in ground test. *Holzforschung* **1999**, *53*, 575–579. [CrossRef]
- García-Iruela, A.; Esteban, L.G.; Fernández, F.G.; de Palacios, P.; Rodríguez-Navarro, A.B.; Sánchez, L.G.; Hosseinpourpia, R. Effect of degradation on wood hygroscopicity: The case of a 400-year-old coffin. *Forests* **2020**, *11*, 712. [CrossRef]

13. Blanchette, R.A. A review of microbial deterioration found in archaeological wood from different environments. *Int. Biodeterior. Biodegrad.* **2000**, *46*, 189–204. [CrossRef]
14. Savory, J.G. Breakdown of timber by ascomycetes and fungi imperfecti. *Ann. Appl. Biol.* **1954**, *41*, 336–347. [CrossRef]
15. Zabel, R.A.; Morrell, J.J. *Wood Microbiology: Decay and Its Prevention*, 2nd ed.; Academic Press: Amsterdam, The Netherlands, 2020.
16. Schmidt, O. *Wood and Tree Fungi: Biology, Damage, Protection, and Use*; Springer: Berlin/Heidelberg, Germany, 2006.
17. Kim, Y.S.; Singh, A.P. Micromorphological characteristics of wood biodegradation in wet environments: A review. *IAWA J.* **2000**, *21*, 135–155. [CrossRef]
18. Daniel, G.; Nilsson, T. Developments in the study of soft rot and bacterial decay. In *Forest Products Biotechnology*; Taylor & Francis: Abingdon, UK, 1998; pp. 37–62.
19. Lucejko, J.J.; Modugno, F.; Ribechini, E.; Tamburini, D.; Colombini, M.P. Analytical instrumental techniques to study archaeological wood degradation. *Appl. Spectrosc. Rev.* **2015**, *50*, 584–625. [CrossRef]
20. High, K.E.; Penkman, K.E.H. A review of analytical methods for assessing preservation in waterlogged archaeological wood and their application in practice. *Herit. Sci.* **2020**, *8*, 1–33. [CrossRef]
21. Macchioni, N.; Pizzo, B.; Capretti, C.; Giachi, G. How an integrated diagnostic approach can help in a correct evaluation of the state of preservation of waterlogged archaeological wooden artefacts. *J. Archaeol. Sci.* **2012**, *39*, 3255–3263. [CrossRef]
22. Chelazzi, D.; Giorgi, R.; Baglioni, P. Nanotechnology for Vasa wood de-acidification. *Macromol. Symp.* **2006**, *238*, 30–36. [CrossRef]
23. Pizzo, B.; Pecoraro, E.; Lazzeri, S. Dynamic mechanical analysis (DMA) of waterlogged archaeological wood at room temperature. *Holzforschung* **2018**, *72*. [CrossRef]
24. Romagnoli, M.; Galotta, G.; Antonelli, F.; Sidoti, G.; Humar, M.; Kržišnik, D.; Čufar, K.; Davidde Petriaggi, B. Micro-morphological, physical and thermogravimetric analyses of waterlogged archaeological wood from the prehistoric village of Gran Carro (Lake Bolsena-Italy). *J. Cult. Herit.* **2018**, *33*, 30–38. [CrossRef]
25. Xia, Y.; Chen, T.Y.; Wen, J.L.; Zhao, Y.L.; Qiu, J.; Sun, R.C. Multi-analysis of chemical transformations of lignin macromolecules from waterlogged archaeological wood. *Int. J. Biol. Macromol.* **2018**, *109*, 407–416. [CrossRef] [PubMed]
26. Lucejko, J.J.; Tamburini, D.; Zborowska, M.; Babiński, L.; Modugno, F.; Colombini, M.P. Oak wood degradation processes induced by the burial environment in the archaeological site of Biskupin (Poland). *Herit. Sci.* **2020**, *8*. [CrossRef]
27. Kržišnik, D.; Brischke, C.; Lesar, B.; Thaler, N.; Humar, M. Performance of wood in the Franja partisan hospital. *Wood Mater. Sci. Eng.* **2019**, *14*, 24–32. [CrossRef]
28. Frontini, F. In situ evaluation of a timber structure using a drilling resistance device. Case study: Kjøpmannsgata 27, Trondheim (Norway). *Int. Wood Prod. J.* **2017**, *8*, 14–20. [CrossRef]
29. Xue, S.; Zhou, H.; Liu, X.; Wang, W. Prediction of compression strength of wood usually used in ancient timber buildings by using resistograph and screw withdrawal tests. *Wood Res.* **2019**, *64*, 249–260.
30. Macias, K.A.; Carvajal, M.T. The influence of granule density on granule strength and resulting compact strength. *Chem. Eng. Sci.* **2012**, *72*, 205–213. [CrossRef]
31. Micromeritics Instrument Corporation. *GeoPyc 1365 Operator Manual*; Micromeritics Instrument Corporation: Norcross, GA, USA, 2017.
32. Mitchell, A.J.; Watson, A.J.; Higgins, H.G. An infrared spectroscopic study of delignification of *Eucalyptus regnans*. *Tappi* **1965**, *48*, 520–532.
33. Humar, M.; Fabčić, B.; Zupančič, M.; Pohleven, F.; Oven, P. Influence of xylem growth ring width and wood density on durability of oak heartwood. *Int. Biodeterior. Biodegrad.* **2008**, *62*, 368–371. [CrossRef]
34. Yasuda, S.; Fukushima, K.; Kakehi, A. Formation and chemical structures of acid-soluble lignin I: Sulfuric acid treatment time and acid-soluble lignin content of hardwood. *J. Wood Sci.* **2001**, *47*, 69–72. [CrossRef]
35. Humar, M.; Petrič, M.; Pohleven, F. Changes of the pH value of impregnated wood during exposure to wood-rotting fungi. *Holz als Roh- und Werkstoff* **2001**, *59*, 288–293. [CrossRef]
36. Repe, B. Classification of soils in Slovenia. *Soil Sci. Annu.* **2020**, *71*, 158–164. [CrossRef]
37. Agencija Republike Slovenije za Okolje/Slovenian Environmental Agency. Archives of Meteorological Data. Available online: <http://meteo.arso.gov.si/met/sl/archive/> (accessed on 17 January 2021).
38. Chafe, S.C. Wood-water relations. *For. Ecol. Manag.* **1990**, *31*, 121–123. [CrossRef]
39. Poljanšek, S.; Jevšenak, J.; Gričar, J.; Levanič, T. Seasonal radial growth of Black pine (*Pinus nigra* Arnold) from Bosnia and Herzegovina, monitored by the pinning method and manual band dendrometers. *Acta Silvae et Ligni* **2019**, *119*, 1–11. [CrossRef]
40. European Committee for Standardisation. *Durability of Wood and Wood-Based Products—Natural Durability of Solid Wood: Guide to Natural Durability and Treatability of Selected Wood Species of Importance in Europe*; European Committee for Standardisation: Brussels, Belgium, 1994.
41. Brischke, C.; Meyer, L.; Alfredsen, G.; Humar, M.; Francis, L.; Flæte, P.-O.; Larsson-Brelid, P. Natural durability of timber exposed above ground—A survey. *Drv. Ind.* **2013**, *64*, 113–129. [CrossRef]
42. Wagenfuhr, R. *Holzatlas*; Fachbuchverlag: Leipzig, Germany, 2007.
43. Čufar, K.; Tišler, V.; Gorišek, Ž. Arheološki les—Njegove lastnosti in raziskovalni potencial. *Arheol. Vestn.* **2002**, *53*, 69–75.
44. Fengel, D.; Wegener, G. *Wood: Chemistry, Ultrastructure, Reactions*; Walter de Gruyter: Berlin, Germany; New York, NY, USA, 2011.
45. Hemmingson, J.; Wong, H. Characterization of photochemically degraded newsprint solubles by <sup>13</sup>C NMR and IR spectroscopy. *Holzforschung* **1989**, *43*, 141–147. [CrossRef]





46. Woźniak, M.; Kwaśniewska-Sip, P.; Krueger, M.; Roszyk, E.; Ratajczak, I. Chemical, biological and mechanical characterization of wood treated with propolis extract and silicon compounds. *Forests* **2020**, *11*, 907. [CrossRef]
47. Blanchette, R.A.; Cease, K.R.; Abad, A.R.; Koestler, R.J.; Simpson, E.; Sams, G.K. An evaluation of different forms of deterioration found in archaeological wood. *Int. Biodeterior.* **1991**, *28*, 3–22. [CrossRef]
48. Ghavidel, A.; Hosseinpourpia, R.; Militz, H.; Vasilache, V.; Sandu, I. Characterization of Archaeological European White Elm (*Ulmus laevis* P.) and Black Poplar (*Populus nigra* L.). *Forests* **2020**, *11*, 1329. [CrossRef]
49. Esteban, L.G.; De Palacios, P.; Fernández, F.G.; Guindeo, A.; Conde, M.; Baonza, V. Sorption and thermodynamic properties of juvenile *Pinus sylvestris* L. wood after 103 years of submersion. *Holzforschung* **2008**, *62*, 745–751. [CrossRef]
50. Anbu, P.; Kang, C.H.; Shin, Y.J.; So, J.S. Formations of calcium carbonate minerals by bacteria and its multiple applications. *SpringerPlus* **2016**, *5*, 1–26. [CrossRef] [PubMed]
51. Sarikaya, M. Biomimetics: Materials fabrication through biology. *Proc. Natl. Acad. Sci. USA* **1999**, *96*, 14183–14185. [CrossRef] [PubMed]
52. Merk, V.; Chanana, M.; Keplinger, T.; Gaan, S.; Burgert, I. Hybrid wood materials with improved fire retardance by bio-inspired mineralisation on the nano- and submicron level. *Green Chem.* **2015**, *17*, 1423–1428. [CrossRef]
53. Turk, J.; Pranjić, A.M.; Tomasin, P.; Škrlep, L.; Antelo, J.; Favaro, M.; Škapin, A.S.; Bernardi, A.; Ranogajec, J.; Chiurato, M. Environmental performance of three innovative calcium carbonate-based consolidants used in the field of built cultural heritage. *Int. J. Life Cycle Assess.* **2017**, *22*, 1329–1338. [CrossRef]





Article

# Characterization of Archaeological European White Elm (*Ulmus laevis* P.) and Black Poplar (*Populus nigra* L.)

Amir Ghavidel <sup>1</sup>, Reza Hosseinpourpia <sup>2,\*</sup>, Holger Militz <sup>3</sup>, Viorica Vasilache <sup>4</sup>  
and Ion Sandu <sup>5,6</sup>

<sup>1</sup> Faculty of Geography and Geology, Doctoral School of Geosciences, “Alexandru Ioan Cuza” University of Iasi, 22 Carol I Blvd., 700506 Iasi, Romania; amir.ghavidelesfahlan@student.uaic.ro

<sup>2</sup> Department of Forestry and Wood Technology, Linnaeus University, Lückligns Plats 1, 351 95 Växjö, Sweden

<sup>3</sup> Wood Biology and Wood Products, University of Göttingen, Buesgenweg 4, D-37077 Göttingen, Germany; hmilitz@gwdg.de

<sup>4</sup> ARHEOINVEST Centrum, Institute of Interdisciplinary Research, “Alexandru Ioan Cuza” University of Iasi, 11 Carol I Blvd., 700506 Iasi, Romania; viorica.vasilache@uaic.ro

<sup>5</sup> Academy of Romanian Scientists (AOSR), 54 Splaiul Independentei St., Sect. 5, 050094 Bucharest, Romania; ion.sandu@uaic.ro

<sup>6</sup> Romanian Inventors Forum, 3 Sf.Petru Movila St, Bloc L11, Et, III, Ap. 3, 700089 Iasi, Romania

\* Correspondence: reza.hosseinpourpia@lnu.se

Received: 17 November 2020; Accepted: 10 December 2020; Published: 14 December 2020



**Abstract:** The present study aims at characterization of freshly-cut and archaeological European white elm and poplar. The archaeological elm sample was buried at a depth of 8–10 m inside of soil with age approximation of ~1800–2000 years old, and the archaeological poplar sample was a part of a boat in a freshwater lake or river with age estimation of ~1000–1200 years. Alteration in the chemical structure of the elm and poplar samples due to the ageing process were confirmed by X-ray photoelectron spectroscopy (XPS). Both archaeological wood (AW) samples illustrated considerably lower cellulose crystallinity than the fresh samples as determined by X-ray diffraction. The sorption behavior of AW and fresh wood (FW) samples were evaluated by means of dynamic vapor sorption (DVS) analysis. Results exhibited a higher equilibrium moisture content (EMC) and sorption hysteresis values in archaeological elm and poplar as compared with the fresh samples. Higher hydrophilicity of the AW samples than the FW ones is attributed to their higher amorphous structure. The extensive degradation of AW samples were also confirmed by scanning electron microscopy (SEM) micrographs.

**Keywords:** X-ray photoelectron spectroscopy (XPS); X-ray diffraction (XRD); dynamic vapor sorption (DVS); archaeological wood; wood conservation and preservation

## 1. Introduction

Wood is an important renewable resource, and it has been the most important material in human's life since ancient times with various applications from constructions to furniture and from traditional household occupations to artefacts. The old wood constructions and artefacts represented worldwide are thus an important part of cultural heritage that must be acknowledged, understood, and conserved in accordance with the technical principles and code of ethics [1].

As defined previously, the term of archaeological wood (AW) refers to a dead wood used by an extinct human culture, that may or may not has been modified for or by use, and that was discarded into a specific natural environment [2–4]. Wood, as an organic material, is susceptible to abiotic

and biotic deterioration. Abiotic factors such as weather, fire, and aggressive chemicals degrade the wood structure, and particular changes occur on the surface [5]. Changes in the ambient humidity cause swelling and shrinkage in wood cells, resulting in changes in the cell dimensions over time, as well as slow hydrolysis of polysaccharide compounds, oxidation of lignin, and leaching of degraded products and extractives from the cell walls [2]. While biotic factors are an essential part of the carbon cycle. A number of different microorganisms such as insects, mites, nematodes, fungi, and bacteria can damage the wood structure. Many fungi can degrade the cellulose fibers, but only a limited number of so-called cellulolytic fungi can break down the highly crystalline part of the cellulose. Bacteria, in addition to wood rot spores, can also weaken wood in such a way that substantial strength losses can be encountered. Three types of wood degrading bacteria are known in the literature based on their specific micro-morphological features: tunneling bacteria, erosion bacteria, and cavitation bacteria [6]. Finding has shown that tunneling bacteria (TB) can be present in conditions similar to soft rot, while erosion bacteria (EB) are capable of rotting wood in environments with very low oxygen supply [7]. When wood is submerged underwater or buried in soil, due to the absence of oxygen, the process of so-called wood fossilization is initiated [8]. The rate of wood fossilization and the degradation level of wood polymers increase by the time of deposition [9]. The chemical composition of AW or subfossil wood and the resulting physical and mechanical properties during long-term contact with the soil imply lower cellulose and higher lignin content in fossil wood as compared with FW [8]. Changes in the chemical structure of AW due to environmental elements or application sites have been studied previously [10]. Popescu et al. [11] reported that the chemical structure of archaeological lime obviously changed during the first ageing period, which is normally around 150 years. Lime wood sample showed the highest percentage of carbon atoms and the lowest content of oxygen atoms on the surface. The extractive content of archaeological lime was also considerably reduced because of oxidation and mild hydrolysis. Lucejko et al. [12] studied the degradation processes induced by the burial environment of archaeological oak. The authors quoted that only small chemical transformation of the polysaccharide component, mainly involving hemicelluloses, occurred during the burial time, which could be due to the heterogeneity and inhomogeneity of the natural composition of oak wood. Kacik et al. [13] evaluated the changes in the cellulose, hemicelluloses, lignin, and extractives contents in 108 to 390 years old fir. They observed higher extractive content and lower amount of hemicelluloses in naturally aged fir wood than the fresh wood. Cellulose, lignin, and hemicellulose are known to degrade over time, and the amounts of these elements decrease in the wood, whereas extractives can remain unchanged. It is possible for the wood to absorb chemicals such as limestone, through storing it in the lumens. Still, the initial wood extractives would not increase and are more likely to decrease depending on the burial site [8]. Evaluation of archaeological elm (*Ulmus* sp.) wood with about 350 years old from Chenghuang Temple, China, showed obvious decreases in carbohydrates and lignin contents, deterioration in microstructures, and alteration in micromechanical properties at the surface layer of wood as a result of ageing process or weathering [14]. Bader and co-workers [15] analyzed the chemical compositions and microstructure-mechanics of load-bearing archaeological oak of the Oseberg Viking ship. They reported although hemicelluloses and amorphous cellulose were clearly degraded in AW, the cell wall stiffness was increased, as determined by nanoindentation. It is known that the combination of oxygen and solar radiation rapidly induces oxidation of lignin and hemicelluloses and also depolymerizes the amorphous part of cellulose [16]. The degraded products are water-soluble and will be easily removed from the wood surface by rain, and as a result discoloration of wood surface occurs [8,17,18]. These deterioration mechanisms depend on the conditions that wood is stored and used. However, even under most favorable conditions, a long-term ageing process can degrade the wood polymers [10].

The hygroscopic structure of wood is attributed to the presence of different hydrophilic polymers in the cell wall, that contain hydroxyl groups. The most hydrophilic polymers in the wood are hemicelluloses followed by amorphous cellulose and lignin [19–21]. Changes in the chemistry of wood cell wall due to the ageing process, i.e., in AW, directly affect its performances. Controlling the

hygroscopicity of AW is a fundamental concern of the conservator [22]. Popescu and Hill [23] analyzed the water vapor sorption of naturally aged *Tilia cordata* Mill. and reported different sorption behavior in the historical wood samples as compared to fresh ones, suggesting a potential annealing reaction associated with plasticization of the cell wall matrix at high moisture content. Sonderegger and colleagues [24] claimed that natural ageing affected the physical and mechanical properties of spruce, fir, and oak wood, but the effect on sorption and swelling behavior of wood was negligible. No differences or marginal shifts on equilibrium moisture content (EMC) of various AW species as compared with FW were reported by Kranitz et al. [25].

Characteristics of AW differ by their place of application (buried, submerged, exposed, etc.), and studying these types of materials bring additional information on the long-term performances of wood products. This knowledge will also help us to provide a proper conservation plan for wooden objects of cultural importance. Therefore, the main aim of the present study was to characterize the archaeological European white elm (*Ulmus laevis* P.) and black poplar (*Populus nigra* L.) wood samples and to compare them with the freshly cut wood samples. The chemical structure and crystallinity of the samples were respectively analyzed by means of XPS spectroscopy and X-ray diffraction methods. Dynamic vapor sorption (DVS) analysis was also conducted to evaluate the sorption behavior of AW and FW samples.

## 2. Materials and Methods

### 2.1. Raw Materials and Samples Preparations

Freshly cut elm (*Ulmus laevis* P.) and poplar (*Populus nigra* L.) wood samples were received from a sawmill. This consisted of  $45 \times 90 \times 4000$  mm (L  $\times$  T  $\times$  R) boards from Romanian growth area Suceava. The defect-free samples (no knots, cracks, reaction wood) with annual growth rings slope of  $<5^\circ$  were taken from heartwood. The moisture contents of FW elm and poplar were 7.66% and 7.79%, respectively. The respective density of FW elm and poplar were  $0.55 \text{ g/cm}^3$  and  $0.42 \text{ g/cm}^3$ . The elm AW sample was collected from sand mines, buried at a depth of 8–10 m in the alluvial soil from the former Somes riverbed, in the region of Satu Mare–Romania and county of Vetiș. Age of the elm AW is estimated to be around 1800 to 2000 years, and its form of application on that place is unclear. The poplar AW sample was received from the historical museum of Iasi–Romania. This sample was part of a boat in a freshwater lake or river. The age of this sample is approximately 1000 to 1200 years. The age of both AW samples were determined by stratigraphic evaluation method based on the landmarks of ceramics and the numismatic pieces found in the layer next to the wooden artefact, also according to the archived documents [3]. It should be noted that because of the specks of dirt and other impurities, such as soil, the external surfaces of both AW samples were removed by 20–30 mm, prior to analysis.

### 2.2. X-Ray Photoelectron Spectroscopy (XPS)

XPS analysis was carried out on the samples measuring  $1 \times 5 \times 5 \text{ mm}^3$  (L  $\times$  T  $\times$  R) by the PHI VersaProbe II spectrometer (Ulvacphi, Inc., Osaka, Japan) using a monochromatic Al-K $\alpha$  source with photonic energy of 1486.6 eV and a base pressure of 2  $\mu\text{Pa}$ , as described previously [10]. All samples were analyzed at room temperature without prior sample surface purification. Two measurements were performed for each wood type, and the average value was calculated.

### 2.3. X-Ray Diffraction Analysis (XRD)

Degree of wood crystallinity was measured with X-ray diffraction analysis using a Philips X'Pert MPD PW 3040 diffractometer (Netherlands) equipped with a PW 3050/10 goniometer, divergence slit  $0.5^\circ$ , anti-scatter slit  $0.5^\circ$ , receiving slit 0.6 mm, secondary graphite monochromator, mask 15 mm, 40 kV activity, and 30 mA with Cu K $\alpha$  radiation. The analysis was performed according to our previous study [10] following the scanning range of  $5\text{--}50^\circ 2\theta$  with a phase width of  $0.02^\circ 2\theta$  in a continuous

mode. Sample spinning was at 1 rps, and the counting time was 4 s per move. Wood samples were milled in a planetary ball mill (P7 premium first, Fritsch) and prepared in 16 mm sample holders using backloading.

#### 2.4. DVS Analysis

Dynamic vapor sorption behavior of wood samples were analyzed using DVS apparatus (DVS advantage, Surface Measurement Systems, London, UK), as described previously [6,10,26–28]. Wood samples were milled and passed through the 2-mm mesh. Approximately 20 mg of the milled samples were placed on a DVS sample holder. Sorption isotherms were recorded at a constant temperature of 25 °C. The relative humidity (RH) was increased in the following sequence: 0%, 5%, 15%, 25%, 35%, 45%, 55%, 65%, 75%, 85%, and 95 % RH, and followed in reverse order to 0% RH. The RH was maintained until the mass change of the specimen per minute was  $<0.001\% \text{ min}^{-1}$  over a period of 10 min and the equilibrium mass of the specimen recorded. At each RH the weight at equilibrium condition was recorded by micro-balance and then equilibrium moisture content (EMC) was assessed, accordingly.

#### 2.5. Scanning Electron Microscope (SEM)

The microstructure of AW and FW elm and poplar samples were evaluated by TESCAN MIRA3 FEG-SEM (Czechia) operating at a 70 Pa vacuum and a 15 kV accelerating voltage. The samples measuring  $10 \times 10 \times 10 \text{ mm}^3$  were cut with a razor blade before imaging, according to our previous study [6].

### 3. Results and Discussion

#### 3.1. XPS

Figure 1 shows the C1s energy level spectra of AW and FW wood samples analyzed by XPS spectroscopy. The conforming surface composition within the C1s energy level is illustrated in Table 1. The C1s signal encompasses four sub-peaks, e.g., C1, C2, C3, and C4 [29]. The C1 is related to the carbon atoms that are bonded with either carbon or hydrogen. The C2 signal assigns to the carbon atom single is bonded with an oxygen atom. The C2 signal in wood sample is related to the carbohydrates, mainly cellulose, and hemicelluloses [29,30]. The carbonyl groups are indicated by C3 stretching band, while carboxyl groups are shown by C4 peak.

The C1 sub-peak area significantly increased in both AW samples. The C1 signal is mainly attributed to extractives and lignin of wood [11]. This fact shows a lower concentration of oxygenated C atoms. Referring to the FTIR results in our previous study [6], this increase indicates that the amount of lignin was increased after the ageing process, which might be related to the reduction in carbohydrate content. The C2 sub-peak in elm sample decreased after the ageing process, while it is slightly increased in archaeological poplar. The absorption in C3 peaks in both AW (elm and poplar) samples are decreased after the ageing process. This indicates that the quantity of carboxyl groups are decreased, which might be due to the oxidation and hydrolysis process in contact with soil, change in humidity and ultra-violet (UV) light degradation [31]. The abiotic degradation of wood by weathering elements such as UV light, however, occurs at maximum 1–2 mm depth [5], while the samples in this study were obtained from a deeper part of the surface. Therefore, other degradation mechanisms than weathering factors must be involved.

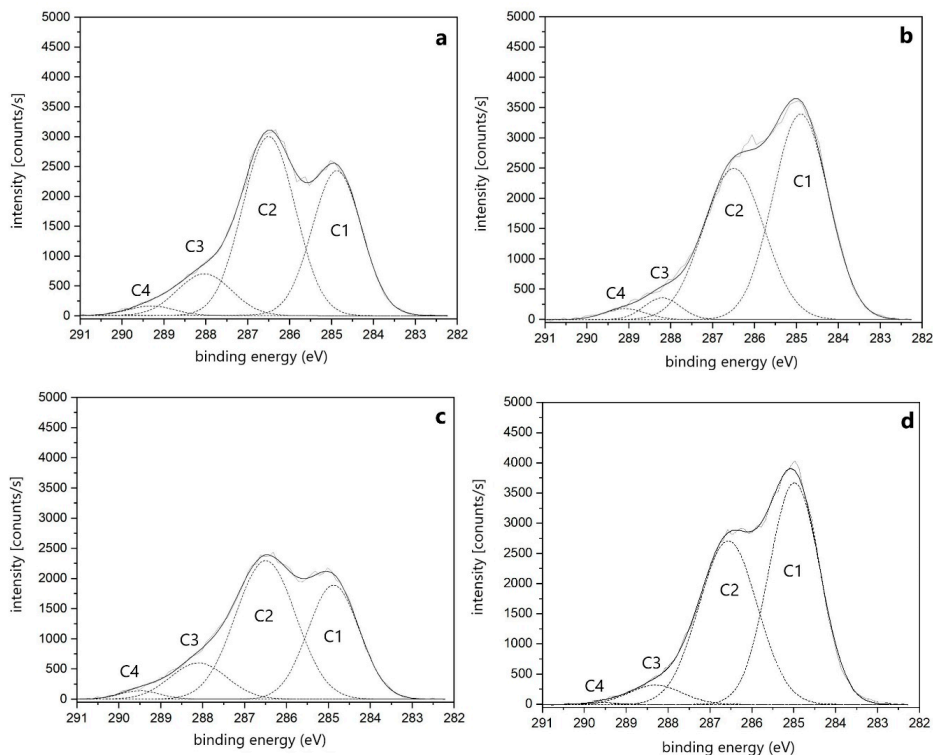


**Figure 1.** High-resolution spectra of the C1s energy level of (a) fresh elm, (b) archaeological elm, (c) fresh poplar, and (d) archaeological poplar.

**Table 1.** Relative surface composition for fresh and archaeological elm and poplar.

Wood Samples	C1 (atm.%)	C2 (atm.%)	C3 (atm.%)	C4 (atm.%)	Atomic Ratio O/C	Cox/Cunox
Fresh elm	36.2 ( $\pm 8.0$ )	51.1 ( $\pm 4.4$ )	10.3 ( $\pm 2.5$ )	2.3 ( $\pm 1.4$ )	0.42	1.75
Archaeological elm	54.1 ( $\pm 2.9$ )	38.9 ( $\pm 3.8$ )	5.2 ( $\pm 0.5$ )	1.8 ( $\pm 0.4$ )	0.32	0.84
Fresh poplar	43.5 ( $\pm 7.0$ )	42.6 ( $\pm 1.3$ )	11.4 ( $\pm 6.6$ )	2.5 ( $\pm 1.0$ )	0.42	1.29
Archaeological poplar	48.8 ( $\pm 2.7$ )	42.0 ( $\pm 4.9$ )	7.2 ( $\pm 5.1$ )	2.0 ( $\pm 2.3$ )	0.28	1.04

The atomic ratio and Cox/Cunox in both AW samples were lower than the FW ones. These differences can be attributed to the oxidation and hydrolysis reactions of carbon-containing compounds in the deeper parts of AWs and migration of the degraded products to the surface during the ageing process [11,30,32].

The O1 energy level spectra of AW and FW samples are shown in Figure 2. The O1 energy level includes two sub-peaks, namely O1 and O2. The O1 sub-peak related to an oxygen atom that is linked with a double bond to a carbon atom, and the O2 sub-peak, with higher binding energy, reflects an oxygen atom linked to a carbon atom by a single bond. An apparent reduction observed in O2 sub-peak of archaeological elm while there were no significant changes observed in the archaeological poplar. This variation is in accordance with the FTIR analysis in our previous study [6], which could be related to the C = O bond in hemicellulose.

The XPS results demonstrate the depolymerization, oxidation, and hydrolysis reactions on the surface of AW samples [11]. These findings are compatible with the FTIR spectroscopic data obtained in our previous study [6], which show that hemicelluloses and amorphous part of cellulose polymers are degraded over the exposure time. Although the crystalline part of cellulose is more stable to degradation, due to the severe ageing process and soil contact, most crystalline regions were degraded. The lignin is a stability polymer and it was no rapid deterioration found due to ageing process [11]. Fors [33] reported that the ratio of lignin to cellulose increases as the wood is degraded. Wood-decay fungi require oxygen to gain ATP for cellular metabolism and hyphal growth,

and also for active expression and secretion of an array of enzymes and metabolites to decompose the wood polymers [34–36]. The AW samples that analyzed in this study collected from the places with a low oxygen content, e.g., under soil or fresh water, and thus it is unlikely that the wood-decay fungi degraded the structure of AW samples. It is well-known that bacteria are more tolerant to conditions considered extreme for most wood-decay fungi. Erosion bacteria is also widely accepted as a destruction agent in AW under conditions with limited oxygen availability [37]. Therefore, it is expected that the degradation in cell wall polymers of archaeological elm and poplar is caused by erosion bacteria. In addition, selective degradation by fungi and moisture changes may occur in archaeological poplar as it was located in aquatic media and then left under humid conditions for some periods. Placing the archaeological poplar in the museum may also cause photo-degradation with visible light [38,39].

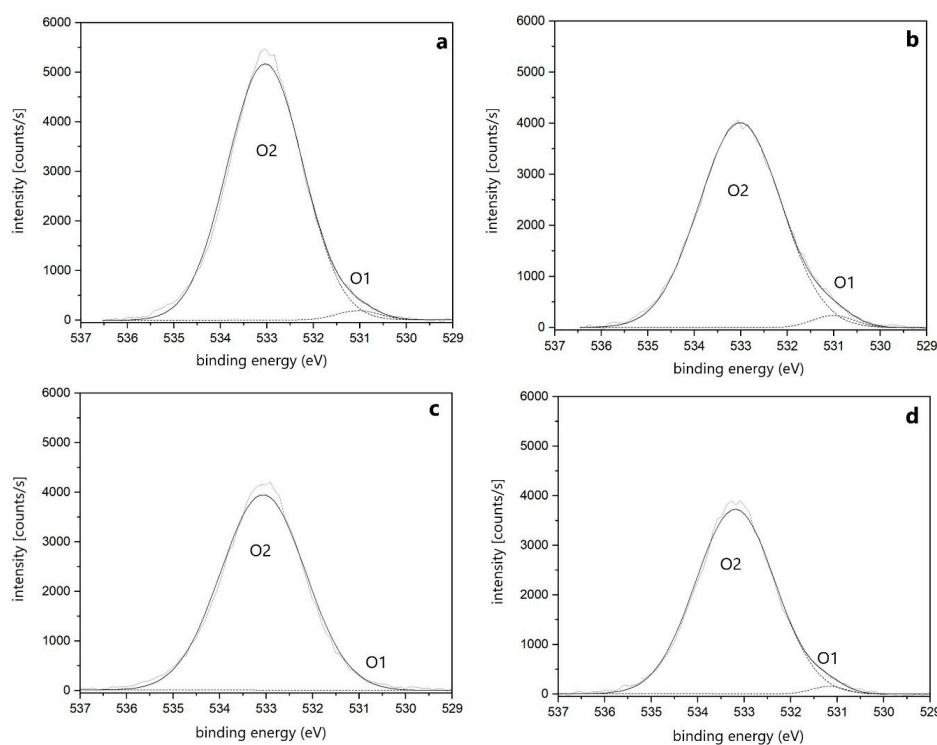


**Figure 2.** High-resolution spectra of the O1s energy level of (a) fresh elm, (b) archaeological elm, (c) fresh poplar, and (d) archaeological poplar.

### 3.2. XRD

The X-ray diffractograms of the AW and FW samples are illustrated in Figure 3a,b. In order to measure the intensities of diffraction bands, to verify the crystalline and amorphous areas, and to determine the crystallite size, the Gaussian profiles were used to deconvolute the diffractograms, as explained previously [10]. The peak intensity and peak expansion are differed in wood species due to the ageing process. Firm peaks observed in the range between  $20.50^\circ$  and  $22.50^\circ$   $2\theta$  in FW of elm and poplar, while the AW displayed much broader and weaker diffraction peaks. The reflection from  $16.14^\circ$  to  $17.94^\circ$   $2\theta$  is assigned to the amorphous part of lignocellulosic materials [40]. The results indicate a much lower degree of crystallinity and greater amorphous regions in the AW samples. In comparison with archaeological poplar, the reflection peaks in archaeological elm is much weaker, which can be related to its age, i.e., approximately 600–800 years older than poplar, and also stronger degree of degradation.

The maximum ( $I_{200}$ ) and minimum ( $I_{am}$ ) intensities of the crystalline cellulose, the crystalline index (CrI) and the crystallite size ( $L$ ) are shown in Table 2. The  $L$  values were smaller for both AW

samples. This decreasing together with the decreasing in CrI indicate the increase of the amorphous domains [41]. The CrI in both AW samples were lower than the FW ones. This might be attributed to the removing of extractives and also to the effects of repetitive ageing processes during absorption and desorption of moisture or liquid water [40], due to the fact that both AW samples were collected from moist conditions. Biological degradation of AW samples can be an additional reason since both elm and poplar specimen were collected from the places with the possible destruction by erosion bacteria [6] and selective fungi degradation, in the case of archaeological poplar.

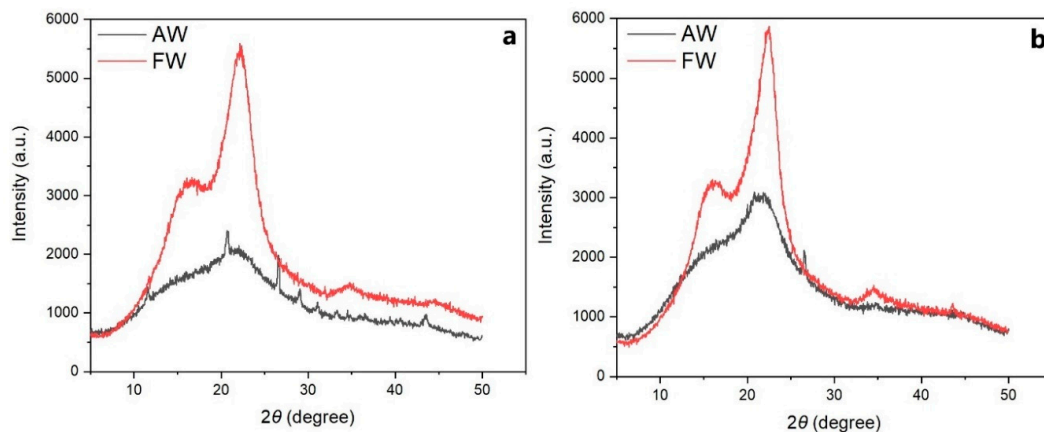


**Figure 3.** X-ray diffractograms from archaeological wood (AW) and fresh wood (FW) of elm (a) and poplar (b).

**Table 2.** Band positions of crystalline and amorphous cellulose and the calculated parameters for the wood samples.

Wood Samples	$I_{200}$	$I_{am}$	CrI (%)	$L$ (200) (nm)
Fresh-elm	20.14	17.26	42.26	8.23
Archaeological-elm	22.06	16.82	26.13	5.69
Fresh-poplar	22.5	18.14	49.91	8.18
Archaeological-poplar	20.78	17.62	29.11	6.85

### 3.3. Sorption Isotherms

The adsorption and desorption isotherms of elm and poplar AW and FW are shown in Figure 4a,b. The isotherm curves of fresh and archaeological elm and poplar samples exhibited a type II sigmoid character of cellulose-containing materials. The ageing phenomena altered the sorption behavior of elm and poplar samples through whole adsorption and desorption runs. Both AW samples showed higher equilibrium moisture content (EMC) values during absorption and desorption processes as compared with the fresh samples throughout the entire hygroscopic ranges. The high absorption and desorption values in AW samples could be explained by the alteration on their chemical structure [42–44], and also disordering their crystalline regions [45]. We found previously that the decomposition in polysaccharides of archaeological elm was more pronounced. A similar chemical change was observed in the archaeological poplar (unpublished results). This together with the XRD results, in Figure 3, confirms that the amorphous parts of AW samples were considerably increased, which will lead to the higher flexibility of cell wall polymer to accommodate water molecules during the sorption processes. A similar trend observed previously in delignified wood micro-veneers [44]. Hydrophilic structure of Scots pine (*Pinus sylvestris*) after degradation by brown-rot fungi showed Chirkova et al. [42]. Analyzing the sorption properties of 103 years old Scots pine showed that because of the degradation of hemicellulose and decreasing in the crystallinity index, the EMC in AW sample was higher than the FW. Most recently, García-Iruela and co-workers [45] quoted that the higher moisture adsorption of AW (*Pinus sylvestris* L. with 400 years old) than the FW is related to the greater availability of active



hydroxyl groups. Biological degradation of the samples due to ageing condition may also enhance the hydrophilic structure of wood polymers, and thus increase the number of active sorption sites.

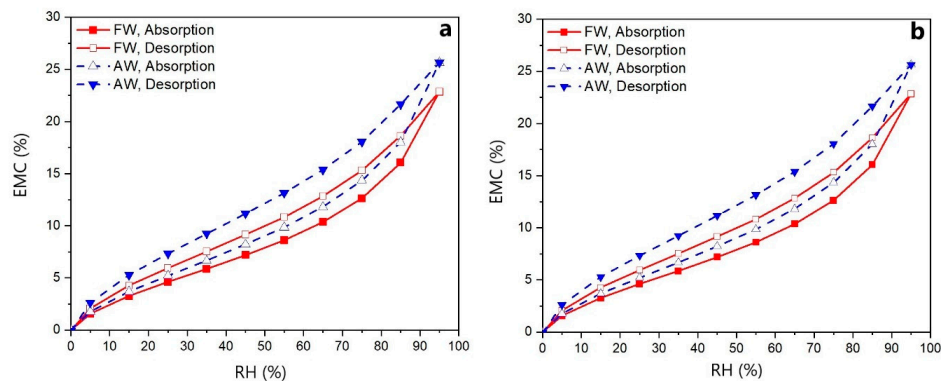


**Figure 4.** Adsorption and desorption isotherms of archaeological and fresh elm (a) and poplar (b) at a given relative humidity (RH) level.

The sorption hysteresis of archaeological and fresh elm and poplar are shown in Figure 5a,b. The AW samples illustrated greater differences between the EMC values during desorption and adsorption runs, which resulted in a larger hysteresis loop area. It is evident that the sorption hysteresis is slightly higher in both archaeological and fresh elm as compared with the ones in poplar. The highest hysteresis value was obtained in the archaeological elm samples. The hysteresis values in fresh and archaeological elm were 3.03% and 3.86%, respectively, whereas poplar samples show the respective values of 2.7% and 3.68%. As indicated in the XRD results, the crystalline structure of wood samples were considerably decreased because of ageing conditions. Therefore, the sorption hysteresis of these samples could be related to the behavior of the highly amorphous matrices, mainly during the desorption run. With regard to the adsorption process, the water molecules are adsorbed by the amorphous structure of wood samples resulting in swollen cell wall matrix. Because of the extensive degradation of AW polymers, the ability of the degraded polymers to rearrange of cell wall matrices during desorption process is inhibited, and thus greater time lag occurs for matrix relation, as postulated by Lu and Pignatello [46]. The different sorption behavior of archaeological elm and poplar might be attributed to the differences in their condition of exposure and degradation mechanisms [47]. A greater hygroscopic behavior and sorption hysteresis of 205 years old *Pinus sylvestris* L. as compared with the FW was reported to be mainly due to the decreases in the crystalline structure of AW [48]. Similar results were reported by García-Iruela and colleagues [45], who explained that the selective degradation mechanisms by fungi and bacteria and also exposure to various humid atmospheres are the main reasons to enhance the amorphous regions, and thus provide more hydrophilic structure in AW than the fresh wood.

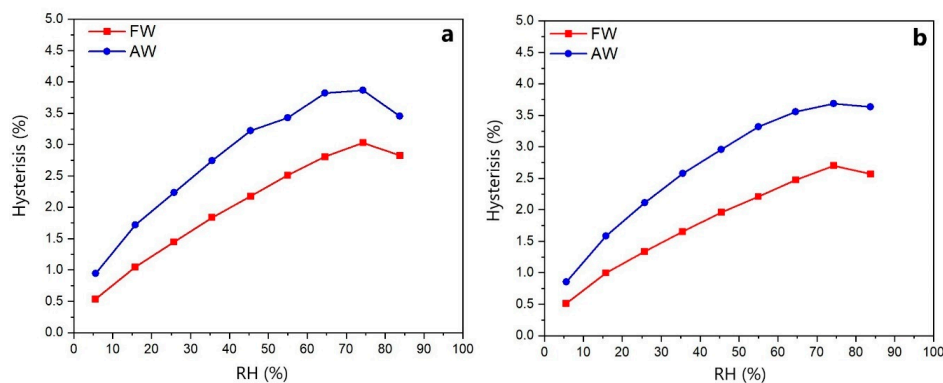


**Figure 5.** Sorption hysteresis of archaeological and fresh elm (a) and polar (b) at a given RH level.

### 3.4. Scanning Electron Microscope (SEM)

SEM micrographs of archaeological and fresh elm and poplar samples are presented in Figures 6a–d and 7a–d. As can be seen in these images, the structures of both wood species were severely degraded because of the ageing conditions. Considerable degradation was observed in the wood rays, particularly in poplar. Those cells are part of the nutrient reserves of the trees and contain a higher quantity of sugars compared to other cell types, such as fibers and vessels [49]. The deteriorated rays indicate that the sugars were the first ones affected by the degradation factors. The destruction in archaeological elm sample can be attributed to the many years of exposure underground, and obvious degradation of cell wall polymers, as reported in our previous study [6]. Although poplar is very low durable species [50], exposure of archaeological poplar to water and also humid conditions may enhance the degradation rates in this sample. Furthermore, local environmental degradation factors such as bacteria, fungi, and pH of the soil (in elm sample) and of the water (in poplar sample) could be considered as additional reasons [8].

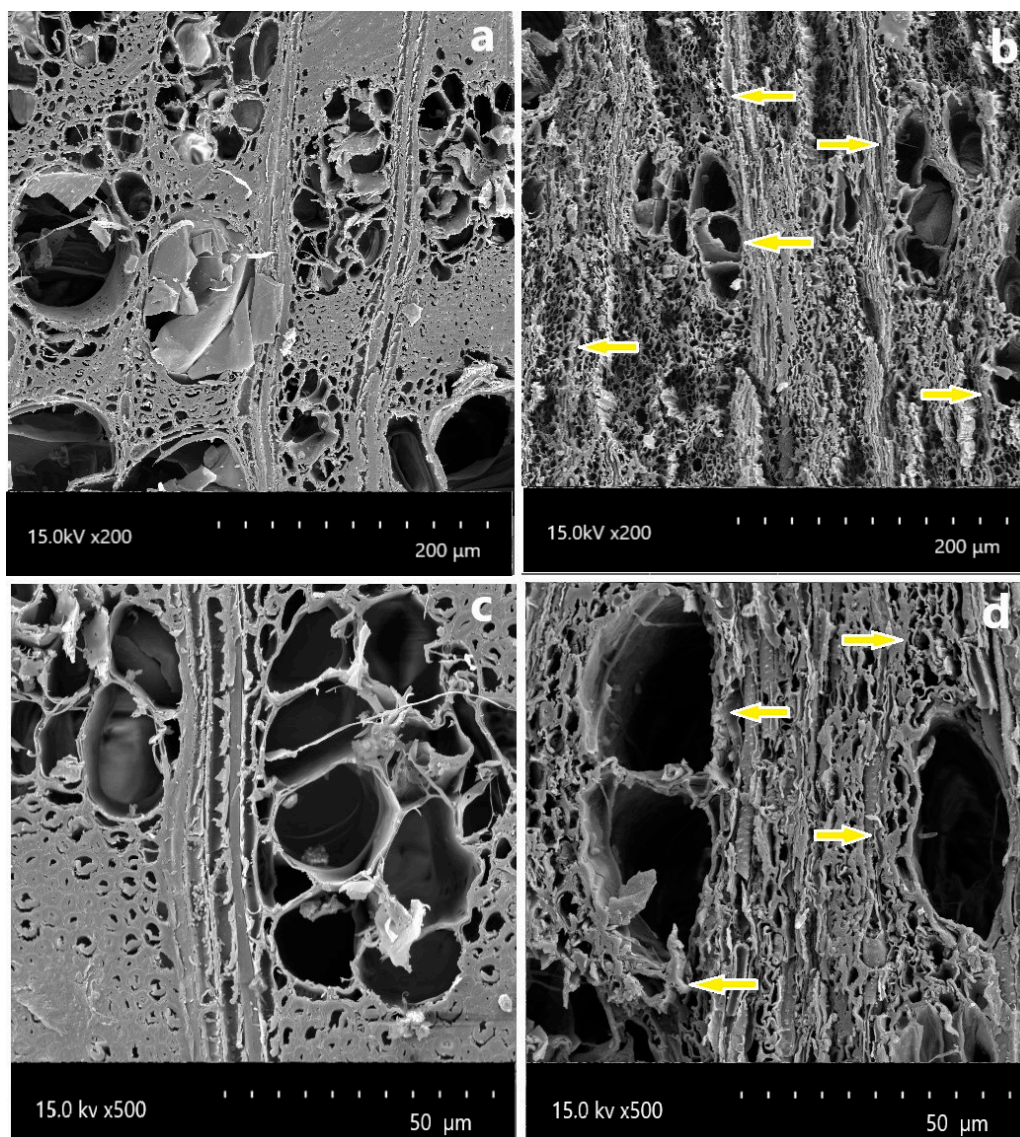


**Figure 6.** Scanning electron microscopy (SEM) micrographs of fresh and archaeological elm at 200 μm (a,b), and 50 μm (c,d) magnification. Arrows indicate the damaged parts of AW.

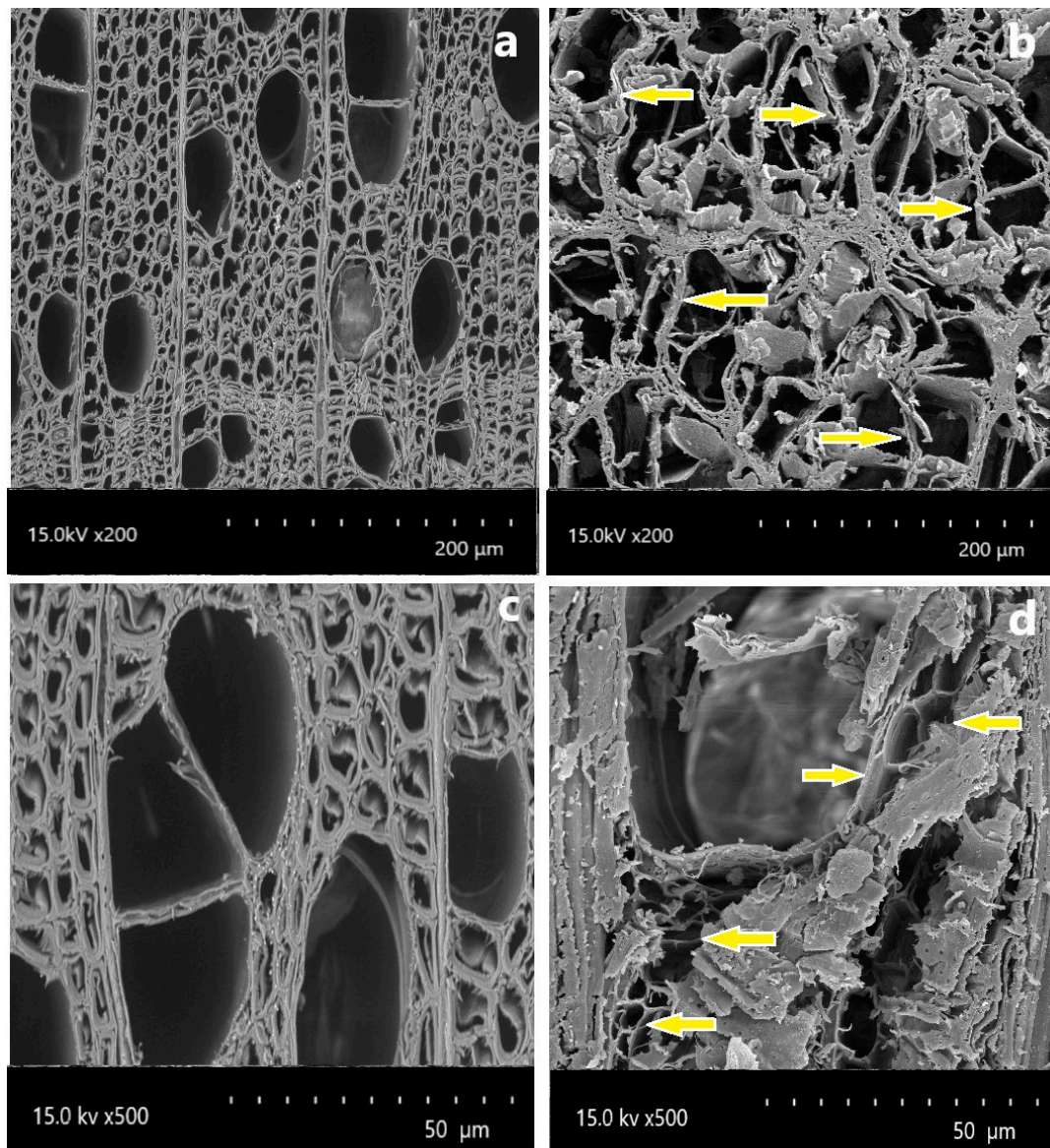


**Figure 7.** Scanning electron microscopy (SEM) micrographs of fresh and archaeological poplar at 200 μm (a,b), and 50 μm (c,d) magnification. Arrows indicate the damaged parts of AW.

#### 4. Conclusions

The fresh and archaeological European white elm (*Ulmus laevis* P.) and black poplar (*Populus nigra* L.) wood samples were studied by means of their chemical and crystalline structures, sorption behavior, and microstructure characters. Depolymerization, oxidation, and hydrolysis reactions occurred in the archaeological samples, as indicated by lower ratios of Cox/Cunox and O/C than fresh samples. The crystalline structure of both elm and poplar samples were also considerably decreased because of the ageing conditions. Accordingly, higher EMC values during adsorption and desorption processes were obtained in the archaeological samples as compared to the fresh ones. The greater sorption hysteresis in archaeological elm and poplar samples than the fresh specimens are expected to be due to the inability of the cell wall to rearrange during the desorption run, because of the severe degradation process. Slight differences were observed in the microstructure of archaeological elm and poplar samples, which are mainly related to their condition of exposure and degradation mechanisms.

Proper conservation of wooden artefacts is dependent upon a knowledge of wood species, microstructure, cell wall chemistry, and its hydrophilic character. This information is critical for

conservators to use a suitable conservation method and chemicals. For instance, polyethylene glycol (PEG) is a conservation agent and it is expected to stabilize in wood by chemical reaction with wood polymers, and thus changes in the chemical structure of wood affect its stabilization. Therefore, our study is anticipated to provide a better understanding on the chemical, physical, and microstructural characters of AW samples exposed at various degradation conditions.

**Author Contributions:** Conceptualization, A.G., R.H.; methodology: A.G., R.H., H.M.; V.V.; validation: A.G., I.S.; investigation: A.G.; resources: A.G., R.H., H.M., I.S.; writing—original draft preparation: A.G., R.H.; writing—review and editing: all authors; All authors have read and agreed to the published version of the manuscript.

**Funding:** This research received no external funding.

**Acknowledgments:** We thank the Department of Wood Biology and Wood Products and the Geoscience Centre, Georg-August-University Göttingen, and the Faculty of Natural Sciences and Technology, University of Applied Sciences and Arts HAWK, Göttingen, for their collaboration and support to perform this research.

**Conflicts of Interest:** The authors declare no conflict of interest.

## References

1. Unger, A.; Schniewind, A.P.; Unger, W. *Conservation of Wood Artifacts*; Springer: Berlin/Heidelberg, Germany, 2001.
2. Walsh-Korb, Z.; Avérous, L. Recent developments in the conservation of materials properties of historical wood. *Prog. Mater. Sci.* **2019**, *102*, 167–221. [CrossRef]
3. Sandu, I.C.A.; Brebu, M.; Luca, C.; Sandu, I.; Vasile, C. Thermogravimetric study on the ageing of lime wood supports of old paintings. *Polym. Degrad. Stab.* **2003**, *80*, 83–91. [CrossRef]
4. Florian, M.L.E. Scope and history of archaeological wood. In *Archaeological Wood: Properties, Chemistry, and Preservation*; Rowell, R.M., Barbour, R.J., Eds.; American Chemical Society: Washington, DC, USA, 1990; pp. 3–32.
5. Reinprecht, L. *Wood Deterioration, Protection and Maintenance*; John Wiley and Sons: West Sussex, UK, 2016.
6. Ghavidel, A.; Gelbrich, J.; Kuqo, A.; Vasilache, V.; Sandu, I. Investigation of archaeological European white elm (*Ulmus laevis*) for identifying and characterizing the kind of biological degradation. *Heritage* **2020**, *3*, 1083–1093. [CrossRef]
7. Björdal, C.G.; Nilsson, T.; Daniel, G.F. Microbial decay of waterlogged archaeological wood found in Sweden—Applicable to archaeology and conservation. *Int. Biodeterior. Biodegrad.* **1999**, *43*, 63–71. [CrossRef]
8. Ghavidel, A.; Hofmann, T.; Bak, M.; Sandu, I.; Vasilache, V. Comparative archaeometric characterization of recent and historical oak (*Quercus* spp.) Wood. *Wood Sci. Technol.* **2020**, *54*, 1121–1137. [CrossRef]
9. Christiernin, M.; Notley, S.M.; Zhang, L.; Nilsson, T.; Henriksson, G. Comparison between 10,000-year old and contemporary spruce lignin. *Wood Sci. Technol.* **2009**, *43*, 23–41. [CrossRef]
10. Ghavidel, A.; Scheglov, A.; Karius, V.; Mai, C.; Tarmian, A.; Vioel, W.; Vasilache, V.; Sandu, I. In-depth studies on the modifying effects of natural ageing on the chemical structure of European spruce (*Picea abies*) and silver fir (*Abies alba*) woods. *J. Wood Sci.* **2020**, *66*, 77. [CrossRef]
11. Popescu, C.M.; Tibirna, C.M.; Vasile, C. XPS characterization of naturally aged wood. *Appl. Surf. Sci.* **2009**, *256*, 1355–1360. [CrossRef]
12. Lucejko, J.J.; Tamburini, D.; Zborowska, M.; Babiński, L.; Modugno, F.; Colombini, M.P. Oak wood degradation processes induced by the burial environment in the archaeological site of Biskupin (Poland). *Herit. Sci.* **2020**, *8*, 1–12. [CrossRef]
13. Kacík, F.; Šmíra, P.; Kačíková, D.; Reinprecht, L.; Nasswetrová, A. Chemical changes in fir wood from old buildings due to ageing. *Cellul. Chem. Technol.* **2014**, *48*, 79–88.
14. Han, L.; Wang, K.; Wang, W.; Guo, J.; Zhou, H. Nanomechanical and topochemical changes in elm wood from ancient timber constructions in relation to natural aging. *Materials* **2019**, *12*, 786. [CrossRef] [PubMed]
15. Bader, T.K.; de Borst, K.; Fackler, K.; Ters, T.; Braovac, S. A nano to macroscale study on structure-mechanics relationships of archaeological oak. *J. Cult. Herit.* **2013**, *14*, 377–388. [CrossRef]

16. Polle, A.; Otter, T.; Sandermann, H. Biochemistry and physiology of lignin synthesis. In *Plant Physiology of Trees*; Rennenberg, H., Eschrich, W., Ziegler, H., Eds.; Backhuys Publishers: Leiden, The Netherlands, 1997; pp. 455–475.
17. Hedges, J.I. The chemistry of archaeological wood. In *Archaeological Wood: Properties, Chemistry, and Preservation*; Rowell, R.M., Barbour, R.J., Eds.; Advances in Chemistry Series 225; American Chemical Society: Washington, DC, USA, 1990; pp. 111–140.
18. Fengel, D. Aging and fossilization of wood and its components. *Wood Sci. Technol.* **1991**, *25*, 153–177. [CrossRef]
19. Hofstetter, K.; Hinterstoisser, B.; Salmén, L. Moisture uptake in native cellulose—The roles of different hydrogen bonds: A dynamic FT-IR study using deuterium exchange. *Cellulose* **2006**, *13*, 131–145. [CrossRef]
20. Hill, C.A.S.; Norton, A.J.; Newman, G. The water vapour sorption properties of Sitka spruce determined using a dynamic vapour sorption apparatus. *Wood Sci. Technol.* **2010**, *44*, 497–514. [CrossRef]
21. Englund, E.T.; Thygesen, L.G.; Svensson, S.; Hill, C.A. A critical discussion of the physics of wood–water interactions. *Wood Sci. Technol.* **2013**, *47*, 141–161. [CrossRef]
22. Bjurhager, I.; Ljungdahl, J.; Wallström, L.; Gamstedt, E.K.; Berglund, L.A. Towards improved understanding of PEG-impregnated waterlogged archaeological wood: A model study on recent oak. *Holzforschung* **2010**, *64*, 243–250. [CrossRef]
23. Popescu, C.M.; Hill, A.S.C. The water vapour adsorption desorption behaviour of naturally aged *Tilia cordata* Mill wood. *Polym. Degrad. Stab.* **2013**, *98*, 1804–1813. [CrossRef]
24. Sonderegger, W.; Kránitz, K.; Bues, C.T.; Niemz, P. Aging effects on physical and mechanical properties of spruce, fir and oak wood. *J. Cult. Herit.* **2015**, *16*, 883–889. [CrossRef]
25. Kranitz, K.; Sonderegger, W.; Bues, C.-T.; Niemz, P. Effects of aging on wood: A literature review. *Wood Sci. Technol.* **2016**, *50*, 7–22. [CrossRef]
26. Hosseinpourpia, R.; Echart, A.S.; Adamopoulos, S.; Gabilondo, N.; Eceiza, A. Modification of pea starch and dextrin polymers with isocyanate functional groups. *Polymers* **2018**, *10*, 939. [CrossRef] [PubMed]
27. Hosseinpourpia, R.; Adamopoulos, S.; Parsland, C. Utilization of different tall oils for improving the water resistance of cellulosic fibers. *J. Appl. Polym. Sci.* **2019**, *136*, 47303. [CrossRef]
28. Hosseinpourpia, R.; Adamopoulos, S.; Mai, C. Effects of acid pre-treatments on the swelling and vapor sorption of thermally modified Scots pine (*Pinus sylvestris* L.) wood. *BioResources* **2018**, *13*, 331–345. [CrossRef]
29. Bodîrlău, R.; Teacă, C.A. Fourier transform infrared spectroscopy and thermal analysis of lignocellulose fillers treated with organic anhydrides. *Rom. J. Phys.* **2009**, *54*, 93–104.
30. Cheng, S.; Huang, A.; Wang, S.; Zhang, Q. Effect of different heat treatment temperatures on the chemical composition and structure of Chinese fir wood. *BioResources* **2016**, *11*, 4006–4016. [CrossRef]
31. Chai, X.S.; Hou, Q.X.; Zhu, J.Y. Carboxyl groups in wood fibers. 2. The fate of carboxyl groups during alkaline delignification and its application for fiber yield prediction in alkaline pulping. *Ind. Eng. Chem. Res.* **2003**, *42*, 5445–5449. [CrossRef]
32. Nzokou, P.; Kamdem, D.P. X-ray photoelectron spectroscopy study of red oak- (*Quercus rubra*), black cherry- (*Prunus serotina*) and red pine- (*Pinus resinosa*) extracted wood surfaces. *Surf. Interface Anal.* **2005**, *37*, 689–694. [CrossRef]
33. Fors, Y. Sulfur-Related Conservation Concerns for Marine Archaeological Wood The Origin, Speciation and Distribution of Accumulated Sulfur with Some Remedies for the Vasa. Ph.D. Thesis, Stockholm University, Stockholm, Sweden, 2008.
34. Kirk, T.K.; Farrell, R.L. Enzymatic “combustion”: The microbial degradation of lignin. *Microbiology* **1987**, *41*, 465–505. [CrossRef]
35. Lundell, T.K.; Mäkelä, M.R.; de Vries, R.P.; Hildén, K.S. Genomics, lifestyles and future prospects of wood-decay and litter-decomposing basidiomycota. In *Advances in Botanical Research*, 1st ed.; Martin, F., Ed.; Academic Press: New York, NY, USA, 2014. [CrossRef]
36. Hammel, K.E.; Cullen, D. Role of fungal peroxidases in biological ligninolysis. *Curr. Opin. Plant Biol.* **2008**, *11*, 349–355. [CrossRef]
37. Kim, Y.S.; Singh, A.P. Wood as cultural heritage material and its deterioration by biotic and abiotic agents. In *Secondary Xylem Biology Origins, Functions, and Applications*; Kim, I.S., Funada, R., Singh, A.P., Eds.; Academic Press: New York, NY, USA, 2016; pp. 233–257.

38. Tolvaj, L.; Varga, D. Photodegradation of timber of three hardwood species caused by different light sources. *Acta Silv. Lignaria Hung.* **2012**, *8*, 145–155. [CrossRef]
39. Tolvaj, L.; Mitsui, K. Light source dependence of the photodegradation of wood. *J. Wood Sci.* **2005**, *51*, 468–473. [CrossRef]
40. Lionetto, F.; Sole, R.D.; Cannoletta, D.; Vasapollo, G.; Maffezzoli, A. Monitoring wood degradation during weathering by cellulose crystallinity. *Materials* **2012**, *5*, 1910–1922. [CrossRef]
41. Bryne, L.E.; Lausmaa, J.; Ernstsson, M.; Englund, F.; Wälinder, M.E.P. Ageing of modified wood. Part 2: Determination of surface composition of acetylated, furfurylated, and thermally modified wood by XPS and ToF-SIMS. *Holzforschung* **2010**, *64*, 305–313. [CrossRef]
42. Chirkova, J.; Irbe, I.; Andersons, B.; Andersone, I. Study of the structure of biodegraded wood using the water vapour sorption method. *Int. Biodeterior. Biodegrad.* **2006**, *58*, 162–167. [CrossRef]
43. Esteban, L.G.; de Palacios, P.; Fernandez, F.G.; Guindeo, A.; Conde, M.; Baonza, V. Sorption and hermodynamic properties of juvenile *Pinus sylvestris* L. wood after 103 years of submersion. *Holzforschung* **2008**, *62*, 745–751. [CrossRef]
44. Hosseinpourpia, R.; Adamopoulos, S.; Mai, C. Dynamic vapour sorption of wood and holocellulose modified with thermosetting resins. *Wood Sci. Technol.* **2016**, *50*, 165–178. [CrossRef]
45. García-Iruela, A.; Esteban, L.G.; Fernández, F.G.; Palacios, P.; Rodríguez-Navarro, A.B.; Sánchez, L.G.; Hosseinpourpia, R. Effect of degradation on wood hygroscopicity: The case of a 400-year-old coffin. *Forests* **2020**, *11*, 712. [CrossRef]
46. Lu, Y.; Pignatello, J.J. Demonstration of the ‘conditioning effect’ in soil organic matter in support of a pore deformation mechanism for sorption hysteresis. *Environ. Sci. Technol.* **2002**, *36*, 4553–4561. [CrossRef]
47. Ghauhan, S.S.; Nagaveni, H.C. Moisture adsorption behaviour of decayed rubber wood. *J. Inst. Wood Sci.* **2009**, *19*, 1–6.
48. Esteban, L.G.; Fernandez, F.G.; Garcia, F.; Casasus, A.G.; Palacios, P.P.; Gril, J. Comparison of the hygroscopic behavior of 205-year-old and recently cut juvenile wood from *Pinus sylvestris* L. *Ann. Forest Sci.* **2006**, *63*, 309–317. [CrossRef]
49. Pettersen, R.C. *The Chemistry of Solid Wood*; Advances in Chemistry Series 20; US Department of Agriculture: Washington, DC, USA, 1984.
50. EN 350. *Durability of Wood and Wood-based Products—Testing and Classification of the Durability to Biological Agents of Wood and Wood-Based Materials*; European Committee for Standardization: Brussels, Belgium, 2016.

**Publisher’s Note:** MDPI stays neutral with regard to jurisdictional claims in published maps and institutional affiliations.





© 2020 by the authors. Licensee MDPI, Basel, Switzerland. This article is an open access article distributed under the terms and conditions of the Creative Commons Attribution (CC BY) license (<http://creativecommons.org/licenses/by/4.0/>).



Review

# Gap-Fillers for Wooden Artefacts Exposed Outdoors—A Review

Magdalena Broda <sup>1,2,\*</sup> , Paulina Kryg <sup>3,4</sup> and Graham Alan Ormondroyd <sup>2</sup> 

<sup>1</sup> Department of Wood Science and Thermal Techniques, Faculty of Forestry and Wood Technology, Poznań University of Life Sciences, 60 637 Poznań, Poland

<sup>2</sup> BioComposites Centre, Bangor University, Deiniol Road, Bangor LL57 2UW, UK; g.ormondroyd@bangor.ac.uk

<sup>3</sup> National Museum of Agriculture and Food Industry in Szreniawa, 62 052 Szreniawa, Poland; p.kryg@muzeum-szreniawa.pl

<sup>4</sup> Department of Wood Chemical Technology, Faculty of Forestry and Wood Technology, Poznań University of Life Sciences, 60 637 Poznań, Poland

\* Correspondence: magdalena.broda@up.poznan.pl

**Abstract:** Conservation of wooden artefacts that are exposed outdoors, mainly in open-air museums, is a very complex and difficult issue that aims to preserve both the integrity and aesthetics of valuable objects. Unceasingly subjected to several factors, such as alternating weather conditions and the activities of microorganisms, algae, and insects, they undergo continuous changes and inevitable deterioration. Their biological and physical degradation often results in the formation of gaps and cracks in the wooden tissue, which creates a need not only for wood consolidation, but also for using specialist materials to fill the holes and prevent further degradation of an object. To ensure effective protection for a wooden artefact, a filling material must both protect the wood against further degradation and adapt to changes in wood dimensions in response to humidity variations. A variety of substances, both organic and inorganic, have been used for conservation and gap filling in historic wooden objects over the years. The filling compounds typically consist of two components, of which one is a filler, and the second a binder. In the case of inorganic fillers, plaster has been traditionally used, while the most popular organic fillers were wood powder, wood shavings, and powdered cork. As with binders, mainly natural substances have been used, such as animal glues or waxes. Nowadays, however, due to the lower biodegradability and better physicochemical properties, synthetic materials are gaining popularity. This article discusses the types of filling compounds currently used for gap filling in wooden artefacts exposed outdoors, outlining their advantages and drawbacks, as well as future perspective compounds. It appears that particularly composite materials based on natural polymers deserve attention as promising filling materials due to their high elasticity, as well as similarity and good adhesion to the wooden surface. Their main shortcomings, such as susceptibility to biodegradation, could be eliminated by using some modern, bio-friendly preservatives, providing effective protection for historic wooden artefacts.

**Keywords:** gap-fillers; gap-filling materials; wooden artefacts; wood conservation; wood exposed outdoors; microballoons; resins; glass beads; cellulose powder; binders



**Citation:** Broda, M.; Kryg, P.; Ormondroyd, G.A. Gap-Fillers for Wooden Artefacts Exposed Outdoors—A Review. *Forests* **2021**, *12*, 606. <https://doi.org/10.3390/f12050606>

Academic Editor: Tripti Singh

Received: 13 April 2021

Accepted: 10 May 2021

Published: 12 May 2021

**Publisher's Note:** MDPI stays neutral with regard to jurisdictional claims in published maps and institutional affiliations.



**Copyright:** © 2021 by the authors. Licensee MDPI, Basel, Switzerland. This article is an open access article distributed under the terms and conditions of the Creative Commons Attribution (CC BY) license (<https://creativecommons.org/licenses/by/4.0/>).

## 1. Introduction

Open-air museums (so-called skansens) play an indispensable role in the preservation and presentation of a threatened heritage of regional or national history. Giving us insights into the natural and cultural past of particular regions and the ethnic groups that were living there, these unique institutions help forge the sense of identity of the people in the area.

The idea for open-air museums in Europe came in the 18th century in Denmark as an evolution of traditional indoor type museums to preserve traditional village architecture in the rapidly developing world and thus maintain the cultural and historical consciousness of people. The first skansen was established in 1867 in Norway. Since that time, open-air



museums began to develop—at first mainly in Scandinavia, and then throughout Europe and the world. Some of them were established to preserve historical buildings in the place of their origin or to save unique archaeological discoveries exactly in the area where they were made, while others were erected from scratch in new suitable places where the interesting objects were transferred to [1–3].

Open-air museums are often called “living museums” as they hold collections of intangible heritage resources, providing an interpretation of how people lived and acted in the past thanks to the achievements of experimental archaeology. They are a specific kind of medium linking culture and people, imparting values, knowledge and experiences of the past to subsequent generations. Their quest is to present historical treasures attractively and extensively, and help visitors appreciate and enjoy the rich heritage of the region. Although the significance of a museum does not rely only on its collection, but also on the philosophical, anthropological and cultural impact on society, the truth is that behind all these ideas are impermanent materials. In the case of open-air museums, the main collections are traditional buildings and structures exposed at large outdoor sites, and the primary material from which they came is usually degradable wood. Therefore, to fulfil their mission, the museums have to find a way to reconcile the intangible and the tangible, and save the wooden historic landmarks from decay, destruction, and ultimately the loss of the artefact [3–5].

The main wooden artefacts presented in open-air museums are various buildings, including cottages, huts, farm buildings, churches, wind- or watermills, as well as smaller structures, such as wayside shrines and crosses, beehives or statues (a few examples of wooden objects from the collections of The National Museum of Agriculture and Food Industry in Szreniawa and its branch—The Museum of Apiculture in Swarzędz, Poland are presented in Figures 1 and 2). Their outdoor exposition unceasingly subjects them to various abiotic and biotic factors that cause them damage.



**Figure 1.** Three examples of wooden beehives from the collection of The Museum of Apiculture in Swarzędz, a branch of The National Museum of Agriculture and Food Industry in Szreniawa, Poland; from the left: a beehive No. MS E-128 called “Chinese”, a beehive No. MS E-63 called “The Priest”, a mushroom-shaped beehive No. MS E-242.



**Figure 2.** Wooden relics from the collection of The Museum of Apiculture in Swarzędz, a branch of The National Museum of Agriculture and Food Industry in Szreniawa, Poland; from the left: a set of figural beehives and an example of an architectural beehive (No. MS E-111).

The objects exhibited in the open air are constantly exposed to changing weather conditions. Precipitation and humidity variations result in alterations in wood dimensions, i.e., cyclic swelling and shrinking, which can cause wood deformation or even cracking (Figures 3A,D,E and 4D). Cracking and deformations impair an artefact's aesthetic, but the object that is cracked all over is also at risk of breaking apart into pieces and disintegrating. The rainfall and high air humidity, but also water that accumulates in cracks, promote further microbial, fungal, or algae infestation, which leads to the decay of wooden tissue and the creation of holes cavities (Figures 3D,E and 4A–C). UV radiation, temperature fluctuations or activity of wood-boring beetles and other insects that occur in the surrounding environment create further damage (Figure 3A–C). As a result, the structural, mechanical, and chemical properties of wooden artefacts deteriorate over time, along with their aesthetic and artistic qualities. Such objects are usually full of cracks and hollows of various shapes and dimensions [6–9]. This creates a need for the application of not only typical wood conservation agents to consolidate wood and preserve the whole artefact, but also special materials to fill the gaps and keep the integrity and aesthetics of valuable objects and prevent their total destruction. Conservation of such types of historical objects is thus a challenging and complex issue requiring specific interdisciplinary knowledge and integrated technical and artistic conservation measures, which together ensure relevant results being concurrently in line with conservation ethics and excellence.



**Figure 3.** Damage on wooden objects exposed in the open air ((A–E): artefacts from the collection of The Museum of Apiculture in Swarzędz, a branch of The National Museum of Agriculture and Food Industry in Szreniawa, Poland).



**Figure 4.** Damage of wooden objects covered with paints ((A–D): artefacts from the collection of The Museum of Apiculture in Swarzędz, a branch of The National Museum of Agriculture and Food Industry in Szreniawa, Poland).

This paper focuses specifically on the gap-filling of wooden artefacts exposed outdoors—an important but often overlooked problem in wood conservation. The article reviews the filling compounds currently applied for gap-filling and discusses their usefulness for wooden objects exhibited in the open air. It revolves around the features of filling materials that are the most required from the conservation perspective, outlines the advantages and drawbacks of these materials, and presents possible future perspectives in this field.

## 2. Materials for Gap Filling in Wooden Objects

Filling gaps in historical artefacts is in line with a philosophical trend based on the idea to conserve historical material rather than replace it. The reasons for gap-filling in wooden objects exposed outdoors are twofold, depending on the state of their preservation. Firstly, when the damage to an object threatens its existence (e.g., loss of stability (Figure 5B,C), deep cracks leading to splits and disintegration (Figure 5A,D)), then conservation considerations prevail, and a structural fill is necessary to provide an object with adequate strength and integrity. On the other hand, when multiple holes and cracks in an object cause the loss of its aesthetic quality and historical character that impedes the right interpretation of the artefact (Figure 6), aesthetic concerns predominate, and a soft, nonstructural fill is desirable [10,11]. Filling materials should then permit the degraded historical artefact to be “reconditioned and retained in place” [12].



**Figure 5.** Structural damage of wooden objects that threatens their existence (artefacts from the collections of The Museum of Apiculture in Swarzędz (B,C), and The National Museum of Agriculture and Food Industry in Szreniawa, Poland (A,D)).

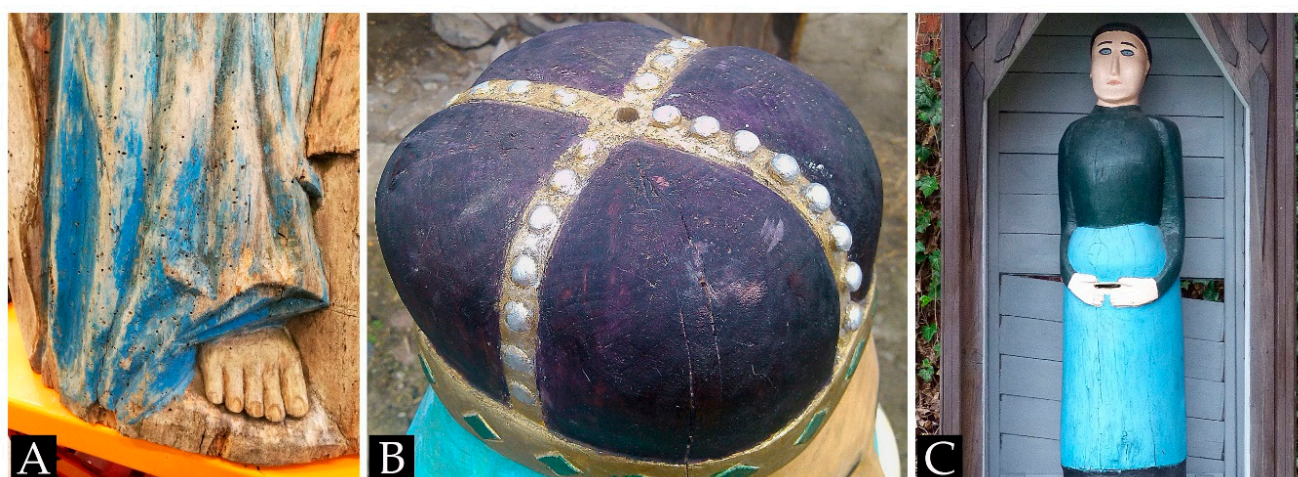


**Figure 6.** Damage that causes loss of the aesthetic quality of wooden objects (artefacts from the collection of The Museum of Apiculture in Swarzędz (C), and The National Museum of Agriculture and Food Industry in Szreniawa, Poland (A,B)).

A variety of materials have been used to fill gaps in wooden artworks exposed outdoors, including organic and inorganic compounds. Historically, mainly natural materials were applied, such as wooden fills, waxes, plaster, chalk, bitumen, concrete, gesso or oil-based putties. Then, due to their better performance, synthetic materials have become more popular; these include various resins (acrylic, epoxy, methacrylic, and vinyl), polyurethane, and silicone rubbers mixed with sawdust or synthetic microballoons [10,12–17]. Recently, as in other areas, a return to nature can be observed in wood conservation. This reflects the application of natural fillers, such as cellulosic materials (paper pulp, microcrystalline cellulose, long fibre tissues, cellulose or wood powder) or minerals (Halloysite nanotubes, silicates) in combination with natural biocides and various binders, including resins, natural oils, waxes, cellulose ethers, and other adhesives [18–27]. Conservators also use commercial ready-mixed compounds that include not only fillers and adhesives, but also additional agents, such as pigments, biocides, emulsifiers or thickeners (e.g., Plastic Wood, Polyfilla, AJK dough), or home-made pastes of confidential composition adjusted to the needs of individual wooden artefacts [13,28,29].

Conservation materials for filling holes and cracks in exterior wooden artworks face much more challenging conditions in comparison with museum interiors. Therefore, their properties should match the requirements imposed by the outdoor environment. Flexibility and cohesive strength proportionate to that of wood are two of the most important features due to the changing outdoor humidity and the resulting swelling and shrinkage of the wood. The ideal material would be one that could respond to these changes, i.e., expand when wood shrinks and shrink when the wood swells. It should adhere well to the void's surface and provide proper fusion with wood tissue. Fillers also need to be resistant to

weathering (ageing) and leaching. Their physico-chemical and mechanical properties should correspond with wood to avoid its damage. Filling materials ought to be removable (conservation ethics require the method to be reversible or at least enabling retreatability), easy to prepare, apply and work, as well as to carve or paint, non-toxic, preferably also easily accessible, and relatively inexpensive [11,18,30–32]. The key to providing proper conservation of a wooden artefact is an individual approach to each case that involves thorough characteristics of an object and its state of preservation, as well as choosing the most appropriate conservation materials and methods tailored to the artefact and that correspond to both aesthetic and conservation requirements [13,17,18].

Fill compounds are two-part systems that consist of a cohesive material (filler) to replace the loss in the wood structure and an adhesive (binder) to affix the material in a conserved object. These two constituents can be separate, as in the case of a properly shaped wooden fill glued into the void using an adhesive, or mixed together into a single filling mass that ensures both filling the loss and adhesion to its surface [10]. Masses are then multi-component mixtures of adhesive(s) and bulking agent(s) blended in the right proportions to provide requested physical and mechanical properties. They can be simple mixtures of chemically inert agents or a blend of compounds that can chemically react with each other or crystallise to form a final filling material with appropriate characteristics. However, in conservation practice, there are also more complex recipes with various interactions between their components [17].

### 2.1. Fillers (Bulking Agents)

The primary function of a filler is to replace the missing wooden tissue and fill cavities in an artefact. However, as mentioned above, fillers are usually mixed with adhesives to form a homogeneous ready-to-use filling paste. In such a case, they serve also other functions, such as:

- increasing the viscosity of an adhesive to obtain a stiffer paste, which facilitates its application and prevents its draining from holes or cracks during the conservation process,
- enabling the filling mass to be carved or sanded to facilitate its further painting or to make its surface similar to the surface of the surrounding wood,
- reducing shrinkage of a filling mass when an adhesive used contains volatile components,
- modifying the mechanical properties of an adhesive, thus the whole filling mass, depending on the filler/adhesive ratio,
- altering the volume of the mass in response to changing moisture conditions, depending on the hygroscopicity of a filler [11,18,33].

Several different bulking agents have been used in gap-filling of wooden artefacts exposed outdoors, including both natural (organic and inorganic) as well as synthetic compounds: wooden fills, wood flour, sawdust, wood shavings, coconut fibres, cork granules, rye flour, cellulose powder, lignin, gypsum, chalk, mineral powders, metal or glass powders, glass beads, glass or phenolic microballoons, synthetic fibres, synthetic polymers (powdered or granulated) [13,18,23,31,33,34].

#### 2.1.1. Wooden Fills

One of the solutions applied for filling gaps in wooden artefacts are fills made of wood that can serve as structural or aesthetic compensation. Seasoned wood, usually of the same species of which the wooden object is made, is carved to an appropriate shape for a tight fit. Then it is mounted in the cavity using an adhesive, and its surface is matched to the surrounding area of an artefact [10].

Although this historically oldest conservation method seems evident and fully adequate, it has several drawbacks. The main problem is a different response of new and historic wood to external conditions, in particular to humidity fluctuations. Degraded historic wood is usually to some extent deprived of highly hygroscopic cellulose and hemicelluloses. Therefore, it is less reactive to moisture, thus less dimensionally responsive to it. When humidity changes, different wood pieces (old and new) contract or expand

independently. More reactive fill made of fresh wood can detach itself from the artefact when it dries under low humidity conditions, creating new crevices leading to further damage of an object. When humidity rises, fresh fill expands, which can enlarge the existing gaps and cracks, and even completely destroy an artefact by splitting it into pieces. To avoid such scenarios, conservators sometimes use fills made of the same type of wood with a similar degree of degradation—historical wood with comparable age or fresh timber after artificial weathering [10,11,13,32].

Other problems with wooden fills relate to their fitting to the cavities in a wooden object and visual matching to its surface. The former is difficult due to the usual irregularities of the voids: no matter how accurately carved and fitted, a filler will always eventually come adrift. The latter is complicated due to the individual grain pattern of each wood piece (grain orientation, the width of annual rings, colour). Considering all the above-mentioned facts, using fills made of wood seems not to be a perfect solution [10,11,13].

#### 2.1.2. Sawdust, Wood Shavings, etc.

Probably the most obvious and popular concept for gap-filling in historic wooden artworks is the utilisation of the same material they are made from due to comparable physico-chemical properties. Except for wooden fills described in the previous paragraph, wood or bark (cork) comminuted to a varying degree is often used in combination with different adhesives (mainly nonaqueous due to high swelling and shrinkage of fragmented wood in aqueous binders). Sawdust, wood shavings, and wood flour are cheap and easily available and thus are commonly found in recipes for moldable filling masses. They increase viscosity as well as enhance the hardness and tensile strength of these conservation materials, facilitating their application and further cutting and curving to an appropriate shape and texture. The size of wood particles is selected depending on the type and size of holes in an artefact [16,17,32].

#### 2.1.3. Cellulose

Various forms of cellulose (nanocellulose fibres and crystals, microcrystalline cellulose, paper pulp) and its derivatives (ethers and esters) have been used in the conservation of wooden artworks for consolidation and coating. For gap-filling, mainly microcrystalline cellulose (MCC) and paper pulp are applied as fillers in combination with different adhesives [21,31,35–37].

Microcrystalline cellulose is a natural, non-toxic, fully biodegradable, and recyclable material industrially manufactured from lignocellulosic biomass, usually agricultural, forest and aquatic residues (e.g., rose stem, sugarcane bagasse, rice and coffee husk, date seeds, brown algae, wood, bamboo fibre, tea waste). Its production involves partial hydrolysis of amorphous regions of native cellulose using strong mineral acids at boiling temperature. As a result, small particles (about 50  $\mu\text{m}$  in dimension and 100–1000  $\mu\text{m}$  in length) of high crystallinity are obtained [38–41].

The high degree of crystallinity renders MCC a perfect reinforcing filler, providing it with high thermochemical stability and resistance to swelling in water combined with low density, high specific strength, and viscosity. Additionally, the widespread availability, the chemical composition identical to that found in wood, and the ease of handling make MCC a frequent conservators' choice for consolidation and gap-filling in wooden objects [18,20–22,36,42].

Results of the research by Cataldi et al. [20,22] on MCC/acrylate composite showed that MCC added as a filler to the commercial acrylate adhesive (Paraloid B72 (Dow Chemical Company, Midland, MI, USA) commonly used in wood conservation), significantly improved its thermo-mechanical behaviour by increasing its glass transition temperature and thermal degradation stability, and reduced linear coefficient of thermal expansion. Simultaneously, the addition of MCC increased the composite's stiffness, resistance to fracture propagation, stress at break, tensile energy to break and creep stability, as well as storage modulus and loss modulus proportionally to the rising filler/binder ratio. The stabilising effect of microcrystalline cellulose resulted from the properties of MCC itself

and from a good filler/binder affinity. When applied as a consolidant for degraded wood, the composite additionally reinforced its structure by reducing the pore radius to the size of the corresponding sound wood and enhanced its mechanical properties (e.g., stiffness, flexure strength, and surface hardness); concurrently, it retained the hydrophobicity of the adhesive, reducing the wood moisture content and volumetric swelling of the treated wood [21]. An MCC/acrylate composite can be then particularly useful as a gap-filler for conservation purposes, “... where elevated dimensional stability and a good energy absorption capability under external loads are required...”, as in the case of many wooden objects exposed outdoors [22].

Among cellulosic materials, paper pulp, sheet paper, newspapers or tissue paper have sometimes been used as fillers and have been combined with various, mainly natural adhesives. Due to the higher amount of amorphous regions in cellulose microfibrils, they are more hygroscopic than MCC, thus more prone to swelling when exposed to moisture [17,18,43]. Fulcher [18], however, showed that paper pulp in combination with Klucel<sup>®</sup> (hydroxypropyl cellulose) as an adhesive makes a great gap-filler that is compatible with wood and fits almost all the conservators' criteria. By changing the filler/binder ratio, we can change the properties of the mass and adjust it to the needs of a particular artefact.

There is a lot of new research on the use of cellulose derivatives as fillers for various composites, e.g., lignin-containing cellulose nanofibrils in combination with polymeric diphenylmethane diisocyanate as a wood adhesive [44], polypropylene/poplar wood flour/microcrystalline cellulose /starch powder or MCC/polyester composites with improved mechanical properties [45,46], etc. The properties of the obtained composites are promising, and some of them can potentially be useful in gap-filling in wooden historical objects.

#### 2.1.4. Plaster and Cement

Plaster has been used in conservation practice since antiquity. The name “plaster” can refer to two different types of calcium compounds: lime plaster made of calcium carbonate ( $\text{CaCO}_3$ ) and gypsum plaster (so-called “plaster of paris”) made of calcium sulfate ( $\text{CaSO}_4$ ). Both are mixed with water (and other ingredients) to prepare a filling putty, but the former shrinks upon drying, while the latter, unlike other materials of this type, expands upon setting. Neither of them applied alone is fully appropriate for the conservation of wooden objects: lime plaster can shrink and crack during drying, sticking out from the hole's surface thus creating new gaps; gypsum plaster, by expanding upon drying, can destroy the surrounding wooden tissue leading to the destruction of a whole object [17]. However, in more modern times, plaster has been often used as a bulking component in various conservation masses for gap-filling: hard-finish plasters based on over-heated gypsum and metal salts with longer setting time (e.g., Mack's cement, Keating's, Keene's cement, Parian, Martin's cement); Portland cement made of calcium carbonate and alumino-silicates (more appropriate for large fills); gesso based on calcium sulfate or carbonate mixed with animal glue as the adhesive (unstable under changeable humidity conditions); composition (so-called “compo”) made of animal glue, linseed oil, and a natural resin mixed with a calcium filler. They have been applied to various outdoor artefacts, including metal, stone, and wooden sculptures and structures, often in combination with different substances according to the needs of the individual pieces of art, but most of them are not suitable for degraded wood and under changeable moisture conditions [17,31].

#### 2.1.5. Microballoons

Microballoons are miniature, non-porous, non-toxic, hollow, and perfectly spherical particles with a very low density and specific surface. They are available in the form of white, free-flowing powder, in a wide range of densities and respective compressive strengths. For art conservation, mainly glass, acrylic and phenolic microballoons have been used, often in combination with thermoplastic and thermosetting resins to provide them with better performance [10,11,13,23,47].



Microballoons are inert compounds easily mixed with resins without using complicated tools and procedures. They decrease the viscosity of the resin–filler mixtures without altering their weight and enable them to form thick, lightweight, and easy workable pastes suitable for various conservation purposes. Depending on the adhesive used, some of the masses can be reversible. Microballoons reduce shrinkage during drying and improve the smoothness of filling masses. They enable them to obtain the texture similar to surrounding wood and facilitate their carving and painting (especially the phenolic ones). They also minimise absorption of the resins used by the porous wood tissue, as well as prevent them from affecting water-sensitive painted surfaces or gesso present in conserved artefacts [10,11,13,18,47–50]. The addition of microballoons affects the compressive, flexural or tensile properties of resins; it has been shown that the increased volume fraction of microballoons increases Young’s modulus, compressive strength, and impact resistance of such mixtures. Microballoons-based masses turned out to be effective for applications where dimensional changes upon changeable moisture conditions are minimal due to the high degree of wood degradation, but also, due to their low compressibility, for filling cracks in more reactive less degraded wood [29,47,50–52].

## 2.2. Adhesives (Binders)

Since adhesives applied for filling gaps in wooden artefacts exposed outdoors have to withstand changeable external conditions, their properties have to satisfy specific requirements. First of all, they should be flexible due to the high dimensional changes of wood caused by humidity fluctuations; their hardness and mechanical strength should be adjusted to the condition of the conserved artefact (the bond between wood and adhesive should be weaker than the wood cohesive strength to ensure the potential damage take place within the adhesive, rather than in the structure of the artefact). Binders cannot stain the surface or change the colour of the artefact and need to be resistant to weathering (ageing) and biodegradation. They cannot affect the wood structure, should be non-toxic, safe to handle, easily available, and cheap. To comply with conservation ethics, adhesives should also be reversible or, at least, retreatable [12,16,31,53].

Adhesives are usually mixed with fillers and excipients to form filling masses (pastes) adjusted to the requirements of specific objects, but some of them, especially synthetic resins, are sometimes used separately. In the past, mainly natural adhesives have been used, such as animal glues, natural oils or waxes. They have been replaced by synthetic polymers (e.g., acrylic, epoxy or vinyl resins, silicones, polyurethanes) with better performance and improved durability. There are also commercial adhesive formulations on the market, with properties suitable for outdoor applications, but still little is known about their endurance, resistance to ageing or reversibility [11,13,16,31,33].

### 2.2.1. Animal Glues

Animal glues were among the first adhesives used in construction, manufacture, and conservation (their history dates back at least to ancient Egypt) and they are still in use to present times. Derived mainly from animal collagen—the most abundant mammalian protein present in bones, tendon, skin, connective tissue, and cartilage—they have different chemical, physical, and mechanical properties depending on their origin and a method of preparation. Nevertheless, they have proven to be extremely useful as adhesives and binding media for various purposes, and under certain conditions, they can be highly durable as evidenced by centuries-old fills or joints found in historical artefacts [17,30,54,55].

Animal glues are natural and water-soluble, which reflects in their properties. They are non-toxic, thermoplastic, as well as reversible and retreatable (unlike synthetic resins) and have great adhesion to the wood surface, which suits the conservation purposes. On the other hand, as a good source of nutrients, they are prone to biodegradation, and their hygroscopicity makes them susceptible to moisture changes, which results in their shrinkage, brittleness, and a tendency to fracture when they dry, or in their softening and bleeding when they undergo plastic deformation under wet conditions. These drawbacks

predispose animal glues to serve mainly as interior adhesives [30,33,55–58]. However, their modification with additives such as inert fillers, plasticisers or pigments can significantly improve their performance (by limiting their dimensional changes upon moisture fluctuations and altering their mechanical properties) and give them the properties necessary for gap fillers for specific outdoor conservation purposes [57]. Animal glues do not stain the wooden surface nor cause wood discolouration and can be easily removed from places where they are undesired. Under optimal external conditions (without significant changes in moisture and temperature and limited risk of biodegradation), they can be stable and durable [30,33,55].

Besides the glues based on mammalian collagen, there is a variety of different animal glues, including casein glue, albumin glue or fish glue, which have been applied as paint media, adhesives for architectural, manufacturing, and conservation purposes, as well as binding media for bole and gesso in gilding [33,55,59].

### 2.2.2. Waxes, Oils, and Natural Resins

Waxes are some of the oldest materials used in monuments craft and conservation—beeswax was used by ancient Egyptian craftsmen or applied by the ancient Romans to fix Greek marble statues damaged during transportation [60]. Apart from beeswax, other natural waxes have been used since the beginning of the 19th century, including those of plant (e.g., carnauba, candelilla, esparto, ouricuri) or animal origin (Chinese insect wax, lanolin, shellac wax, spermaceti); nowadays, mineral waxes originated from natural deposits (ozokerite or montan wax) or extracted from crude oil are also in use in the form of paraffin (larger crystalline size) or microcrystalline wax (smaller crystalline size) [17,61].

Waxes are used as coatings, binders or consolidation agents for degraded wood and can be suitable as gap fillers for wooden objects which are not subjected to high temperatures (close to or exceeding the melting point of waxes) [17,31,55,60]. They are non-toxic, inert, chemically stable, resistant to organic solvents, and hydrophobic. They are the traditional choice in conservation since they do not shrink upon setting, can be colour matched to the surrounding surface, and easily removed (due to their low bonding strength and lack of tension between the fill and the surrounding wood). On the other hand, the hydrophobic nature prevents them from expanding or contracting along with wood movements caused by humidity fluctuations, which can lead to falling out of wax fills. Unfortunately, waxes melt and leak out under higher temperatures and significantly increase the weight of a conserved artefact; they are prone to dust accumulation and can be easily scratched because they have poor mechanical resistance. However, their filling performance can be improved when they are mixed with fillers and adhesives [17,55,56,62,63].

Linseed oil (so-called flax oil or flaxseed oil) has also been widely used in wood craft and conservation. It is non-toxic and water-resistant, ubiquitous, easily available and relatively cheap, and as a drying oil that can polymerise into a solid form when exposed to oxygen from the air, it is perfect for various purposes: for finishing wood surfaces, for wood impregnation when blended with resins, other oils or solvents, as a plasticiser and hardener in putties and other filling masses, or as a pigment binder in paints and gildings. However, the development of synthetic resins with better performance significantly limited its application in the past few decades [55,56,62].

Natural tree resins were also utilised in the past for art craft and conservation. Although relatively thermo-chemically stable, they have insufficient flexibility and adhesion to wood to serve as components of gap-fillers in wooden objects [31].

### 2.2.3. Cellulose Ethers and Esters

Cellulose, as mentioned above, can serve as a filler, but its soluble derivatives—ethers and esters—are also used as adhesives or consolidants in wood conservation.

Cellulose ethers are water-soluble polymers produced by chemical modification of cellulose. The modification process includes extraction of cellulose from natural fibres (cotton, wood), treatment with an alkaline solution, and then reaction with various etherification reagents. The process disrupts hydrogen bonds in cellulose, which allows other compounds to bond with glucose units, but also results in a significant reduction of cellulose crystallinity. The resulting products are hygroscopic white powders applied as thickeners, stabilisers, and viscosity modifiers in a variety of industries, and their properties are similar to some synthetic or natural water-soluble polymers (polyurethanes, polyacrylates, polyvinyl alcohol or carrageenan, xanthan gum, locust bean gum) [18,58,64,65].

In wood conservation, mainly methyl and hydroxypropyl cellulose are used as consolidation agents or adhesives; however, other ethers have been recently tested [18,23,24,36,55,66,67]. The most common compound is Klucel<sup>®</sup> (hydroxypropyl cellulose), available in a wide range of grades and viscosity; however, because high-molecular-weight Klucel<sup>®</sup> (types H and M) was found unstable, mainly the low molecular G type is in use. Klucel<sup>®</sup> is soluble in water or ethanol; it has been applied as an adhesive in combination with paper pulp, microballoons, and cellulose powder, or a mixture thereof, for filling losses in wooden objects exposed mainly in museum interiors [18,68–70]. It was shown to be susceptible to ageing/weathering, similar to cellulose or other cellulose ethers [18].

Studies on Klucel<sup>®</sup> G mixed with ground chalk revealed that such a mass is prone to slump and shrink upon drying; therefore, is not suitable as a gap-filler [13]. On the other hand, as shown by Fulcher [18], a blend of Klucel<sup>®</sup> G with paper pulp meets almost all the criteria set for gap fillers for wooden artefacts. The fill is compatible with wood and responds to moisture fluctuations similarly to wood. Therefore, potentially, it could be used outdoors. Its hardness and strength can be adjusted to the requirements of the object by changing the concentration of an adhesive, and it can be prepared using a variety of solvents suitable for individual artefacts. The important thing is that the fill should be considered a system, and its properties are not a sum of the properties of its components because individual ingredients—a bulking agent, an adhesive, and a solvent—affect each other, modifying the resulting material and its reactions to the surrounding environment. Kryg et al. [23] studied fills composed of Klucel<sup>®</sup> G and wood powder or glass microballoons as bulking agents, using acetone or water as solvents. The results show that the properties of the examined fills differed significantly depending on the solvent and the filler/adhesive ratio. Because all the fills were susceptible to water, none of them was suitable for external application.

Among other cellulose derivatives sometimes used in conservation are cellulose esters: nitrate and acetate. They dry quickly and degrade easily by discolouring and releasing acidic vapours, become brittle in time and prone to cracks, and their binding properties are relatively weak. To improve its filling performance, cellulose nitrate was sometimes plasticised with other materials; mixed with wood dust served as a filling mass called “Plastic Wood”. Today, however, there are plenty of better adhesives. Therefore, cellulose esters are not a primary choice as adhesives for wood conservation [17,56,58].

#### 2.2.4. Synthetic Resins

Synthetic resins are liquid, semi-liquid or soft solid viscous substances industrially produced in polymerisation, polycondensation or polyaddition reactions. They are mixtures of prepolymers (oligomers and short polymers) that contain highly reactive functional groups, which enable their further polymerisation and cross-linking in the process called curing. It leads to the formation of rigid polymers as final products. Depending on the chemical structure and the production method, there are various classes of synthetic resins, including acrylic, epoxy, vinyl, polyurethane, etc. Considering their reversibility, there are two different types of resins: thermoplastic, which softens upon heating and hardens again—they are easily moulded, and therefore are suitable for filling purposes—and thermosetting, which undergo irreversible hardening by curing. Synthetic resins are applied widely as adhesives, coatings, cross-linkers, etc. They are also used in art conservation as

consolidants, adhesives or protectives and are considered as more resistant to degradation and better performing compared to natural adhesives [30,31,53,58,71]. Some of the most common synthetic resins in wood conservation are described below.

- Acrylic resins

Acrylic resins are thermoplastic or thermosetting polymers commonly used in artwork conservation. They are colourless, transparent, inert, reversible, insoluble in water, but easily soluble in organic solvents including fast-drying acetone or safe for finishes or paints xylene, which are frequently used in wooden artwork conservation. They have good adhesion and mechanical properties. Although highly resistant to temperature, acids and alkalis, in the long term they are prone to microbial degradation, UV radiation, and mechanical damage to some extent, which can change their physical and mechanical characteristics [20,22,30,61,72,73].

Paraloid B72 (methyl-acrylate/ethylene methyl-acrylate copolymer) is the most popular acrylic resin applied in conservation and restoration owing to its flexibility, good optical properties, and removability combined with higher photo-thermal oxidation stability and lower water sorption than other members of this resin family. It performs well as a consolidant for degraded wood, a barrier coating or protective layer for different surfaces, but is also useful as an adhesive, including its application for gap-filling masses in combination with different bulking agents [20–22,31,72,74]. When mixed with microcrystalline cellulose, it can form an innovative thermoplastic composite with enhanced thermal stability and mechanical performance (including an increase of the elastic modulus and storage modulus, as well as improved creep stability) proportional to the concentration of MCC. Although MCC increased the moisture content of the composite, it also had a stabilising effect on it. The results show that the addition of MCC is an efficient way to improve the performance of acrylic resins used for conservation purposes where dimensional stability and energy absorption capability under external loads are necessary, which relates to some of the requirements for gap-fillers for wooden artefacts exposed outdoors [20,22]. A study by Kryg et al. [23] revealed that a blend of higher concentrations of Paraloid B72 and glass microballoons, although not highly flexible, was relatively dimensionally stable upon drying and exposure to water vapour and liquid water (despite high absorption of moisture) and was quite easy to finish; these features make it potentially useful as a gap-filler for external use. On the other hand, the blends of Paraloid B72 and wood powder turned out to be soft and fragile, difficult in finishing, and highly sensitive to moisture. Only those with a binder concentration of 50% were relatively compact and stable under humid conditions [23].

There is also a variety of commercial fillers based on acrylic polymers that are potentially useful in filling losses in wooden objects. These ready-to-use fillers contain various binders, bulking agents, and additional substances. The problem is that their composition is a trade secret; therefore, it is hard to predict their properties under certain conditions. Although they are usually recommended by manufacturers for particular applications, there are limited references for their use in wood conservation [15].

- Epoxy resins

Epoxy resins are reactive polymers or pre-polymers that contain epoxy groups. They are soluble in organic solvents, and their solubility depends on their molar mass. Low-molecular-weight liquid resins are soluble in toluene, xylene, benzene, acetone, cyclohexanone, etc. Higher-molecular-weight solid-state resins are soluble in acetone and cyclohexanone, and partially soluble in aromatic hydrocarbons. Due to reactive epoxy groups, epoxy resins can cross-link with themselves or with several different chemicals (e.g., acids, alcohols, amines, phenols, thiols, etc.) in the process called curing or hardening, forming a thermosetting polymer as a final product. Epoxy polymers are insoluble, relatively resistant to weathering, moisture, and UV radiation, with enhanced mechanical properties and thermo-chemical resistance. Therefore, they are employed widely in different industries, i.e., as adhesives, coatings, and components of composite materials [61,75].

Epoxy resins are also useful in wood conservation and applied as adhesives (e.g., for conservation of panel paintings), consolidants or fillers. Different formulations can make them compatible with concrete, glass, stone, wood, or other materials. Since they are thermosetting polymers, they should be considered irreversible, which is against conservation rules. Nevertheless, in some cases, where the strengthening of an artefact is a primary aim, the principle of irreversibility becomes secondary, and the application of epoxies can be approved. Irreversibility can be sometimes bypassed by coating the surface of a hole in wood with a reversible coating which enables the fill to be easily removed if necessary. The only problem that remains then is the proper adhesive strength between the coating and wood and between the coating and a fill [11–14,33,63,72].

Epoxy resins should not be used alone as fills for wooden objects because they can penetrate wooden tissue, thus irreversibly change the properties of wood (they are not flexible enough when they polymerise, making wood rigid, brittle, and prone to rupture). However, when combined with various fillers and additives that increase their viscosity, they can make a gap-filling paste ideal for filling voids, holes, checks, and splits of different origin in wooden objects. Epoxy-based masses adhere well to a wooden surface and are relatively durable and long-lasting, which makes them a good choice for external applications. They are easy to work with (sanding, carving, etc.), leaving a nice finished surface; they can also be coloured by adding pigments to resins or painting the surface of an already cured mass [11,13,16,61,76,77]. Unfortunately, they are not free from drawbacks. First of all, even when mixed with fillers (e.g., microballoons), they can still have high compression modulus. Under humid conditions, the surrounding wood can be stressed because it cannot expand while absorbing moisture, which may result in its warping or crushing. On the other hand, when such wood dries, tensile stress can cause check formation between the fill and wood [13,14]. Additionally, due to the different mechanical characteristics of microballoons and epoxy matrix, the stresses localised in various parts of the composite itself can cause cracks and voids in the fill [51]. Other concerns are the previously mentioned irreversibility, yellowing when exposed to heat or light (important for art or historical artefacts where epoxies are visible on the surface), and the heat released during the curing process [13,33,77]. Nevertheless, epoxy-based masses have been applied frequently for gap-filling in wooden artefacts exposed outdoors, and, in some cases (e.g., in applications where wooden artefact remains in a moderately stable relative humidity or when wood does not undergo significant dimensional changes upon changes in moisture conditions), they can be the best choice [13,14,77,78].

- Polyurethanes

Polyurethanes are synthetic resins produced via polyaddition reaction of dialcohols or polyols and polyisocyanates. Depending on the chemical composition, both thermosetting plastics and elastomers are available with different properties. Therefore, they can be used in a wide range of industrial applications. Generally, they have medium viscosity, which makes them easy to mix and process, but also to cast and shape. They can be combined with various additives, including inhibitors, pigments or fillers, to give them properties required for specific applications. They have a short curing time and do not shrink much upon curing; however, their adhesive properties are not as good as those of epoxy resins [55,79–83].

Polyurethane resins can be used to produce polyurethane foams, which are commonly used as insulating materials in construction. In accordance with their mechanical characteristics, particularly their rigidity, stiffness, and compressive and tensile properties, they can be categorised as flexible, semi-rigid or rigid foams [82,84]. Their good dimensional stability, high durability, low weight, low thermic coefficient, good moisture and compression resistance, and easy workability make them also suitable for filling gaps in wooden artefacts. Polyurethane foams adhere well to wood and are resistant to high temperatures, UV radiation, and chemicals. However, their moisture properties are not compatible with wood. They should be applied layer by layer to the dry wood surface to limit temperature rise and ensure the proper foaming process. Cured foams are easily workable with all tools

typically used for wood and can be painted. They can also be mechanically removed from an object when necessary [84,85].

- Vinyl resins

The term “vinyl resin” refers to different compounds, usually vinyl acetate, vinyl chloride, vinyl ether, vinyl butyral or copolymer blends of these. They can be used in dispersions, emulsions, and solutions and also mixed with different additives (e.g., pigments) to tailor their properties to specific applications. They polymerise easily at ambient or elevated temperatures, and once cured, they are flexible and resistant to water and various chemicals. They adhere well to different surfaces and therefore are commonly employed as adhesives and coatings for various purposes [73,86].

Vinyl resins have found application as consolidants and fillers in wood conservation since the early 1950s. Some examples include a mixture of polyvinyl acetate with sawdust and gypsum applied for filling cracks and holes made by wood-destroying insects, or a blend of polyvinyl butyral, glass microballoons, and pigments applied for filling losses in ancient dry wooden furniture [31,33]. There are also different commercial ready-mixed vinyl filling masses intended for patching plaster or wallboard in the construction industry, which can be adapted for wood conservation. These materials are flexible, have good working properties, and great adhesion to wood. However, they are irreversible, susceptible to UV and heat ageing (they become yellow and brittle), and may be swelled by water, thus damaging paints or gildings and swelling the adjacent wood layers [33]. They may also shrink significantly upon curing and become much harder than low-density wood. All these make them less desirable as gap-fillers [15,30,76].

- Silicone resins

Owing to exceptionally stable silicon-carbon and silicon-oxygen bonds, semi-organic silicone resins are particularly resistant to oxidation and thermal decomposition. Depending on the type of functional groups attached to the silicon atom, various polymers with different properties can be obtained and further modified via their reactive groups (alkyd, polyester, acrylic, and epoxy) to enhance their durability. They have high thermo-chemical stability and are resistant to external factors (humidity, UV radiation). These versatile materials are applied in almost all industry branches, as well as in art conservation [73,87–89].

Among silicon resins, particularly RTV (room-temperature-vulcanising silicone) silicones are suitable for filling losses in wooden objects. These dimethyl siloxanes are commonly available as proprietary formulations in most hardware stores. They are easy to apply, water-resistant, with long-term flexibility, and relatively stable when used outdoors. They do not penetrate wood tissue and can be easily removed by pulling them out of the voids. Their compression modulus is lower than that of most wood, and they can form a perfect, inert, durable, and elastic fill. However, they have poor working and finishing properties. To improve these, they can be blended with various additives, including pigments and fillers. The addition of fillers (e.g., powdered fibreglass or glass microballoons) increases their viscosity. This provides the surface with enough roughness to enable its finishing (sanding, carving, etc.) and painting with acrylic paints [13,16,30,63].

### 3. Summary

To summarise the information mentioned above, Table 1 presents the most important advantages and disadvantages of individual compounds of different filling materials in the context of gap-filling in wooden objects exhibited in the open air.

**Table 1.** A summary of advantages and disadvantages of different materials for filling gaps in wooden artefacts exposed outdoors. Some examples of their application in conservation practice are given in parentheses.

Filling Material/Example of Its Application in Conservation Practice	Advantages	Drawbacks
<b>Fillers</b>		
wooden fills (Chik Kwai Study Hall in Hong Kong [32], The Castle of Racconigi [90], wooden elements in Royal Palace in Wilanów [91], wooden monument in the World War II cemetery in Radomlje [78])	compatible with the wood of the same age and species	different response on moisture than historic wooden tissue if inappropriately chosen, needs to be precisely shaped to ensure proper joint, difficult to match the grain pattern
sawdust, wood shavings (Chik Kwai Study Hall in Hong Kong [32], wooden elements in Royal Palace in Wilanów [91], wooden monument in the World War II cemetery in Radomlje [78])	compatible with wood, easily available, cheap, enhance mechanical performance and workability of moldable filling masses	hygroscopic, appropriate for nonaqueous binders (due to high swelling and shrinkage of fragmented wood in contact with water)
cellulose	non-toxic, easily applicable, compatible with wood, thermo-chemically stable, resistant to swelling in water, low density, high viscosity and specific strength	-
plaster and cement	non-toxic, readily available easily applicable, forms easy workable pastes	lime plaster shrinks and cracks during drying; gypsum plaster expands upon drying and thus can destroy the surrounding wooden tissue; not suitable for degraded wood and under changeable moisture conditions
microballoons (Totem pole from Canadian Museum of Civilization [11])	non-toxic, low density, light weight, form easily workable pastes, can be reversible, reduce shrinkage during drying, improve smoothness and mechanical performance of filling masses, easily paintable, easily mixed with various resins	-
<b>Adhesives (Binders)</b>		
animal glues	natural, non-toxic, completely reversible, excellent adhesion to the wood surface, do not stain wood	prone to biodegradation, extremely hygroscopic, very sensitive to moisture and temperature fluctuations (swelling and shrinkage)
waxes, oils and natural resins	non-toxic, chemically stable, resistant to moisture and water, reversible, do not change colour upon ageing	vulnerable to dust accumulation, poor mechanical resistance, low bond strength, not resistant to heat
cellulose ethers and esters	compatible with wood, response to moisture fluctuations similar to wood, good adhesion	prone to shrink upon drying, become brittle over time, poor penetration into wood
acrylic resins (wooden gateway from the historical centre of Brasov [56])	flexible, high photo-thermal stability, good adhesion and mechanical properties, inert, reversible	prone to biodegradation in the long term, UV radiation, and mechanical damage
epoxy resins (Totem pole from Canadian Museum of Civilization [11], Chik Kwai Study Hall in Hong Kong [32], the wooden monument in the World War II cemetery in Radomlje [78])	easy to be carved, sanded or finishing after setting, durable, easily workable, resistant to weathering, good mechanical properties	irreversible after curing, easily penetrate wood tissue—not appropriate to use alone since they change wood properties
polyurethanes (Ionic capitals from Mount Pleasant, a historic house in Fairmount Park, Philadelphia [16])	easy to mix, process, cast, and shape, dimensionally stable upon drying, resistant to high temperatures, UV radiation and chemicals, durable, good moisture and compression resistance	insoluble in solvents once cured, moisture properties different from wood

Table 1. Cont.

Filling Material/Example of Its Application in Conservation Practice	Advantages	Drawbacks
vinyl resins (adornments in towers of Royal Palace at Wilanów [92], wooden elements in Royal Palace in Wilanów [91])	quite soft, flexible, easily workable, resistant to water and chemicals, good adhesion	in mixtures with different compounds can be irreversible, susceptible to UV and heat ageing, shrink upon drying, may be swelled by water and destroy gildings and paints
silicone resins (wooden doors attributed to the Spanish Colonial period from a historic farmstead south of San Antonio [63])	high thermo-chemical stability, resistance to external factors, elastic, do not penetrate the wood fibres, inert after curing, compression modulus lower than wood, resistant to water, easily reversed by mechanically pulling them out of the gap, durable (at least 10 years when used outdoors)	poor working properties, low compatibility with paint, may penetrate wood before curing

#### 4. Conclusions

The presented survey leads to the conclusion that although the materials applied for filling losses in wooden artefacts exposed outdoors are highly diverse, none of them fully comply with all conditions required for outdoor application in wood or meet all requirements of conservation ethics, perhaps because none of them was intended for such a purpose. The most common problem of filling materials concerns their compatibility with wood, mainly susceptibility to moisture and the relating dimensional changes, as well as mechanical properties. Excessive shrinkage or swelling of fills in response to humidity fluctuations, different from wood behaviour may threaten the integrity of wooden artefacts. The same relates to differences in flexibility, compression or tensile strength. Another serious drawback involves poor adhesion of fills to the wood surface or insufficient cohesion of the fill itself; they can lead to gap formation between wood and filling mass or within a fill, further microbial infestations due to the presence of water collected in new cracks and, as a consequence, degradation of the wooden object. Susceptibility to weather conditions and biodegradation, causing changes in wood colour or damaging paints and gildings on the wood surface as well as irreversibility, complete the list of shortcomings. Therefore, there is a constant need to develop new, more effective gap-fillers to properly protect priceless historical wooden objects for future generations.

It can be concluded that among the most promising materials are blends and composites made up of various substances, particularly natural compounds compatible with wood. Depending on the composition and the ratios of individual components, the properties of such materials could be potentially adjusted to the needs and requirements of specific applications. Broad research has been conducted recently on composites based on both natural and synthetic components for various purposes that proves the possibility of developing materials with desired characteristics [79–81,83,93–96]. However, as pointed out by Fulcher [18], it should be remembered that such filling composites, “... should be considered as a system, and its properties are not a sum of the properties of its components, because individual ingredients—a bulking agent, an adhesive and a solvent—affect each other, modifying the resulting material and its reactions to the surrounding environment”.

Having efficient, safe, and verified conservation materials and methods is essential to preserve our cultural heritage, but, even if there are some good filling materials, there is still not enough scientific data on their long-term behaviour and durability. Therefore, close cooperation between scientists and conservators is necessary to understand both the needs of cultural heritage artefacts and the properties of materials proposed for their conservation and make all the process being in line with conservation ethics, because “Conservation practice seeks to understand and preserve tangible cultural property, whereas conservation ethics seek to understand and preserve intangible cultural property” [5].



**Author Contributions:** Conceptualisation, M.B. and P.K.; writing—original draft preparation, M.B., P.K. and G.A.O.; writing—review and editing, P.K., M.B. and G.A.O.; visualisation, P.K. and M.B.; supervision, M.B. All authors have read and agreed to the published version of the manuscript.

**Funding:** This research received no external funding.

**Institutional Review Board Statement:** Not applicable.

**Informed Consent Statement:** Not applicable.

**Conflicts of Interest:** The authors declare no conflict of interest. The funders had no role in the design of the study; in the collection, analyses, or interpretation of data; in the writing of the manuscript, or in the decision to publish the results.

## References

1. Ali, Z.M.; Zawawi, R. Contributions of Open Air Museums In Preserving Heritage Buildings: Study of Open-Air Museums in South East England. *JDBE* **2010**, *7*. Available online: <https://ejournal.um.edu.my/index.php/jdbe/article/view/5298> (accessed on 10 April 2021).
2. Paardekooper, R. *The Value of an Archaeological Open-Air Museum Is in Its Use: Understanding Archaeological Open-Air Museums and Their Visitors*; Sidestone Press: Leiden, The Netherlands, 2012.
3. Sevan, O. Open Air Museums as Ways of Preserving and Transmitting the Spirit of Place. In Proceedings of the 16th ICOMOS General Assembly and International Symposium: ‘Finding the Spirit of Place—Between the Tangible and the Intangible’, Quebec, QC, Canada, 29 September–4 October 2008.
4. Hurt, R.D. Agricultural Museums: A New Frontier for the Social Sciences. *Hist. Teach.* **1978**, *11*, 367–375. [CrossRef]
5. Rivers, S. Conservation of Japanese Lacquer in Western Collections—Conserving Meaning and Substance. In Proceedings of the Preprints of the 14th Triennial Meeting of the ICOM Committee for Conservation, The Hague, The Netherlands, 12–16 September 2005; James & James: London, UK, 2005; pp. 1083–1086.
6. Schmidt, O. *Wood and Tree Fungi: Biology, Damage, Protection, and Use*; Springer Science & Business Media: Berlin/Heidelberg, Germany, 2006.
7. Tolvaj, L.; Popescu, C.-M.; Molnar, Z.; Preklet, E. Effects of Air Relative Humidity and Temperature on Photodegradation Processes in Beech and Spruce Wood. *BioResources* **2016**, *11*, 296–305. [CrossRef]
8. Witomski, P. Konserwacja Zachowawcza a Trwałość Budowli Drewnianych. *Bud. I Arch.* **2015**, *14*, 157–164. [CrossRef]
9. Wermuth, J.A. Simple and Integrated Consolidation Systems for Degraded Wood. In *Archaeological Wood*; Advances in Chemistry; American Chemical Society: Washington, DC, USA, 1989; Volume 225, pp. 301–359. ISBN 978-0-8412-1623-5.
10. Podmaniczky, M.S. Structural Fills for Large Wood Objects: Contrasting and Complementary Approaches. *JAIC* **1998**, *37*, 111–116. [CrossRef]
11. Barclay, R.; Mathias, C. An Epoxy/Microballoon Mixture for Gap Filling in Wooden Objects. *JAIC* **1989**, *28*, 31–42. [CrossRef]
12. Phillips, M.W.; Selwyn, J.E. *Epoxy Resins for Wood Repairs in Historic Buildings*; Office of Archeology and Historic Preservation, Heritage Conservation and Recreation Service, US Department of the Interior, Technical Preservation Services Division: Washington DC, USA, 1978.
13. Grattan, D.W.; Barclay, R.L. A Study of Gap-Fillers for Wooden Objects. *Stud. Conserv.* **1988**, *33*, 71–86. [CrossRef]
14. Cleary, R. Considering the Use of Epoxies in the Repair of Historic Structural Timber. Master’s Thesis, University of Pennsylvania, Philadelphia, PA, USA, 2014.
15. Craft, M.L.; Solz, J.A. Commercial Vinyl and Acrylic Fill Materials. *JAIC* **1998**, *37*, 23–34. [CrossRef]
16. Deurenberg-Wilkinson, R.M. Choosing an Adhesive for Exterior Woodwork Through Mechanical Testing. *JAIC* **2015**, *54*, 74–90. [CrossRef]
17. Thornton, J. A Brief History and Review of the Early Practice and Materials of Gap-Filling In the West. *JAIC* **1998**, *37*, 3–22. [CrossRef]
18. Fulcher, K. An Investigation of the Use of Cellulose-Based Materials to Gap-Fill Wooden Objects. *Stud. Conserv.* **2017**, *62*, 210–222. [CrossRef]
19. Fulcher, K.E. Survey on Material Used to Fill Wooden Objects during Conservation. *J Open Archaeol Data* **2014**, *3*. [CrossRef]
20. Cataldi, A.; Dorigato, A.; Deflorian, F.; Pegoretti, A. Effect of the Water Sorption on the Mechanical Response of Microcrystalline Cellulose-Based Composites for Art Protection and Restoration. *J. Appl. Polym. Sci.* **2014**, *131*. [CrossRef]
21. Cataldi, A.; Deflorian, F.; Pegoretti, A. Microcrystalline Cellulose Filled Composites for Wooden Artwork Consolidation: Application and Physic-Mechanical Characterization. *Mater. Des.* **2015**, *83*, 611–619. [CrossRef]
22. Cataldi, A.; Dorigato, A.; Deflorian, F.; Pegoretti, A. Thermo-Mechanical Properties of Innovative Microcrystalline Cellulose Filled Composites for Art Protection and Restoration. *J. Mater. Sci.* **2014**, *49*, 2035–2044. [CrossRef]
23. Kryg, P.; Mazela, B.; Broda, M. Dimensional Stability and Moisture Properties of Gap-Fillers Based on Wood Powder and Glass Microballoons. *Stud. Conserv.* **2020**, *65*, 142–151. [CrossRef]

24. Infurna, G.; Cavallaro, G.; Lazzara, G.; Milioto, S.; Dintcheva, N.T. Bionanocomposite Films Containing Halloysite Nanotubes and Natural Antioxidants with Enhanced Performance and Durability as Promising Materials for Cultural Heritage Protection. *Polymers* **2020**, *12*, 1973. [CrossRef] [PubMed]
25. Cavallaro, G.; Milioto, S.; Lazzara, G. Halloysite Nanotubes: Interfacial Properties and Applications in Cultural Heritage. *Langmuir* **2020**, *36*, 3677–3689. [CrossRef]
26. Broda, M. Natural Compounds for Wood Protection against Fungi—A Review. *Molecules* **2020**, *25*, 3538. [CrossRef]
27. Bettina, G.F.; Giambra, B.; Cavallaro, G.; Lazzara, G.; Megna, B.; Fakhrullin, R.; Akhatova, F.; Fakhrullin, R. Restoration of a XVII Century's Predella Reliquary: From Physico-Chemical Characterization to the Conservation Process. *Forests* **2021**, *12*, 345. [CrossRef]
28. Fulcher, K. The Diverse Use of AJK Dough in Conservation. *J. Inst. Conserv.* **2014**, *37*, 32–42. [CrossRef]
29. Abdallah, M.; Kamal, H.M.; Abdrabou, A. Investigation, Preservation and Restoration Processes of an Ancient Egyptian Wooden Offering Table. *IJCS* **2016**, *7*, 1047–1064.
30. Williams, D.C. Some Experiences with Flexible Gap-Filling Adhesives for the Conservation of Wood Objects. In Proceedings of the Facing the Challenges of Panel Paintings Conservation: Trends, Treatments, and Training, Los Angeles, CA, USA, 17–18 May 2009.
31. Unger, A.; Schniewind, A.; Unger, W. *Conservation of Wood Artifacts: A Handbook*; Springer Science & Business Media: Berlin/Heidelberg, Germany, 2001.
32. Leung, E.S.; Yeung, E.S.; Chan, S.W. Strike a Balance—Repair or Replace? *Adv. Mater. Res.* **2010**, *133*, 997–1002.
33. Young, C.; Ackroyd, P.; Hibberd, R.; Gritt, S. The Mechanical Behaviour of Adhesives and Gap Fillers for Re-Joining Panel Paintings. *Natl. Gallery Tech. Bull.* **2002**, *23*, 83–96.
34. Huuhilo, T.; Martikka, O.; Butylina, S.; Kärki, T. Mineral Fillers for Wood–Plastic Composites. *Wood Mater. Sci. Eng.* **2010**, *5*, 34–40. [CrossRef]
35. Antonelli, F.; Galotta, G.; Sidoti, G.; Zikeli, F.; Nisi, R.; Petriaggi, B.D.; Romagnoli, M. Cellulose and Lignin Nano-Scale Consolidants for Waterlogged Archaeological Wood. *Front. Chem.* **2020**, *8*. [CrossRef] [PubMed]
36. Hamed, S.A.A.K.M.; Hassan, M.L. A New Mixture of Hydroxypropyl Cellulose and Nanocellulose for Wood Consolidation. *J. Cult. Herit.* **2019**, *35*, 140–144. [CrossRef]
37. Fierascu, R.C.; Doni, M.; Fierascu, I. Selected Aspects Regarding the Restoration/Conservation of Traditional Wood and Masonry Building Materials: A Short Overview of the Last Decade Findings. *Appl. Sci.* **2020**, *10*, 1164. [CrossRef]
38. Haldar, D.; Purkait, M.K. Micro and Nanocrystalline Cellulose Derivatives of Lignocellulosic Biomass: A Review on Synthesis, Applications and Advancements. *Carbohydr. Polym.* **2020**, *250*, 116937. [CrossRef]
39. Collazo-Bigliardi, S.; Ortega-Toro, R.; Boix, A.C. Isolation and Characterisation of Microcrystalline Cellulose and Cellulose Nanocrystals from Coffee Husk and Comparative Study with Rice Husk. *Carbohydr. Polym.* **2018**, *191*, 205–215. [CrossRef]
40. Katakjwala, R.; Mohan, S.V. Microcrystalline Cellulose Production from Sugarcane Bagasse: Sustainable Process Development and Life Cycle Assessment. *J. Clean. Prod.* **2020**, *249*, 119342. [CrossRef]
41. Rasheed, M.; Jawaid, M.; Karim, Z.; Abdullah, L.C. Morphological, Physiochemical and Thermal Properties of Microcrystalline Cellulose (MCC) Extracted from Bamboo Fiber. *Molecules* **2020**, *25*, 2824. [CrossRef] [PubMed]
42. El Hadidi, N.; Abdel-Monem, H.; Mohamed, M.; Hashem, G. Retreatment and Conservation of a Wooden Panel Previously Treated with Bees Wax. *Adv. Res. Conserv. Sci.* **2020**, *1*, 48–65. [CrossRef]
43. Artal-Isbrand, P. So Delicate yet so Strong and Versatile—the Use of Paper in Objects Conservation. *JAIC* **2018**, *57*, 112–126. [CrossRef]
44. Chen, H.; Nair, S.S.; Chauhan, P.; Yan, N. Lignin Containing Cellulose Nanofibril Application in PMDI Wood Adhesives for Drastically Improved Gap-Filling Properties with Robust Bondline Interfaces. *Chem. Eng. J.* **2019**, *360*, 393–401. [CrossRef]
45. Asgari, A.; Hemmasi, A.; Bazayr, B.; Taleipour, M.; Nourbakhsh, A. Inspecting the Properties of Polypropylene/ Poplar Wood Flour Composites with Microcrystalline Cellulose and Starch Powder Addition. *BioResources* **2020**, *15*, 4188–4204.
46. Karakus, K.; Atar, İ.; Başboğa, İ.H.; Bozkurt, F.; Mengeloğlu, F. Wood Ash and Microcrystalline Cellulose (MCC) Filled Unsaturated Polyester Composites. *Kast. Univ. J. For. Fac.* **2017**, *17*, 282–289. [CrossRef]
47. Hatchfield, P. Note on a Fill Material for Water Sensitive Objects. *JAIC* **1986**, *25*, 93–96. [CrossRef]
48. Iaccarino Idelson, A.; Pannuzi, S.; Brunetto, A.; Galanti, G.; Giovannone, C.; Massa, V.; Serino, C.; Vischetti, F. Use of 3D technologies within the conservation of the ancient windows of the basilica of s. Sabina in rome. Construction of exhibition stands in carbon composite on a milled structure. *Int. Arch. Photogramm. Remote Sens. Spat. Inf. Sci.* **2017**, *XLII-5/W1*, 593–598. [CrossRef]
49. Nabil, E. Scientific Methods for the Treatment of Ibis Mummy's Wooden Coffin. *Egypt. J. Archaeol. Restor. Stud.* **2020**, *10*, 9–21. [CrossRef]
50. Carlisle, K.B.; Chawla, K.K.; Gladysz, G.M.; Koopman, M. Structure and Mechanical Properties of Micro and Macro Balloons: An Overview of Test Techniques. *J. Mater. Sci.* **2006**, *41*, 3961–3972. [CrossRef]
51. Huang, R.; Li, P. Elastic Behaviour and Failure Mechanism in Epoxy Syntactic Foams: The Effect of Glass Microballoon Volume Fractions. *Compos. Part B Eng.* **2015**, *78*, 401–408. [CrossRef]
52. Hsu, H.-H.; Sully, D. Fusing and Refreshing the Memory: Conserving a Chinese Lacquered Buddha Sculpture in London. *Stud. Conserv.* **2016**, *61*, 124–130. [CrossRef]
53. Nakhla, S.M. A Comparative Study of Resins for the Consolidation of Wooden Objects. *Stud. Conserv.* **1986**, *31*, 38–44. [CrossRef]

54. Schellmann, N. Consolidation of Stressed and Lifting Decorative Coatings on Wood. The Effect on Consolidant Choice on the Structural Integrity of Multilayered East Asian Lacquer Coatings with Gesso-Like Foundation Layers. Ph.D. Thesis, Hochschule der Bildenden Künste Dresden, Dresden, Germany, 2012.
55. Rivers, S.; Umney, N. *Conservation of Furniture*; Routledge: Oxfordshire, UK, 2007.
56. Tuduce-Traistaru, A.-A.; Campean, M.; Timar, M.C. Compatibility Indicators in Developing Consolidation Materials with Nanoparticle Insertions for Old Wooden Objects. *Int. J. Conserv. Sci.* **2010**, *1*, 219–226.
57. Schellmann, N.C. Animal Glues: A Review of Their Key Properties Relevant to Conservation. *Stud. Conserv.* **2007**, *52*, 55–66. [CrossRef]
58. McGlinchey, C. Polymers in Conservation. *Encycl. Archaeol. Sci.* **2018**, 1–3. [CrossRef]
59. Jeszeová, L.; Bauerová-Hlinková, V.; Baráth, P.; Puškárová, A.; Bučková, M.; Kraková, L.; Pangallo, D. Biochemical and Proteomic Characterization of the Extracellular Enzymatic Preparate of *Exiguobacterium Undae*, Suitable for Efficient Animal Glue Removal. *Appl. Microbiol. Biotechnol.* **2018**, *102*, 6525–6536. [CrossRef]
60. Webb, M. Methods and Materials for Filling Losses on Lacquer Objects. *JAIC* **1998**, *37*, 117–133. [CrossRef]
61. Szczepińska, K. Historycznie Stosowane Impregnaty Do Wzmocnienia Zniszczonego Drewna Polichromowanego—Próba Przeglądu. Część II: Impregnaty Syntetyczne. *Acta Univ. Nicolai Copernic. Zabytkozn. I Konserw.* **2015**, 469–508. [CrossRef]
62. Szczepińska, K. Historycznie stosowane impregnaty do wzmocnienia zniszczonego drewna polichromowanego—próba przeglądu. Część I: Impregnaty naturalne. *Acta Univ. Nicolai Copernic.* **2014**, 569. [CrossRef]
63. Storch, P.S. Fills for Bridging Structural Gaps in Wooden Objects. *J. Am. Inst. Conserv.* **1994**, *33*, 71–75. [CrossRef]
64. Majewicz, T.G.; Erazo-Majewicz, P.E.; Podlas, T.J. Cellulose Ethers. *Encycl. Polym. Sci. Technol.* **2002**. [CrossRef]
65. Shaghaleh, H.; Xu, X.; Wang, S. Current Progress in Production of Biopolymeric Materials Based on Cellulose, Cellulose Nanofibers, and Cellulose Derivatives. *RSC Adv.* **2018**, *8*, 825–842. [CrossRef]
66. Walsh, Z.; Janeček, E.-R.; Jones, M.; Scherman, O.A. Natural Polymers as Alternative Consolidants for the Preservation of Waterlogged Archaeological Wood. *Stud. Conserv.* **2017**, *62*, 173–183. [CrossRef]
67. Cavallaro, G.; Lazzara, G.; Milioto, S.; Parisi, F. Halloysite Nanotubes for Cleaning, Consolidation and Protection. *Chem. Rec.* **2018**, *18*, 940–949. [CrossRef] [PubMed]
68. Elston, M. Technology and Conservation of a Polychromed Wooden Sarcophagus. In Proceedings of the Conservation in Ancient Egyptian Collections, London, UK, 20–21 July 1995; pp. 13–21.
69. Gänsicke, S.; Hatchfield, P.; Hykin, A.; Svoboda, M.; Tsu, C.M.-A. The Ancient Egyptian Collection at the Museum of Fine Arts, Boston. Part 2, A Review of Former Treatments at the MFA and Their Consequences. *JAIC* **2003**, *42*, 193–236. [CrossRef]
70. Johnson, C.; Head, K.; Green, L. The Conservation of a Polychrome Egyptian Coffin. *Stud. Conserv.* **1995**, *40*, 73–81. [CrossRef]
71. Cappitelli, F.; Zanardini, E.; Sorlini, C. The Biodeterioration of Synthetic Resins Used in Conservation. *Macromol. Biosci.* **2004**, *4*, 399–406. [CrossRef]
72. Ellis, J.L.; Ball, A. Comparison of Two Wood Filler Types with Respect to Relative Shrinkage across Variations in Temperature, in Humidity and within Wood Species. *Int. Wood Prod. J.* **2011**, *2*, 115–119. [CrossRef]
73. Bentley, J. 2—Organic film formers. In *Paint and Surface Coatings*, 2nd ed.; Lambourne, R., Strivens, T.A., Eds.; Woodhead Publishing Series in Metals and Surface Engineering; Woodhead Publishing: Cambridge, UK, 1999; pp. 19–90. ISBN 978-1-85573-348-0.
74. Crisci, G.M.; La Russa, M.F.; Malagodi, M.; Ruffolo, S.A. Consolidating Properties of Regalrez 1126 and Paraloid B72 Applied to Wood. *J. Cult. Herit.* **2010**, *11*, 304–308. [CrossRef]
75. May, C. *Epoxy Resins: Chemistry and Technology*; Routledge: Oxfordshire, UK, 2018.
76. Fox, M. Searching for the Filler of My Dreams—An Odyssey in Gaps and Glues. *J. Vertebr. Paleontol.* **2001**, *21*, 51A. Available online: <http://preparation.paleo.amnh.org/assets/Fox-gapfillerpaper.pdf> (accessed on 10 April 2021).
77. Ellis, L.; Heginbotham, A. An Evaluation of Four Barrier-Coating and Epoxy Combinations in the Structural Repair of Wooden Objects. *J. Am. Inst. Conserv.* **2004**, *43*, 23–37. [CrossRef]
78. Pamic, R.; Pohleven, F. Protection through Construction of a Wooden Monument in Radomlje (Slovenia). *Drewno Prace Nauk. Doniesienia Komun.* **2015**, 58. [CrossRef]
79. Santamaria-Echart, A.; Fernandes, I.; Barreiro, F.; Corcuera, M.A.; Eceiza, A. Advances in Waterborne Polyurethane and Polyurethane-Urea Dispersions and Their Eco-Friendly Derivatives: A Review. *Polymers* **2021**, *13*, 409. [CrossRef]
80. Brzeska, J.; Tercjak, A.; Sikorska, W.; Mendrek, B.; Kowalczyk, M.; Rutkowska, M. Degradability of Polyurethanes and Their Blends with Polylactide, Chitosan and Starch. *Polymers* **2021**, *13*, 1202. [CrossRef]
81. Członka, S.; Kairytė, A.; Miedzińska, K.; Strakowska, A.; Adamus-Włodarczyk, A. Mechanically Strong Polyurethane Composites Reinforced with Montmorillonite-Modified Sage Filler (*Salvia officinalis* L.). *Int. J. Mol. Sci.* **2021**, *22*, 3744. [CrossRef]
82. Randall, D.; Lee, S. *The Polyurethanes Book*; Wiley-Blackwell: Hoboken, NJ, USA, 2002.
83. Alinejad, M.; Henry, C.; Nikafshar, S.; Gondaliya, A.; Bagheri, S.; Chen, N.; Singh, S.K.; Hodge, D.B.; Nejad, M. Lignin-Based Polyurethanes: Opportunities for Bio-Based Foams, Elastomers, Coatings and Adhesives. *Polymers* **2019**, *11*, 1202. [CrossRef]
84. Xu, Z.; Tang, X.; Gu, A.; Fang, Z. Novel Preparation and Mechanical Properties of Rigid Polyurethane Foam/Organoclay Nanocomposites. *J. Appl. Polym. Sci.* **2007**, *106*, 439–447. [CrossRef]
85. Soldenhoff, B. Zastosowanie Sztucznych Pianek Poliuretanowych do Uzupełniania Ubytków Drewna w Obiektach Zabytkowych. *Acta Univ. Nicolai Copernic. Nauk. Humanist. Spo/Lecz. Zabytkozn. I Konserw.* **1979**, *7*, 145–153.

86. Buchheit, R.G. 18—Corrosion Resistant Coatings and Paints. In *Handbook of Environmental Degradation of Materials*, 2nd ed.; Kutz, M., Ed.; William Andrew Publishing: Oxford, UK, 2012; pp. 539–568. ISBN 978-1-4377-3455-3.
87. Robeyns, C.; Picard, L.; Ganachaud, F. Synthesis, Characterization and Modification of Silicone Resins: An “Augmented Review”. *Prog. Org. Coat.* **2018**, *125*, 287–315. [CrossRef]
88. Broda, M.; Dąbek, I.; Dutkiewicz, A.; Dutkiewicz, M.; Popescu, C.-M.; Mazela, B.; Maciejewski, H. Organosilicons of Different Molecular Size and Chemical Structure as Consolidants for Waterlogged Archaeological Wood—A New Reversible and Retreatable Method. *Sci. Rep.* **2020**, *10*, 1–13. [CrossRef]
89. Barclay, R.L.; Grattan, D.W. A Silicone Rubber/Microballoon Mixture for Gap Filling in Wooden Objects. In Proceedings of the ICOM Committee for Conservation: 8th Triennial Meeting, Sydney, Australia, 6–11 September 1987; Preprints. Volume 1, pp. 183–187.
90. Bertolini Cestari, C.; Marzi, T. Conservation of Historic Timber Roof Structures of Italian Architectural Heritage: Diagnosis, Assessment, and Intervention. *Int. J. Arch. Herit.* **2018**, *12*, 632–665. [CrossRef]
91. Czajnik, M.; Rudniewski, P.; Tworek, D. Niektóre Zagadnienia z Prac Nad Konserwacją Elementów Drewnianych. *Ochrona Zabytków* **1962**, *33*, 77–85.
92. Ważny, J. Badanie Wpływu Impregnacji Vinoflexem MP-400 Na Właściwości Techniczne Drewna Wystroju Rzeźbiarskiego Wież Palacu w Wilanowie. *Ochrona Zabytków* **1970**, *23/2*, 83–88. Available online: <http://yadda.icm.edu.pl/yadda/element/bwmeta1.element.desklight-dd146a1e-5cc0-49c9-b7cc-f1fec13ec597> (accessed on 10 March 2021).
93. Sarraj, S.; Szymiczek, M.; Machoczek, T.; Mrówka, M. Evaluation of the Impact of Organic Fillers on Selected Properties of Organosilicon Polymer. *Polymers* **2021**, *13*, 1103. [CrossRef]
94. Réh, R.; Krišták, L.; Sedliačik, J.; Bekhta, P.; Božiková, M.; Kunecová, D.; Vozárová, V.; Tudor, E.M.; Antov, P.; Savov, V. Utilization of Birch Bark as an Eco-Friendly Filler in Urea-Formaldehyde Adhesives for Plywood Manufacturing. *Polymers* **2021**, *13*, 511. [CrossRef] [PubMed]
95. Hejna, A.; Barczewski, M.; Kosmela, P.; Mysiukiewicz, O.; Kuzmin, A. Coffee Silverskin as a Multifunctional Waste Filler for High-Density Polyethylene Green Composites. *J. Compos. Sci.* **2021**, *5*, 44. [CrossRef]
96. Bejenari, I.; Dinu, R.; Montes, S.; Volf, I.; Mija, A. Hydrothermal Carbon as Reactive Fillers to Produce Sustainable Biocomposites with Aromatic Bio-Based Epoxy Resins. *Polymers* **2021**, *13*, 240. [CrossRef] [PubMed]



MDPI  
St. Alban-Anlage 66  
4052 Basel  
Switzerland  
Tel. +41 61 683 77 34  
Fax +41 61 302 89 18  
[www.mdpi.com](http://www.mdpi.com)

*Forests* Editorial Office  
E-mail: [forests@mdpi.com](mailto:forests@mdpi.com)  
[www.mdpi.com/journal/forests](http://www.mdpi.com/journal/forests)



MDPI  
St. Alban-Anlage 66  
4052 Basel  
Switzerland

Tel: +41 61 683 77 34  
Fax: +41 61 302 89 18

[www.mdpi.com](http://www.mdpi.com)



ISBN 978-3-0365-3152-6